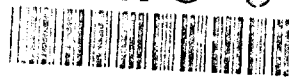


AD-A275 046



ESL-TR-91-26

ASPHALTIC CONCRETE PERFORMANCE UNDER HEAVY FIGHTER AIRCRAFT LOADING

D.A. TIMIAN, S.M. DASS, W.C. DASS, R.H. SUES, M.B. HARDY, J.G. MURFEE

HEADQUARTERS AIR FORCE CIVIL
ENGINEERING SUPPORT AGENCY
HQ AFCEA/RACO
139 BARNES DRIVE
TYNDALL AFB FL 32403-5319

FEBRUARY 1993

FINAL REPORT

APRIL 1988 - NOVEMBER 1990

APPROVED FOR PUBLIC RELEASE:
DISTRIBUTION UNLIMITED

94-02294



ENGINEERING RESEARCH DIVISION
Air Force Civil Engineering Support Agency
Civil Engineering Laboratory
Tyndall Air Force Base, Florida 32403



94 1 25 096

NOTICE

PLEASE DO NOT REQUEST COPIES OF THIS REPORT FROM HQ AFCESA/RA (AIR FORCE CIVIL ENGINEERING SUPPORT AGENCY). ADDITIONAL COPIES MAY BE PURCHASED FROM:

**NATIONAL TECHNICAL INFORMATION SERVICE
5285 PORT ROYAL ROAD
SPRINGFIELD, VIRGINIA 22161**

FEDERAL GOVERNMENT AGENCIES AND THEIR CONTRACTORS REGISTERED WITH DEFENSE TECHNICAL INFORMATION CENTER SHOULD DIRECT REQUESTS FOR COPIES OF THIS REPORT TO:

**DEFENSE TECHNICAL INFORMATION CENTER
CAMERON STATION
ALEXANDRIA, VIRGINIA 22314**

EXECUTIVE SUMMARY

A. OBJECTIVE

One approach to reducing rutting is the use of a mix design technique that explicitly considers the loading which will be applied to the pavement. This study was designed to investigate the relative differences in performance of two mix design methods when the mixes are subject to high pressure tires.

B. BACKGROUND

Rutting of asphaltic concrete pavements is rapidly becoming a cause for concern among Air Force (AF) civil engineers. Modern fighter aircraft often have operating tire pressures well above the capacity of the existing pavements. Research efforts are under way to identify cost-effective alternatives for the design of asphaltic concrete mixtures under these high pressure tires.

C. SCOPE

Pavement test sections were constructed and trafficked by high pressure tires. Variations in test sections included mix design, airfield design, and wheel loading. Pavement loading and performance were monitored throughout trafficking. The collected data was reduced for evaluation of rutting performance and resistance.

D. METHODOLOGY

Two mix design methods, the heavy-duty Marshall and the gyratory, were investigated for this project. The Marshall technique is an impact method and was selected because it is the most frequently used design method for AF pavements. The gyratory uses a kneading action and was selected because it had showed promise in an earlier study.

E. TEST DESCRIPTION

Pavement test sections were designed and constructed at Tyndall AFB to study the rutting damage. Variations between test sections included mix design procedure, airfield design, and wheel loading. The mix design procedures were the heavy-duty Marshall and the gyratory. Airfield designs included 4-inch and 6-inch flexible pavements along with a 6-inch asphaltic overlay on 12 inches of Portland cement concrete. Two lanes were trafficked, one for an empty F-15C/D, the other for a fully loaded F-15C/D. This report documents the analysis of the test data from the fully loaded F-15C/D lane.

A single-wheel loadcart laden with 29500 pounds of lead weight was towed back and forth by a modified front-wheel drive truck. The single wheel was an aircraft tire set to an inflation pressure of 355 psi. The loadcart position, velocity, and applied load was monitored continuously throughout the trafficking. The load was trafficked across a 4-foot wide lane using a normal distribution. Histograms of loadcart position were calculated for comparison to the pavement response. The forward passes of the loadcart averaged 13 mph while those passes conducted in reverse gear averaged 9 mph. The dynamic load applied to the pavement varied from 22000 to 37000 pounds due to the vertical oscillation of the trafficking loadcart. However, the average dynamic load, 29600 pounds, was similar to the static load of 29500 pounds.

Environmental measurements were also taken continuously throughout the trafficking. Although radiation intensity, wind speed and direction were monitored, they were not used in this analysis. Five thermocouples were placed to monitor the temperature at the pavement surface and at several depths below the surface. Ambient temperature was also recorded at six feet above surface. Because most of the trafficking was conducted during the hot summer months, the average ambient temperature was 87.4°F, while the average pavement surface temperature was found to be 112.8°F.

The permanent pavement response to the trafficking was monitored with a profilograph, which measures the contour of the pavement surface across the traffic lane. Profilograph measurements were taken prior to trafficking for original conditions, at intermittent pass levels, and at the end of trafficking for final conditions. Cores from the asphaltic concrete were also taken at different pass levels to determine the change in air voids with traffic.

Damage parameters were defined to provide a consistent set of variables that quantify the pavement surface response. They included maximum rut depth, maximum upheaval, rut width, rut area, and upheaval area. These damage parameters were then used to correlate damage to the applied loading. Statistical methods were employed to rank order the test sections by degree of damage. A multivariate analysis was conducted to determine the significance of the test variables on the pavement damage in light of the damage variability within each test section and other sources of variability such as environment, material properties, and loading. A Pearson pairwise correlation analysis of the the test variables was also performed to help interpret the results from the multivariate analysis and to further quantify the relative importance of the test variables and their relationship to each other.

F. RESULTS

A nonlinear relationship between damage and passes was found for all test sections. The damage measures revealed an increase in the accumulated damage at the ends of the traffic lane, reflecting the acceleration/deceleration of the loadcart. The lateral position histograms showed a slightly skewed distribution. The greater the asymmetry in loading, the greater was the observed damage. The temperature did not vary much during trafficking hours, therefore conclusions regarding the rate of rutting versus temperature could not be made.

The damage varied significantly between test sections, with the most obvious factors being the mix design and the granular layer support. For both mix designs, the composite test sections performed better than their flexible counterparts. The difference can be attributed to the rutting in the granular layers of the flexible sections. Sixty percent of the flexible test section rutting was in the granular layers.

The significance of the mix design procedure on the pavement response can be seen by comparing the damage profiles from the composite test sections. The Marshall mix section experienced three times the rutting of the gyratory mix despite having less traffic. The gyratory sections formed broad ruts, characteristic of densification. The Marshall sections formed multiple ruts, characteristic of plastic flow. The cores removed from the test sections showed the severely rutted Marshall mix to have densities greater than 98 percent theoretical maximum while the stable gyratory mix had densities below this critical value.

G. CONCLUSIONS

The laboratory compactive effort used to select the amount of binder (asphalt) must equal that from the expected traffic. The problem with the Marshall compaction procedure is that the impact method cannot create laboratory densities similar to those found under high pressure tires. Further increasing the Marshall compactive effort will only degrade the aggregate. The gyratory testing machine applies higher compactive effort through kneading without degrading the aggregate. The mix designer is able to select the amount of binder appropriate for the traffic.

This study has shown that pavements can be designed using gyratory methods and that these surfaces have superior performance to Marshall mix designs. Even though the gyratory sections were compacted to only 92 percent of the theoretical maximum density, the gyratory sections outperformed the Marshall sections. Heavier field compaction equipment for gyratory mixes may further minimize surface rutting. Lower asphalt costs in the leaner gyratory mixes may offset the additional cost of purchasing gyratory testing equipment.

Independent of the mix design method, the granular layers were found to contribute about sixty percent of the rutting in the 6-inch flexible sections. Improvements in granular layer performance are needed to improve the overall performance of flexible airfield pavements under high pressure tires.

PREFACE

This report, entitled "Asphalt Concrete Performance under Heavy Fighter Aircraft Loading" was prepared by Applied Research Associates (ARA) under a Scientific and Technical Assistance (SETA) contract and funded under Contract Number F08635-88-C-0067 by the Air Force Civil Engineering Support Agency, Civil Engineering Laboratory, Tyndall Air Force Base, Florida 32403-5319. The work was a joint effort between the Air Force and its SETA contractor. Co-Principal investigators were David Timian of ARA and Jim Murfee of the Air Force. Dr Robb Sues and ARA's Southeast Division handled the statistical analyses.


Groups contributing to the design included Texas Transportation Institute, Army COE Waterways Experiment Station, Resource International, Inc, and the University of North Carolina at Charlotte. Most of the construction and loadcart operation was done by the Civil Engineering Laboratory Operations Branch. Data acquisition expertise was supplied by ARA's Rocky Mountain, New England, and Southwest Divisions.

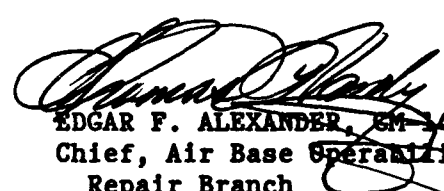
This report covers work performed between April 1988 and November 1990. The AFCESA/RD project officer was Jim Murfee.


This report has been reviewed by the Public Affairs Office and is releasable to the National Technical Information Service (NTIS). At NTIS, it will be available to the general public, including foreign nationals.

This technical report has been reviewed and is approved for publication.


JIM MURFEE, GS-13
Project Officer


FELIX T. UHLIR III, Lt Col, USAF
Chief, Engineering Research Division


EDGAR F. ALEXANDER, SM-14
Chief, Air Base Operability and
Repair Branch


FRANK P. GALLAGHER III, Colonel, USAF
Director, Air Force Civil Engineering
Laboratory

DTIC QUALITY INSPECTED 5

vii

(The reverse of this page is blank)

Accession For	
NTIS GRA&I	<input checked="checked" type="checkbox"/>
DTIC TAB	<input type="checkbox"/>
Unannounced	<input type="checkbox"/>
Justification	
By	
Distribution/	
Availability Codes	
Dist	Avail and/or Special
A-1	

TABLE OF CONTENTS

Section	Title	Page
I	INTRODUCTION.....	1
	A. OBJECTIVE.....	1
	B. BACKGROUND.....	1
	C. SCOPE/APPROACH.....	1
II	TEST DESCRIPTION.....	3
	A. DESIGN.....	3
	B. CONSTRUCTION.....	5
	C. ASPHALTIC CONCRETE.....	5
	D. BASE COURSE.....	6
	E. SUBGRADE.....	6
III	MEASUREMENT AND DATA ACQUISITION TECHNIQUES.....	14
	A. LOADCART INSTRUMENTATION.....	14
	B. ENVIRONMENTAL INSTRUMENTATION.....	15
	C. PROFILOGRAPH.....	16
	D. MATERIAL PROPERTIES.....	16
IV	DATA REDUCTION AND ANALYSIS.....	28
	A. VELOCITY.....	28
	B. LATERAL POSITION.....	29
	C. TEMPERATURE.....	33
	D. LOAD.....	33
	E. PAVEMENT PROFILES.....	34
	F. DAMAGE PARAMETERS.....	35
	G. EFFECTS OF COMPACTIVE EFFORT.....	40
	H. MULTIVARIATE ANALYSIS.....	42
V	CONCLUSIONS AND RECOMMENDATIONS.....	155
	A. DATA ACQUISITION EFFORTS.....	155
	B. RELATIONSHIP BETWEEN LOADING AND DAMAGE.....	155
	C. EFFECT OF MIX DESIGN ON PERFORMANCE.....	156
	D. SIGNIFICANCE OF RUTTING IN BASE LAYERS.....	157
	E. CONCLUSIONS AND RECOMMENDATIONS.....	157
	REFERENCES.....	158

APPENDICES

A	FALLING WEIGHT DEFLECTOMETER DATA.....	159
B	CORE DENSITY DATA.....	169
C	TEMPERATURE DATA AND HISTOGRAMS.....	177
D	THREE DIMENSIONAL PROFILOGRAPH PLOTS.....	241
E	REGRESSION PLOTS OF DAMAGE PARAMETERS VERSUS TRAFFIC...	255
F	BOX PLOTS OF DAMAGE PARAMETERS.....	291
G	RESULTS FROM PEARSON PAIRWISE CORRELATION ANALYSIS.....	311
H	RESULTS OF STEPWISE REGRESSION MODELS.....	341

LIST OF FIGURES

Figure	Title	Page
1	Layout of Test Sections	13
2	Loadcart With Optical Sensor Attached	22
3	Pavement Marking Pattern	23
4	Load Wheel Support Structure with Loadcells.....	24
5	Profilograph System	25
6	Posttest Marshall Mix Design Results	26
7	Trench Side View in the Marshall 4-Inch Flexible Test Section	27
8	Trench Side View in the Gyratory 4-Inch Flexible Test Section	27
9	Initial Segment of a Calculated Velocity Profile	62
10	Typical Velocity Profile, Forward and Reverse	63
11	Velocity Histograms for Stations 0-48 at Pass Level 2589	64
12	Velocity Histograms for Stations 562-612 at Pass Level 2589.....	65
13	Velocity Histograms for Stations 240-384 at Pass Level 2589.....	66
14	Velocity Histograms at Pass Levels 2589, 5817, and 10350	67
15	Data Acquisition and Algorithm for Calculating Lateral Position	68
16	Potential Y Position Error Caused by Optical Sensor Sampling Distance.....	69
17	Mode-Centered Histograms for Station 364	70
18	Comparison of Target and Actual Load Distributions	78
19	Typical Variation of Traffic Mode, Mean, and Standard Deviation	79
20	Mode and Mean of Lateral Position Versus Station	80
21	Normalized Lateral Position Histograms for 4-Inch Flexible Marshall Section.....	82
22	Normalized Lateral Position Histograms for 6-Inch Flexible Marshall Section.....	83
23	Normalized Lateral Position Histograms for 6-Inch Composite Marshall Section.....	84
24	Normalized Lateral Position Histograms for 6-Inch Composite Gyratory Section.....	85
25	Normalized Lateral Position Histograms for 6-Inch Flexible Gyratory Section.....	86
26	Normalized Lateral Position Histograms for 4-Inch Flexible Gyratory Section.....	87
27	Ambient and Surface Temperature Histograms	88
28	Midheight and Interface Temperature Histograms	89

LIST OF FIGURES

Figure	Title	Page
29	Six- and Twelve-Inch Depth Into Base Course Temperature Histograms.....	90
30	Average Daily Temperature for All Trafficking Days.....	91
31	Variation of Load During Pass 2500	92
32	Rut Progression in 4-Inch Flexible Marshall Section	93
33	Rut Progression in 6-Inch Flexible Marshall Section	94
34	Rut Progression in 6-Inch Composite Marshall Section ...	95
35	Rut Progression in 4-Inch Flexible Gyratory Section	96
36	Rut Progression in 6-Inch Flexible Gyratory Section	97
37	Rut Progression in 6-Inch Composite Gyratory Section ...	98
38	Representative Profile for Marshall Mix Design 4-Inch Flexible	99
39	Representative Profile for Marshall Mix Design, 6-Inch Flexible	100
40	Representative Profile for Marshall Mix Design, Composite.....	101
41	Representative Profile for Gyratory Mix Design Composite.....	102
42	Representative Profile for Gyratory Mix Design, 6-Inch Flexible.....	103
43	Representative Profile for Gyratory Mix Design, 4-Inch Flexible.....	104
44	Estimated Base Course Rut Profile, 6-Inch Marshall Mix Design.....	105
45	Estimated Base Course Rut Profile, 6-Inch Gyratory Mix Design.....	106
46	Damage Parameters.....	107
47	Rut Depth Regression Analysis for 6-Inch Composite Marshall Section.....	108
48	Maximum Upheaval Height Regression Analysis for 6-Inch Composite Marshall Section.....	109
49	Upheaval and True Rut Depth from the Marshall 4-Inch Flexible Section at the Final Pass Level.....	110
50	Upheaval and True Rut Depth from the Gyratory 4-Inch Flexible Section at the Final Pass Level.....	111
51	Upheaval and True Rut Depth from the Marshall 6-Inch Flexible Section at the Final Pass Level.....	112
52	Upheaval and True Rut Depth from the Marshall Composite Section at the Final Pass Level.....	113
53	Upheaval and True Rut Depth from the Gyratory Composite Section at the Final Pass Level.....	114

LIST OF FIGURES

Figure	Title	Page
54	Upheaval and True Rut Depth from the Gyratory 6-Inch Flexible Section at the Final Pass Level.....	115
55	True Rut Depths from 4-Inch Flexible Sections.....	116
56	True Rut Depths from 6-Inch Flexible Sections.....	117
57	True Rut Depths from Composite Sections.....	118
58	True Rut Depth vs Station at Pass Levels 1554 and 4784..	119
59	Boxplot of Rut Depth for Pass Level 2324.....	120
60	Boxplot of Rut Depth for Pass Level 4784.....	121
61	Boxplot of Rut Depth for Pass Level 9715.....	122
62	True Rut Depths from Gyratory Test Sections.....	123
63	True Rut Depths from Marshall Test Sections.....	124
64	Relationship Between True Rut Location and the Mode and Mean for Marshall Sections.....	125
65	Relationship Between True Rut Location and the Mode and Mean for Gyratory Sections.....	126
66	Affected and Rut Widths from the Marshall Test Sections.	127
67	Affected and Rut Widths from the Gyratory Test Sections.	128
68	Areas Calculated for the Marshall Sections at Final Pass Level.....	129
69	Areas Calculated for the Gyratory Sections at Final Pass Level.....	130
70	Boxplot Comparison of Rut Area From Each Test Section at Traffic Level 4784.....	131
71	Boxplot Comparison of Upheave Area From Each Test Section at Traffic Level 4784.....	132
72	Rut and Upheave Areas for the 4-Inch Flexible Test Sections.....	133
73	Rut and Upheave Areas for the 6-Inch Flexible Test Sections.....	134
74	Rut and Upheave Areas for the Gyratory Composite Test Section.....	135
75	Rut and Upheave Areas for the Marshall Composite Test Section.....	136
76	Rut and Upheave Areas for the Gyratory Composite Test Section Through Traffic Level 10350.....	137
77	Effects of Compactive Effort on Asphalt Content.....	138
78	Effectiveness of Four Levels of Compaction on Gyratory Mix from Paver.....	139
79	Density Change With Traffic, Gyratory Test Sections.....	140
80	Post-Traffic Densities, Composite Test Sections.....	141

LIST OF FIGURES

Figure	Title	Page
81	Matrix of Data Points Available for Analysis.....	142
82	ANOVA Generated Predictions of Rut Depth Versus Observed Damage.....	143
83	ANOVA Generated Predictions of Rut Area Versus Observed Damage.....	144
84	Pavement Impulse Stiffness Modulus Versus Station.....	145
85	Initial Bulk Density Data and Interpolated Values Versus Station.....	146
86	Asphalt Content Data and Interpolated Values Versus Station.....	147
87	Theoretical Maximum Density and Interpolated Values Versus Station.....	148
88	Asphalt Volume Data and Interpolated Values Versus Station.....	149
89	Voids Total Mix Data and Interpolated Values Versus Station.....	150
90	Voids Filled Data and Interpolated Values Versus Station	151
91	True Rut Depth Versus Standard Deviation of Lateral Position of Loadcart.....	152
92	True Rut Area Versus Standard Deviation of Lateral Position of Loadcart.....	153
93	Pavement Thickness Variation.....	154

LIST OF TABLES

Table	Title	Page
1	MATERIAL PROPERTY SUMMARY OF DESIGN ASPHALTIC CONCRETE...	7
2	BASE COURSE SPECIFICATIONS AND TEST RESULTS.....	8
3	AVERAGE ASPHALT CONTENT AND REFERENCE GRADATION VALUES FROM UNCOMPACTED MIX.....	9
4	AVERAGE MARSHALL PROPERTIES.....	9
5	AVERAGE GYRATORY PROPERTIES.....	10
6	AVERAGE VALUES OF DENSITY, ASPHALT CONTENT, AND VOID PARAMETERS FROM FIELD CORES.....	11
7	AVERAGE RESILIENT MODULUS VALUES OF FIELD CORES.....	12
8	PROFILOGRAPH INCREMENTS.....	19
9	FALLING WEIGHT DEFLECTOMETER TEST RESULTS.....	20
10	AVERAGE DENSITY VALUES OF CORES REMOVED FROM LOADED F-15 LANE.....	21
11	SAMPLE OPTISENSOR DATA FOR A PASS WITH AN EXTRA STRIPE...	54
12	EFFECT OF EXTRA POINT ON LATERAL POSITION.....	55
13	AVERAGE VALUES AND STANDARD DEVIATIONS OF TEMPERATURE MEASUREMENTS FOR 10350 PASSES OF TRAFFIC.....	56
14	STATIONS FOR REPRESENTATIVE TEST SECTIONS.....	56
15	DAMAGE RANK ORDERS AT VARIOUS PASS LEVELS.....	57
16	TEST VARIABLES USED TO DESCRIBE ANTECEDENT CONDITIONS IN MANOVA.....	58
17	R-SQUARE STATISTIC FOR EACH DAMAGE MEASURE - ALL VARIABLES.....	59
18	R-SQUARE STATISTIC FOR EACH DAMAGE MEASURE - VARIABLE SUBSET 1.....	59
19	R-SQUARE STATISTIC FOR EACH DAMAGE MEASURE - VARIABLE SUBSET 2.....	59
20	PEARSON PAIRWISE CORRELATION COEFFICIENTS FOR SIX DAMAGE MEASURES.....	60
21	STEPWISE REGRESSION VARIABLE RANK ORDERING.....	61

SECTION I

INTRODUCTION

A. OBJECTIVE

One approach to reducing rutting is the use of a mix design technique that explicitly considers the loading which will be applied to the pavement. Previous laboratory work sponsored by the Air Force Engineering and Services Center suggested that rational mix designs could significantly reduce the rutting potential of asphaltic concrete (1). The study reported in this paper was designed to investigate the relative differences in performance of two mix design methods when the mixes are subjected to high-pressure aircraft tire loadings. The Marshall technique was used because it is the most frequently used design technique for AF pavements; the gyratory technique was selected because it showed promise in the earlier study. Conclusions from the laboratory work were verified in this study through a field test using simulated aircraft loading conditions.

B. BACKGROUND

Rutting of asphaltic concrete pavements is rapidly becoming a cause for concern among Air Force (AF) civil engineers. Modern fighter aircraft often have operating tire pressures well above the capacity of the existing pavements. Because about forty percent of Air Force taxiways are asphaltic concrete, any increase in the rate of rutting will require major reconstruction costing millions of dollars. Research efforts are under way to identify cost-effective alternatives for the design of asphaltic concrete mixtures to resist rutting under increased tire pressures.

C. SCOPE/APPROACH

Pavement test sections were designed and constructed at Tyndall AFB to study the rutting damage caused by both empty and fully loaded F-15 C/D aircraft with high pressure tires. Variations between test sections included mix design procedure, airfield design, and wheel loading. The mix design procedures used were the Marshall method with heavy-duty criteria and the gyratory method. Airfield designs included 4-inch and 6-inch flexible pavements and a 6-inch asphaltic concrete overlay on 12 inches of Portland cement concrete.

The loadcars and pavement were instrumented to monitor the loading and pavement response during trafficking. Using computerized data acquisition systems, the loading data was recorded for each pass of the loadcart. Response measurements were recorded at periodic intervals during trafficking.

All of the collected data was reduced and stored using a database management system. This report focuses on the analysis of the test data from the fully loaded F-15 lane. Statistical analysis techniques were used to develop representative loading and response functions for all sections. Statistical methods were also used to investigate the correlations between loading functions, material properties, and response measurements.

This report documents pavement loading and response measurement techniques, data reduction procedures, analysis methodology, and results. All tables and figures for each section are located at the end of the section for the reader's convenience. Section II describes the test section design and construction. Section III presents the types of instrumentation used to make the trafficking measurements and presents the material properties measured during and after trafficking. Section IV describes how the raw data was reduced into a usable form, presents typical values for each of the parameters, and details the relationships between loading and damage for each of the test sections. Section V discusses the conclusions about pavement rutting that were developed from this study. Supporting data is supplied in the appendices. A complete set of mode-centered histograms and profilograph data are maintained in two unpublished appendices.

SECTION 11

TEST DESCRIPTION

The test sections for this project were designed to compare the rutting damage caused by high pressure tires between various airfield pavement designs. These designs include flexible pavements and asphaltic overlays of rigid pavements. Two mix designs, two aircraft loadings, and three airfield designs are tested in this study resulting in a total of twelve test sections.

This section summarizes the procedures used to design and construct the test sections. The as-built pavement section and material properties have been determined and are reported for use in analyzing test section response. The material property information is the result of extensive quality control in the laboratory and field investigations before, during, and after construction. The laboratory testing is comprised of general classification tests combined with Marshall and gyratory design tests. The field testing includes surveying, density, profilograph, Falling Weight Deflectometer (FWD), and Seismic Cone Penetration Tests (SCPT). A detailed presentation of the data can be found in the design and construction report (2).

A. DESIGN

The project was designed to test two asphaltic concrete mixtures under several construction and load variations. Two mix design procedures chosen for use in this project are the Marshall design using heavy-duty criteria and the gyratory design procedure. All other material variables are eliminated by using the same materials and the same construction techniques. The airfield design types, illustrated in Figure 1, include 4-inch and 6-inch flexible pavements over 12 inches of base course, and a 6-inch asphaltic concrete overlay on a 12-inch thick Portland cement concrete slab. The flexible pavement sections extend from each end of the PCC slab. All sections with Marshall mix are located on the east end and all sections with gyratory mix are located on the west end. Elevations measured at the site are based on a benchmark located south of the concrete slab. The elevation of this benchmark was arbitrarily assumed to be 10 feet for convenience. The sections were designed to provide two trafficking lanes.

1. Asphalt Mix Design

The aggregate was selected and supplied under contract with Florida ASphalt and Paving Company (FAPCO) with ARA completing the quality control tests to determine the aggregate acceptability. The selected aggregate was supplied in three separate sizes, identified as #67, #8910 (both Alabama limestones), and DRAVO, a crushed limestone from Perry, Florida. An acceptable blend of the aggregate was determined by an iterative trial and

error procedure and tested to see if it met the grain size limits called for in the test plan. The LA abrasion resistance, ASTM C 131 (3), of blended material was determined to be 28.3 percent loss, well below the limit of 40 percent loss. The specific gravity of each aggregate was determined according to ASTM C 127 and C 128 (3) along with the weighted average for the aggregate mix. Table 1 lists the design aggregate gradation and specific gravities.

Grade AC-20 asphalt cement was used in the design and production of the mix. The properties of the asphalt used are: penetration = 0.57 millimeter ASTM D 5 (4), specific gravity = 1.0293 ASTM D 70 (4), kinematic viscosity = 471.8 centistokes ASTM D 2170 (5), and the softening point = 128° Fahrenheit ASTM D 36 (4).

The asphalt mix design procedures are specified in the test plan as: Military Standard 620A, Method 100 (6), 75 blow compaction, for the Marshall mix, and ASTM D 3387 (5), using 300 psi compaction pressure, for the gyratory mix. The resulting asphalt contents for each mix are 6.4 percent of the total weight for the Marshall and 5.1 percent of the total weight for the gyratory. The resulting properties for each mix at the design asphalt content are also summarized in Table 1.

2. Base Course Design

The material used for the base course was shipped from northern Alabama due to the lack of acceptable material in the local area. The delivered material was tested for conformance to the base course specifications as listed in the test plan. The requirements and the results of the tests are listed in Table 2. Specific gravity tests, ASTM C 127 and C 128 (3), reveal an average value of 2.707 for this material. The optimum moisture content was determined to be 6.0 percent, resulting in an optimum density of 141 pounds per cubic foot (pcf) using Modified Proctor compaction, ASTM D 1557 (4).

3. Subgrade

Local materials consisting of clean sand were used for fill subgrade. The material was hauled in from a borrow pit approximately 1/2 mile from the test sections and is classified as clean sand (Unified Classification SP). A Modified Proctor test found the optimum moisture content to be 4.5 percent at an optimum density of 97.5 pcf.

B. CONSTRUCTION

Test section construction began in May 1988, with the Air Force's Operations Group (RDCO) removing the asphaltic concrete overlay from the previous test. ARA surveyed the site and placed grade stakes for the fill subgrade. RDCO transported clean sand from the borrow pit and placed it in 6-inch lifts. These lifts were watered and compacted with a vibratory roller until a maximum density was reached. ARA verified the compaction of the fill subgrade with a nuclear density gauge after each lift.

The base course material had been stored in stockpiles on the Portland cement concrete (PCC) slab. The transition sections between the flexible sections and the rigid pavement were constructed before placement of the base course over the fill subgrade. The transitions were designed to minimize the effects of changing pavement layers along the traffic lane. The base course thickness was increased to 36 inches for the 10 feet closest to the PCC slab. The base course thickness was gradually decreased to 12 inches over the next 5 feet. The base course material under the flexible sections was placed in 6-inch lifts by RDCO. ARA performed density checks and surveyed each lift upon completion.

Before the placement of the asphalt concrete, profilograph measurements were made every 2 feet over the flexible section base course by ARA. The PCC slab elevations were measured at three points every 2 feet along each traffic lane. Prime coat was applied to the base course material by FAPCO one week before placement of the asphaltic concrete. The application rate was 0.43 gallons per square yard and 0.35 gallons per square yard on the east and west ends, respectively. Tack coat was applied by FAPCO on each lift immediately before paving. The application rate for the tack coat was set to not exceed 0.05 gallons per square yard.

C. ASPHALTIC CONCRETE

The asphaltic concrete was manufactured at the FAPCO batch plant located on East 15th Street, Panama City, Florida. Before production began, the plant was calibrated using standard procedures with assistance of personnel from the US Army Corps of Engineers Waterways Experiment Station (WES). All cold feed bins were emptied and cleaned before being filled with the specified aggregate. FAPCO placed and compacted the asphaltic concrete in two lifts. ARA monitored the density during compaction with a nuclear density gauge. RDCP and ARA sampled the hot mix at selected points. ARA conducted extraction, grain size distribution, and compaction tests while paving was taking place. ARA also removed 4-inch diameter cores from the pavement after it had cooled for density correlations.

Several types of tests were performed on samples of the delivered mix. These tests included Marshall and gyratory compaction, theoretical maximum density, asphalt content by extraction, grain size distribution, bulk density, stability, and flow. The average asphalt content values and reference gradation data extracted from uncompacted mix is presented for all sections in Table 3. The average bulk density, stability, flow, and theoretical maximum density of the Marshall samples are shown in Table 4. The gyratory stability index, gyratory compaction index, stability, flow, and theoretical maximum density are shown in Table 5 for the gyratory samples. Table 6 presents the average bulk density, asphalt content, theoretical maximum density, asphalt volume, voids total mix, and voids filled, calculated from cores extracted from the test sections. Actual data is provided in Reference (2).

Resilient modulus tests were conducted on one core from each test section according to ASTM D 4123. The tests were conducted at 40, 71, 104 and 120 degrees Fahrenheit using 0.05 and 0.10 second-load durations and 1-, 2-, and 3-second cycle times. The data shows the expected trend of decreasing modulus with increasing temperature. A comparison between the Marshall and gyratory samples reveals a slightly higher modulus for the gyratory mixture as shown in Table 7.

A comparison of the grain distribution data from the plant calibration and the data from tests conducted during paving reveals the presence of excess fine material. This occurrence could have been caused by breakdown of the DRAVO material during the hot mixing process. The LA Abrasion test results did not reveal this breakdown because only the larger aggregates are tested.

D. BASE COURSE

Base course material was placed in 6-inch lifts and sprayed with water from a gravity feed water and P-4 crash fire fighting vehicle prior to rolling with a vibratory roller. A peak density was typically achieved after six to eight coverages.

E. SUBGRADE

The subgrade material was placed in 6- to 9-inch lifts using the scrapers which transported the sand from the borrow pit. A gravity feed water truck was used to saturate the sand just before compaction with a vibratory roller. The watering and compaction was repeated until a maximum density was reached as determined by a nuclear gauge.

TABLE 1. MATERIAL PROPERTY SUMMARY OF DESIGN ASPHALTIC CONCRETE.

AGGREGATE

SIEVE DESIGNATION	CRITERIA	PERCENT PASSING DESIGN
3/4"	100	99.9
1/2"	82-96	88.9
3/8"	75-89	79.0
# 4	59-73	62.0
# 8	46-60	52.6
# 16	34-48	41.2
# 30	24-38	30.2
# 50	15-27	21.1
# 100	8-18	12.5
# 200	3-6	5.6

SPECIFIC GRAVITY

ASPHALT	1.0293
AGGREGATE BULK (weighted average of blend)	2.591
APPARENT AGGREGATE	2.764

MATERIAL PROPERTY	MARSHALL	GYRATORY
Unit Weight of Aggregate Only (pcf)	---	144.5
Density (pcf)	148.7	153.9
Flow (.01 inch)	9.5	10.4
Gyratory Stability Index	---	1.02
Stability (lbs)	3000	5500
Voids Filled (%)	82.0	80.6
Voids Total Mix (%)	3.3	1.9

TABLE 2. BASE COURSE SPECIFICATIONS AND TEST RESULTS.

GRADATION OF AGGREGATES

SIEVE DESIGNATION	MINIMUM AND MAXIMUM %	ACTUAL %
1 INCH	100	100.0
1/2 INCH	40-70	65.9
# 4	20-50	33.7
# 10	15-40	22.2
# 40	5-25	12.4
# 200	0-10	6.6

LOS ANGELES ABRASION

Maximum Wear %	40.0
Actual Wear %	27.4

INDEX PROPERTIES

TEST	SPECIFICATION	ACTUAL
Liquid Limit	Non-Plastic - 25	13.8
Plasticity Index	0-5	0
Maximum Dry Density	Peak	141.0 pcf
Optimum Moisture Content	- - - -	6.0%
Apparent Specific Gravity	- - - -	2.707

**TABLE 3. AVERAGE ASPHALT CONTENT AND REFERENCE GRADATION
VALUES FROM UNCOMPACTED MIX.**

SECTION NUMBER	MIX TYPE	LIFT LAYER	NUMBER OF SAMPLES	ASPHALT CONTENT	PERCENT PASSING #8	PERCENT PASSING #200
1	MARSHALL	TOP	2	6.27	47.2	8.4
2	MARSHALL	TOP	4	6.28	48.6	9.1
	MARSHALL	BOTTOM	2	6.57	59.3	11.5
3	MARSHALL	TOP	10	6.47	49.7	10.0
	MARSHALL	BOTTOM	2	6.07	57.6	11.2
4	GYRATORY	TOP	8	5.17	51.0	10.5
	GYRATORY	BOTTOM	2	5.08	59.1	11.2
5	GYRATORY	TOP	3	4.84	57.8	10.8
	GYRATORY	BOTTOM	1	5.41	61.6	11.6
6	GYRATORY	TOP	1	5.09	60.2	11.4

TABLE 4. AVERAGE MARSHALL PROPERTIES.

SECTION NUMBER	LIFT LAYER	NUMBER OF SAMPLES	BULK DENSITY (pcf)	STABILITY (lbs)	FLOW (in)	THEORETICAL MAXIMUM DENSITY (pcf)
1	TOP	1	155.4	3128	.17	159.2
2	TOP	3	155.3	2914	.15	158.7
	BOTTOM	1	149.8	3226	.14	157.6
3	TOP	6	154.7	2746	.14	158.2
	BOTTOM	2	150.6	2945	.13	158.6
7	TOP	2	155.4	2639	.14	158.6
8	TOP	2	155.1	2827	.14	158.6
	BOTTOM	1	150.1	3080	.10	158.3
9	TOP	6	154.5	2863	.13	158.9
	BOTTOM	4	150.5	3094	.11	158.2

TABLE 5. AVERAGE GYRATORY PROPERTIES.

SECTION NUMBER	LIFT LAYER	NUMBER OF SAMPLES	BULK DENSITY (pcf)	GSI ¹	GCI ²	STABILITY (lbs)	FLOW (in)	TMD ³ (pcf)
4	TOP	4	157.0	1.060	0.990	5001	.12	161.9
	BOTTOM	2	154.8	1.026	0.987	5818	.15	161.5
5	TOP	3	156.0	1.032	0.988	5984	.11	162.0
	BOTTOM	1	154.7	0.999	0.987	5400	.15	161.4
6	TOP	1	151.9	0.983	0.987	5044	.10	161.7
10	TOP	5	156.9	1.056	0.986	5755	.11	161.5
	BOTTOM	2	153.8	1.016	0.986	6116	.11	162.0
11	TOP	4	158.1	0.783	0.987	5776	.11	161.9
	BOTTOM	1	153.5	1.010	0.987	6690	.12	163.4
12	TOP	2	158.2	1.054	0.986	6385	.11	162.2

¹ Gyratory Stability Index

² Gyratory Compaction Index

³ Theoretical Maximum Density

TABLE 6. AVERAGE VALUES OF DENSITY, ASPHALT CONTENT,
AND VOID PARAMETERS FROM FIELD CORES.

SECTION NUMBER	MIX & LIFT ¹	BULK DENSITY (pcf)	ASPHALT CONTENT (%)	THEORETICAL MAXIMUM DENSITY (pcf)	ASPHALT VOLUME ² (%)	VOIDS TOTAL MIX (%)	VOIDS FILLED (%)
1	M T	150.6	6.27	158.8	14.70	5.17	74.01
2	M T	153.0	6.29	158.9	14.98	3.71	80.46
	M B	148.5	6.57	158.4	15.17	6.28	70.89
3	M T	151.6	6.45	158.5	15.22	4.40	77.97
	M B	148.8	6.09	158.7	14.11	6.24	69.51
4	G T	148.9	5.18	162.1	12.02	8.20	59.80
	G B	146.3	5.09	161.5	11.59	9.40	55.26
5	G T	148.9	4.85	161.6	11.23	7.85	59.16
	G B	146.8	5.41	161.4	12.36	9.07	57.74
6	G T	144.9	5.09	161.7	11.49	10.38	52.58
7	M T	153.4	6.51	158.6	15.55	3.25	82.72
8	M T	152.4	6.46	158.6	15.32	3.91	79.71
	M B	148.2	6.83	158.3	15.76	6.38	71.27
9	M T	152.6	6.24	158.6	14.83	3.81	79.66
	M B	148.9	6.46	158.5	14.97	6.03	71.49
10	G T	151.6	5.13	161.5	12.11	6.11	66.57
	G B	147.1	5.00	162.3	11.44	9.41	54.96
11	G T	149.3	5.26	162.4	12.23	8.06	60.29
	G B	146.0	4.97	163.4	11.30	10.63	51.54
12	G T	148.4	5.12	162.3	11.83	8.57	58.02

¹ Mix Type M = Marshall, G = Gyratory
Lift T = Top, B = Bottom

² Asphalt Specific Gravity = 1.0293

TABLE 7. AVERAGE RESILIENT MODULUS VALUES (PSI) OF FIELD CORES.

TEST TEMPERATURE (°F)	MIX DESIGN	SAMPLING TIME (SEC)	CYCLE TIME		
			3-SEC	2-SEC	1-SEC
41	MARSHALL	0.05	1.85E+06	1.64E+06	1.72E+06
		0.10	1.21E+06	1.09E+06	1.13E+06
	GYRATORY	0.05	1.70E+06	1.78E+06	1.96E+06
		0.10	1.19E+06	1.36E+06	1.53E+06
74	MARSHALL	0.05	3.41E+05	3.35E+05	3.80E+05
		0.10	2.37E+05	2.45E+05	2.66E+05
	GYRATORY	0.05	4.27E+05	4.26E+05	4.51E+05
		0.10	2.98E+05	3.09E+05	3.33E+05
104	MARSHALL	0.05	7.47E+04	8.24E+04	6.46E+04
		0.10	5.91E+04	6.67E+04	5.36E+04
	GYRATORY	0.05	1.24E+05	1.21E+05	1.26E+05
		0.10	9.87E+04	1.06E+05	1.08E+05

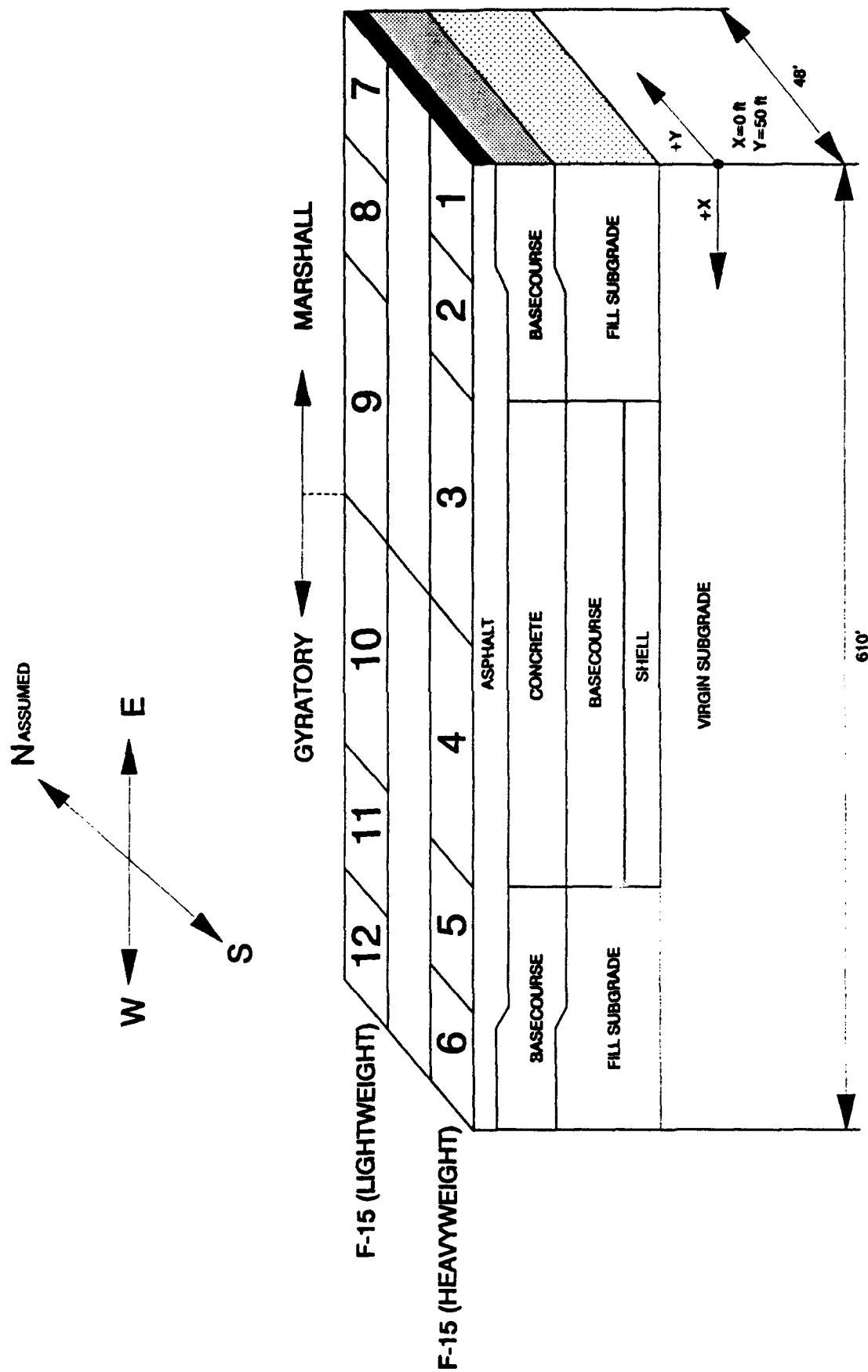


Figure 1. Layout of Test Sections.

SECTION III

MEASUREMENT AND DATA ACQUISITION TECHNIQUES

One of the primary purposes of this project was to investigate the rutting processes in asphaltic concrete pavements. Data from both the loading applied to the pavement and the pavement response was observed to evaluate these processes. To better quantify rutting, several types of measurements were made, including loadcart position, velocity, applied load, temperature, pavement deformation, and asphaltic concrete material properties. Descriptions of how these measurements were made are presented in the following subsections.

A. LOADCART INSTRUMENTATION

Loadcarts were used at Tyndall AFB to apply the load. They consisted of a front-wheel drive truck with a modified rear frame which held the selected amount of weight. The weight was almost completely supported by an aircraft tire which was mounted through an axle to the rear frame. Computerized data acquisition systems were designed and installed in F-15 loadcarts to monitor the loadings applied to the pavement. These computers were used to record data from each pass and to provide the operator feedback on how the systems were working. The information was gathered from two channels of instrumentation, an optical sensor and loadcells. All the data was saved and reduced as described in Section IV.

1. Optical Sensor

Loadcart position and velocity data was calculated from the output of an optical sensor mounted to the loadcarts, as shown in Figure 2. The sensor responded to white patterns marked on the black pavement by putting out a voltage which was monitored by the computer. The pattern marked on the pavement is illustrated in Figure 3. The optical sensor provides a high voltage whenever a stripe in the pattern is encountered and a low voltage otherwise. The relative times at which the high voltages were first encountered was recorded by the computer. At the end of each loadcart pass the data was stored on a floppy disk and checked for completeness. The automated completeness check involved counting the number of high voltage readings stored and writing the number to the screen. The loadcart operator could then verify that the correct number of pavement markings were encountered. Any deviations from the expected number signaled problems in the system which were then corrected.

2. Loadcells

Static measurements of the wheel loads and tire pressure were made before trafficking began. The total wheel loads used for each of the loadcars were 19000 and 29500 pounds for the empty F-15 and fully loaded F-15 loadcars, respectively. These high wheel loads were produced by stacking lead ingots, weighing either 1950 or 3900 pounds each, on the loadcar frame just above the load tire. The total static axle load was measured at a truck scale located on Tyndall AFB. The positions of the weights were marked and recorded so that the same configuration of weight could be produced at the field test site. Each day before trafficking began the configuration of the weights and the tire pressure were checked by the loadcar operators. Any variations in the position of the weights and the tire pressure were corrected. The tire pressures used were 190 and 355 psi for the empty F-15 and fully loaded F-15 loadcars, respectively.

Dynamic variations of the wheel load were anticipated before trafficking. Loadcells were mounted in the structure of the wheel support, as shown in Figure 4, in order to measure these variations while the loadcar was moving. Two loadcells, one in front of and one behind the load wheel, were wired to electrically average the response to the load variations. This electrical average was monitored by the second channel of the computer data acquisition system. Installation of the loadcells was completed before weights were added to the loadcar. The loadcells were placed in the proper position and the connection bolt was tightened enough to just register load on the loadcells. The output of the loadcells was monitored as the weights were applied to provide a calibration relationship. This calibration was used to calculate the variations in the wheel load.

B. ENVIRONMENTAL INSTRUMENTATION

Because asphaltic concrete material properties are temperature sensitive, the amount of rutting depends on pavement temperature. An environmental monitoring station was set up next to the 6-inch flexible Marshall design portion of the trafficking test sections. A data recorder monitored the output of the environmental sensors and saved the values at continuous 30 minute intervals throughout trafficking.

Five thermocouples were placed to monitor the temperature at different depths below the surface of the pavement: the surface, the midheight, the asphaltic concrete-base course interface, 6 inches into the base course, and 12 inches into the base course. An additional thermocouple was used to monitor the ambient conditions (approximately 6 feet above the pavement surface).

Three other environmental sensors were monitored throughout the test. The measurements included solar radiation intensity, wind speed, and wind direction. These latter measurements were made as a part of the environmental monitoring program, however they have not been used in connection with this study.

C. PROFILOGRAPH

The long-term pavement response to the trafficking was monitored with a profilograph, which measures the contour of the pavement across the traffic lane. The elevations of the end points of the profiles were measured with a rod and level. Variations in elevation across the profile were recorded using two different methods throughout the study. One method used a calibrated roller which rotated 1 inch for every foot of travel across the lane. A wheel and guide system followed the contour of the pavement, tracing the exact elevation variations on a sheet of paper attached to the roller. These hardcopy profilographs were digitized and stored on floppy disks. The second method utilized a computer data acquisition system in conjunction with the profilograph to directly store the profile data in digital format, as shown in Figure 5. The roller was replaced with a wire wound linear variable differential transducer (LVDT) with a 150-inch maximum displacement. The wheel and guide system had a direct current differential transducer (DCDT) attached. The output from these transducers was recorded by computer and stored on floppy disk.

Profilograph measurements were made prior to and periodically throughout trafficking. Table 8 lists the traffic levels where profile data was acquired. Also included in Table 8 are the starting and ending stations for each set of profilograph measurements. The starting and ending stations change with increasing traffic level because portions of the test sections were removed from trafficking as they became unsafe. Profilograph Set 21 is defined as the last profilograph at each station.

D. MATERIAL PROPERTIES

An extensive field and laboratory testing program provided a considerable amount of information on the material properties of the test sections. These tests were performed before, during, and after construction, and during and after trafficking. The pretrafficking material properties have been summarized in Section II with complete details documented in the construction report (2). Posttest mix designs, trafficked core tests, falling weight deflectometer (FWD) tests, and trench cuts were performed during and after the trafficking portion of the test. The results of these investigations are presented in the following paragraphs.

1. Posttest Mix Designs

The asphaltic concrete mixture delivered to the site contained excess dust, as defined by material passing through the #200 sieve. A posttest mix design using the Marshall procedure was performed to determine the effect of the excess fine material on the optimum asphalt content. Figure 6 presents the results of these tests. Optimum asphalt content for the Marshall procedure posttest was 5.8 percent, which is 0.6 percent lower than the optimum asphalt content determined in the original mix design series and in the constructed mat. This value is lower because excess dust tends to reduce the required asphalt. Insufficient material remained to complete the posttest mix design using the gyratory procedure. Based on the gyratory stability index of field samples compacted in the gyratory machine, the optimum asphalt content for the gyratory mix would also have been lower.

2. FWD Data

Nondestructive testing with the FWD was performed periodically throughout the construction and trafficking portions of the test at specified stations in each lane. FWD results recorded before trafficking have been summarized in an earlier report (7). FWD testing was not possible on sections where the surface profile had become too irregular, because such irregularity causes a nonuniform loading on the FWD plate. The peak deflection data is summarized in Appendix A in the form presented in Table 9, which is a sample set of FWD data. Other important information documented with the FWD data includes date, time, temperature, pass level, and impulsive force for each test. The impulse stiffness modulus (ISM), a measure of the applied load divided by the maximum displacement, for each load, has been calculated and is also included in Appendix A.

3. Core Densities

Cores were removed from the test sections periodically throughout trafficking. The samples taken before trafficking were used by Resource International, Inc., and the University of North Carolina at Charlotte for rut prediction and modeling. ARA performed bulk density tests on each of the cores prior to shipping. Table 10 lists the densities of a sampling of cores removed from the fully loaded F-15 lane at various traffic levels (top 4-inch lifts). The values presented in Table 10 are averages for all cores removed from that station at that traffic level. The individual density values are included as Appendix B.

4. Trenches

Upon completion of the trafficking portion of the test, several locations were selected for destructive testing. The asphaltic concrete was cut with a concrete saw and pulled off with a backhoe. The backhoe was then used to excavate the base course and a small layer of subgrade. The sides of the resulting trenches were cleaned and examined. Figures 7 and 8 show the sides of trenches in the 4-inch flexible Marshall and gyratory sections, respectively. The rutting in the asphaltic concrete and in the base course can be easily detected. Measurements made in the trench reveal that approximately sixty percent of the total rutting could be traced to the granular layers. In the trench at Station 474, base course rutting was not perceptible to the eye. However, there was degradation of base course in the upper 6-inch lift that was trafficked and some increase in dry bulk density under that station.

TABLE 8. PROFILOGRAPH INCREMENTS.

PROFILOGRAPH SET #	TRAFFIC LEVEL (passes)	STARTING STATION (ft)	ENDING STATION (ft)
01	0	0	610
03	70	0	610
04	112	0	610
05	224	0	610
06	420	0	610
07	448	0	610
08	882	0	610
09	1554	0	610
11	2324	0	610
21A	2589	0	36
21B	3049	38	84
12	3286	86	610
13	3942	86	610
15	4784	86	610
21C	5137	86	190
16	5370	192	610
21D	5817	192	334
17	6808	336	610
18	8080	336	610
21E	9715	336	348
21E	9715	528	610
19	9716	336	610
21F	10350	350	526

TABLE 9. FALLING WEIGHT DEFLECTOMETER TEST RESULTS.

SECTION 1

Thickness Base = 12 inches
Date = 10/04/88

Thickness Asphalt Concrete = 4 inches
Surface Temperature = 65.3°F

STATION feet	TIME hr	LOAD lbs	D1	D2	DEFLECTIONS (mils)					D7	ISM kips/in
0	922	9711	13.03	6.65	3.39	2.20	1.69	1.34	1.14	745.3	
0	922	9536	12.36	6.54	3.31	2.20	1.77	1.38	1.14	771.5	
0	922	14558	18.82	10.04	5.20	3.43	2.80	2.13	1.73	773.5	
0	922	18945	23.98	12.80	6.69	4.37	3.50	2.76	2.32	790.0	
0	922	26605	33.58	17.91	9.41	6.22	4.65	3.82	3.19	792.3	
12	923	9488	12.83	6.81	3.31	2.20	1.61	1.30	1.10	739.5	
12	923	9409	12.32	6.61	3.39	2.28	1.69	1.42	1.18	763.7	
12	923	14399	18.90	10.20	5.16	3.39	2.56	2.05	1.73	761.9	
12	923	18770	24.69	13.11	6.65	4.33	3.35	2.72	2.28	760.2	
12	923	26431	34.76	18.15	9.33	5.94	4.49	3.70	3.15	760.4	
23	925	9520	13.58	7.40	3.27	2.09	1.61	1.18	1.18	701.0	
23	925	9377	12.76	7.13	3.23	2.01	1.57	1.10	1.10	734.9	
23	925	14320	19.53	10.91	5.12	3.27	2.48	2.13	1.69	733.2	
23	925	18722	24.84	13.78	6.57	4.21	3.27	2.76	2.24	753.7	
23	925	26129	34.76	19.09	9.21	5.79	4.80	3.70	3.11	751.7	
35	926	9393	12.87	7.13	3.50	2.40	1.81	1.46	1.18	729.8	
35	926	9313	12.24	6.93	3.54	2.48	1.93	1.50	1.22	760.9	
35	926	14240	18.62	10.47	5.31	3.58	2.76	2.17	1.77	764.8	
35	926	18675	23.66	13.39	6.97	4.72	3.54	2.91	2.48	789.3	
35	926	25668	32.95	18.70	9.80	6.50	4.84	3.90	3.31	779.0	
47	927	9377	13.50	7.83	3.82	2.44	1.85	1.42	1.26	694.6	
47	927	9313	12.91	7.64	3.78	2.40	1.85	1.42	1.30	721.4	
47	927	14240	19.80	11.61	5.75	3.62	2.76	2.32	1.89	719.2	
47	927	18611	25.47	14.88	7.48	4.76	3.70	3.07	2.60	730.7	
47	927	25827	35.98	20.67	10.35	6.57	4.96	4.09	3.43	717.8	
58	929	9091	12.36	7.28	3.70	2.36	1.73	1.34	1.06	735.5	
58	929	9202	11.97	7.20	3.66	2.40	1.73	1.38	1.10	768.8	
58	929	14113	18.90	11.14	5.87	3.70	2.68	2.13	1.77	746.7	
58	929	18532	24.49	14.41	7.60	4.92	3.66	2.91	2.48	756.7	
58	929	25843	34.45	20.28	10.55	6.73	4.92	3.94	3.31	750.2	

TABLE 10. AVERAGE DENSITY VALUES (PCF) OF CORES REMOVED FROM LOADED F-15 LANE.

MIX TYPE	DESIGN TYPE	THICKNESS (inch)	STATION (feet)	DENSITY VALUE AT PASS LEVEL									
				0	2589	3049	4600	5137	5817	7500	9715	10350	
MARSHALL	FLEXIBLE	4	25	150.5	155.6								
			49	150.6		154.7							
	COMPOSITE	6	94	151.1			156.2						
			141	154.8									
			173	153.1			156.0						
			213	151.9									
			215	152.1									
			257	151.9				156.0					
			261	151.4									
			279	147.5				156.2					
GYRATORY	COMPOSITE	6	305	154.3			155.0		155.4				
			331	151.1					158.1				
			369	149.2						157.6			
			377	146.9			155.1			156.4		156.4	
			401	148.9									
			415	148.9									
			426	146.5			155.8			156.8		157.1	
			445	150.8									
			449	149.8									
			FLEXIBLE	6	496	151.1			157.4			157.9	
510	146.6												
567	144.8												
591	145.0									151.3			

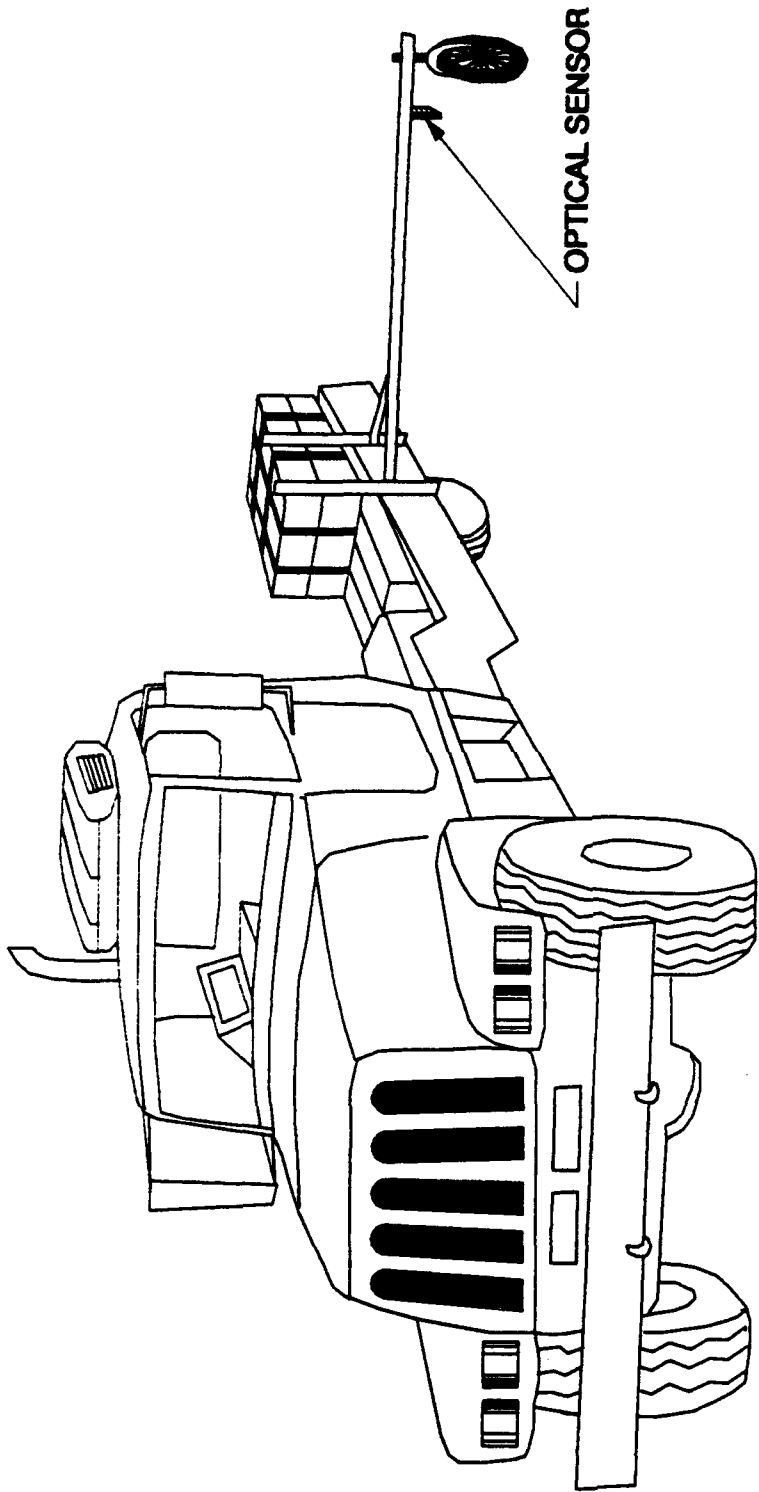


Figure 2. Loadcart With Optical Sensor Attached.

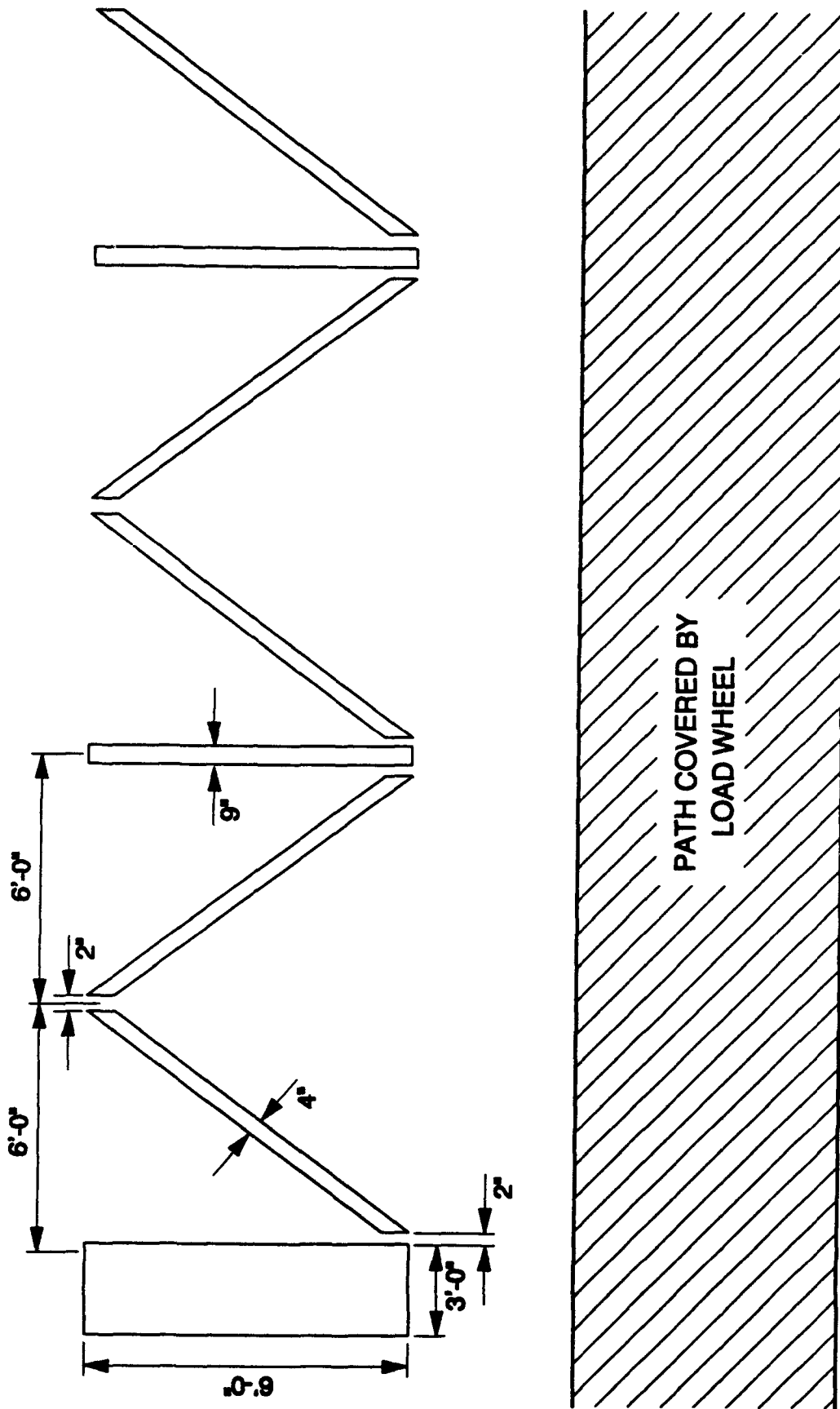


Figure 3. Pavement Marking Pattern.

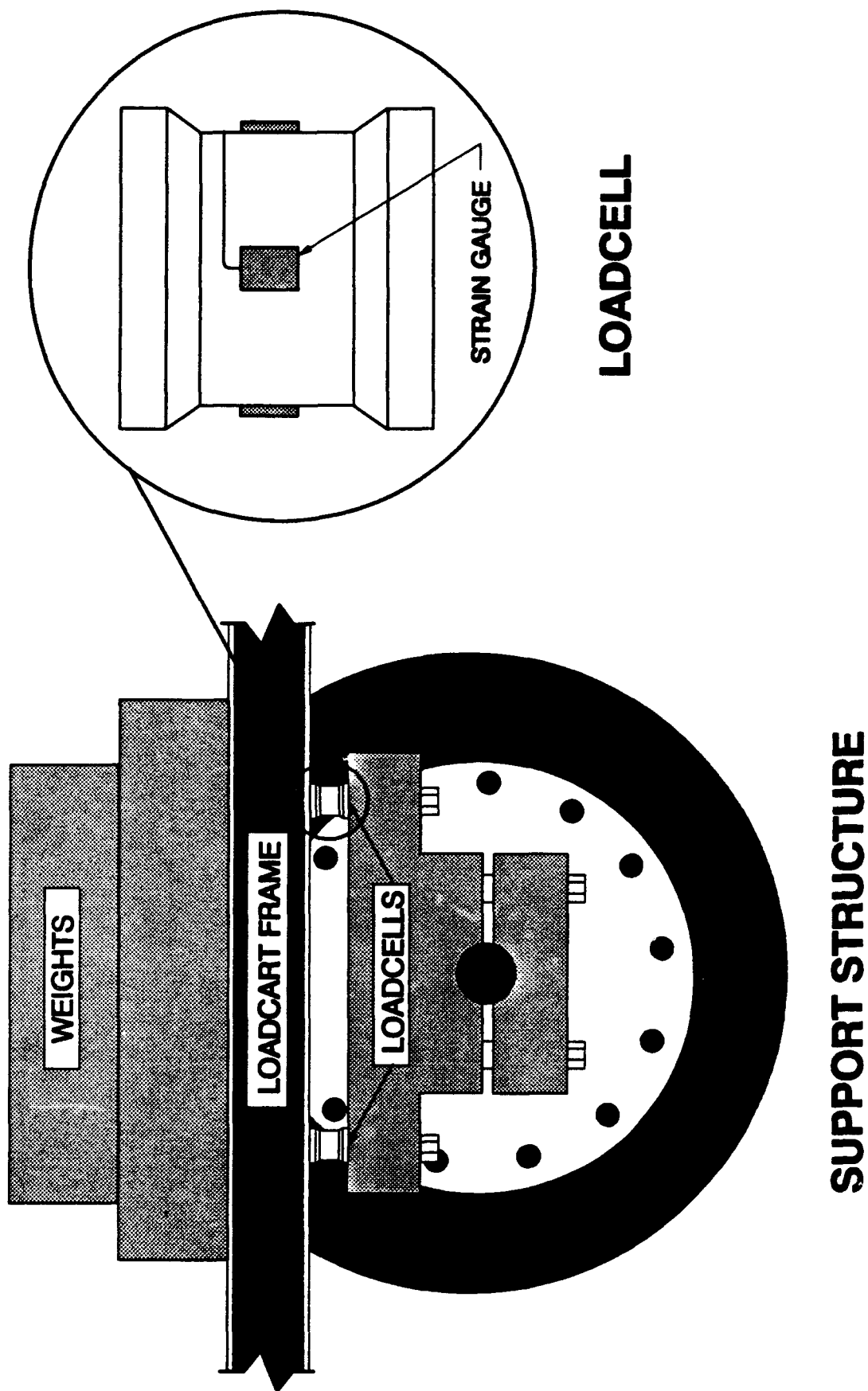


Figure 4. Load Wheel Support Structure With Loadcells.

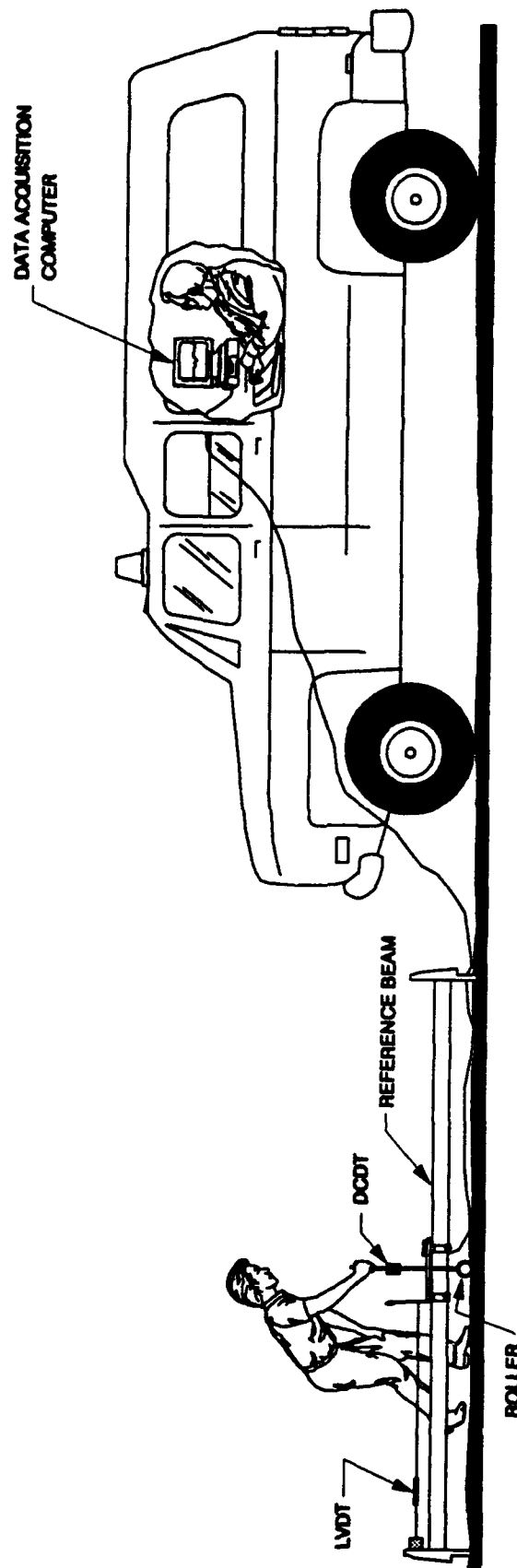
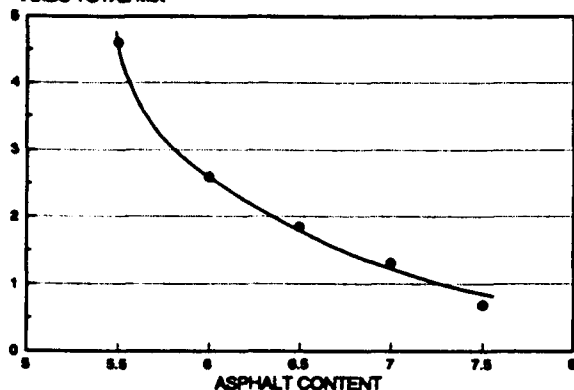
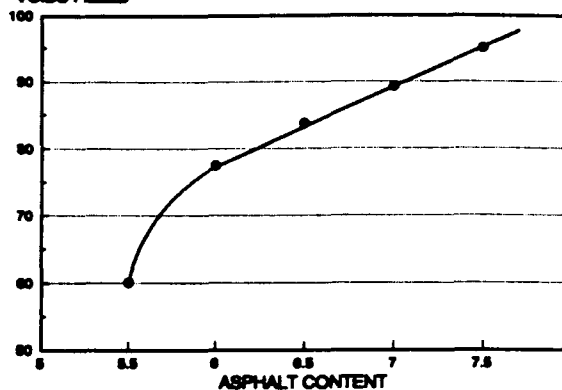


Figure 5. Profilograph System.

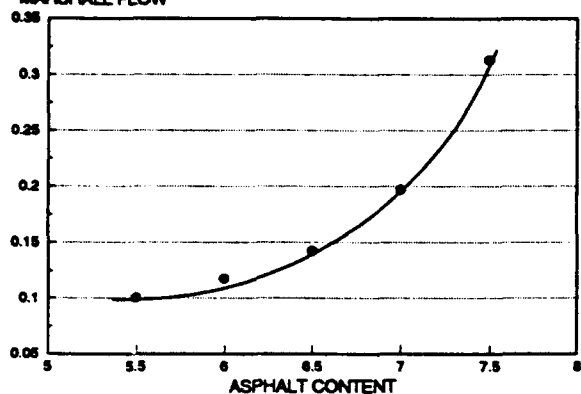
VOIDS TOTAL MIX



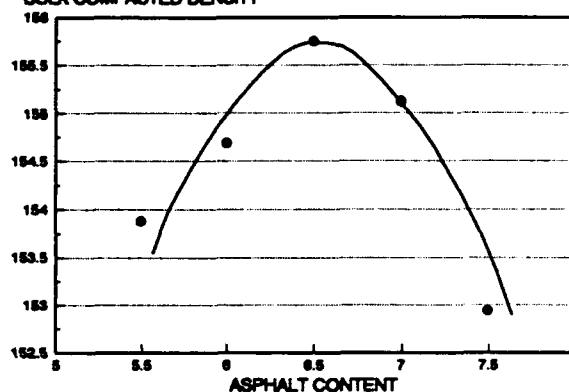
VOIDS FILLED



MARSHALL FLOW



BULK COMPACTED DENSITY



DESIGN ASPHALT CONTENT DETERMINATION

PROPERTY	TARGET	% AC
STABILITY	PEAK	5.75
VTM	4%	5.55
VF	75%	5.85
DENSITY	PEAK	6.5

AVG = 5.91

REQUIREMENTS TO MEET ACCEPTABILITY CRITERIA

PROPERTY	TARGET	% AC
STABILITY	>1800 lbs.	NO CHANGE
VTM	3 - 5%	5.81
VF	70 - 80%	NO CHANGE
FLOW	0.08 - 0.16	NO CHANGE

DESIGN ASPHALT CONTENT - 5.8%

MARSHALL STABILITY

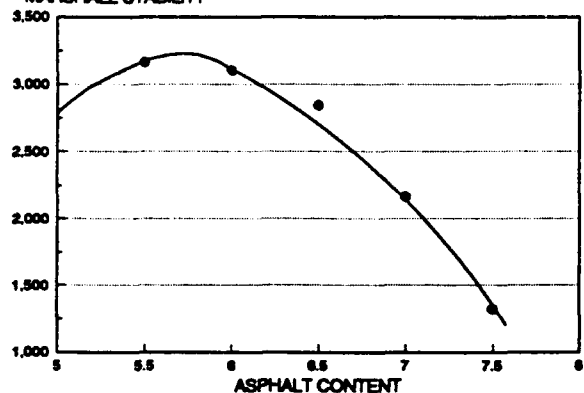


Figure 6. Posttest Marshall Mix Design Results.

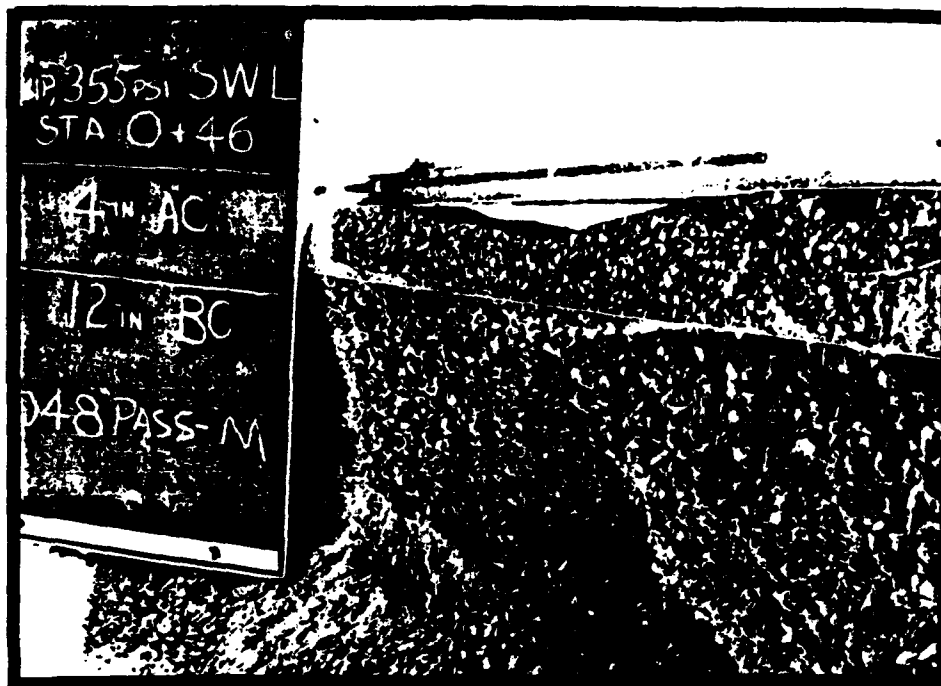


Figure 7. Trench Side View in the Marshall 4-inch Flexible Test Section.

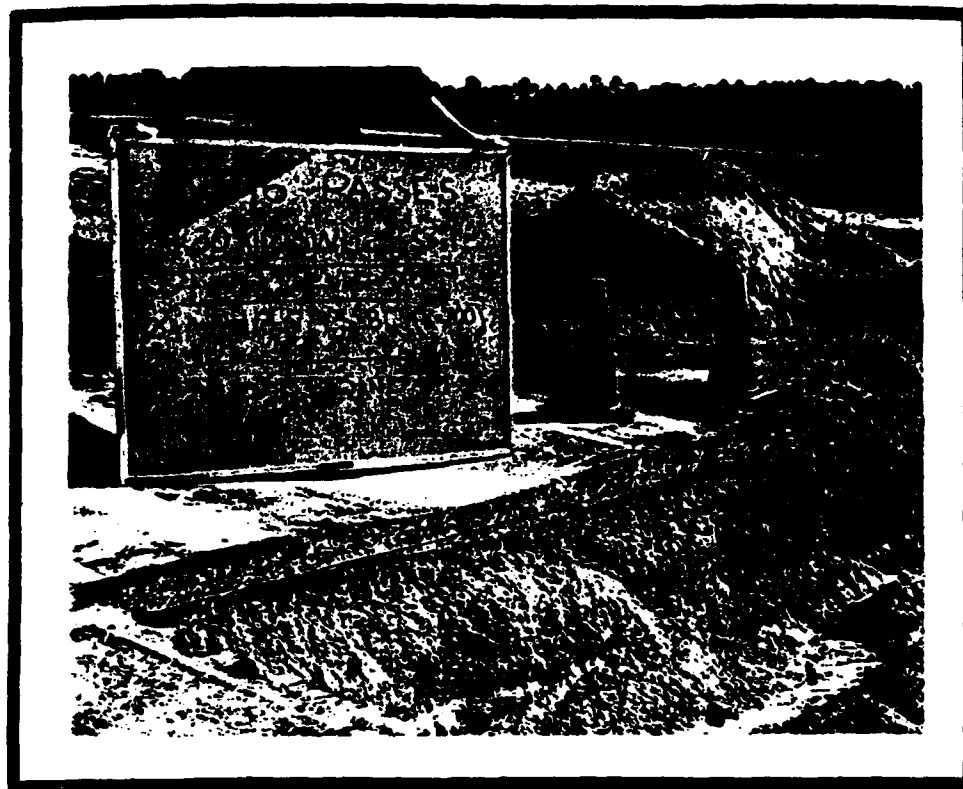


Figure 8. Trench Side View in the Gyratory 4-inch Flexible Test Section.

SECTION IV

DATA REDUCTION AND ANALYSIS

Some of the data recorded from the measurements described in Section III required conversion into a form that would be useful to engineers and scientists. This usable form of the data was maintained in a database for ease in querying and overall management of the various data types. Loadcart velocity and lateral position were obtained from the optical sensor data. Loadcells provided a measure of the dynamic fluctuations in the wheel load. Environmental instrumentation recorded the temperatures needed to estimate the in situ pavement material properties. The rutting of the test sections was monitored by profilograph. Algorithms used to convert this data into usable form are explained in this section. In addition, overall results from each type of measurement are presented and discussed for the fully loaded F-15 lane. Results from the empty F-15 lane will be presented in a later report.

A. VELOCITY

The velocity of the loadcart was calculated from the timing data produced by the optical sensor. The output from the optical sensor was sampled at a specified data acquisition rate. This rate served as a clock for determining the relative time at which each white stripe was detected. The velocity over the M-shapes was then calculated as the time it took the loadcart to traverse the pattern divided by the 12-foot distance between each vertical stripe of the pattern. This calculation procedure assumes: (1) the velocity was constant over each M-shaped pattern and (2) the distance traveled by the loadcart was 12 feet for all M-shaped patterns. Any deviations from these assumptions will be a source of error in the reduced loadcart position data.

The assumption of a constant velocity over each M-shape was valid over most of the trafficked length. However, this assumption does not hold true during the acceleration and deceleration portion of each pass. It was not uncommon to find a 1 to 2 mph difference in the calculated velocity from one M-shape to the next during the acceleration and deceleration stages. To minimize the error in the position calculations caused by this variable velocity, a modified velocity value was used in the calculation of the loadcart position as it passed the first angled leg of the M-shape. This modification was not necessary for determining the loadcart position while passing over the second angled leg, because the time data used comes from the central portion of the M-shape where the actual velocity is most likely to agree with the calculated velocity. Figure 9 illustrates the initial portion of a velocity profile as calculated by the data reduction code. This variation in velocity is assumed to actually occur in the field. A modified

velocity value was calculated only when the difference in velocity between two adjacent M-shapes was 1 mph or greater. The rate of change (slope) in the velocity between the two M-shapes was used to adjust the velocity to more accurately represent the true velocity of the loadcart as it passed over the first angled leg of the M-shape.

Because the loadcart naturally deviated from the intended straight path as it traversed the test sections, an increase in the true distance traveled resulted. The error caused by this deviation is very small. A 3-foot deviation in Y position over a 12-foot length causes only a three percent error in the velocity calculation. Visual observations by test personnel and Y position calculations verified that maximum lateral deviations were on the order of inches across any 12-foot section and therefore would not significantly affect calculated results.

The average velocity of the loadcart while traveling forward was generally 13 mph and consistently about 9 mph while moving backwards, as shown in Figure 10. The maximum backwards velocity attainable was limited by the reverse gear. The acceleration and deceleration zones typically extended about 36 feet (three M-shaped patterns) into each end of the test sections. Forward passes and reverse passes were labeled with odd and even pass numbers, respectively.

Velocity histograms were developed for the acceleration/deceleration zones of the trafficked length. Figure 11 shows the velocity histograms for Stations 0-48 at Pass Level 2589. Stations 0-12 have a wider range in velocity values while Stations 36-48 are outside the zone of any acceleration/deceleration effects. The velocity histograms for Stations 562-612 at Pass Level 2589 are illustrated in Figure 12. These histograms also indicate that the first 36 feet are within the acceleration/deceleration zone. Further from the ends of the lane the concentrations in velocities around 9 and 13 mph correspond to the nominal reverse and forward velocities. For comparison, Figure 13 shows the velocity histograms from two 12-foot sections located outside the range of acceleration/deceleration. The histograms for these same two sections are repeated in Figure 14, complete to their final pass level. Stations 372-384 show an increase in the number of velocity occurrences at 10-12 mph after Pass Level 5817. Although this section is centrally located to the entire test section length, Stations 0-336 were no longer trafficked after Pass 5817 because of excessive rutting. Therefore, after Pass 5817, Stations 372-384 fell within a new acceleration/deceleration zone.

B. LATERAL POSITION

The lateral position of the loadcart was calculated each time the loadcart passed either of the two angled stripes within each M-shaped pattern

(Figure 15). Using the optical sensor data, the velocity was first calculated for each M-shaped pattern as previously described. By using the difference in time at which each angled stripe was detected, coupled with the calculated velocity, two separate longitudinal distances were determined for each M-shape. These distances are located between the first vertical member of the M-shape (e.g., Point 4) and the adjacent internal angled stripe (Point 5), and between the two internal, angled stripes (Points 5 and 6). The lateral Y position of the loadcart was then determined algebraically based on these intermediate longitudinal distances, as described in Figure 15. The intermediate longitudinal distances from the M-shape pattern were then recalculated to correspond to the station designations along the length of the test path.

Errors in the calculated lateral positions could be caused by several factors including the assumed constant velocity across any one M-shape, missing the true edge of a white stripe due to the sampling rate, or extraneous points detected by the optical sensor where no white stripe actually exists. The lateral position calculations were corrected for acceleration/deceleration and are considered accurate. Figure 16a shows a hypothetical path of the optical sensor as it crossed over a white stripe of the M-shape, with sampling locations highlighted. Note that for a constant velocity, the sampling rate can be expressed in terms of samples per inch instead of samples per second. The distance between samples then becomes the maximum potential error by which the optical sensor may miss the start of a white line. This error will be reflected in the lateral position calculations because these calculations are based on the time interval between the start of adjacent white lines as detected by the optical sensor. Figure 16b shows the magnitude of this error for various loadcart velocities, using the sampling rate used in this study (150 Hz). For a velocity of approximately 13 mph, the maximum potential error in lateral position is about 1.5 inches.

Another source of error in the lateral position data was spurious detection of white stripes by the optical sensor. These extra data points were probably due to either light reflecting off the flat faces of the gravel in the pavement mix, or water puddles. For those passes containing a minimal number of extra data points, the erroneous points were easily recognized and were deleted. Table 11 is an example of data for a pass having an extra white stripe found by the optical sensor. The "icount value" in this table is the time (in counts) at which the optical sensor detected a white stripe. The "delta value" is the difference in time (in counts) between finding each white stripe. Note that the delta values maintain a pattern throughout the data on this pass which reflect the characteristic nature of an M-shaped pattern. The extra white stripe found is Data Point number 72. The effect of this extra white stripe is shown in Table 12. The lateral position data for this pass averages about 35 inches, however, beginning at Station 332 and beyond, the data is obviously wrong. By deleting the erroneous data point the proper

timing pattern in the delta value (and hence the Y position values) will be restored. However, for some passes with several extra white stripes, this judgment was not easily applied and the data was left as is. For these cases, the lateral position data was obviously incorrect from the point of the extraneous data and throughout the remainder of the pass. The erroneous portion of these passes was removed from the database so as not to bias results. Less than ten percent of all lateral position data was omitted from the database.

1. Histograms

An important step in reducing the optisensor data to a manageable volume was the calculation of load position histograms. These load histograms show the number of passes versus the Y position of the load tire for a given station. Load histograms were determined for stations and pass levels that corresponded to the stations and pass levels at which profilographs were taken. The applied loads (in histogram format) could then be directly compared with the measured rut profiles and corresponding damage parameters.

The bar width for the load histograms was selected based on two considerations. First, from basic statistics considerations (8), the following equation can be used to estimate the appropriate number of intervals (k) for plotting the histogram of a given data set,

$$k = 1 + 3.3 \log(n)$$

where n is the number of data points in the set. At the first pass level of interest, 70 passes, just seven intervals would satisfy this criterion. Given the measurement extent of 72 inches across the lane, seven intervals corresponds to a histogram bar width of 10.3 inches. At the highest pass level, 10350 passes, using this equation results in 14 intervals that are each 5.1 inches wide. The second consideration in determining a bar width was a physical one, tire width. The footprint of the fully loaded F-15 tire was approximately 8 inches wide. Because this width was also in the range of statistically-reasonable histogram bar widths, one tire width (8 inches) was used to calculate all load histograms.

A computer code was written to automatically compute and plot the load histograms from the optisensor data. For each pass at a given station, the available X and Y position data (these data had been stored only at locations where the optisensor crossed an angled white stripe) was interpolated to find Y position at the station of interest. Seventy-two 1-inch bins across the traffic lane were used to count passes at each station. From the 1-inch bins, histograms could then be constructed with an arbitrary positioning in the Y-direction. For this study, the load histograms were calculated and positioned either about the mode of the load distribution or

about the position of the peak true rut depth (at that station, up to that pass level). The first type of histogram insures that the central bar of the histogram will usually be the largest (resulting in histograms with a consistent shape). The second type allows the number of passes in one tire width directly above the peak rut to be determined (important in evaluating some of the rut prediction methods).

Mode-centered load histograms have been computed and plotted for all 1030 combinations of pass levels and stations for which profilographs are available.¹ A sample of this histogram data is shown in Figure 17 for Station 364. Note that the beginning and ending positions of the load histograms shown in Figure 17 shift with the mode of the traffic distribution. With these histograms, the build-up of loadcart traffic can be traced from start to finish. The last histogram shows the distribution of completed traffic. The final histogram from Station 364 is compared with the intended traffic distribution in Figure 18.

Variations in the mode, mean, and standard deviation of the traffic distribution are shown in Figure 19 for Station 364, which is typical of other stations. The mode and mean oscillate early in trafficking due to the small number of data points. After about 1000 passes, however, the traffic distribution stabilizes and the mode, mean, and standard deviation do not change much. The observation that the mode and mean are several inches apart is also typical of most stations, a result of the typically asymmetric (skewed) load distributions.

When taken in series, the load histograms also provide summary information about the wander of the loadcart (i.e., variation in Y position down the traffic lane) during trafficking. The mode and mean Y position of the traffic distributions are plotted versus station in Figure 20 for several intermediate pass levels and for the final pass level achieved at all stations. This load position information is compared in subsequent analysis to the lateral position of peak rut depth.

To consider the overall loading applied to each type of pavement, representative load distributions were developed on a section by section basis. These distributions were developed by counting any part of the tire which passes over the 1-inch wide bins set up to track the lateral location. Each loadcart pass would then contribute to the total passes in eight of the 1-inch bins. By simultaneously considering all stations within a selected longitudinal distance, the number of total observations greatly increases and the distributions can be presented in 1-inch increments. Representative distributions for each length of pavement with an equal final pass count are

1. All the mode-centered histograms are documented in an unpublished supplement to this report, Appendix I.

shown in Figures 21 through 26 for Sections 1 through 6, respectively. The dotted lines on each distribution represent plus or minus two standard deviations from the average distribution and indicate the relative variability in load distribution from station to station within a given section. With the exception of Stations 336-348 (Figure 24a), the variation within each length of pavement is small. The variation in load position in the length between Stations 336-348 is probably due to its shorter length and subsequently less reliable averaging within the 1-inch bins.

C. TEMPERATURE

Temperature measurements made throughout the trafficking portion of the study were loaded into the project database. The data was linked with the trafficking history data and sorted to provide the number of passes in each temperature increment. Figures 27 through 29 present the number of passes ("occurrences") versus the temperature data in histogram format for the final pass level. The complete set of histograms for each measurement type is found in Appendix C, along with the actual data at each traffic level when profilographs were taken. The average value of temperature for each measurement location and its standard deviation is presented in Table 13. These values were calculated over the complete trafficking portion of the test, so the actual average for sections which were removed from the test early may be slightly different. The average temperature presented for the pavement midheight is 103.5°F. Figure 30 is a plot of average daily temperature values for the pavement surface, pavement midheight, and ambient conditions throughout trafficking. As can be seen in the figure, the temperatures fluctuated around the average pavement temperatures throughout the course of the test.

D. LOAD

Visual observation of the loadcart traveling down the test sections revealed an almost continuous vertical oscillation of the entire loadcart. The loadcells mounted on the loadwheel support structure recorded the variations in the load applied to the tire. The tire transferred the wheel load to the pavement, although it is not certain how the tire pressure varied during the dynamic loading. The maximum magnitude of the load variation was nearly eighty percent of the static wheel load. The calibrated output of the loadcells from the fully loaded F-15 loadcart for a given pass is shown in Figure 31. The load varied a total of 15 kips, from 22 to 37 kips. However, the average and standard deviation for this pass were 29.6 and 1.8 kips, respectively. Based on this measurement, the static weight of 29.5 kips is actually a very good approximation of the load for the complete pass. It should also be noted that although a sampling rate of 150 Hz was used, only every other data point was retained in order to maintain a reasonable and manageable quantity of data.

E. PAVEMENT PROFILES

The profilograph provided a means of recording the permanent pavement response to the load. Profiles were taken prior to trafficking to represent original conditions, at intermittent pass levels throughout the trafficking, and at the end of trafficking to represent final conditions. The original and final profilographs were taken at 2-foot intervals while those taken at the intermittent pass levels were at 4-, 8-, or 10-foot intervals depending upon the variability of the response in each section. Profiles were measured across a 10-foot wide area, which was centered over the approximately 4-foot wide trafficking zone.

Between each test section exists a transitional zone created during construction. These transitional zones did not necessarily respond in the same manner as the adjacent pavement. Therefore, a central group of stations were selected to represent each test section to ensure that the results would not be misrepresented by transitional zone stations.² Table 14 lists the test sections, their associated station numbers (eliminating transitional zones) and the final number of passes. The final level of passes changes with station number because the test lanes were shortened as trafficking progressed. Also, the first 20 feet of the Marshall 4-inch test section performed poorly in terms of rutting in comparison to the remainder of that test section and was not considered representative of that section.

Figures 32 through 34 illustrate typical rutting progression for several stations from the Marshall mix design test sections. Figure 32 shows profilograph data from the 4-inch flexible, Figure 33 shows the 6-inch flexible, and Figure 34 is from the composite test section. Again, note that the final pass levels vary for each location. The Marshall mix design tended to develop multiple ruts (more than one prominent rut) in both the composite and flexible test sections. In the composite sections, there was a smaller overall magnitude in rut depth than the flexible sections. This difference was substantial because, in the flexible sections, a large portion of the rutting occurred in the base support layers.

Figures 35 through 37 illustrate typical rutting progression for several stations from the gyratory mix design test sections. Figure 35 shows profilograph data from the 4-inch flexible section, Figure 36 from the 6-inch flexible section, and Figure 37 from the composite test section. The gyratory mix appears to allow a smooth transition from the original surface elevation to its final state, resulting in a single, shallow broad depression with a small amount of upheaval (if any). The overall magnitude of the rutting was

2. The original and final profilographs taken at all stations are available in an unpublished supplement to this report, Appendix J. Selected figures in Appendix J also contain the profilographs taken at intermittent pass levels.

least in the gyratory composite test section. It appears that most of the rutting in the flexible sections occurred in the base course.

Representative profiles were computed for the six sections at or near the end of trafficking and are shown in Figures 38 through 43. Where a portion of the section was removed from trafficking, the representative profile was calculated at the pass level where the most stations could be included. In order to develop these representative profiles, all of the profiles were first normalized to the original pavement surface. That is, the rutting displacements for each profile were replaced by the relative displacement from the original pavement surface. Next, the normalized profiles were used to compute the longitudinal mean and standard deviation of the rut depth for each inch of lateral position along the rut, resulting in the "representative" profiles. The three curves shown in each figure are the mean rut depth for the subsection and the mean plus and minus two standard deviations. The representative profiles clearly depict the shape of the ruts at the end of trafficking and also the variability of rutting within a subsection.

A comparison of the rutting in the 6-inch composite and 6-inch flexible sections provides an estimate of the amount of the base course rutting. Assuming that the rutting in the composite sections is representative of the behavior of the asphaltic concrete, a subtraction of the representative composite rutting from the representative flexible rutting reveals the base course rutting. Figures 44 and 45 show the resulting estimated base course rutting for the Marshall and gyratory sections, respectively. The Marshall comparison was made at a slightly different traffic level (5817 passes for the composite and 5137 passes for the flexible section) and the gyratory comparison was made at the same traffic level (10350 passes). The maximum base course rutting in the 6-inch flexible Marshall section shown in Figure 44 is approximately 1.5 inches. This amount corresponds to sixty-five percent of the total rutting in the Marshall section. The maximum base course rutting in the 6-inch flexible gyratory section is approximately 0.5 inch, corresponding to fifty-nine percent of the total rutting in the 6-inch flexible gyratory section.

In addition to the representative profiles, three-dimensional plots were produced for each subsection to allow visualization of the rutting in an exaggerated scale. These plots are included as Appendix D. The plots show the multiple-rut channels that developed in some of the subsections and also the lateral wander of peak rut depth that developed in some subsections.

F. DAMAGE PARAMETERS

Damage parameters were created to provide a consistent set of variables that quantify the rut profiles. These damage parameters were then used to

correlate damage to the applied loading. The damage parameters are based on the change in profile from original conditions. Figure 46 illustrates the damage parameters that were calculated from the profilograph data.

Three vertical displacements were measured on each rut profile. Two of these measurements focus on the rutting depths. The true rut depth refers to the maximum difference between the original profile and the measured profile at any point along the profile. The apparent rut depth defines the magnitude of the rut as it would be measured in the field using a straight edge and ruler. This measurement would therefore include upheaval. The third vertical measurement taken was the maximum amount of upheaval above the original profile on either side of the true rut depth. For each profile, the lateral position of all these measurements was also determined.

A least-squares regression analysis was completed relating each damage parameter to total number of passes. The regressions were found to have a better correlation coefficient if the natural log of total passes were related to the damage parameter. Figures 47 and 48 present these regressions for two damage parameters, rut depth and maximum upheaval, from the 6-inch composite Marshall section. The remainder of the regressions are presented in Appendix E. The plots show a nonlinear relationship between load and rut depth as expected.

The calculated upheaval and true rut depth for the Marshall 4-inch flexible test section at the final pass level is shown in Figure 49. Note that the final pass level was 2589 passes for Stations 0-36 and 3049 passes for the remainder of the section. The initial 20 feet experienced more upheaval and true rut depth than Stations 38-64, even though it had 500 fewer passes. This increased magnitude of rut depth and upheaval is believed to be due to its location within the acceleration/deceleration zone. It appears that a lower velocity accelerated the degradation of the pavement, although an additional factor may be the loading frequency. The loading frequency is different for the end zones than the central portions of the trafficked length. The end zones were loaded twice within a relatively short span of time, whereas those portions in the center had evenly spaced and longer time periods between loadings. This increased magnitude of pavement degradation at the acceleration/deceleration zone was not significant in the gyratory 4-inch flexible test section. Figure 50 shows the vertical displacements for the gyratory 4-inch section at its final pass level of 9715 passes. All displacements are within a reasonably close range although there is a general increase in rut depth towards the end of the test section. Figures 51 and 52 show the displacements from the Marshall 6-inch flexible and composite test sections, respectively, at the final pass level. Although the composite test section had a smaller true rut magnitude, even with more passes, its magnitude of upheaval was far greater than the flexible test section. This probably reflects the inability of the PCC base to deflect. The gyratory composite test

section, Figure 53, did not exhibit a noticeable increase in upheaval magnitude in comparison to its flexible counterpart, Figure 54. Additionally, the rut magnitude was much less for the composite section.

The true rut depths from the two mix designs for each type of test section are compared in Figures 55 through 57. The data are only presented up to the maximum number of passes incurred by the Marshall mix design. Regardless of pass level, the gyratory mix design consistently exhibited a smaller amount of true rut depth than the Marshall mix design. Also, the rate of rutting in the gyratory test sections appears to flatten with pass level whereas the Marshall seems to increase as the rutting progresses.

For both mix designs, the composite test sections performed better than their flexible counterparts. Figure 58 compares the rut depth from both mix designs at two pass levels, 1554 and 4784. The Marshall 4-inch flexible section has no data for the 4784 pass level since all trafficking was halted by Pass Level 3049. The figure indicates the superior performance of the composite test sections and, in particular, the superior performance of the gyratory composite at Pass Level 4784. The differences in performance between the flexible and composite sections can be attributed to the rutting in the granular base layers of the flexible sections.

These results are also summarized in Figures 59 through 61 which show boxplots of rut depth across the six sections at three different traffic levels (2324, 4784, and 9715 passes). Box plots are not shown for some Marshall test sections at Traffic Levels 4784 and 9715 because trafficking had stopped before these traffic levels. The box plots show the 25th, 50th and 75th percentile values of damage as horizontal lines and the mean damage as a blackened square. The central vertical lines extend from the box as far as the data extends, to a distance of at most 1.5 interquartile ranges (an interquartile range is the distance between the 25 and 75th sample percentiles). The plots clearly illustrate the relative damage for the six sections and the variability of the damage within a section. All three figures indicate that the least amount of variability was in the composite sections. Damage variability was particularly low in the gyratory composite section.

The true rut depths for all the test sections from the gyratory mix design are summarized in Figure 62. The composite test section exhibited approximately half the rutting of the 6-inch flexible and about a third of the 4-inch flexible rutting. The 4-inch test section also showed a wider variation in its response than the composite test section. Wide variations in response were also found for the Marshall mix design, as shown in Figure 63. The Marshall mix seems to have changed behavior once a true rut of approximately one inch was induced. After that point the true rut depth would either: (1) increase at an extraordinary rate due to the channelization of

traffic in the rut; or (2) diminish, reflecting a broadening of the rut width due to an omission of passes directly in the rut. Note that after rutting became extreme in the Marshall sections, the loadcart was sometimes intentionally steered to just either side of the rut so as not to cause extreme wear on the sides of the loadcart tires.

The mean and mode of the lateral load position histograms were compared to the peak rut depth location and are shown in Figures 64 and 65. The mode tracked the rut depth much better than the mean, as would be expected, since the histograms were slightly skewed.

The apparent rut depth is the vertical displacement measured below two points of maximum elevation across the rut (Figure 46). The apparent rut depth was calculated in anticipation of the need to determine the remaining life, in terms of rutting, of a particular taxiway based on field measurements of apparent rut depth. However, it was found that the apparent rut depth is sensitive to the original pavement crown location and the amount of upheaval. Therefore it was not considered a good parameter in determining taxiway lifespan, although it still is important in determining the current safety and serviceability of the taxiway.

Two damage parameters related to rut width were also calculated from the profiles, affected width and rut width. The affected width was selected to describe the distance across the lane which showed significant deformation (rut or upheave). The determination of this width was based on a change in elevation of less than 2.5 percent of the true rut depth or 0.05 inches, whichever was greatest. The 0.05-inch cutoff value was chosen based on the accuracy of the profilograph instrumentation, the accuracy of the digitizing of the profilographs, and the naturally occurring roughness of the pavement surface. When a subsequent profilograph did not match smoothly to the original profilograph, the affected width calculations were too large. For these cases, the affected widths were scaled by hand, employing engineering judgment.

The rut width was calculated as the width between the two points of maximum elevation to either side of the point where the true rut depth was greatest. This strict definition did not adequately describe the rut widths for the Marshall mix design sections where there were multiple ruts. For these multiple rut cases, the rut widths for final profilographs were scaled directly from the profilographs. Figures 66 and 67 illustrate the rut and affected widths for the final pass level of the Marshall and gyratory mix designs, respectively. The box plots comparing rut width across the sections at three different traffic levels can be found in Appendix F. In the Marshall composite sections, the rut width is consistently about 45 inches, whereas in the flexible sections the rut width is larger (about 50 inches). For the gyratory mix design the rut width is about 60 inches, seemingly independent of

the base material. For both mix designs, the affected widths are highly variable, ranging from 50 to 90 inches for the Marshall and from 60 to 100 inches in the gyratory test sections. This variation is well illustrated in the box plots for rut width. High variability in rut width is mostly due to the resolution of the profilographs and the ability to perfectly align subsequent profiles.

Two areas were calculated for each profile, anticipating that they could be related to the amount of densification within the asphaltic concrete. The first is the area of upheaval and the second is the true rut area. These areas were calculated as either a positive or negative change in elevation across the affected width of each profile. Figures 68 and 69 present the rut area and upheaval area at the final pass level for the Marshall and gyratory sections, respectively. Figures 70 and 71 show box plots comparing rut area and upheaval area across the test sections at Traffic Level 4784 (see Appendix F for box plots at additional traffic levels). The figures reveal that the Marshall sections upheaved significantly more than the gyratory (exceeding a factor of three for the average upheaval area), for both the flexible and the composite sections. For rut area, the magnitudes are similar at the same traffic level. An important observation, however, is that the gyratory areas do not significantly increase at the higher traffic levels. In fact, the rut areas at the final traffic levels for the gyratory and Marshall sections are similar even though the final pass level for the gyratory sections is two to four times that of the Marshall sections. This is investigated further in the paragraphs below.

To quantitatively compare the damage for the six test sections, a statistical means separation analysis was performed. This analysis determines whether or not the average damage in a particular section is significantly different from the average damage observed in all the other sections (considering the damage variability) and then rank orders the damage in the six sections. The analysis included the Multiple T Test, The Waller-Duncan K-ratio T Test, and Tukey's Studentized Range Test. The tests were performed on all six damage measures, for the three traffic levels shown in the box plots. The results are summarized in Table 15. The table shows the rank order of the test sections, from least to greatest damage. Brackets are used to group sections for which the difference in damage was not statistically significant.

The results in the tables confirm the observations made earlier:

- (1) rut depth is significantly greater for the Marshall than the gyratory sections when other design parameters are held constant (i.e., asphalt thickness and base layer design)
- (2) rut areas are generally not significantly different for the two

mix designs when other design parameters are held constant (i.e., the Marshall test sections exhibited narrower and deeper rutting than gyratory but the breadth of the gyratory influence compensates for the deeper Marshall ruts

- (3) upheaval areas are greater for the Marshall mix than the gyratory regardless of other parameters.

Table 15 shows that, for rut depth, the 4-inch flexible gyratory design is roughly equivalent to the 6-inch flexible Marshall mix design. Thus, the gyratory design allows a savings of 2 inches of asphalt for the same performance as measured by rut depth.

Figure 72 shows the rut and upheaval areas for the 4-inch flexible test sections to Pass Level 6000. Both mixes have approximately the same amount of rut and upheaval area through Pass Level 3049 when the Marshall trafficking was halted, although the gyratory rut depth was less than the Marshall. Despite the variability in the affected width calculation, the gyratory design must have a broader basin of rutting than the Marshall. For the 6-inch flexible test sections shown in Figure 73, both mixes appear to have the same magnitude of rut and upheaval areas for only the first 1000 passes. Thereafter, the Marshall areas continued to increase at a faster rate than did the gyratory mix. The gyratory composite and Marshall composite test sections are shown in Figure 74 and Figure 75, respectively, up to Pass Level 6000 when the trafficking in the Marshall test section was halted. For the first 5000 passes both test sections have about the same amount of rut area. After that point, the Marshall clearly shows an increase in rutting. The difference in the response of the gyratory and Marshall composite sections is more apparent in the upheaval area. The gyratory design appears to maintain a relatively small amount of upheaval while the Marshall upheaval area is twice the gyratory. The gyratory maintains this relatively small amount of upheaval throughout the trafficking as shown in Figure 76.

In summary, the flexible test sections exhibit an immediate response to trafficking as evidenced by its rut area as a function of pass level. This immediate response in the flexible sections is present regardless of mix type or pavement thickness. The composite test sections did not show this immediate increase in rut area. This difference between the flexible and composite response time is attributed to granular layer rutting. In theory, granular base course materials (not modified) should have an initial, immediate response to trafficking due to their unbound nature.

G. EFFECTS OF COMPACTIVE EFFORT

In design of asphalt mixtures, once an aggregate has been selected, different increments of binder are added and specimens of the mixture are

compacted to determine the effects of overfilling and underfilling the voids in the aggregate. Density and voids filled with binder are two of the parameters used in this analysis. Figure 77 presents data from the test sections regarding the effect of compactive effort on the performance of the mix. The curve in Figure 77 represents the Marshall compactive effort used to design the mixture for the test sections. The top cluster of data points represents the density of the pavement as determined from cores taken from the gyratory test section ruts after traffic. Note that the voids filled are similar for the post traffic gyratory and the optimum Marshall binder content. However, the means by which the voids were filled was attained differently. The voids filled for the gyratory post-trafficking was achieved by compaction whereas the Marshall design curve achieved its voids filled by additional binder. This difference is seen by their performance under trafficking. When F-15 traffic was applied, the gyratory mix remained stable, but the Marshall mix did not. Hence, the laboratory compactive effort used to select the amount of binder must equal that of the traffic. Designing an asphalt mixture using a level of compactive effort which does not simulate the applied traffic may not provide the true optimum design asphalt content. The problem associated with the Marshall compaction procedure is that the impact method cannot reach the density levels achieved under high pressure tires. Further increasing the Marshall compactive effort degrades the aggregate. The gyratory testing machine applies higher compactive effort without degrading the aggregate and can simulate any traffic. The mix designer is then able to select the amount of binder appropriate for the traffic.

Specimens of the gyratory mix were taken from the paver and compacted in the laboratory with both Marshall and gyratory methods. The specimen air voids were compared to core voids of the same mix taken after construction of the mat and after traffic from the F-15. Figure 78 dramatically shows the effectiveness of gyratory compaction and inadequacy of Marshall compaction to match the density of the traffic. Figure 78 also shows that the 20-ton rubber tired (RT) roller used to compact the mat achieved an average of over seven percent air voids. Current Department of Defense (DOD) specifications (6) allow for payment deductions for greater than seven percent air voids. These penalties should be relaxed or greater compaction effort used to compact the mats, or both, if gyratory methods are to be implemented by DOD.

Cores removed from the test sections reveal the difference in behavior of the Marshall and gyratory mixes. Figure 79 illustrates the change in density as a function of pass level for the gyratory test section. The density information is provided in terms of percent theoretical maximum density because it takes into account the slight variation in the as-built asphalt content. As indicated, the gyratory sections densify under traffic. However, at a density level of ninety-eight percent of the theoretical maximum the densification rate decreased to almost zero. The mixture designed for the gyratory test sections was able to support the applied traffic without

failure. The data also reveals that a higher initial compactive effort in the gyratory test sections could eliminate most of the initial asphaltic concrete densification. It is not known if the 4-inch data is valid due to lack of additional data. Figure 80 compares the final densities attained by both mix designs. The Marshall mix, which had rutted so severely that trafficking was stopped, had densities greater than ninety-eight percent theoretical maximum while the stable gyratory had densities below this point.

H. MULTIVARIATE ANALYSIS

A multivariate statistical analysis was conducted to determine the significance of the test variables on rut damage in light of the damage variability within the sections and other sources of variability such as environment, material properties, and loading. These results also form a basis for developing improved rut damage prediction models. The statistical analysis techniques used were MANOVA (Multivariate ANalysis Of VAriance), Pearson pairwise correlation analysis, and stepwise regression with multivariate incremental R-square measures. The MANOVA was used for initial screening and identification of the test variables, while the correlation and stepwise regressions were used to further quantify the relative importance of the test variables.

The database for this analysis consisted of damage measures (response variables) and test variables (antecedent conditions). The antecedent conditions are the measures of load, environment, material properties, and pavement geometry that are used to explain the observed damage.

Figure 81 illustrates the 1030 observations of rut damage data available for the analysis, corresponding to the profilograph measurements made at the various stations at various pass levels. For each point in the figure the six damage measures as previously described (as shown in Figure 46) were evaluated. These included true rut depth (DT), maximum upheave area (HU1), second maximum upheave (HU2), rut width (WR), upheave area (A2), and true rut area (A1). To describe the antecedent conditions (loading, environmental, and pavement) for the multivariate analysis, 51 test variables were compiled. In total, input for the analysis therefore consisted of a matrix of 57 variables (51 test variables plus six damage measures) by 1030 observations. Due to some missing upheave area (A2) damage measures, only 1009 observations were available for that damage measure.

The test variables can be categorized into three groups: load variables, environment variables, and pavement material and geometry variables. Each of the test variables are listed in Table 16 and briefly described below.

Seven test variables were used for characterizing the pavement loading. These seven variables included the number of passes, the natural log of the

number of passes, and five variables for describing the lateral distribution or position of the load. The primary description of load was total number of passes. The natural logarithm of the total passes was included because earlier work showed a log-linear relation between damage and pass level.

The purpose of including the position variable was to study the effect of the load lateral spread on damage. The lateral spread is characterized by both the lateral position standard deviation and the lateral position variance. An additional measure, quasiskew, was also evaluated. Quasiskew is a measure designed to identify asymmetry in the load histogram; it is defined as:

$$Q = |(\bar{y} - y_{\text{mode}})| / \sigma_y$$

where Q = quasiskew,
 \bar{y} = mean load position,
 y_{mode} = modal (most frequent) load position, and
 σ_y = load position standard deviation.

The environmental parameters used in the multivariate analysis consisted of the number of passes at different temperature intervals. Earlier work has shown that the interaction of load and temperature is important in modeling pavement damage. This study looked at the effects of this interaction. Interaction cells were defined at each pass level and 10-degree temperature intervals. For example, as shown in Table 16, the number of passes for which pavement surface temperature was between 80 and 90 degrees was used as an interaction cell. Cumulative pass numbers were produced for each temperature type and 10-degree temperature interval, for each of the twenty pass levels at which profiles were taken. Only the eight intervals from 70 degrees to 150 degrees contained passes and for any given temperature type only those intervals that had a nonzero total number of passes were used as variables in the analysis. For example, as shown in Table 16, ambient temperature is characterized by four variables plus average ambient temperature. The average for each temperature type and pass level was estimated as:

$$t_{\text{ave}} = \sum (n_i \times t_i) / \sum n_i$$

where t_{ave} = weighted average temperature,
 t_i = the midpoint temperature of temperature interval i , and
 n_i = the cumulative count of passes for interval i .

Thus, a weighted average temperature was obtained at each of the twenty pass levels.

Eleven variables were used in an initial (Phase I) analysis to describe the pavement configuration and material properties. As shown in Table 16

these included: mix type, design type, design thickness, asphalt content, asphalt volume, total voids, voids filled, theoretical maximum density, bulk density, base course FWD ISM, and pavement FWD ISM. This set of variables is augmented in a later (Phase II) analyses to include aggregate gradation and constructed asphalt thickness. The first two variables, mix type and design type, are categorical variables, that is, they do not take on continuous numeric values as for the other variables. For multivariate analysis, the standard approach to handling such variables is to represent each value of a categorical variable by an indicator (0-1) variable. This approach was used for the MANOVA.

Falling weight deflectometer (FWD) and pavement material property measurements were not taken at all stations and so were estimated for intervening stations by piecewise linear interpolation. The Impulse Stiffness Modulus (ISM) was measured at the top of the base course to represent the underlying granular layers and also again at the top of the pavement to represent all pavement layers. When repeated measurements were taken at a station, mean values were used. Sections 1 and 6 do not have lower lift thickness measurements because a 4-inch thick pavement was laid in one lift at the same time as the top 4-inch layer of the other sections. Thus, the material properties are based on the top asphalt lift only for consistency.

1. MANOVA of Six Damage Measures

The first step in the statistical analysis was a MANOVA to screen the significance of all the test variables on the six damage measures, both individually and collectively. Due to the large number of test variables, a two phased approach was used in the MANOVA. This was necessary because many of the variables are expressible as linear combinations of other variables and are highly correlated with each other. This has the tendency to mask the importance of some variables and can lead to incorrect conclusions. In the first phase, an analysis where all the test variables were included was performed. In the second phase, the results of Phase I were used to select subsets of those test variables that were relatively independent of one another. The dataset used in the Phase I analysis (Figure 81) was also used for the Phase II analysis.

Because the initial analysis used all of the test variables it was expected that many would not be significant. Individual Analysis Of Variance (ANOVA) results were produced for each of the six damage measures. In each case a damage prediction model was developed based on the data and the test variables. Although the resulting models are not necessarily useful for damage prediction, they can be used to investigate the importance of the test variables. For each there is an R-Square statistic which measures the proportion of the damage variation explained by the model. The R-Square statistic was significant in all cases at any standard confidence level.

Table 17 shows the R-Square statistic for each of the damage measures from the Phase I analysis.

The ANOVA results indicate that the test variables explain the variation in damage across the test sections, particularly rut depth (DT) and rut area (A1). Figures 82 and 83 confirm this, showing the damage predicted by the ANOVA generated regression relationship versus observed damage. It should be noted that the significance of upheave area was reduced by the inclusion of the gyratory composite (Section 4), which did not exhibit plastic flow but did rut some.

The results of the ANOVA also showed that the main effects of only a small subset of the variables were estimable, because of the lack of independence among many of the test variables. For purposes of understanding the test results and developing predictive models, the significant variables identified in this initial analysis are not necessarily the best variables to rely on. This is because the analysis may arbitrarily identify as significant only one of a pair of highly correlated variables. In some instances this may be due to confounding in the experimental variables. Engineering judgment must be used to sort out the important variables and select subsets for further analysis.

Based on the Phase I analysis, two different variable sets were selected and used in Phase II. Both sets included a core of fifteen basic test variables that were found to be significant in the initial screening analyses, and a group of seven additional variables, different for each set. Note that several of the variables in the core group are functionally dependent. However, these were retained at this stage based on the initial screening analyses. The following analyses were used to further reduce and rank order the significant variables.

The core variables included the two categorical variables:

- (1) mix type (Marshall vs. gyratory) and
- (2) design type (flexible vs. composite)

and thirteen other numeric variables:

- (1) design thickness
- (2) natural log of number of passes
- (3) load lateral position standard deviation
- (4) load lateral position variance
- (5) load lateral position quasiskew
- (6) base course FWD ISM
- (7) pavement FWD ISM
- (8) top lift bulk density

- (9) top lift asphalt content (%)
- (10) top lift theoretical maximum density
- (11) top lift asphalt volume (%)
- (12) top lift total voids (%), and
- (13) top lift voids filled (%).

Two different groups of seven additional variables were used in conjunction with the core variables. These seven variables represent different combinations of pass number and trafficking temperature information. The first group contained:

- (1) number of passes
- (2) average temperature 12 inches into the base course
- (3) average temperature 6 inches into the base course
- (4) average temperature at base course-pavement interface
- (5) average temperature midheight in the pavement
- (6) average temperature at the pavement surface, and
- (7) average ambient temperature.

As described earlier, these average temperatures are weighted according to the number of passes at 10-degree temperature intervals. The second group of variables contained the cumulative number of passes when the surface temperature was:

- (1) 80-90 degrees
- (2) 90-100 degrees
- (3) 100-110 degrees
- (4) 110-120 degrees
- (5) 120-130 degrees
- (6) 130-140 degrees, and
- (7) 140-150 degrees.

Note that in this second group, total number of passes need not be included since it is simply the sum of the passes at the seven different temperature intervals. Additionally, only surface temperature was used for this initial analysis since the temperatures at the other locations are highly correlated with it.

With these two sets of variables it was now possible to compute multivariate statistics of the overall effect of each test variable on the damage measures collectively. Several test statistics were used to assess the significance of the test variables. These test statistics included, Wilk's Lambda, Pillai's Trace, Hotelling-Lawley Trace, and Roy's Greatest Root. All of the test statistics tended to indicate the same relative significance for the test variables.

The MANOVA produced individual ANOVAs from the first variable subset for each of the six damage measures and the multivariate significance tests for the effects of the test variables on the six damage measures collectively. All test variable main effects were estimable, but several were nonsignificant in the individual ANOVAs, that is, some variables were not significant for some damage measures. The ANOVA for each damage measure was significant at any standard confidence level. Table 18 shows the R-Square statistic for each of the damage measures from the ANOVA. The reductions in R-Square from the Phase I analysis results from using far fewer variables. However, the individual estimations of the main effects are far more reliable in this analysis.

The results of the MANOVA indicated that all twenty-two test variables were significant, that is, in terms of contribution to overall damage as measured by all six damage measures.

As with the first variable subset, individual ANOVAs were conducted for each of the six damage measures from the second variable subset and a MANOVA was performed for the effect of the test variables on the six damage measures, collectively. Again, all test variable main effects were estimable, but several were nonsignificant in the individual ANOVAs. The ANOVA for each damage measure was significant at any standard confidence level. Table 19 shows the R-Square statistic for each of the damage measures from the ANOVAs. As in the previous analysis, the R-Square values are smaller than those from the Phase I analysis. Again, this results from using fewer variables.

The results of the MANOVA, indicated that twenty-one of the twenty-two test variables were significant, that is, in terms of contribution to overall damage as measured by all six damage measures. The number of passes when pavement surface temperatures were between 140 and 150 degrees was not found to be significant. This is most likely because there was only a small number of passes at this temperature interval.

2. Pearson Pairwise Correlation Analysis

A Pearson pairwise correlation analysis of all the variables was also performed to help in explaining the results of the MANOVA and to further quantify the relative importance of the test variables and their relationship to each other. This analysis is a basic multivariate technique to compute correlation coefficients for all possible pairs of numeric variables in the data. Again, to include information about the two categorical variables, mix type and design type, two indicator variables were computed. The mix type indicator variable was set to zero for the Marshall mix and one for the gyratory mix. Similarly the design type indicator variable was set to zero for

the flexible design and one for the composite design. Also, three additional variables were added at this stage:

- (1) actual asphaltic concrete layer thickness, taken as the difference in pavement surface elevation to the base course surface elevation
- (2) dust (percent aggregate in the asphalt mix passing a #200 sieve)
- (3) sand (percent aggregate in the asphalt mix passing a #8 sieve and retained on the #200 sieve)

Appendix G contains the results of the correlation analysis in the form of a matrix entitled "Pairwise Correlations of All Possible Pairs of Non-Zero Variables." For each pair of variables, the matrix contains three numeric entries. The first entry is the Pearson correlation coefficient. The second entry is the "p-value" for the test of significance of the correlation coefficient. For small p-values, usually < 0.05 , the hypothesis that the correlation coefficient is zero is rejected. The third entry is the number of observations available for computation of the correlation coefficient.

Guided by the initial ANOVA and MANOVA results, several interesting observations can be drawn from the correlation analysis. The objective of the correlation analysis is to identify variables that could be used in a rut damage prediction model.

First, there is a very strong and significant correlation between design type (i.e., flexible vs. composite) and the pavement falling weight deflectometer measurements. The correlation coefficients are approximately 0.99. This indicates that the FWD measurement is an excellent indicator of the base support type, independent of the pavement surface mix type. This is further borne out by the lack of correlation between the FWD measurement and the mix type (nearly zero). Figure 84 illustrates this graphically, showing the pavement FWD readings taken across the test sections. Note that the plot shows the raw data as circles and the interpolated values used in the ANOVA as crosses.

Next the correlation between the damage measures and the FWD measurements can be examined. The FWD measurement correlates well with rut area (correlation coefficient of approximately seventy percent) and is also somewhat correlatable to rut depth (approximately fifty percent). This is true only because of the overwhelming influence of design type, i.e. difference between the underlying PCC and aggregate support shown in Figure 84. There was no correlation between FWD ISM and rutting within a given test section.

Finally, it is seen that the mix type is highly correlated with all of the asphalt properties, including bulk density, asphalt content, theoretical maximum density, asphalt volume, total voids, and filled voids. This correlation indicates that these measured properties were significantly different for the two different mixes and could, therefore, form the basis for a quantitative model. This is portrayed graphically in Figures 85 through 90.

Based on the correlation analysis, the pairwise relationship among the six damage measures can also be examined. Table 20 shows the correlation among the six damage measures, extracted from the matrix in Appendix G. The analysis verifies the expected correlation between rut depth and rut area and also the expected correlation between upheaval height and upheaval area. It also shows that there is a strong correlation between the two upheaval height measures. However, for several of the measures, the correlation is not particularly high, for example, the upheaval measures versus rut depth measures versus rut width. Thus, depending on the relative importance of each of the damage measure in describing the functionality of the pavement, it may be desirable to retain all six measures in further analysis and development of prediction models.

3. Stepwise Regression Analysis for Variable Rank Ordering

A stepwise regression analysis was performed to build the largest, most explanatory model for each of the six damage measures. Starting with the most important test variable, new test variables were added until no more significant ones could be found. During this process if any test variable lost its significance by virtue of being in combination with others in the model, it was removed, and the process continued. This analysis was used to rank the test variables in terms of their importance in explaining observed damage. It can also be used to build the best predictive model with the least number of variables.

As for the MANOVA, the stepwise analysis was performed in two phases. The stepwise analysis was begun (Phase I) using both variable subsets used in the MANOVA Phase II analysis. The results of this Phase I analysis were used in conjunction with the correlation and MANOVA results to identify a reduced set of variables for the Phase II stepwise analysis.

The results of the Phase I analysis showed that the temperature measurements contributed relatively little to explaining the damage variation in the test sections. On closer examination this should be expected because of the manner in which the test was conducted. There was not a sufficient variation in temperature at different stages of trafficking to quantify the relative contribution of the number of passes at the different temperature intervals. Most of the rutting occurred early on and the temperature did not

vary widely. Hence, the temperature variables were deleted in the Phase II stepwise regression analysis.

Several additional variables were also deleted for the Phase II stepwise regression analysis based on the results of the correlation analysis and the functional relationship among several of the asphalt property descriptors. The variables that were deleted included: total voids, voids filled, asphalt volume, base course FWD ISM, mix type indicator (Marshall versus gyratory), and design type indicator (flexible versus composite). The latter three variables were deleted because the correlation analysis showed that pavement FWD ISM is a good indicator of design type regardless of mix design and that mix type is adequately characterized by the remaining asphalt variables of asphalt content, bulk density, and theoretical maximum density.

Hence, the final retained variable set for the Phase II stepwise analysis represents a set of relatively independent variables that can be measured in a field evaluation. The best models found for each damage measure are listed in Appendix H. Also shown in Appendix H are the R-Square statistic for each model and the mean square error (mse) of the estimated unexplained variation. The F-test statistic shown for each variable measures the significance of its parameter estimate and is a good indicator of the test variable's relative importance and proportion of explained variation attributable to that test variable. Used with a normally distributed error term having a mean of zero and variance equal to the mean square error, these models would provide reliable predictions or simulations of damage for pavements and conditions within the ranges of the test measurements.

The overall importance of each final test variable on all of the damage measures collectively was calculated using multivariate incremental R-square measures or average "percentage of damage variation explained" by the test variable. These measures were calculated as:

$$\text{OVERALL IMPORTANCE} = 100/6 * \sum [(R\text{-square} * F) / \sum F]$$

where the outer sum is over the six damage measures, the inner sum is over all significant test variables within each the damage measure model, and F is the order-independent F-test statistic for the significance of the parameter estimate of each test variable. The results are shown in Table 21. Also shown are the number of damage measure models for which each variable was significant, as well as statistics for that variable across those models.

4. Conclusions from Multivariate Analysis

Immediately apparent is the importance of the base support as quantified by the pavement FWD measurements. This importance is expected based on the results of the MANOVA and correlation analysis, and the fact that

a large percentage of the total permanent pavement displacement of the flexible sections occurred in the base layers. The results show that the base support is the single most important variable when the set of six damage parameters is considered collectively. However, these results do not provide a basis for studying the relative importance of base course properties (as measured by the FWD) to rutting in flexible pavements because the correlation does not hold within pavement types (i.e. for the flexible and composite pavements separately). Surprisingly, in regards to using the FWD as a predictor of rutting potential, it should be noted that the pavement FWD measurements could not discern mix design type.

The measures for the loading (passes and log of passes) collectively explain roughly twelve percent of the damage variation. This number is not as large as might be expected because this analysis identifies those variables that explain the variation of damage in the dataset. Although the dataset captures the variation in damage with number of passes, number of passes does not account for differences in damage for the different test sections. Also, the rate of damage tends to level off as trafficking progresses, so that pass number can explain less damage variation as trafficking progresses. The regression analysis results for damage versus passes for the individual sections more clearly shows the relationship between loading and damage.

Taken together, the five pavement material measures (bulk density, theoretical maximum density, asphalt content, and the two aggregate gradation variables, sand and dust) explain about fifteen percent of the damage variation. This contribution is expected since the density and asphalt content measures were shown earlier to discriminate between the Marshall and gyratory mix design. The gradation measures contribute to explaining rut damage variation within a section.

The significance of the load distribution spread and shape (as measured by the variance, standard deviation, and quasiskew) on damage is not clear at this point. While there is a statistically significant contribution, it is relatively small. These results can be explained by examining the correlations between the load spread and damage measures shown in Figures 91 and 92. Although the correlation analysis does show a greater correlation between load spread and rut depth than for load spread and rut area, as would be expected, the correlations are very small for both. This is most likely a result of the small variation in load spread during the course of trafficking as can be seen in the figures. An important observation, however, is that quasi skew, which is a measure of load distribution asymmetry is in all cases positively correlated in the damage as might be expected. Hence, the indication is that an asymmetric load distribution will lead to greater damage.

Asphalt thickness was found to explain only about two percent of the damage variation when considering all six test sections. The contribution of asphalt thickness is overshadowed by the much greater effects of base support and mix design types. However, within a given section, for a particular pavement design, thickness may be a very significant variable. For this reason an additional study was performed to investigate the importance of asphalt thickness.

This study was conducted by performing a MANOVA and then individual ANOVAs for each section. The analysis examined the effect of thickness by evaluating how the damage variation is explained by four variables: section identifier (ID), actual asphalt thickness, number of passes, and log of number of passes. Figure 93 shows a plot of the actual asphalt thickness for the test sections. The section ID is included in the variable set for the MANOVA since this effectively "factors out" the effect of design difference, leaving only the variation within a section to be explained. Considering all six sections and all six damage measure, the MANOVA showed that asphalt thickness was highly significant in explaining damage variation within a section. Next, the individual ANOVAs were performed. The results of this analysis showed that asphalt thickness was again significant for all sections, except that it is only marginally so for the 4-inch flexible Marshall section and the 6-inch gyratory composite section.

As mentioned earlier, the test conditions did not provide sufficient data to quantify the effects of temperature. There was not a sufficient variation in temperature at different stages of trafficking to quantify the relative contributions of the number of passes at the different temperatures intervals.

The results and conclusions of the multivariate statistical analysis can be summarized as follows:

- (1) Pavement FWD measurements can differentiate between different base layer designs, regardless of the surface course design.
- (2) Mat asphalt content, bulk density, and theoretical maximum density may be key indicators for predicting surface rutting. However, this conclusion requires further evaluation.
- (3) Load asymmetry was found to be positively correlated with all damage measures for all sections. Hence damage prediction models should incorporate an allowance for expected trafficking asymmetry.
- (4) Multiple damage measures should be retained for further analysis and development of pavement performance evaluation models.

- (5) Actual thickness of the asphalt layer is significant in explaining rut damage variation within a section.
- (6) Pavement aggregate gradation is significant in explaining rut damage variation.
- (7) The quantitative effect of temperature on rut damage could not be evaluated.
- (8) The effect of load magnitude on rut damage has not yet been quantified.

TABLE 11. SAMPLE OPTISENSOR DATA FOR A PASS WITH AN EXTRA STRIPE.

PASS NUMBER = 4929, LANE = Heavyweight
 NUMBER OF LINES FOUND = 134
 NUMBER OF LINES EXPECTED = 133

DATA PT.#	ICOUNT VALUE	DELTA VALUE	DATA PT.#	ICOUNT VALUE	DELTA VALUE	DATA PT.#	ICOUNT VALUE	DELTA VALUE
1	1137	1137	46	3673	39	91	5159	44
2	1233	96	47	3714	41	92	5182	23
3	1332	99	48	3792	78	93	5207	25
4	1379	47	49	3825	33	94	5247	40
5	1428	49	50	3858	33	95	5273	26
6	1523	95	51	3920	62	96	5300	27
7	1565	42	52	3948	28	97	5340	40
8	1610	45	53	3976	28	98	5366	26
9	1694	84	54	4033	57	99	5390	24
10	1735	41	55	4060	27	100	5434	44
11	1778	43	56	4088	28	101	5458	24
12	1860	82	57	4139	51	102	5482	24
13	1899	39	58	4163	24	103	5528	46
14	1940	41	59	4188	25	104	5551	23
15	2020	80	60	4237	49	105	5573	22
16	2059	39	61	4258	21	106	5623	50
17	2100	41	62	4281	23	107	5644	21
18	2180	80	63	4330	49	108	5666	22
19	2220	40	64	4351	21	109	5716	50
20	2260	40	65	4373	22	110	5737	21
21	2340	80	66	4421	48	111	5758	21
22	2380	40	67	4442	21	112	5809	51
23	2421	41	68	4465	23	113	5830	21
24	2500	79	69	4513	48	114	5850	20
25	2539	39	70	4535	22	115	5901	51
26	2581	42	71	4557	22	116	5921	20
27	2659	78	72	4584	27	117	5943	22
28	2698	39	73	4605	21	118	5993	50
29	2740	42	74	4626	21	119	6014	21
30	2817	77	75	4649	23	120	6036	22
31	2858	41	76	4696	47	121	6085	49
32	2900	42	77	4718	22	122	6107	22
33	2979	79	78	4742	24	123	6129	22
34	3019	40	79	4788	46	124	6177	48
35	3060	41	80	4811	23	125	6199	22
36	3139	79	81	4834	23	126	6222	23
37	3178	39	82	4884	50	127	6273	51
38	3218	40	83	4905	21	128	6296	23
39	3301	83	84	4927	22	129	6322	26
40	3338	37	85	4977	50	130	6377	55
41	3378	40	86	4998	21	131	6403	26
42	3463	85	87	5021	23	132	6432	29
43	3502	39	88	5068	47	133	6500	68
44	3542	40	89	5091	23	134	6532	32
45	3634	92	90	5115	24	135	0	0

TABLE 12. EFFECT OF EXTRA POINT ON LATERAL POSITION.

PASS NUMBER = 4929, LANE = Heavyweight

X POS. FEET	Y POS. INCHES	TIME SECONDS	X POS. FEET	Y POS. INCHES	TIME SECONDS
608.972	39.165	0.343	345.407	33.943	21.889
603.143	34.881	1.003	339.214	35.735	22.209
597.214	36.265	1.643	332.604	43.587	22.503
591.085	34.186	2.276	327.975	44.870	22.683
585.199	36.448	2.856	321.606	31.561	22.963
579.269	36.399	3.416	318.573	76.044	23.116
573.229	36.086	3.976	309.505	32.765	23.576
567.229	35.914	4.523	306.375	73.670	23.736
561.300	35.230	5.056	297.500	32.830	24.196
555.300	36.770	5.589	294.625	76.670	24.349
549.319	35.001	6.123	285.665	30.846	24.823
543.356	37.446	6.656	282.827	79.089	24.969
537.375	34.330	7.189	273.606	31.561	25.443
531.375	37.670	7.723	270.573	76.044	25.596
525.281	35.462	8.263	261.342	34.726	26.063
519.318	36.991	8.789	258.177	71.296	26.223
513.205	36.368	9.329	249.239	35.966	26.669
507.318	36.991	9.849	245.830	67.125	26.836
501.225	36.130	10.389	237.020	38.588	27.276
495.450	38.570	10.903	233.536	63.605	27.456
489.245	35.895	11.456	225.056	38.160	27.896
483.356	37.446	11.983	221.992	69.074	28.056
477.281	35.462	12.523	213.311	35.096	28.509
471.318	36.991	13.049	210.247	72.138	28.669
465.375	34.330	13.576	201.470	33.193	29.129
459.150	34.970	14.129	198.691	77.459	29.276
453.448	33.452	14.643	189.665	30.846	29.749
447.229	35.914	15.209	186.827	79.089	29.896
441.568	32.014	15.736	177.665	30.846	30.369
435.112	34.512	16.349	174.956	80.638	30.509
429.138	37.172	16.883	165.636	31.200	30.989
422.980	32.933	17.403	163.027	81.496	31.123
417.309	35.121	17.843	153.766	29.634	31.596
411.260	36.293	18.256	150.897	79.931	31.743
405.375	34.330	18.629	141.636	31.200	32.216
399.268	36.384	19.009	138.766	78.366	32.363
393.113	37.476	19.376	129.505	32.765	32.836
387.171	35.223	19.716	126.636	76.800	32.983
381.278	35.489	20.043	117.625	31.330	33.449
375.089	34.237	20.369	114.750	78.170	33.603
369.407	33.943	20.663	105.721	30.176	34.096
363.085	34.186	20.989	102.721	77.824	34.269
357.474	33.143	21.276	93.723	30.159	34.809
351.144	34.901	21.596	90.893	79.890	35.003

TABLE 13. AVERAGE VALUES AND STANDARD DEVIATIONS OF TEMPERATURE MEASUREMENTS FOR 10350 PASSES OF TRAFFIC.

MEASUREMENT TYPE	DEPTH BELOW SURFACE (in)	AVERAGE VALUE (°F)	STANDARD DEVIATION (°F)
Ambient	72 (above surface)	87.4	4.4
Surface	0	112.8	13.5
Midheight	3	103.5	10.8
Interface	6	97.6	7.8
Six Inch	12	92.9	3.8
Twelve Inch	24	92.0	4.4

TABLE 14. STATIONS FOR REPRESENTATIVE TEST SECTIONS.

SECTION NUMBER	MIX DESIGN	SECTION TYPE	REPRESENTATIVE PROFILES	
			STATION	FINAL PASS LEVEL
1	MARSHALL	4-INCH FLEXIBLE ASPHALTIC CONCRETE	20-36	2589
			38-64	3049
2	MARSHALL	6-INCH FLEXIBLE ASPHALTIC CONCRETE	78-84	3049
			86-140	5137
3	MARSHALL	6-INCH COMPOSITE ASPHALTIC CONCRETE OVER 12-INCH PORTLAND CEMENT	156-190	5137
			192-304	5817
4	GYRATORY	6-INCH COMPOSITE ASPHALTIC CONCRETE OVER 12-INCH PORTLAND CEMENT	326-334	5817
			336-348	9715
			350-454	10350
5	GYRATORY	6-INCH FLEXIBLE ASPHALTIC CONCRETE	470-526	10350
			528-532	9715
6	GYRATORY	4-INCH FLEXIBLE ASPHALTIC CONCRETE	548-610	9715

TABLE 15. DAMAGE RANK ORDERS AT VARIOUS PASS LEVELS.

a) 2324 PASSES

DAMAGE	RUT DEPTH	MAXIMUM UPHEAVAL	RUT WIDTH	RUT AREA	UPHEAVAL AREA
least	6CG	4FG	6CG	6CG	4FG
	6CM	6FG	6CM	6CM	6FG
	6FG	6CG	4FM	6FG	6CG
	4FG	6FM	6FM	6FM	4FM
	6FM	4FM	6FG	4FG	6FM
most	4FM	6CM	4FG	4FM	6CM

b) 4784 PASSES

DAMAGE	RUT DEPTH	MAXIMUM UPHEAVAL	RUT WIDTH	RUT AREA	UPHEAVAL AREA
least	6CG	6CG	6CM	6CM	6CG
	6FG	6FG	6FM	6CG	6FG
	6CM	4FG	6CG	6FG	4FG
	4FG	6FM	6FG	6FM	6FM
most	6FM	6CM	4FG	4FG	6CM

c) 9715 PASSES

DAMAGE	RUT DEPTH	MAXIMUM UPHEAVAL	RUT WIDTH	RUT AREA	UPHEAVAL AREA
least	6CG	6CG	6CG	6CG	6CG
	6FG	6FG	6FG	6FG	6FG
most	4FG	4FG	4FG	4FG	4FG

Brackets indicate groups of data which are not significantly different.

4 = 4" overlay
6 = 6" overlay

F = flexible section
C = composite section

M = Marshall mix design
G = Gyratory mix design

TABLE 16. TEST VARIABLES USED TO DESCRIBE ANTECEDENT CONDITIONS IN MANOVA.

Load	Mode Lateral Position, Mean Lateral Position, Lateral Position Standard Deviation, Lateral Position Variance, Quasiskew, Number of Passes, Log of Number of Passes	
Environment	Number of Passes in 10° F Temperature Intervals	
	Location	Intervals
	Ambient	70-80, 80-90, 90-100, 100-110, average
	Surface	80-90, 90-100, 100-110, 110-120, 120-130, 130-140, 140-150, average
	Pavement Midheight	80-90, 90-100, 100-110, 110-120, 120-130, average
	Base Course/Pavement Interface	70-80, 80-90, 90-100, 100-110, 110-120, average
	6" into Base Course	80-90, 90-100, average
	12" into Base Course	70-80, 80-90, 90-100, 100-110, average
Pavement Material and Geometry	Mix Type, Design Type, Design Thickness, Asphalt Content, Asphalt Volume, Total Voids, Voids Filled, Theoretical Maximum Density, Bulk Density, Base Support FWD ISM, Pavement FWD ISM	

TABLE 17. R-SQUARE STATISTIC FOR EACH DAMAGE MEASURE - ALL VARIABLES.

Damage Measure	R-Square
True Rut Depth (DT)	0.8349
Maximum Upheave (HU1)	0.6171
Second Maximum Upheave (HU2)	0.6236
Rut Width (WR)	0.4102
Upheave Area (A2)	0.5979
True Rut Area (A1)	0.8463

TABLE 18. R-SQUARE STATISTIC FOR EACH DAMAGE MEASURE - VARIABLE SUBSET 1.¹

Damage Measure	R-Square
True Rut Depth (DT)	0.7460
Maximum Upheave (HU1)	0.5513
Second Maximum Upheave (HU2)	0.5583
Rut Width (WR)	0.4001
Upheave Area (A2)	0.5391
True Rut Area (A1)	0.8295

TABLE 19. R-SQUARE STATISTIC FOR EACH DAMAGE MEASURE - VARIABLE SUBSET 2.¹

Damage Measure	R-Square
True Rut Depth (DT)	0.7622
Maximum Upheave (HU1)	0.5517
Second Maximum Upheave (HU2)	0.5576
Rut Width (WR)	0.3771
Upheave Area (A2)	0.5350
True Rut Area (A1)	0.8350

¹ All "p" values ≤ 0.0001 , where the "p" values are probability significance levels associated with each damage measure model.

TABLE 20. PEARSON PAIRWISE CORRELATION COEFFICIENTS FOR SIX DAMAGE MEASURES.

		DT	HU1	HU2	WR	A2	A1
True Rut Depth	(DT)	1.00	0.36	0.31	0.19	0.27	0.78
Maximum Upheave 1*	(HU1)		1.00	0.83	-0.16	0.90	-0.04
Maximum Upheave 2*	(HU2)			1.00	-0.17	0.89	-0.11
Rut Width	(WR)				1.00	-0.18	0.45
Upheave Area	(A1)	SYMMETRIC				1.00	-0.10
True Rut Area	(A2)						1.00

* Two maximum upheave measurements are calculated: one to either side of the maximum rut depth.

TABLE 21. STEPWISE REGRESSION VARIABLE RANK ORDERING.

VARIABLE	OVERALL ¹ IMPORTANCE	MODEL IMPORTANCE			N-MODELS ²
		MEAN	STANDARD DEVIATION	MINIMUM	MAXIMUM
PAVEMENT STRUCTURE	14.4	14.4	20.9	1.0	54.2
Ln(passes)	8.5	10.2	11.3	3.6	30.4
ACC BULK DENSITY	5.1	5.1	4.2	0.7	10.4
ASPHALT CONTENT	4.5	4.5	2.6	2.1	8.6
PASSES	3.6	4.3	7.7	0.6	18.1
ALL SAND (% PASSING #8)	3.4	4.1	3.1	0.5	7.1
ASPHALT THICKNESS	2.3	2.7	4.5	0.2	10.6
ALL DUST (% PASSING #200)	1.6	2.4	0.9	1.6	3.7
ACC THEORETICAL MAXIMUM DENSITY	0.8	2.3	0.2	2.1	2.4
LOAD QUASISKEW	0.5	0.5	0.2	0.3	0.9
LOAD LATERAL VARIANCE	0.2	0.6	0.5	0.2	1.0
LOAD LATERAL STANDARD DEVIATION	0.2	0.5	0.5	0.1	0.9

¹ Percent of variation expected - all damage measures.² Number of damage measure models for which the variable is significant.

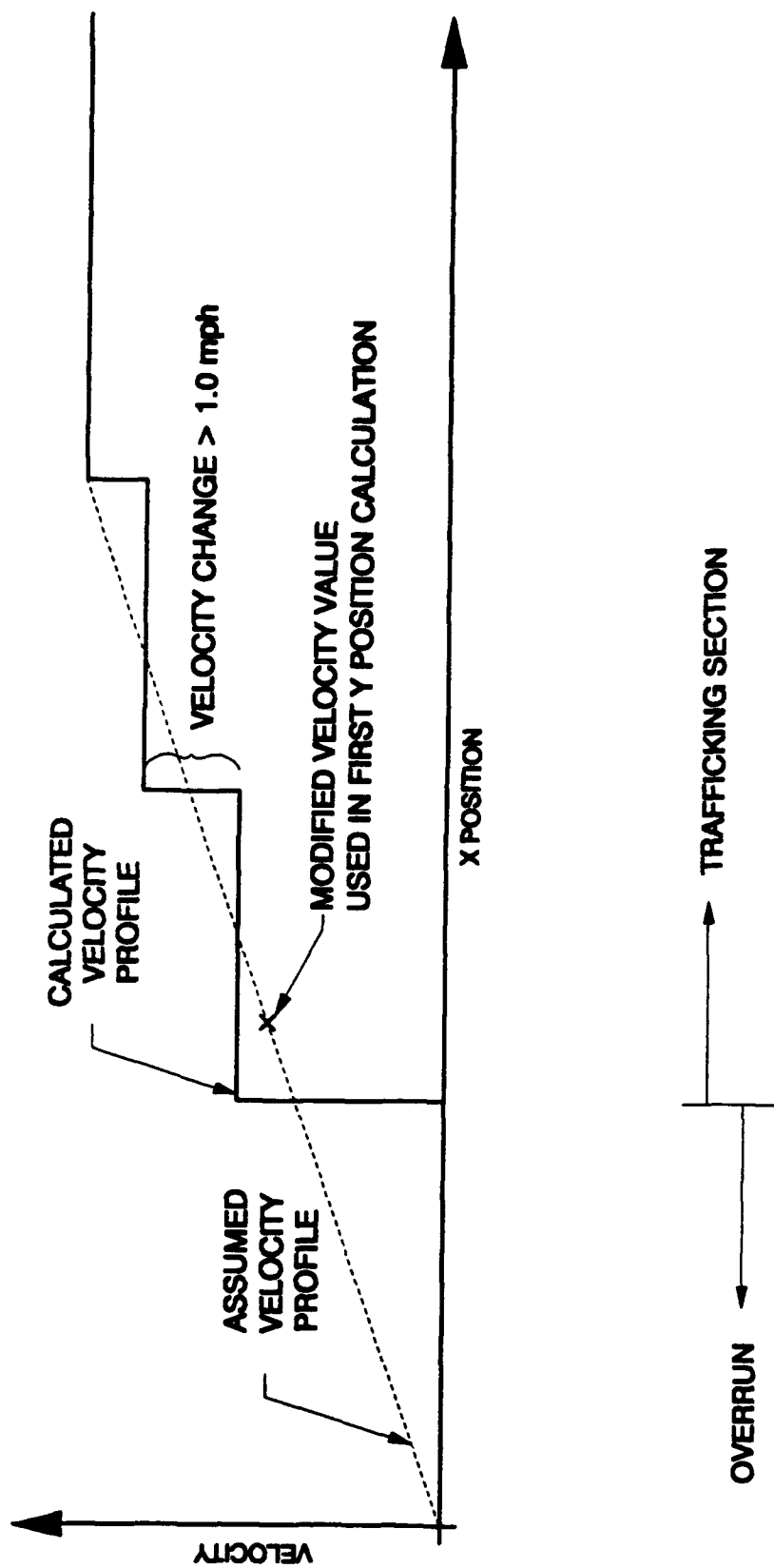


Figure 9. Initial Segment of a Calculated Velocity Profile.

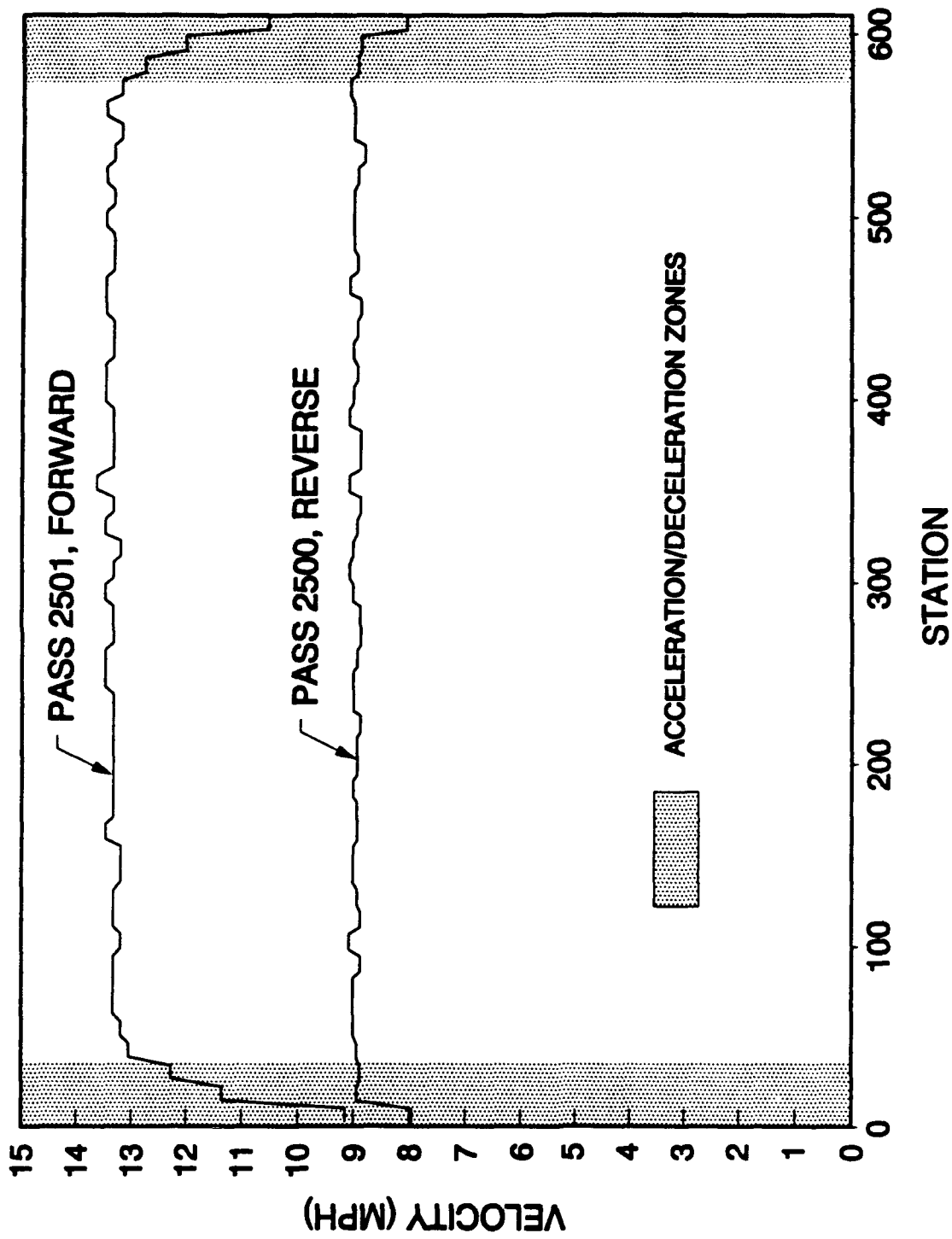


Figure 10. Typical Velocity Profile, Forward and Reverse.

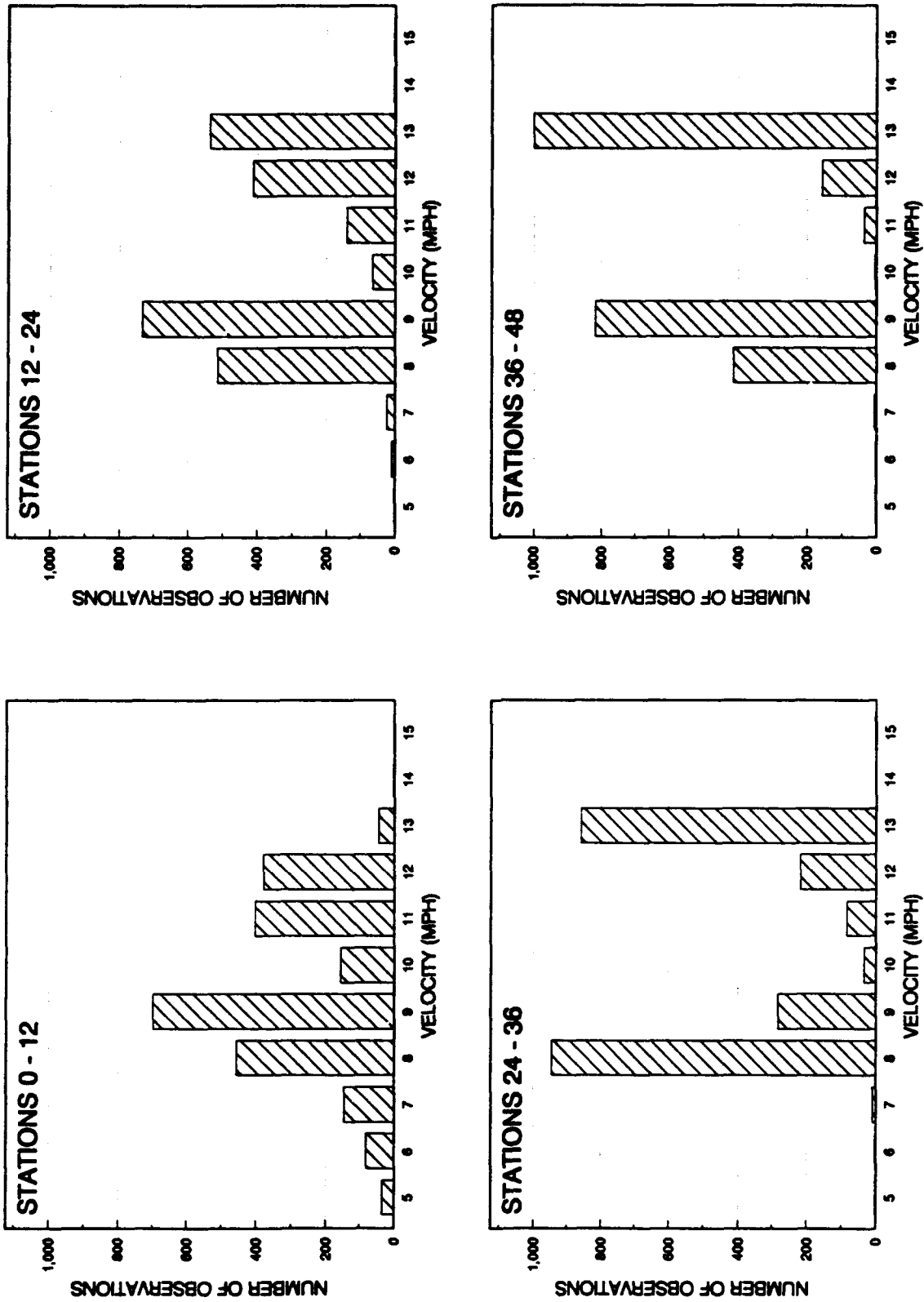


Figure 11. Velocity Histograms for Stations 0-48 at Pass Level 2589.

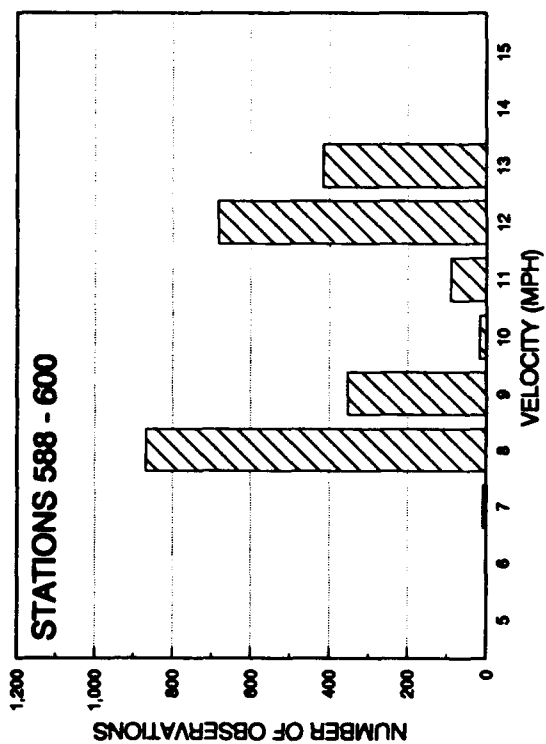
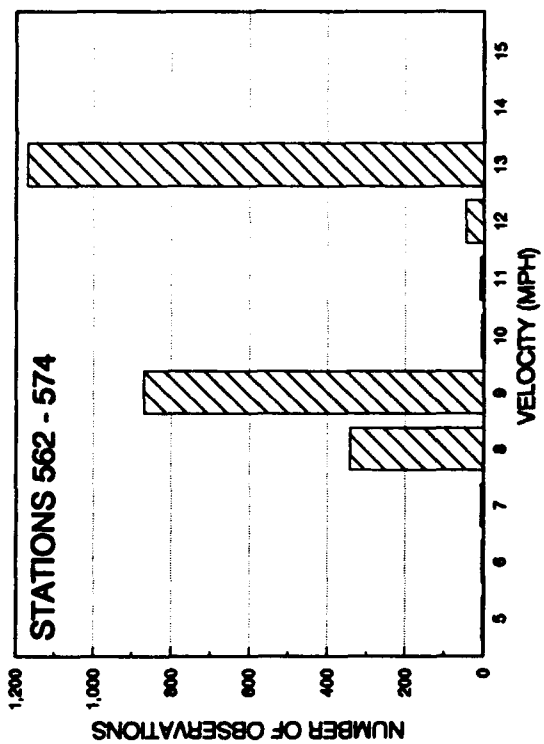
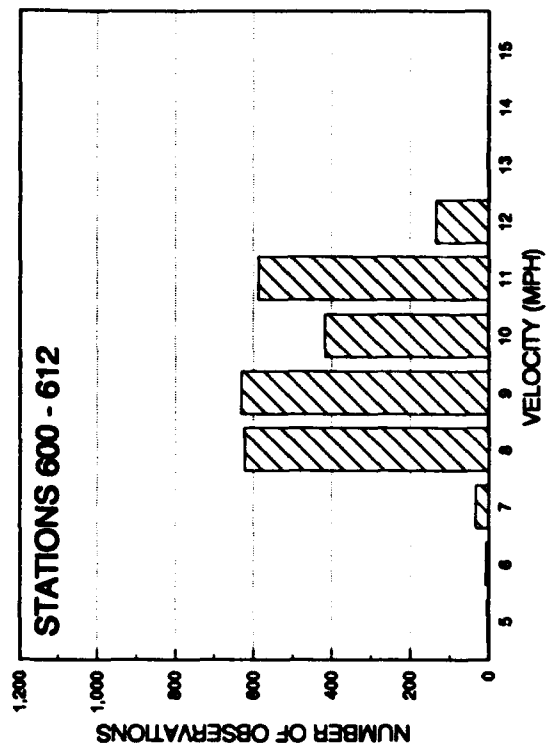
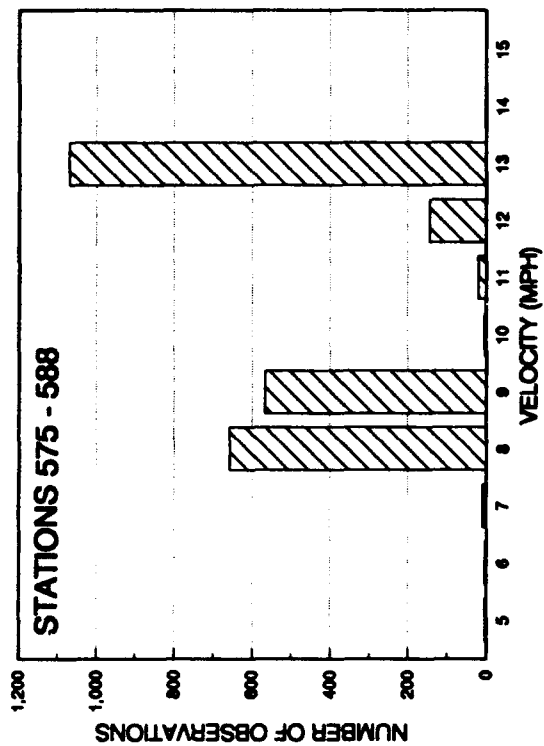


Figure 12. Velocity Histograms for Stations 562-612 at Pass Level 2589.

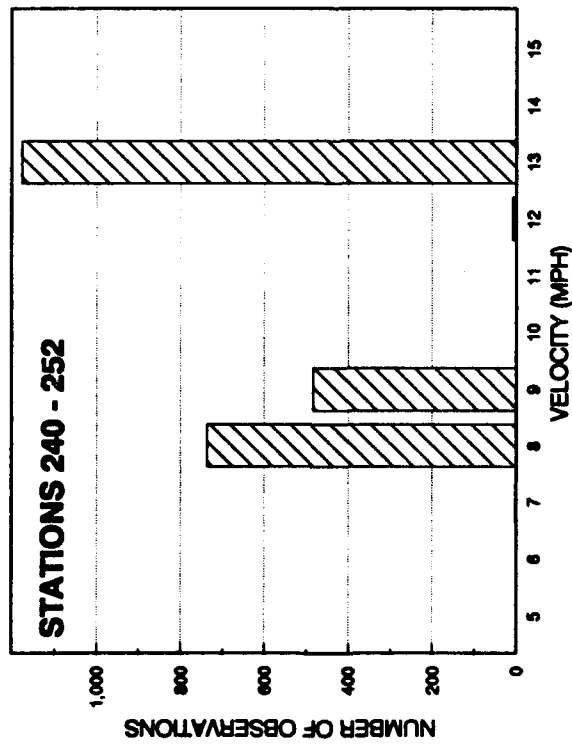
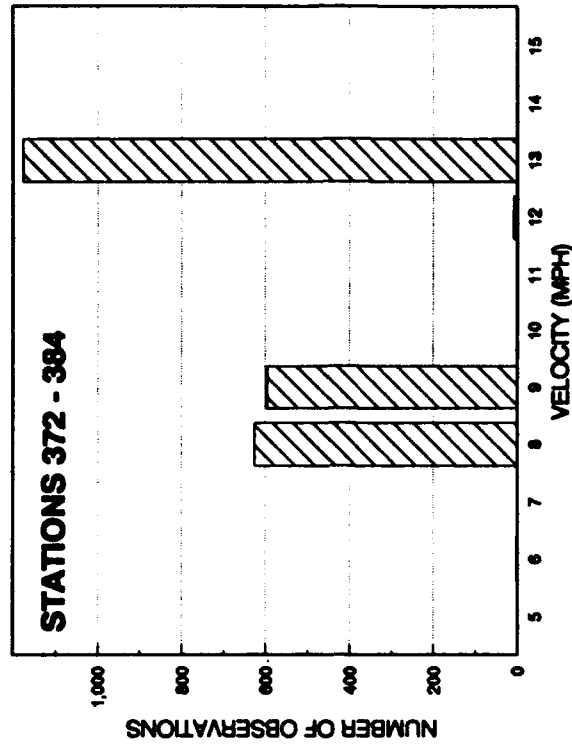


Figure 13. Velocity Histograms for Stations 240-384 at Pass Level 2589.

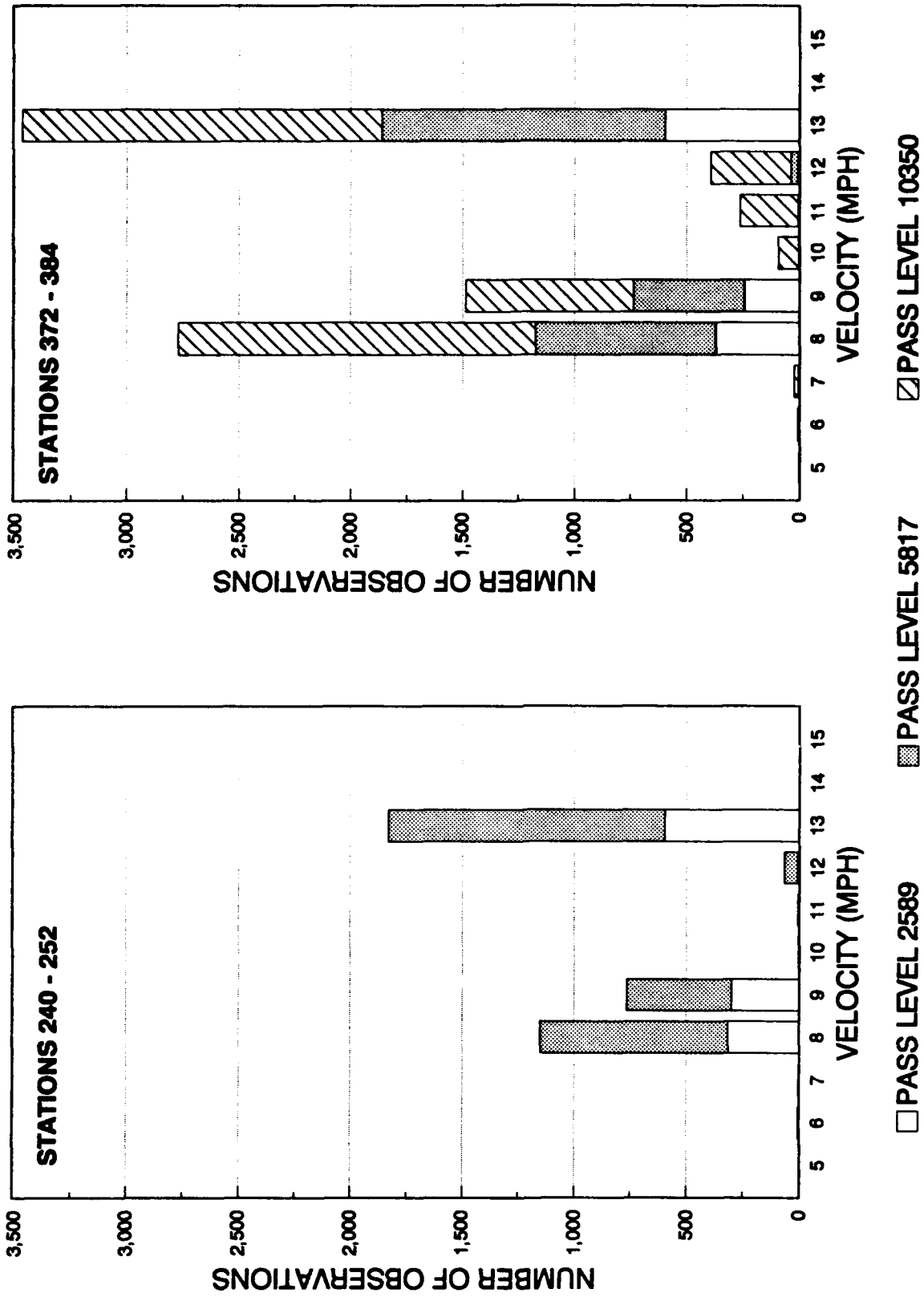
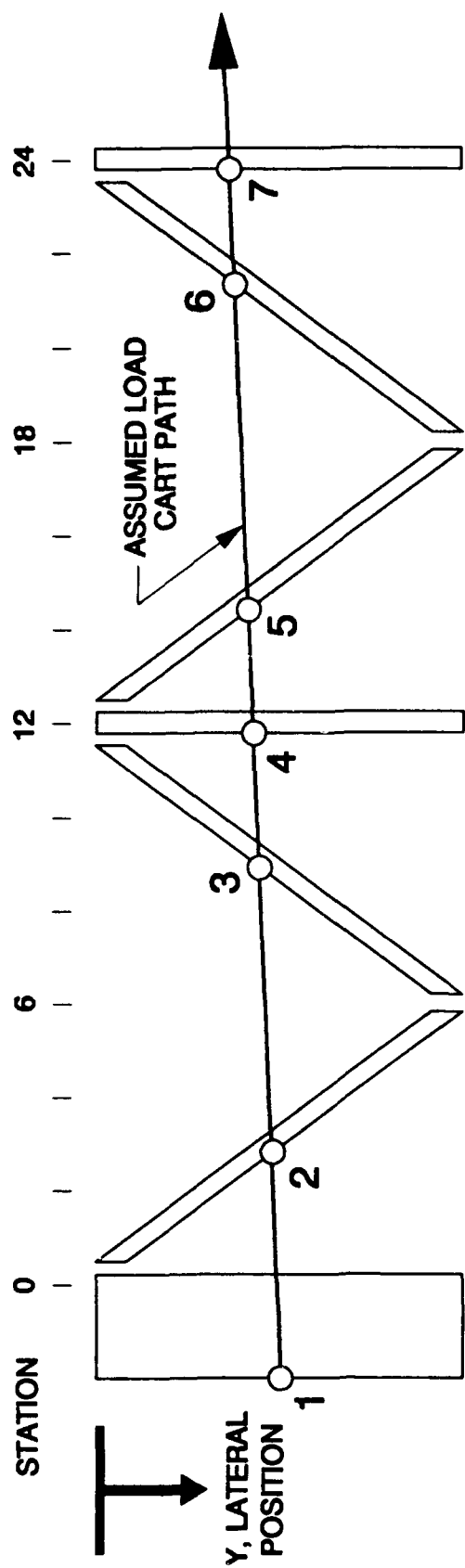


Figure 14. Velocity Histograms at Pass Levels 2589, 5817, and 10350.

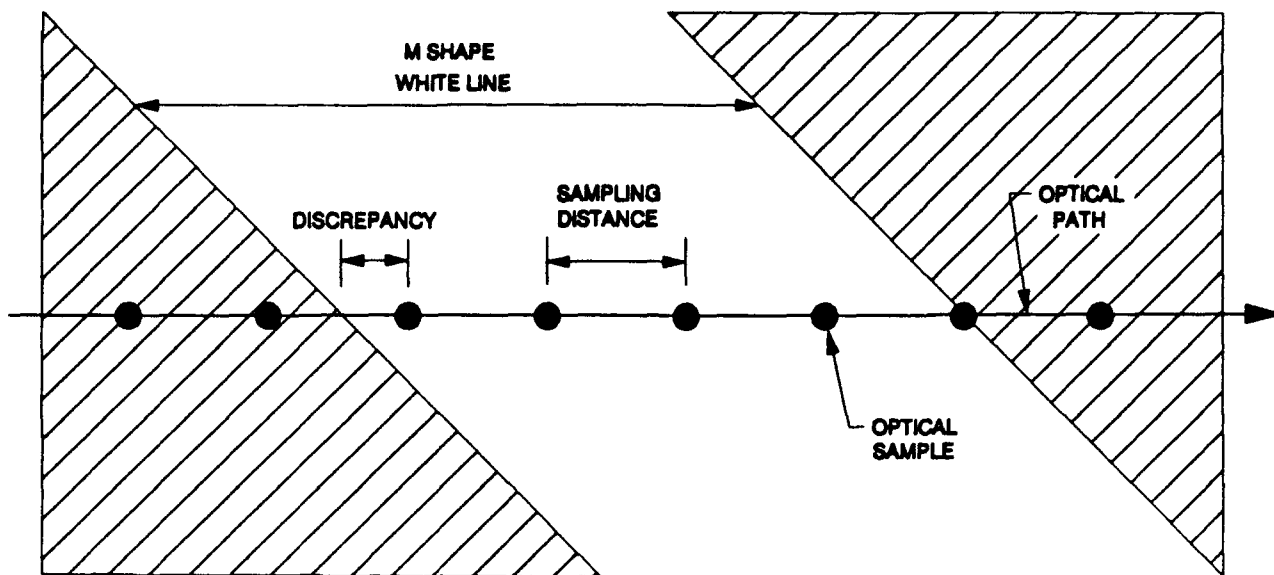


PATTERN A

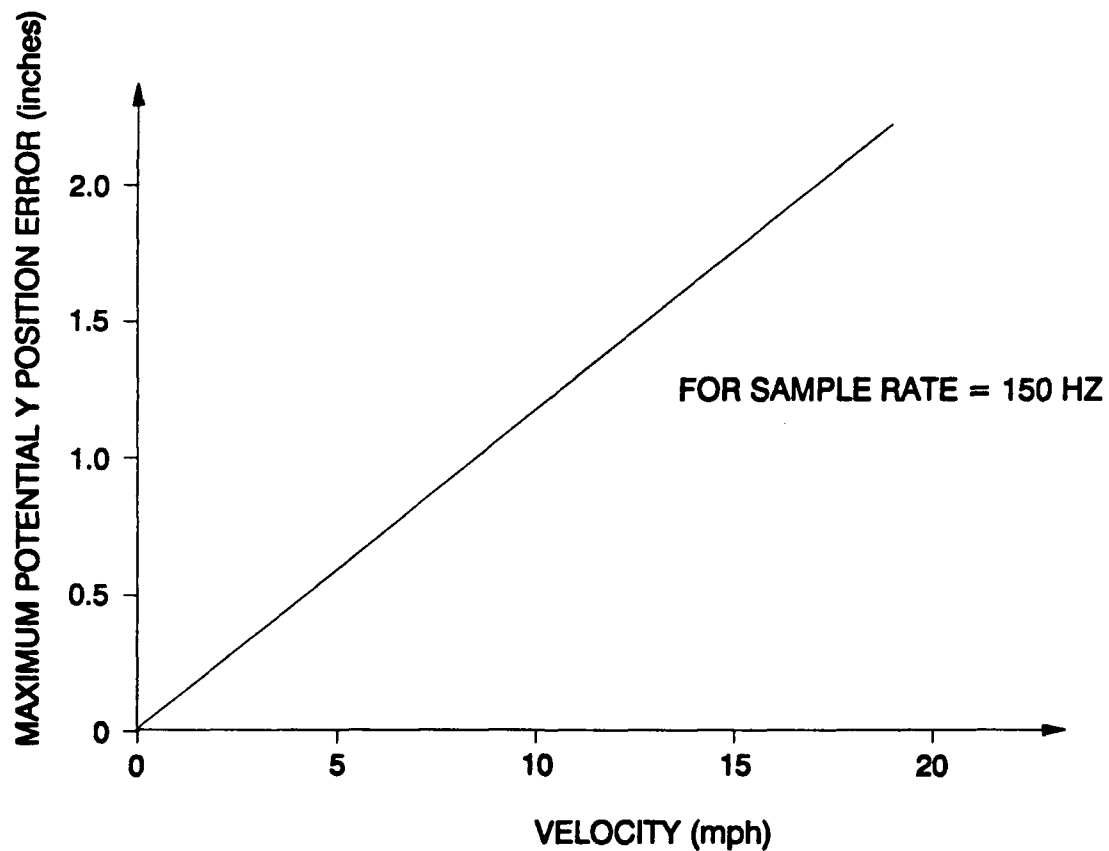
PATTERN B

LATERAL POSITION(2) = (VELOCITY(A)xCOUNT(2-1)) / SAMPLE RATE
 LATERAL POSITION(3) = (VELOCITY(A)xCOUNT(3-2)) / SAMPLE RATE
 LATERAL POSITION(5) = (VELOCITY(B)xCOUNT(5-4)) / SAMPLE RATE ... ETC

Figure 15. Data Acquisition and Algorithm for Calculating Lateral Position.



(a) Sampling Distance.



(b) Maximum Potential Y Position Error.

Figure 16. Potential Y Position Error Caused by Optical Sensor Sampling Distance.

STATION = 364

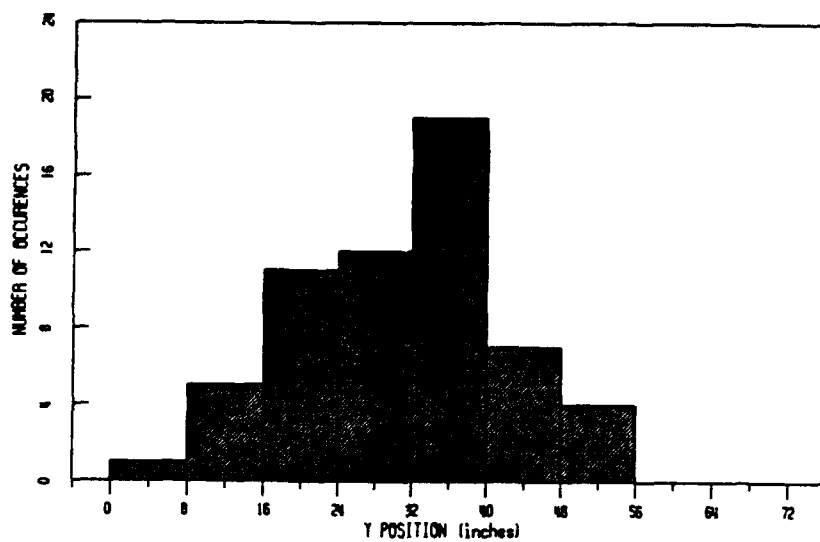
PASS ■ = 70

■ OBS = 59

MODE = 36

MEAN = 31.15

STDEV = 11.40



STATION = 364

PASS ■ = 112

■ OBS = 88

MODE = 36

MEAN = 30.57

STDEV = 10.06

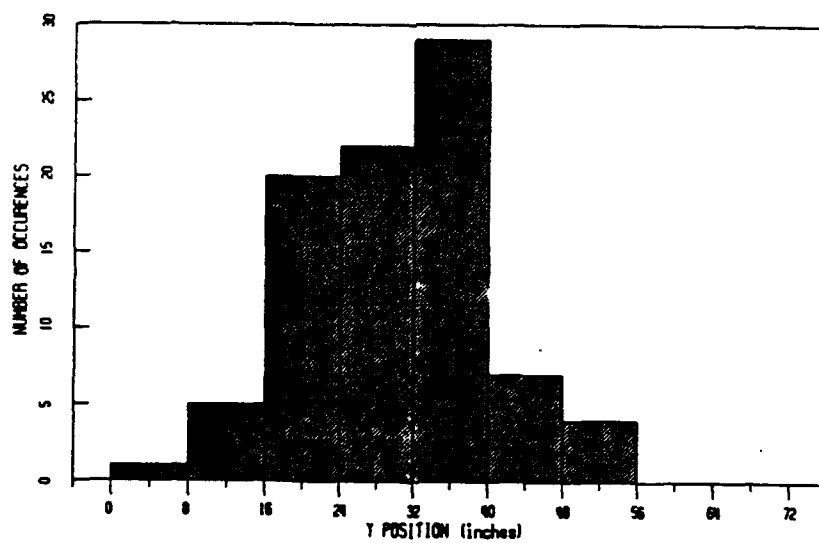


Figure 17. Mode-Centered Histograms for Station 364.

STATION = 364

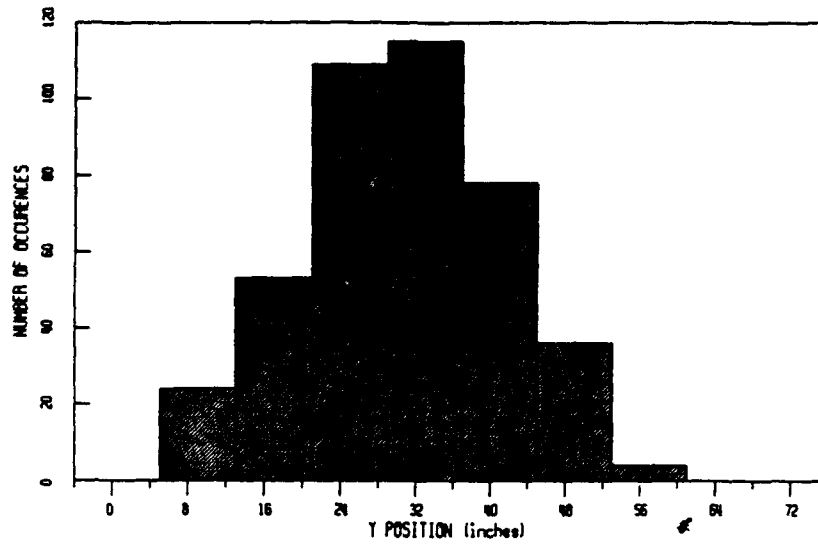
MODE = 33

PASS = 448

MEAN = 31.52

OBS = 419

STDEV = 10.45



STATION = 364

MODE = 31

PASS = 882

MEAN = 31.30

OBS = 817

STDEV = 10.08

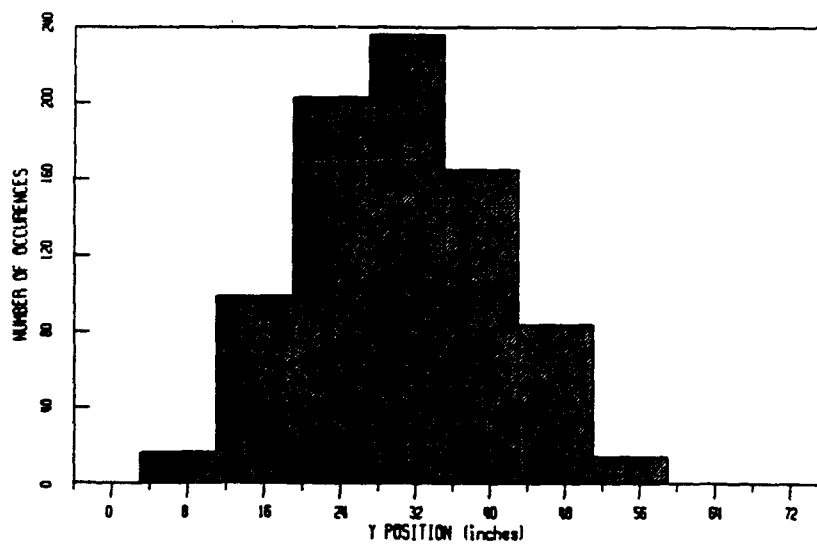
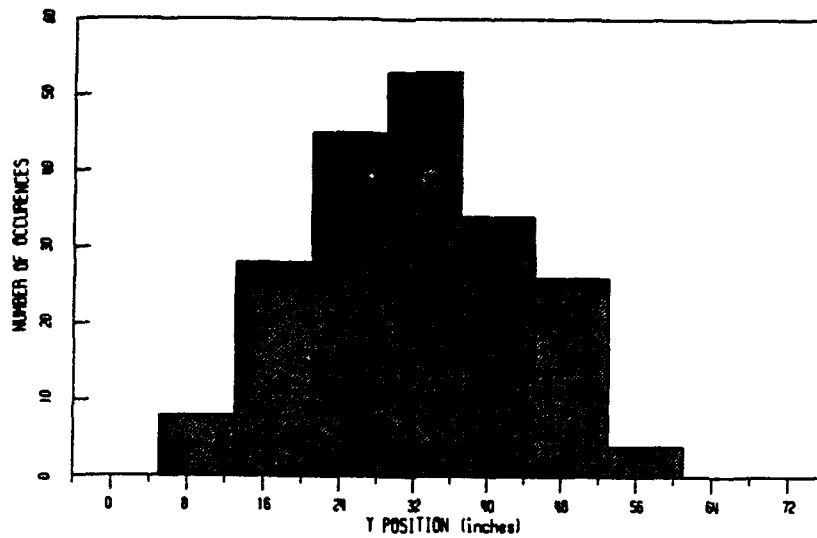


Figure 17. Mode-Centered Histograms for Station 364 (Continued).

STATION = 364
PASS ■ = 224
■ OBS = 198

MODE = 33
MEAN = 32.93
STDEV = 11.02



STATION = 364
PASS ■ = 420
■ OBS = 393

MODE = 33
MEAN = 31.84
STDEV = 10.42

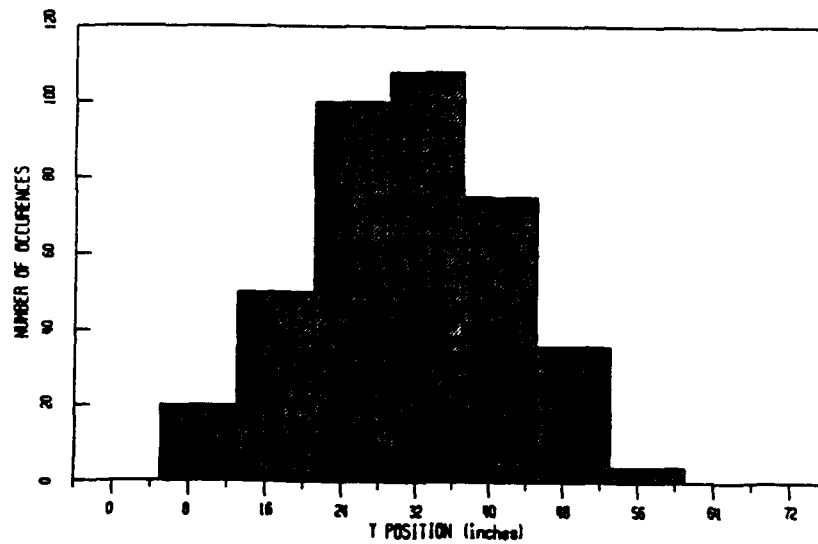
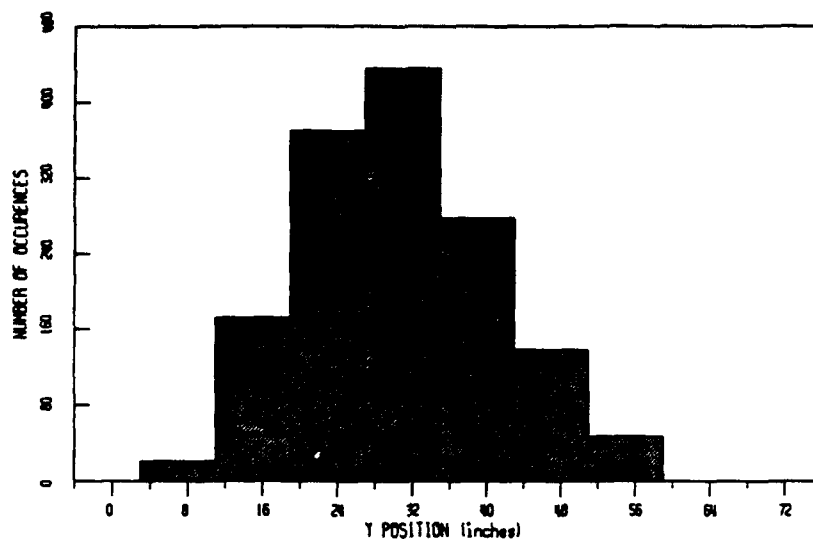


Figure 17. Mode-Centered Histograms for Station 364 (Continued).

STATION = 364
PASS = 1554
OBS = 1462

MODE = 31
MEAN = 31.55
STDEV = 10.30



STATION = 364
PASS = 2324
OBS = 2193

MODE = 29
MEAN = 31.64
STDEV = 10.10

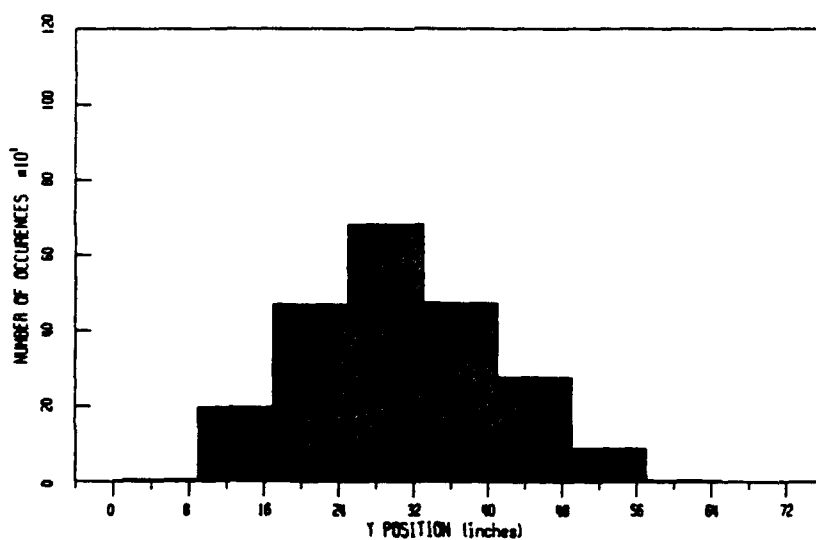
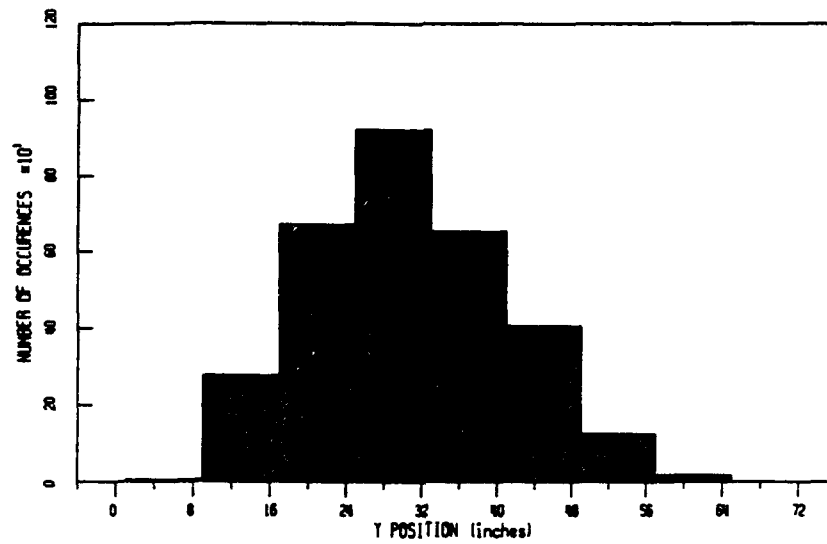


Figure 17. Mode-Centered Histograms for Station 364 (Continued).

STATION = 364
PASS # = 3286
OBS = 3077

MODE = 29
MEAN = 31.82
STDEV = 10.32



STATION = 364
PASS # = 3942
OBS = 3599

MODE = 27
MEAN = 31.54
STDEV = 10.35

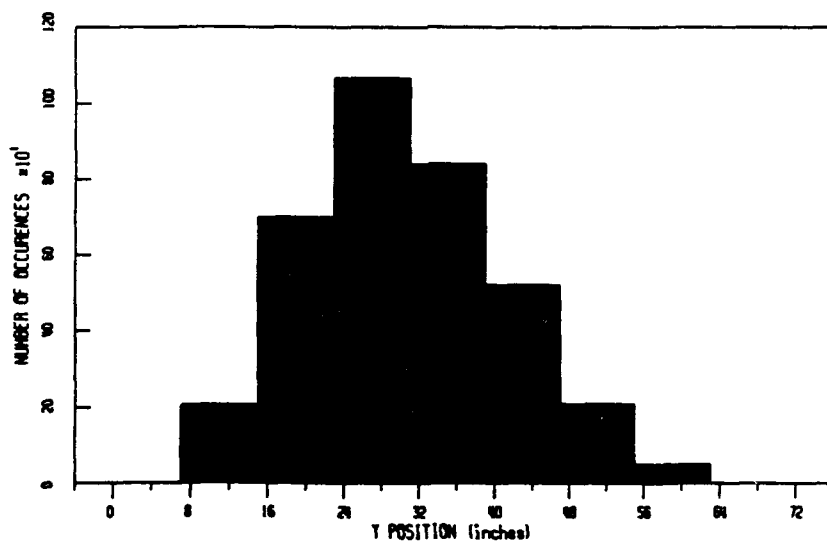
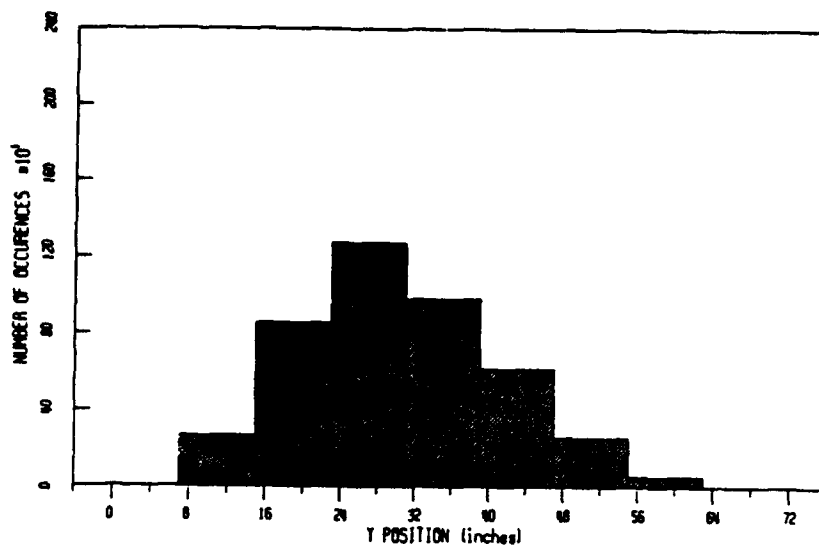


Figure 17. Mode-Centered Histograms for Station 364 (Continued).

STATION = 364
 PASS ■ = 4784
 ■ OBS = 4318

MODE = 27
 MEAN = 31.33
 STDEV = 10.43



STATION = 364
 PASS ■ = 5370
 ■ OBS = 4824

MODE = 27
 MEAN = 31.38
 STDEV = 10.49

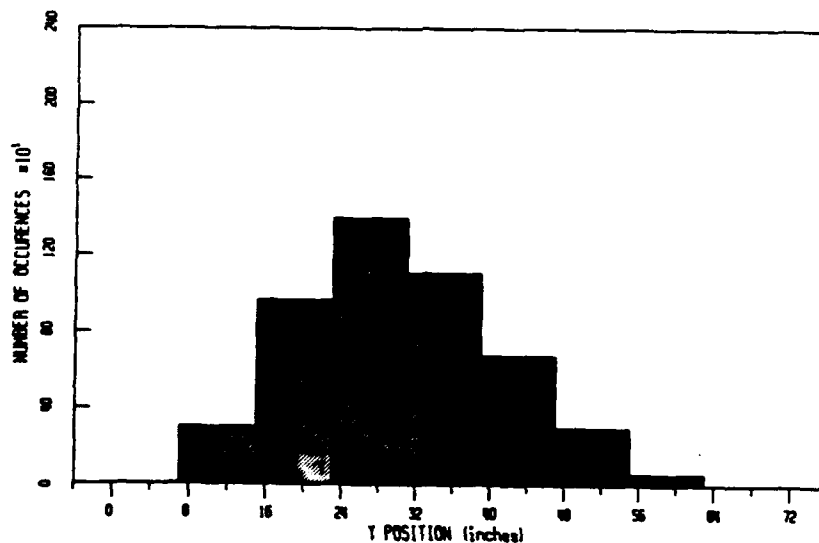
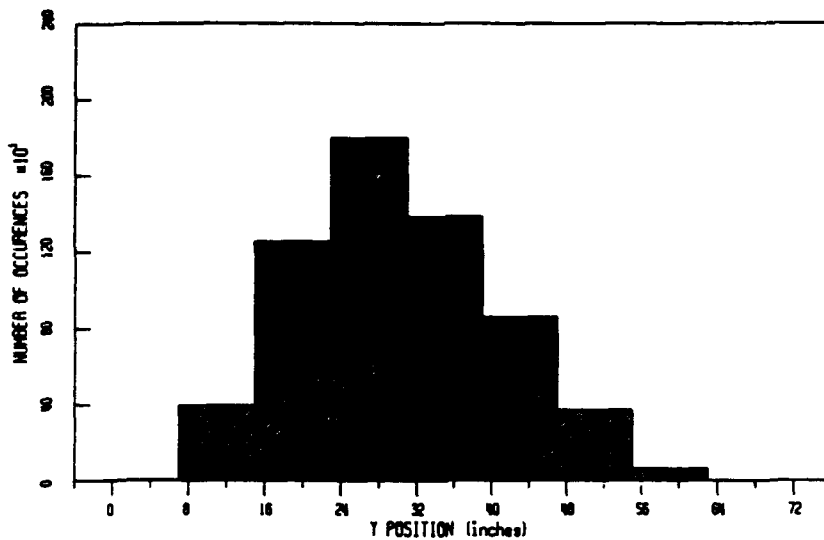


Figure 17. Mode-Centered Histograms for Station 364 (Continued).

STATION = 364
 PASS * = 6808
 * OBS = 6140

MODE = 27
 MEAN = 31.18
 STDEV = 10.44



STATION = 364
 PASS * = 8080
 * OBS = 7297

MODE = 27
 MEAN = 31.22
 STDEV = 10.46

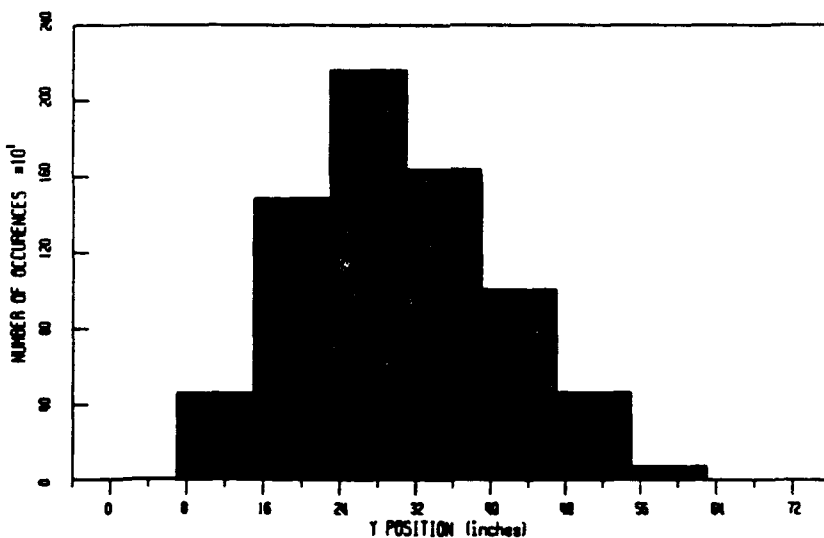
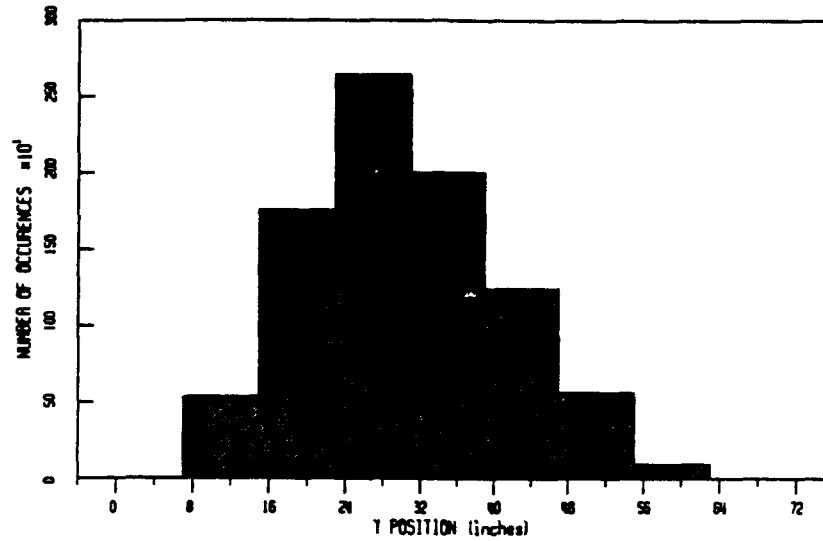


Figure 17. Mode-Centered Histograms for Station 364 (Continued).

STATION = 364
PASS = 9716
OBS = 8844

MODE = 27
MEAN = 31.37
STDEV = 10.43



STATION = 364
PASS = 10350
OBS = 9331

MODE = 27
MEAN = 31.59
STDEV = 10.44

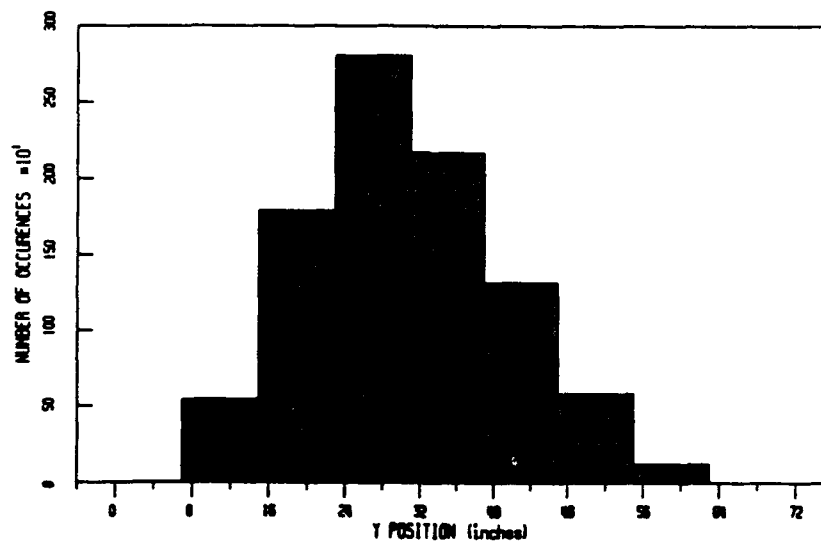
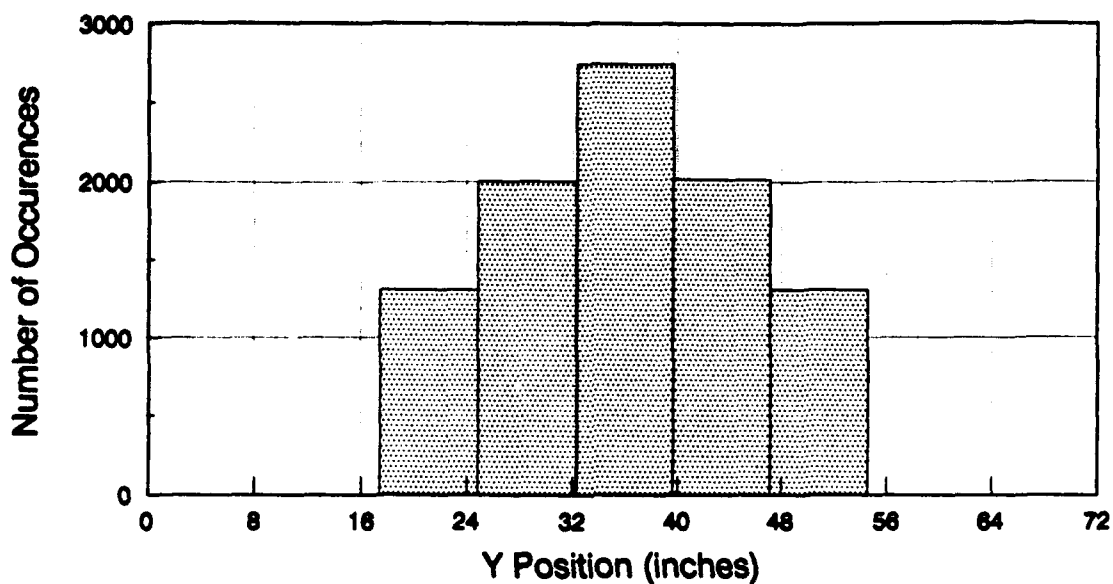
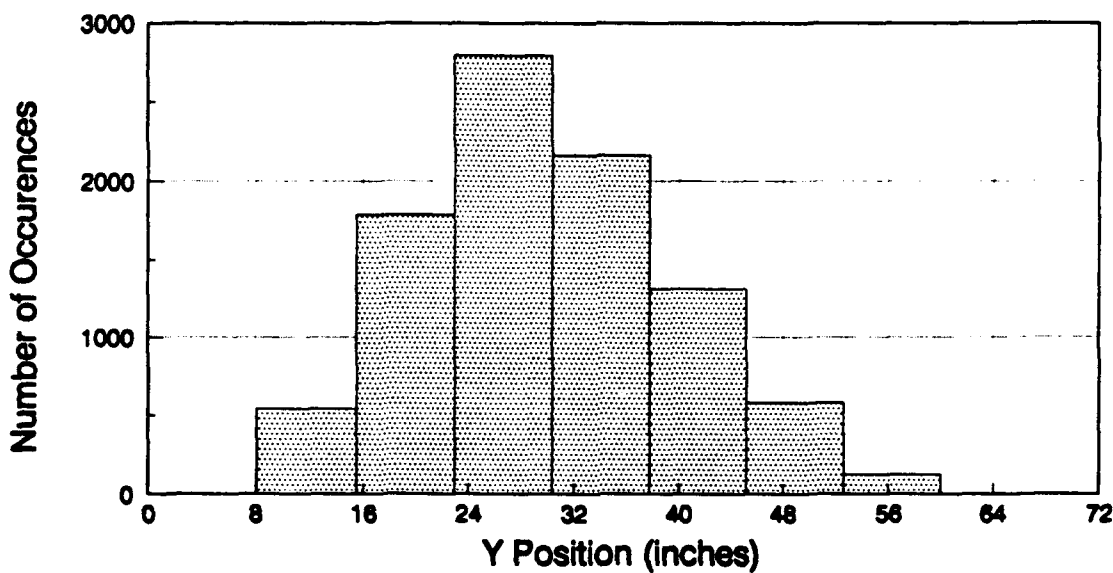


Figure 17. Mode-Centered Histograms for Station 364 (Concluded).



(a) Target Distribution of Traffic During Testing.



(b) Station 364, 10350 Passes.

Figure 18. Comparison of Target and Actual Load Distributions.

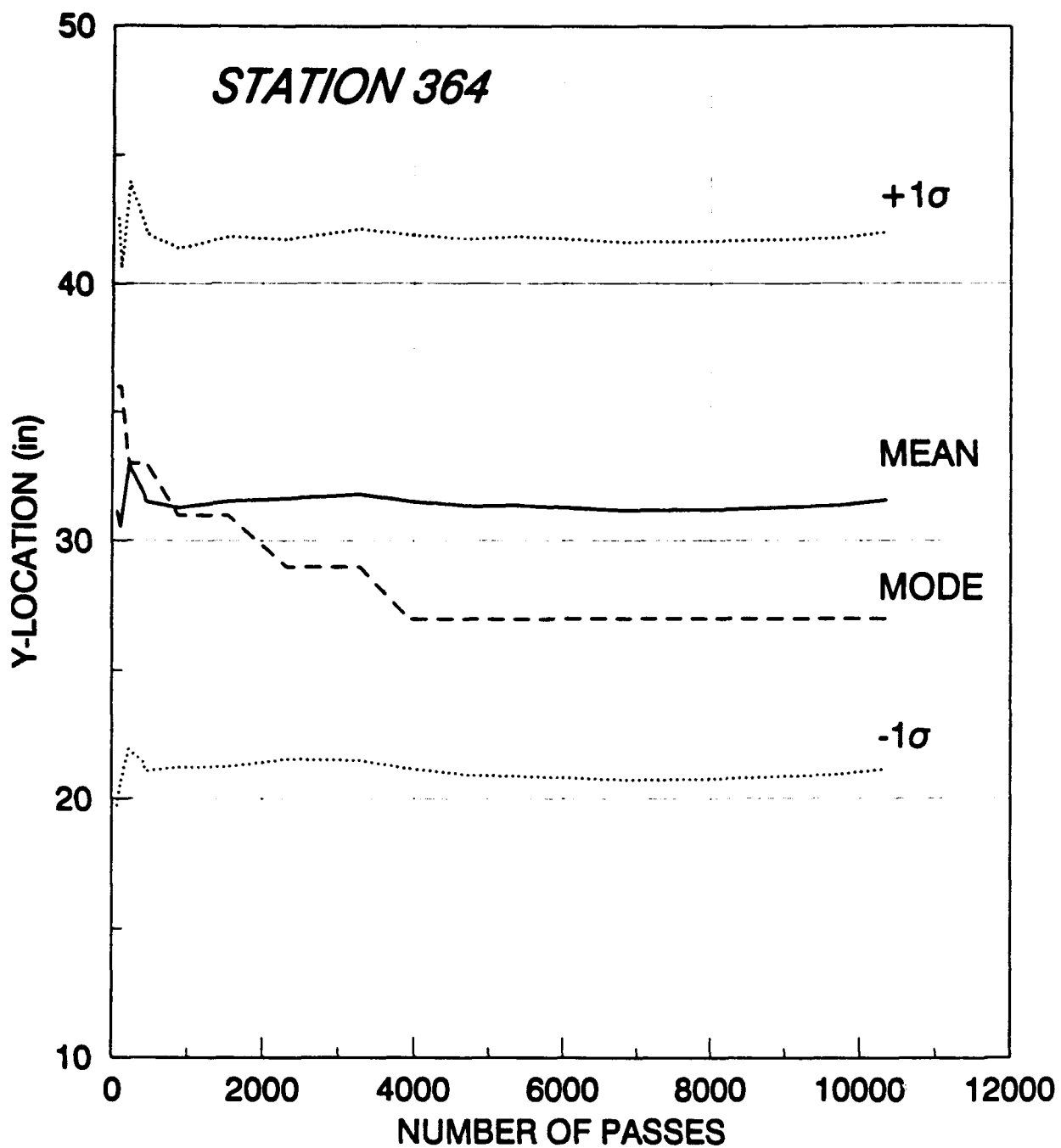
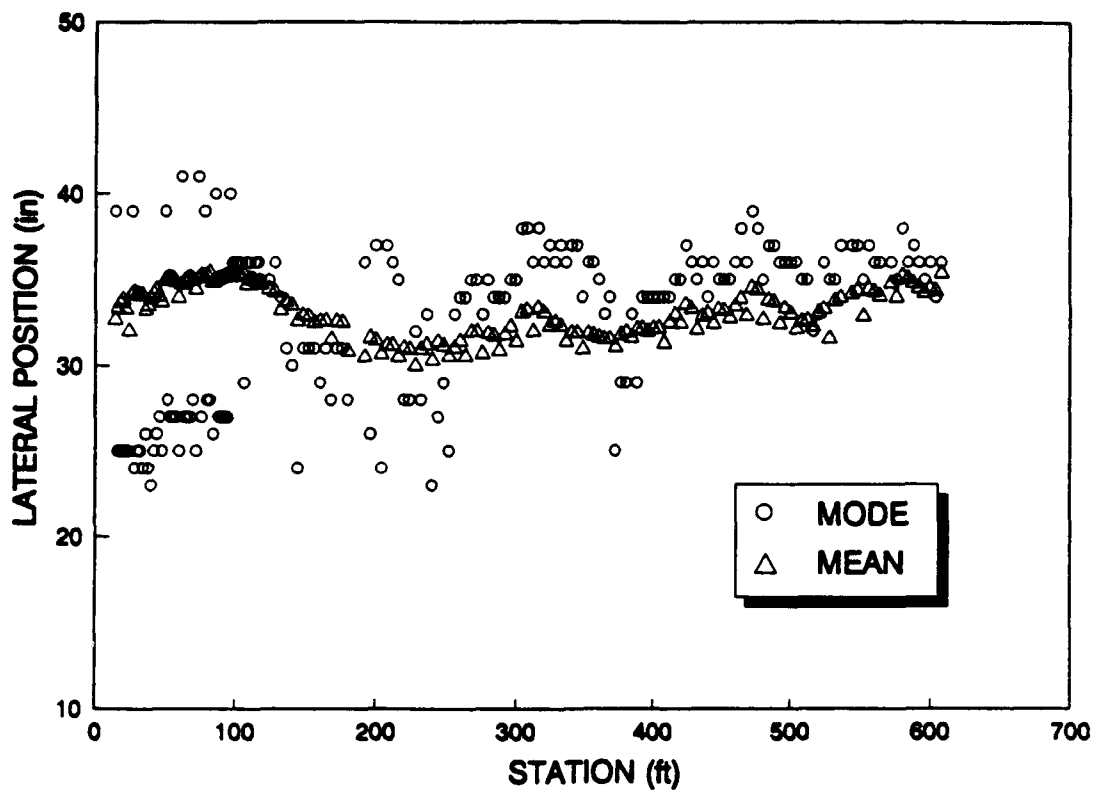
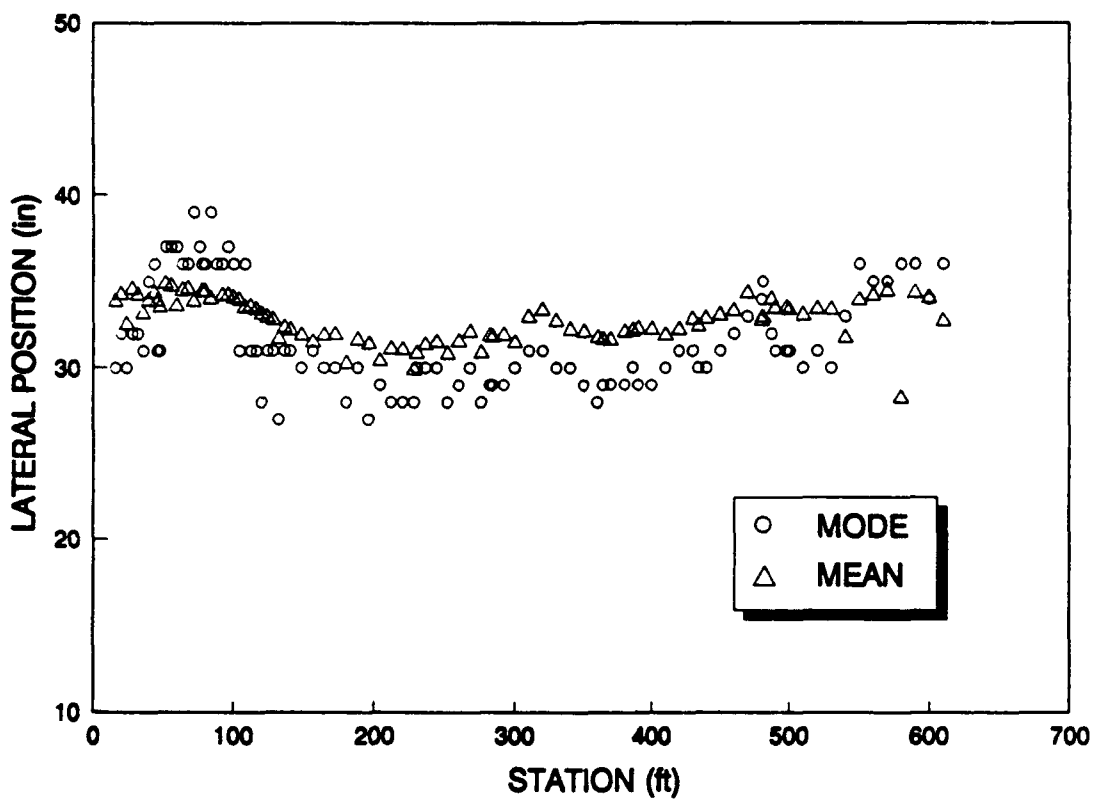


Figure 19. Typical Variation of Traffic Mode, Mean, and Standard Deviation.

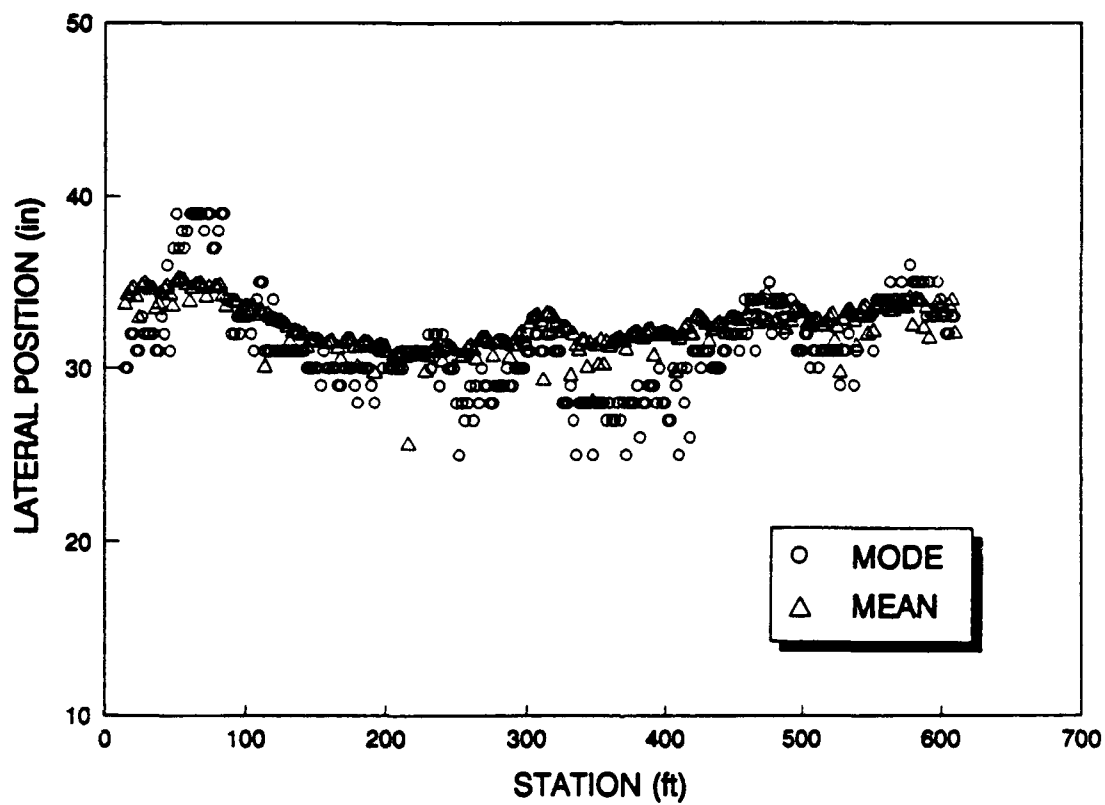


(a) Pass Level 448



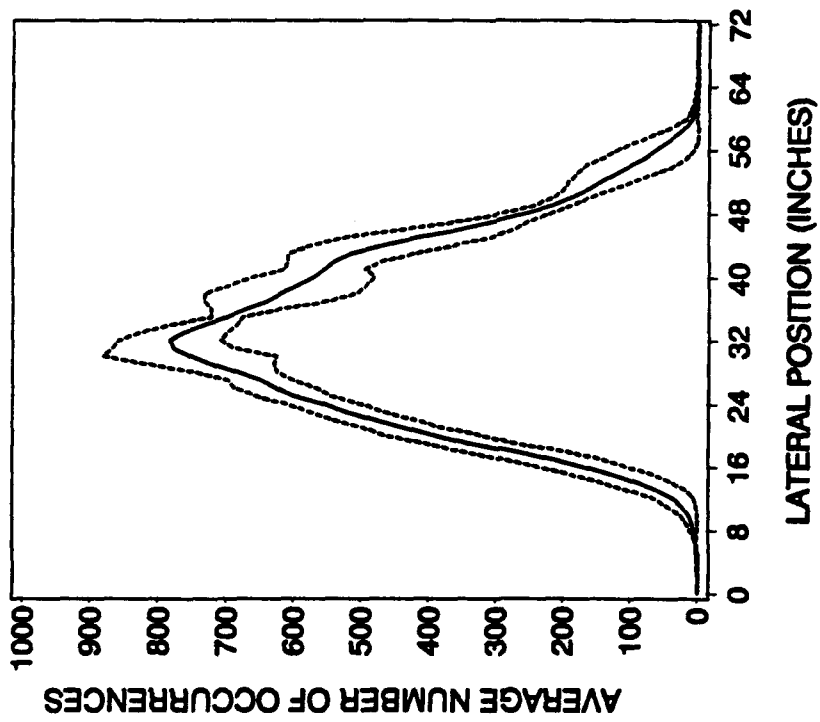
(b) Pass Level 2324

Figure 20. Mode and Mean of Lateral Position Versus Station.

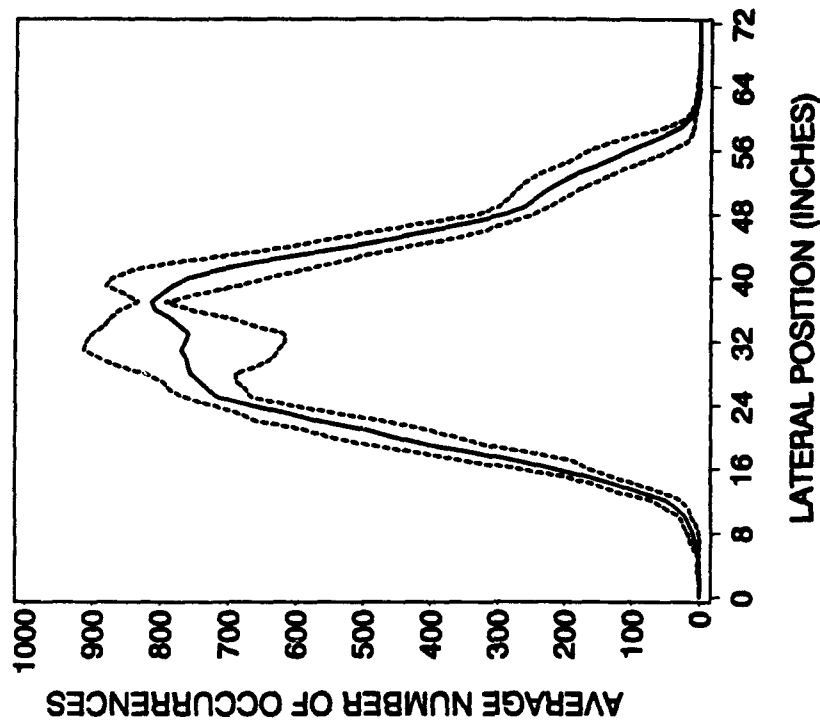


(c) Final Pass Level Achieved at Each Station.

Figure 20. Mode and Mean of Lateral Position Versus Station (Concluded).

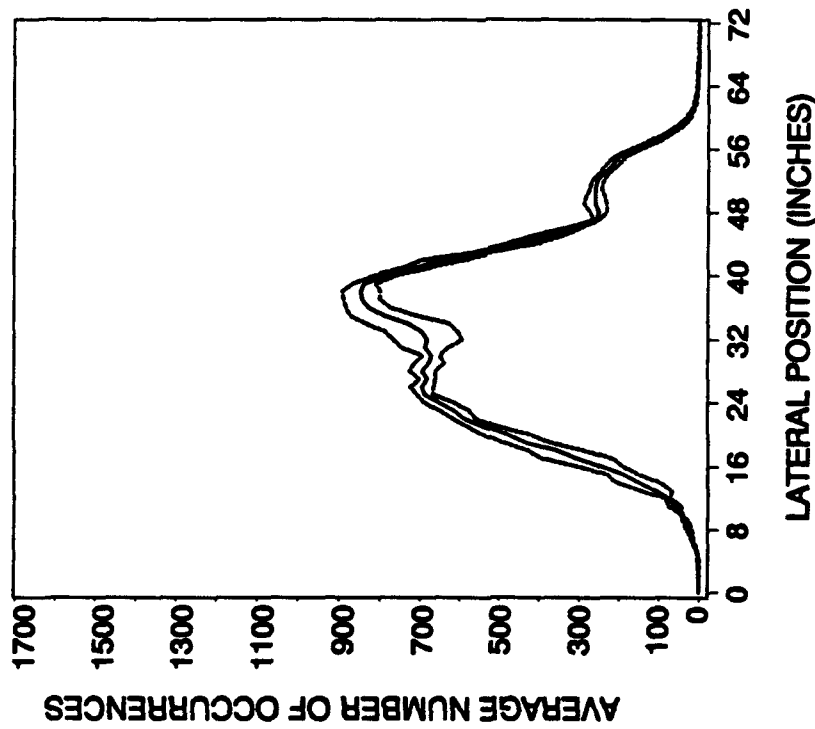


(a) Stations 0-36, 2589 Passes.

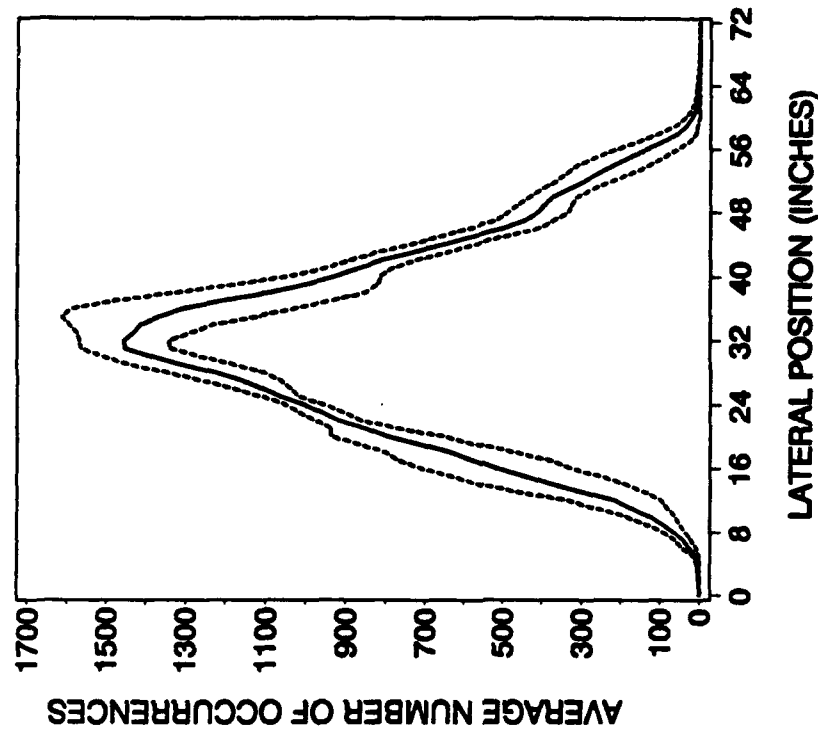


(b) Stations 38-64, 3049 Passes.

Figure 21. Normalized Lateral Position Histograms for 4-Inch Flexible Marshall Section.

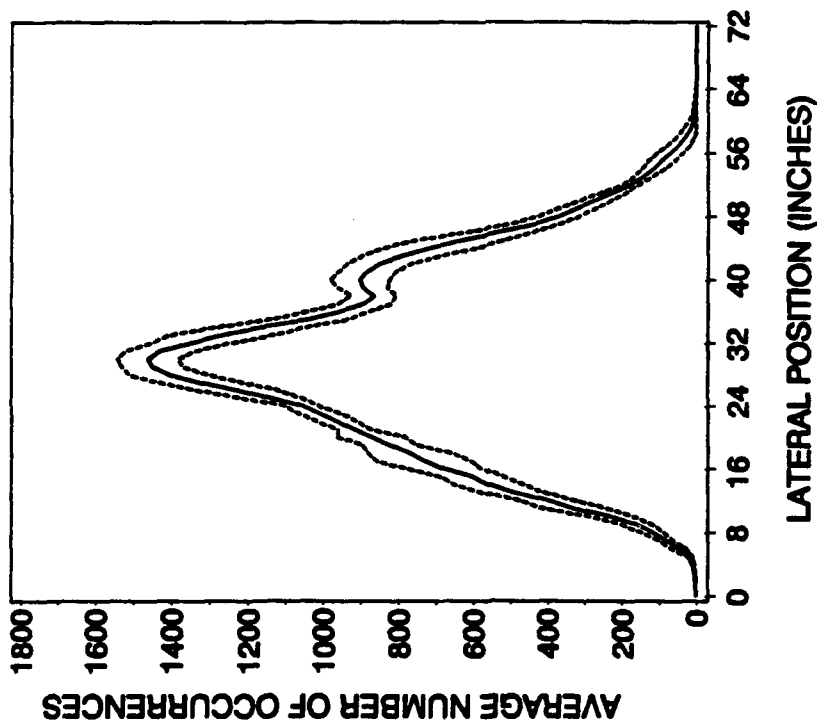


(a) Stations 78-84, 3049 Passes.

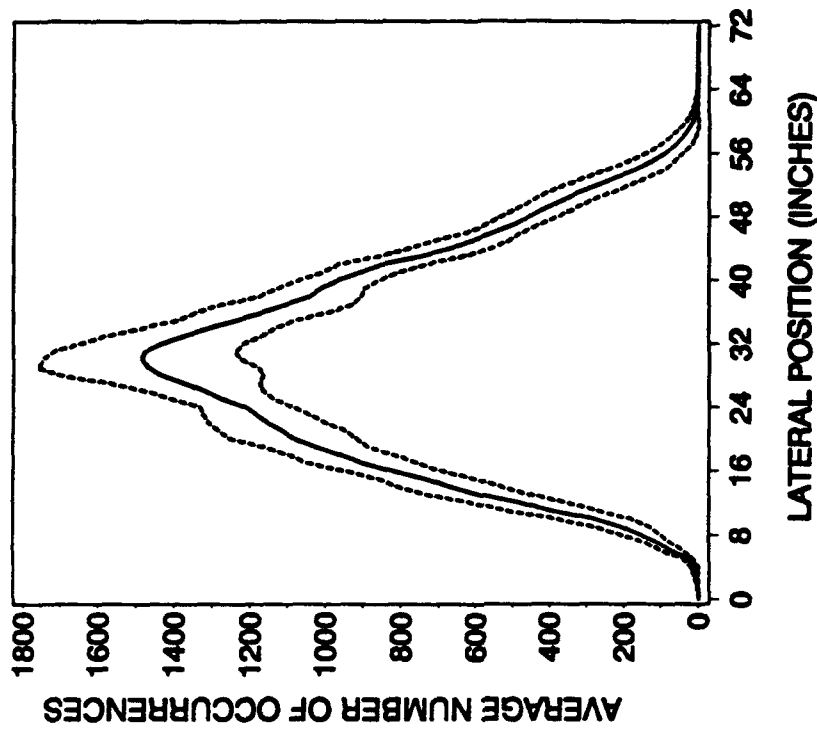


(b) Stations 86-140, 5137 Passes.

Figure 22. Normalized Lateral Position Histograms for 6-Inch Flexible Marshall Section.

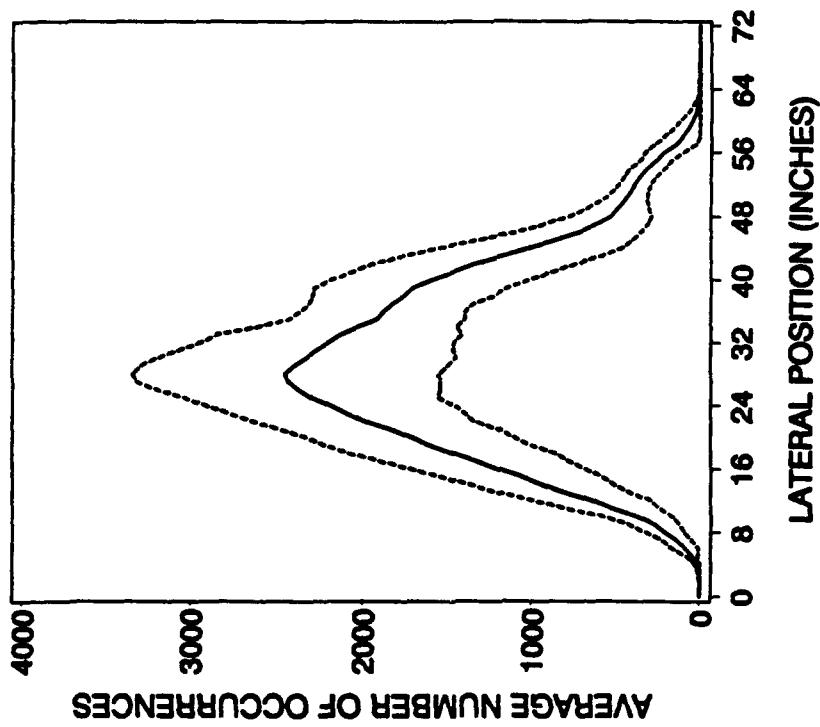


(a) Stations 156-190, 5137 Passes.

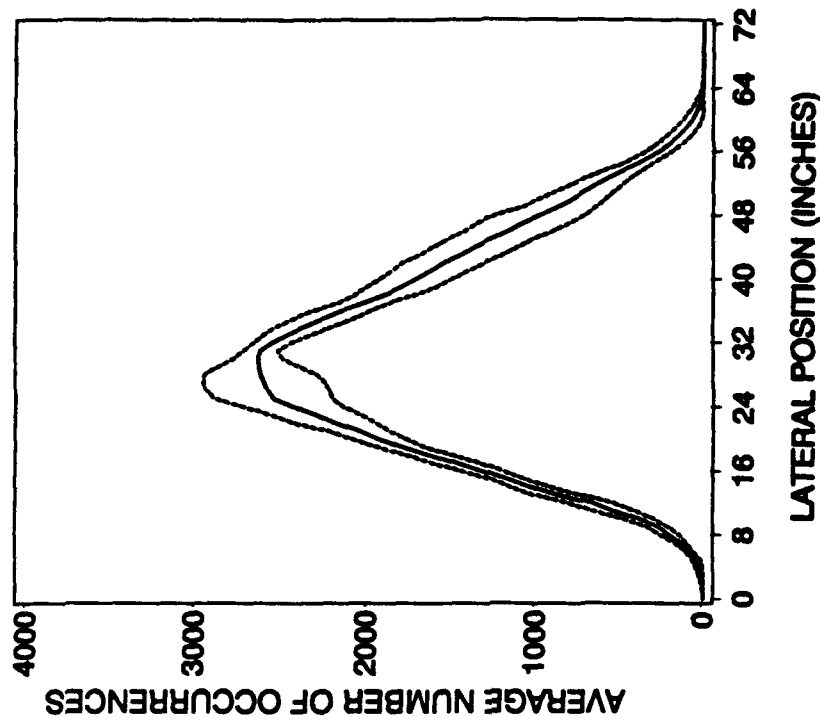


(b) Stations 192-304, 5817 Passes.

Figure 23. Normalized Lateral Position Histograms for 6-Inch Composite Marshall Section.

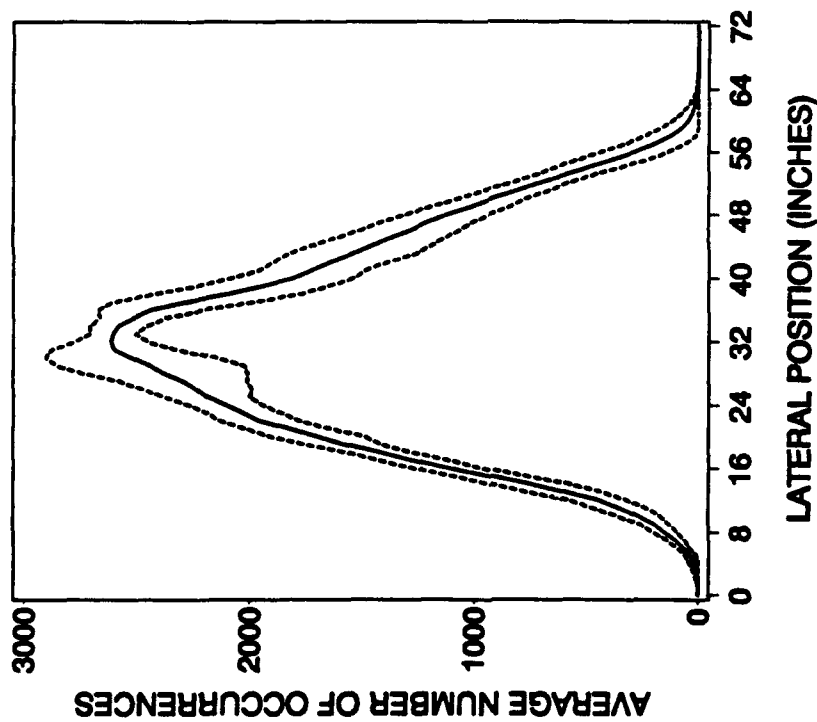


(a) Stations 336-348, 9715 Passes.

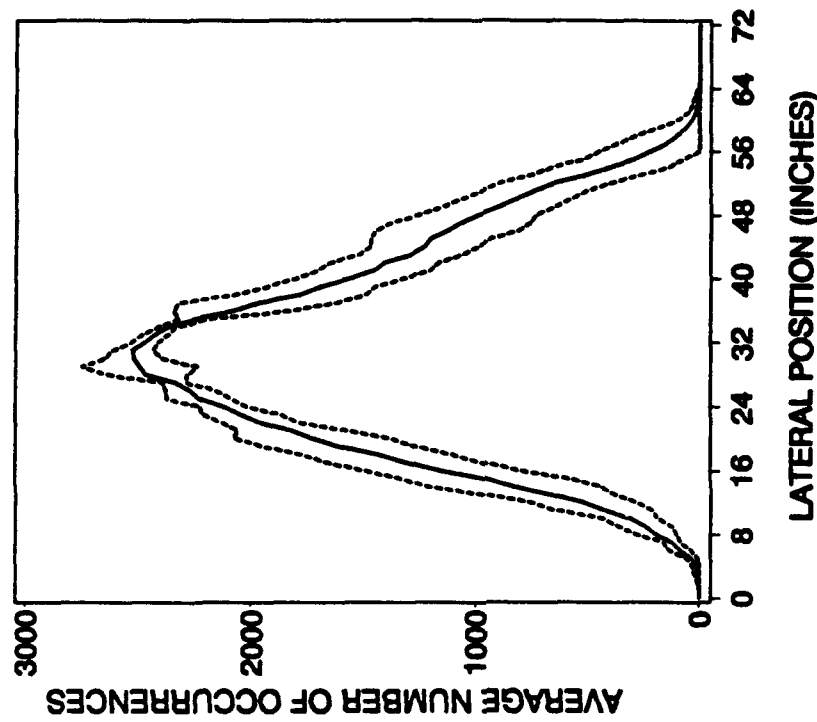


(b) Stations 350-454, 10350 Passes.

Figure 24. Normalized Lateral Position Histograms for 6-Inch Composite Gyrotary Section.

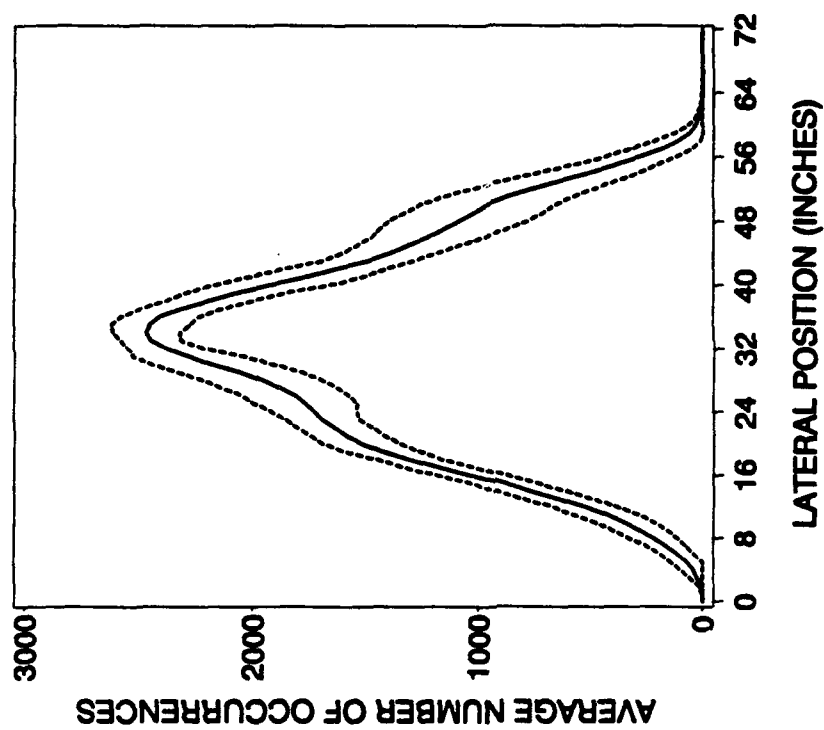


(a) Stations 470-526, 10350 Passes.



(b) Stations 528-532, 9715 Passes.

Figure 25. Normalized Lateral Position Histograms for 6-Inch Flexible Gyratory Section.



(a) Stations 548-610, 9715 Passes.

Figure 26. Normalized Lateral Position Histograms for 4-Inch Flexible Gyratory Section.

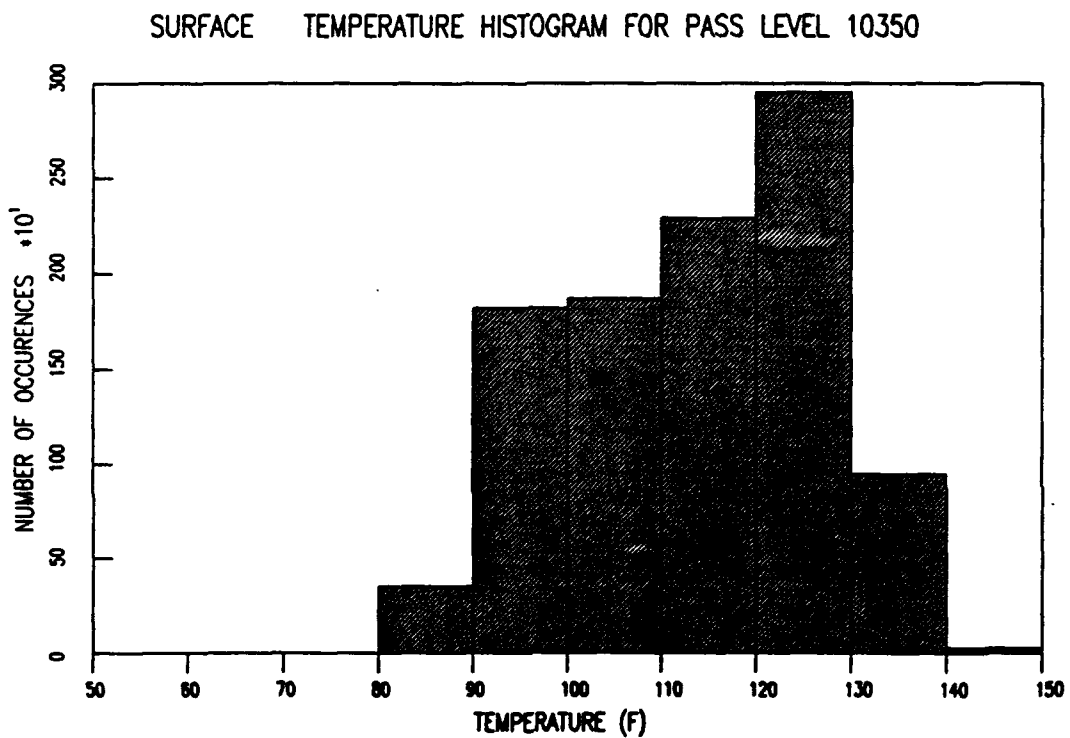
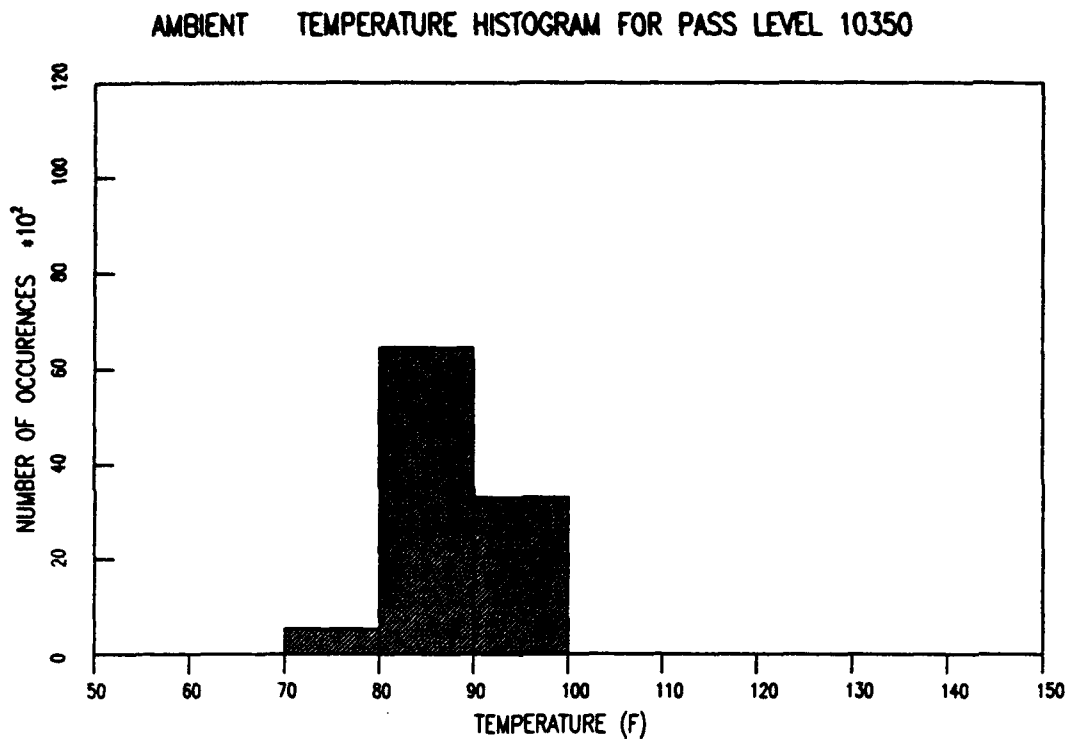
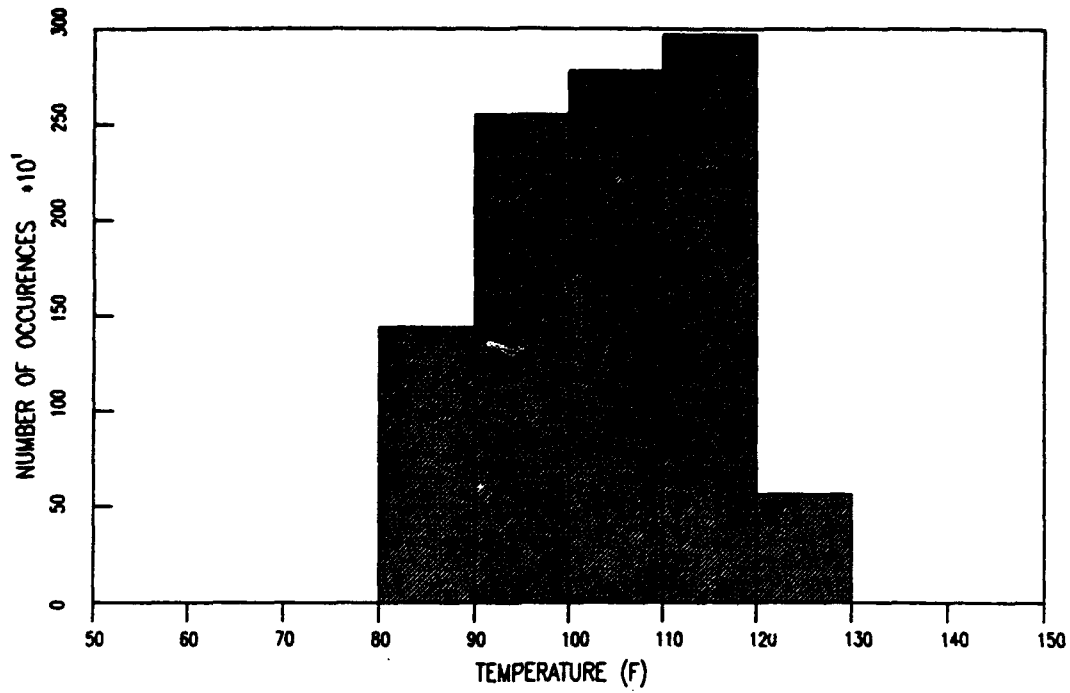


Figure 27. Ambient and Surface Temperature Histograms.

MIDHEIGHT TEMPERATURE HISTOGRAM FOR PASS LEVEL 10350



INTERFACE TEMPERATURE HISTOGRAM FOR PASS LEVEL 10350

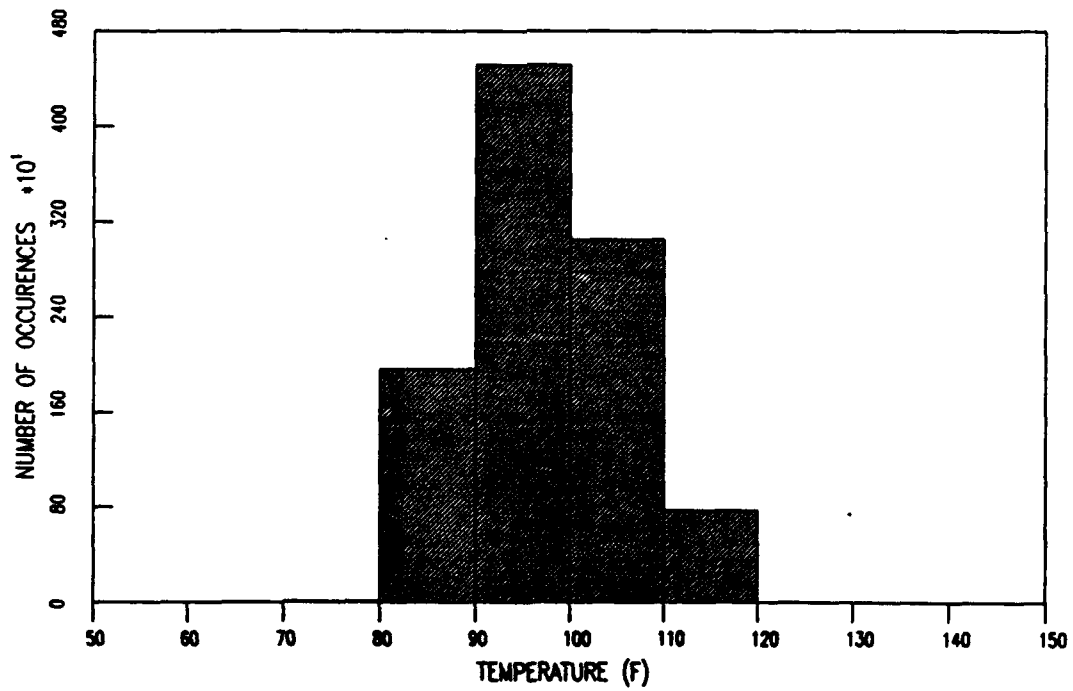
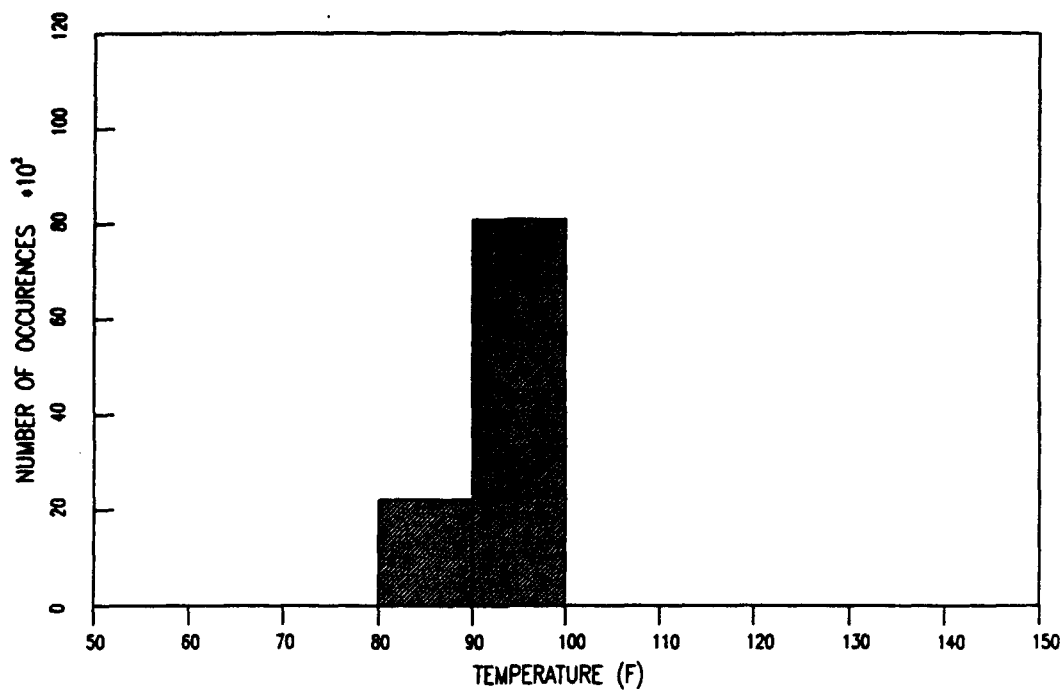


Figure 28. Midheight and Interface Temperature Histograms.

6-INCH TEMPERATURE HISTOGRAM FOR PASS LEVEL 10350



12-INCH TEMPERATURE HISTOGRAM FOR PASS LEVEL 10350

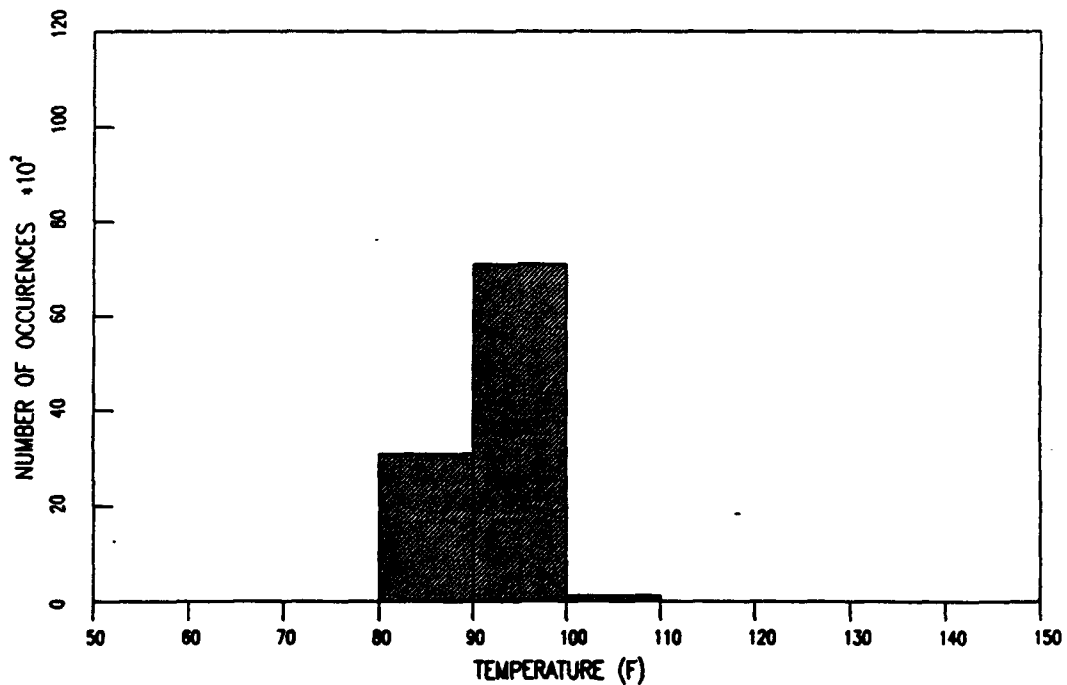


Figure 29. Six- and Twelve-Inch Depth into Base Course Temperature Histograms.

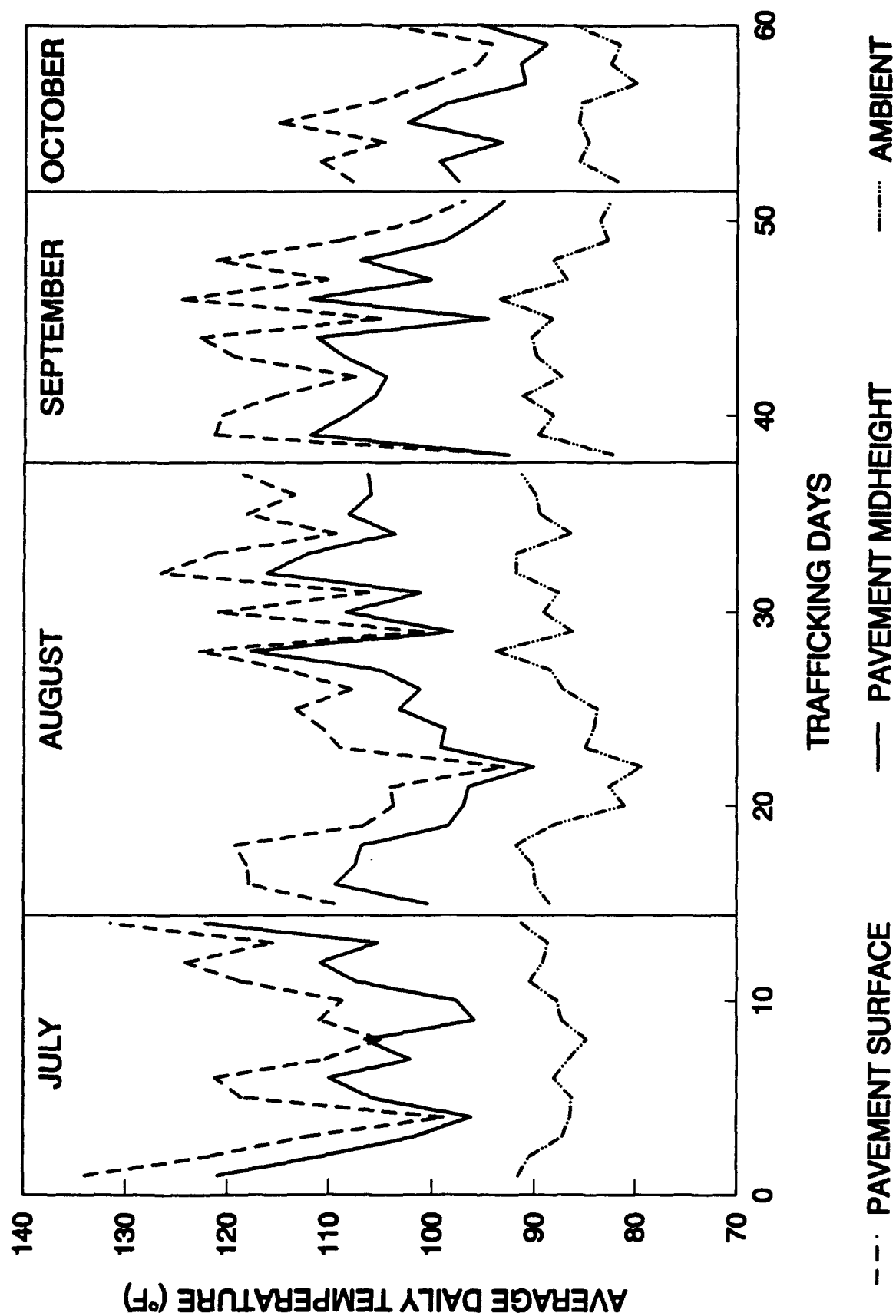


Figure 30. Average Daily Temperature for All Trafficking Days.

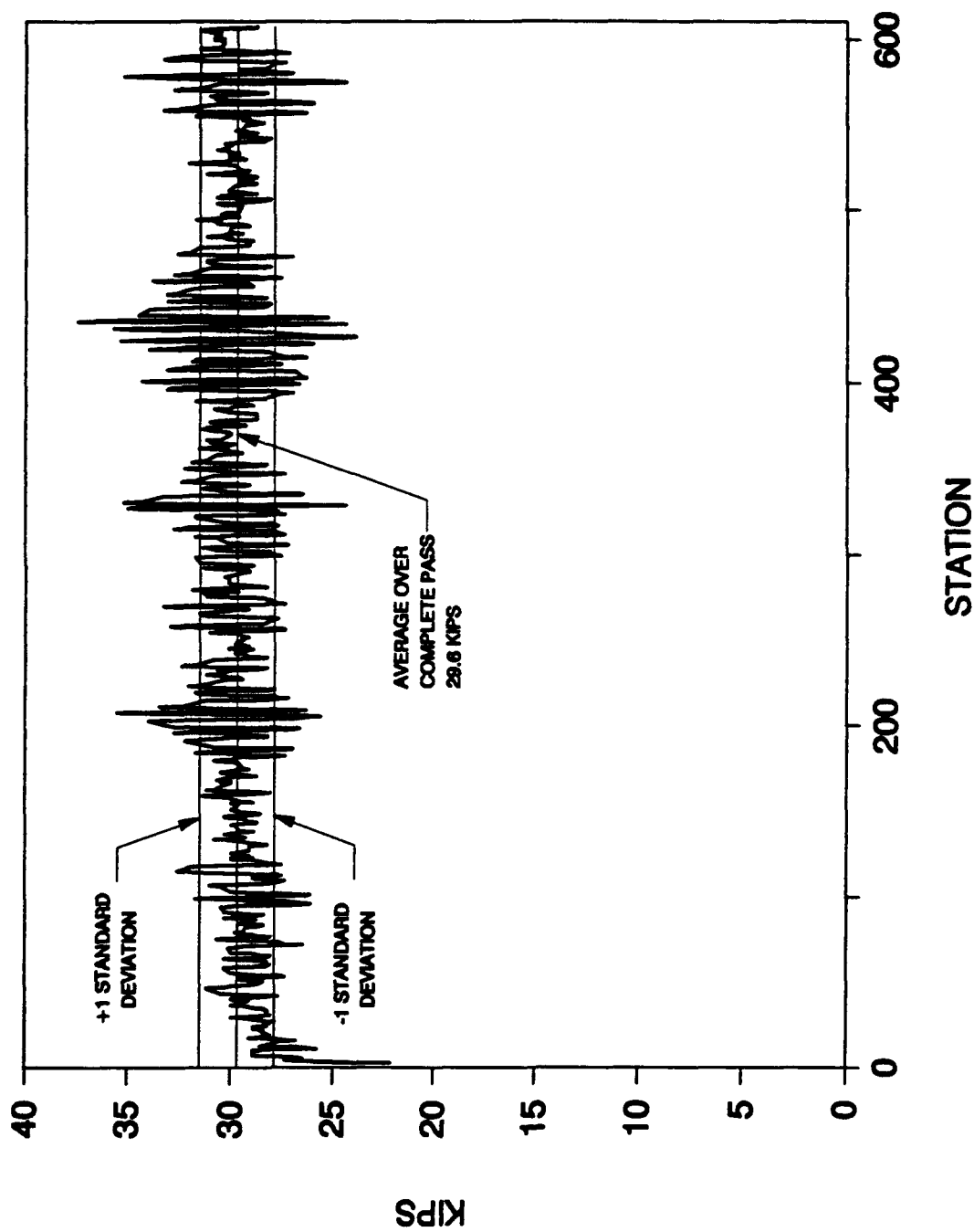
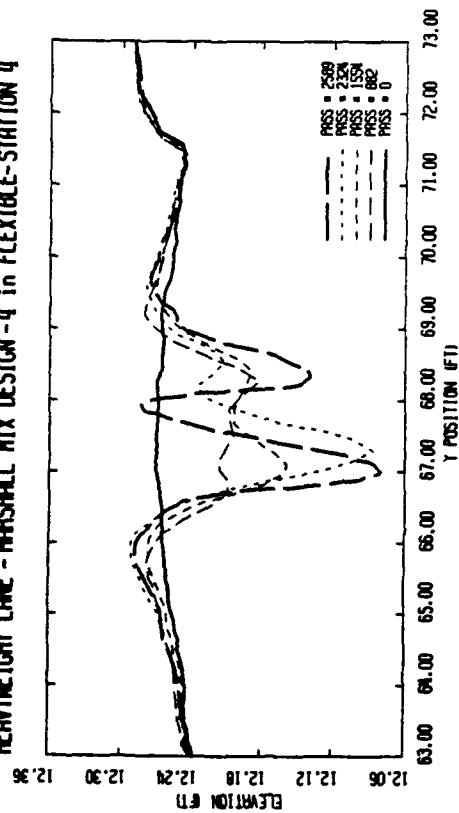
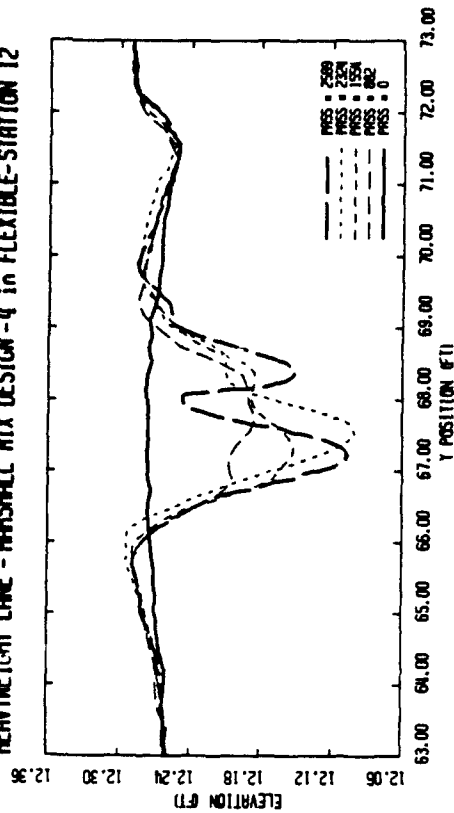


Figure 31. Variation of Load During Pass 2500.

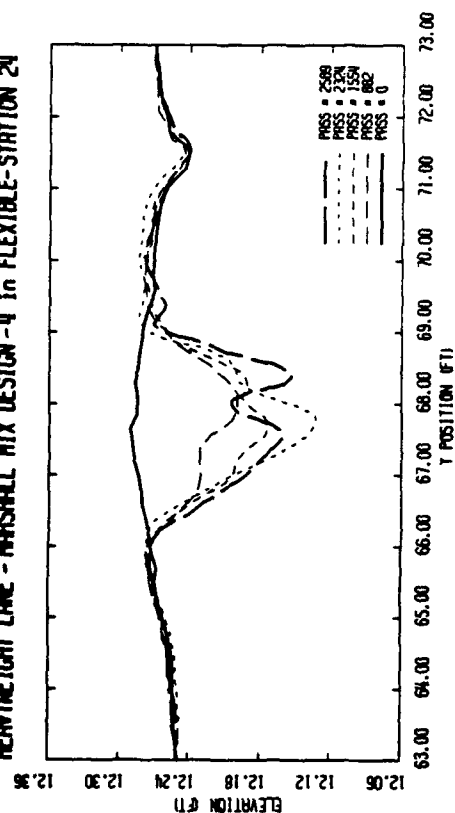
HEAVYWEIGHT LANE - MARSHALL MIX DESIGN -4 in FLEXIBLE-STATION 4



HEAVYWEIGHT LANE - MARSHALL MIX DESIGN -4 in FLEXIBLE-STATION 12



HEAVYWEIGHT LANE - MARSHALL MIX DESIGN -4 in FLEXIBLE-STATION 24



HEAVYWEIGHT LANE - MARSHALL MIX DESIGN -4 in FLEXIBLE-STATION 36

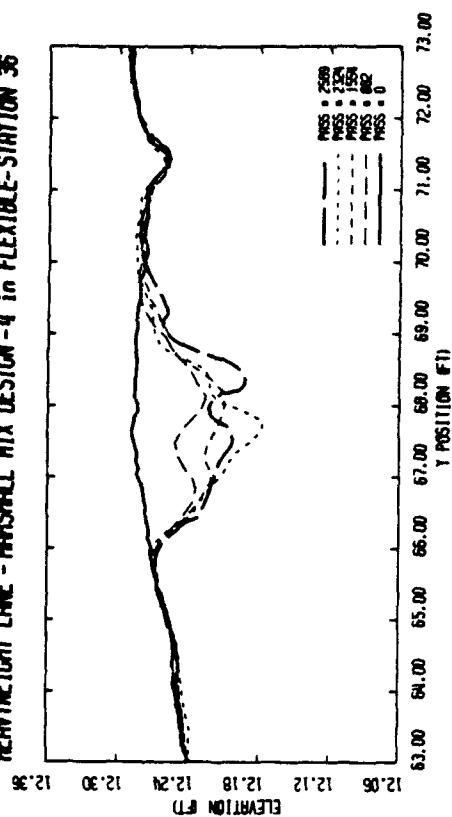


Figure 32. Rut Progression in 4-Inch Flexible Marshall Section.

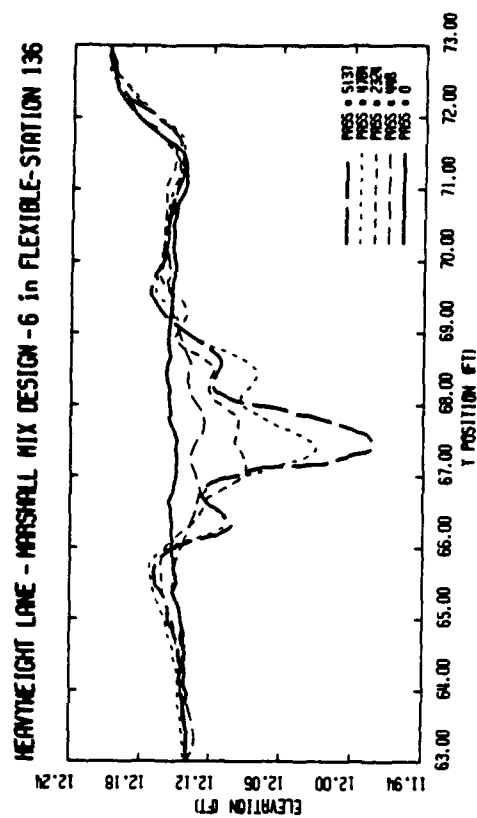
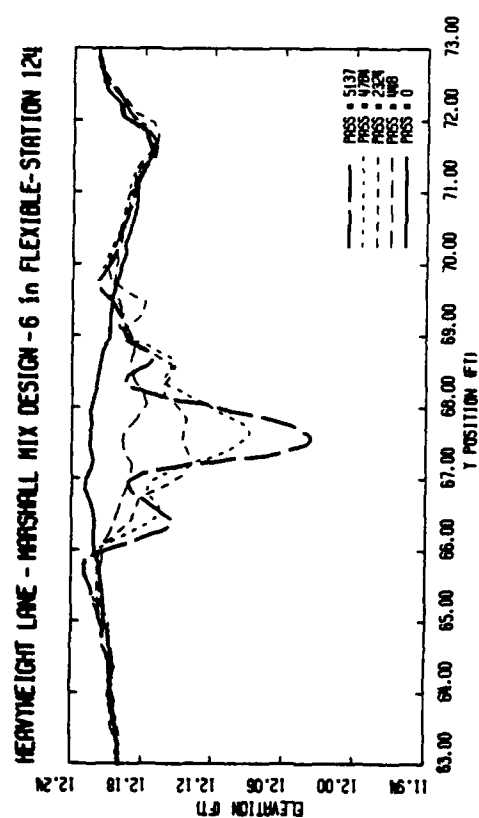
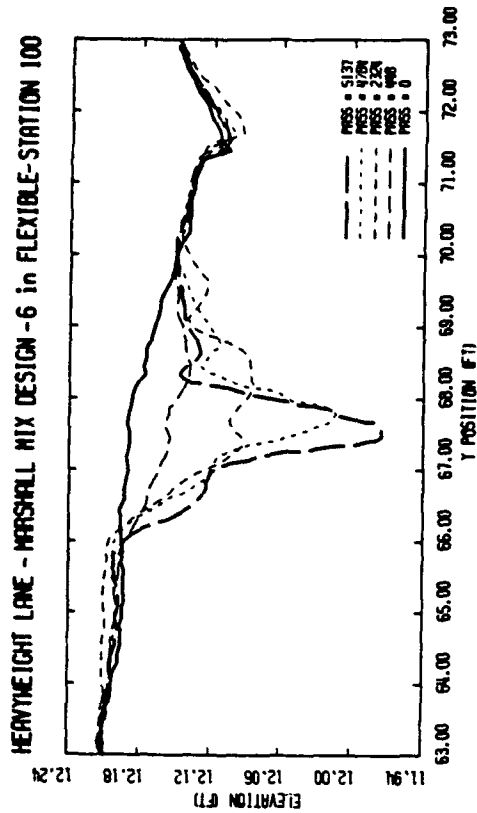
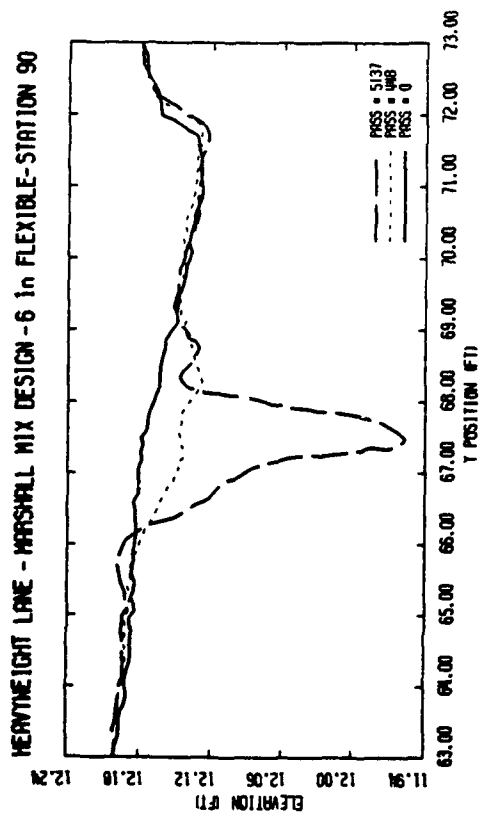


Figure 33. Rut Progression in 6-Inch Flexible Marshall Section.

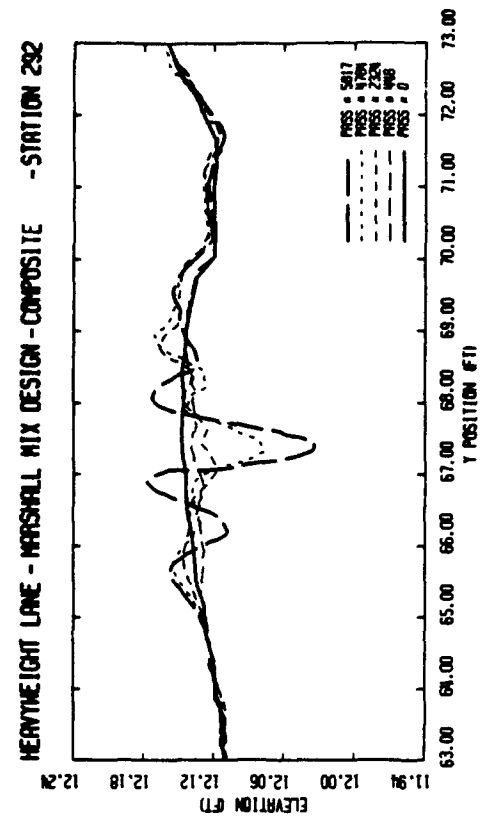
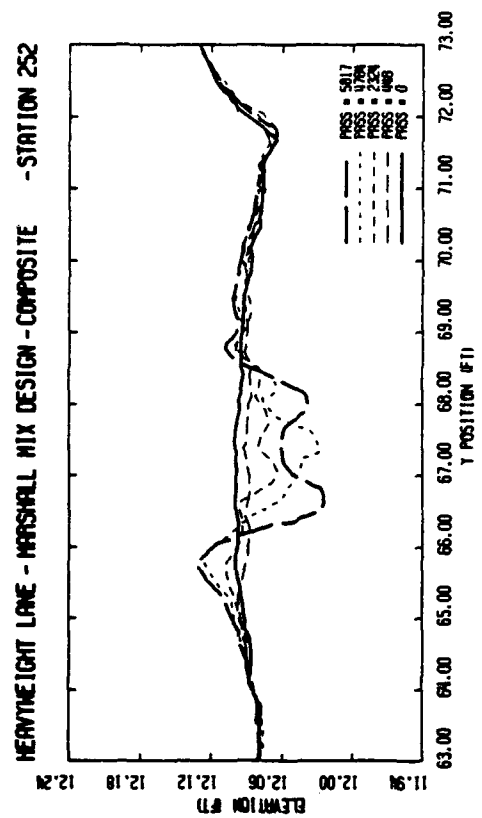
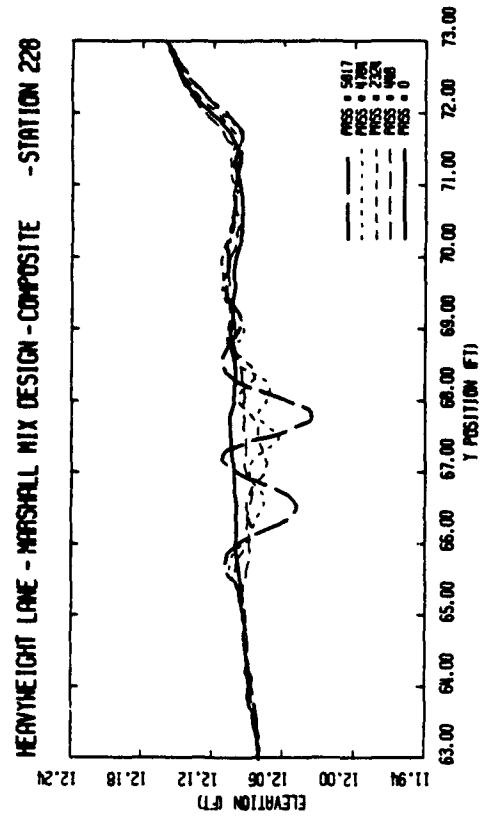
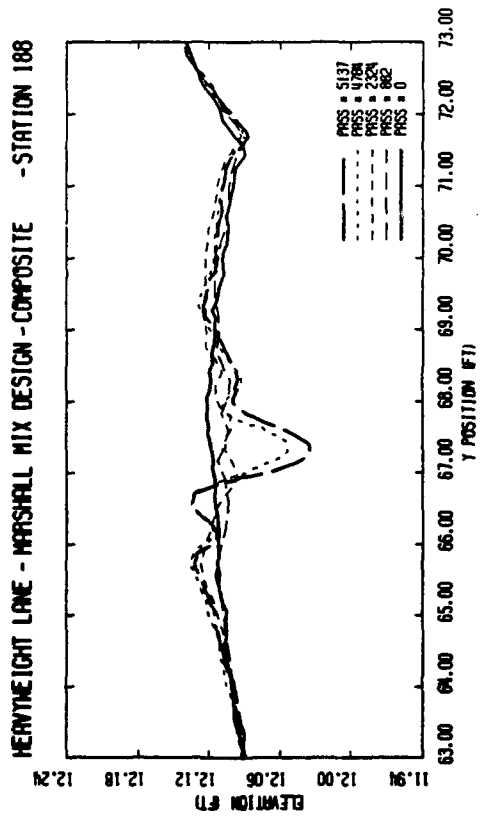


Figure 34. Rut Progression in 8-Inch Composite Marshall Section.

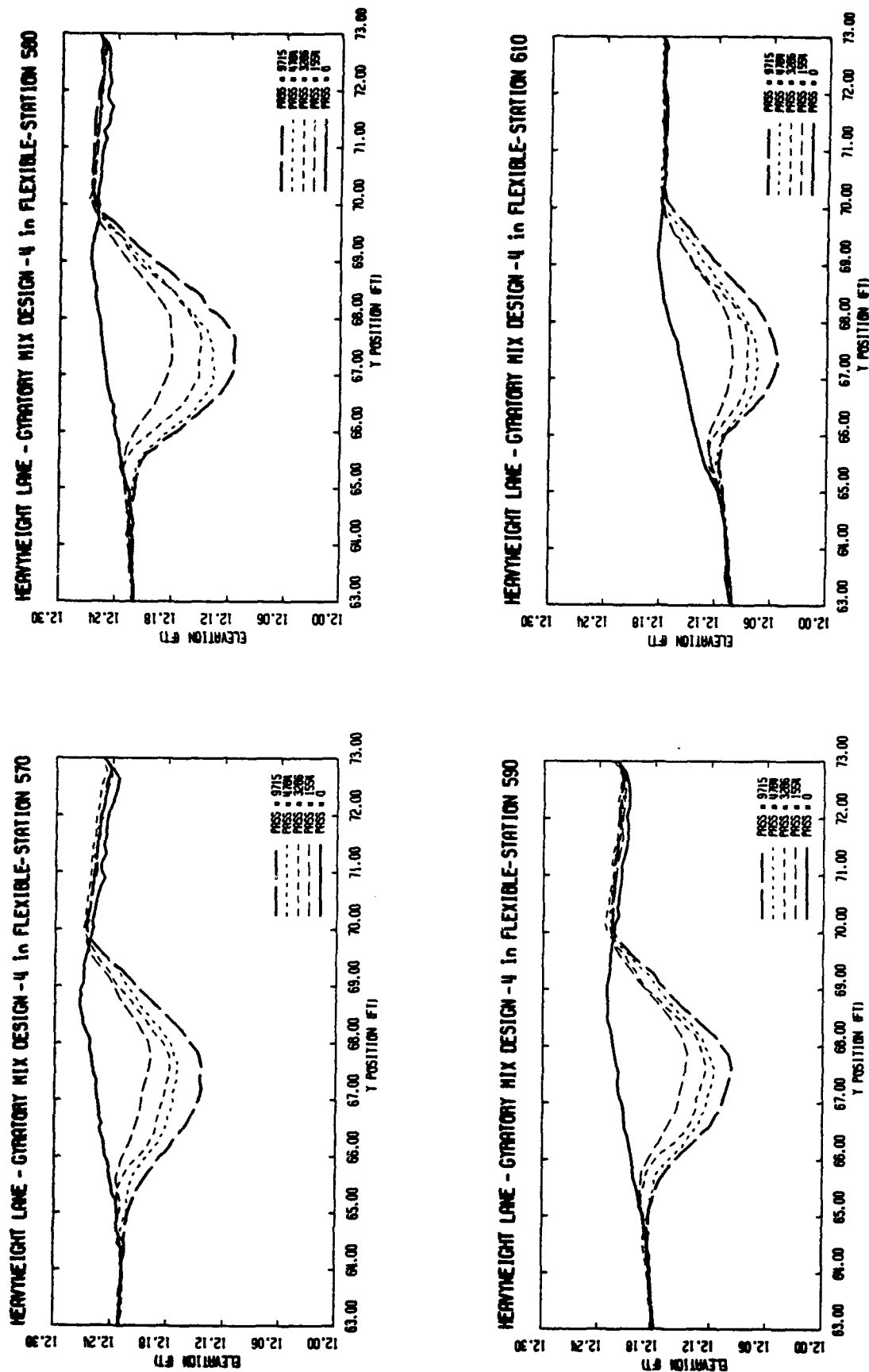


Figure 35. Rut Progression in 4-Inch Flexible Gyratory Section.

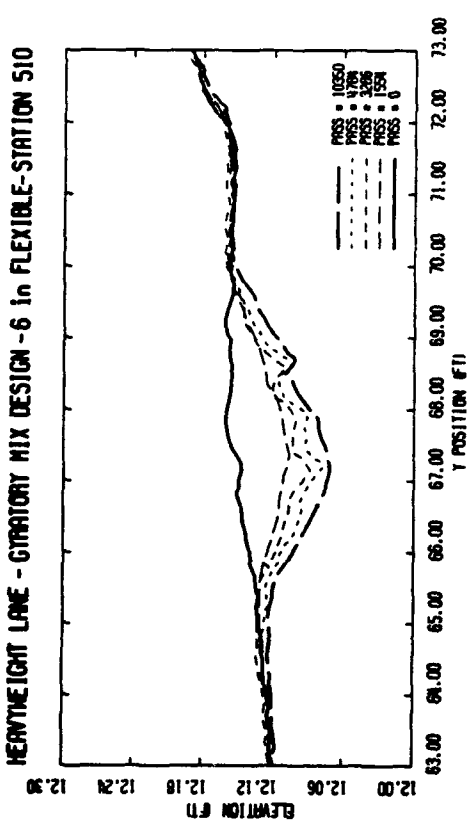
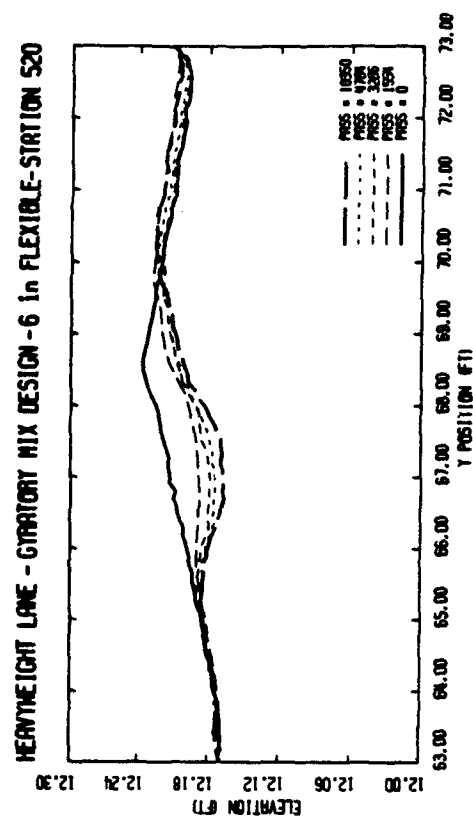
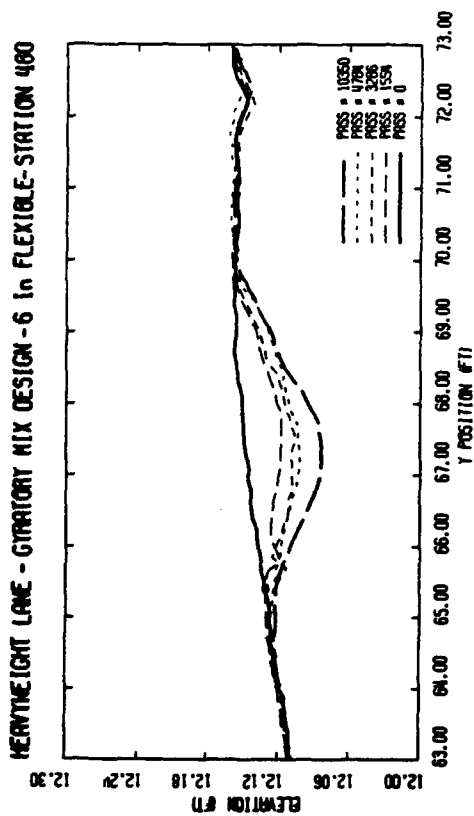
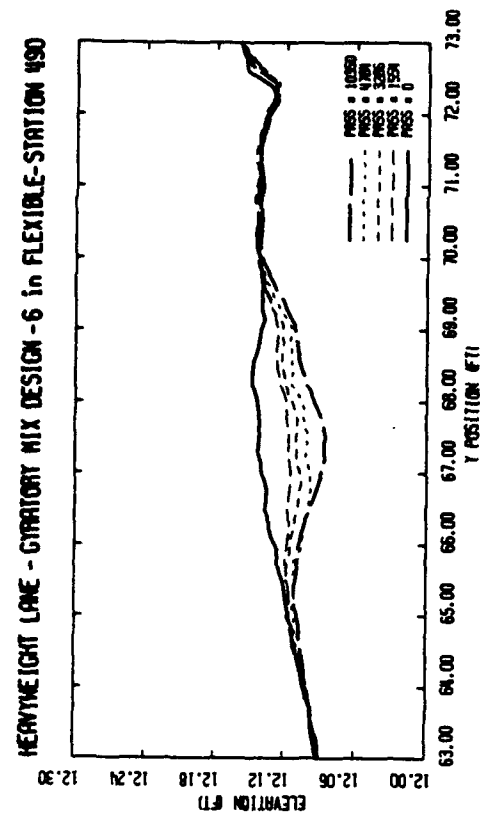


Figure 36. Rut Progression in 6-Inch Flexible Gyratory Section.

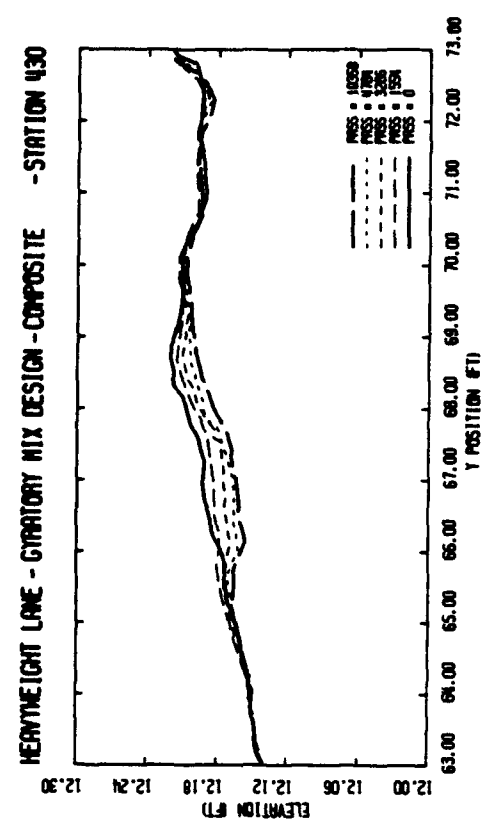
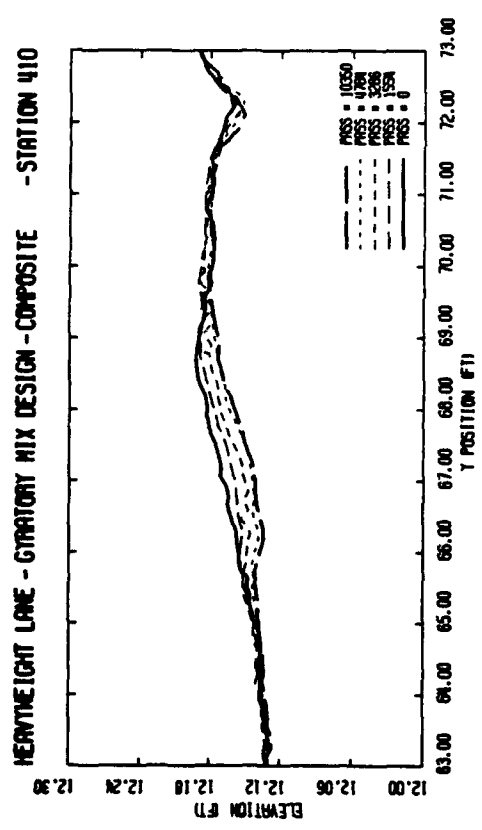
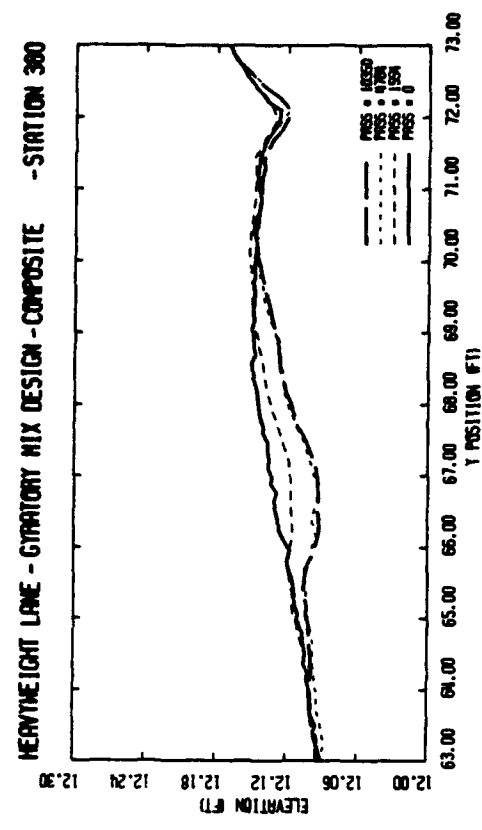
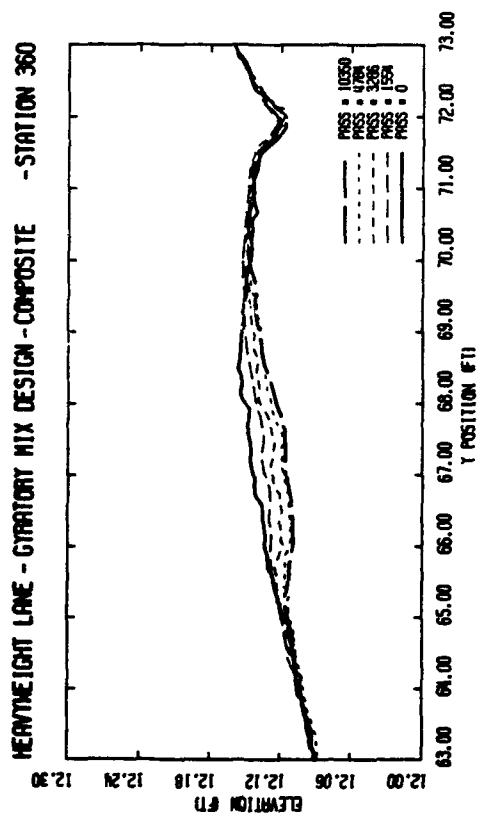


Figure 37. Rut Progression in 6-Inch Composite Gyratory Section.

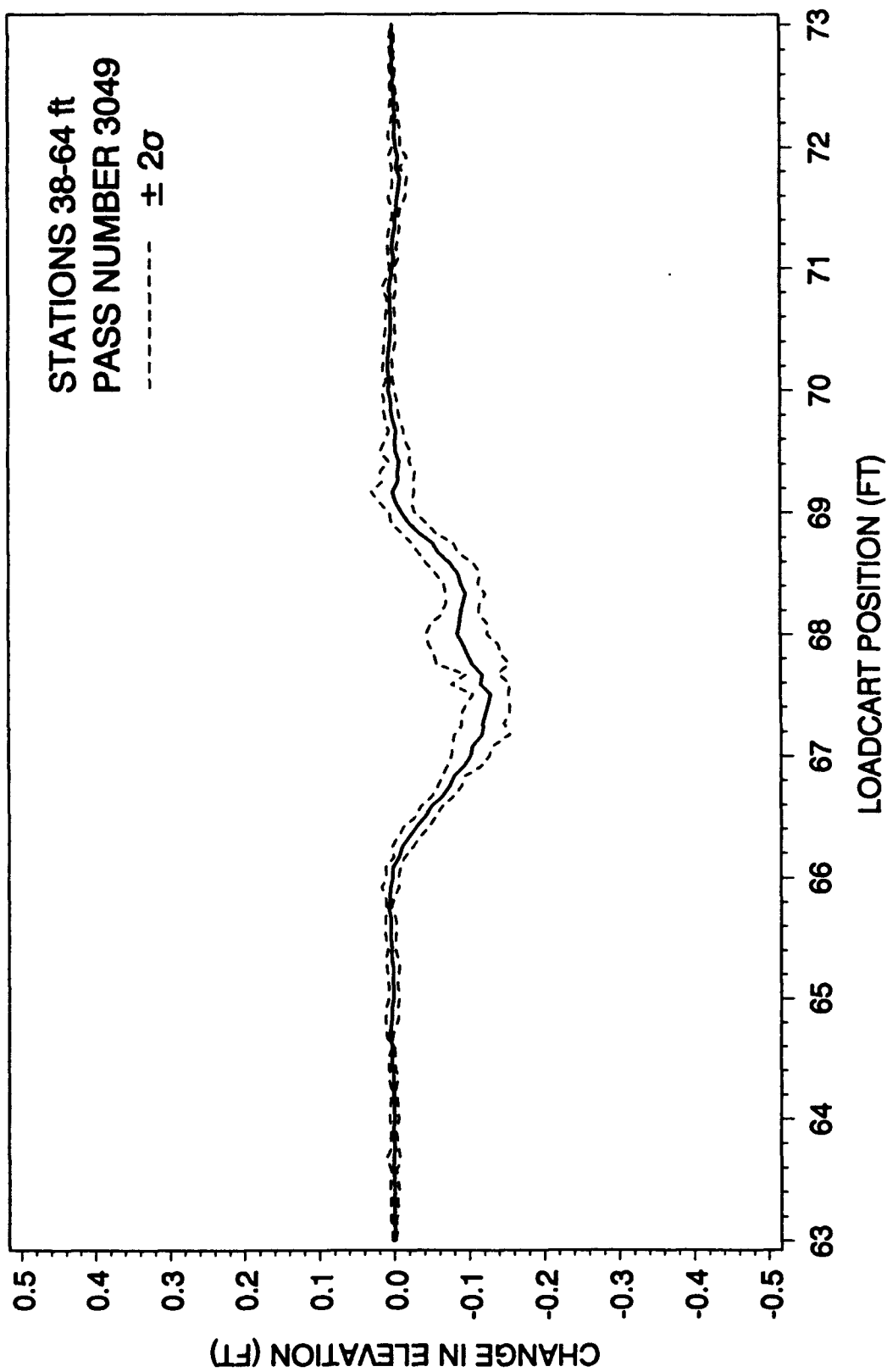


Figure 38. Representative Profile for Marshall Mix Design, 4-Inch Flexible.

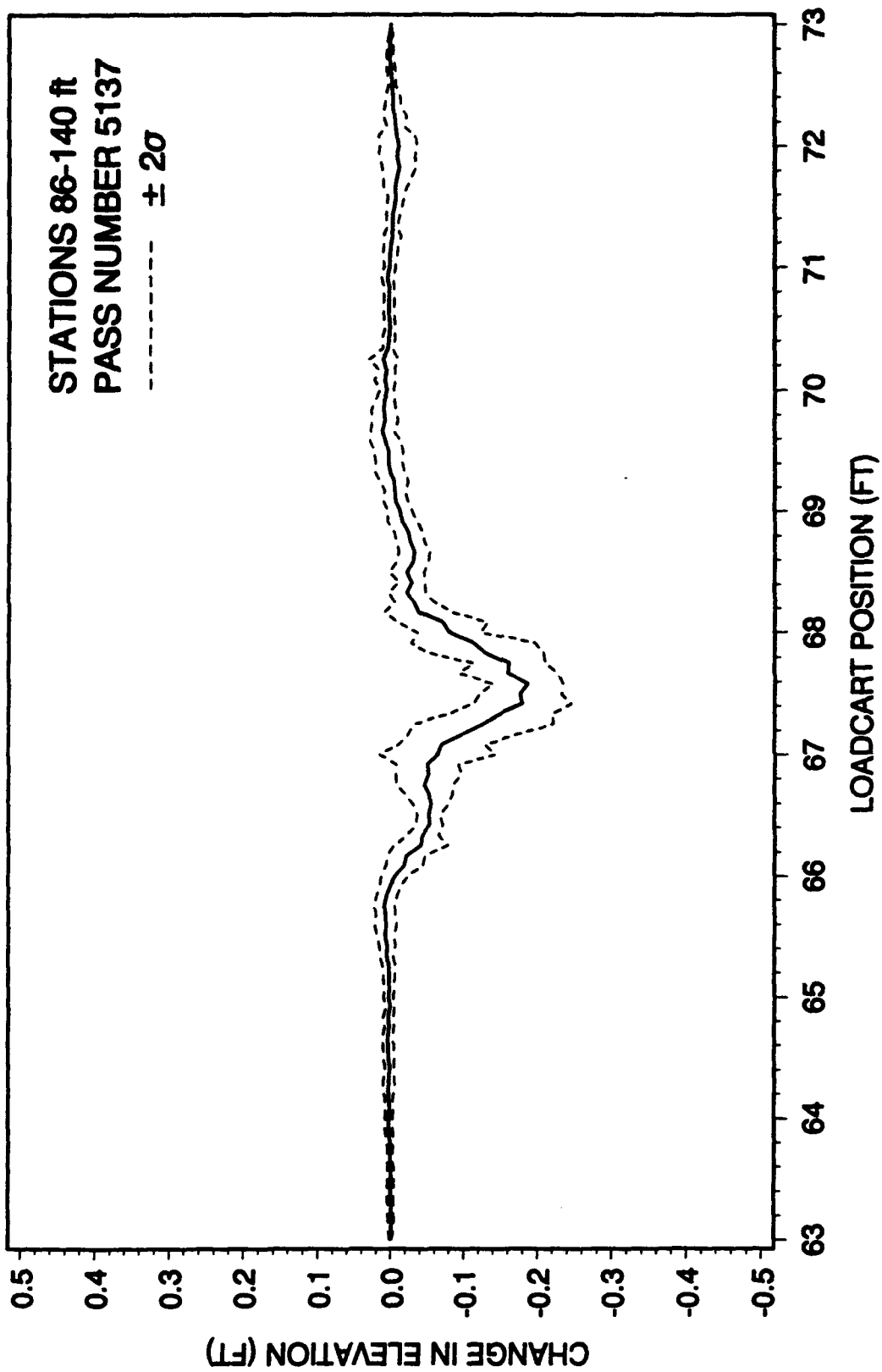


Figure 39. Representative Profile for Marshall Mix Design, 6-Inch Flexible.

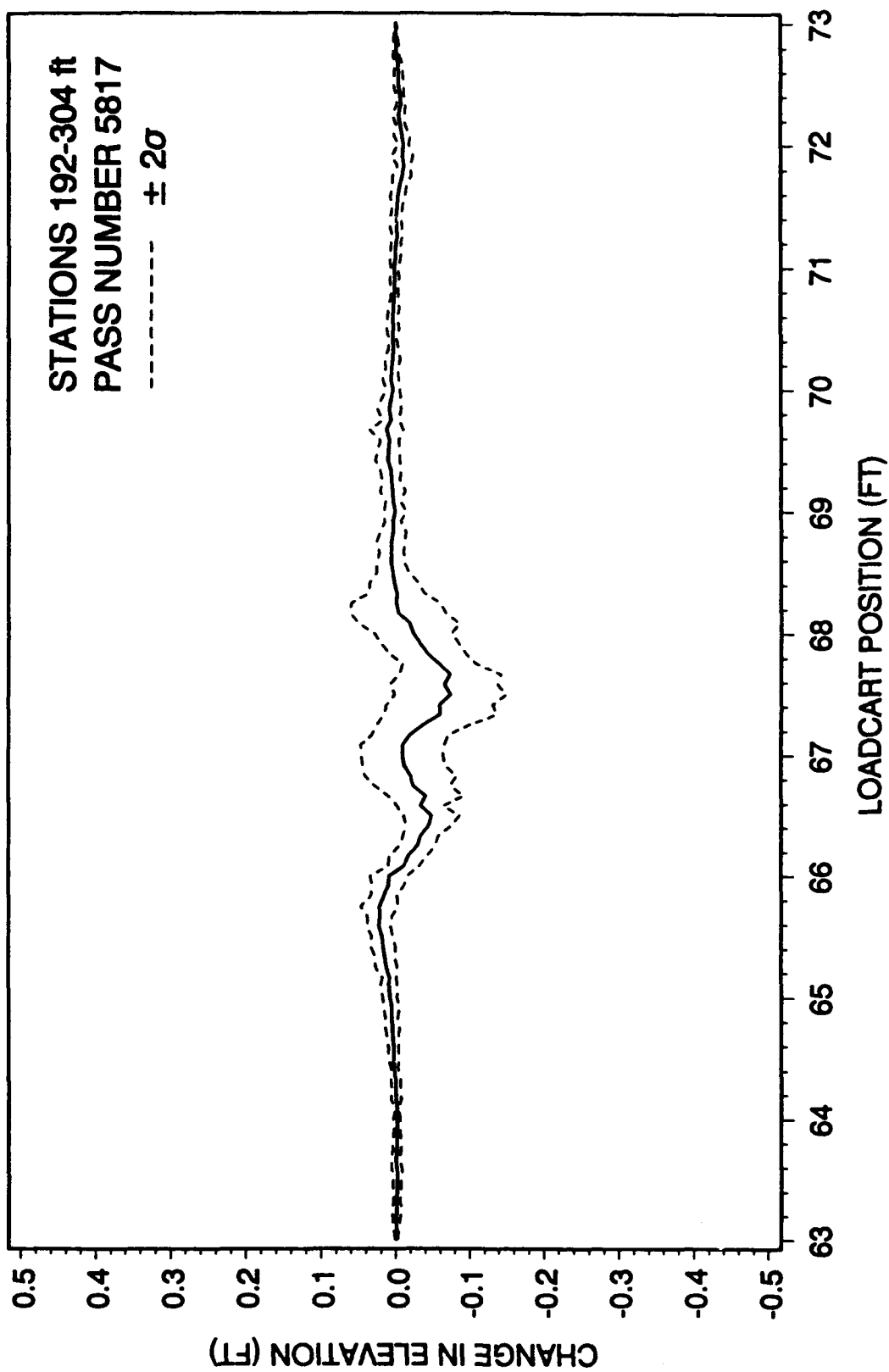


Figure 40. Representative Profile for Marshall Mix Design, Composite.

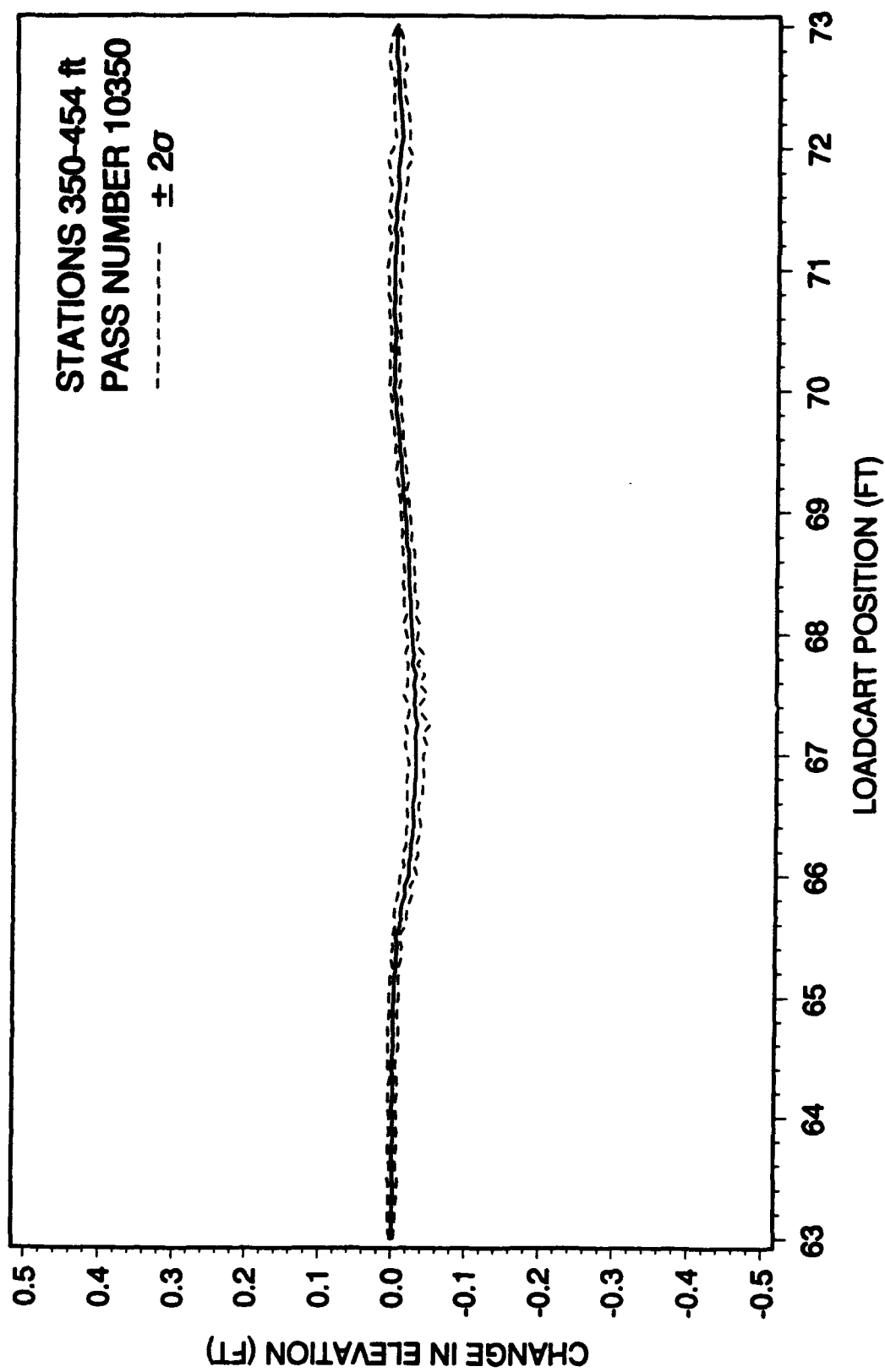


Figure 41. Representative Profile for Gyratory Mix Design, Composite.

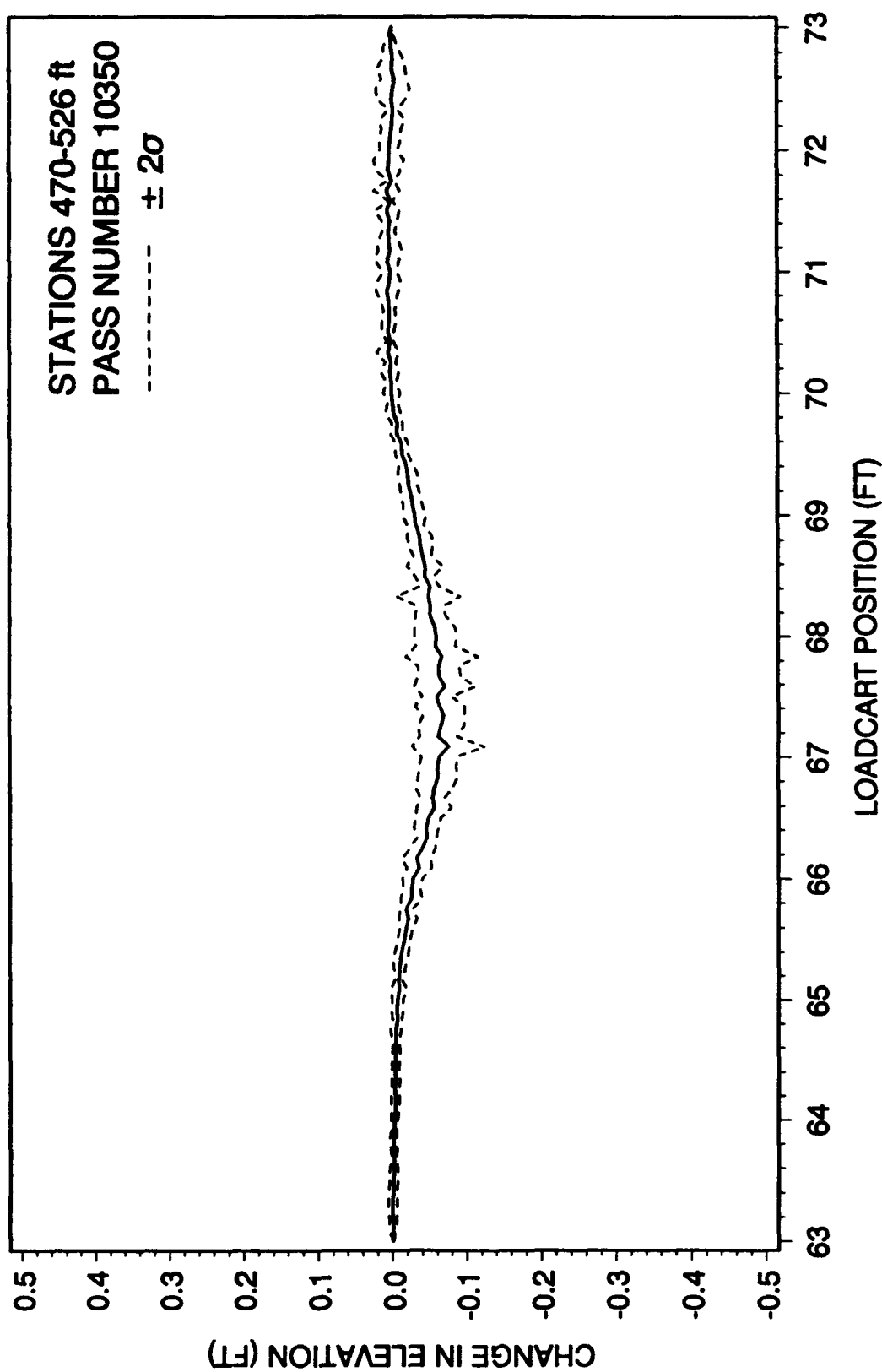


Figure 42. Representative Profile for Gyrotratory Mix Design, 6-Inch Flexible.

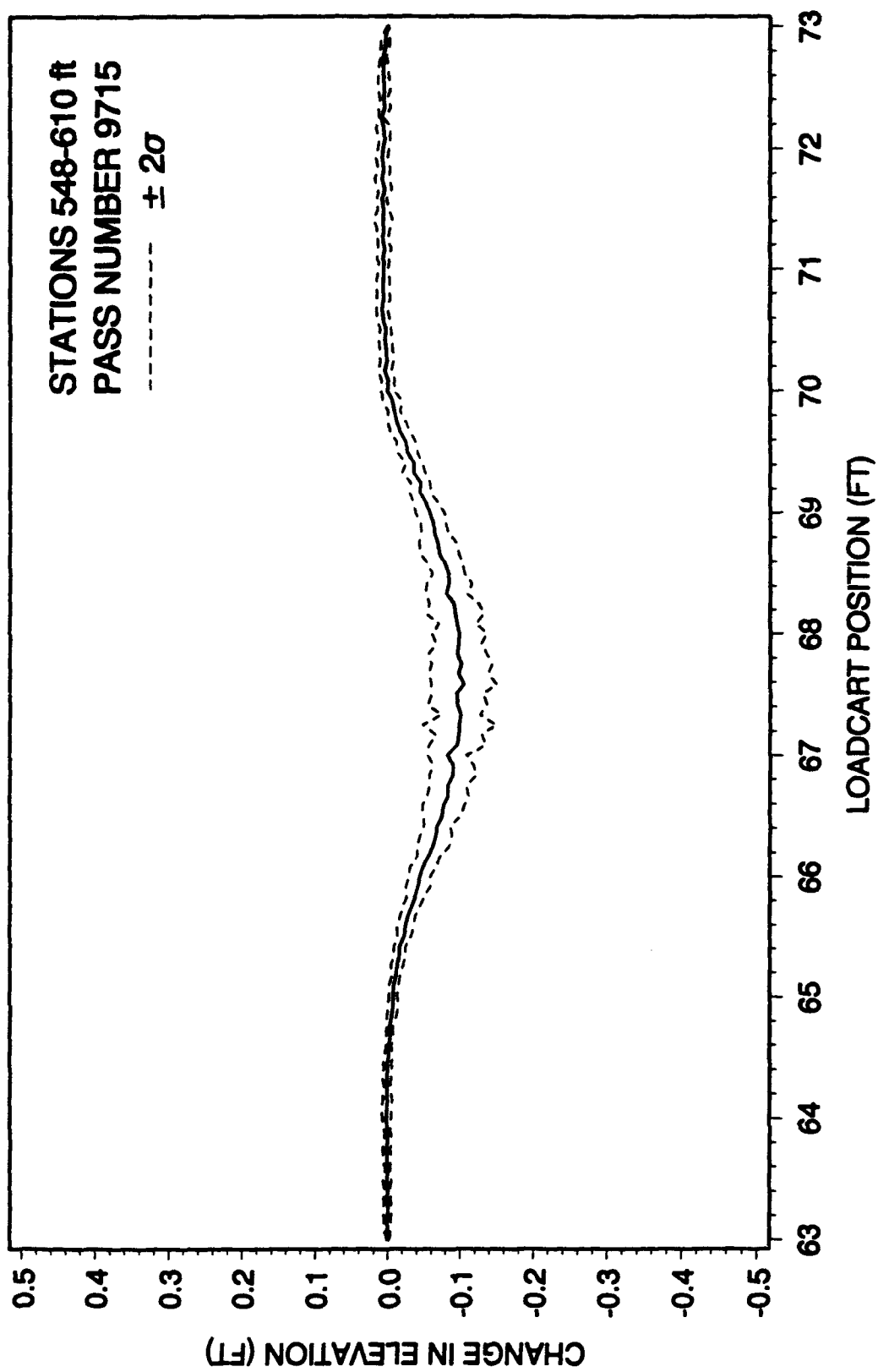


Figure 43. Representative Profile for Gyratory Mix Design, 4-Inch Flexible.

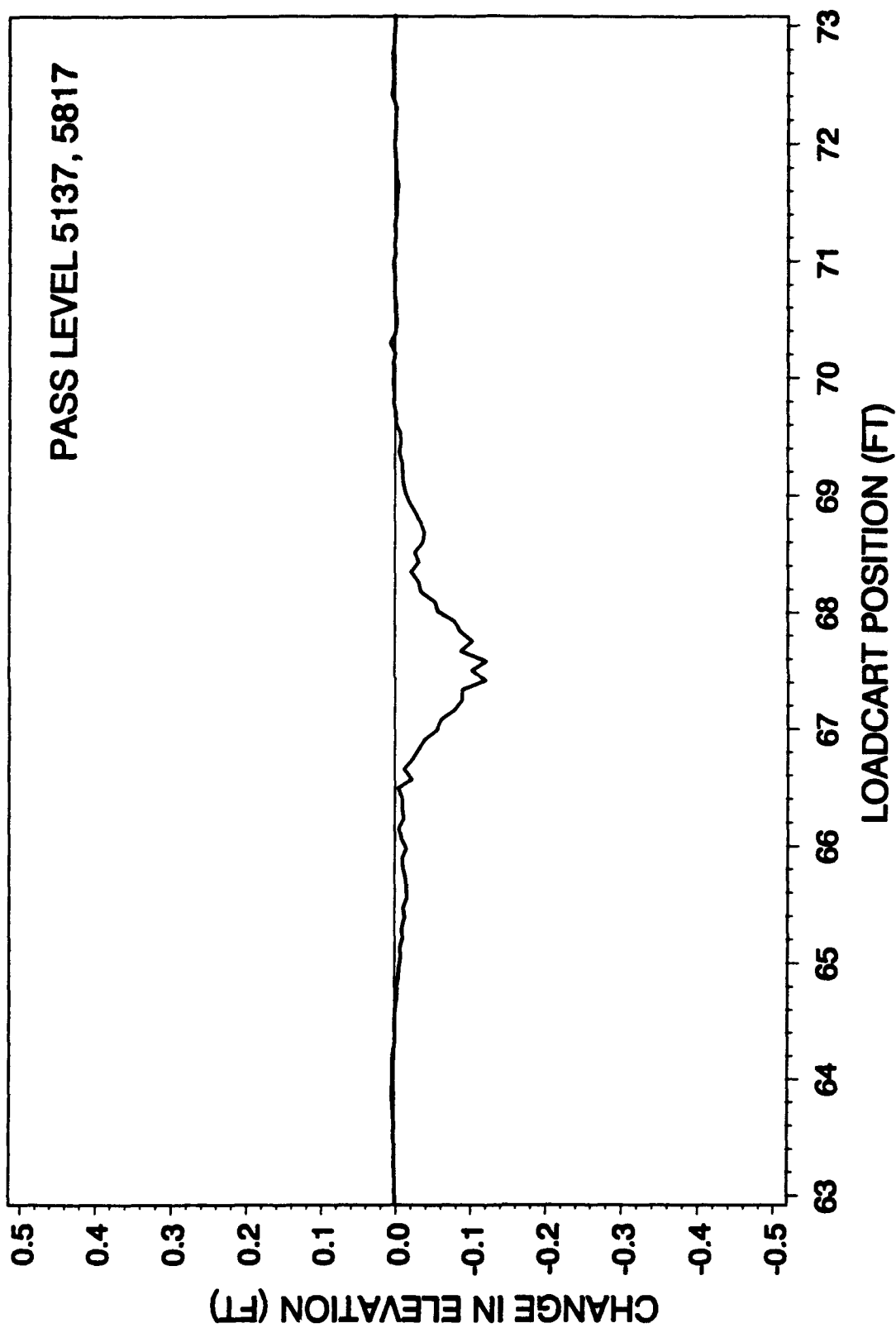


Figure 44. Estimated Base Course Rut Profile, 6-Inch Marshall Mix Design.

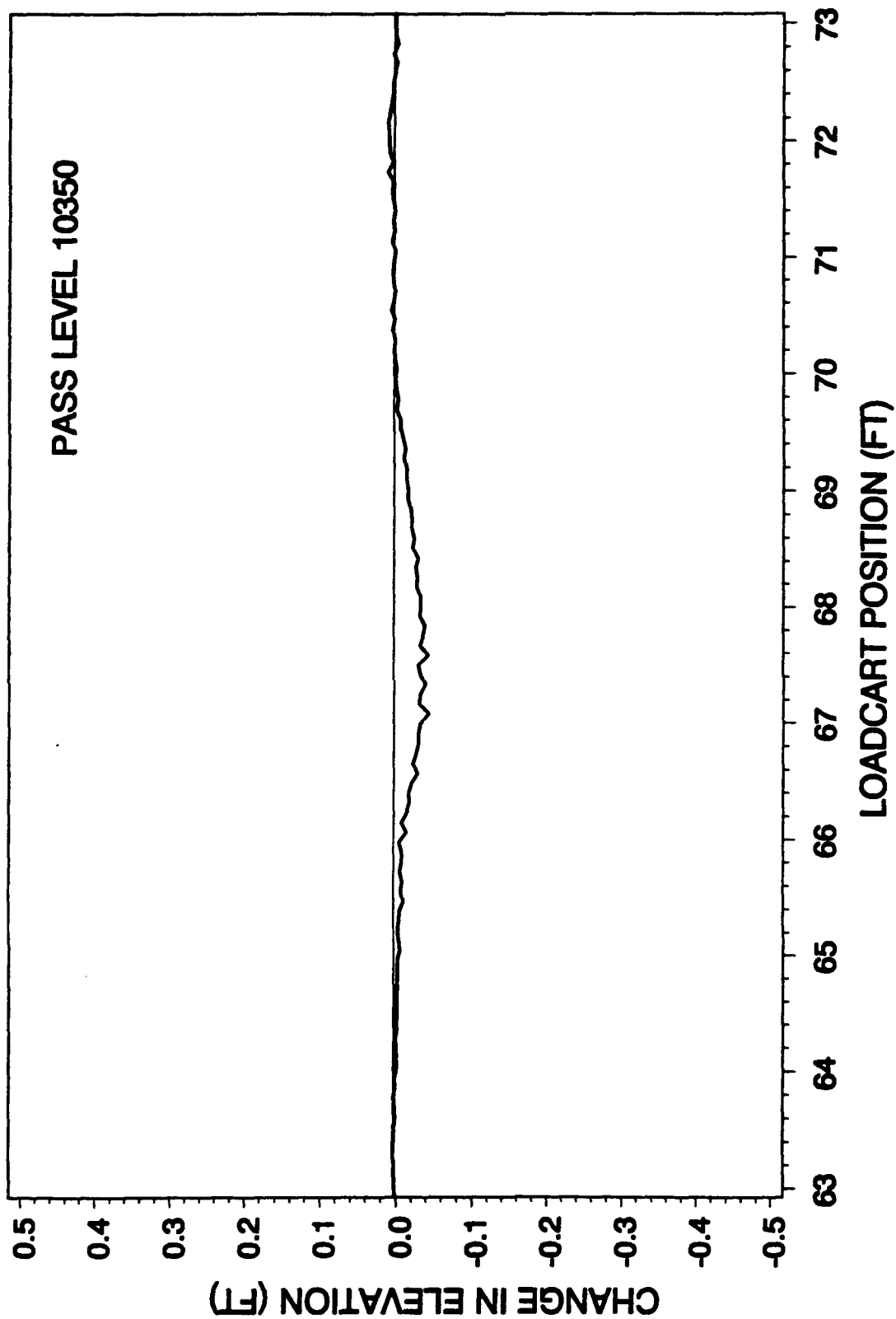
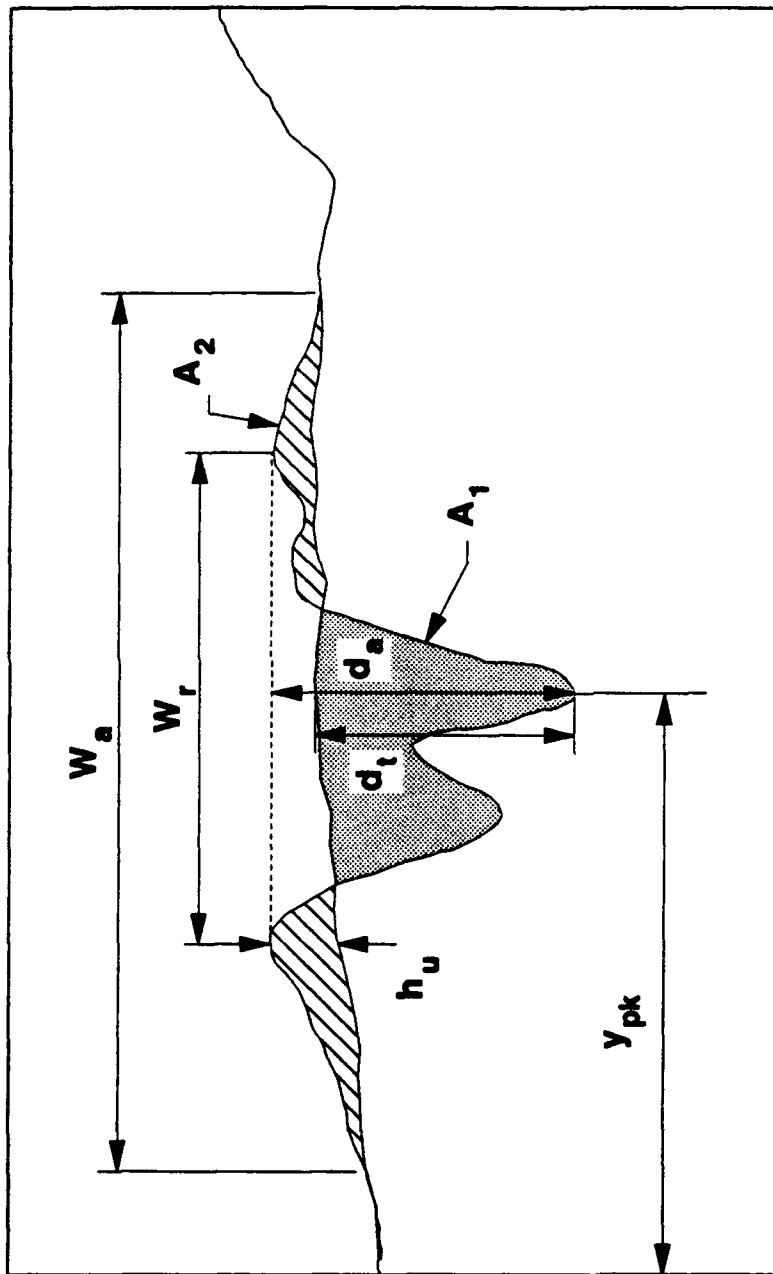


Figure 45. Estimated Base Course Rut Profile, 6-Inch Gyratory Mix Design.



A_1 - TRUE RUT AREA d_t - TRUE RUT DEPTH d_a - APPARENT RUT DEPTH
 A_2 - AREA OF UPHEAVAL w_r - RUT WIDTH w_a - AFFECTED WIDTH
 h_u - HEIGHT OF UPHEAVAL y_{pk} - LATERAL POSITION OF TRUE RUT DEPTH

Figure 46. Damage Parameters.

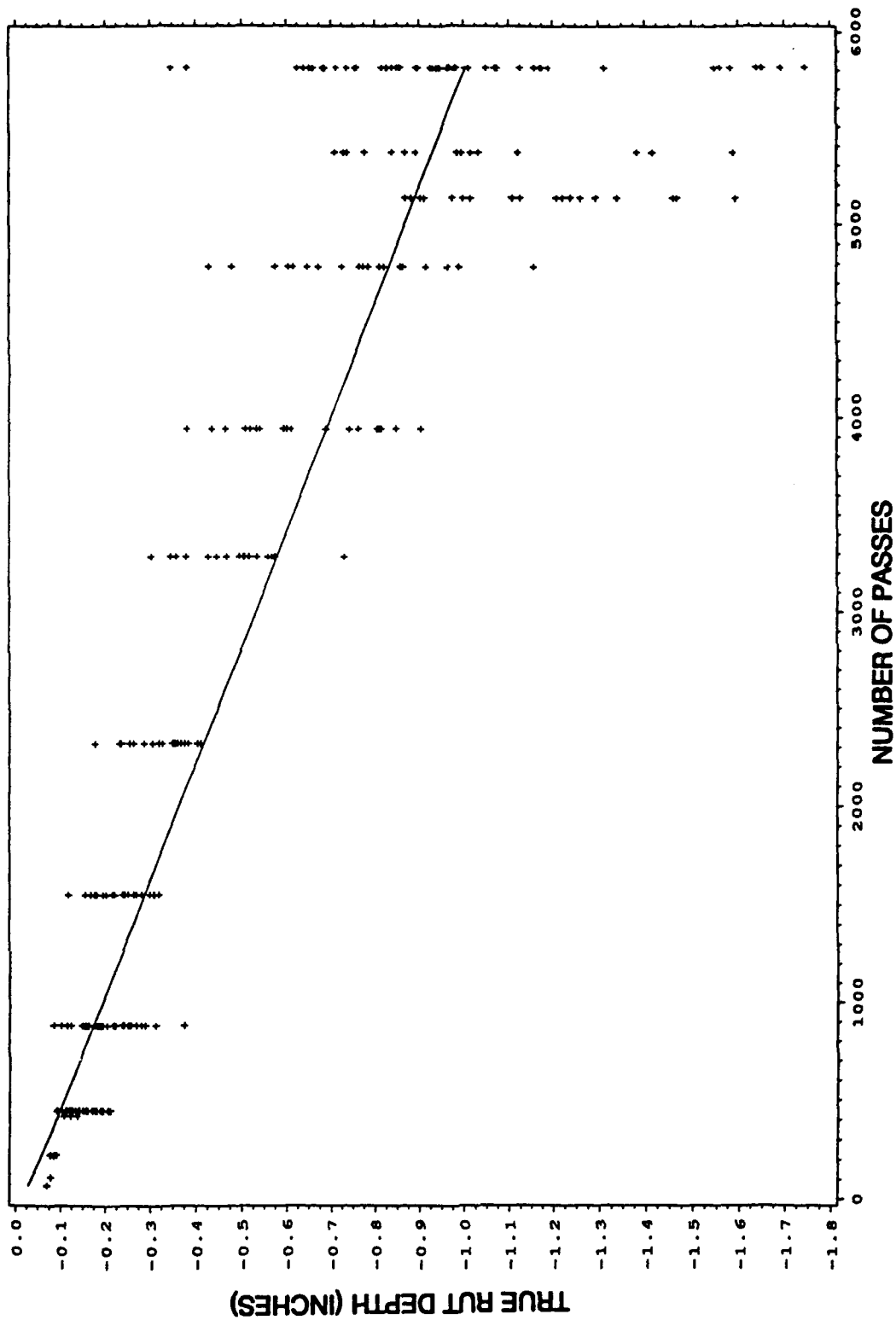


Figure 47. Rut Depth Regression Analysis for 6-Inch Composite Marshall Section.

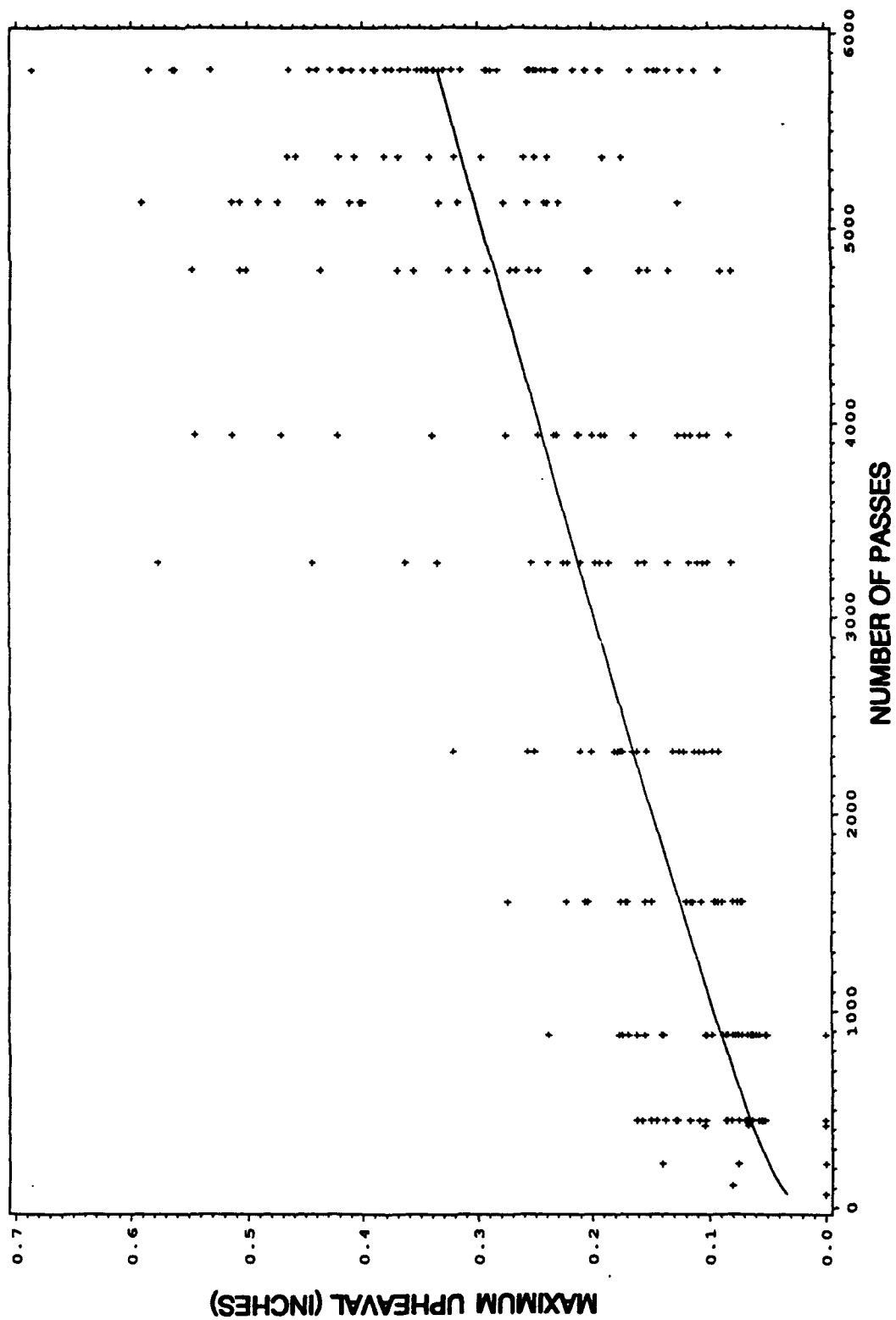


Figure 48. Maximum Upheaval Height Regression Analysis for 6-Inch Composite Marshall Section.

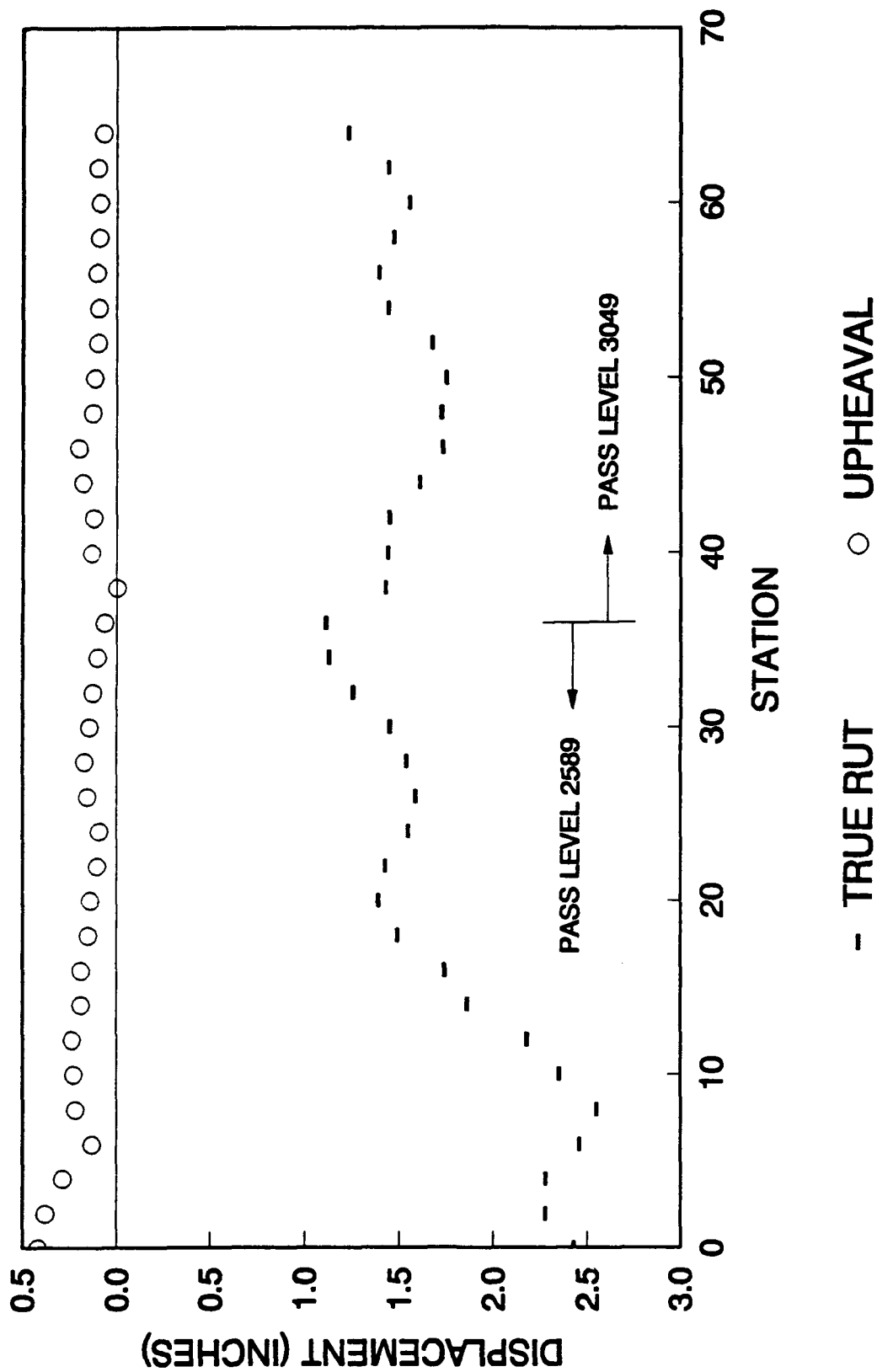


Figure 49. Upheaval and True Rut Depth from the Marshall 4-Inch Flexible Section at the Final Pass Level.

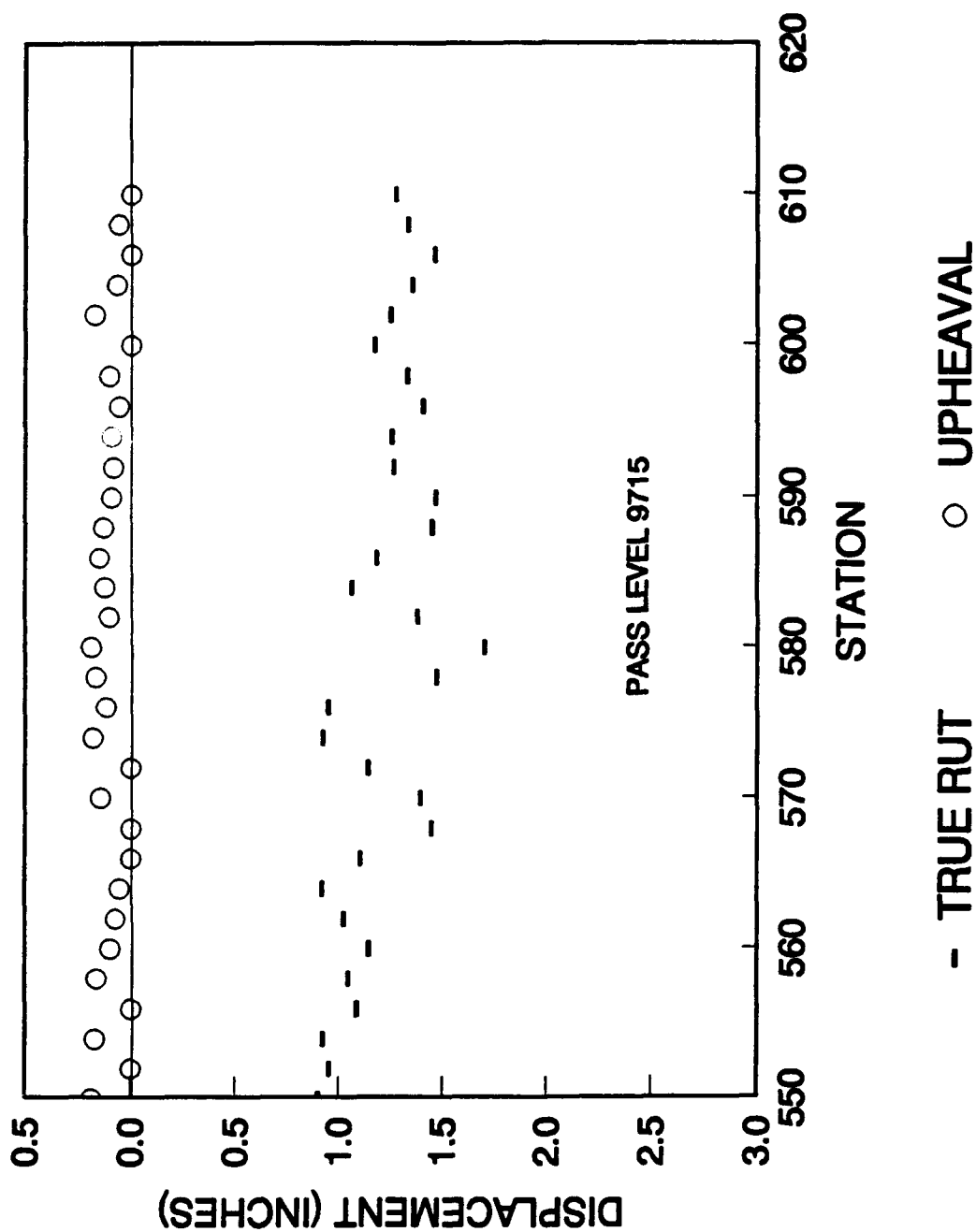


Figure 50. Upheaval and True Rut Depth for the Gyratory 4-Inch Flexible at Final Pass Level.

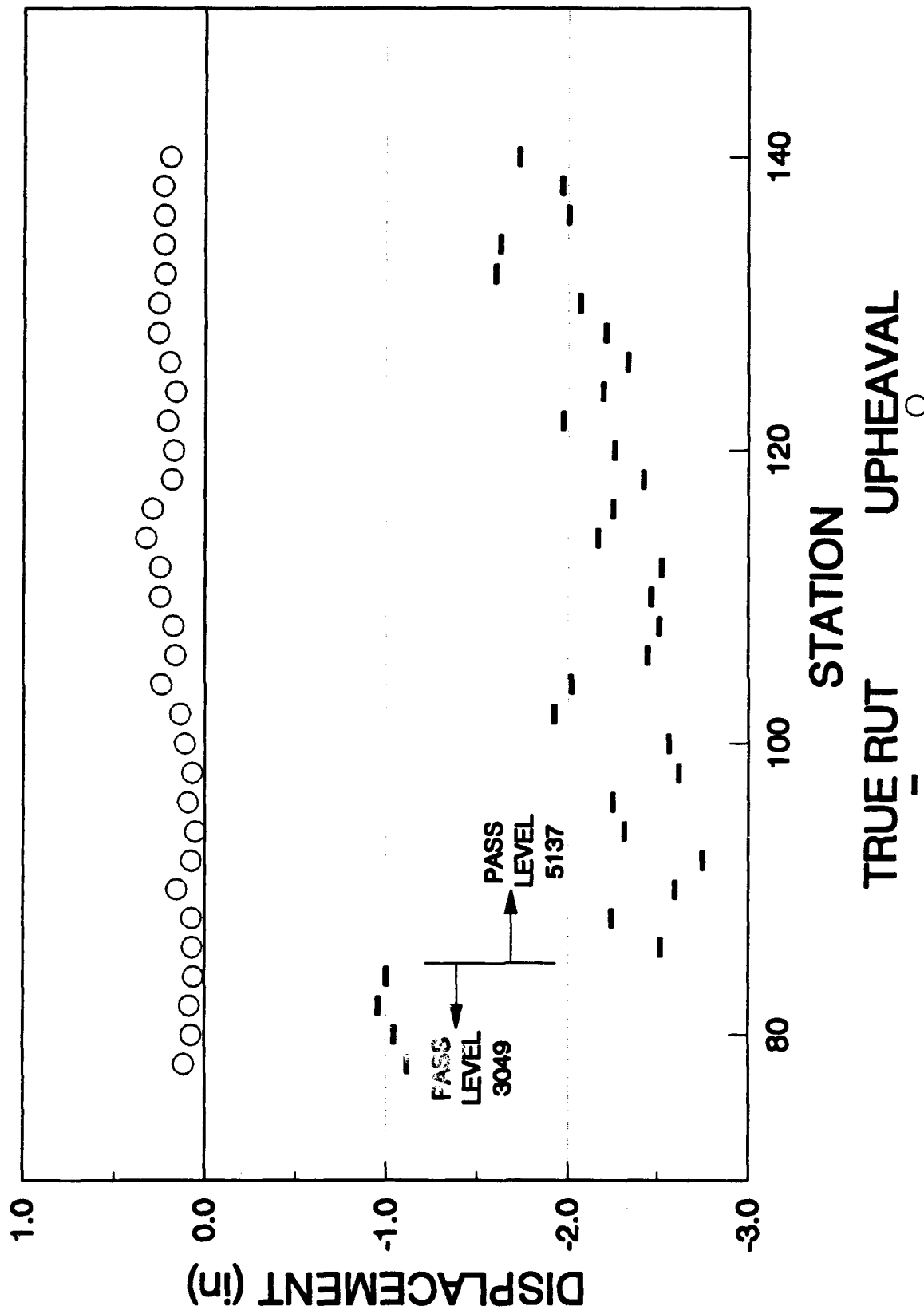


Figure 51. Upheaval and True Rut Depth from the Marshall 6-Inch Flexible Section at the Final Pass Level.

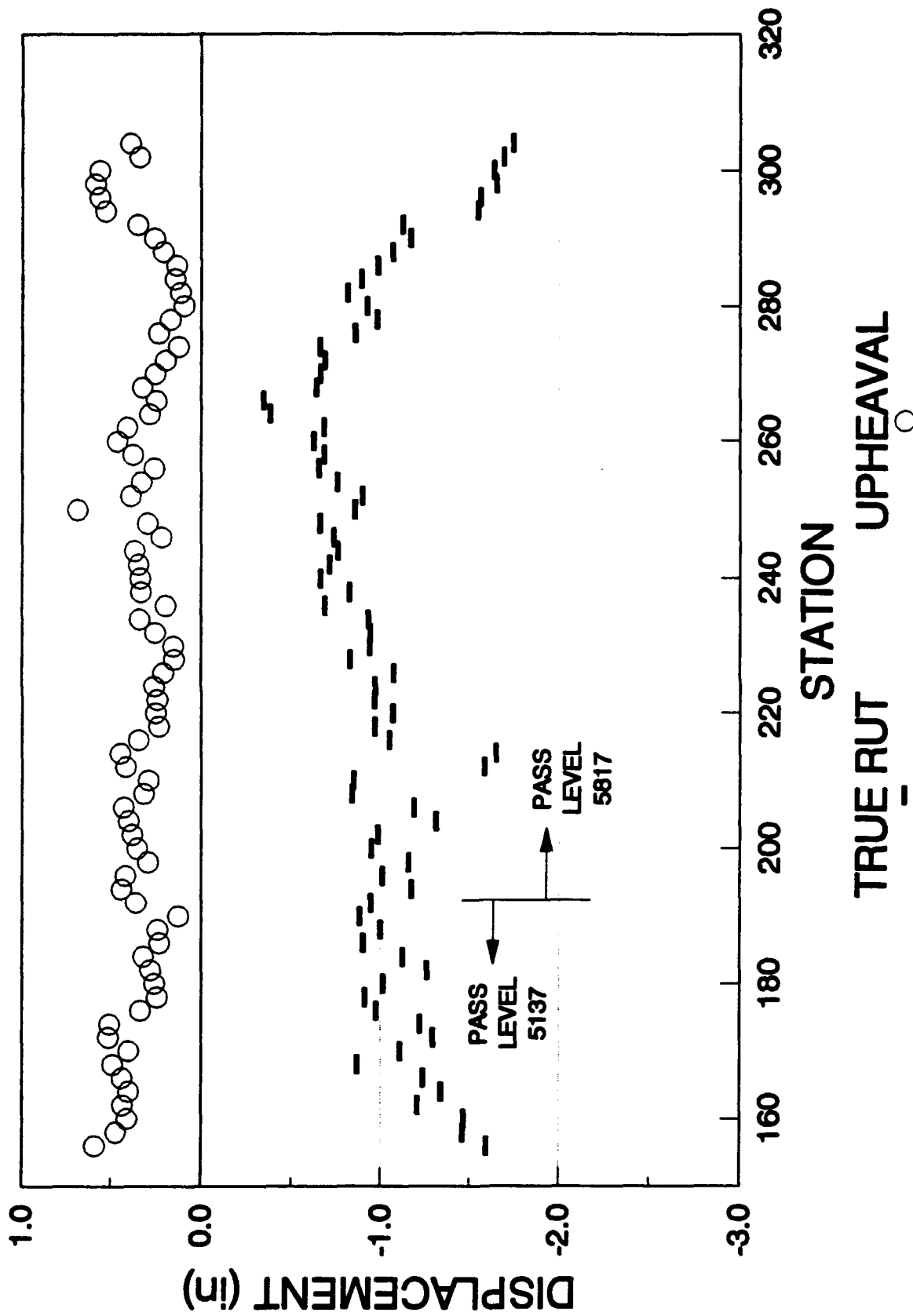


Figure 52. Upheaval and True Rut Depth from the Marshall Composite Test Section at the Final Pass Level.

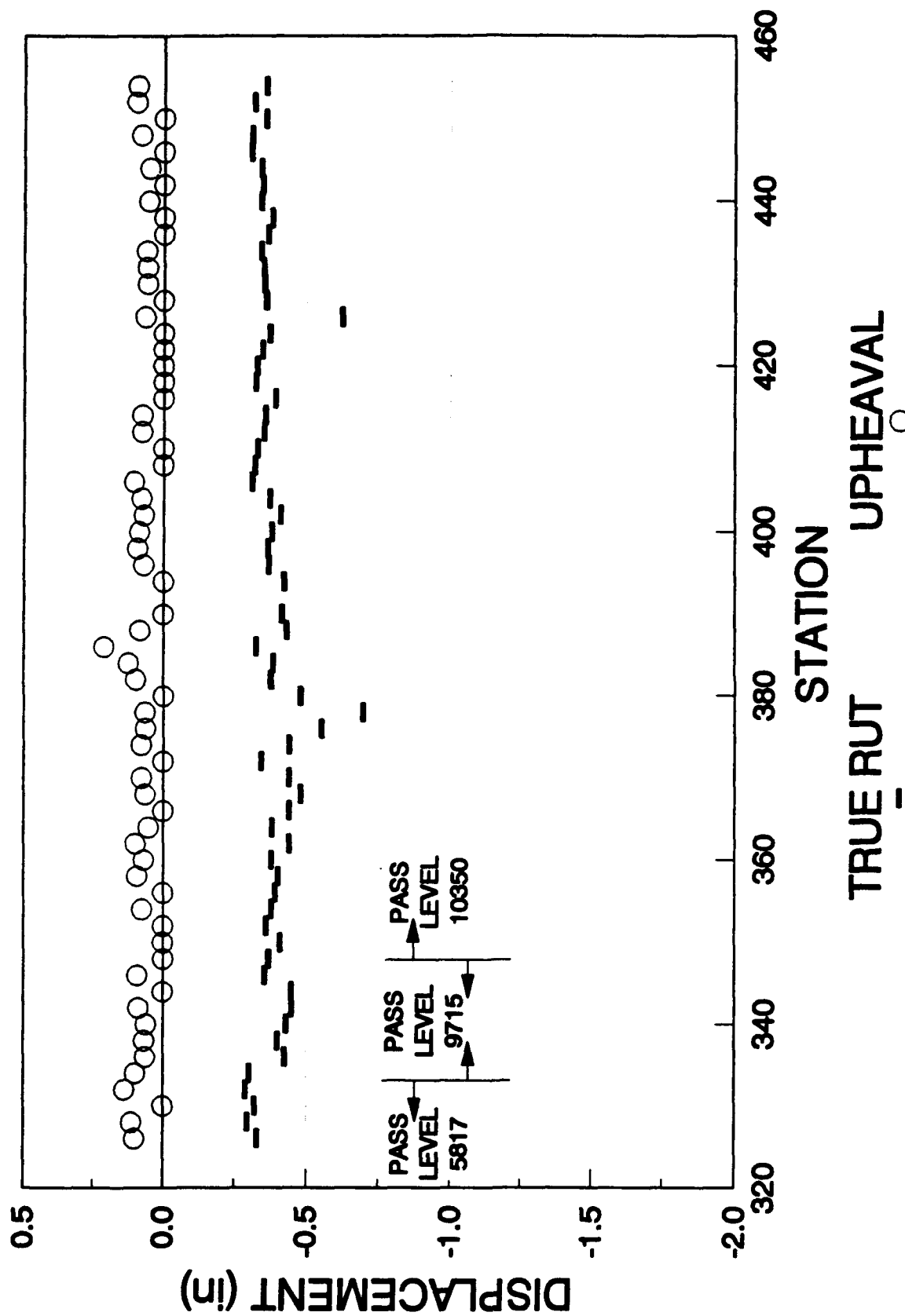


Figure 53. Upheaval and True Rut Depth from the Gyratory Composite Test Section at the Final Pass Level.

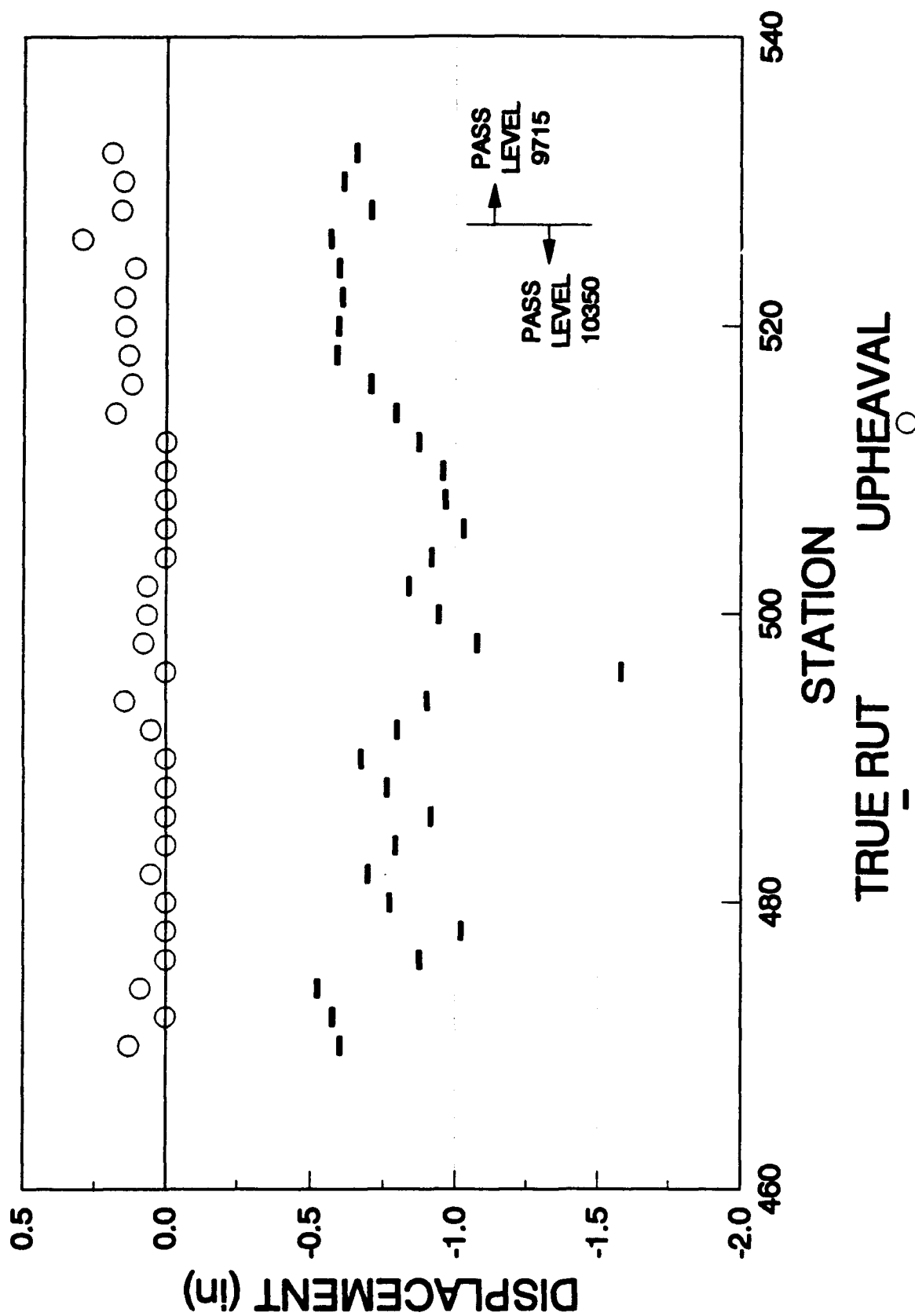


Figure 54. Upheaval and True Rut Depth from the Gyratory 6-Inch Flexible Section at the Final Pass Level.

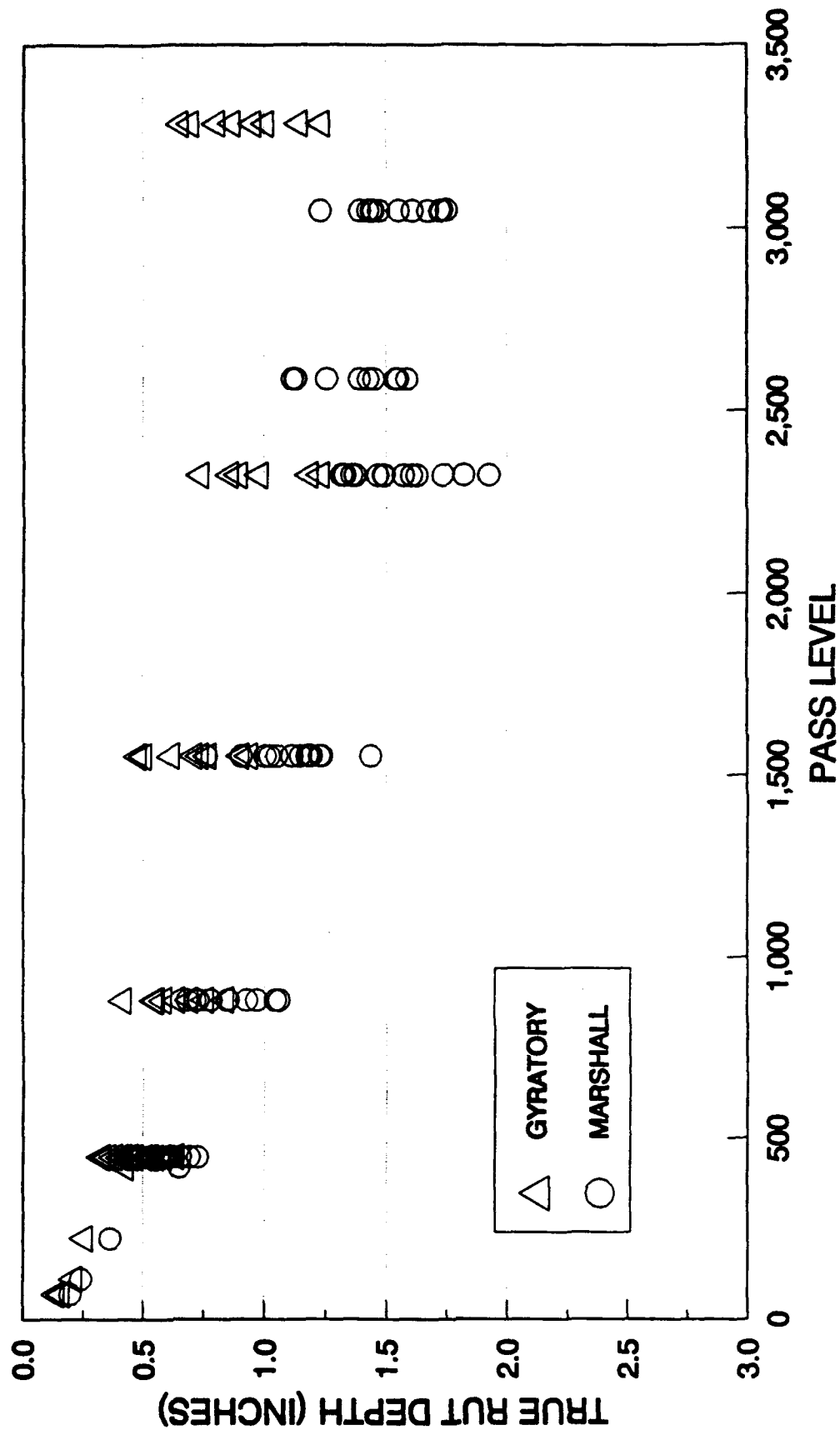


Figure 55. True Rut Depths from 4-Inch Flexible Sections.

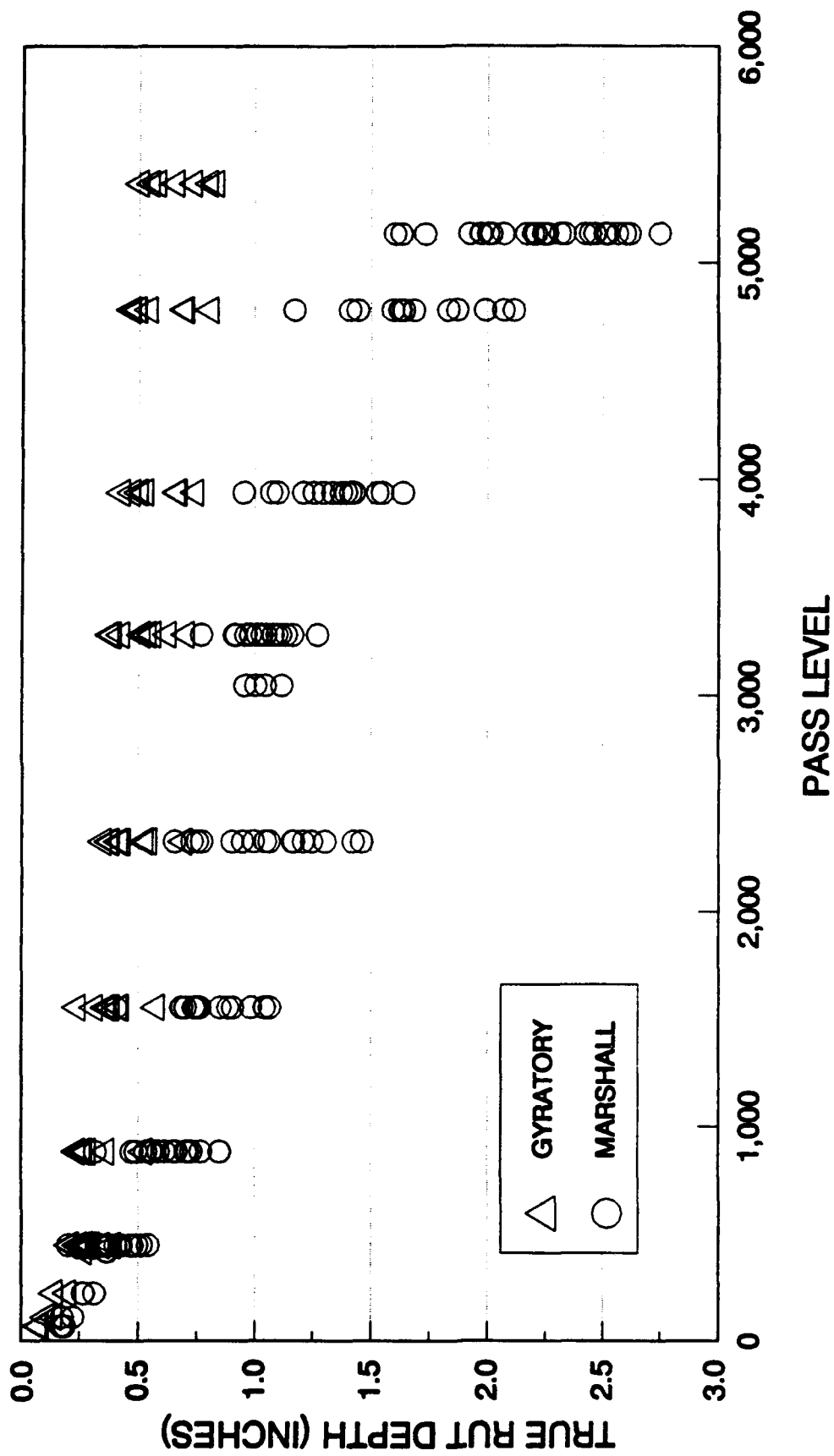


Figure 56. True Rut Depths from 6-Inch Flexible Sections.

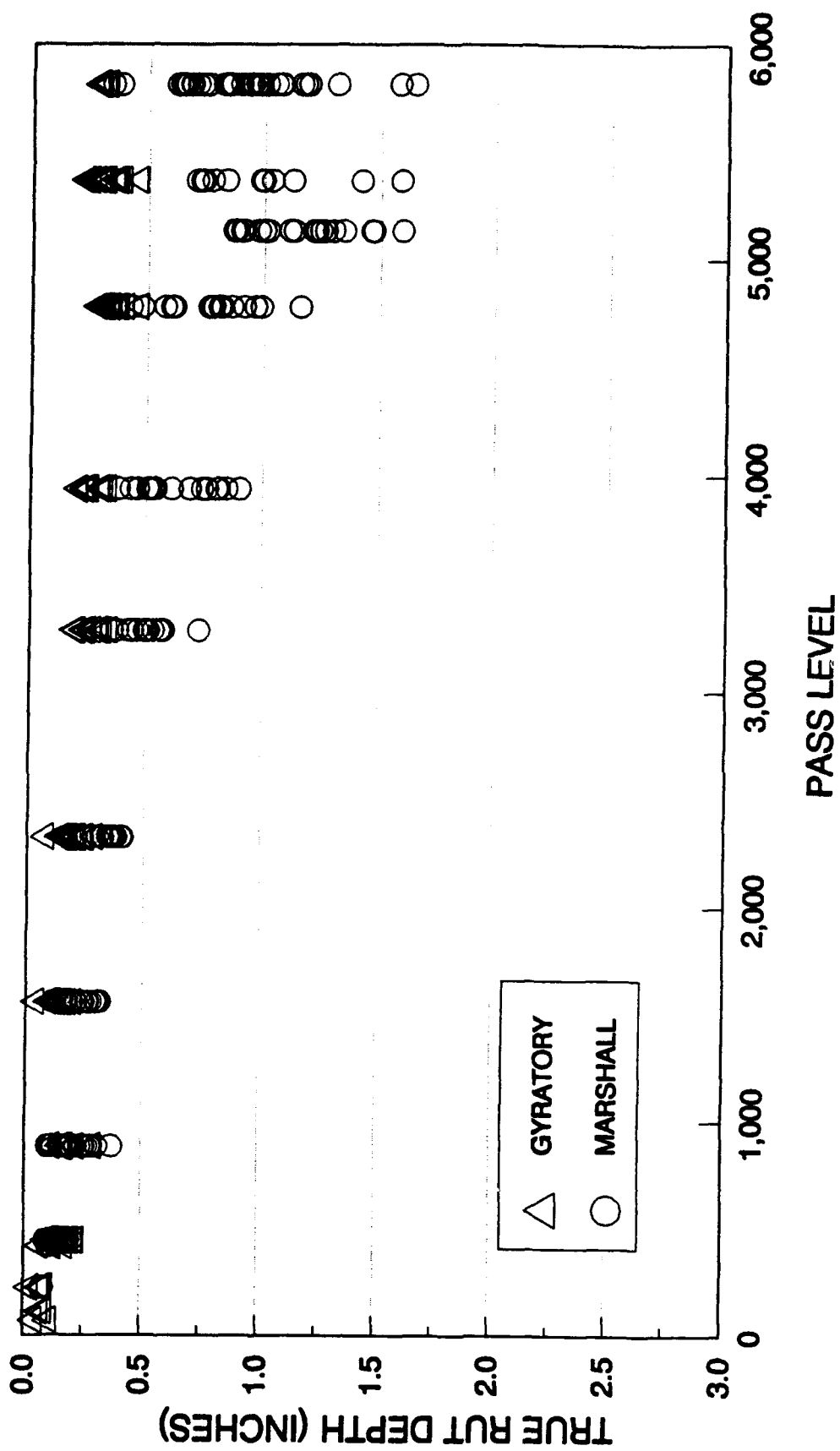


Figure 57. True Rut Depths from Composite Sections.

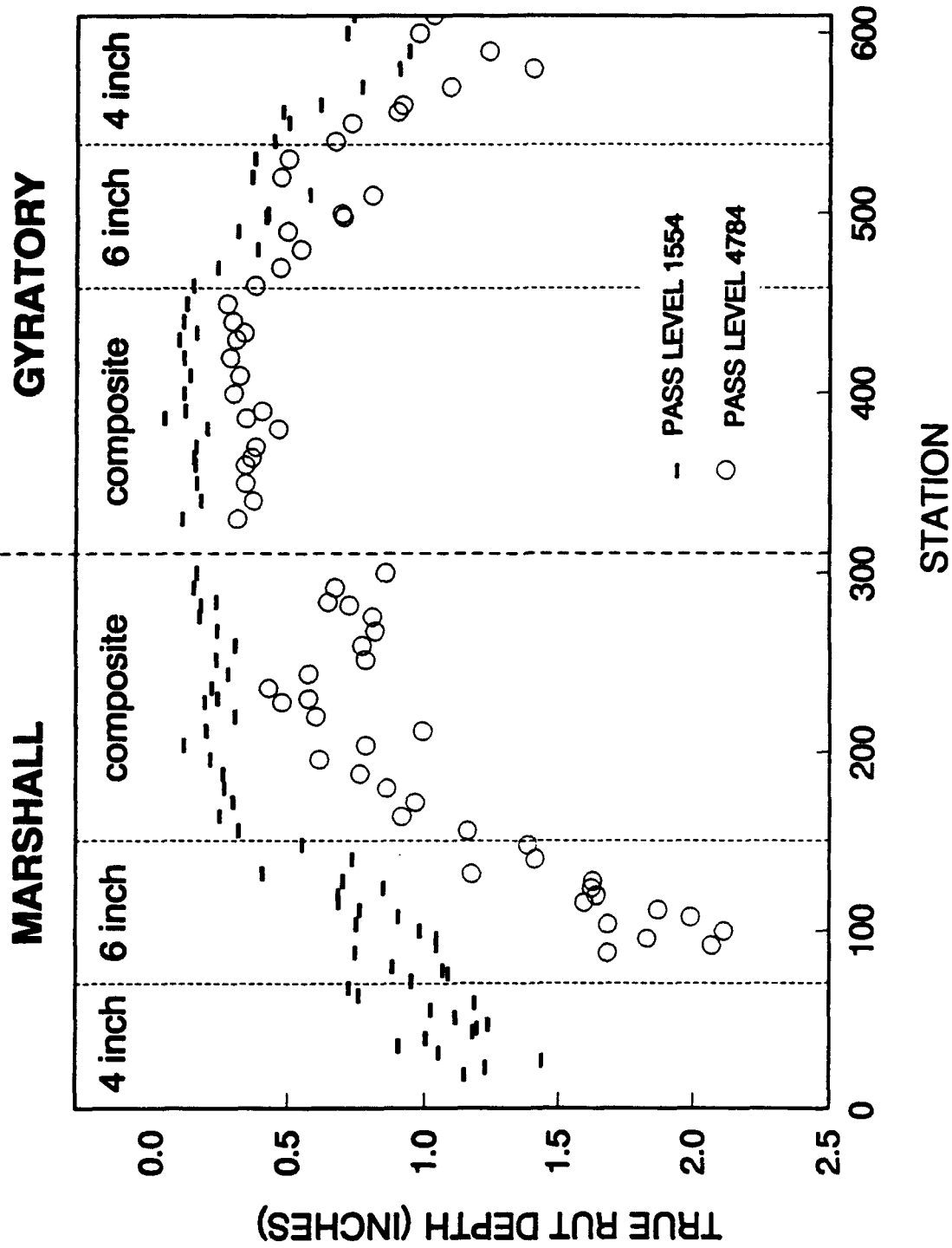


Figure 58. True Rut Depth Versus Station at Pass Level 1554 and 4784.

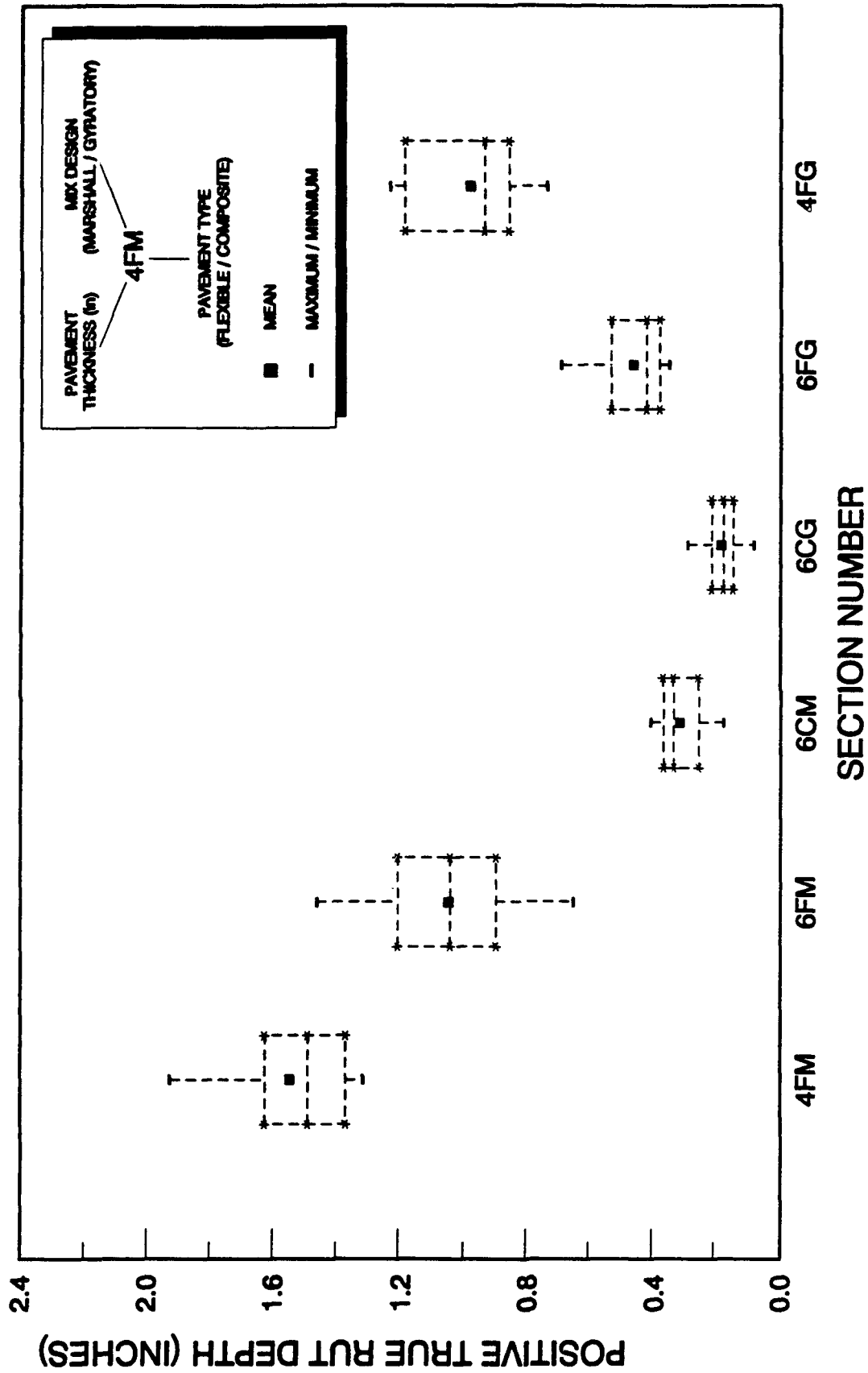


Figure 59. Boxplot of Rut Depth for Pass Level 2324.

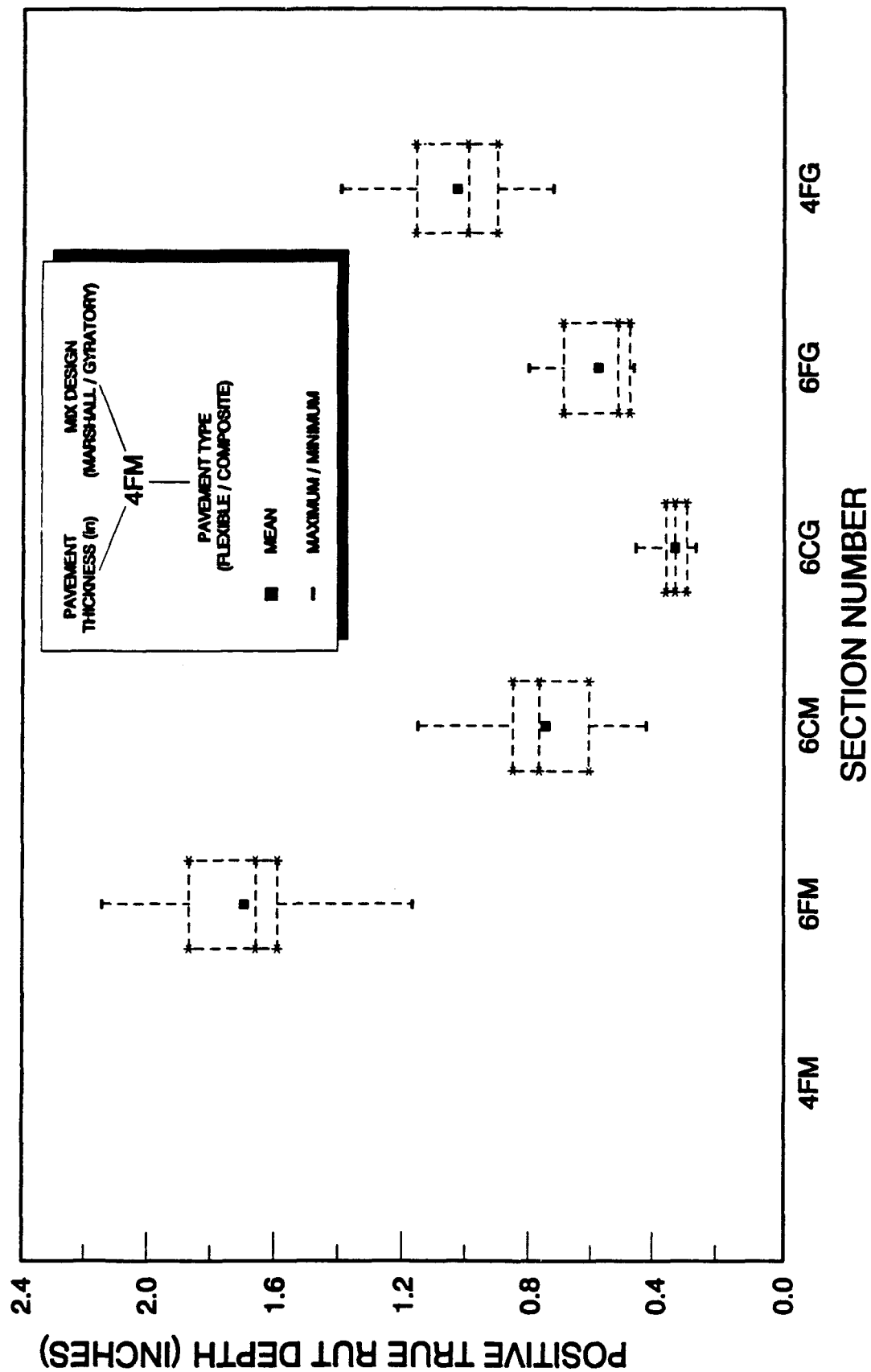


Figure 60. Boxplot of Rut Depth for Pass Level 4784.

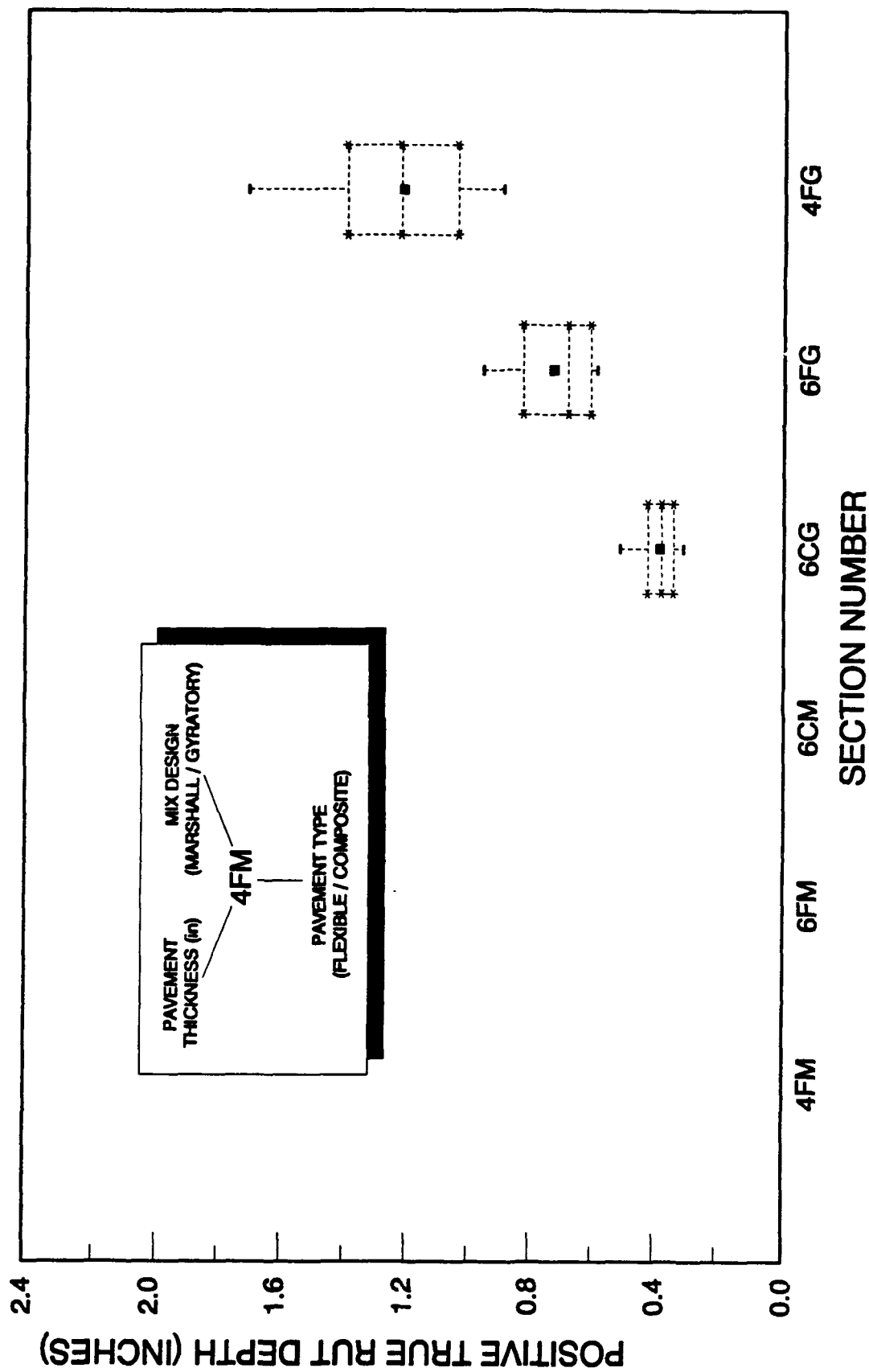


Figure 61. Boxplot of Rut Depth for Pass Level 9715.

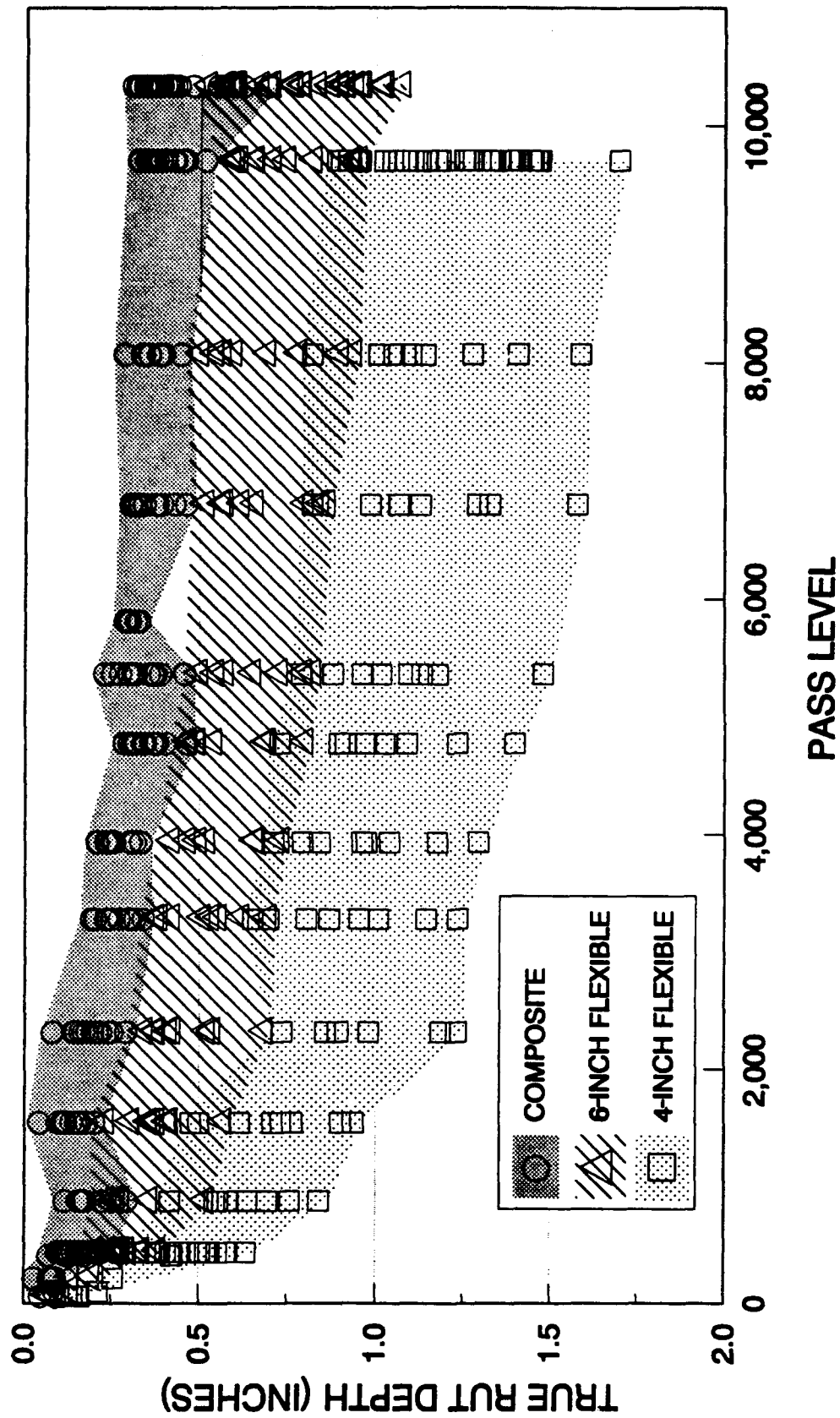


Figure 62. True Rut Depths from Gyratory Test Sections.

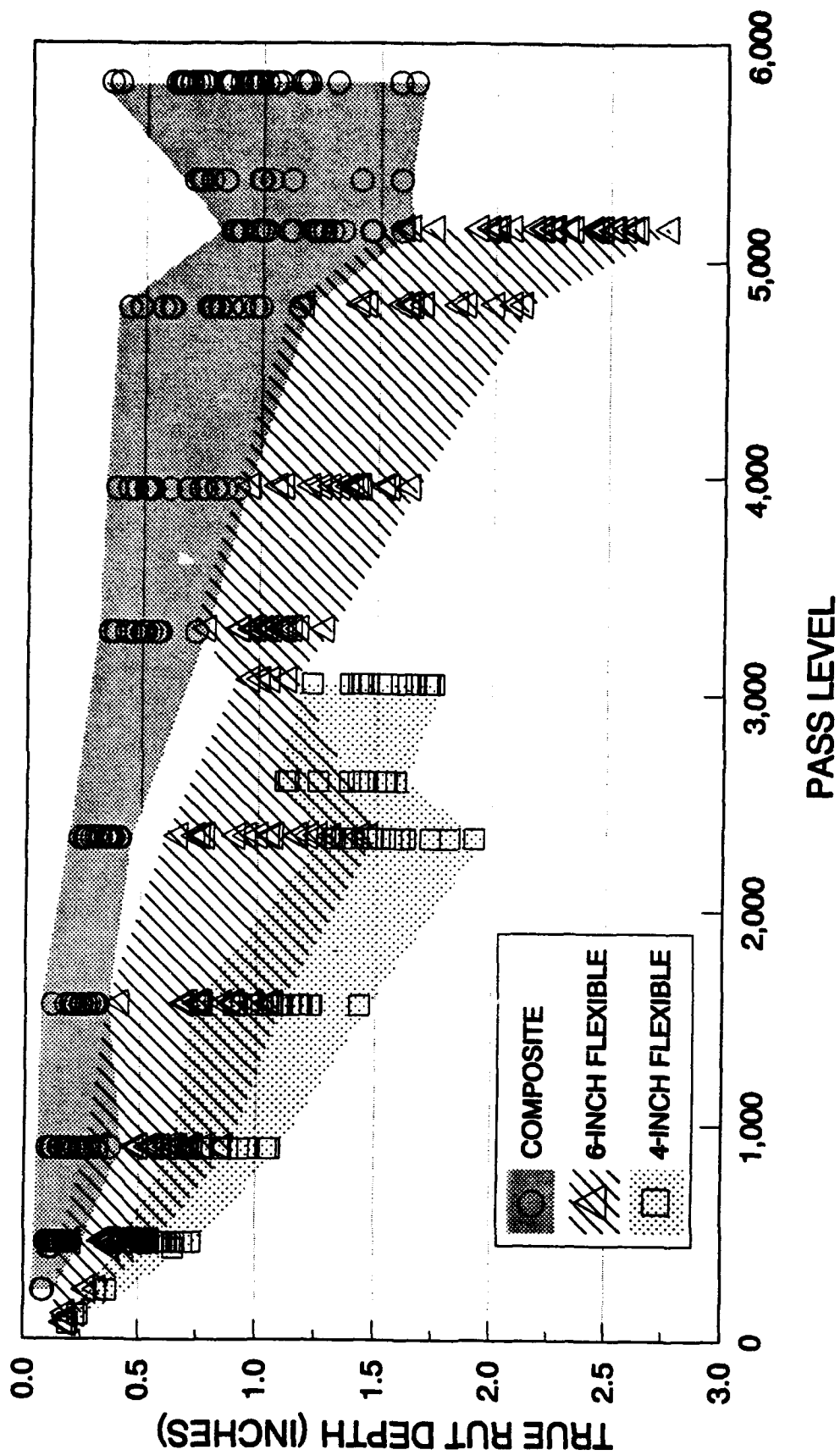


Figure 63. True Rut Depths from Marshall Test Sections.

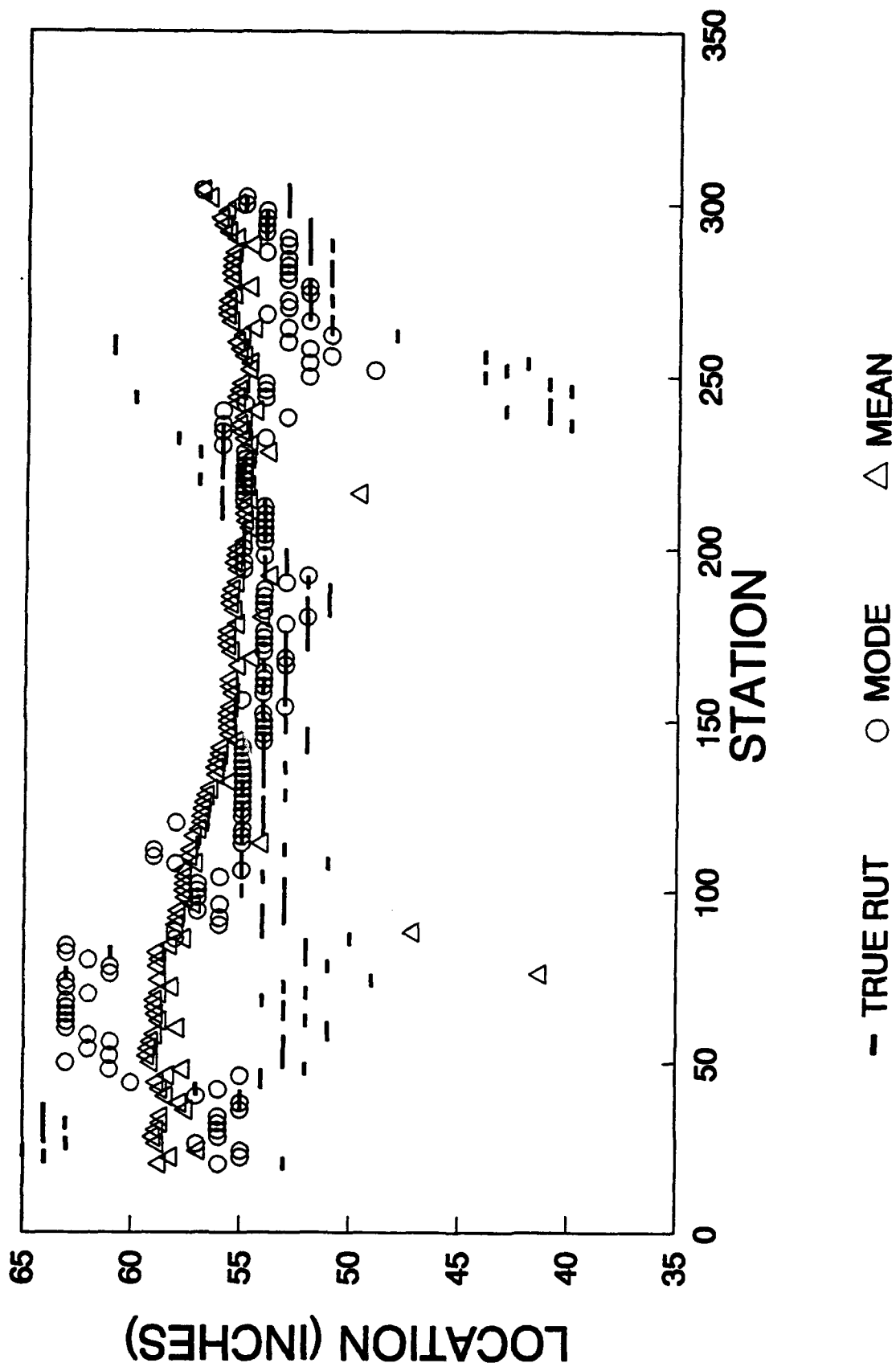


Figure 64. Relationship Between True Rut Location and the Mode and Mean for Marshall Sections.

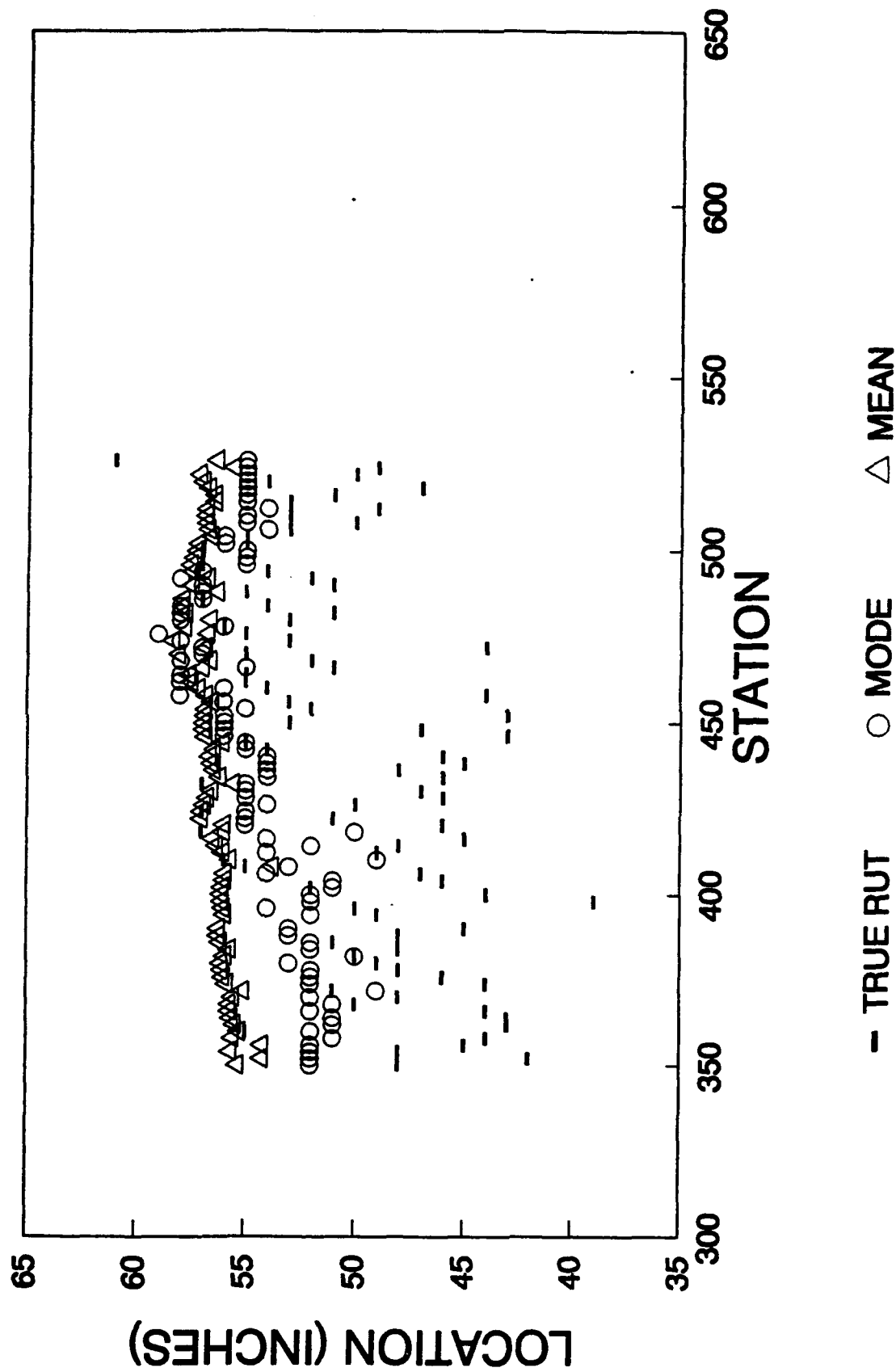


Figure 65. Relationship Between True Rut Location and the Mode and Mean for Gyratory Sections.

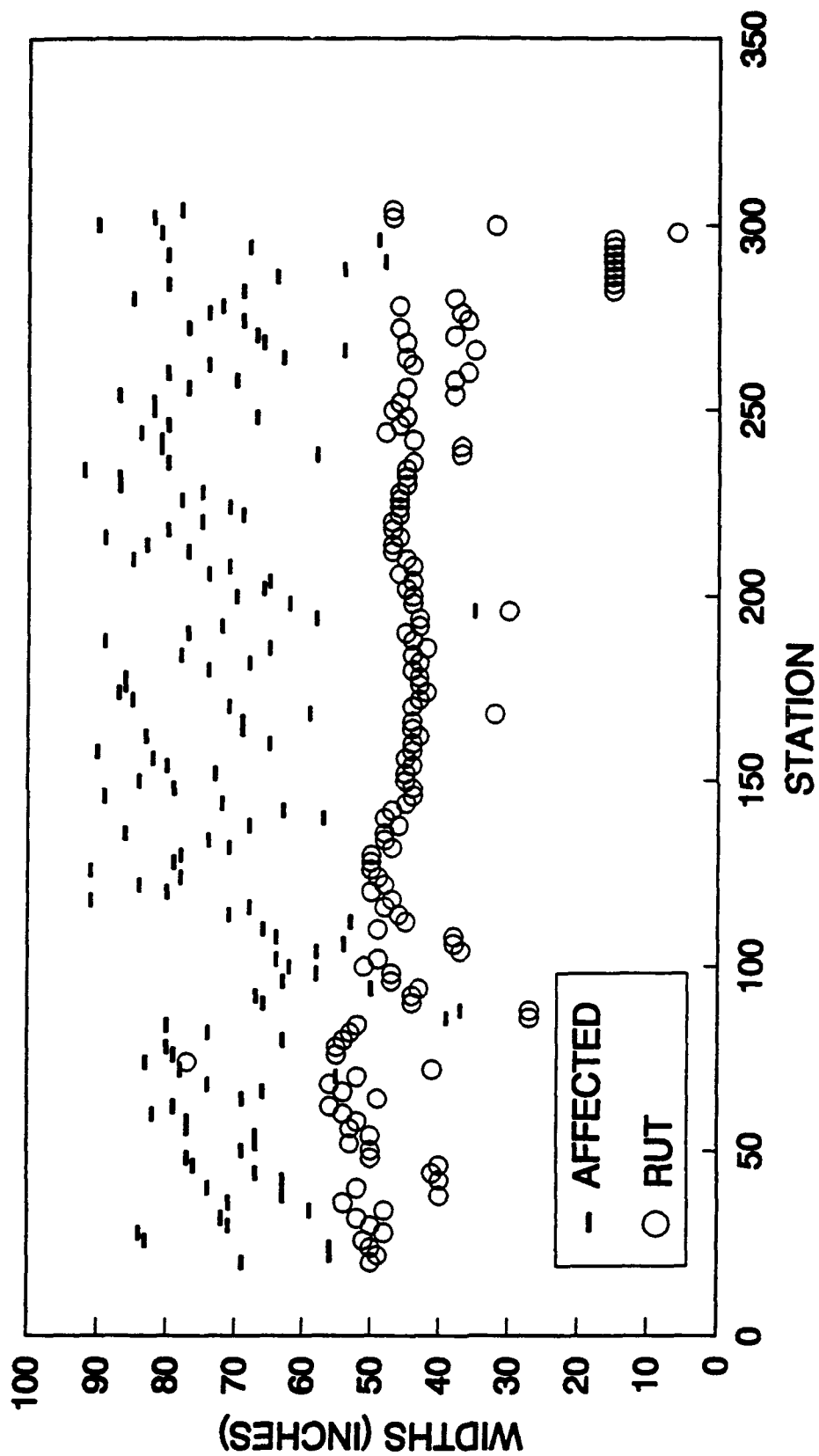


Figure 66. Affected and Rut Widths from the Marshall Test Sections.

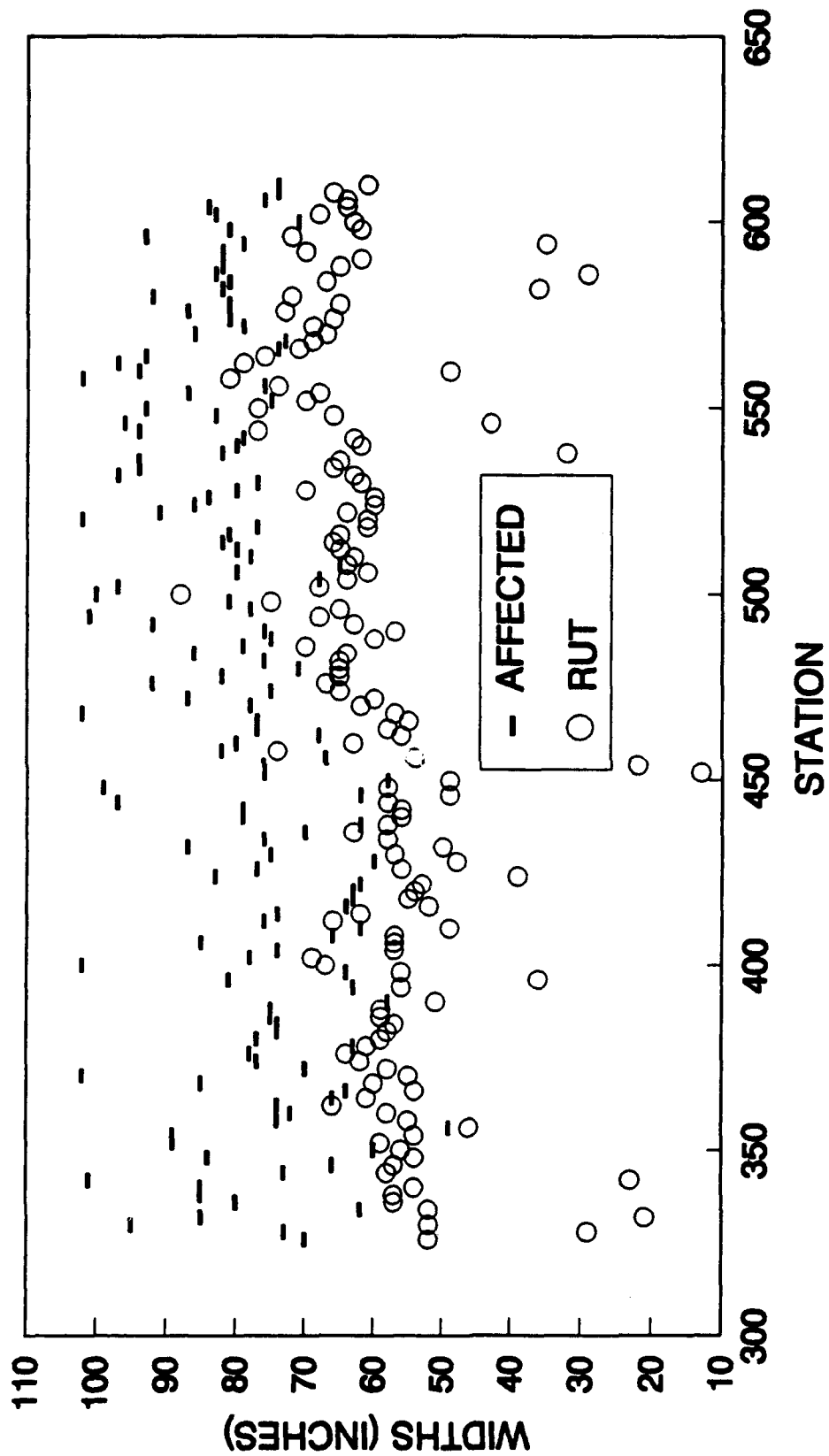


Figure 67. Affected and Rut Widths from the Gyration Test Sections.

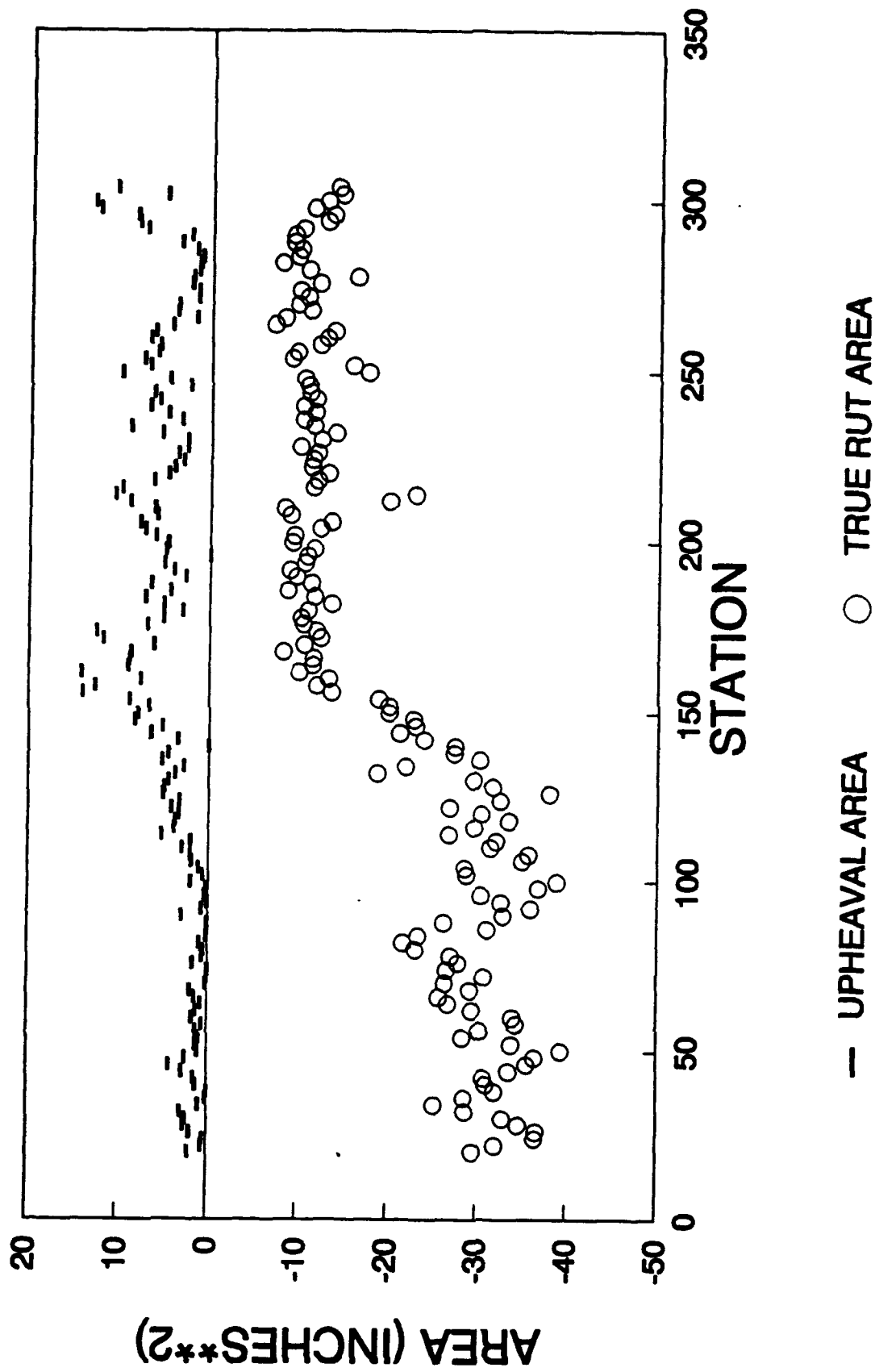


Figure 68. Areas Calculated for the Marshall Sections at Final Pass Level.

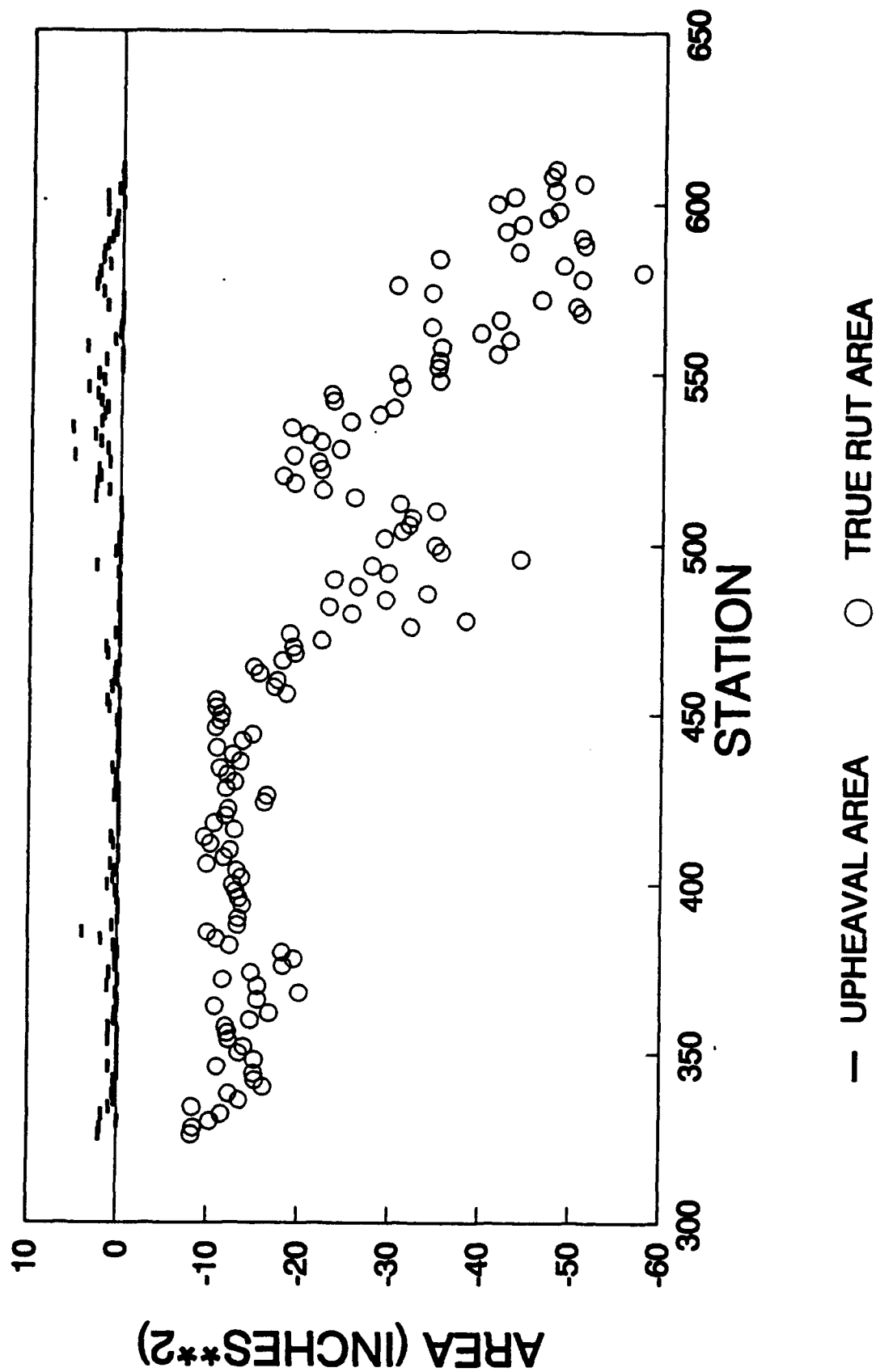


Figure 69. Areas Calculated for the Gyratory Sections at Final Pass Level.

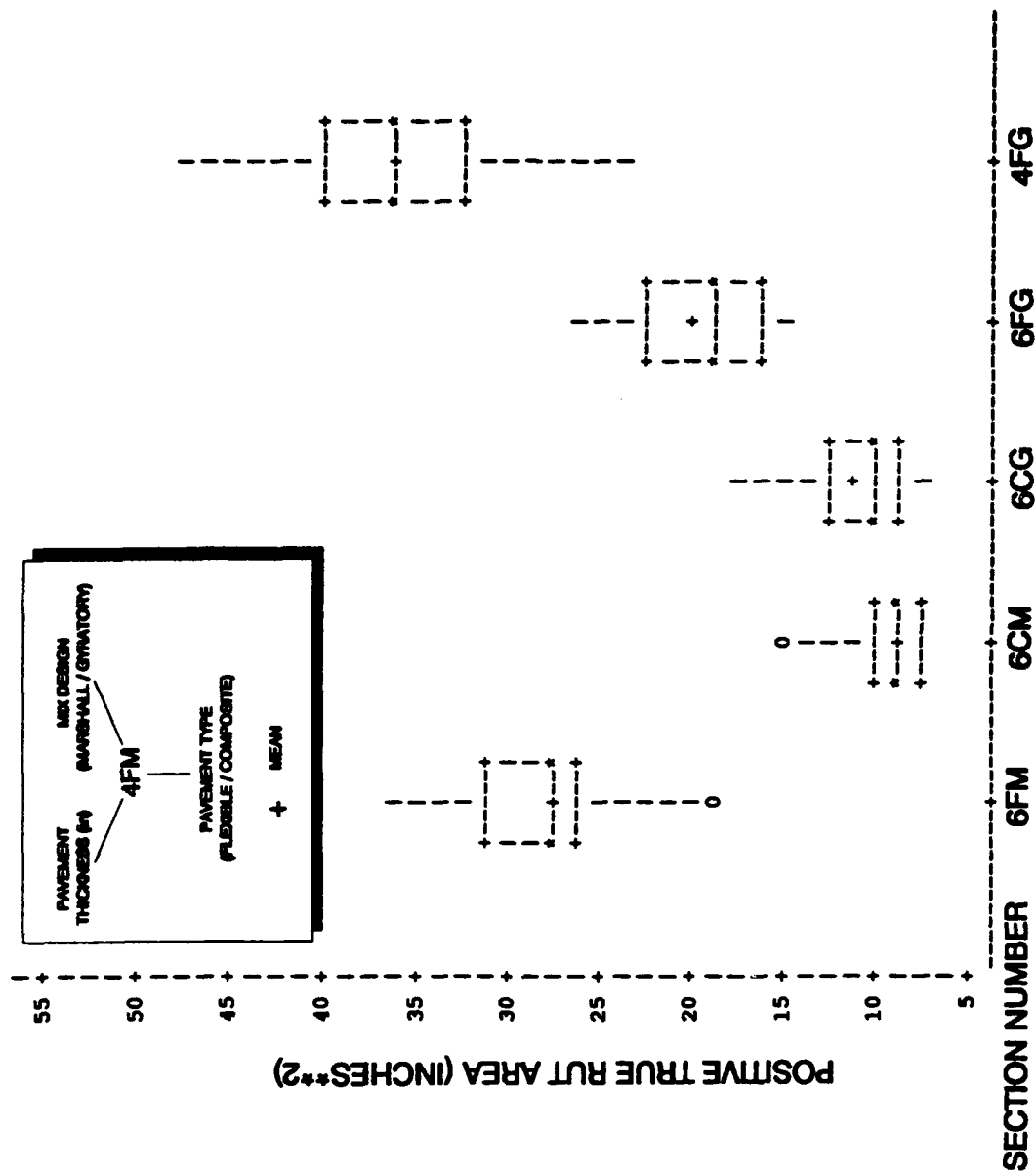


Figure 70. Boxplot Comparison of Rut Area From Each Test Section at Traffic Level 4784.

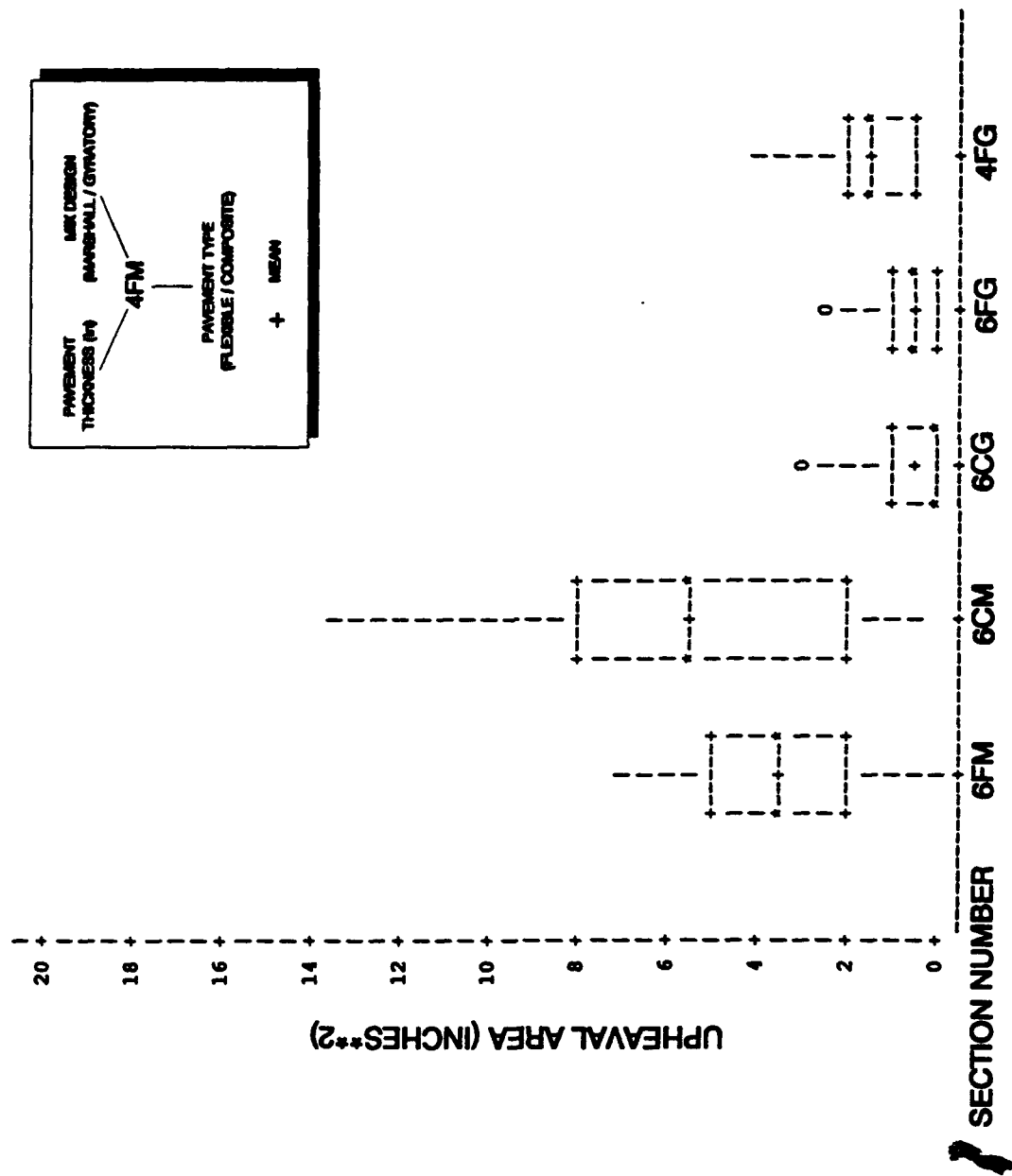


Figure 71. Boxplot Comparison of Upheave Area From Each Test Section at Traffic Level 4784.

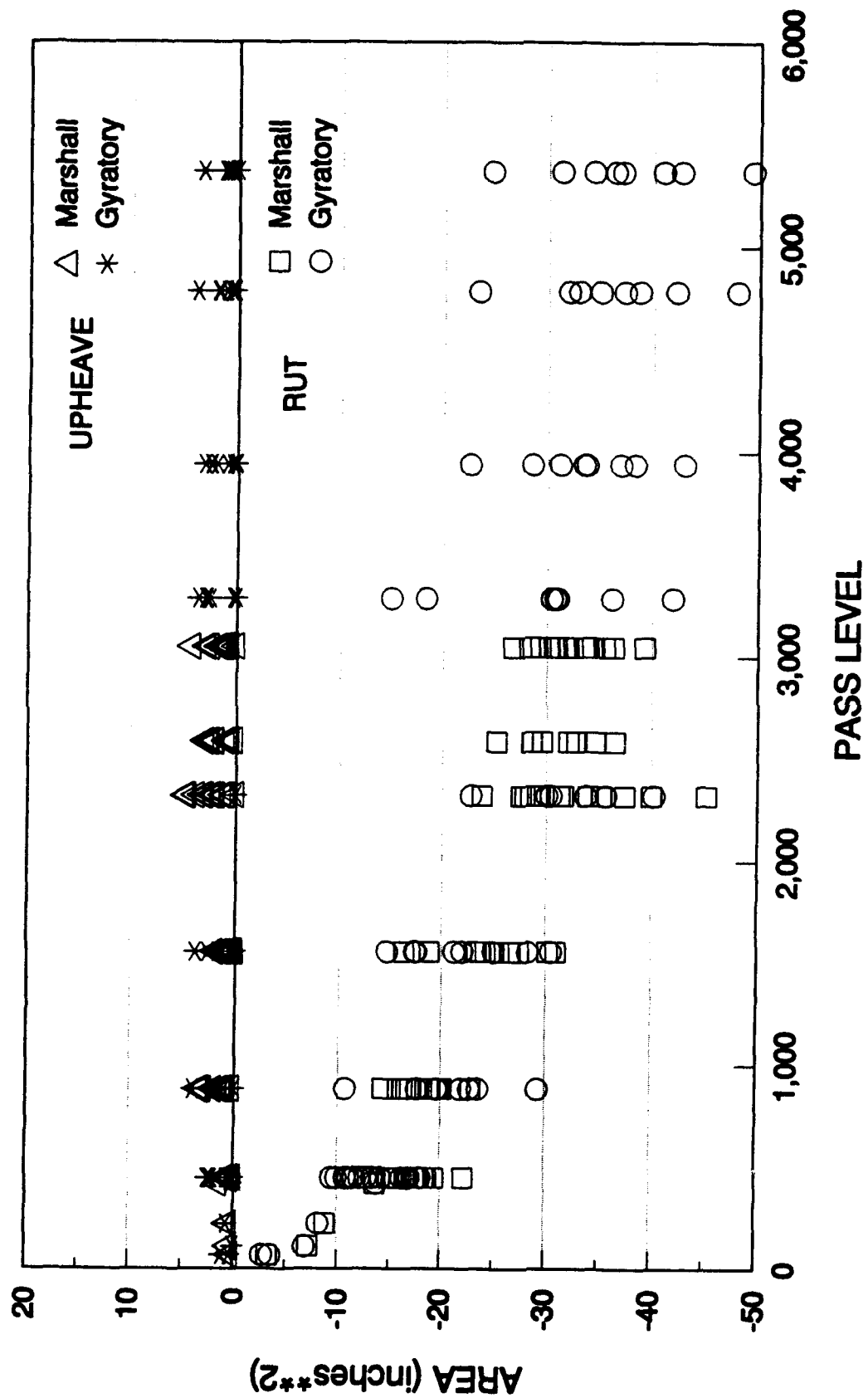


Figure 72. Rut and Upheave Areas For the 4-Inch Flexible Test Sections.

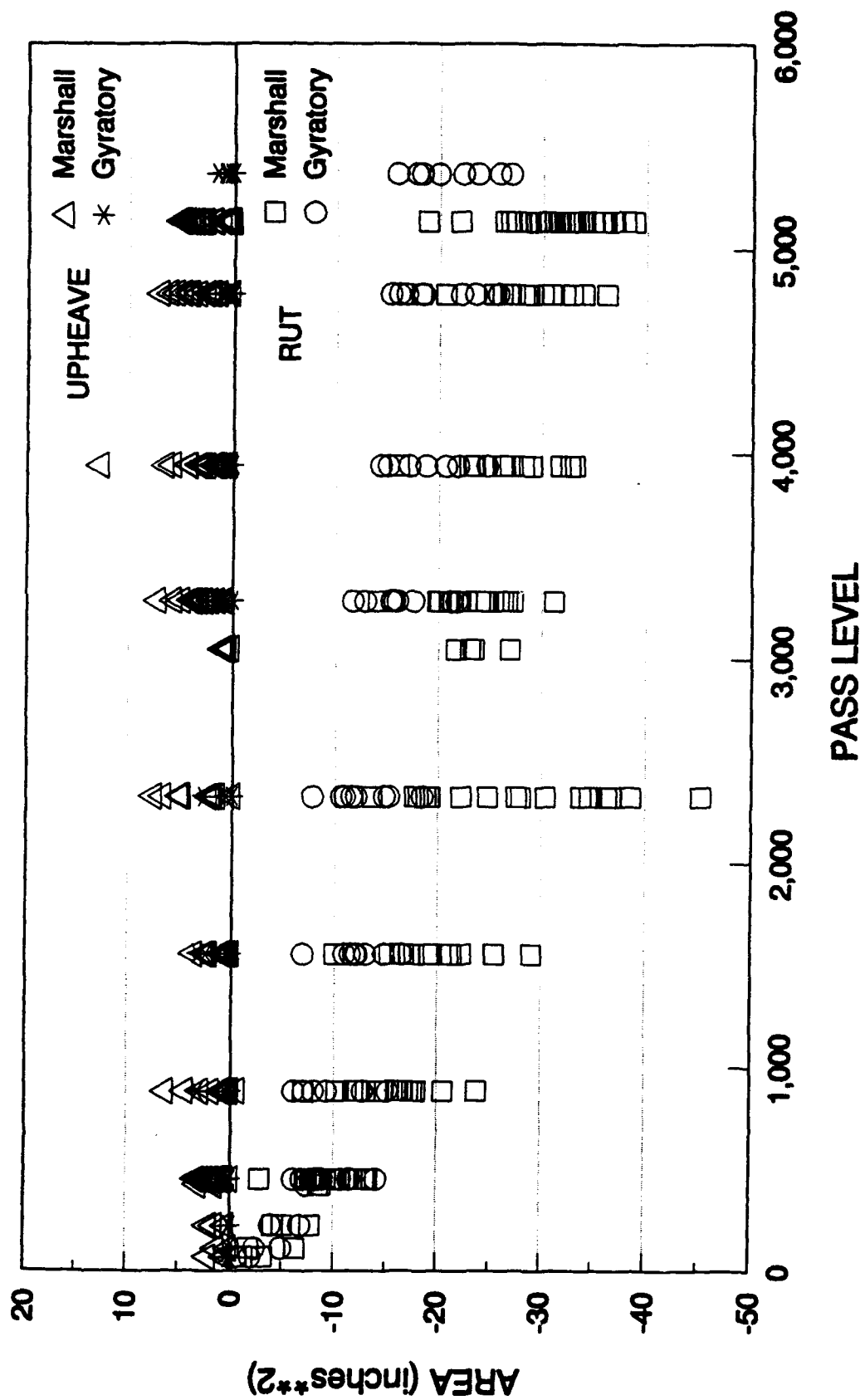


Figure 73. Rut and Upheave Areas For the 6-Inch Flexible Test Sections.

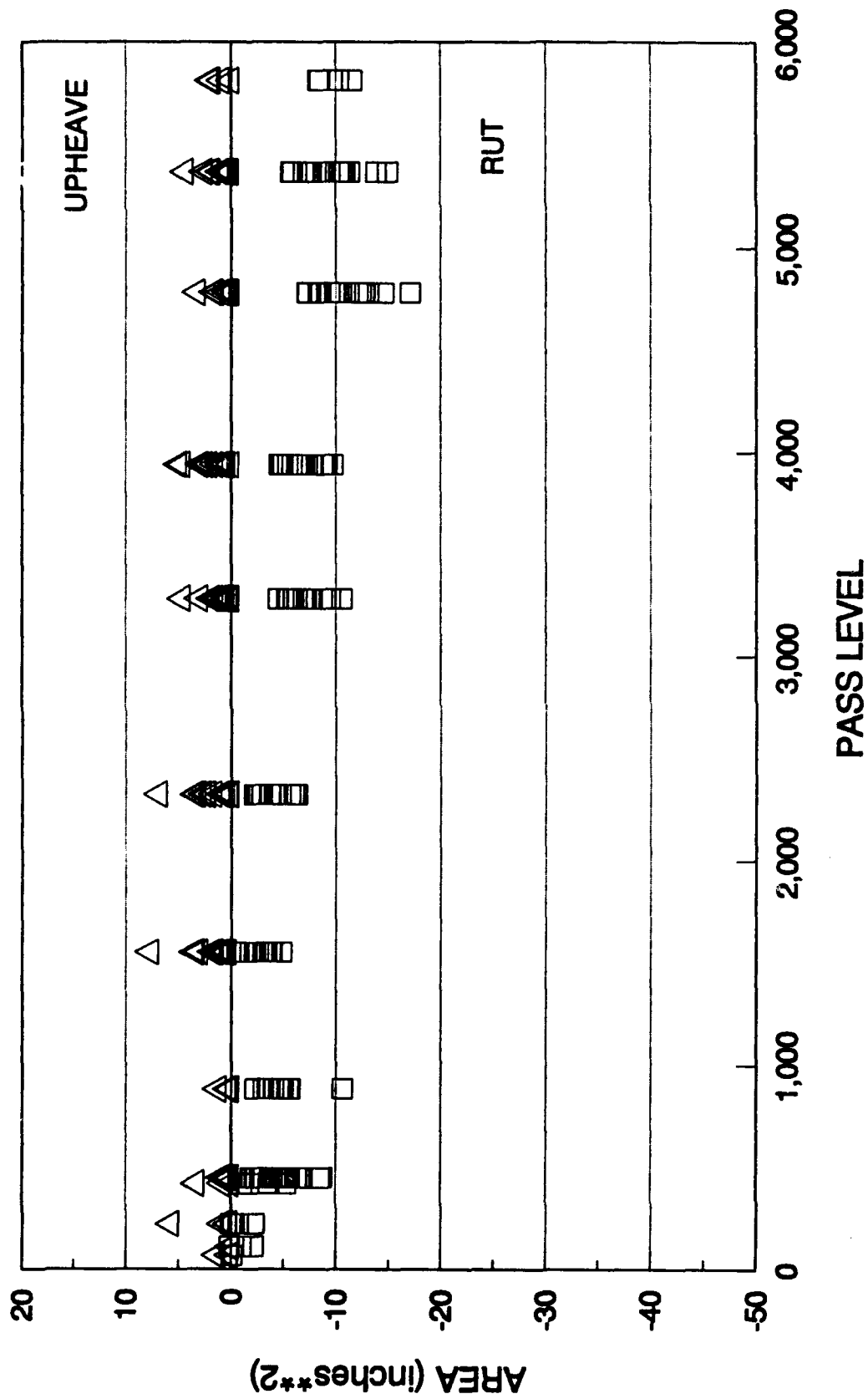


Figure 74. Rut and Upheave Areas For the Gyratory Composite Test Sections.

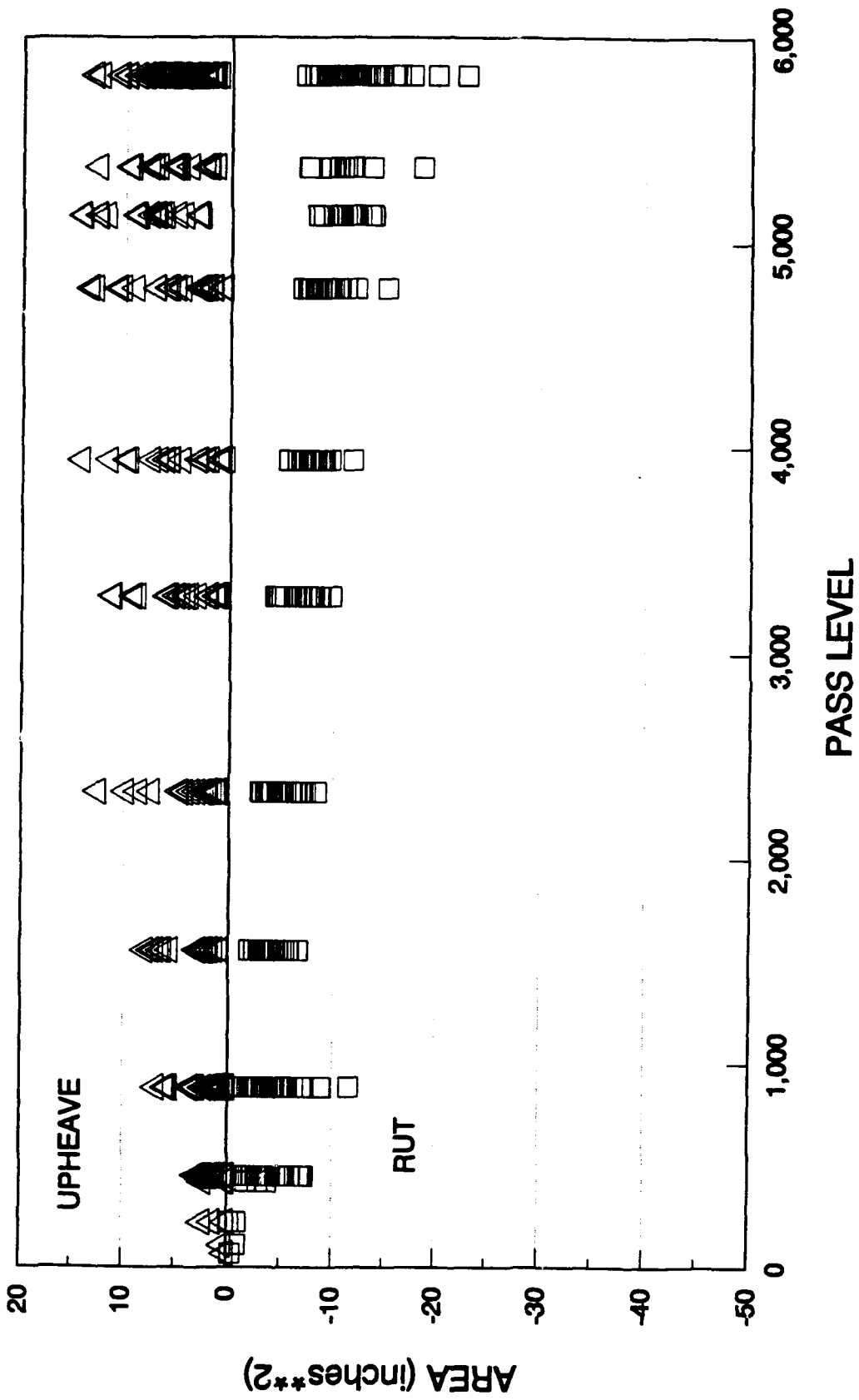


Figure 75. Rut and Upheave Areas For the Marshall Composite Test Sections.

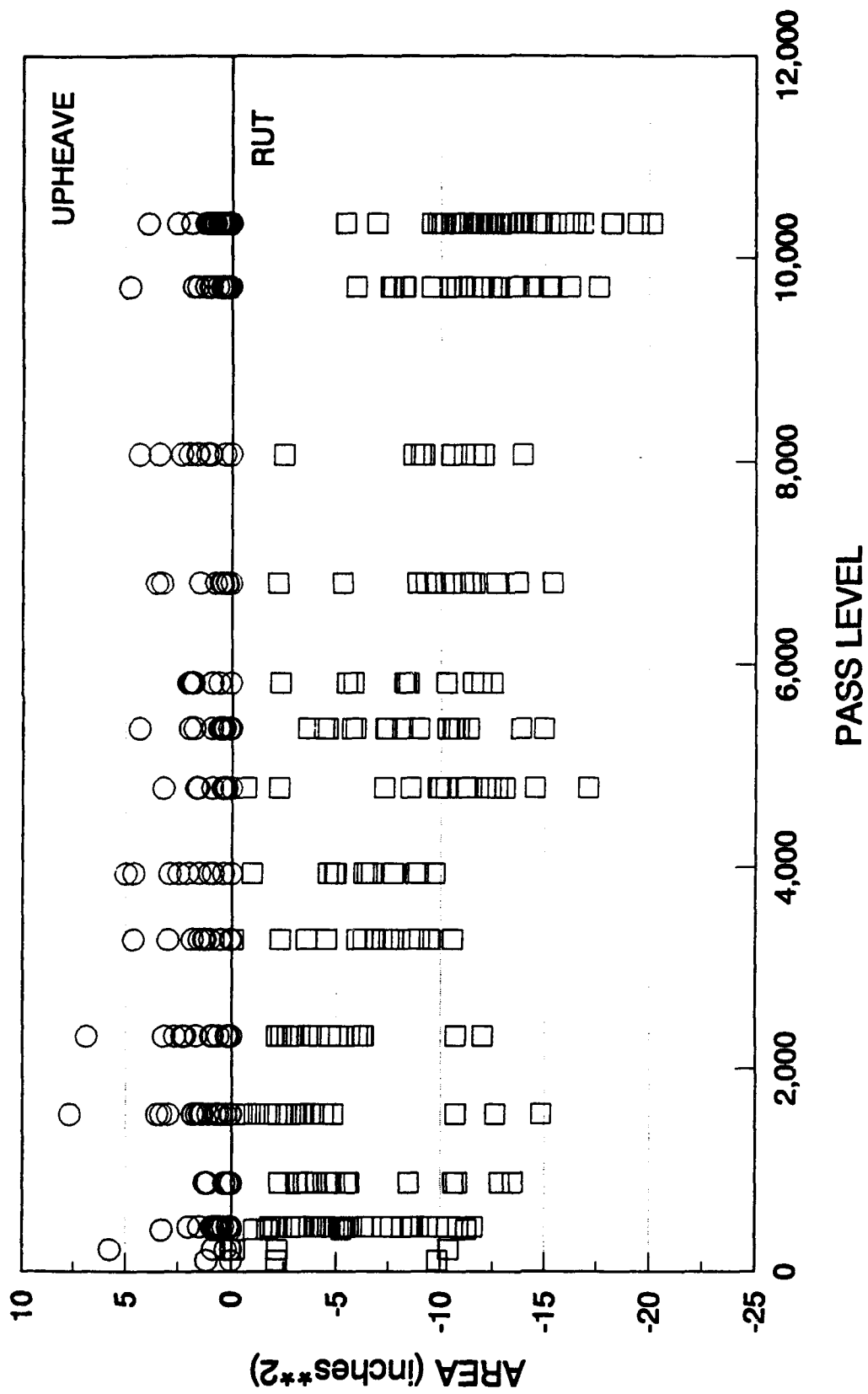


Figure 76. Rut and Upheave Areas for the Gyratory Composite Test Section Through Pass Level 10350.

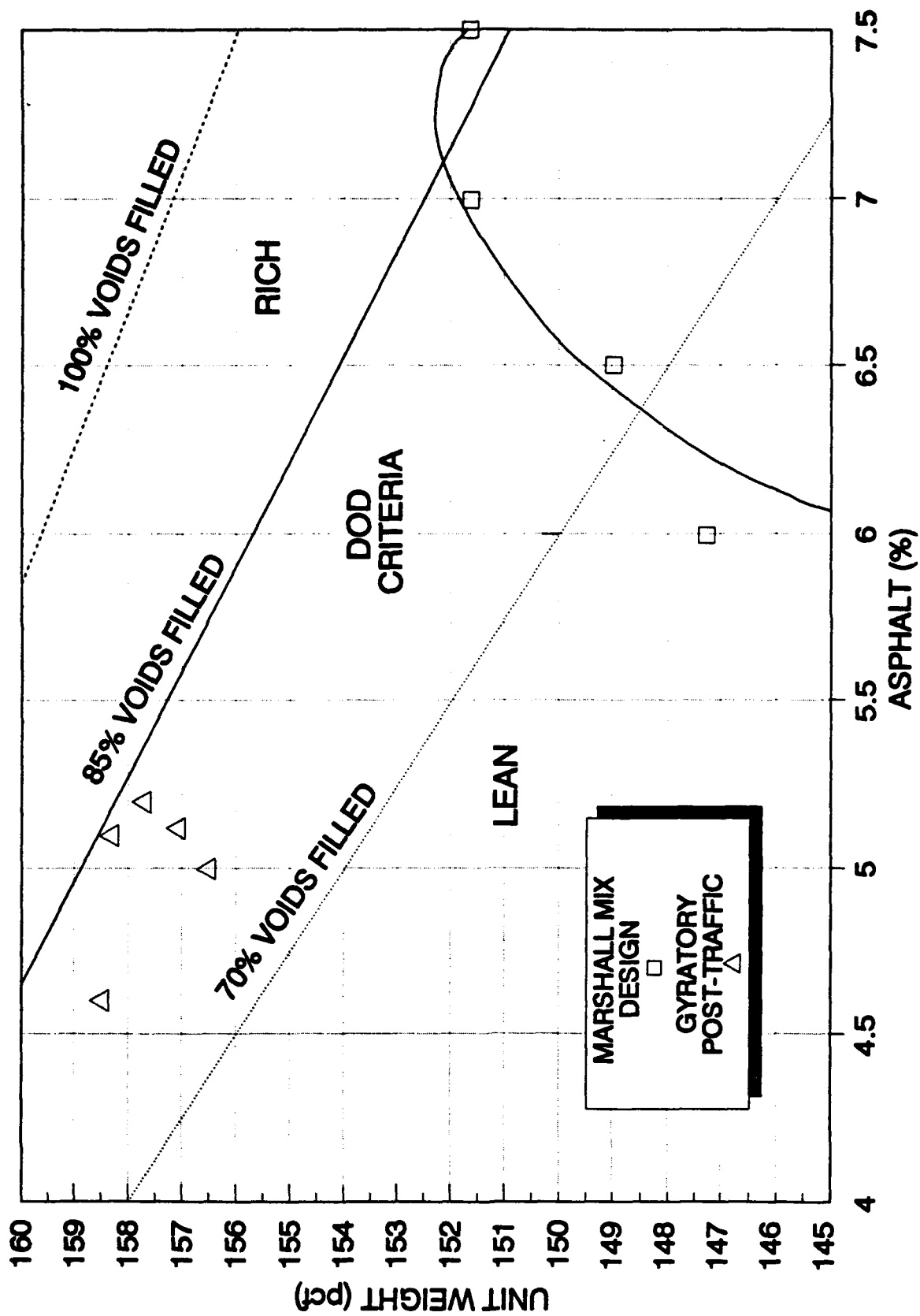


Figure 77. Effects of Compactive Effort on Asphalt Content.

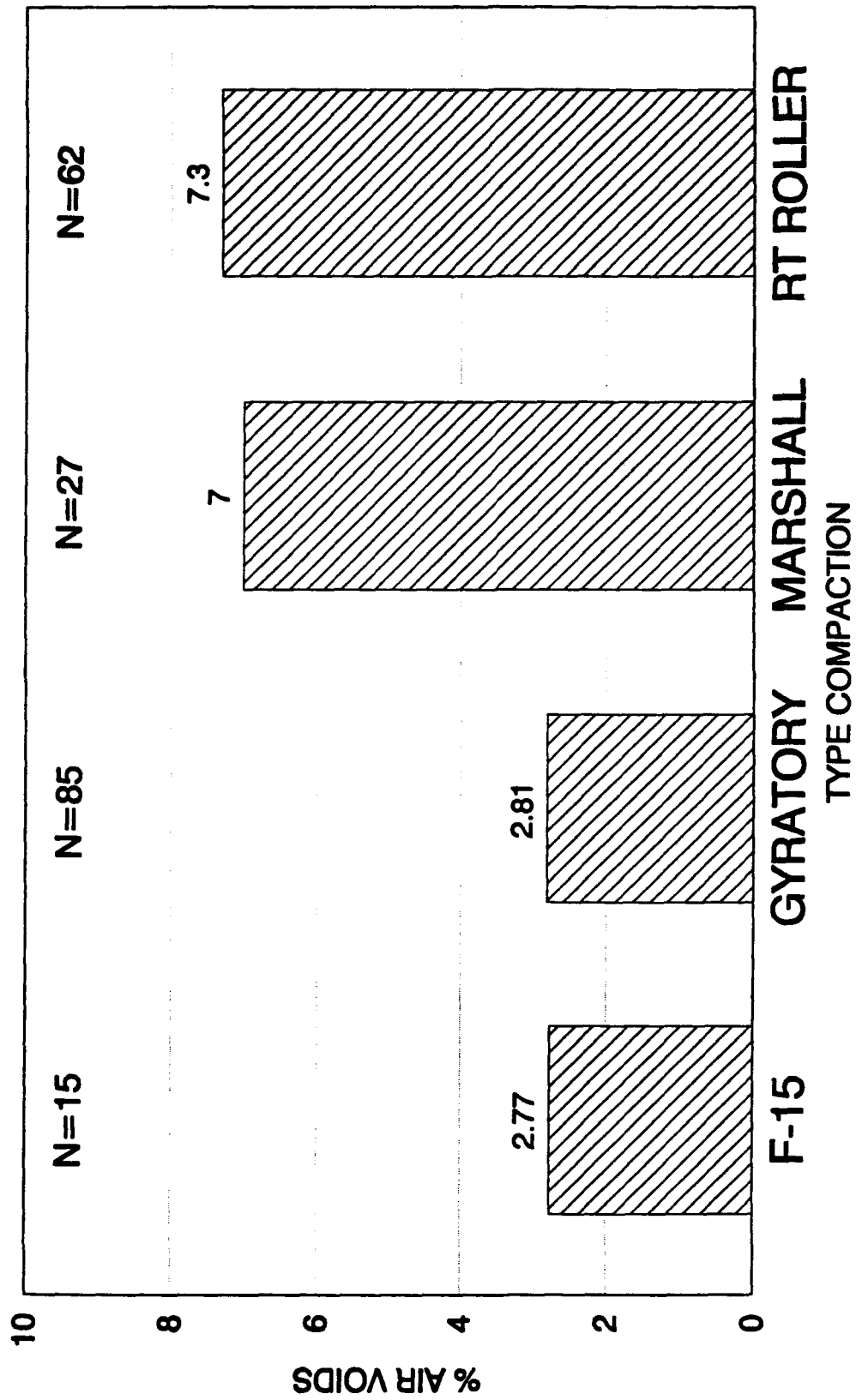


Figure 78. Effectiveness of Four Levels of Compaction on Gyratory Mix from Paver.

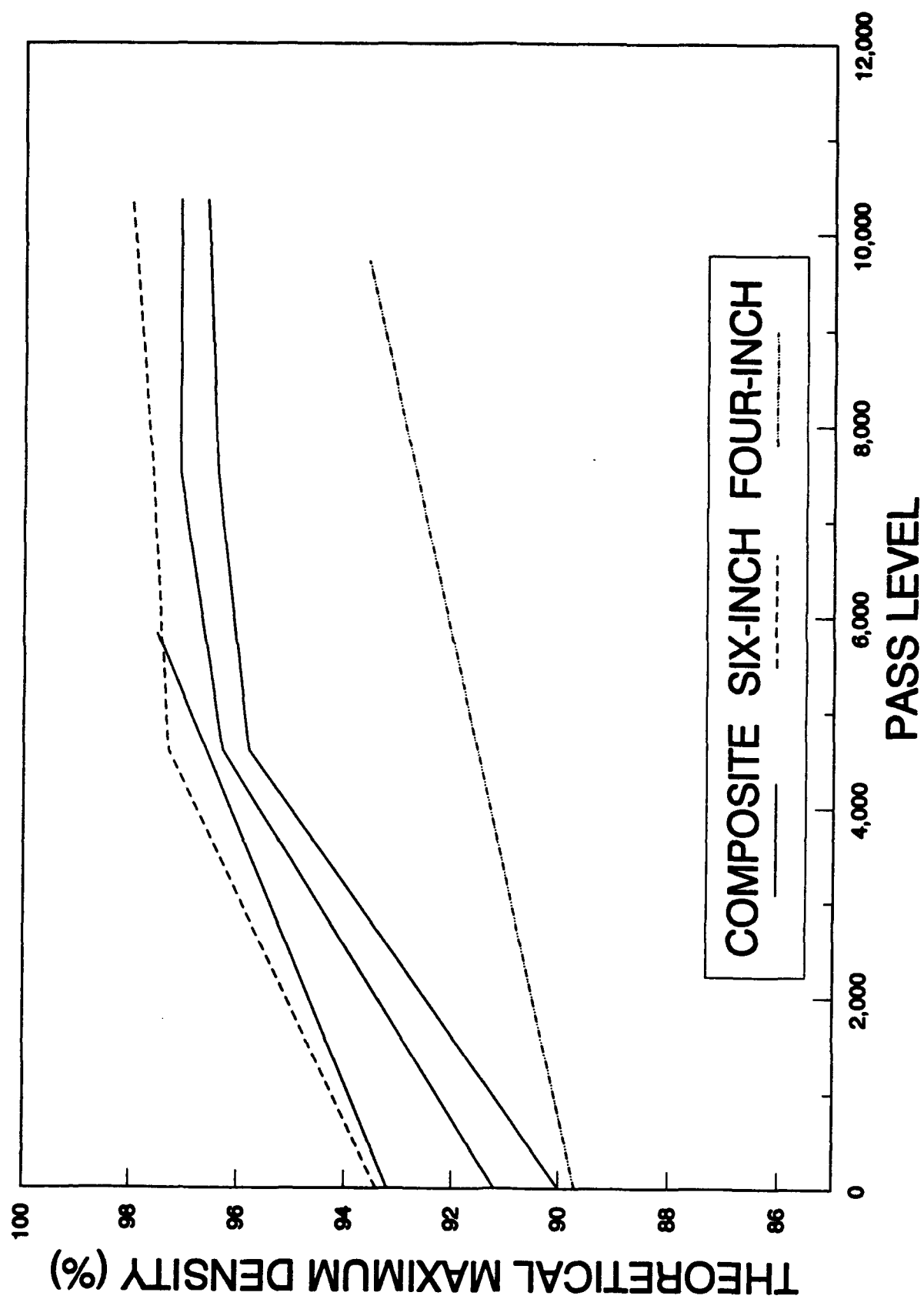


Figure 79. Density Change With Traffic, Gyrotray Test Sections.

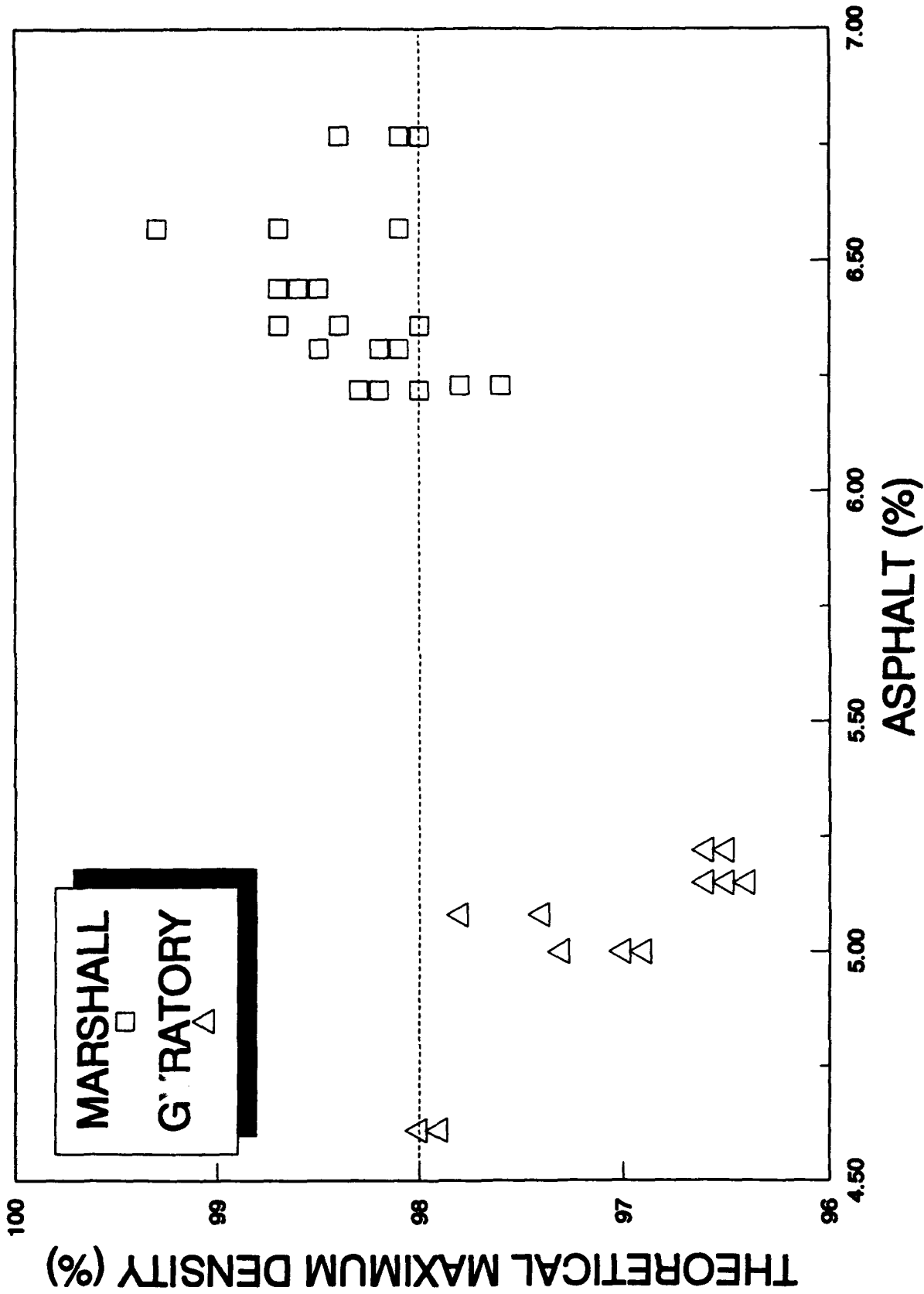


Figure 80. Post-Traffic Densities, Composite Test Sections.

1030 DATA POINTS

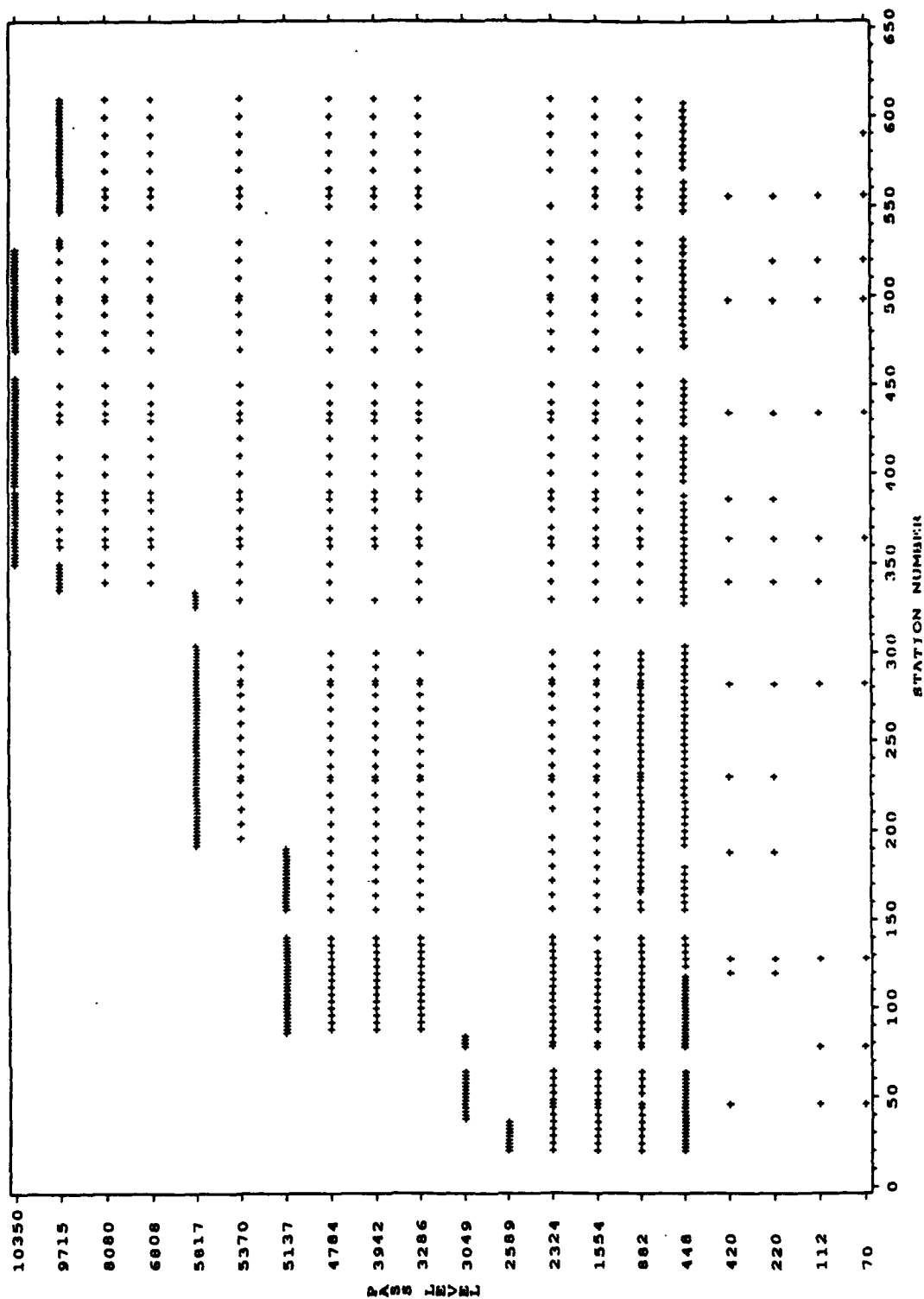


Figure 81. Matrix of Data Points Available for Analysis.

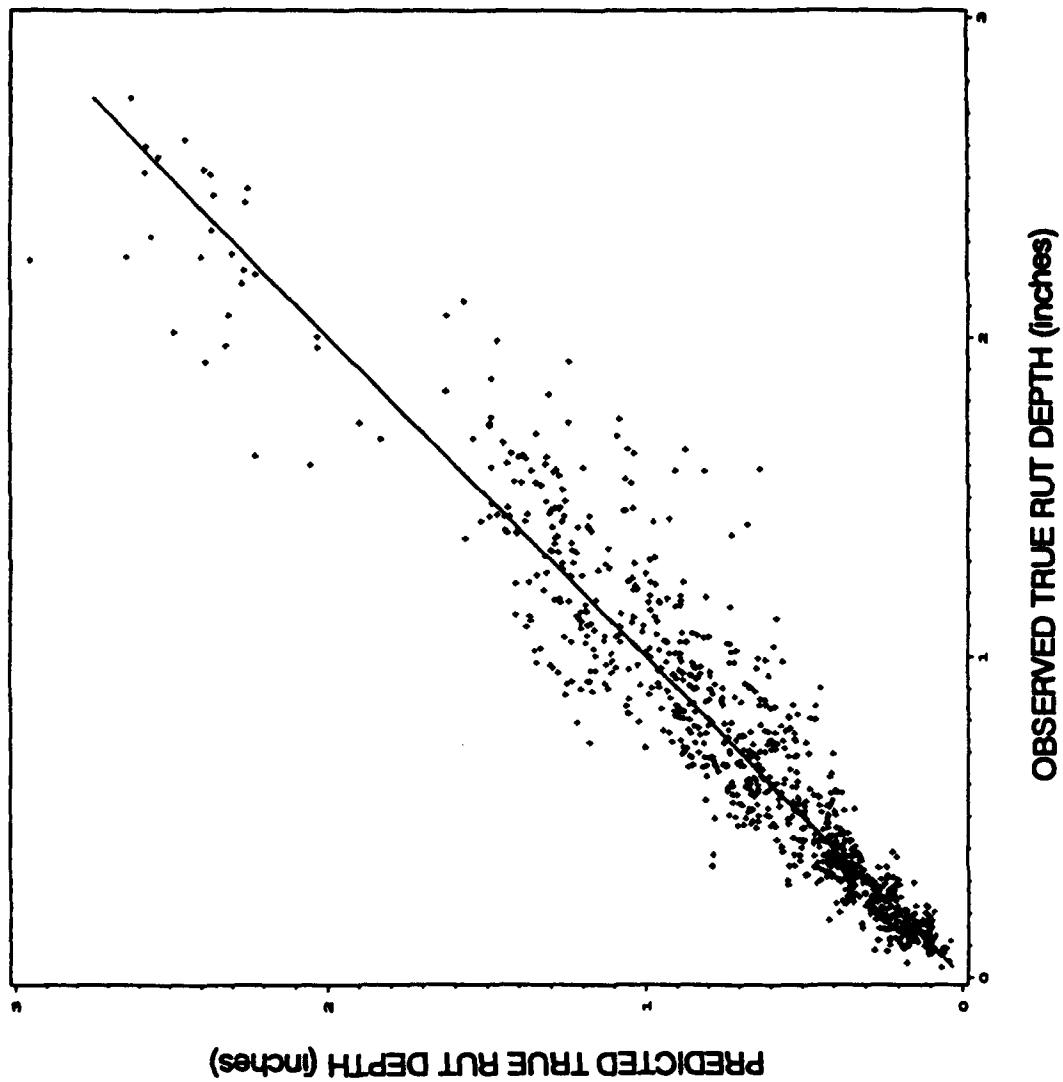


Figure 82. ANOVA Generated Predictions of Rut Depth Versus Observed Damage.

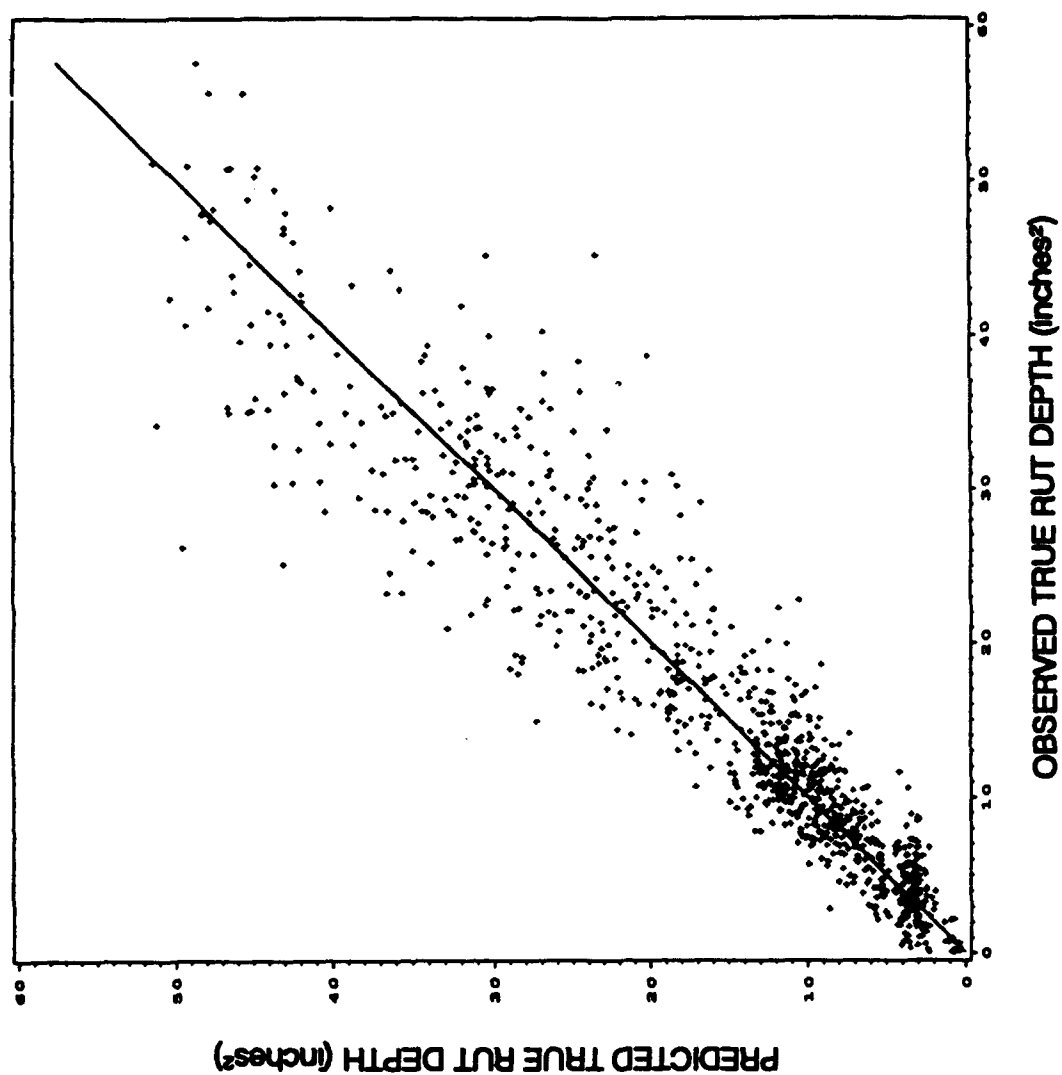


Figure 83. ANOVA Generated Predictions of Rut Area Versus Observed Damage.

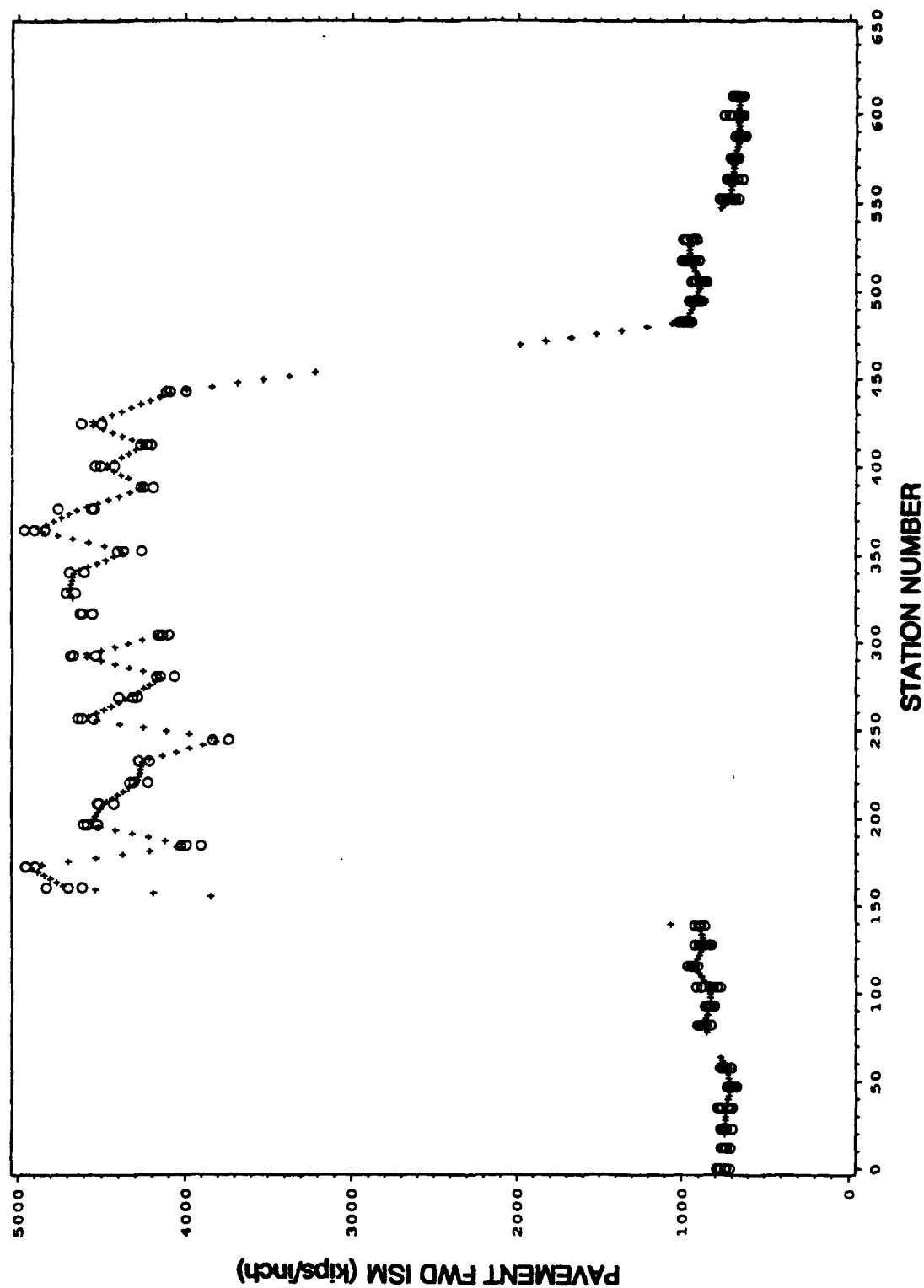


Figure 84. Pavement Impulse Stiffness Modulus Versus Station.

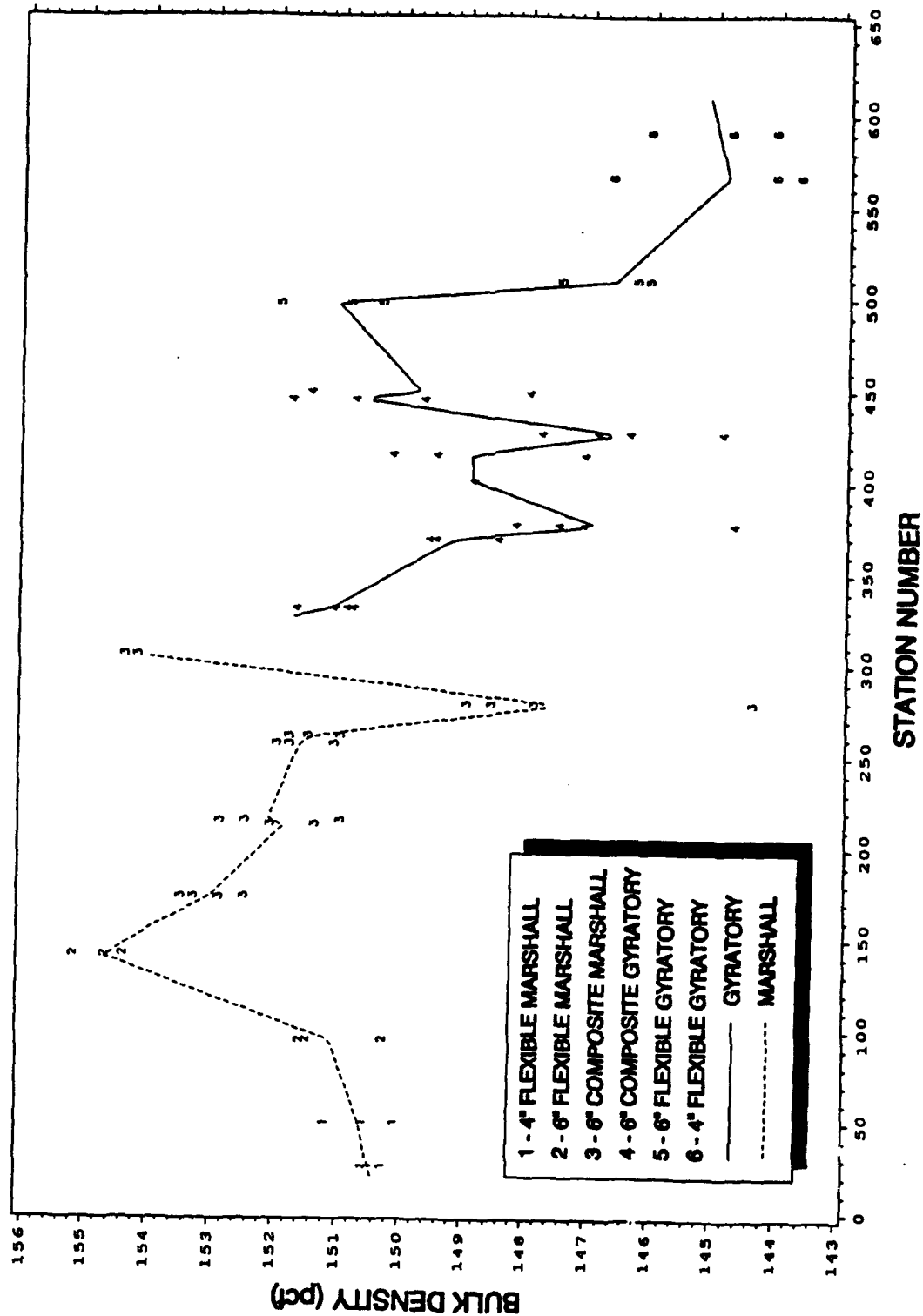


Figure 85. Initial Bulk Density Data and Interpolated Values Versus Station.

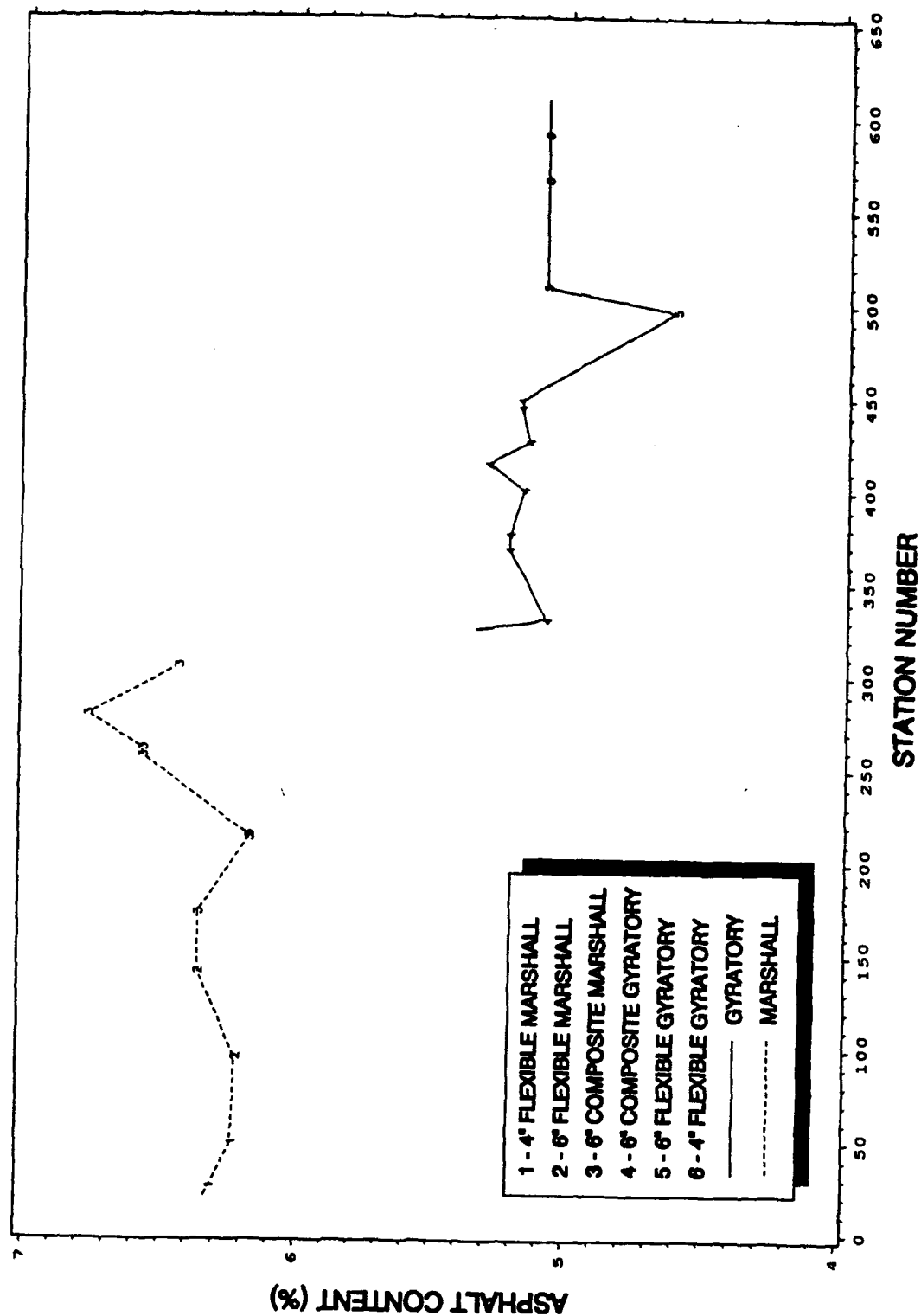


Figure 86. Asphalt Content Data and Interpolated Values Versus Station.

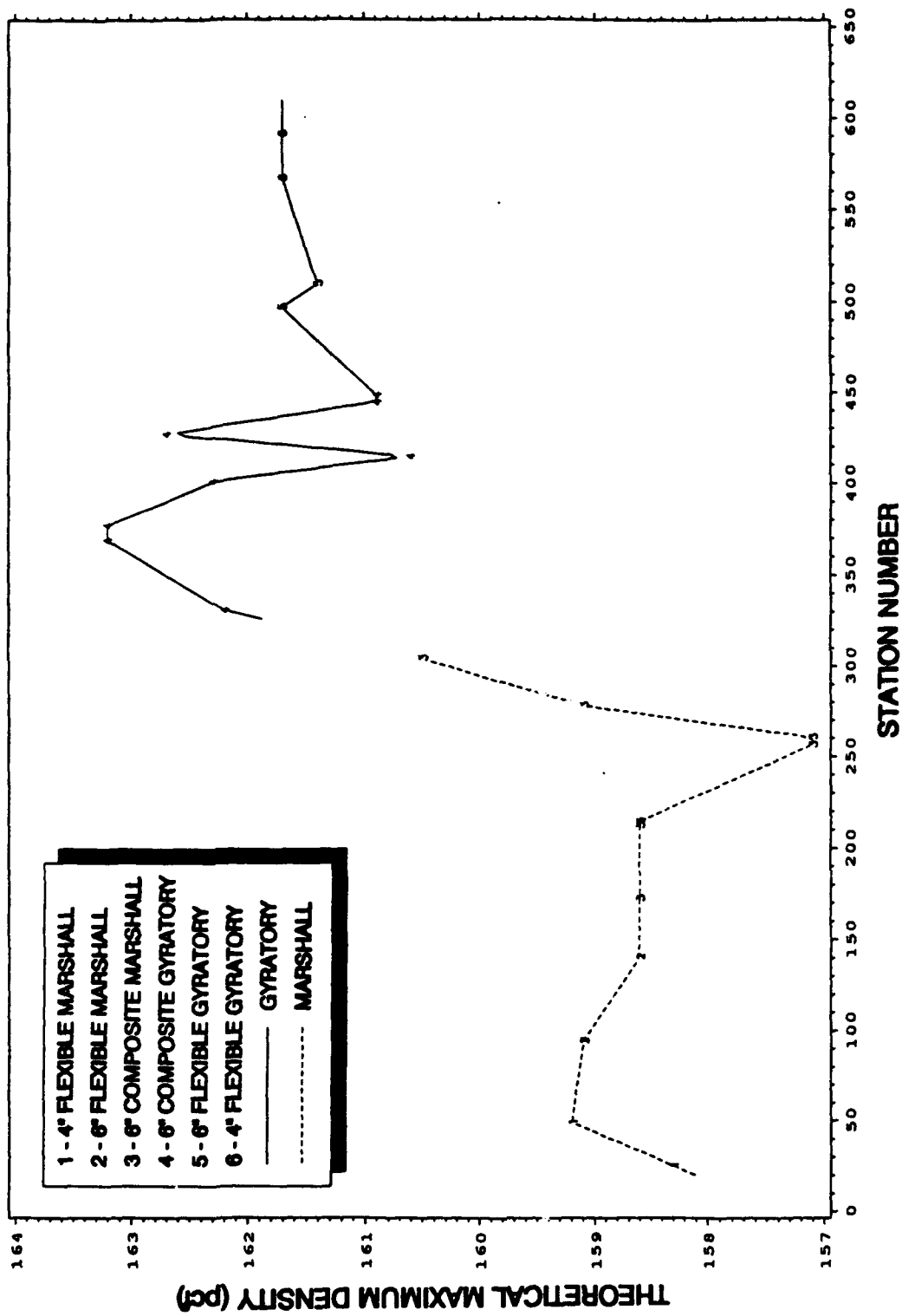


Figure 87. Theoretical Maximum Density and Interpolated Values Versus Station.

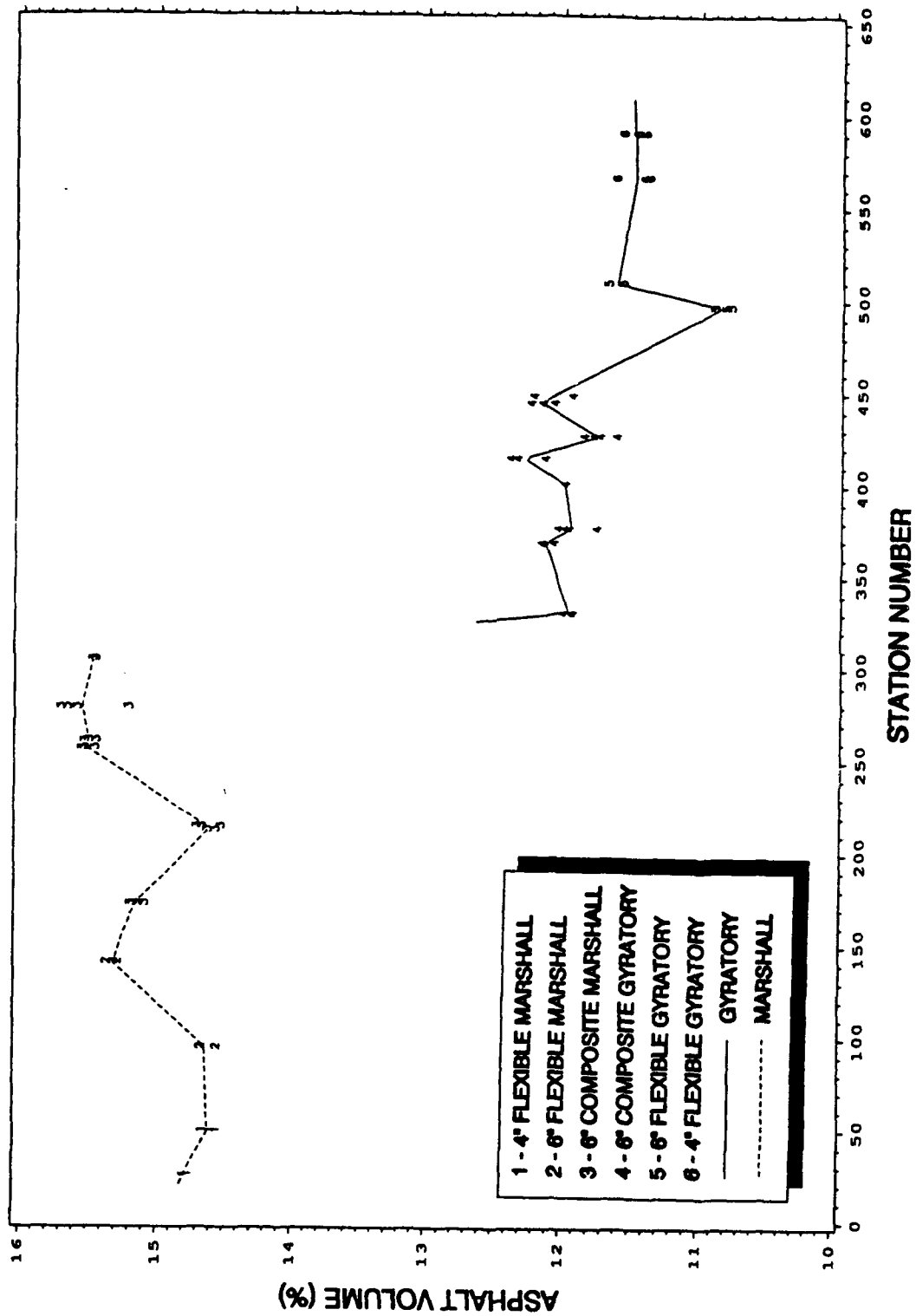


Figure 88. Asphalt Volume Data and Interpolated Values Versus Station.

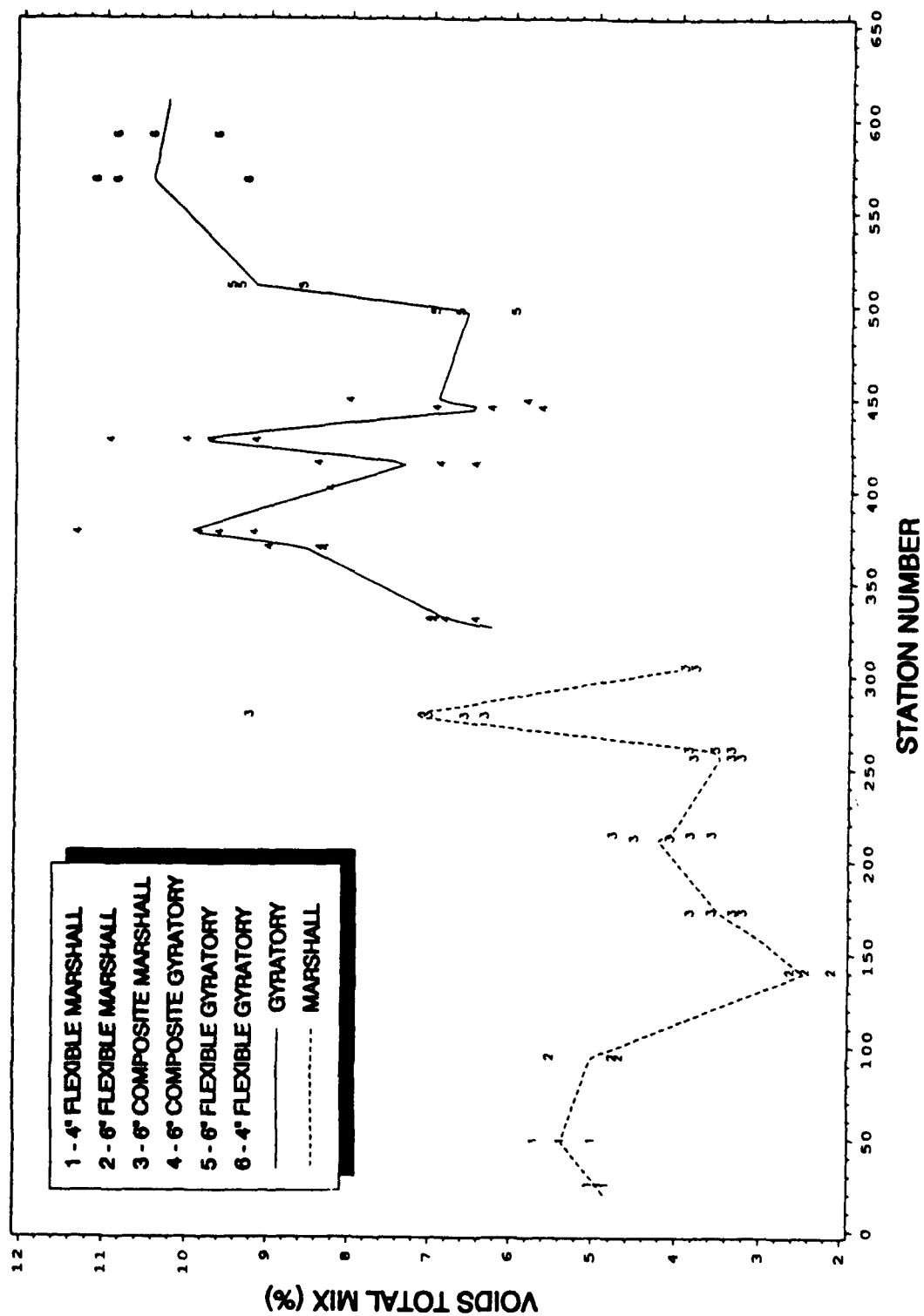


Figure 89. Voids Total Mix Data and Interpolated Values Versus Station.

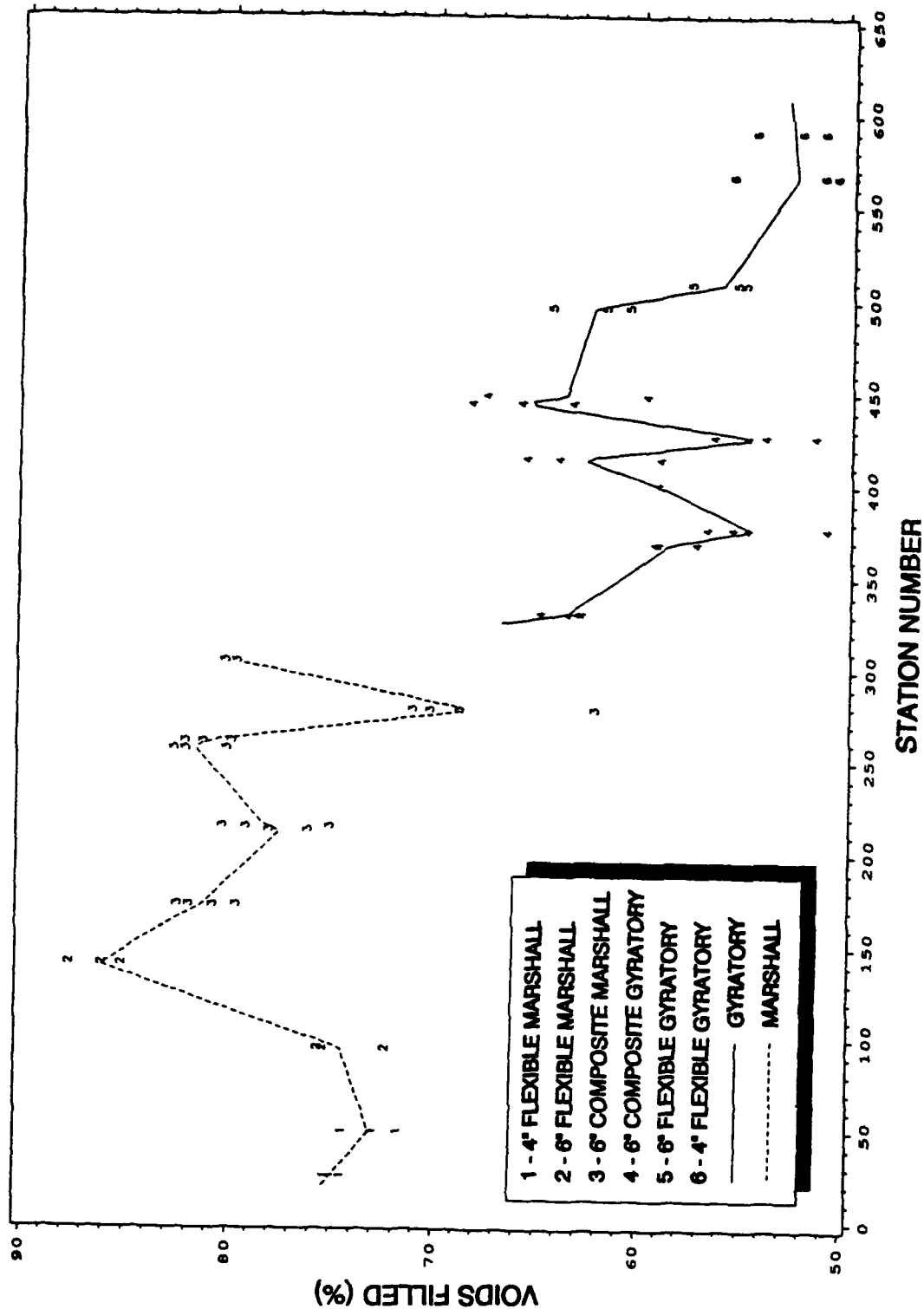


Figure 90. Voids Filled Data and Interpolated Values Versus Station.

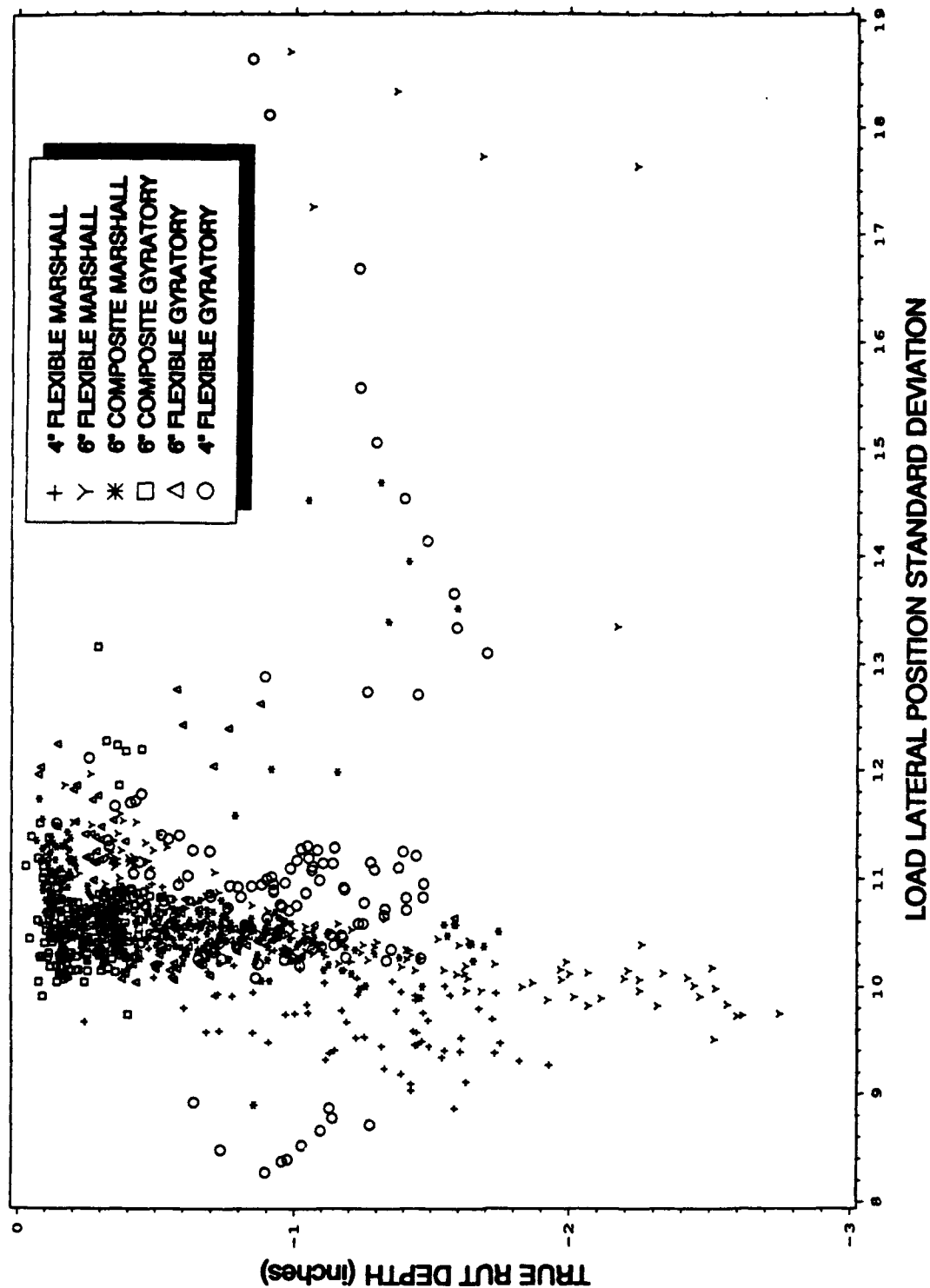


Figure 91. True Rut Depth Versus Standard Deviation of Lateral Position of Loadcart.

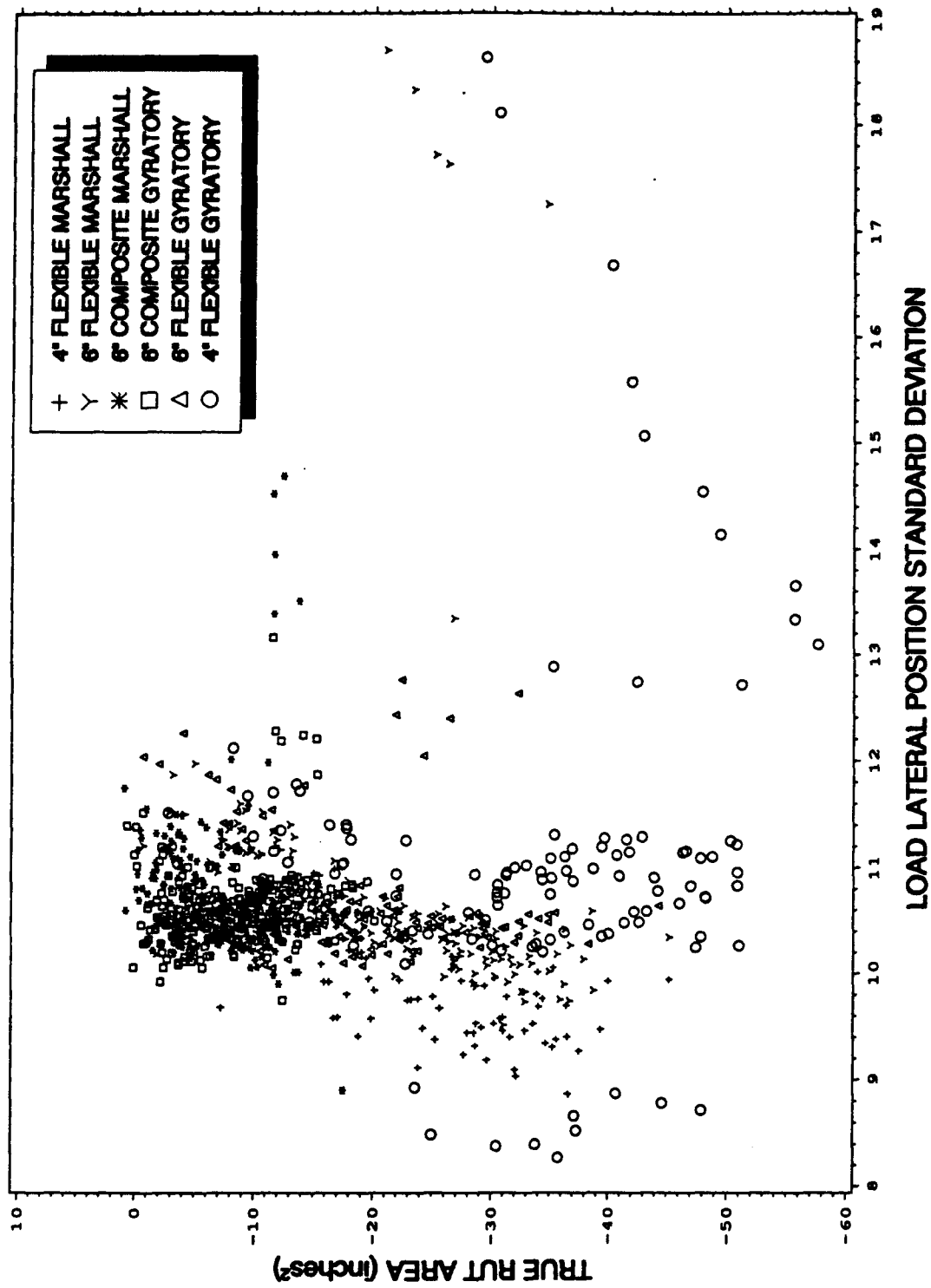


Figure 92. True Rut Area Versus Standard Deviation of Lateral Position of Loadcart.

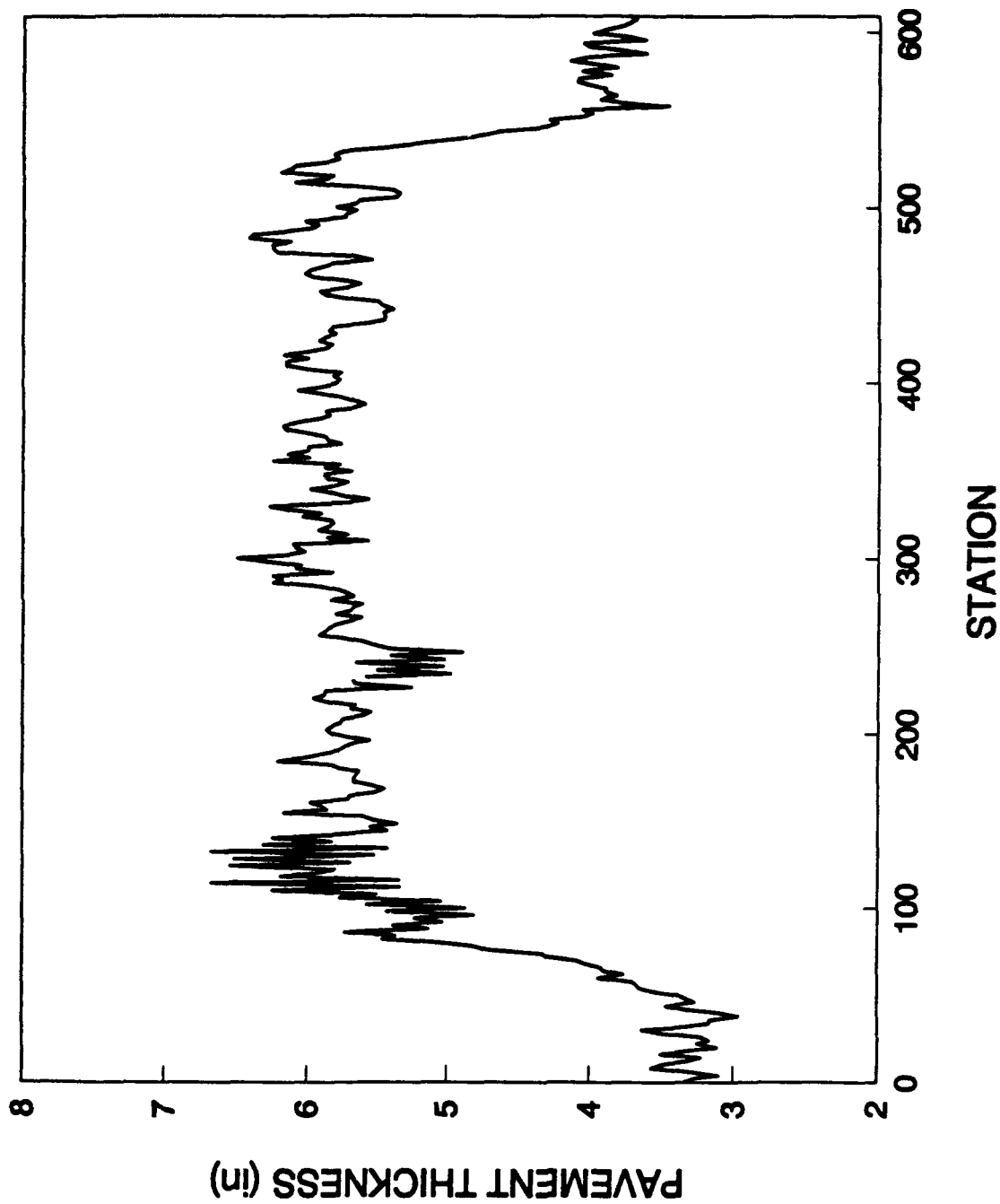


Figure 83. Pavement Thickness Variation.

SECTION V

CONCLUSIONS AND RECOMMENDATIONS

This field study of rutting in asphaltic pavements provided a significant amount of data from which several important conclusions can be drawn. The quality control aspects during construction provided test sections with consistent material properties throughout their length. Instrumentation efforts were successful in providing data on many, if not all, of the important variables associated with pavement performance. The data reduction processes used current technology to provide a complete database from which information can be drawn by future researchers. The analysis of the data incorporated both traditional and statistical techniques, providing a multifaceted review of results.

A. DATA ACQUISITION EFFORTS

A low-cost, high-output data acquisition system was developed for loadcart application. This system provided longitudinal and lateral position, velocity, and dynamic load variation for each pass of the loadcart. The data was loaded in a project database providing a means of comparing loading and damage data. In addition, an extensive set of FWD data was acquired, monitoring the pavement stiffness throughout the study.

B. RELATIONSHIP BETWEEN LOADING AND DAMAGE

All of the damage measures for each section were correlated to the applied loading (traffic level and loadcart position). A nonlinear relationship between damage and passes was found for all cases, with the rate of damage typically decreasing with increasing traffic. The loadcart velocity was bimodal, reflecting forward and backward directions. Profile damage measures revealed an increase in the accumulated damage at the ends of the traffic lane, reflecting the acceleration/deceleration portion of the passes. Lateral position data was reduced into histograms, which show a slightly skewed distribution. The greater the asymmetry in loading, the greater was the observed damage. The mode of the position histograms was the best indicator of the peak rut lateral location. The average of the loadcell data over the length of the pass averaged around the static weight, however oscillations as great as eighty percent above and below the static wheel load were detected. Further analyses to detect possible patterns of load fluctuations and the relationship to rut variation are planned.

The temperature did not vary as much as expected during trafficking, therefore conclusions regarding the rate of rutting versus temperature could not be made. However, the pavement midheight temperature averaged 103.5°F and rutting occurred rapidly. Today's high tire pressure aircraft will continue to cause significant rutting problems in similar environmental conditions. Further study is required to fully quantify the relative performance of gyratory designed pavements under various temperature conditions.

C. EFFECT OF MIX DESIGN ON PERFORMANCE

The analysis presented in Section IV showed that the applied loading across all of the sections did not vary significantly. However, the damage did vary significantly between sections, with the most obvious factors being the asphalt concrete mix design and base support. The gyratory sections formed broad ruts, characteristic of densification. Marshall sections formed multiple ruts, characteristic of plastic flow, with one rut eventually becoming primary. Comparisons between the composite sections, which reveal the behavior directly attributed to the mix design procedure, show that the Marshall mix sections experienced three times the rutting of the gyratory mix. The Marshall sections failed at or below 5800 passes of the loadcart. The gyratory sections had withstood between two and four times the passes of the Marshall sections when the trafficking was stopped because of dropping ambient temperatures.

Comparisons between the mix types for each of the similar sections reveal several important findings. The gyratory sections consistently had less rut depth than the Marshall counterpart although their rut areas were similar in magnitude. This indicates the broad width of the gyratory damage zone relative to the Marshall sections. The rate of damage increased with traffic in the Marshall sections and decreased with traffic in the gyratory sections. The upheaval area in the Marshall sections was three times higher than the upheaval area in the gyratory sections, despite less traffic in the Marshall sections. The gyratory sections had experienced at least twice the traffic.

This study has shown that pavements can be designed using gyratory methods and constructed with conventional equipment. It has also demonstrated that these surfaces have superior performance to Marshall designs. Common arguments preventing the widespread use of the gyratory mix design procedure include the expense of equipping a laboratory with a gyratory compaction device and the problem of inadequate compaction. The gyratory mixture used in this study called for twenty percent less asphalt cement than the Marshall mix. This decrease in binder represented a three percent savings on the in-place cost of the asphaltic concrete. Similar savings on a paving project would offset the initial cost of the gyratory compactor.

Although the behavior of the gyratory mixtures under the applied traffic shown in this study should alleviate concerns of inadequate compaction, heavier equipment will be required to meet current DOD criteria for compaction. The gyratory mixture was not compacted to its design density during construction, probably because of the equipment used. For the Air Force, the compaction problem may be academic. The substantial increase in life span of pavements which are currently rutting after only eight months of operation will compensate for relatively small reductions in life span due to excess permeability.

D. SIGNIFICANCE OF RUTTING IN BASE LAYERS

A comparison of representative profiles between the 6-inch flexible and 6-inch composite sections shows that sixty percent of the rutting experienced in the flexible sections can be traced to the granular layers. Visual observations of the base course conditions were made in trenches at the end of trafficking, and base course rutting was identified at all locations. Statistical analysis also showed the importance of the base support type for its contribution in resisting rutting. An additional investigation is planned to determine the cause of, and methods to reduce granular layer rutting.

E. CONCLUSIONS AND RECOMMENDATIONS

This experiment has shown that rutting of asphalt mixtures can be prevented if the mix is designed with laboratory compaction equal to that of the traffic. Failure of the Marshall sections was attributed to inadequate laboratory compaction during mix design. This was exacerbated somewhat by manufactured fines which prevented construction of mixtures at optimum binder content. In this field study, gyratory designed airfield pavements performed about three times better than Marshall designed pavements in terms of surface rutting. Even at compaction to ninety-two percent of the theoretical maximum density (one percent below DOD criterion), the gyratory sections outperformed the Marshall sections. Heavier field compaction equipment for gyratory mixes may further minimize surface rutting. Lower asphalt costs in the leaner gyratory mixes may offset the additional cost of purchasing gyratory design equipment. Independent of the mix design method, granular layers were found to contribute about sixty percent of the rutting in the 6-inch flexible sections. Improvements in base layer performance are needed to improve the overall performance of flexible airfield pavements under fighter aircraft loading. To account for failure mechanisms other than rutting, cooler weather and long term performance of gyratory designed pavements should also be evaluated. Additional performance data (in-service test sections) will be needed to support Air Force-wide application of gyratory design methods.

REFERENCES

1. Regan, G. L., A Laboratory Study of Asphalt Concrete Mix Design for High-Contact Pressure Aircraft Traffic, ESL-TR-85-66, U.S. Army Waterways Experiment Station, for the Air Force Engineering and Services Center, Tyndall AFB, Florida, June 1987.
2. Timian, D. A., Design and Construction of Pavement Test Sections for the Study of High Pressure Tire Effects, Applied Research Associates, Inc., for the Air Force Engineering and Services Center, Tyndall AFB, Florida, May 1989.
3. ASTM, Annual Book of ASTM Standards. Concrete and Aggregates. Volume 04.02, American Society for Testing and Materials, Philadelphia, Pennsylvania, 1988.
4. ASTM, Annual Book of ASTM Standards. Roofing, Waterproofing, and Bituminous Materials. Volume 04.04, American Society for Testing and Materials, Philadelphia, Pennsylvania, 1988.
5. ASTM, Annual Book of ASTM Standards. Road and Paving Materials. Traveled Surface Characteristics. Volume 04.03, American Society for Testing and Materials, Philadelphia, Pennsylvania, 1988.
6. Military Standard 620-A, Military Standard Test Methods for Bituminous Paving Materials, U.S. Army Engineer Research Laboratories, Mobility Command, Fort Belvoir, Virginia, 1966.
7. Anderson, M. and Timian, D. A., "Backcalculated Moduli for High Pressure Tire Effects Sections," Applied Research Associates, Inc., for the Air Force Engineering and Services Center, Tyndall AFB, Florida, September 1989.
8. Benjamin, J. R. and Cornell, C. A., Probabability, Statistics, and Decision for Civil Engineers, McGraw-Hill Book Company, New York, 1970, p. 8.

APPENDIX A

FALLING WEIGHT DEFLECTOMETER DATA

APPENDIX A. FALLING WEIGHT DEFLECTOMETER TEST RESULTS

SECTION 1

Thickness Base = 12 inches Thickness Asphalt Concrete = 4 inches
Date = 26 June 1989 Surface Temperature = 89.6 °F

STATION feet	TIME hr	LOAD lbs	DEFLECTIONS (mils)							ISM kips/in
			D ₁	D ₂	D ₃	D ₄	D ₅	D ₆	D ₇	
0	1412	9075	13.15	5.51	3.27	2.28	1.77	1.46	1.22	690.1
0	1412	9027	12.56	5.39	3.23	2.28	1.73	1.46	1.22	718.7
0	1412	11602	16.22	7.09	4.17	2.87	2.24	1.81	1.50	715.3
0	1412	18563	26.34	11.34	6.61	4.49	3.46	2.76	2.36	704.7
0	1412	26017	35.51	15.87	9.29	6.26	4.80	3.90	3.27	732.7
12	1413	8948	13.94	5.75	3.23	2.28	1.73	1.30	1.06	641.9
12	1413	8932	13.35	5.75	3.23	2.28	1.81	1.38	1.14	669.1
12	1413	11523	16.93	7.32	4.13	2.83	2.24	1.69	1.38	680.6
12	1413	18484	27.17	11.73	6.57	4.41	3.46	2.68	2.24	680.3
12	1413	25970	37.32	16.38	9.29	6.14	4.72	3.66	3.11	695.9
23	1414	8948	13.11	5.75	3.07	2.24	1.77	1.34	1.14	682.5
23	1414	8916	12.52	5.59	3.07	2.09	1.69	1.38	1.18	712.1
23	1414	11443	15.87	7.24	3.90	2.64	2.13	1.73	1.42	721.0
23	1414	18357	25.39	11.54	6.26	4.17	3.31	2.68	2.32	723.0
23	1414	25668	34.80	15.91	8.74	5.83	4.57	3.78	3.19	737.6
35	1415	8821	13.27	5.63	3.31	2.32	1.73	1.42	1.22	664.7
35	1415	8821	12.68	5.55	3.39	2.32	1.73	1.46	1.22	695.7
35	1415	11332	15.79	7.17	4.17	2.91	2.20	1.77	1.54	717.7
35	1415	18293	25.31	11.54	6.77	4.69	3.50	2.83	2.36	722.8
35	1415	25620	34.33	16.06	9.53	6.50	4.88	3.94	3.31	746.3
47	1416	8900	13.54	6.30	3.39	2.32	1.93	1.54	1.26	657.3
47	1416	8900	13.11	6.22	3.43	2.36	1.93	1.54	1.26	678.9
47	1416	11396	16.57	7.91	4.33	3.03	2.44	1.85	1.38	687.7
47	1416	18389	26.38	12.80	6.93	4.69	3.82	3.07	2.48	697.1
47	1416	25684	36.10	17.72	9.61	6.50	5.16	4.17	3.46	711.5
58	1417	8853	11.97	5.91	3.54	2.52	1.85	1.50	1.30	739.6
58	1417	8821	11.61	5.83	3.50	2.44	1.81	1.50	1.22	759.8
58	1417	11443	15.04	7.56	4.49	3.11	2.32	1.85	1.50	760.8
58	1417	18404	24.25	12.17	7.13	4.88	3.66	2.83	2.40	758.9
58	1417	25795	33.54	16.97	9.96	6.77	5.08	4.02	3.35	769.1

APPENDIX A. FALLING WEIGHT DEFLECTOMETER TEST RESULTS

SECTION 2

Thickness Base = 12 inches
Date = 26 June 1989

Thickness Asphalt Concrete = 6 inches
Surface Temperature = 89.6 °F

STATION feet	TIME hr	LOAD lbs	DEFLECTIONS (mils)							ISM kips/in
			D ₁	D ₂	D ₃	D ₄	D ₅	D ₆	D ₇	
82	1418	8789	10.91	5.91	3.50	2.52	1.77	1.42	1.14	805.6
82	1418	8868	10.67	5.91	3.54	2.60	1.93	1.46	1.14	831.1
82	1418	11443	14.17	7.64	4.57	3.19	2.36	1.73	1.42	807.6
82	1418	18404	23.90	12.28	7.28	5.00	3.74	2.83	2.36	770.0
82	1418	25858	32.99	17.09	10.16	6.97	5.16	4.02	3.35	783.8
93	1420	8868	11.22	6.57	3.31	2.17	1.61	1.38	1.14	790.4
93	1420	8837	10.79	6.38	3.27	2.05	1.57	1.30	1.10	819.0
93	1420	11443	14.21	8.23	4.33	2.72	2.13	1.69	1.38	805.3
93	1420	18246	22.83	13.07	6.85	4.29	3.31	2.68	2.20	799.2
93	1420	26192	31.89	18.11	9.61	6.02	4.61	3.74	3.11	821.3
104	1421	8868	12.13	5.79	3.23	2.20	1.65	1.38	1.06	731.1
104	1421	8821	11.61	5.67	3.23	2.24	1.69	1.42	1.10	759.8
104	1421	11459	15.20	7.52	4.21	2.87	2.24	1.73	1.42	753.9
104	1421	18420	24.29	12.01	6.69	4.53	3.39	2.72	2.28	758.3
104	1421	26176	34.21	16.69	9.37	6.26	4.65	3.70	3.11	765.2
116	1422	8932	13.82	5.08	3.03	2.09	1.54	1.26	1.06	646.3
116	1422	8868	12.95	4.96	2.99	2.05	1.57	1.30	1.06	684.8
116	1422	11507	16.50	6.65	3.98	2.72	2.05	1.65	1.30	697.4
116	1422	18373	26.73	10.71	6.34	4.29	3.31	2.56	2.13	687.4
116	1422	26002	36.61	15.08	8.86	5.94	4.53	3.54	2.87	710.2
128	1423	8821	16.14	5.55	3.07	2.01	1.50	1.22	0.94	546.5
128	1423	8837	15.39	5.43	3.07	1.97	1.77	1.18	0.91	574.2
128	1423	11443	19.92	7.28	4.13	2.68	2.05	1.54	1.26	574.4
128	1423	18373	32.64	11.97	6.69	4.25	3.11	2.52	2.05	562.9
128	1423	25970	44.37	16.69	9.37	5.94	4.33	3.35	2.72	585.3
139	1424	8932	14.06	5.24	2.60	1.73	1.34	1.18	0.98	635.3
139	1424	8884	13.15	5.04	2.48	1.65	1.30	1.14	0.91	675.6
139	1424	11475	16.77	6.69	3.27	2.09	1.69	1.38	1.14	684.3
139	1424	18436	26.77	10.83	5.31	3.39	2.64	2.13	1.93	688.7
139	1424	25827	36.26	14.92	7.40	4.72	3.66	2.87	2.48	712.3

APPENDIX A. FALLING WEIGHT DEFLECTOMETER TEST RESULTS

SECTION 3

Thickness Concrete = 12 inches Thickness Asphalt Concrete = 6 inches
Date = 28 June 1989 Surface Temperature = 89.6 °F

STATION feet	TIME hr	LOAD lbs	DEFLECTIONS (mils)							ISM kips/in
			D ₁	D ₂	D ₃	D ₄	D ₅	D ₆	D ₇	
161	1320	9107	6.89	1.57	1.61	1.54	1.42	1.18	1.02	1321.8
161	1320	9091	6.69	1.65	1.69	1.61	1.46	1.26	1.10	1358.9
161	1320	11729	8.27	2.01	2.05	1.89	1.69	1.46	1.22	1418.3
161	1320	18802	12.76	3.23	3.31	3.07	2.76	2.36	2.05	1473.5
161	1320	26208	17.01	4.57	4.72	4.29	3.82	3.31	2.80	1540.7
173	1322	9027	5.75	1.65	1.85	1.65	1.46	1.30	1.14	1569.9
173	1322	8980	5.39	1.69	1.81	1.65	1.46	1.30	1.14	1666.0
173	1322	11602	6.85	2.01	2.20	1.93	1.69	1.50	1.22	1693.7
173	1322	18675	10.94	3.43	3.62	3.23	2.83	2.44	2.13	1707.0
173	1322	25938	14.80	4.84	5.04	4.49	3.98	3.43	2.87	1752.6
185	1323	8996	4.88	1.97	1.93	1.73	1.54	1.38	1.18	1843.4
185	1323	9043	4.61	1.93	1.89	1.69	1.46	1.30	1.10	1961.6
185	1323	11682	5.91	2.44	2.36	2.17	1.93	1.65	1.38	1976.6
185	1323	18818	9.29	3.86	3.78	3.39	2.95	2.52	2.20	2025.6
185	1323	26272	12.56	5.39	5.31	4.76	4.13	3.58	3.03	2091.7
197	1325	9059	4.76	1.89	1.89	1.69	1.46	1.30	1.06	1903.2
197	1325	9027	4.57	1.89	1.89	1.69	1.46	1.26	1.06	1975.3
197	1325	11697	5.87	2.52	2.44	2.17	1.93	1.61	1.34	1992.7
197	1325	18802	9.21	3.98	3.90	3.46	2.95	2.52	2.17	2041.5
197	1325	26733	12.52	5.55	5.39	4.84	4.17	3.54	2.95	2135.2
209	1326	9012	5.08	1.81	1.81	1.61	1.42	1.26	1.06	1774.0
209	1326	8964	4.80	1.81	1.81	1.61	1.38	1.26	1.06	1867.5
209	1326	11650	5.98	2.36	2.28	2.05	1.81	1.54	1.26	1948.2
209	1326	18706	9.45	3.86	3.82	3.39	2.95	2.56	2.20	1979.5
209	1326	26367	12.91	5.35	5.28	4.69	4.06	3.46	2.91	2042.4
221	1328	9091	4.69	1.85	1.81	1.65	1.42	1.26	1.06	1938.4
221	1328	9027	4.45	1.77	1.73	1.54	1.34	1.18	0.98	2028.5
221	1328	11729	5.75	2.28	2.24	2.05	1.77	1.57	1.30	2039.8
221	1328	18865	9.21	3.78	3.74	3.31	2.91	2.48	2.13	2048.3
221	1328	26892	12.56	5.16	5.08	4.53	3.98	3.39	2.83	2141.1
233	1329	9043	4.17	2.05	1.93	1.73	1.65	1.38	1.14	2168.6
233	1329	9012	4.06	1.97	1.89	1.69	1.54	1.30	1.10	2219.7
233	1329	11697	5.31	2.52	2.44	2.17	1.97	1.65	1.42	2202.8
233	1329	18818	8.66	3.98	3.86	3.46	3.03	2.60	2.24	2173.0
233	1329	26923	11.89	5.47	5.28	4.72	4.13	3.54	2.95	2264.3

APPENDIX A. FALLING WEIGHT DEFLECTOMETER TEST RESULTS

SECTION 3

Thickness Concrete = 12 inches Thickness Asphalt Concrete = 6 inches
Date = 28 June 1989 Surface Temperature = 89.6 °F

STATION feet	TIME hr	LOAD lbs	DEFLECTIONS (mils)							ISM kips/in
			D ₁	D ₂	D ₃	D ₄	D ₅	D ₆	D ₇	
245	1330	9059	4.84	2.09	2.05	1.85	1.65	1.42	1.14	1871.7
245	1330	9059	4.53	1.97	1.93	1.73	1.50	1.26	1.02	1999.8
245	1330	11666	5.79	2.56	2.52	2.24	1.97	1.69	1.38	2014.9
245	1330	18881	9.25	4.09	4.02	3.54	3.07	2.64	2.24	2041.2
245	1330	26955	12.64	5.71	5.55	4.92	4.25	3.62	3.03	2132.5
257	1333	9457	4.96	1.69	1.73	1.57	1.34	1.26	1.10	1906.7
257	1333	9361	4.76	1.77	1.77	1.57	1.34	1.26	1.10	1966.6
257	1333	11904	6.18	2.28	2.28	2.05	1.81	1.61	1.34	1926.2
257	1333	18865	9.53	3.62	3.58	3.19	2.80	2.36	2.05	1979.5
257	1333	26812	12.95	5.08	5.04	4.53	3.98	3.39	2.87	2070.4
269	1335	8948	4.80	1.69	1.81	1.61	1.42	1.22	1.06	1864.2
269	1335	8980	4.61	1.69	1.81	1.61	1.42	1.26	1.02	1947.9
269	1335	11634	5.75	2.20	2.32	2.09	1.81	1.57	1.34	2023.3
269	1335	18865	8.98	3.58	3.74	3.35	2.91	2.48	2.13	2100.8
269	1335	26955	12.20	4.96	5.08	4.53	3.94	3.39	2.83	2209.4
281	1336	9091	4.02	1.89	1.85	1.61	1.38	1.22	0.98	2261.4
281	1336	9027	4.06	1.97	1.97	1.73	1.46	1.34	1.14	2223.4
281	1336	11570	5.20	2.52	2.32	2.05	1.81	1.50	1.22	2225.0
281	1336	18611	8.58	4.06	3.90	3.43	2.95	2.48	2.13	2169.1
281	1336	25858	11.85	5.71	5.47	4.84	4.13	3.50	2.87	2182.1
293	1337	8964	5.20	1.97	1.93	1.69	1.54	1.30	1.10	1723.8
293	1337	8932	5.04	2.01	1.93	1.69	1.54	1.30	1.06	1772.2
293	1337	11618	6.26	2.52	2.36	2.17	1.93	1.61	1.34	1855.9
293	1337	18722	9.72	3.98	3.82	3.35	2.99	2.48	2.05	1926.1
293	1337	26685	13.31	5.47	5.39	4.76	4.09	3.50	2.91	2004.9

APPENDIX A. FALLING WEIGHT DEFLECTOMETER TEST RESULTS

SECTION 4

Thickness Concrete = 12 inches Thickness Asphalt Concrete = 6 inches
Date = 28 June 1989 Surface Temperature = 89.6 °F

STATION feet	TIME hr	LOAD lbs	DEFLECTIONS (mils)							ISM kips/in
			D ₁	D ₂	D ₃	D ₄	D ₅	D ₆	D ₇	
305	1341	8964	9.76	1.65	1.81	1.65	1.42	1.26	1.10	918.4
305	1341	8948	9.49	1.69	1.85	1.65	1.42	1.30	1.10	942.9
305	1341	11586	11.22	2.17	2.28	2.05	1.81	1.54	1.30	1032.6
305	1341	18675	16.38	3.50	3.62	3.27	2.76	2.36	1.97	1140.1
305	1341	26478	21.73	5.00	5.16	4.61	4.02	3.39	2.76	1218.5
317	1342	8964	8.54	1.34	1.77	1.57	1.38	1.22	1.06	1049.6
317	1342	8900	8.35	1.38	1.77	1.57	1.38	1.22	1.06	1065.9
317	1342	11539	10.12	1.77	2.09	1.89	1.65	1.42	1.26	1140.2
317	1342	18659	15.83	2.99	3.54	3.19	2.76	2.32	2.01	1178.7
317	1342	26303	21.50	4.25	4.92	4.41	3.82	3.27	2.72	1223.4
329	1343	9027	4.17	1.85	1.77	1.57	1.34	1.22	1.02	2164.7
329	1343	8980	4.02	1.85	1.77	1.57	1.34	1.22	1.02	2233.8
329	1343	11666	5.20	2.44	2.28	2.05	1.81	1.54	1.30	2243.5
329	1343	18865	8.27	3.86	3.70	3.27	2.80	2.40	2.05	2281.1
329	1343	27050	11.34	5.43	5.16	4.57	3.94	3.31	2.76	2385.4
341	1344	8948	4.61	1.81	1.77	1.57	1.38	1.26	1.10	1941.0
341	1344	8884	4.25	1.73	1.57	1.46	1.30	1.10	0.94	2090.4
341	1344	11602	5.51	2.40	2.13	1.97	1.77	1.50	1.30	2105.6
341	1344	18675	8.70	3.66	3.54	3.15	2.76	2.40	2.09	2146.6
341	1344	26399	11.89	5.08	4.80	4.29	3.82	3.27	2.76	2220.3
353	1345	8996	4.29	1.81	1.73	1.57	1.38	1.22	1.06	2097.0
353	1345	8916	4.21	1.89	1.81	1.65	1.46	1.30	1.10	2117.8
353	1345	11666	5.31	2.28	2.20	1.97	1.73	1.50	1.26	2197.0
353	1345	18802	8.39	3.78	3.58	3.23	2.83	2.44	2.13	2241.0
353	1345	26621	11.50	5.24	4.96	4.45	3.94	3.39	2.87	2314.9
365	1346	9027	4.09	1.69	1.65	1.50	1.34	1.18	1.02	2207.1
365	1346	8884	3.94	1.69	1.65	1.50	1.34	1.18	1.02	2254.8
365	1346	11682	4.96	2.01	1.97	1.77	1.57	1.38	1.18	2355.2
365	1346	18802	7.87	3.23	3.15	2.83	2.48	2.17	1.89	2389.1
365	1346	26764	10.94	4.61	4.49	4.06	3.58	3.11	2.68	2446.4

APPENDIX A. FALLING WEIGHT DEFLECTOMETER TEST RESULTS

SECTION 4

Thickness Concrete = 12 inches Thickness Asphalt Concrete = 6 inches
Date = 28 June 1989 Surface Temperature = 89.6 °F

STATION feet	TIME hr	LOAD lbs	DEFLECTIONS (mils)							ISM kips/in
			D ₁	D ₂	D ₃	D ₄	D ₅	D ₆	D ₇	
377	1347	8980	4.49	1.77	1.61	1.42	1.50	1.14	1.02	2000.0
377	1347	8900	4.37	1.85	1.69	1.50	1.57	1.18	1.10	2036.6
377	1347	11650	5.43	2.20	2.05	1.81	1.81	1.42	1.26	2145.5
377	1347	18865	8.58	3.54	3.27	2.91	2.76	2.24	1.97	2198.7
377	1347	26844	11.85	4.92	4.69	4.21	3.74	3.27	2.80	2265.3
389	1349	9186	4.17	1.81	1.77	1.61	1.42	1.26	1.10	2202.9
389	1349	9059	3.98	1.77	1.69	1.54	1.34	1.22	1.02	2276.1
389	1349	11507	4.96	2.17	2.17	1.89	1.69	1.54	1.22	2320.0
389	1349	18659	8.11	3.58	3.50	3.11	2.76	2.36	2.01	2300.7
389	1349	25922	11.22	4.96	4.84	4.29	3.82	3.27	2.72	2310.3
401	1350	8948	3.94	1.93	1.81	1.65	1.54	1.30	1.06	2271.1
401	1350	8932	3.78	1.81	1.69	1.54	1.34	1.18	1.02	2363.0
401	1350	11634	4.88	2.36	2.17	1.93	1.73	1.50	1.22	2423.8
401	1350	18722	7.68	3.70	3.50	3.15	2.76	2.36	2.05	2437.8
401	1350	26415	10.59	5.24	4.92	4.37	3.86	3.35	2.83	2494.3
413	1351	8948	4.21	2.13	2.01	1.77	1.54	1.34	1.14	2125.4
413	1351	8948	4.06	2.05	1.93	1.69	1.42	1.26	1.06	2203.9
413	1351	11618	5.31	2.72	2.60	2.32	2.05	1.73	1.42	2187.9
413	1351	18786	8.43	4.41	4.13	3.70	3.23	2.76	2.32	2228.5
413	1351	26590	11.57	6.02	5.67	5.08	4.37	3.70	3.15	2298.2
425	1353	8964	3.98	1.85	1.77	1.57	1.38	1.22	1.02	2252.3
425	1353	8900	3.94	1.93	1.85	1.65	1.42	1.30	1.10	2258.9
425	1353	11650	4.92	2.44	2.28	2.05	1.81	1.57	1.30	2367.9
425	1353	18786	7.88	3.82	3.66	3.27	2.83	2.44	2.05	2408.5
425	1353	26812	10.67	5.39	5.08	4.53	3.98	3.43	2.87	2512.8
443	1354	8980	4.33	2.05	1.89	1.69	1.46	1.30	1.10	2073.9
443	1354	8996	4.21	2.05	1.89	1.69	1.46	1.30	1.10	2136.8
443	1354	11650	5.43	2.60	2.44	2.09	1.81	1.57	1.34	2145.5
443	1354	18881	8.78	4.25	3.90	3.39	2.91	2.48	2.13	2150.5
443	1354	26892	12.05	5.98	5.51	4.76	4.09	3.46	2.91	2231.7

APPENDIX A. FALLING WEIGHT DEFLECTOMETER TEST RESULTS

SECTION 5

Thickness Base = 12 inches
Date = 26 June 1989

Thickness Asphalt Concrete = 6 inches
Surface Temperature = 89.6 °F

STATION feet	TIME hr	LOAD lbs	DEFLECTIONS (mils)							ISM kips/in
			D ₁	D ₂	D ₃	D ₄	D ₅	D ₆	D ₇	
483	1426	8996	10.31	5.20	3.07	2.28	1.69	1.30	1.10	872.6
483	1426	8900	9.80	5.04	2.99	2.20	1.69	1.30	1.02	908.2
483	1426	11539	12.76	6.65	3.94	2.76	2.13	1.69	1.38	904.3
483	1426	18484	20.63	10.87	6.38	4.41	3.39	2.68	2.24	896.0
483	1426	26447	28.27	15.08	8.90	6.14	4.57	3.62	2.95	935.5
495	1427	8868	10.55	5.67	2.80	1.81	1.42	1.18	0.98	840.6
495	1427	8853	10.24	5.63	2.87	1.89	1.50	1.26	1.02	864.6
495	1427	11475	13.31	7.36	3.78	2.48	1.93	1.57	1.30	862.1
495	1427	18468	21.61	11.77	6.02	3.94	2.95	2.40	2.01	854.6
495	1427	25874	29.96	16.42	8.58	5.59	4.25	3.46	2.83	863.6
506	1428	8900	10.79	5.31	2.91	2.01	1.57	1.22	1.02	824.8
506	1428	8853	10.39	5.31	2.91	2.01	1.65	1.26	1.06	852.1
506	1428	11523	13.50	6.77	3.82	2.64	2.05	1.61	1.34	853.6
506	1428	18452	22.17	11.18	6.38	4.21	3.23	2.56	2.17	832.3
506	1428	26367	30.75	15.91	9.13	6.10	4.53	3.66	3.11	857.5
518	1429	8884	10.87	5.16	2.91	2.05	1.61	1.30	1.10	817.3
518	1429	8884	10.47	5.16	2.99	2.17	1.69	1.34	1.10	848.5
518	1429	11443	13.39	6.69	3.90	2.80	2.17	1.65	1.34	854.6
518	1429	18373	21.54	10.91	6.34	4.41	3.39	2.64	2.20	853.0
518	1429	26415	29.69	15.24	8.94	6.10	4.61	3.58	2.95	889.7
530	1430	8916	10.55	5.08	2.99	2.09	1.57	1.34	1.18	845.1
530	1430	8884	10.08	4.88	2.87	2.01	1.50	1.30	1.06	881.3
530	1430	11491	13.07	6.50	3.78	2.64	2.05	1.57	1.30	879.2
530	1430	18484	21.54	10.71	6.18	4.25	3.15	2.60	2.13	858.1
530	1430	26303	30.31	15.20	8.78	5.98	4.53	3.62	2.95	867.8

APPENDIX A. FALLING WEIGHT DEFLECTOMETER TEST RESULTS

SECTION 6

Thickness Base = 12 inches
Date = 26 June 1989

Thickness Asphalt Concrete = 4 inches
Surface Temperature = 89.6 °F

STATION feet	TIME hr	LOAD lbs	DEFLECTIONS (mils)							ISM kips/in
			D ₁	D ₂	D ₃	D ₄	D ₅	D ₆	D ₇	
553	1431	8996	10.91	5.55	3.23	2.32	1.77	1.38	1.14	824.6
553	1431	8853	10.55	5.67	3.15	2.36	1.81	1.38	1.10	839.1
553	1431	11491	13.94	7.32	4.21	3.03	2.36	1.81	1.46	824.3
553	1431	18452	23.23	11.77	6.69	4.69	3.62	2.80	2.24	794.3
553	1431	26415	32.17	16.38	9.41	0.42	5.08	3.78	2.95	821.1
564	1433	8932	12.40	5.98	3.11	2.09	1.54	1.42	1.18	720.3
564	1433	8868	11.93	5.87	3.11	2.09	1.54	1.42	1.18	743.3
564	1433	11507	15.63	7.68	4.09	2.72	2.09	1.77	1.38	736.2
564	1433	18500	24.84	12.40	6.46	4.25	3.31	2.64	2.24	744.8
564	1433	26351	33.62	16.97	9.09	5.91	4.57	3.66	3.07	783.8
576	1433	8932	13.27	6.26	3.62	2.44	1.73	1.42	1.10	673.1
576	1433	8868	12.72	6.14	3.58	2.44	1.73	1.42	1.06	697.2
576	1433	11507	16.54	8.11	4.65	3.11	2.28	1.73	1.34	695.7
576	1433	18420	26.93	13.31	7.44	4.92	3.54	2.83	2.24	684.0
576	1433	26256	37.09	18.70	10.47	6.81	4.88	3.86	3.11	707.9
588	1435	8932	12.83	6.26	3.39	2.24	1.73	1.34	1.10	696.2
588	1435	8932	12.36	6.02	3.31	2.28	1.69	1.34	1.10	722.7
588	1435	11507	16.22	7.99	4.41	3.03	2.28	1.81	1.46	709.4
588	1435	18389	26.22	12.76	6.89	4.61	3.46	2.76	2.32	701.3
588	1435	26272	36.34	17.80	9.61	6.30	4.69	3.78	3.11	722.9
600	1435	8868	11.97	5.91	3.46	2.48	1.93	1.38	1.10	740.9
600	1435	8884	11.46	5.59	3.46	2.40	1.77	1.34	1.02	775.2
600	1435	11507	15.16	7.52	4.53	3.15	2.28	1.77	1.38	759.0
600	1435	18389	25.08	12.32	7.28	5.04	3.74	2.87	2.32	733.2
600	1435	26303	35.00	17.24	10.00	6.81	5.08	3.94	3.15	751.5
611	1436	8916	11.65	5.83	3.54	2.48	1.85	1.38	1.06	765.3
611	1436	8916	11.30	5.75	3.58	2.56	1.93	1.46	1.14	789.0
611	1436	11491	14.88	7.56	4.57	3.27	2.44	1.85	1.46	772.2
611	1436	18404	24.72	12.28	7.28	5.00	3.70	2.87	2.32	744.5
611	1436	26319	34.49	17.24	10.08	6.81	5.00	3.86	3.15	763.1

APPENDIX A. FALLING WEIGHT DEFLECTOMETER TEST RESULTS

SECTION 5

Thickness Base = 12 inches Thickness Asphalt Concrete = 6 inches
Date = 5 September 1989 Surface Temperature = 94.1 °F

STATION feet	TIME hr	LOAD lbs	DEFLECTIONS (mils)							ISM kips/in
			D ₁	D ₂	D ₃	D ₄	D ₅	D ₆	D ₇	
518	1226	9488	10.87	6.97	3.90	2.52	1.85	1.46	1.18	872.9
518	1226	9425	10.35	6.69	3.82	2.48	1.77	1.42	1.14	910.6
518	1226	12079	13.27	8.62	4.88	3.31	2.40	1.77	1.50	910.2
518	1226	19088	21.06	13.90	7.87	5.16	3.74	3.07	2.48	906.4
518	1226	26399	27.91	18.66	10.83	7.09	5.16	3.94	3.27	945.9
530	1225	9345	11.61	7.05	3.86	2.48	1.77	1.46	1.18	804.9
530	1225	9282	10.91	6.65	3.78	2.48	1.81	1.54	1.18	850.8
530	1225	11872	14.02	8.58	4.88	3.27	2.40	1.81	1.46	846.8
530	1225	18913	22.64	13.78	7.80	5.16	3.78	2.83	2.32	835.4
530	1225	25858	30.08	18.31	10.59	6.81	5.04	3.90	3.19	859.6

SECTION 6

Thickness Base = 12 inches Thickness Asphalt Concrete = 4 inches
Date = 5 September 1989 Surface Temperature = 94.1 °F

STATION feet	TIME hr	LOAD lbs	DEFLECTIONS (mils)							ISM kips/in
			D ₁	D ₂	D ₃	D ₄	D ₅	D ₆	D ₇	
553	1219	9361	14.92	7.52	3.70	2.40	1.85	1.42	1.14	627.4
553	1219	9313	13.54	7.17	3.70	2.40	1.77	1.46	1.18	687.8
553	1219	12031	17.13	9.17	4.76	3.07	2.28	1.85	1.50	702.3
553	1219	19120	26.30	14.41	7.48	4.80	3.58	2.83	2.40	727.0
553	1219	26367	33.62	19.17	10.16	6.50	4.80	3.86	3.27	784.3
564	1214	9647	13.82	7.56	3.86	2.48	1.69	1.61	1.26	698.0
564	1214	9600	13.35	7.40	3.82	2.44	1.69	1.57	1.22	719.1
564	1214	12270	17.01	9.45	4.92	3.19	2.36	1.81	1.46	721.3
564	1214	19358	26.22	14.72	7.64	4.84	3.58	2.99	2.48	738.3
564	1214	26399	33.66	19.33	10.16	6.54	5.00	3.86	3.27	784.3

APPENDIX B

CORE DENSITY DATA

TABLE B1. PRETRAFFIC BULK DENSITIES - HEAVYWEIGHT LANE

CORE IDENTIFICATION	MIX	LIFT	SECTION	BULK DENSITY (pcf)
A0+25B	M	T	1	150.50
A0+25D	M	T	1	150.60
A0+25F	M	T	1	150.30
A0+49B	M	T	1	150.60
A0+49D	M	T	1	151.20
A0+49F	M	T	1	150.10
A0+95B	M	T	2	150.30
A0+95D	M	T	2	151.60
A0+95F	M	T	2	151.50
A1+41B	M	T	2	155.20
A1+41D	M	T	2	154.70
A1+41F	M	T	2	154.40
A0+95B	M	B	2	146.10
A0+95D	M	B	2	146.10
A0+95F	M	B	2	150.80
A1+41B	M	B	2	148.40
A1+41D	M	B	2	148.80
A1+41F	M	B	2	150.50
A1+73A	M	T	3	153.50
A1+73C	M	T	3	153.30
A1+73E	M	T	3	152.90
A1+73G	M	T	3	152.50
A2+13B	M	T	3	151.40
A2+13D	M	T	3	152.10
A2+13F	M	T	3	152.10
A2+15B	M	T	3	151.00
A2+15D	M	T	3	152.90
A2+15F	M	T	3	152.50
A2+57B	M	T	3	151.80
A2+57D	M	T	3	152.00
A2+57F	M	T	3	151.80
A2+61B	M	T	3	151.50
A2+61D	M	T	3	151.80
A2+61F	M	T	3	151.00
A2+79A	M	T	3	144.40
A2+79C	M	T	3	149.00

TABLE B1. PRETRAFFIC BULK DENSITIES - HEAVYWEIGHT LANE (Continued.)

CORE IDENTIFICATION	MIX	LIFT	SECTION	BULK DENSITY (pcf)
A2+79E	M	T	3	148.60
A2+79G	M	T	3	147.90
A3+05B	M	T	3	154.20
A3+05D	M	T	3	154.40
A3+05F	M	T	3	154.20
A1+73A	M	B	3	147.80
A1+73C	M	B	3	147.30
A1+73E	M	B	3	150.10
A1+73G	M	B	3	149.10
A2+13B	M	B	3	144.70
A2+13D	M	B	3	146.30
A2+13F	M	B	3	148.00
A2+15B	M	B	3	144.00
A2+15D	M	B	3	146.10
A2+15F	M	B	3	146.30
A2+57B	M	B	3	148.40
A2+57D	M	B	3	151.50
A2+57F	M	B	3	151.60
A2+61B	M	B	3	150.00
A2+61D	M	B	3	151.60
A2+61F	M	B	3	151.60
A2+79A	M	B	3	147.80
A2+79C	M	B	3	148.90
A2+79E	M	B	3	150.80
A2+79G	M	B	3	149.50
A3+05B	M	B	3	149.00
A3+05D	M	B	3	150.40
A3+05F	M	B	3	150.90
A3+31A	G	T	4	150.80
A3+31C	G	T	4	151.10
A3+31E	G	T	4	151.70
A3+31G	G	T	4	150.90
A3+69B	G	T	4	148.50
A3+69D	G	T	4	149.50
A3+69F	G	T	4	149.60

TABLE B1. PRETRAFFIC BULK DENSITIES - HEAVYWEIGHT LANE (Continued.)

CORE IDENTIFICATION	MIX	LIFT	SECTION	BULK DENSITY (pcf)
A3+77A	G	T	4	144.70
A3+77C	G	T	4	147.10
A3+77E	G	T	4	147.50
A3+77G	G	T	4	148.20
A4+01C	G	T	4	148.90
A4+15B	G	T	4	147.10
A4+15D	G	T	4	150.20
A4+15F	G	T	4	149.50
A4+27A	G	T	4	144.90
A4+27C	G	T	4	146.40
A4+27E	G	T	4	147.80
A4+27G	G	T	4	146.90
A4+45B	G	T	4	149.70
A4+45D	G	T	4	150.80
A4+45F	G	T	4	151.80
A4+49C	G	T	4	148.00
A4+49G	G	T	4	151.50
A3+31A	G	B	4	144.80
A3+31C	G	B	4	144.60
A3+31E	G	B	4	144.70
A3+31G	G	B	4	145.30
A3+69B	G	B	4	144.50
A3+69D	G	B	4	146.00
A3+69F	G	B	4	147.20
A3+77A	G	B	4	142.60
A3+77C	G	B	4	145.20
A3+77E	G	B	4	146.60
A3+77G	G	B	4	145.90
A4+01C	G	B	4	146.40
A4+15B	G	B	4	147.30
A4+15D	G	B	4	148.10
A4+15F	G	B	4	147.80
A4+27C	G	B	4	146.00
A4+27E	G	B	4	147.60
A4+27G	G	B	4	147.30
A4+45B	G	B	4	148.40
A4+45D	G	B	4	147.50
A4+45F	G	B	4	148.60

TABLE B1. PRETRAFFIC BULK DENSITIES - HEAVYWEIGHT LANE (Continued)

CORE IDENTIFICATION	MIX	LIFT	SECTION	BULK DENSITY (pcf)
A4+49C	G	B	4	146.70
A4+49G	G	B	4	146.40
A4+97B	G	T	5	150.40
A4+97D	G	T	5	150.90
A4+97F	G	T	5	152.00
A5+10B	G	T	5	146.10
A5+10D	G	T	5	146.30
A5+10F	G	T	5	147.50
A4+97B	G	B	5	146.80
A4+97D	G	B	5	147.20
A4+97F	G	B	5	148.00
A5+10B	G	B	5	144.70
A5+10D	G	B	5	146.20
A5+10F	G	B	5	147.70
A5+67B	G	T	6	144.10
A5+67D	G	T	6	143.70
A5+67F	G	T	6	146.70
A5+91B	G	T	6	144.10
A5+91D	G	T	6	144.80
A5+91F	G	T	6	146.10

TABLE B2. BULK DENSITIES AFTER APPROXIMATELY 4600 PASSES.
HEAVYWEIGHT LANE

CORE IDENTIFICATION	MIX	LIFT	SECTION	BULK DENSITY (pcf)
A3+05H	M	T	3	155.6
A3+05I	M	T	3	155.2
A3+05J	M	T	3	154.1
A3+05H	M	B	3	153.1
A3+05I	M	B	3	152.3
A3+05J	M	B	3	153.0
A3+78H	G	T	4	155.7
A3+78I	G	T	4	155.0
A3+78J	G	T	4	154.5
A3+78H	G	B	4	150.1
A3+78I	G	B	4	148.5
A3+78J	G	B	4	148.8
A4+26H	G	T	4	155.6
A4+26I	G	T	4	156.2
A4+26J	G	T	4	155.7
A4+26J	G	B	4	150.8
A4+26H	G	B	4	150.8
A4+26I	G	B	4	151.0
A4+96H	G	T	5	157.6
A4+96I	G	T	5	157.6
A4+96J	G	T	5	156.9
A4+96J	G	B	5	150.6
A4+96H	G	B	5	151.9
A4+96I	G	B	5	151.0

**TABLE B3. BULK DENSITIES AFTER APPROXIMATELY 7500 PASSES.
HEAVYWEIGHT LANE**

CORE IDENTIFICATION	MIX	LIFT	SECTION	BULK DENSITY (pcf)
A3+79K	G	T	4	156.7
A3+79K	G	B	4	150.7
A3+79L	G	T	4	156.7
A3+79L	G	B	4	150.5
A3+79M	G	T	4	155.9
A3+79M	G	B	4	149.3
A4+27K	G	T	4	156.9
A4+27K	G	B	4	151.6
A4+27L	G	T	4	157.1
A4+27L	G	B	4	151.8
A4+27M	G	T	4	156.5
A4+27M	G	B	4	151.7
A4+95K	G	T	5	158.1
A4+95L	G	T	5	158.0
A4+95M	G	T	5	157.6
A4+95K	G	B	5	151.6
A4+95L	G	B	5	152.2
A4+95M	G	B	5	152.3

APPENDIX C

TEMPERATURE DATA AND HISTOGRAMS

APPENDIX C. NUMBER OF PASSES RECORDED IN 10-DEGREE TEMPERATURE RANGES.

MEASUREMENT TYPE	PASS LEVEL	TEMPERATURE RANGES (°F)							
		LOW - 70 HIGH - 80	80 90	90 100	100 110	110 120	120 130	130 140	140 150
AMBIENT	70	0	44	26	0	0	0	0	0
AMBIENT	112	0	86	26	0	0	0	0	0
AMBIENT	220	0	194	26	0	0	0	0	0
AMBIENT	420	0	394	26	0	0	0	0	0
AMBIENT	448	0	422	26	0	0	0	0	0
AMBIENT	882	0	678	202	0	0	0	0	0
AMBIENT	1554	77	1033	428	12	0	0	0	0
AMBIENT	2324	199	1669	437	12	0	0	0	0
AMBIENT	2589	199	1864	507	12	0	0	0	0
AMBIENT	3049	199	2186	630	12	0	0	0	0
AMBIENT	3286	199	2190	863	12	0	0	0	0
AMBIENT	3942	199	2574	1135	12	0	0	0	0
AMBIENT	4784	199	2817	1730	12	0	0	0	0
AMBIENT	5137	220	3082	1794	12	0	0	0	0
AMBIENT	5370	220	3185	1924	12	0	0	0	0
AMBIENT	5817	220	3353	2203	12	0	0	0	0
AMBIENT	6808	220	3773	2774	12	0	0	0	0
AMBIENT	8080	374	4355	3308	12	0	0	0	0
AMBIENT	9715	461	5894	3308	12	0	0	0	0
AMBIENT	10350	535	6455	3308	12	0	0	0	0
SURFACE	70	0	0	4	18	22	10	16	0
SURFACE	112	0	0	12	34	22	28	16	0
SURFACE	220	0	0	21	38	66	69	26	0
SURFACE	420	0	0	21	89	138	120	52	0
SURFACE	448	0	0	21	103	152	120	52	0
SURFACE	882	0	0	39	178	244	345	74	0
SURFACE	1554	0	71	124	293	422	498	142	0
SURFACE	2324	0	165	211	509	668	622	142	0
SURFACE	2589	0	173	258	535	740	734	142	0
SURFACE	3049	0	233	349	651	789	799	206	0
SURFACE	3286	0	233	349	655	805	900	322	0
SURFACE	3942	0	233	503	740	977	975	467	25
SURFACE	4784	0	244	613	880	1111	1130	755	25
SURFACE	5137	0	244	735	937	1211	1201	755	25
SURFACE	5370	0	244	735	937	1211	1341	848	25
SURFACE	5817	0	259	780	1045	1251	1580	848	25
SURFACE	6808	0	259	880	1187	1431	2051	946	25
SURFACE	8080	0	351	984	1313	1689	2741	946	25
SURFACE	9715	0	351	1374	1815	2209	2955	946	25
SURFACE	10350	0	351	1820	1869	2291	2955	946	25

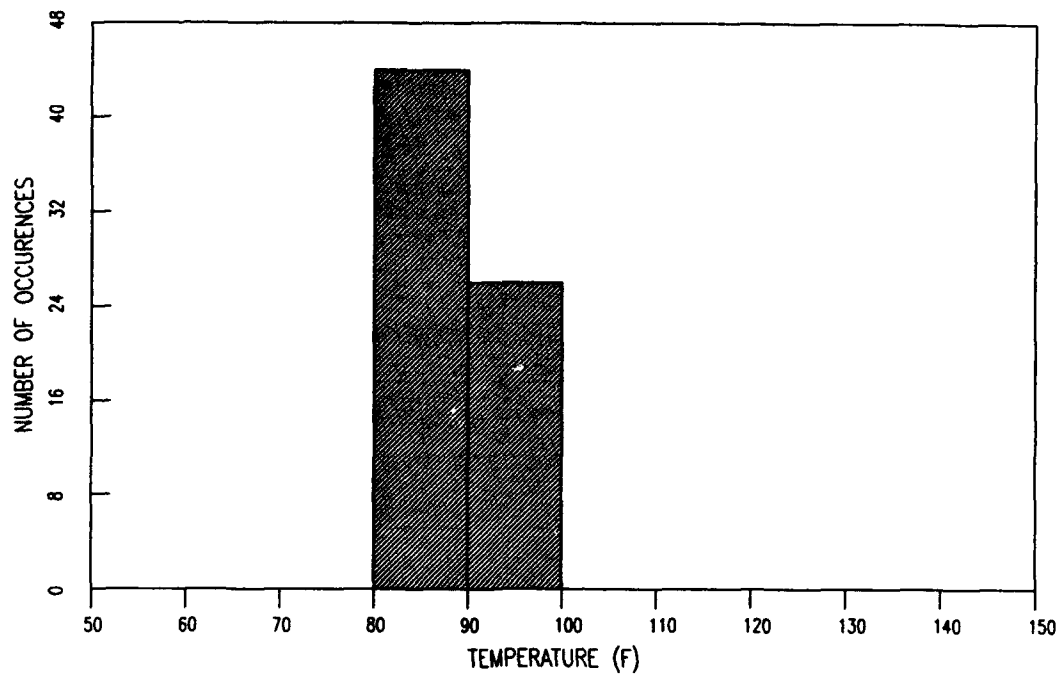
APPENDIX C. NUMBER OF PASSES RECORDED IN 10-DEGREE TEMPERATURE RANGES.

MEASUREMENT TYPE	PASS LEVEL	TEMPERATURE RANGES (°F)							
		LOW - 70 HIGH - 80	80 90	90 100	100 110	110 120	120 130	130 140	140 150
MIDHEIGHT	70	0	0	24	20	19	7	0	0
MIDHEIGHT	112	0	0	48	22	35	7	0	0
MIDHEIGHT	220	0	0	90	64	59	7	0	0
MIDHEIGHT	420	0	0	134	160	68	58	0	0
MIDHEIGHT	448	0	0	148	174	68	58	0	0
MIDHEIGHT	882	0	8	270	241	274	87	0	0
MIDHEIGHT	1554	0	100	435	506	360	149	0	0
MIDHEIGHT	2324	0	260	658	758	492	149	0	0
MIDHEIGHT	2589	0	285	743	794	611	149	0	0
MIDHEIGHT	3049	0	309	991	842	694	191	0	0
MIDHEIGHT	3286	0	309	991	873	761	330	0	0
MIDHEIGHT	3942	0	340	1109	1073	904	494	0	0
MIDHEIGHT	4784	0	376	1342	1191	1286	563	0	0
MIDHEIGHT	5137	0	397	1511	1231	1406	563	0	0
MIDHEIGHT	5370	0	397	1511	1268	1602	563	0	0
MIDHEIGHT	5817	0	446	1619	1361	1799	563	0	0
MIDHEIGHT	6808	0	546	1900	1404	2366	563	0	0
MIDHEIGHT	8080	0	786	1982	1818	2900	563	0	0
MIDHEIGHT	9715	0	1204	2254	2685	2969	563	0	0
MIDHEIGHT	10350	0	1443	2554	2781	2969	563	0	0
INTERFACE	70	0	0	42	21	7	0	0	0
INTERFACE	112	0	16	60	29	7	0	0	0
INTERFACE	220	0	16	144	53	7	0	0	0
INTERFACE	420	0	16	224	128	52	0	0	0
INTERFACE	448	0	16	238	142	52	0	0	0
INTERFACE	882	0	55	386	358	81	0	0	0
INTERFACE	1554	0	116	803	505	126	0	0	0
INTERFACE	2324	0	386	1083	722	126	0	0	0
INTERFACE	2589	0	401	1231	824	126	0	0	0
INTERFACE	3049	0	430	1522	921	154	0	0	0
INTERFACE	3286	0	430	1553	988	293	0	0	0
INTERFACE	3942	0	434	1793	1246	447	0	0	0
INTERFACE	4784	0	469	2130	1562	597	0	0	0
INTERFACE	5137	0	547	2282	1682	597	0	0	0
INTERFACE	5370	0	547	2319	1878	597	0	0	0
INTERFACE	5817	0	547	2526	2118	597	0	0	0
INTERFACE	6808	0	587	2909	2589	694	0	0	0
INTERFACE	8080	0	909	3380	2987	773	0	0	0
INTERFACE	9715	9	1479	4364	3050	773	0	0	0
INTERFACE	10350	9	1963	4515	3050	773	0	0	0

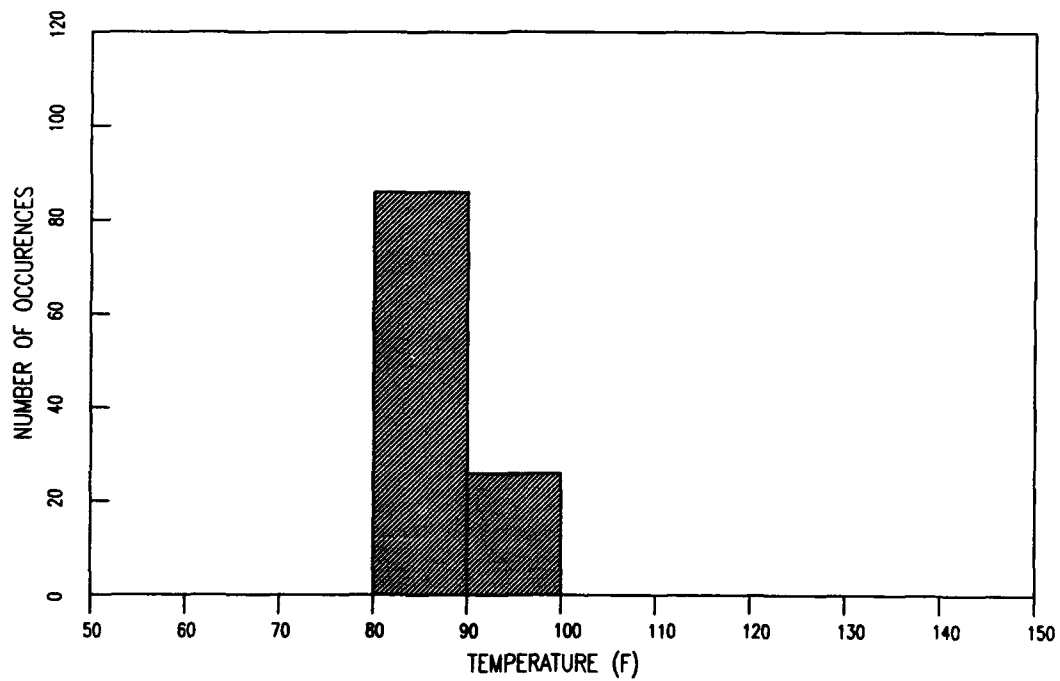
APPENDIX C. NUMBER OF PASSES RECORDED IN 10-DEGREE TEMPERATURE RANGES.

MEASUREMENT TYPE	PASS LEVEL	TEMPERATURE RANGES (°F)							
		LOW - 70 HIGH - 80	80 90	90 100	100 110	110 120	120 130	130 140	140 150
6 INCH	70	0	0	70	0	0	0	0	0
6 INCH	112	0	34	78	0	0	0	0	0
6 INCH	220	0	48	172	0	0	0	0	0
6 INCH	420	0	48	372	0	0	0	0	0
6 INCH	448	0	48	400	0	0	0	0	0
6 INCH	882	0	108	772	0	0	0	0	0
6 INCH	1554	0	108	1442	0	0	0	0	0
6 INCH	2324	0	236	2081	0	0	0	0	0
6 INCH	2589	0	236	2346	0	0	0	0	0
6 INCH	3049	0	236	2791	0	0	0	0	0
6 INCH	3286	0	236	3028	0	0	0	0	0
6 INCH	3942	0	236	3684	0	0	0	0	0
6 INCH	4784	0	250	4508	0	0	0	0	0
6 INCH	5137	0	250	4858	0	0	0	0	0
6 INCH	5370	0	250	5091	0	0	0	0	0
6 INCH	5817	0	250	5538	0	0	0	0	0
6 INCH	6808	0	250	6529	0	0	0	0	0
6 INCH	8080	0	250	7799	0	0	0	0	0
6 INCH	9715	0	1576	8099	0	0	0	0	0
6 INCH	10350	0	2211	8099	0	0	0	0	0
12 INCH	70	0	42	28	0	0	0	0	0
12 INCH	112	0	84	28	0	0	0	0	0
12 INCH	220	0	192	28	0	0	0	0	0
12 INCH	420	0	392	28	0	0	0	0	0
12 INCH	448	0	420	28	0	0	0	0	0
12 INCH	882	0	651	229	0	0	0	0	0
12 INCH	1554	1	785	764	0	0	0	0	0
12 INCH	2324	1	1083	1233	0	0	0	0	0
12 INCH	2589	1	1083	1498	0	0	0	0	0
12 INCH	3049	1	1083	1943	0	0	0	0	0
12 INCH	3286	1	1083	2137	43	0	0	0	0
12 INCH	3942	1	1083	2715	121	0	0	0	0
12 INCH	4784	1	1112	3524	121	0	0	0	0
12 INCH	5137	1	1133	3853	121	0	0	0	0
12 INCH	5370	1	1133	4086	121	0	0	0	0
12 INCH	5817	1	1133	4533	121	0	0	0	0
12 INCH	6808	1	1133	5524	121	0	0	0	0
12 INCH	8080	1	1133	6794	121	0	0	0	0
12 INCH	9715	1	2459	7094	121	0	0	0	0
12 INCH	10350	1	3094	7094	121	0	0	0	0

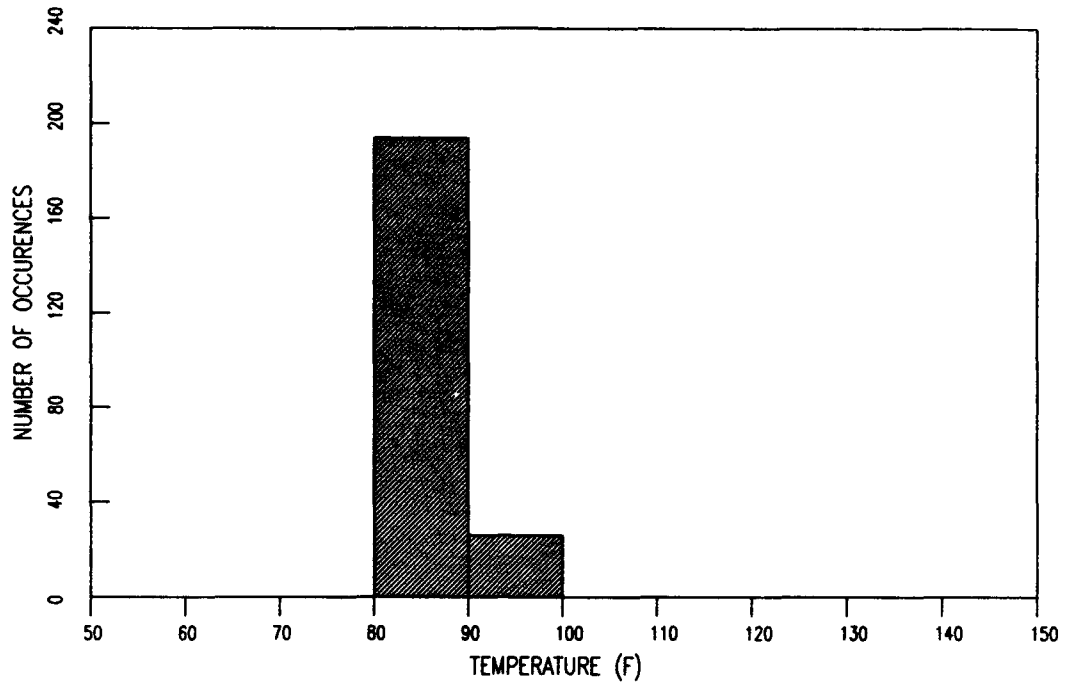
AMBIENT TEMPERATURE HISTOGRAM FOR PASS LEVEL 70



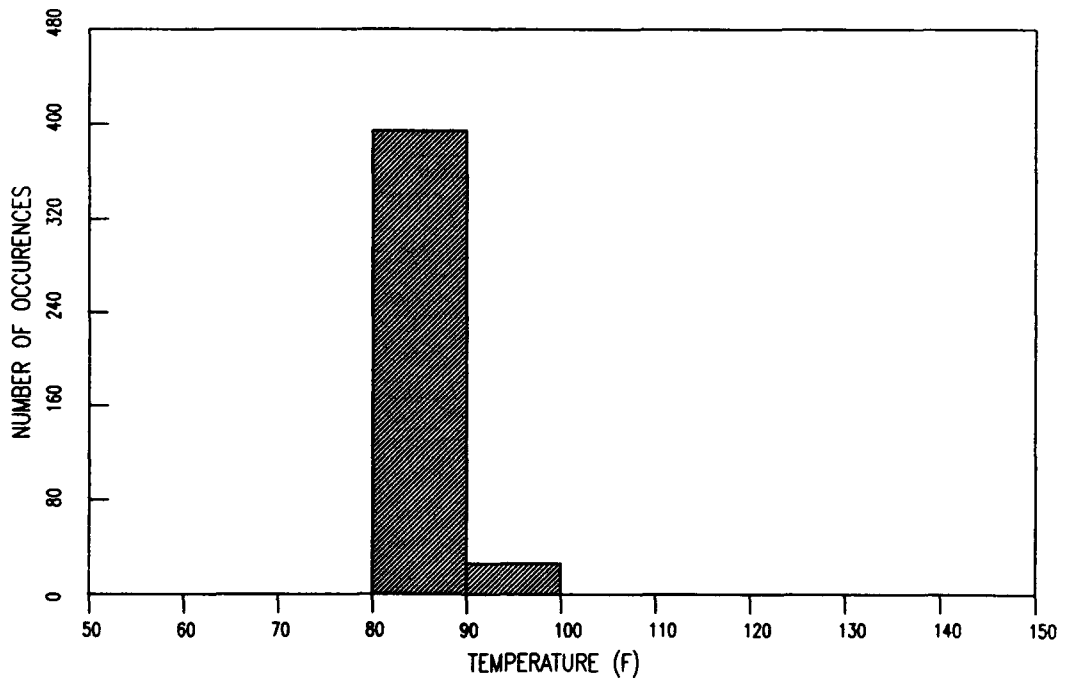
AMBIENT TEMPERATURE HISTOGRAM FOR PASS LEVEL 112



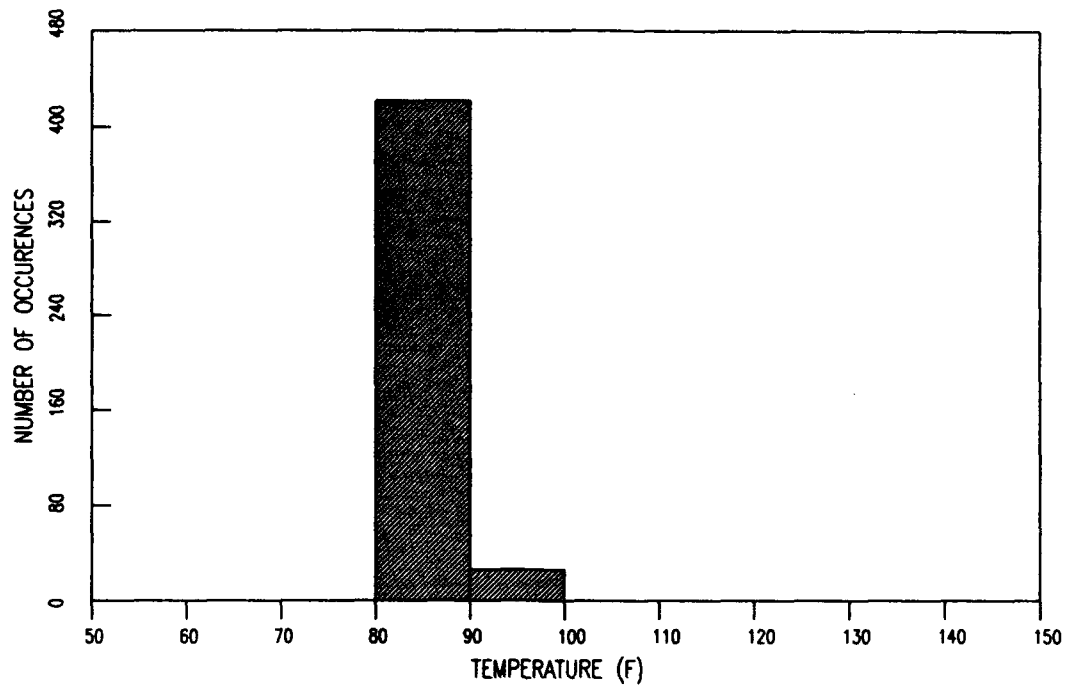
AMBIENT TEMPERATURE HISTOGRAM FOR PASS LEVEL 220



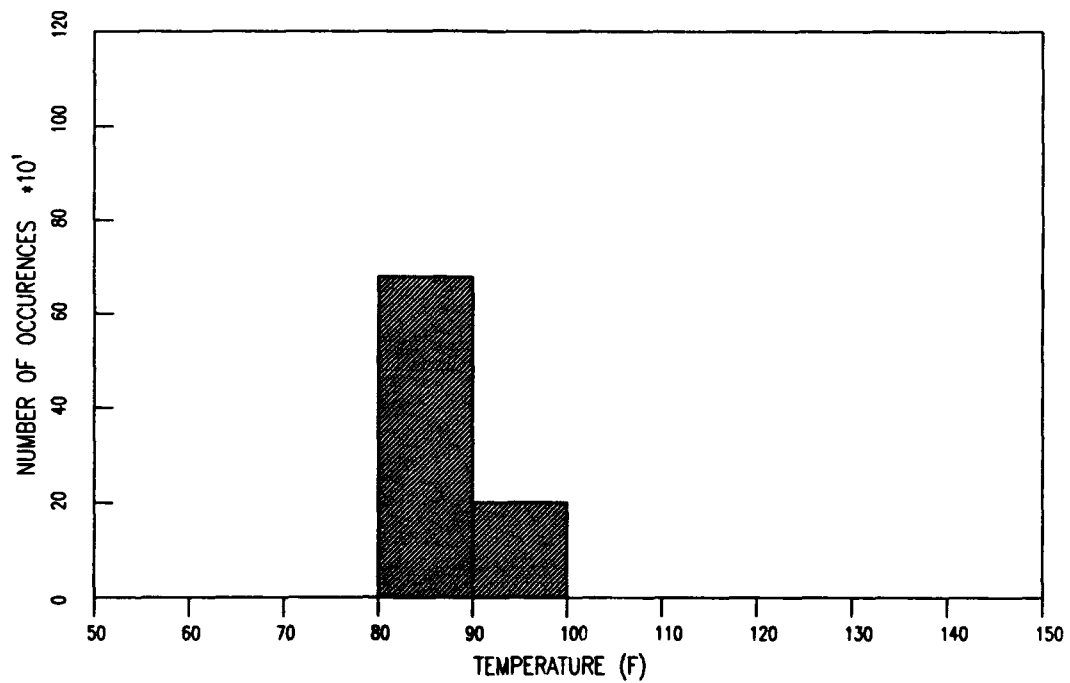
AMBIENT TEMPERATURE HISTOGRAM FOR PASS LEVEL 420



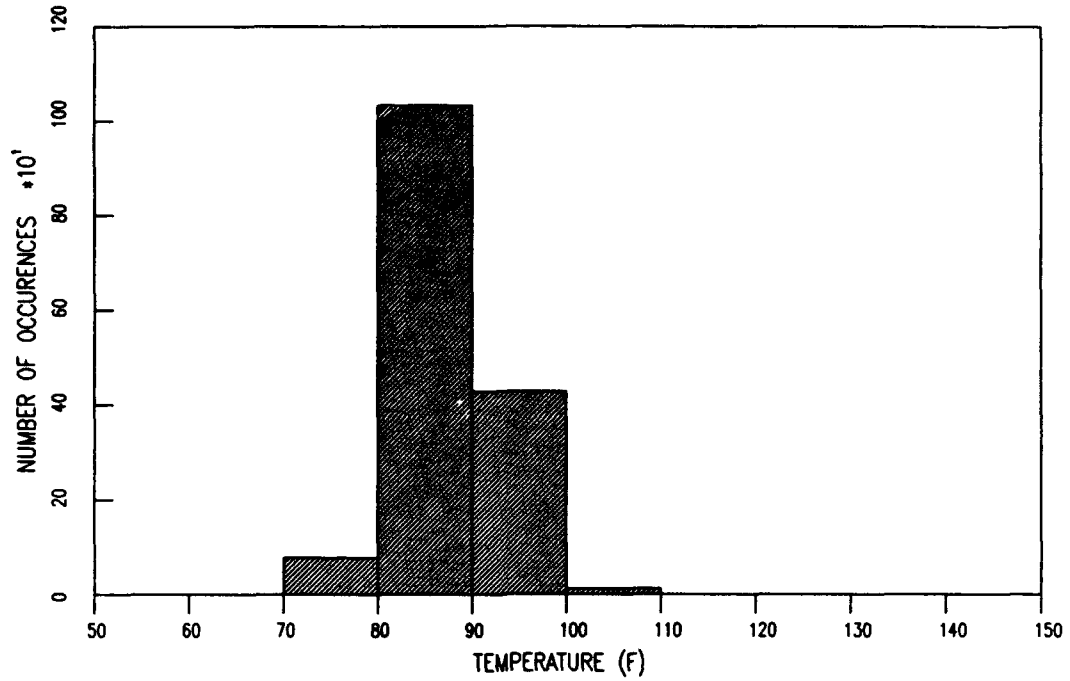
AMBIENT TEMPERATURE HISTOGRAM FOR PASS LEVEL 448



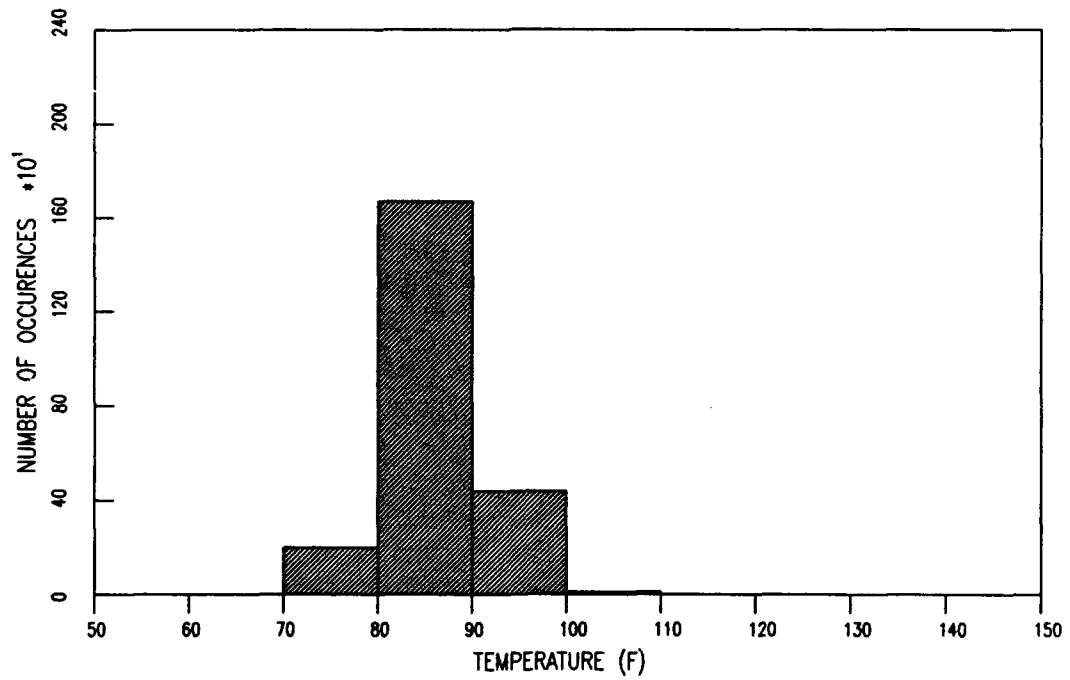
AMBIENT TEMPERATURE HISTOGRAM FOR PASS LEVEL 882



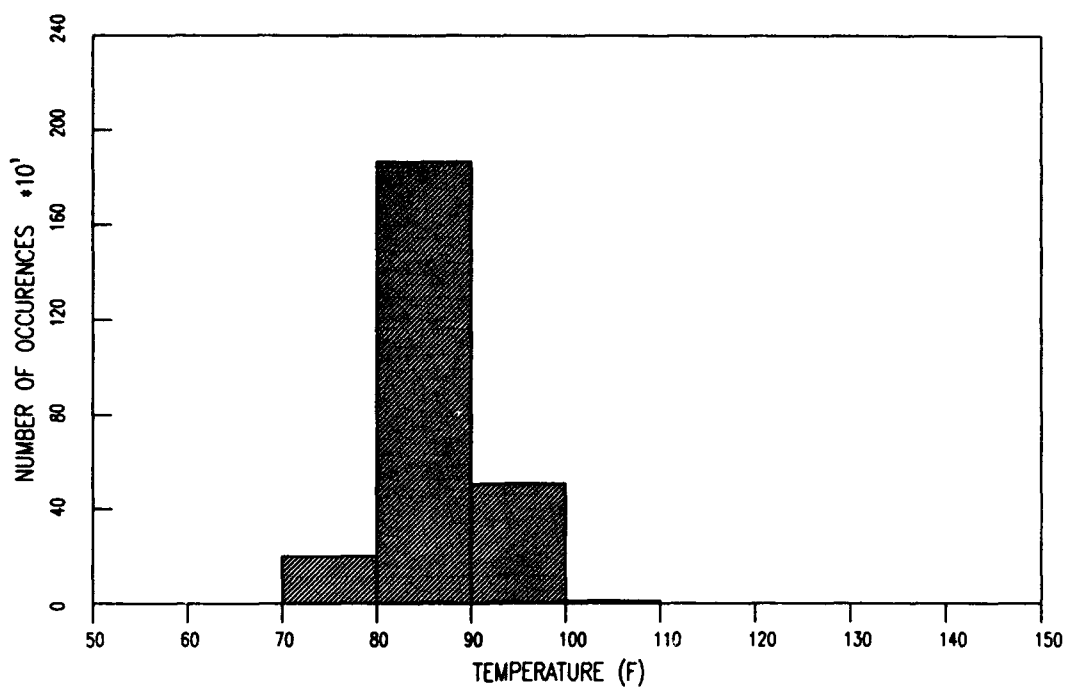
AMBIENT TEMPERATURE HISTOGRAM FOR PASS LEVEL 1554



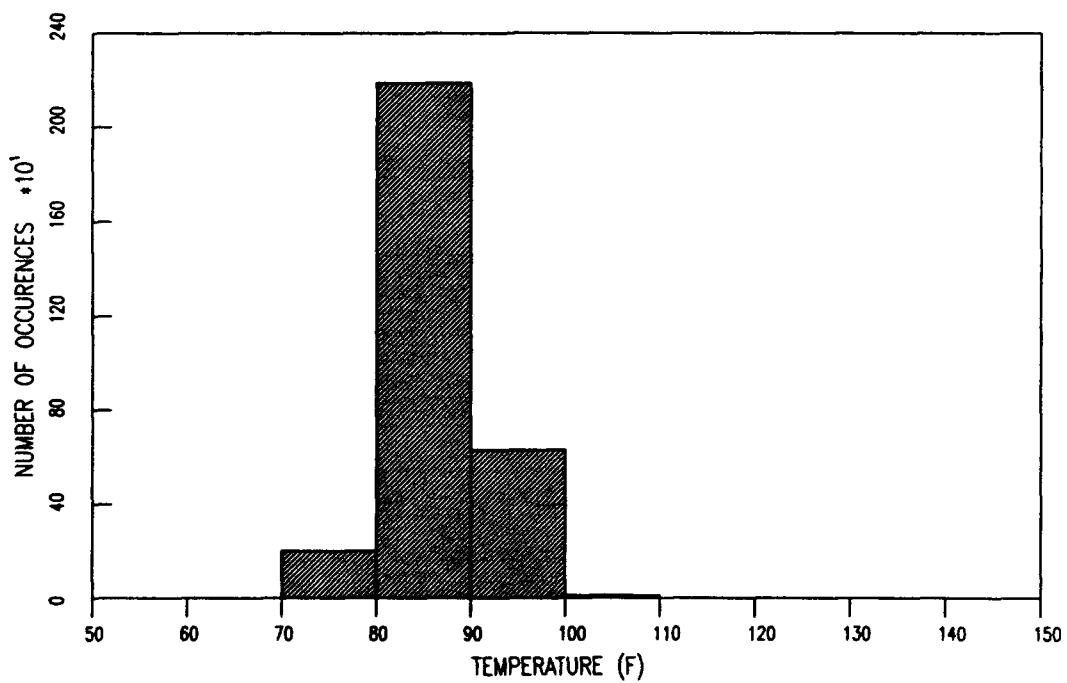
AMBIENT TEMPERATURE HISTOGRAM FOR PASS LEVEL 2324



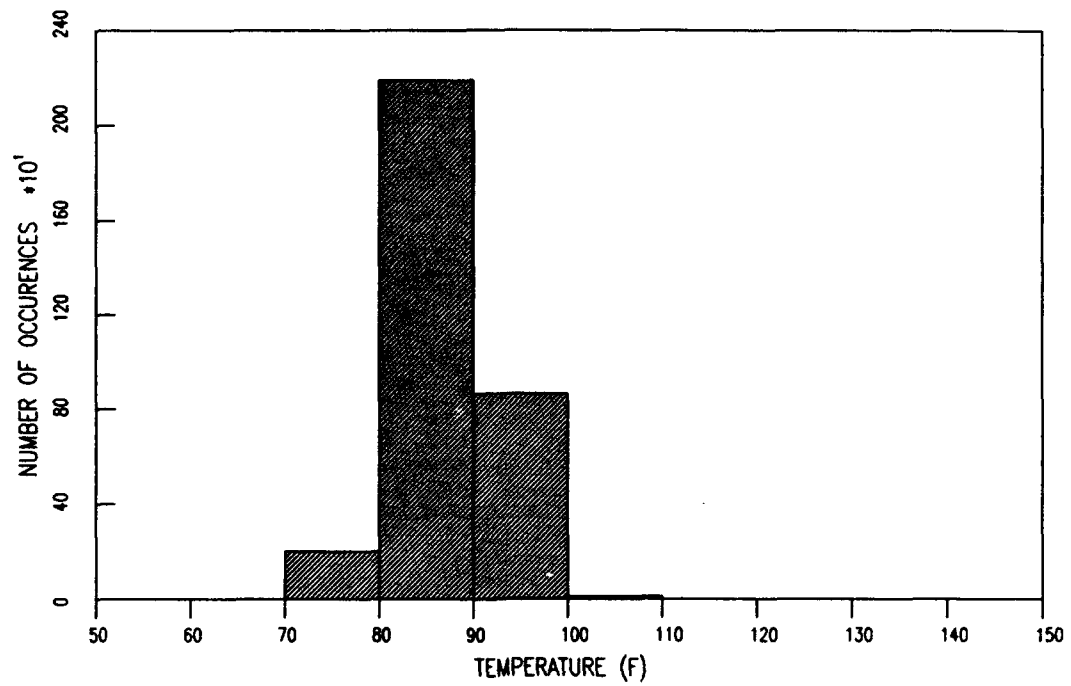
AMBIENT TEMPERATURE HISTOGRAM FOR PASS LEVEL 2589



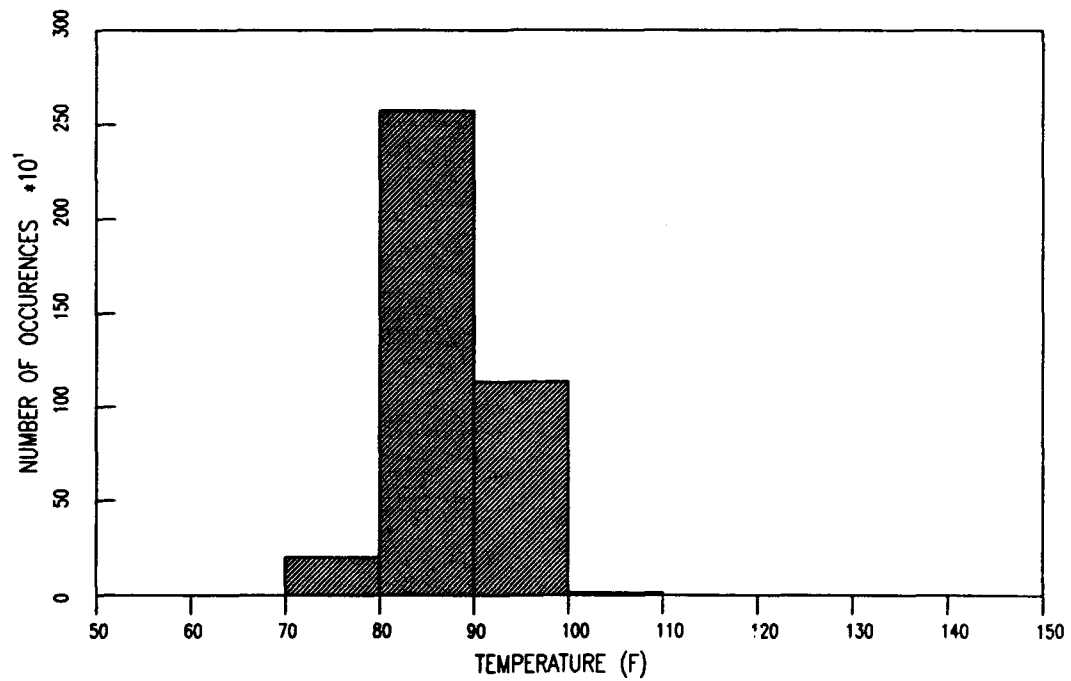
AMBIENT TEMPERATURE HISTOGRAM FOR PASS LEVEL 3049



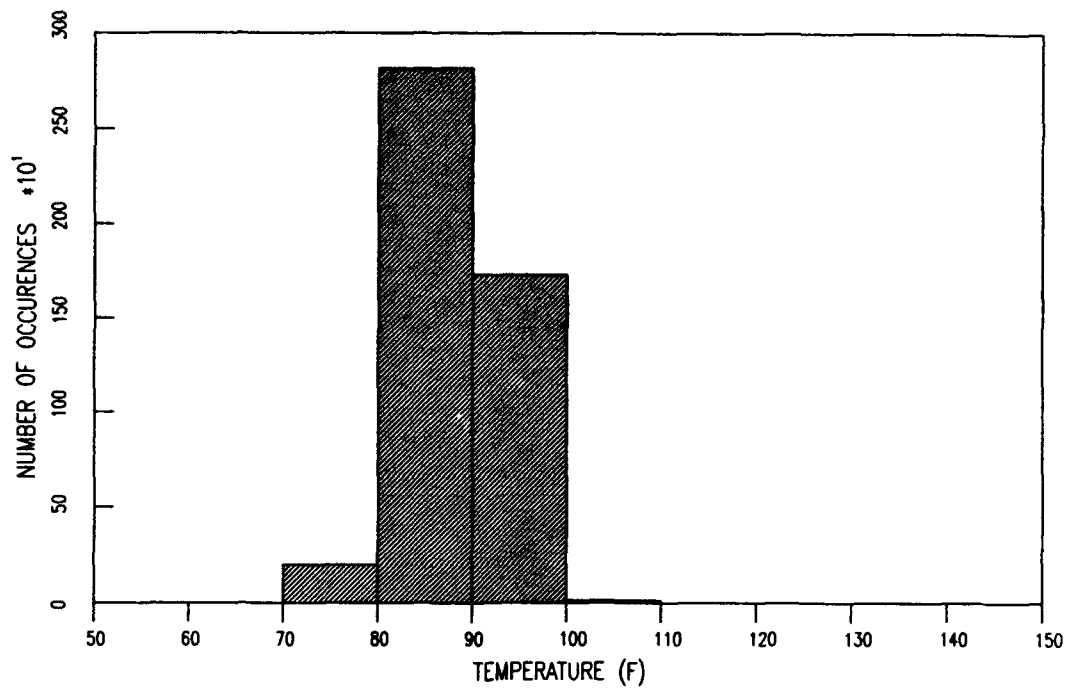
AMBIENT TEMPERATURE HISTOGRAM FOR PASS LEVEL 3286



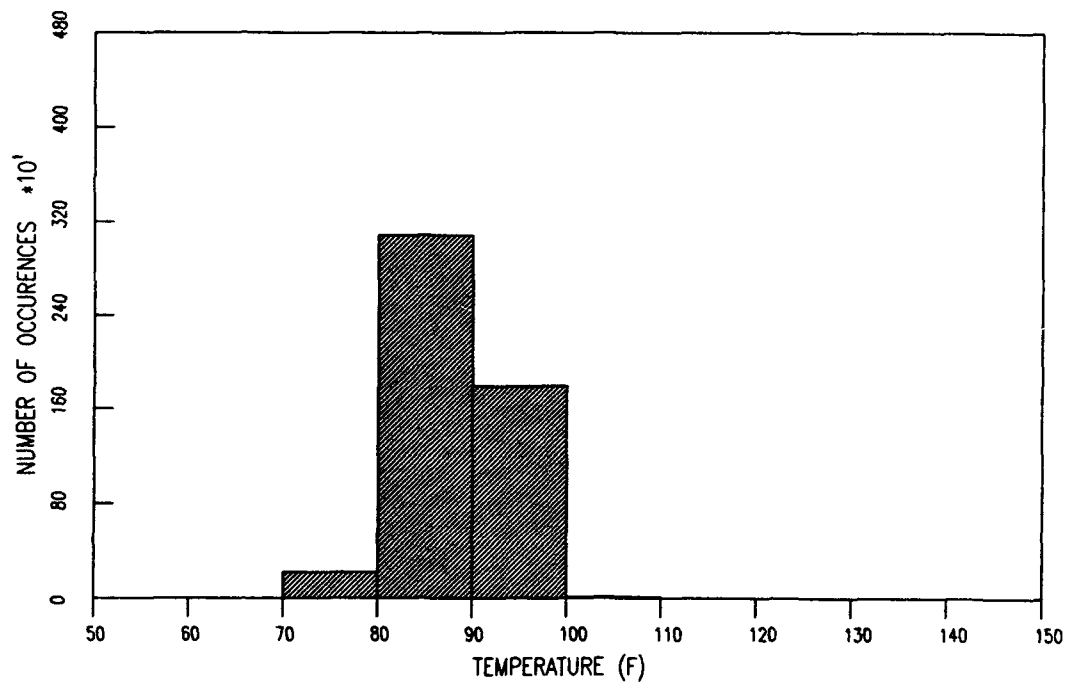
AMBIENT TEMPERATURE HISTOGRAM FOR PASS LEVEL 3942



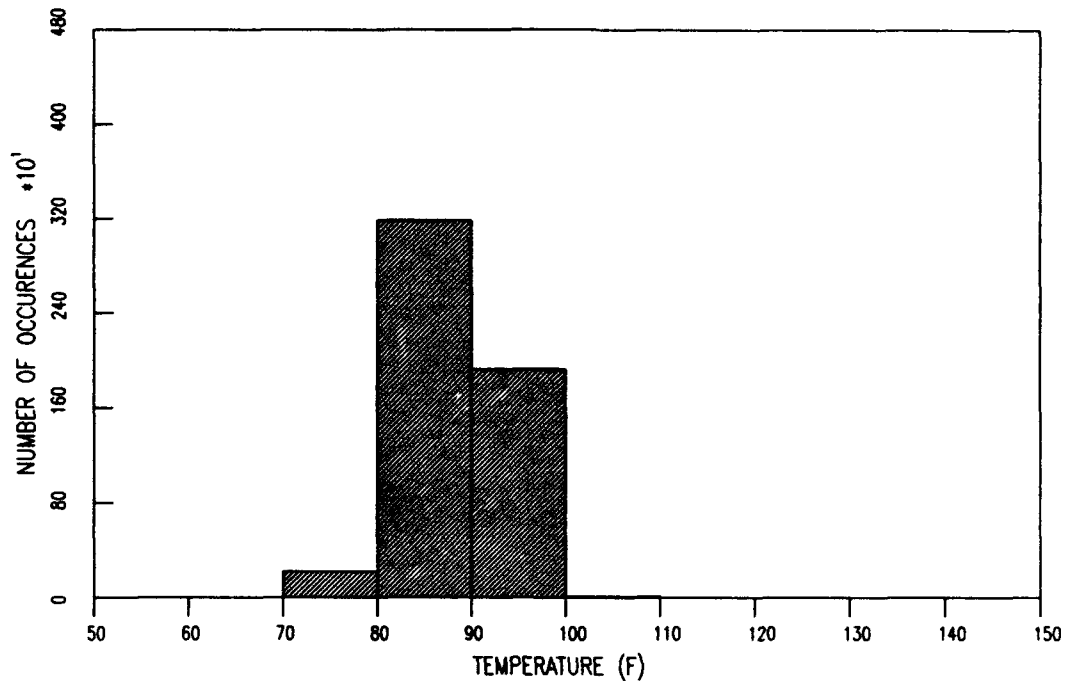
AMBIENT TEMPERATURE HISTOGRAM FOR PASS LEVEL 4784



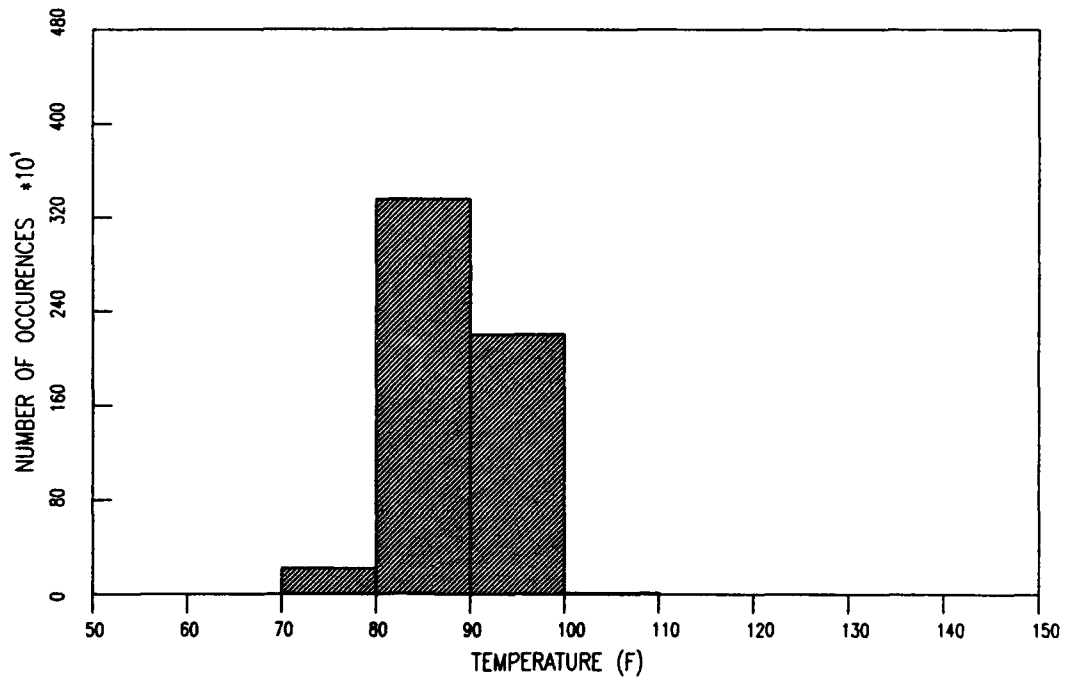
AMBIENT TEMPERATURE HISTOGRAM FOR PASS LEVEL 5137



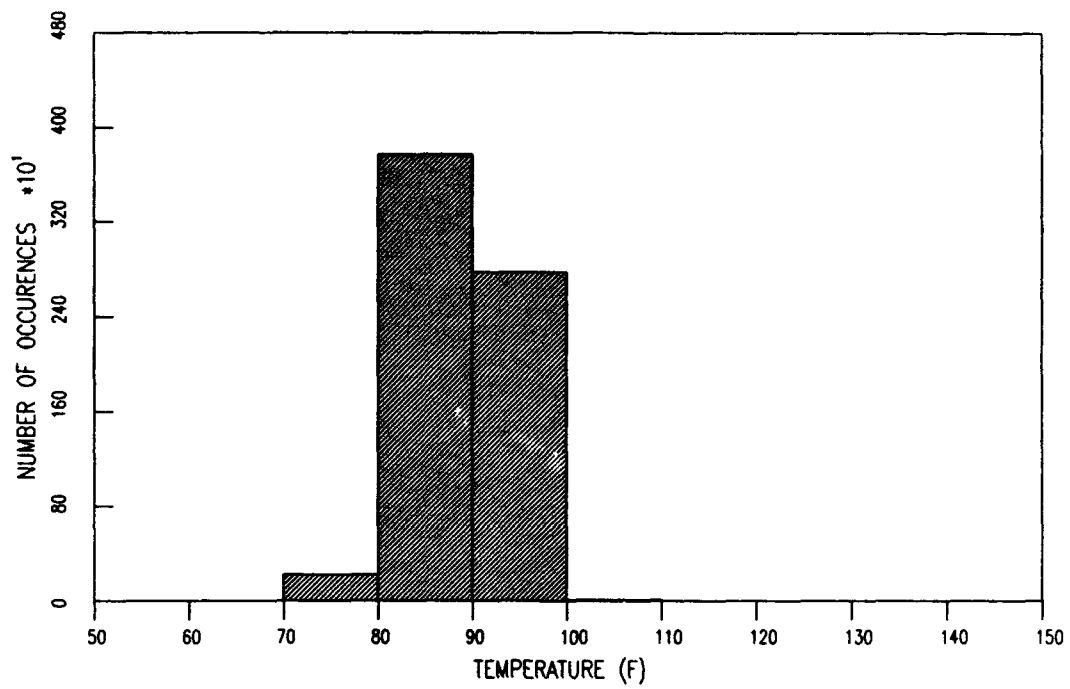
AMBIENT TEMPERATURE HISTOGRAM FOR PASS LEVEL 5370



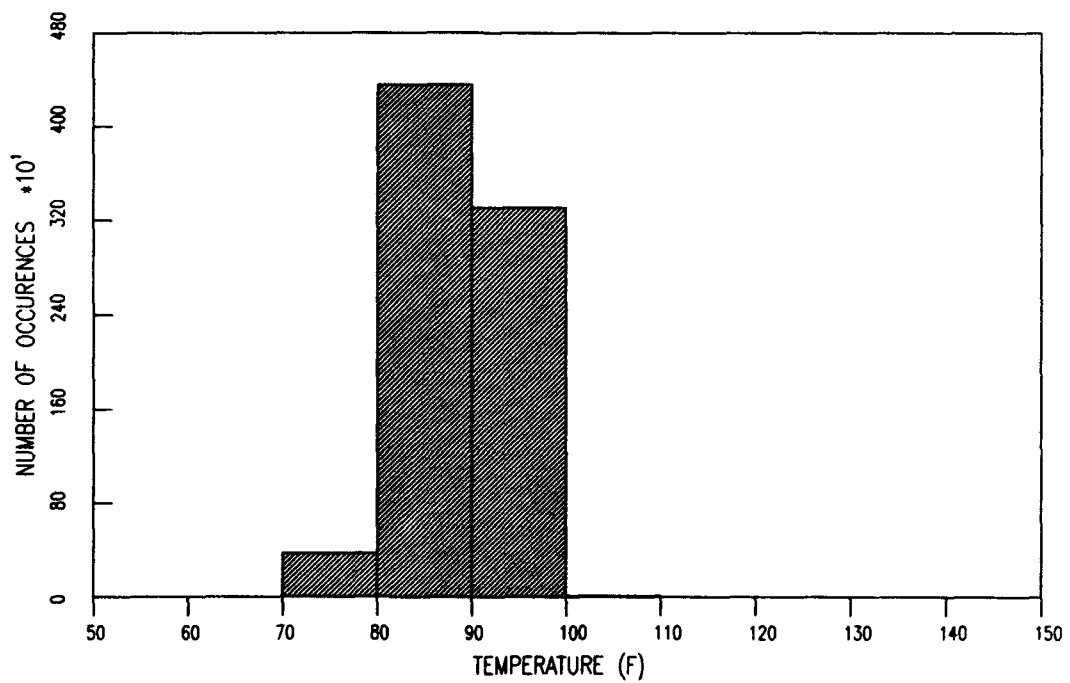
AMBIENT TEMPERATURE HISTOGRAM FOR PASS LEVEL 5817



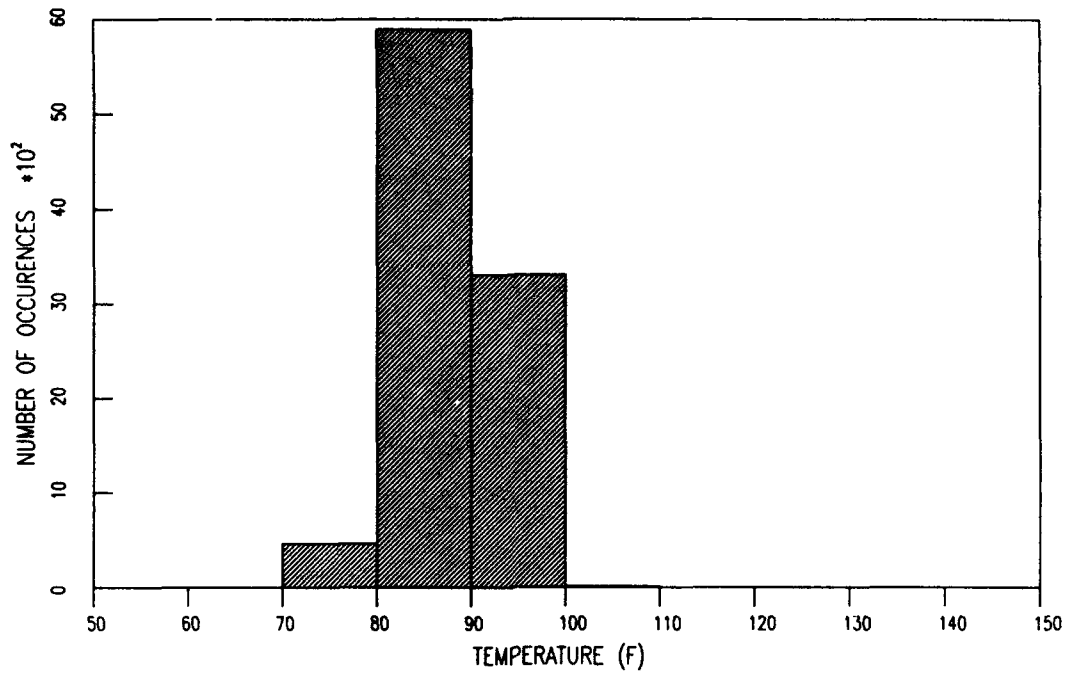
AMBIENT TEMPERATURE HISTOGRAM FOR PASS LEVEL 6808



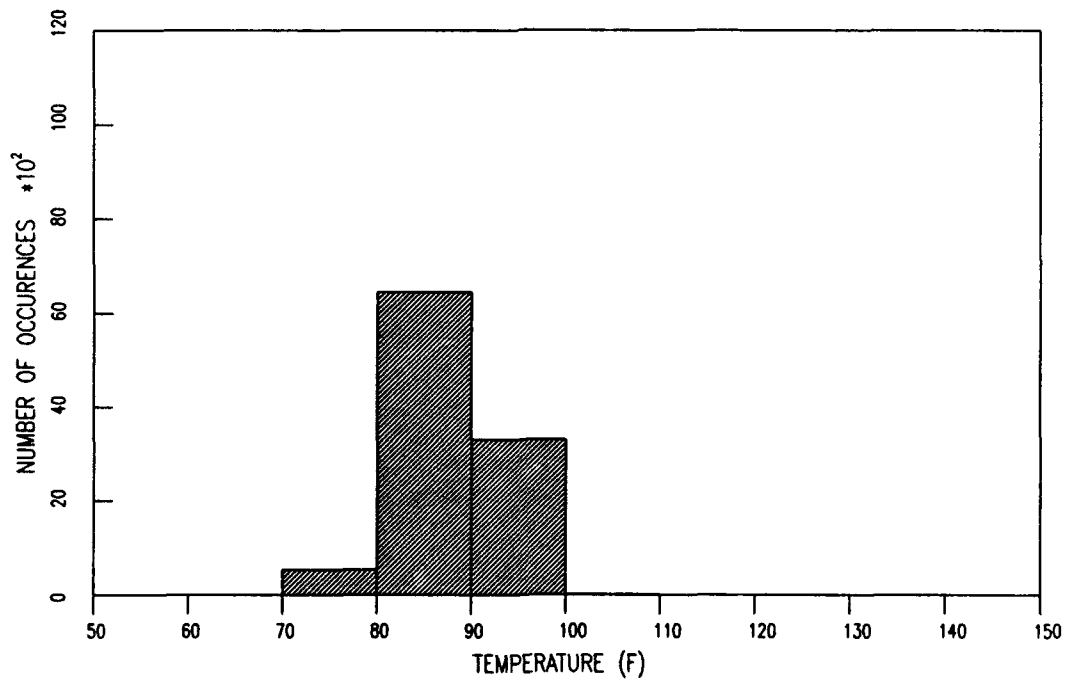
AMBIENT TEMPERATURE HISTOGRAM FOR PASS LEVEL 8080



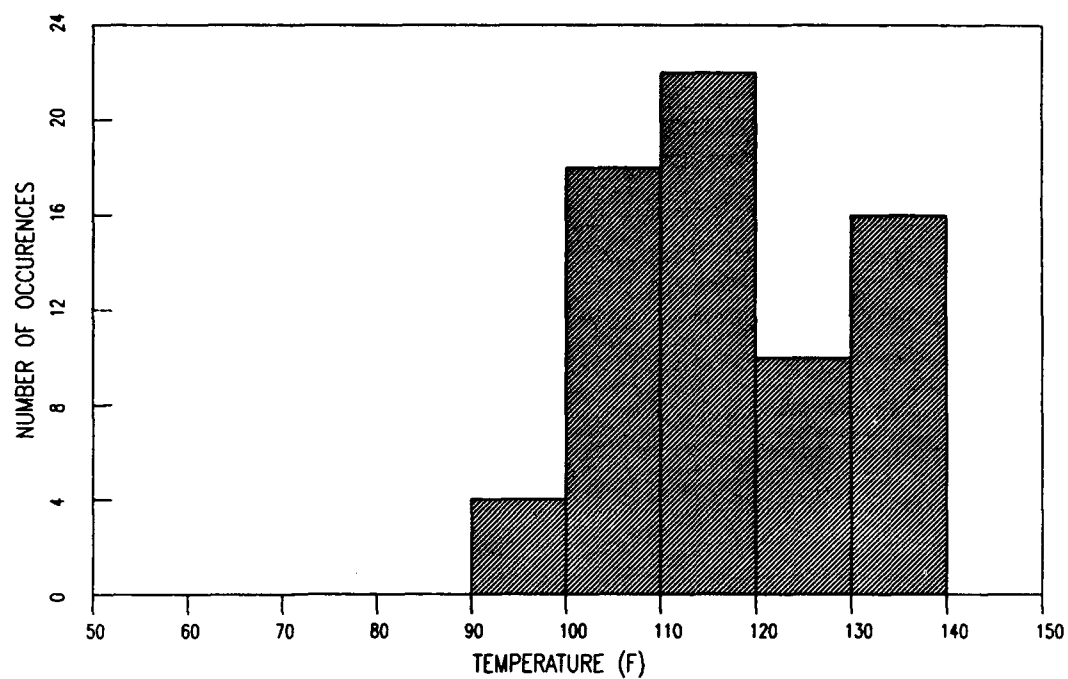
AMBIENT TEMPERATURE HISTOGRAM FOR PASS LEVEL 9715



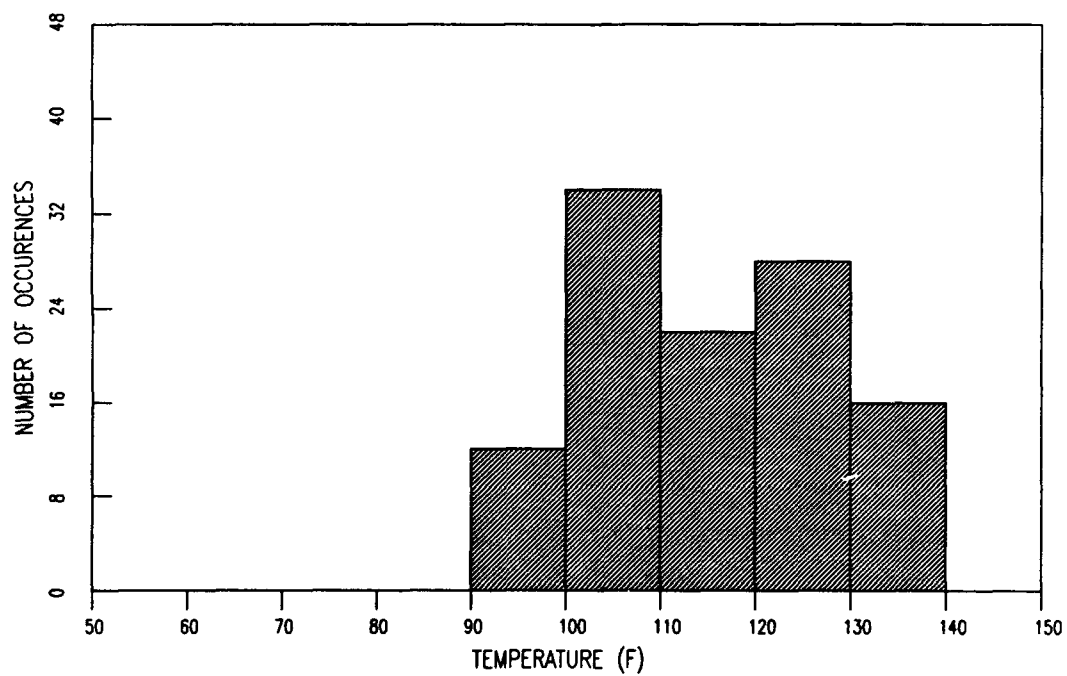
AMBIENT TEMPERATURE HISTOGRAM FOR PASS LEVEL 10350



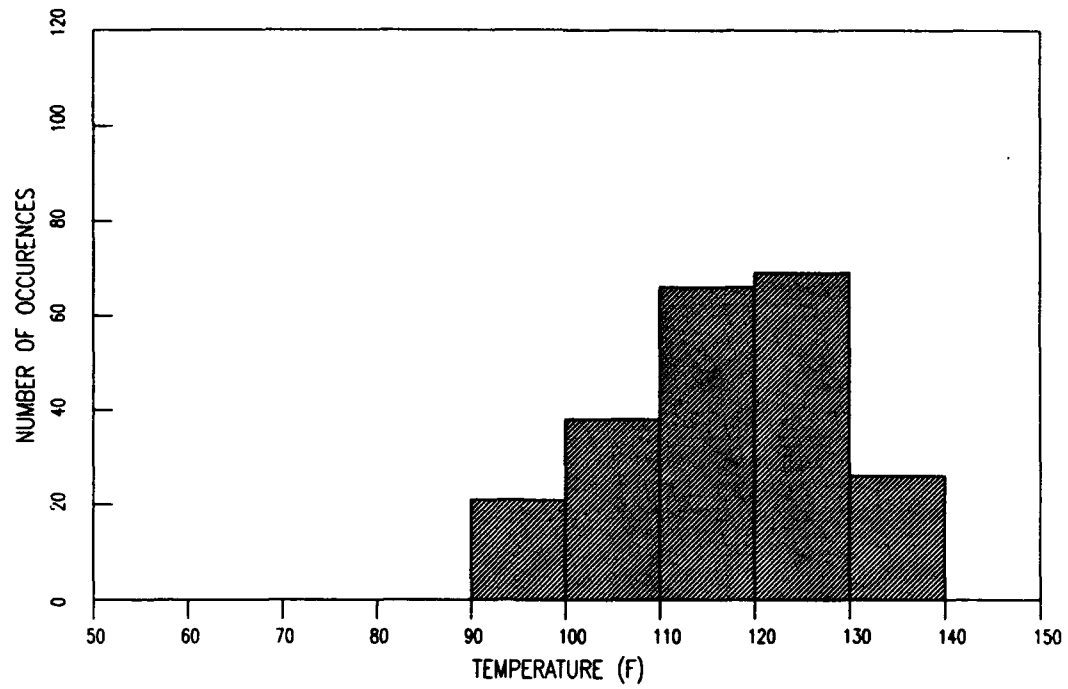
SURFACE TEMPERATURE HISTOGRAM FOR PASS LEVEL 70



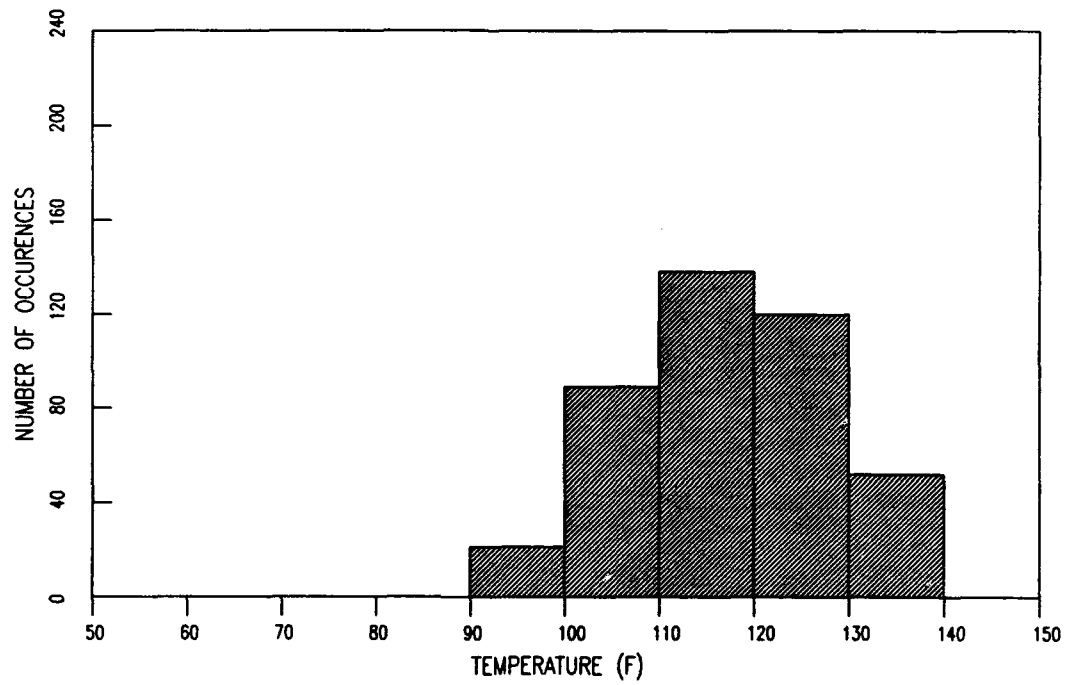
SURFACE TEMPERATURE HISTOGRAM FOR PASS LEVEL 112



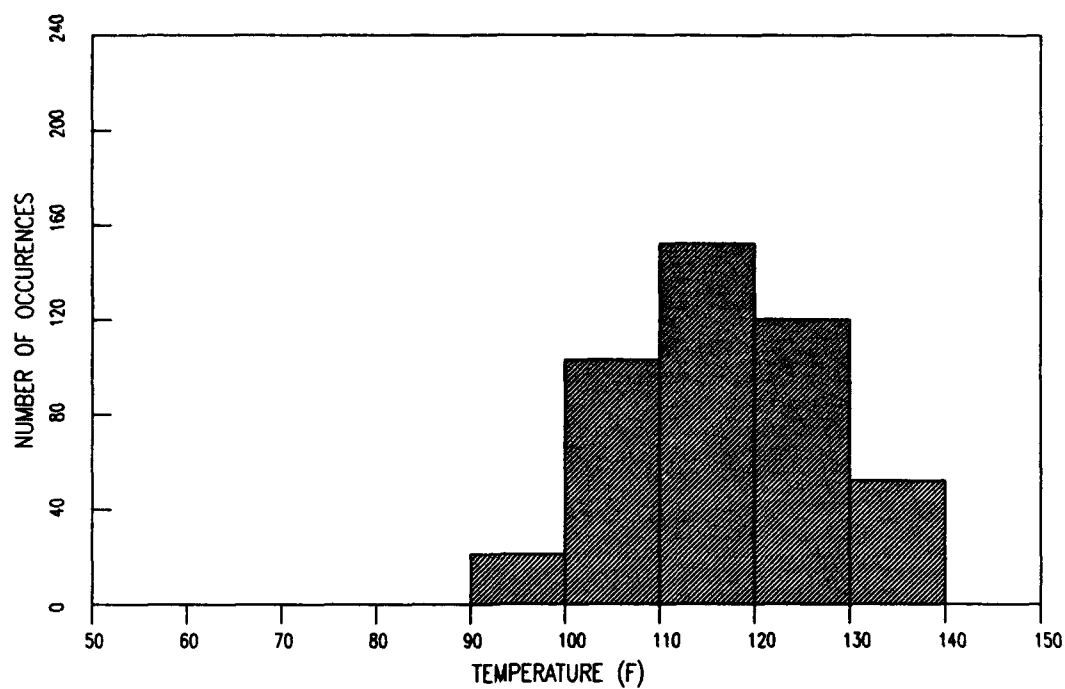
SURFACE TEMPERATURE HISTOGRAM FOR PASS LEVEL 220



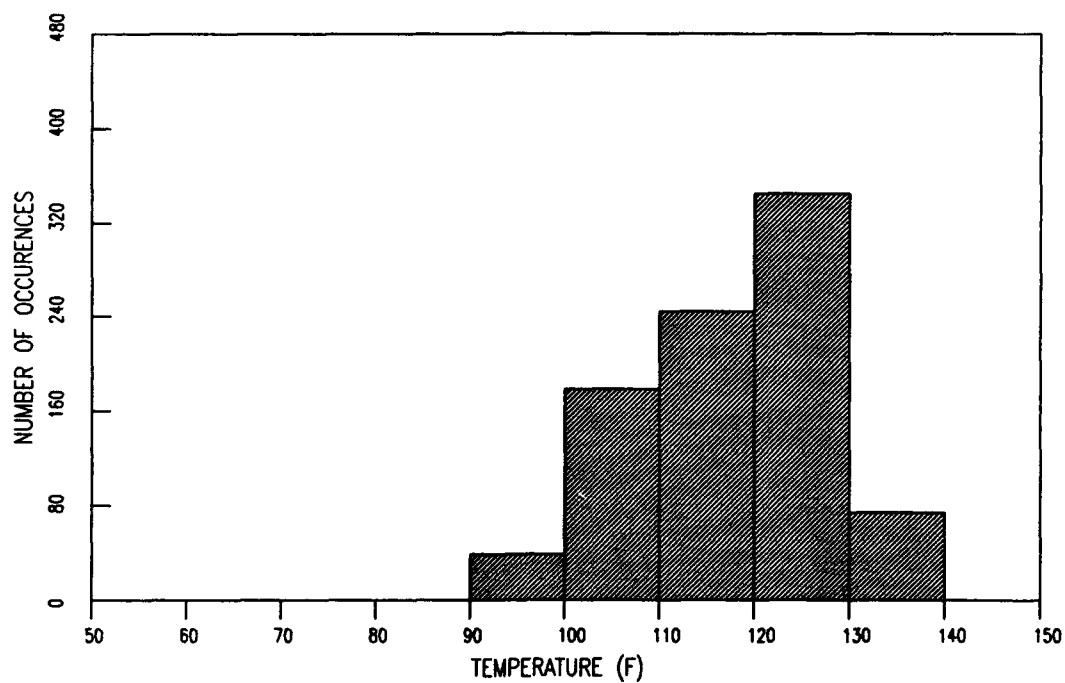
SURFACE TEMPERATURE HISTOGRAM FOR PASS LEVEL 420



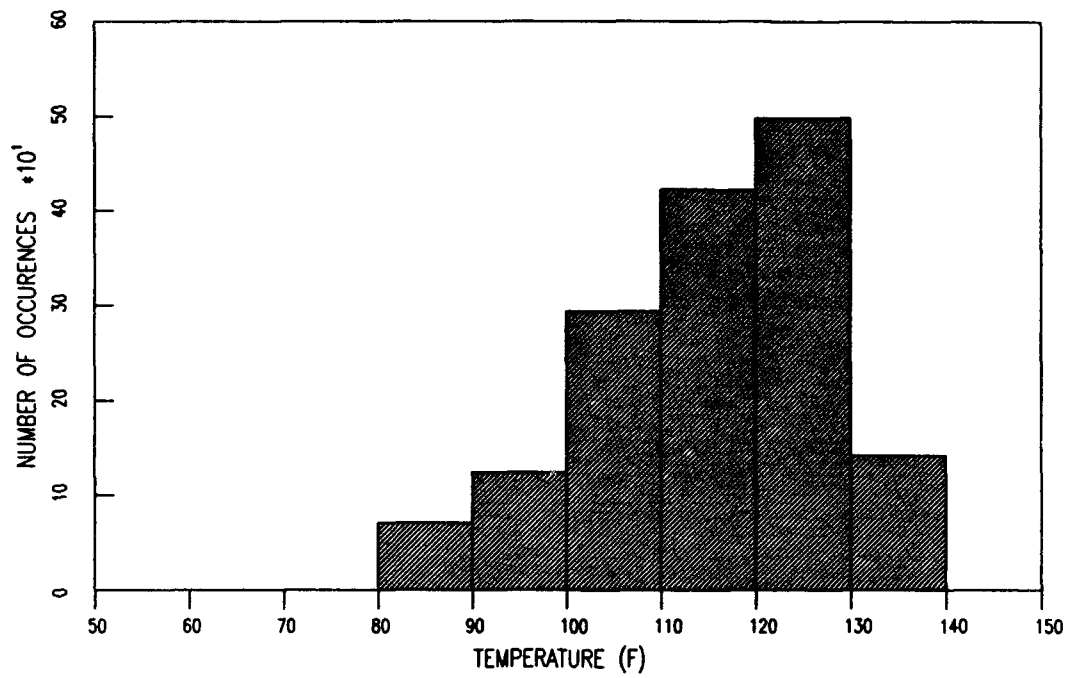
SURFACE TEMPERATURE HISTOGRAM FOR PASS LEVEL 448



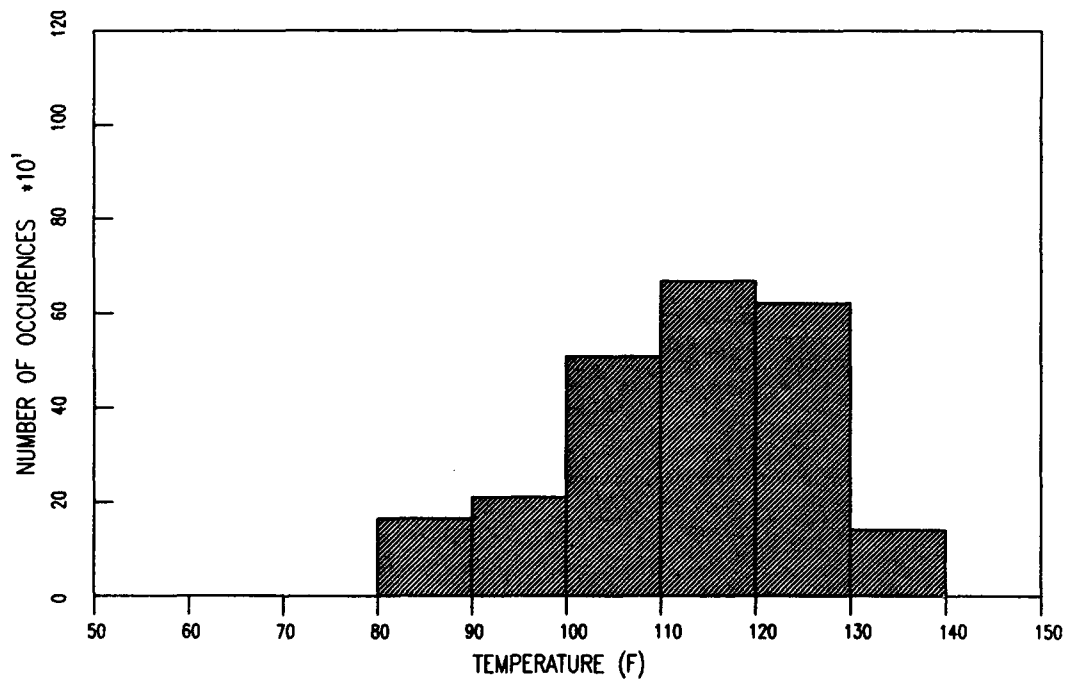
SURFACE TEMPERATURE HISTOGRAM FOR PASS LEVEL 882



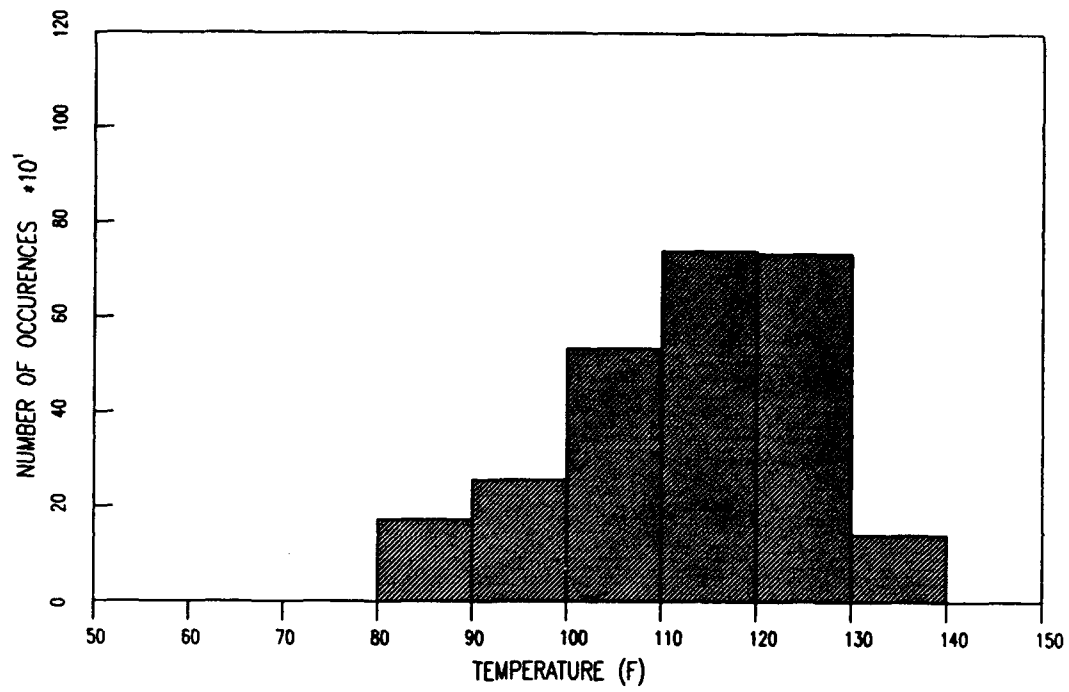
SURFACE TEMPERATURE HISTOGRAM FOR PASS LEVEL 1554



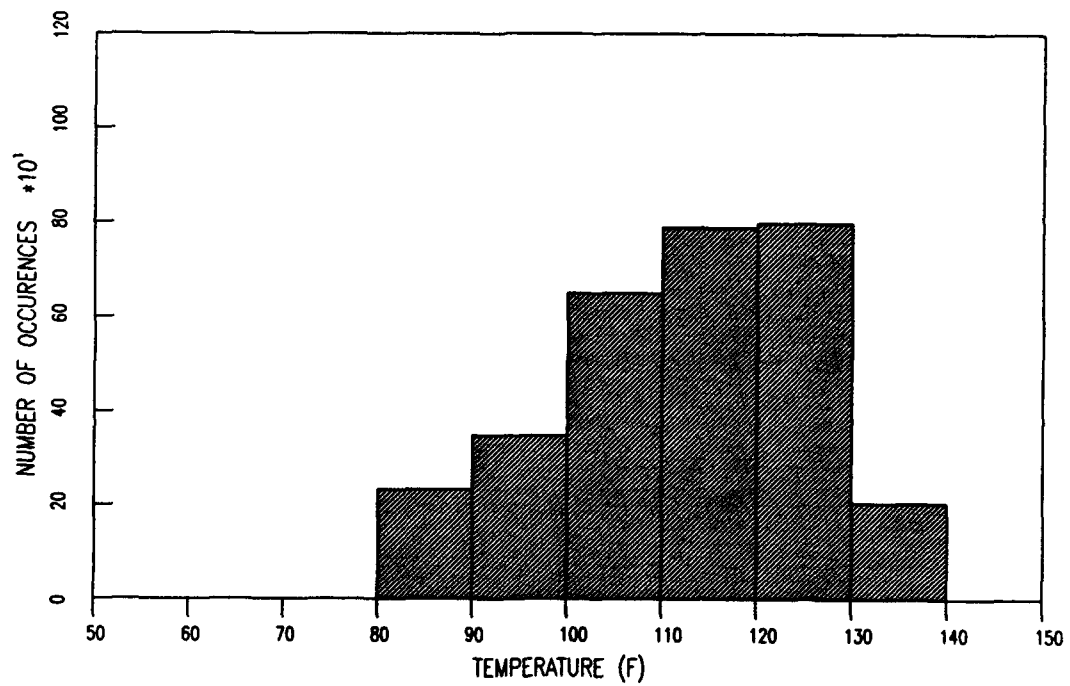
SURFACE TEMPERATURE HISTOGRAM FOR PASS LEVEL 2324



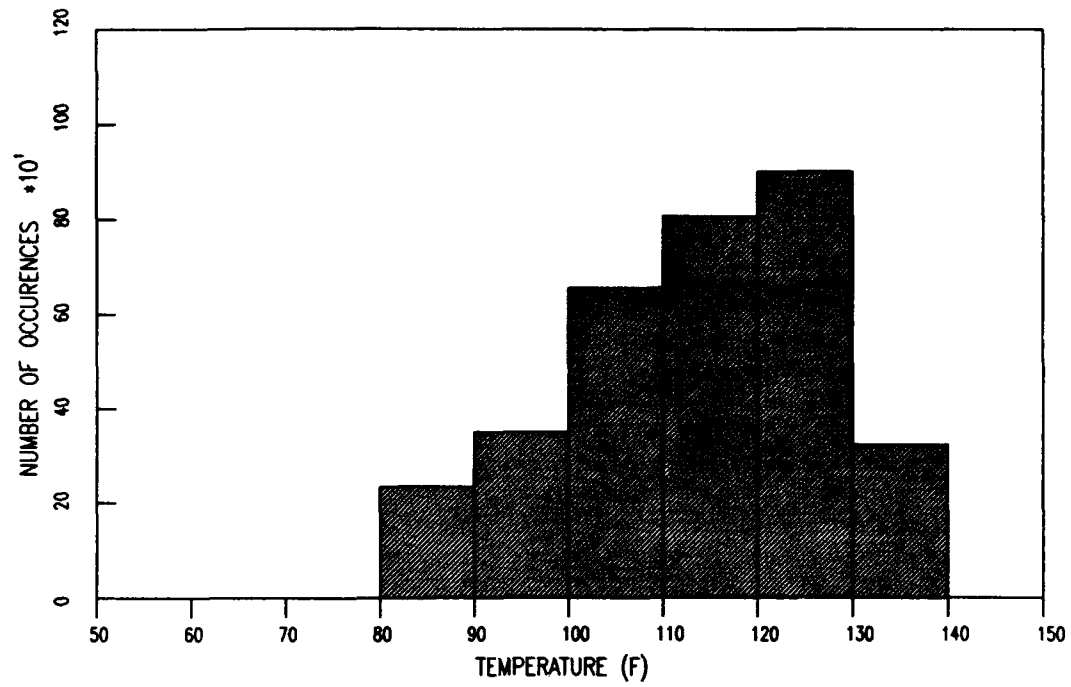
SURFACE TEMPERATURE HISTOGRAM FOR PASS LEVEL 2589



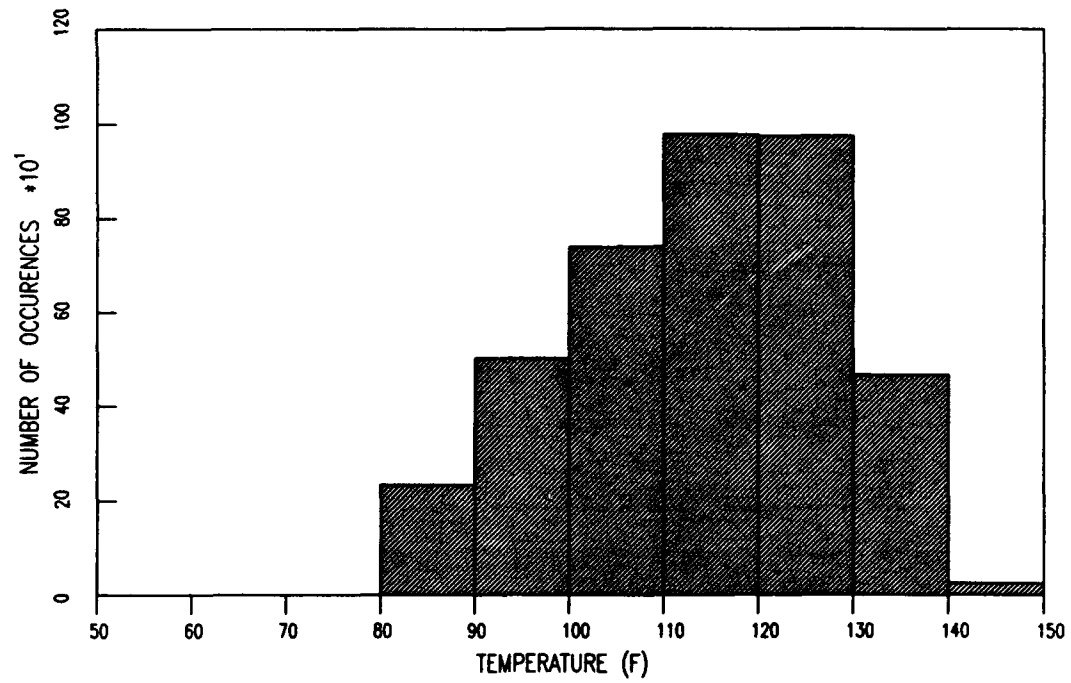
SURFACE TEMPERATURE HISTOGRAM FOR PASS LEVEL 3049



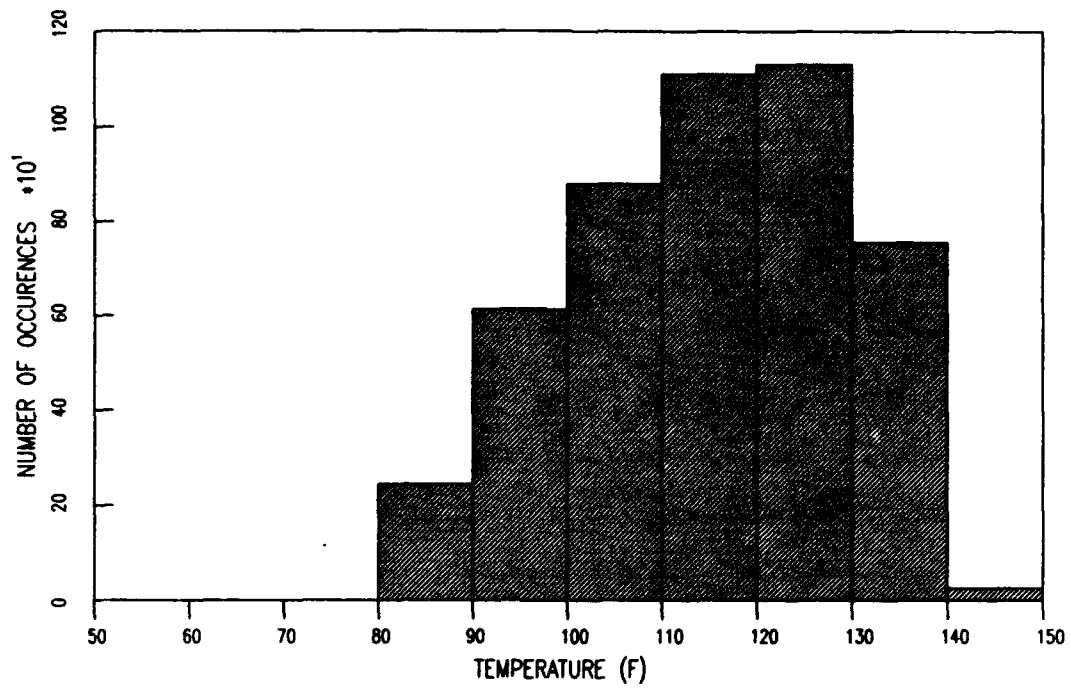
SURFACE TEMPERATURE HISTOGRAM FOR PASS LEVEL 3286



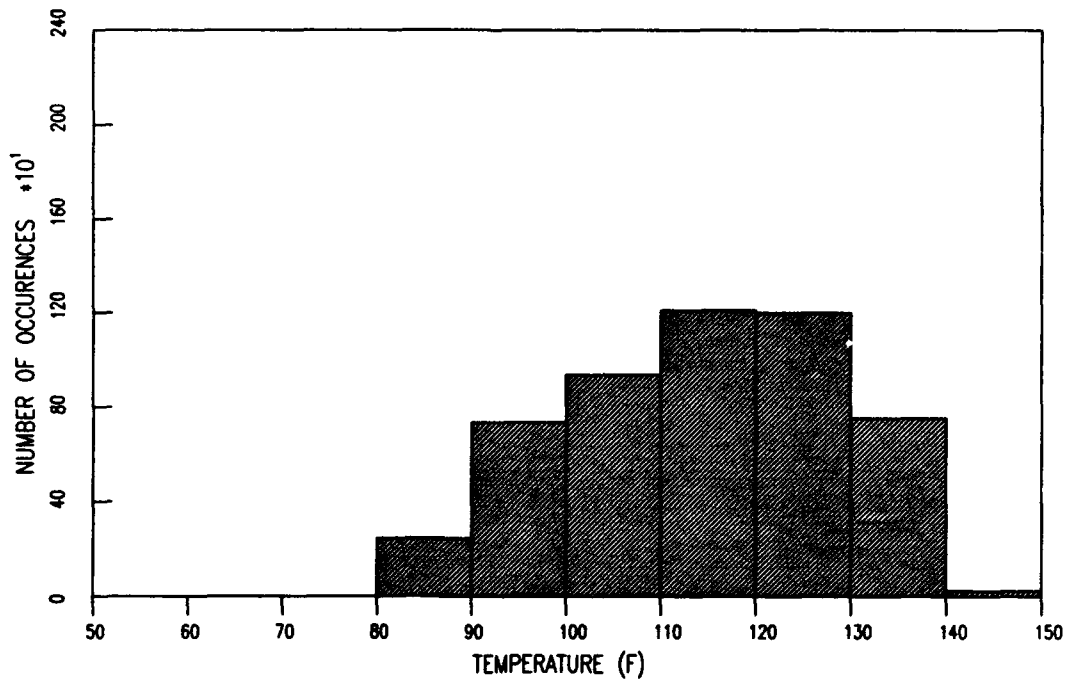
SURFACE TEMPERATURE HISTOGRAM FOR PASS LEVEL 3942



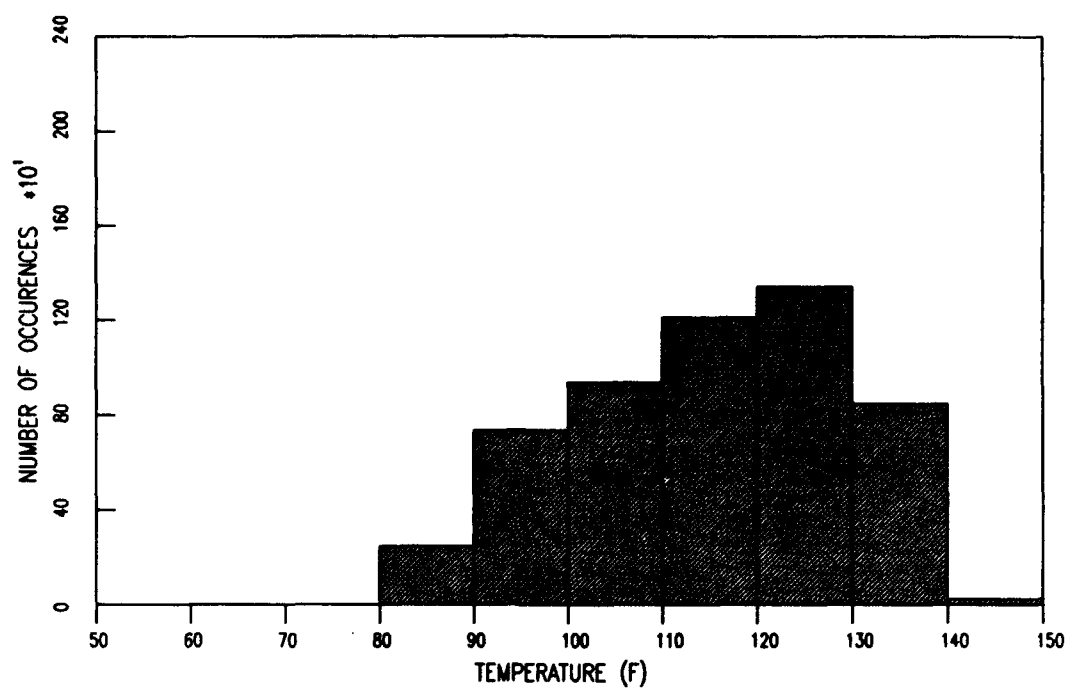
SURFACE TEMPERATURE HISTOGRAM FOR PASS LEVEL 4784



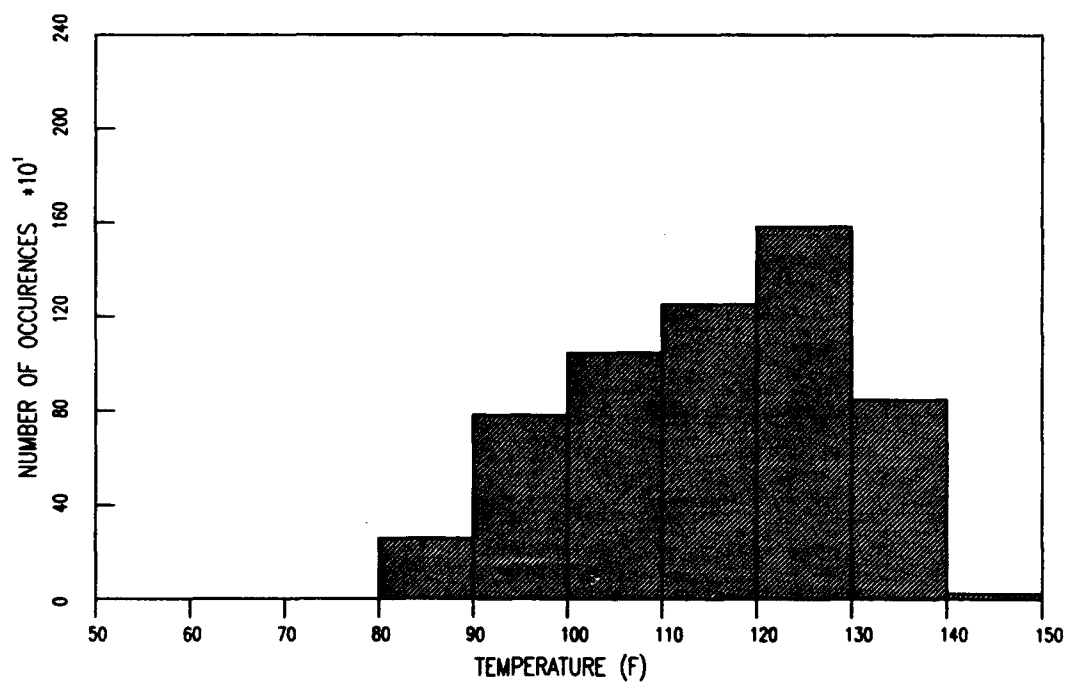
SURFACE TEMPERATURE HISTOGRAM FOR PASS LEVEL 5137



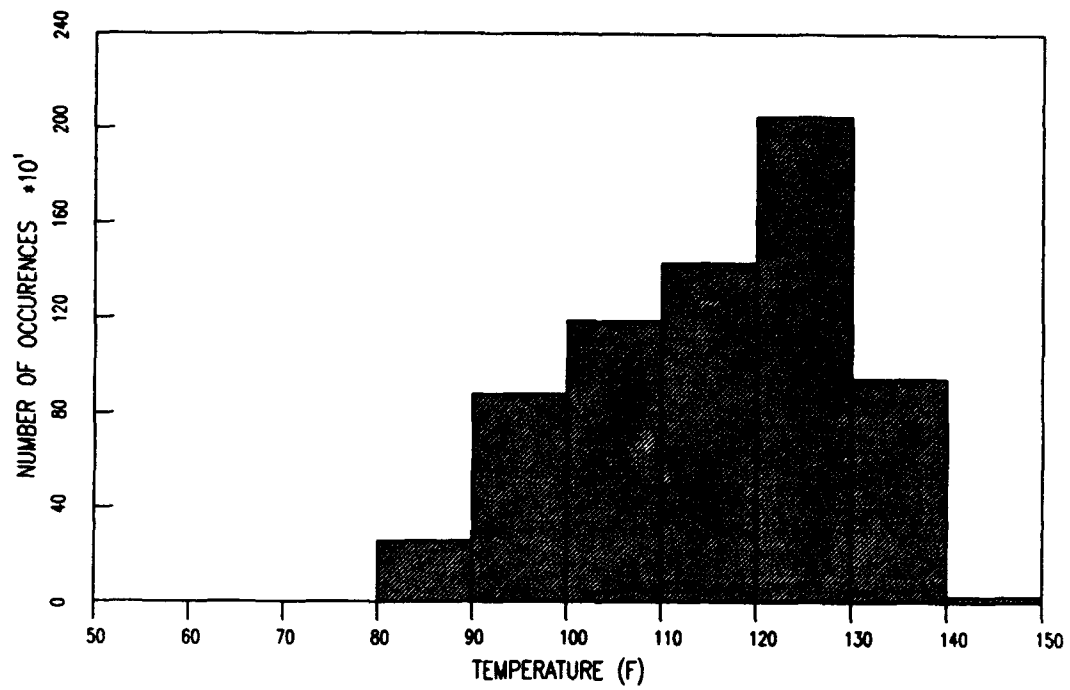
SURFACE TEMPERATURE HISTOGRAM FOR PASS LEVEL 5370



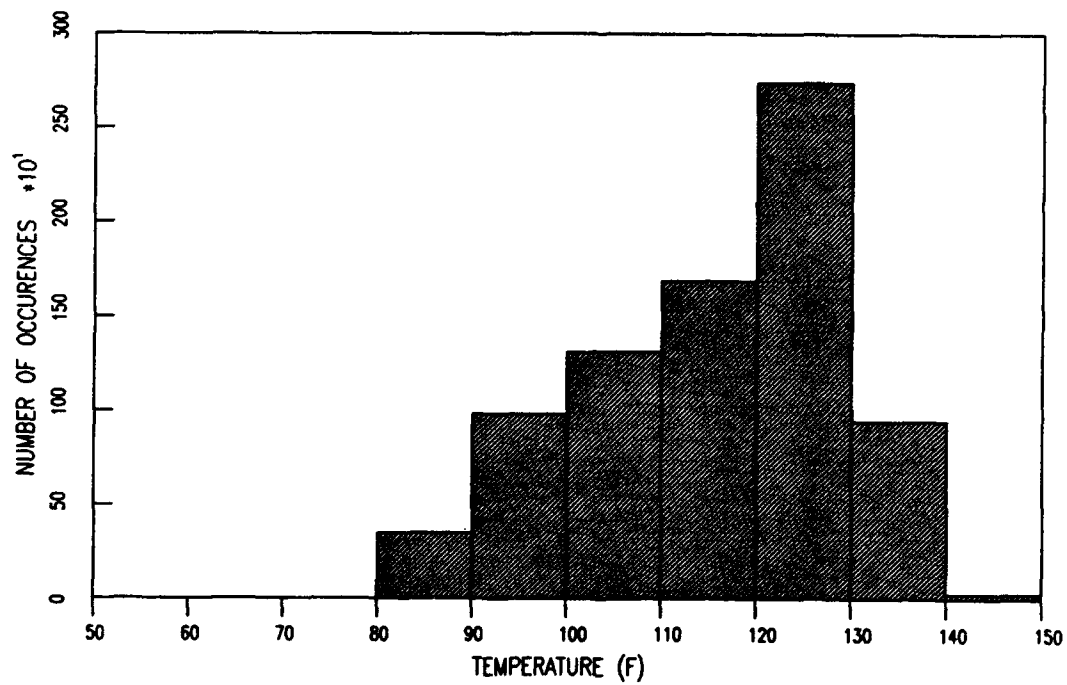
SURFACE TEMPERATURE HISTOGRAM FOR PASS LEVEL 5817



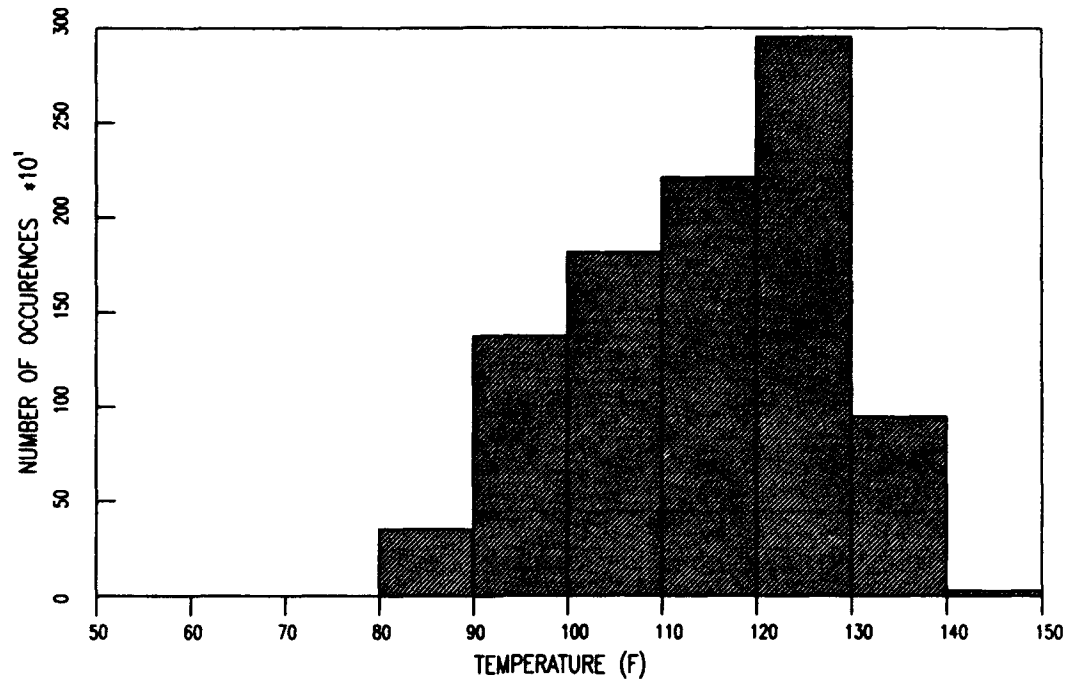
SURFACE TEMPERATURE HISTOGRAM FOR PASS LEVEL 6808



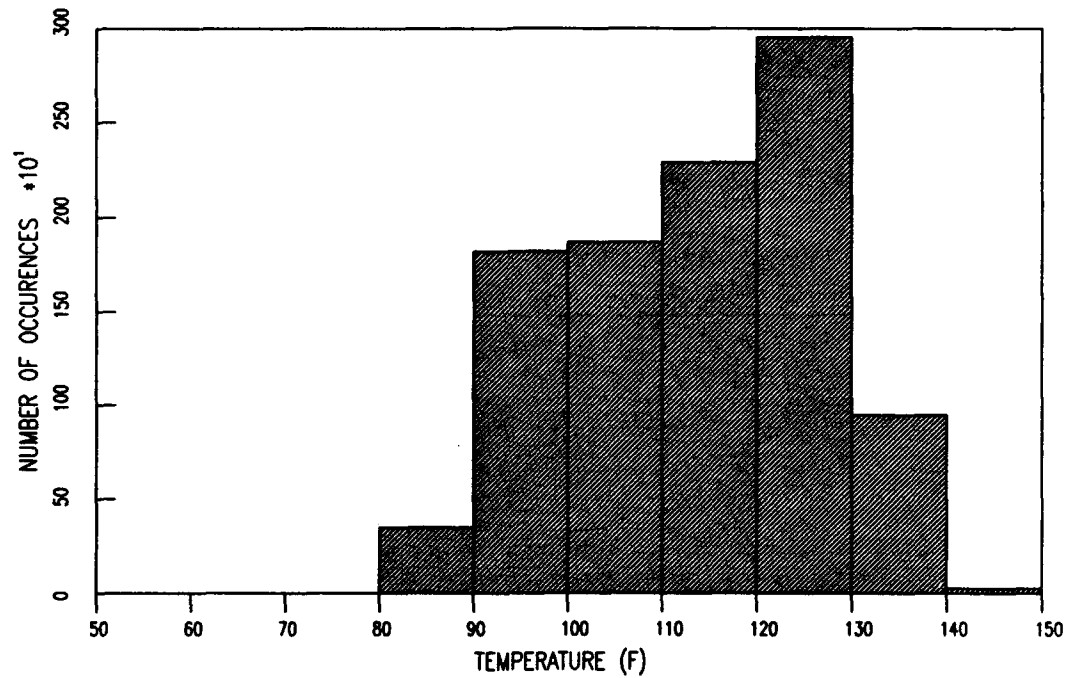
SURFACE TEMPERATURE HISTOGRAM FOR PASS LEVEL 8080



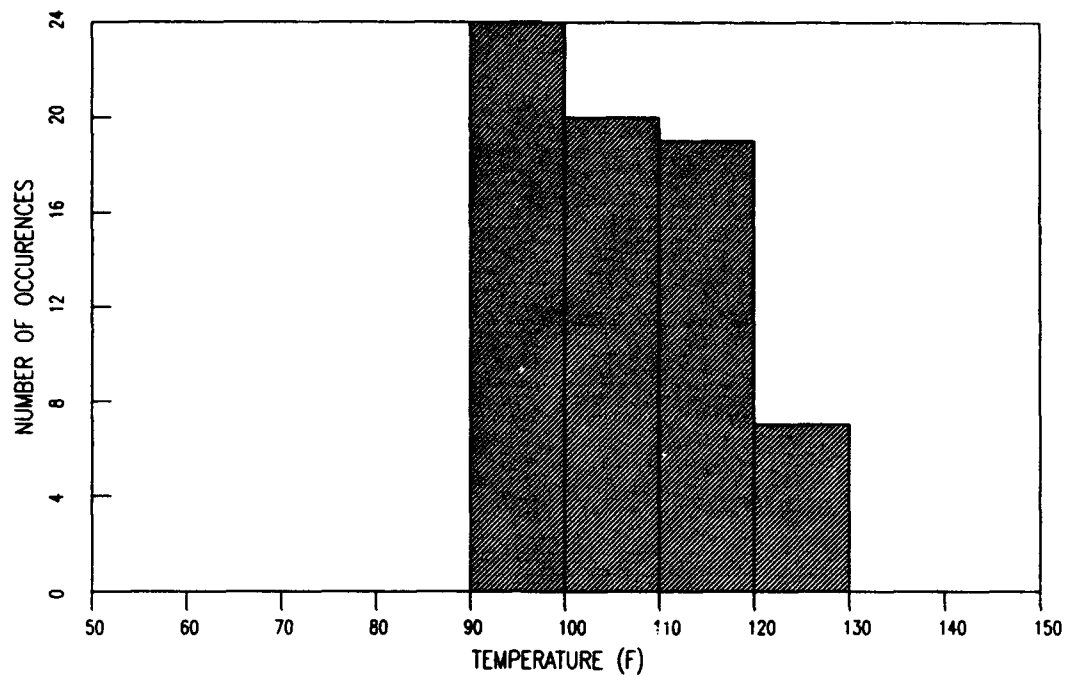
SURFACE TEMPERATURE HISTOGRAM FOR PASS LEVEL 9715



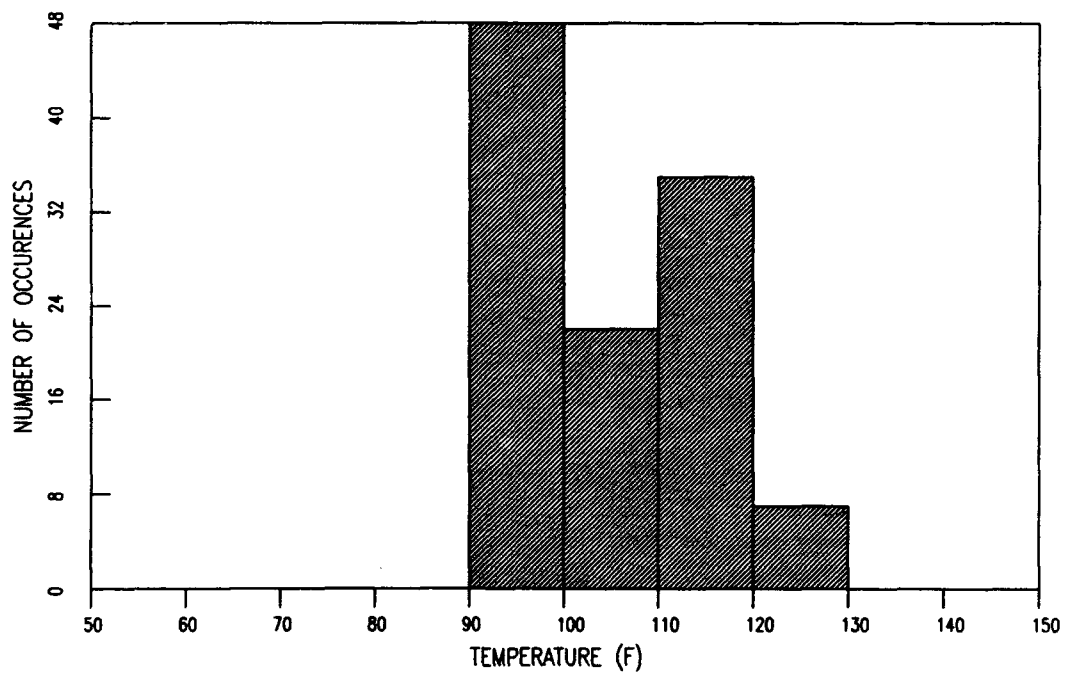
SURFACE TEMPERATURE HISTOGRAM FOR PASS LEVEL 10350



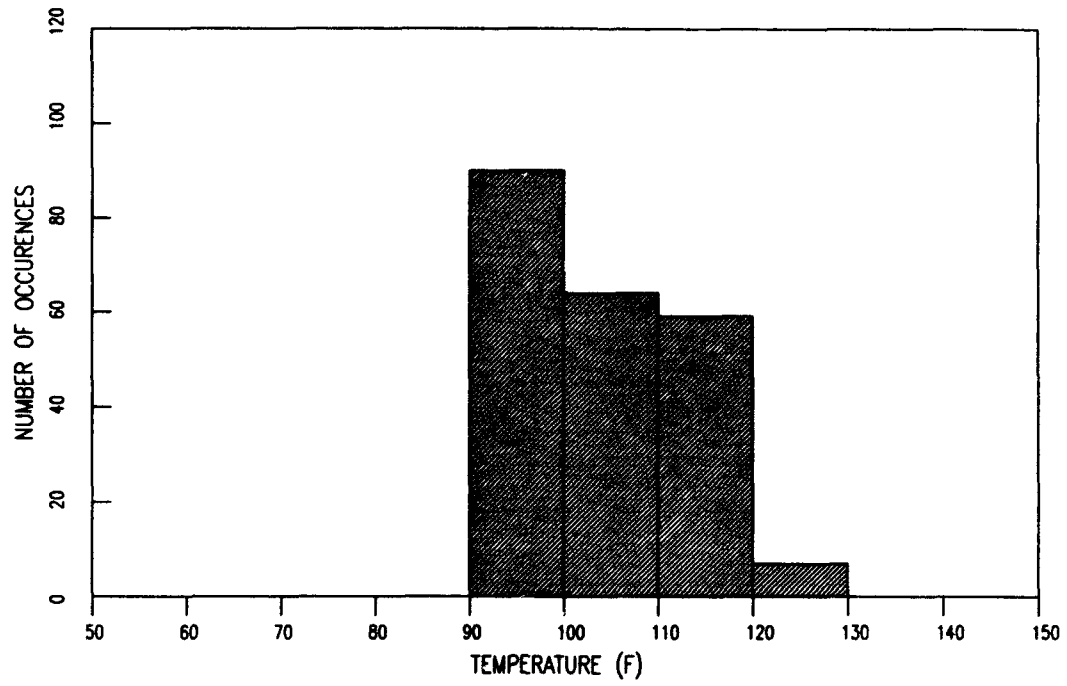
ASPHALT MIDHEIGHT TEMPERATURE HISTOGRAM FOR PASS LEVEL 70



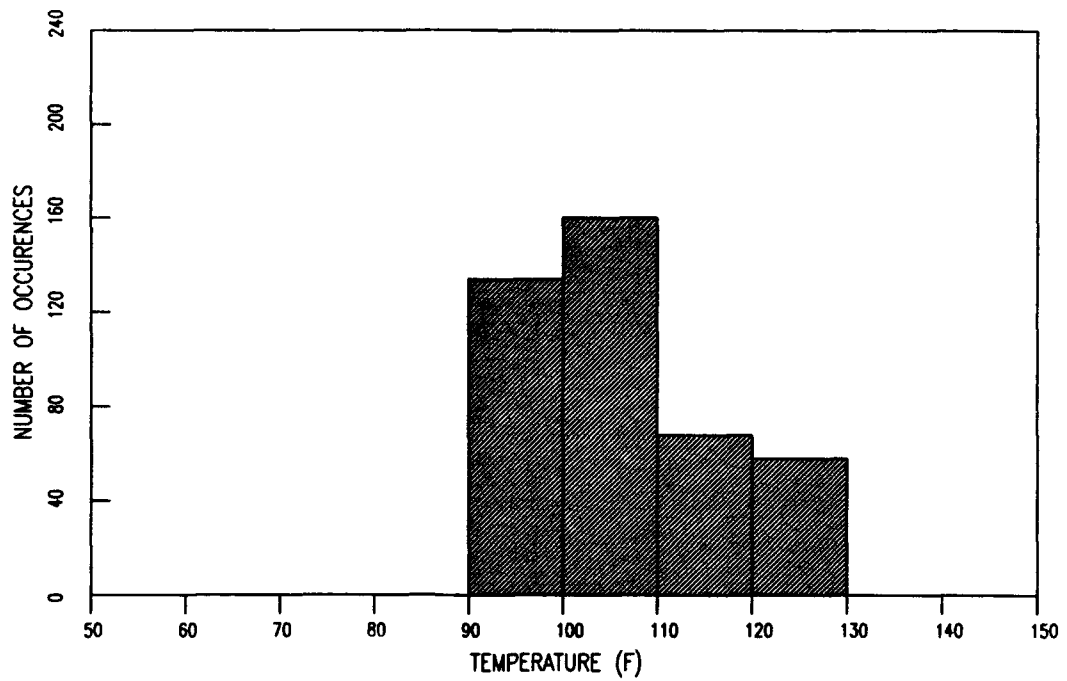
ASPHALT MIDHEIGHT TEMPERATURE HISTOGRAM FOR PASS LEVEL 112



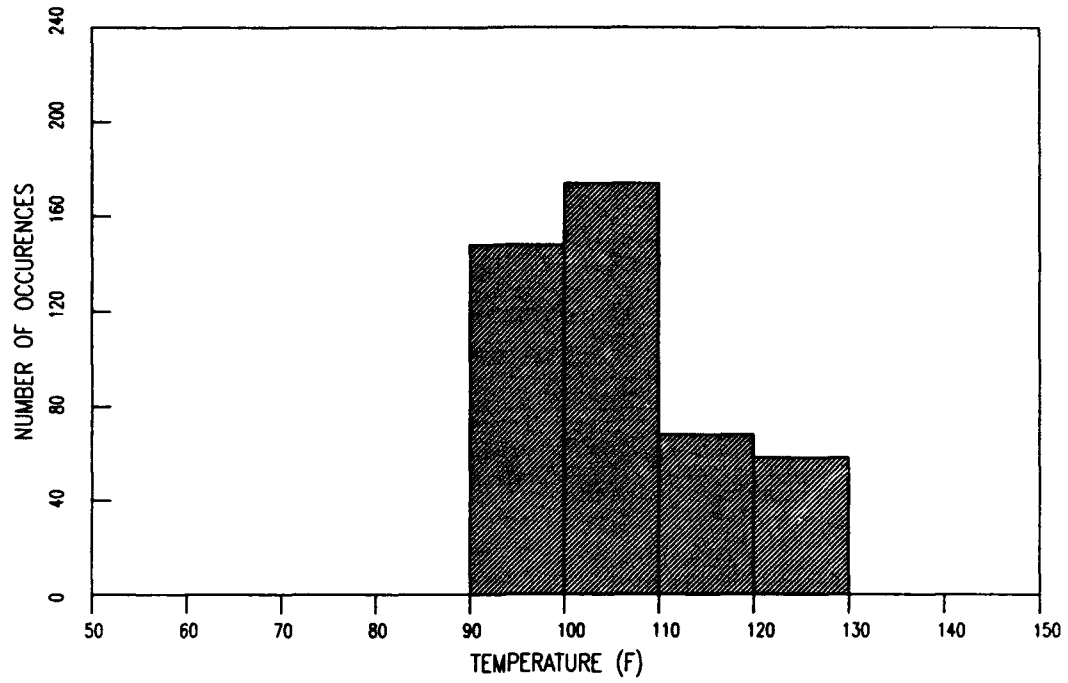
ASPHALT MIDHEIGHT TEMPERATURE HISTOGRAM FOR PASS LEVEL 220



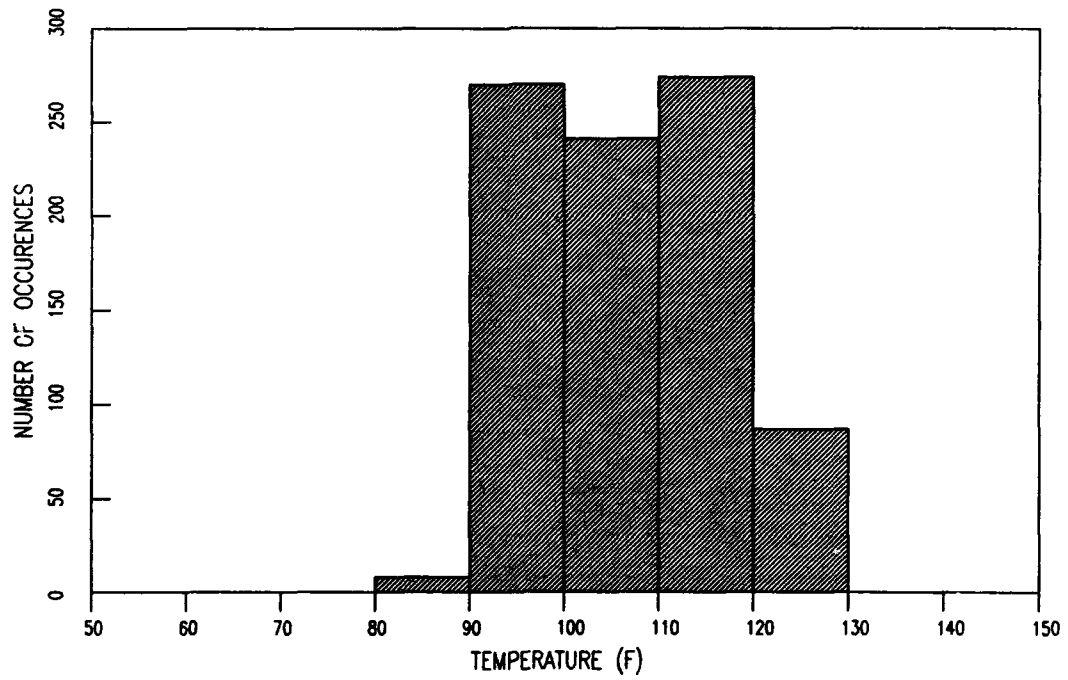
ASPHALT MIDHEIGHT TEMPERATURE HISTOGRAM FOR PASS LEVEL 420



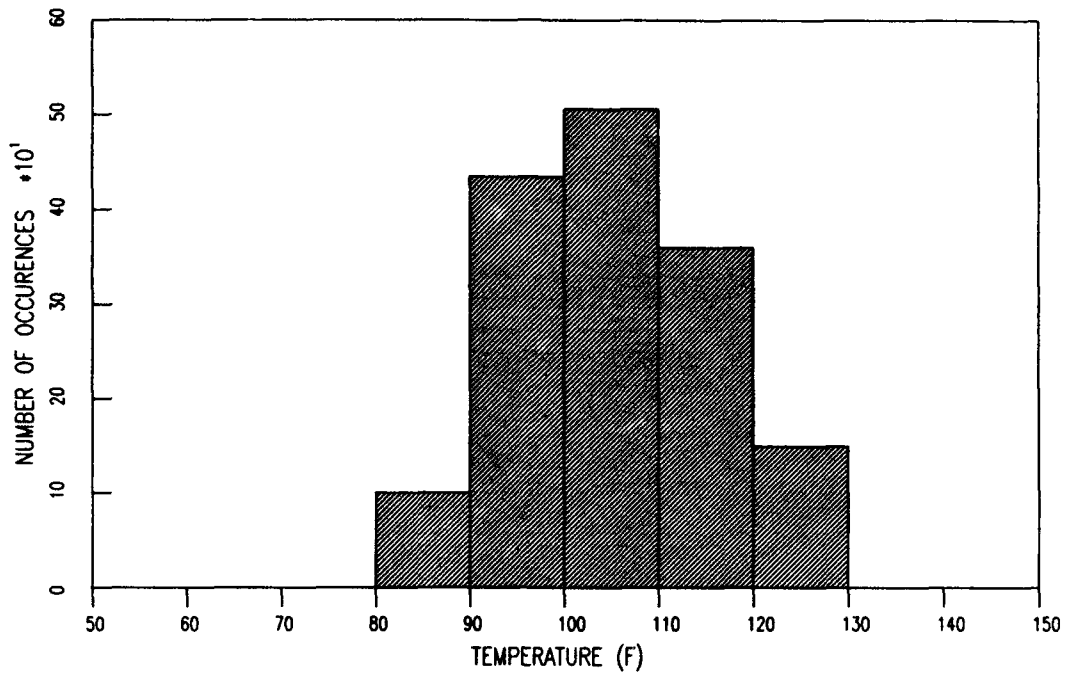
ASPHALT MIDHEIGHT TEMPERATURE HISTOGRAM FOR PASS LEVEL 448



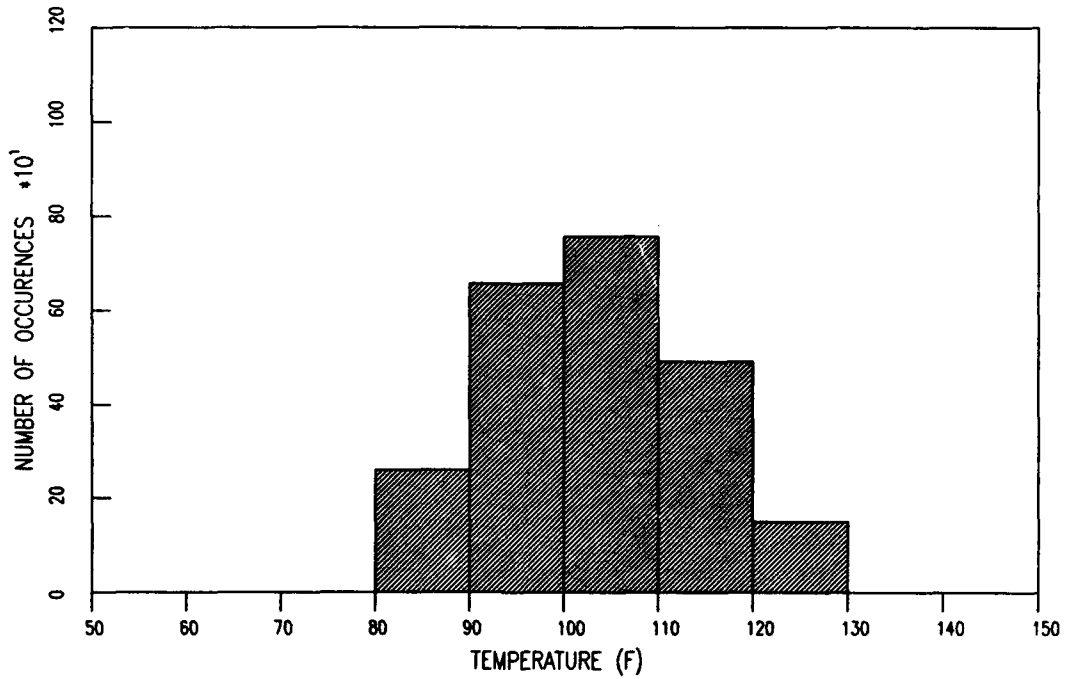
ASPHALT MIDHEIGHT TEMPERATURE HISTOGRAM FOR PASS LEVEL 882



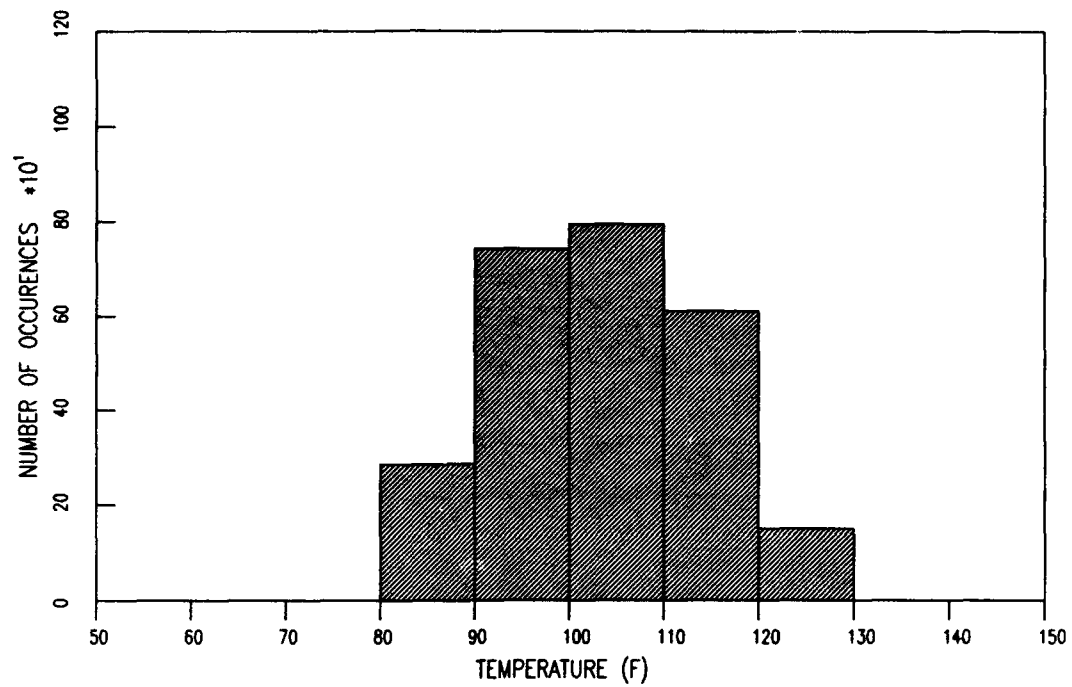
ASPHALT MIDHEIGHT TEMPERATURE HISTOGRAM FOR PASS LEVEL 1554



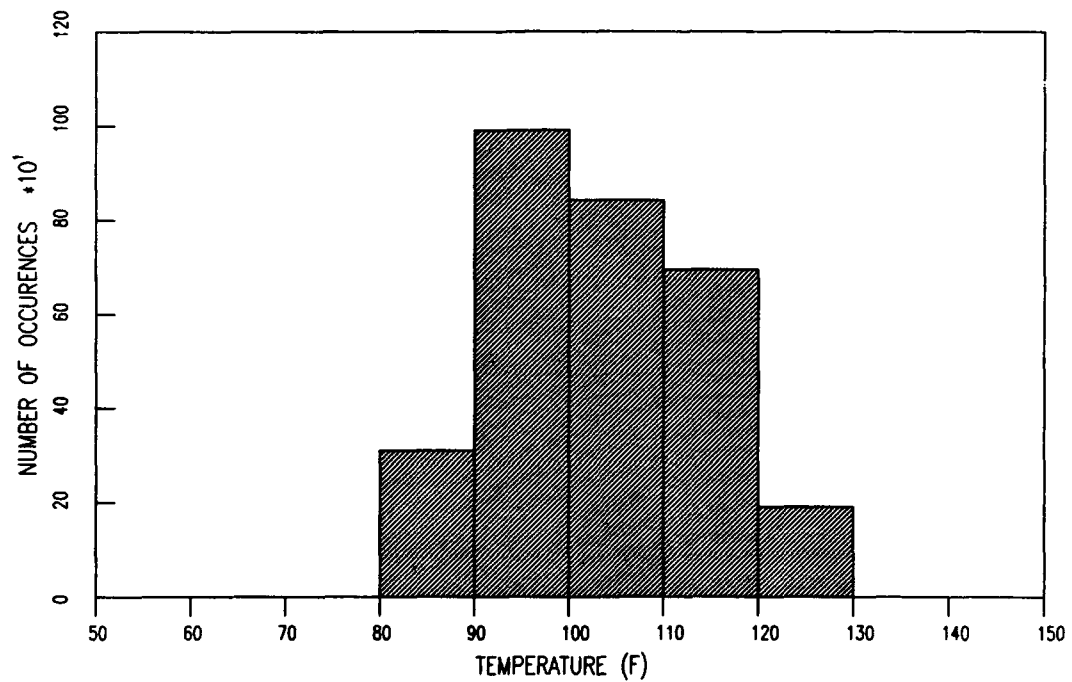
ASPHALT MIDHEIGHT TEMPERATURE HISTOGRAM FOR PASS LEVEL 2324



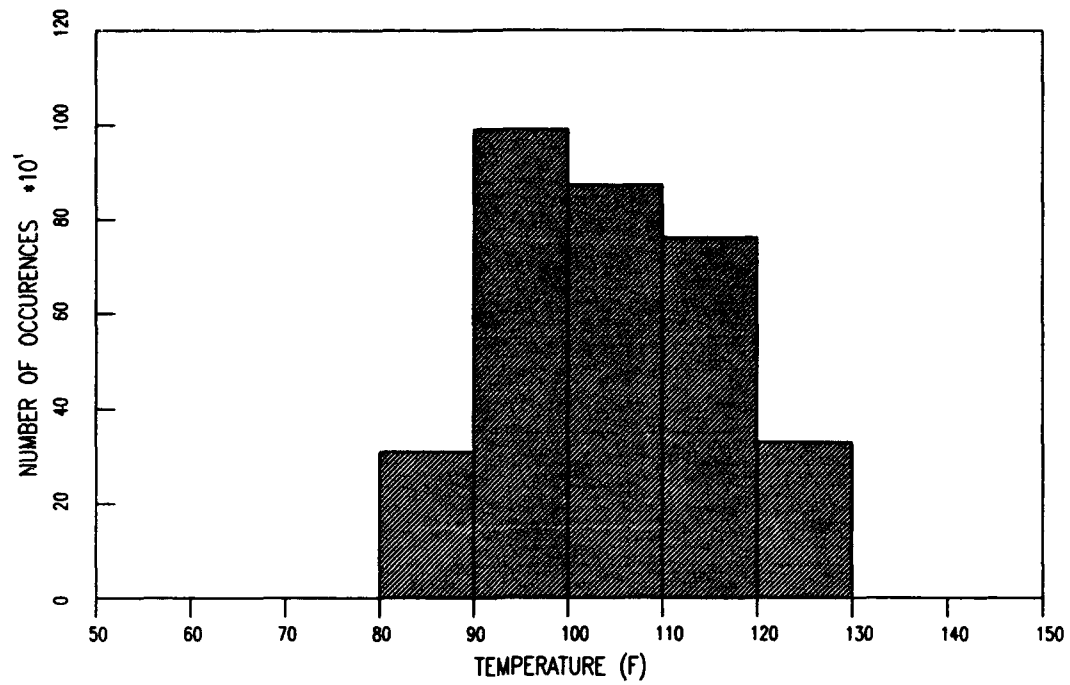
ASPHALT MIDHEIGHT TEMPERATURE HISTOGRAM FOR PASS LEVEL 2589



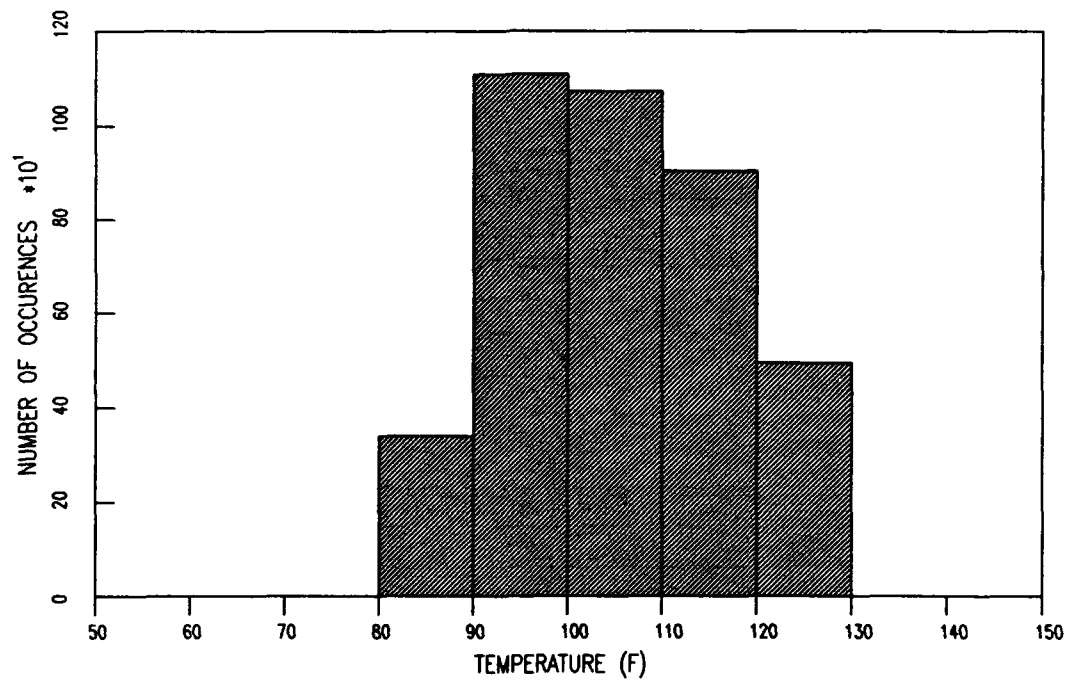
ASPHALT MIDHEIGHT TEMPERATURE HISTOGRAM FOR PASS LEVEL 3049



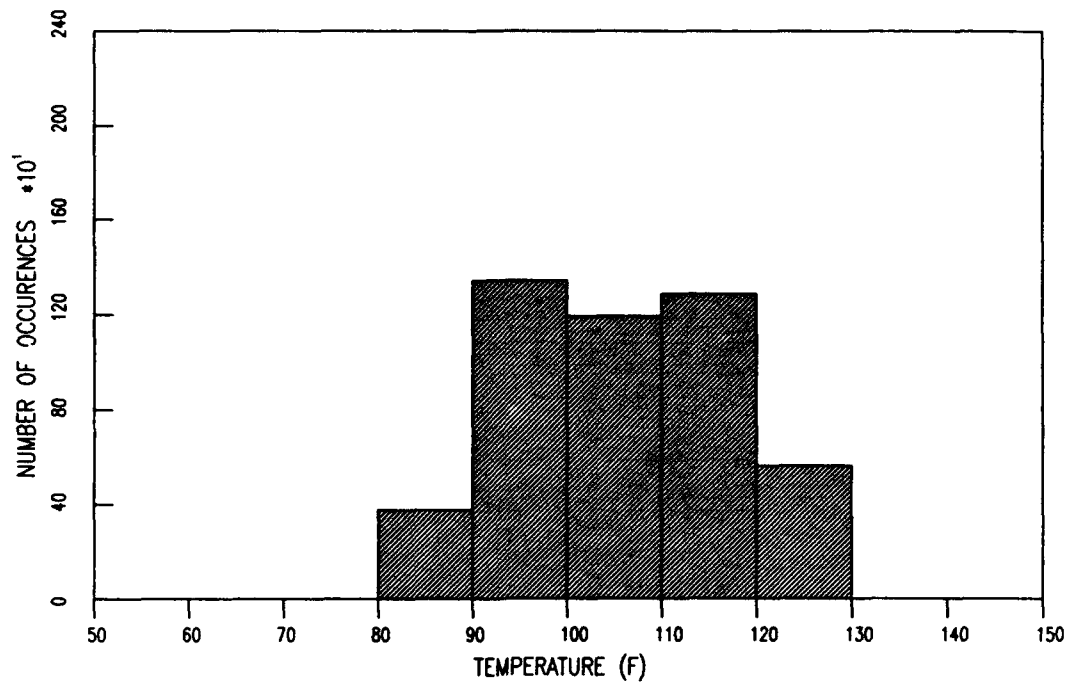
ASPHALT MIDHEIGHT TEMPERATURE HISTOGRAM FOR PASS LEVEL 3286



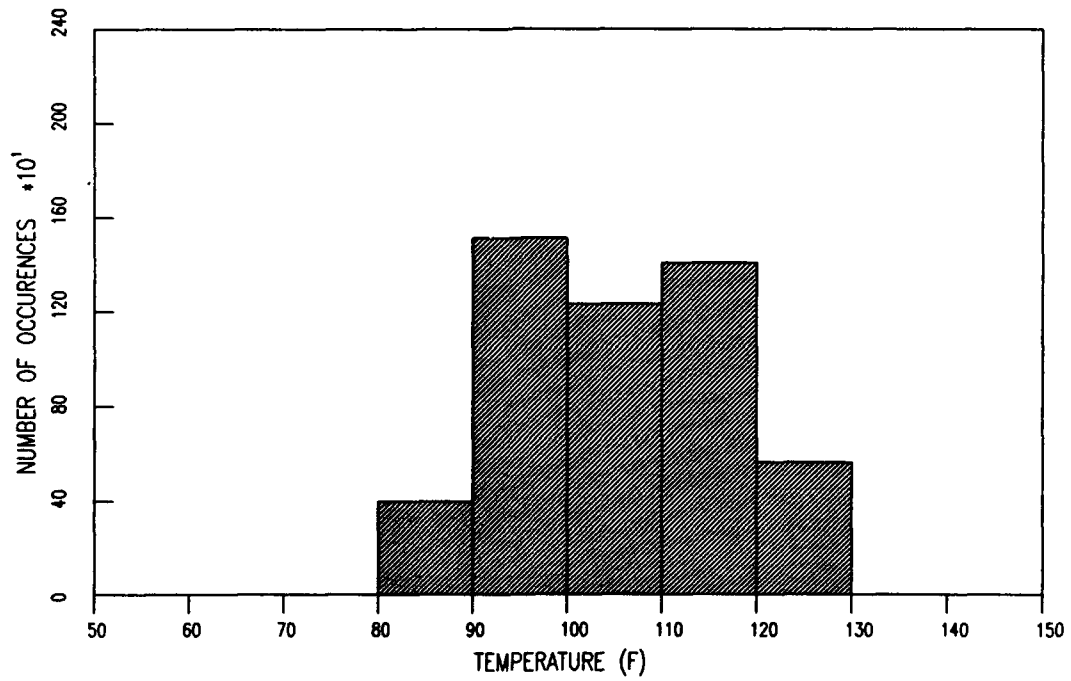
ASPHALT MIDHEIGHT TEMPERATURE HISTOGRAM FOR PASS LEVEL 3942



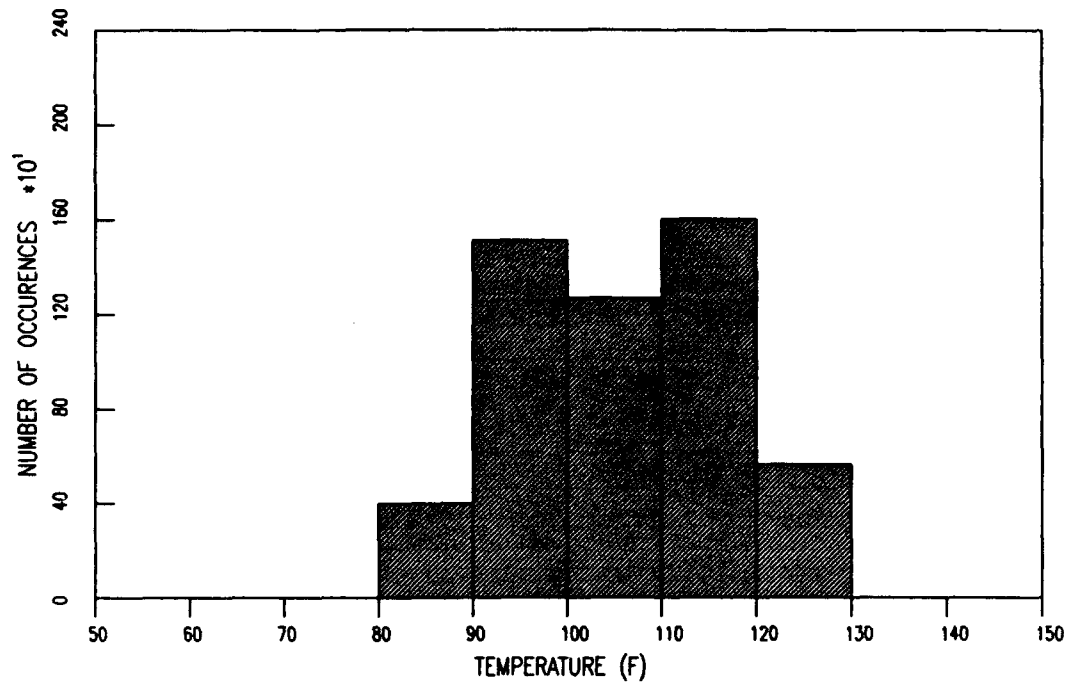
ASPHALT MIDHEIGHT TEMPERATURE HISTOGRAM FOR PASS LEVEL 4784



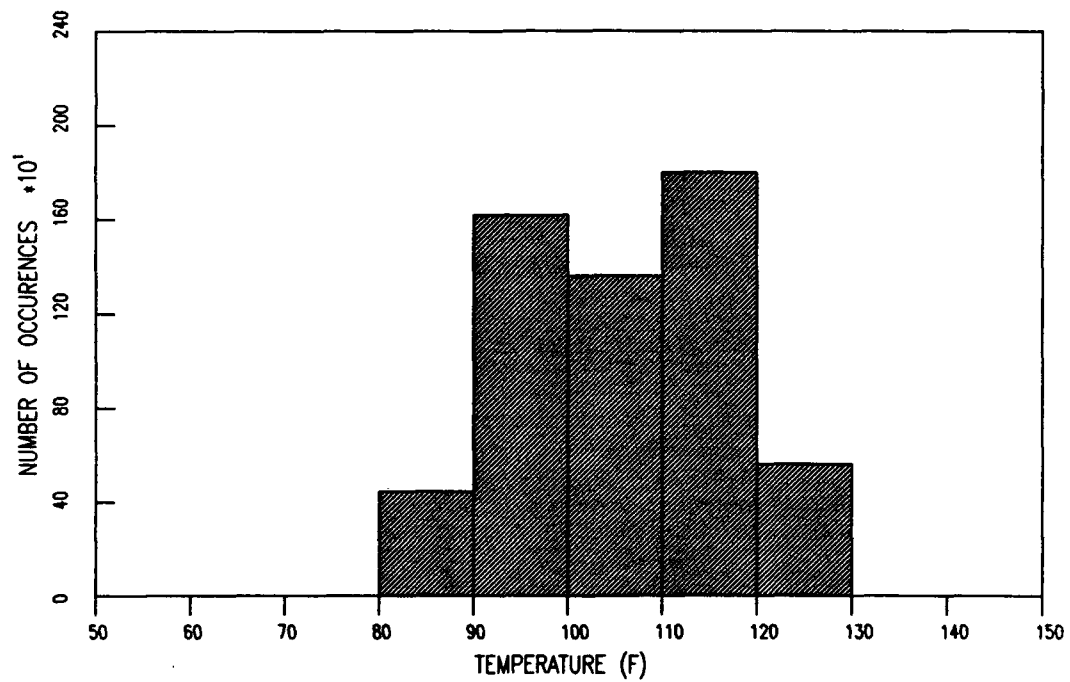
ASPHALT MIDHEIGHT TEMPERATURE HISTOGRAM FOR PASS LEVEL 5137



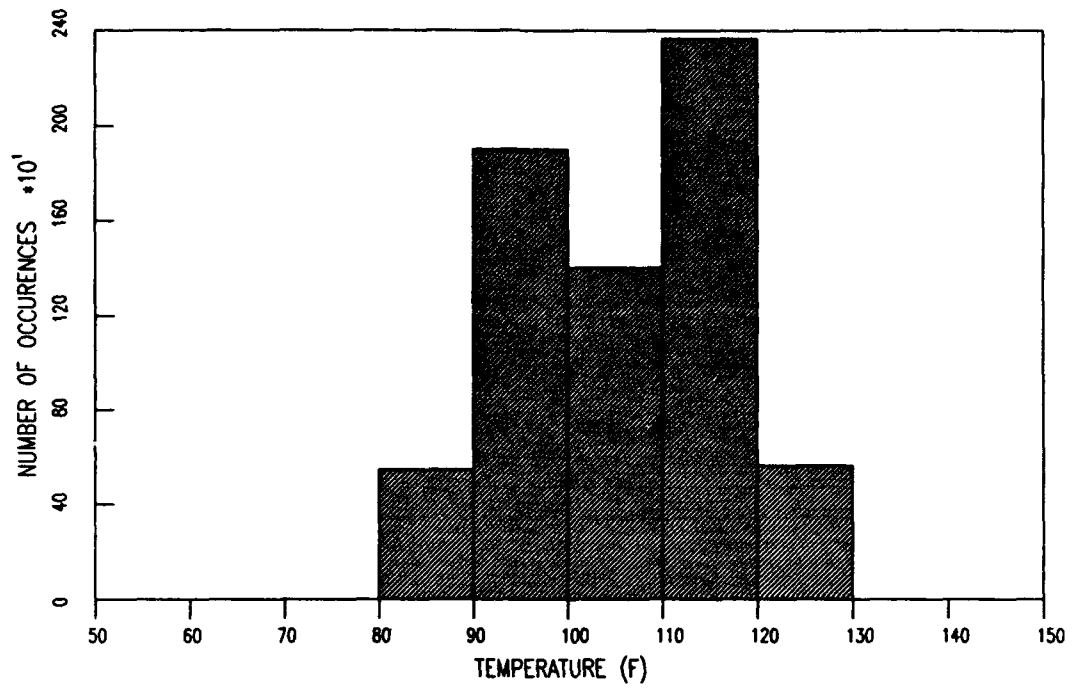
ASPHALT MIDHEIGHT TEMPERATURE HISTOGRAM FOR PASS LEVEL 5370



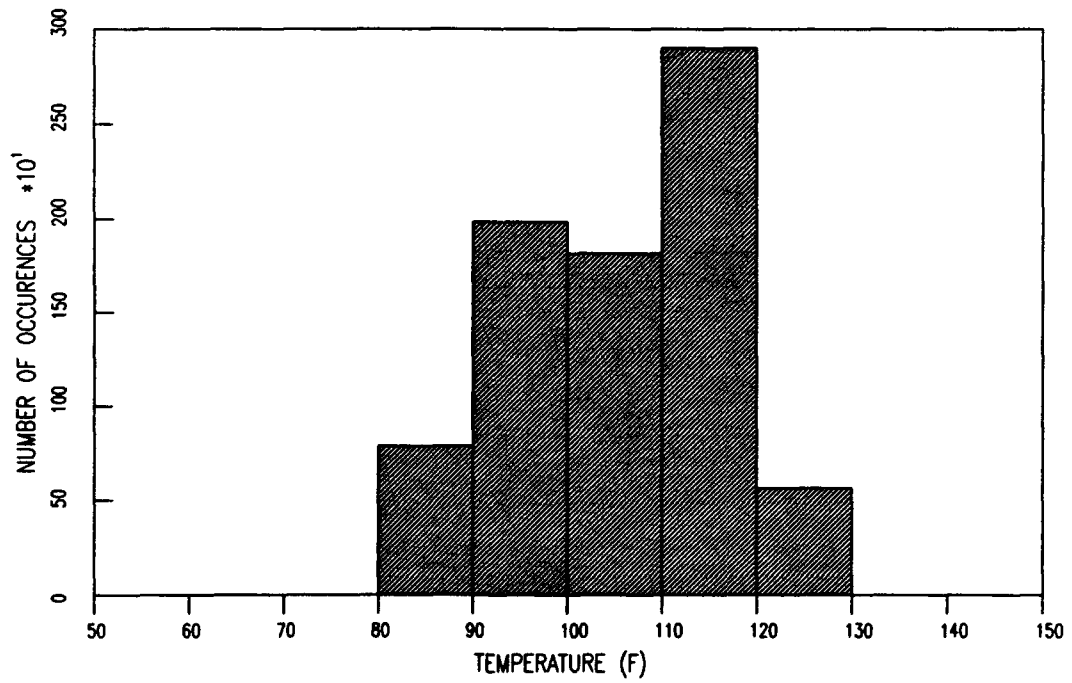
ASPHALT MIDHEIGHT TEMPERATURE HISTOGRAM FOR PASS LEVEL 5817



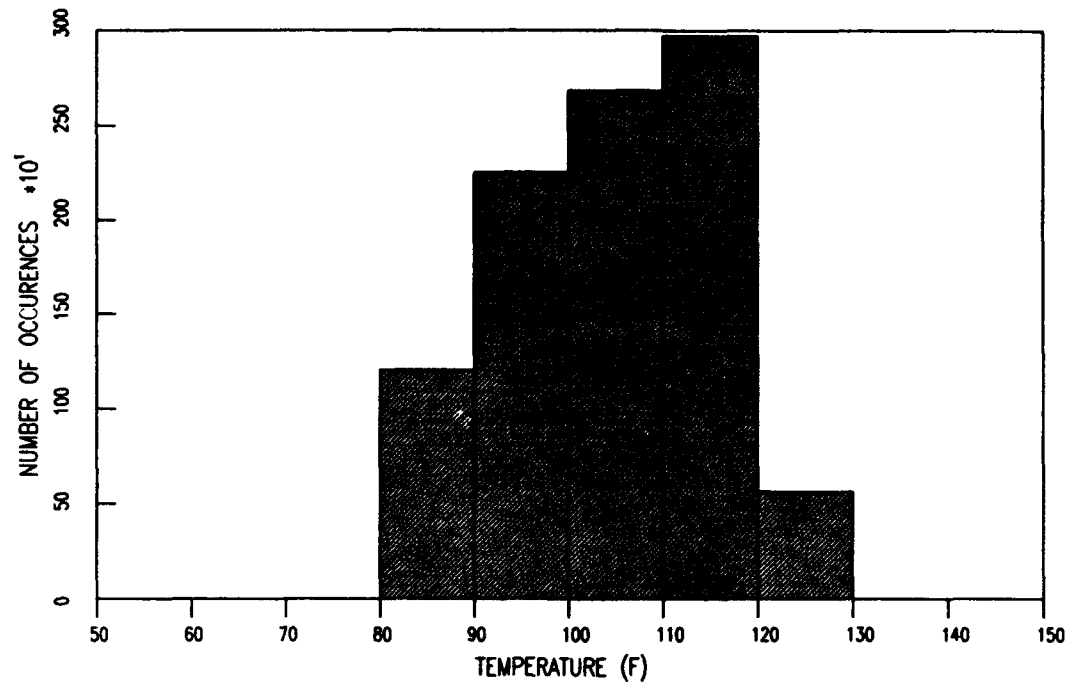
ASPHALT MIDHEIGHT TEMPERATURE HISTOGRAM FOR PASS LEVEL 6808



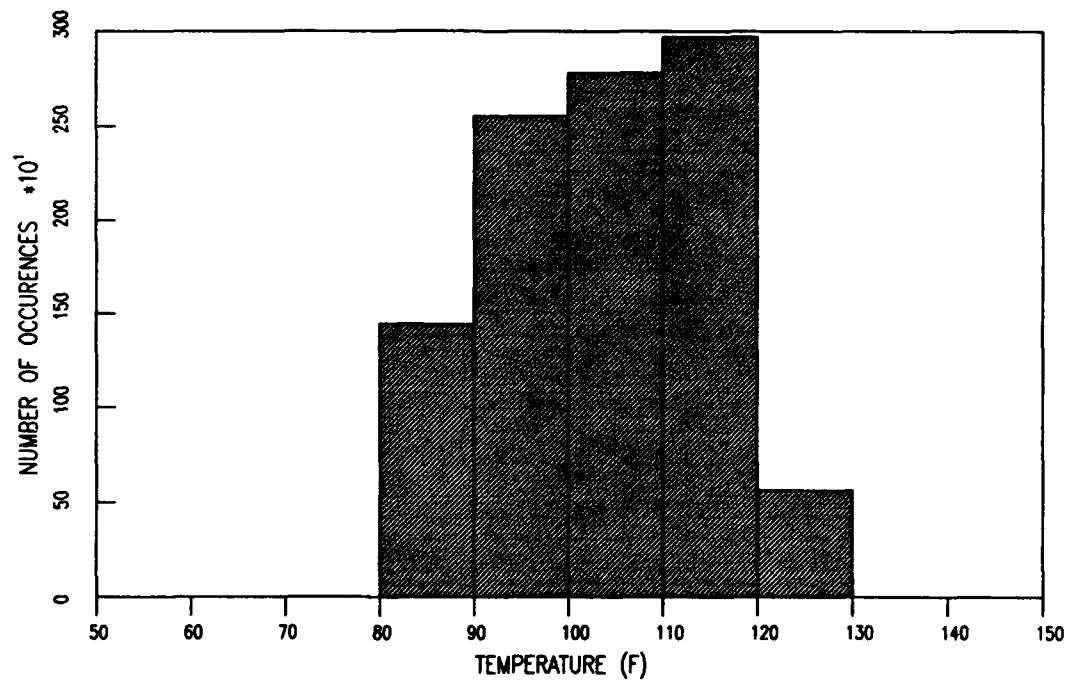
ASPHALT MIDHEIGHT TEMPERATURE HISTOGRAM FOR PASS LEVEL 8080



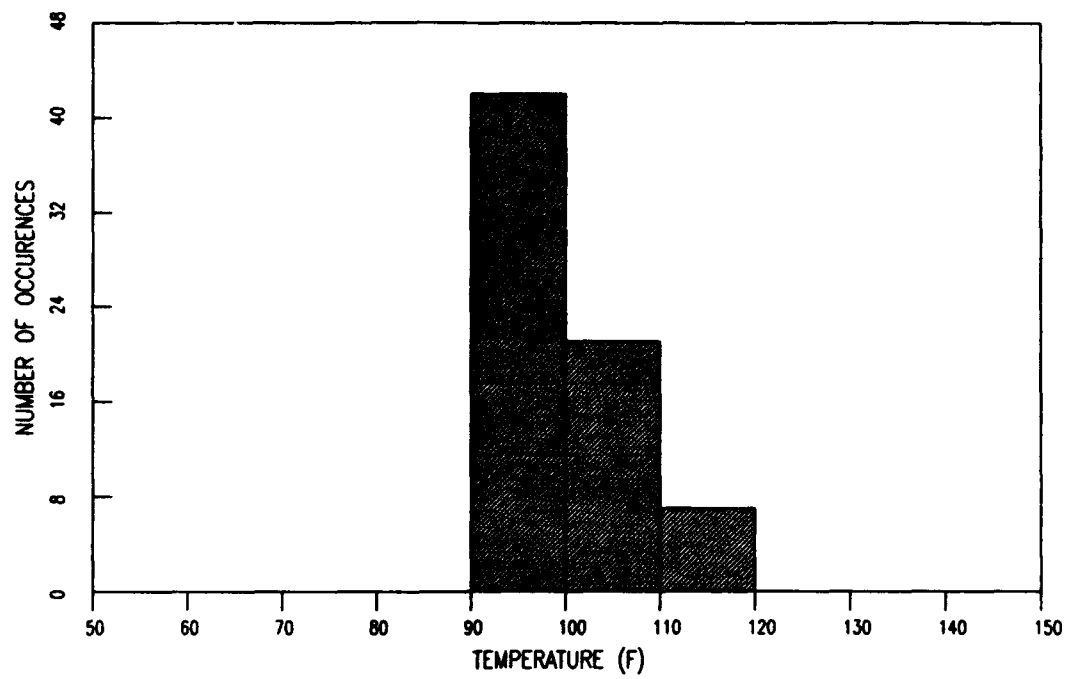
ASPHALT MIDHEIGHT TEMPERATURE HISTOGRAM FOR PASS LEVEL 9715



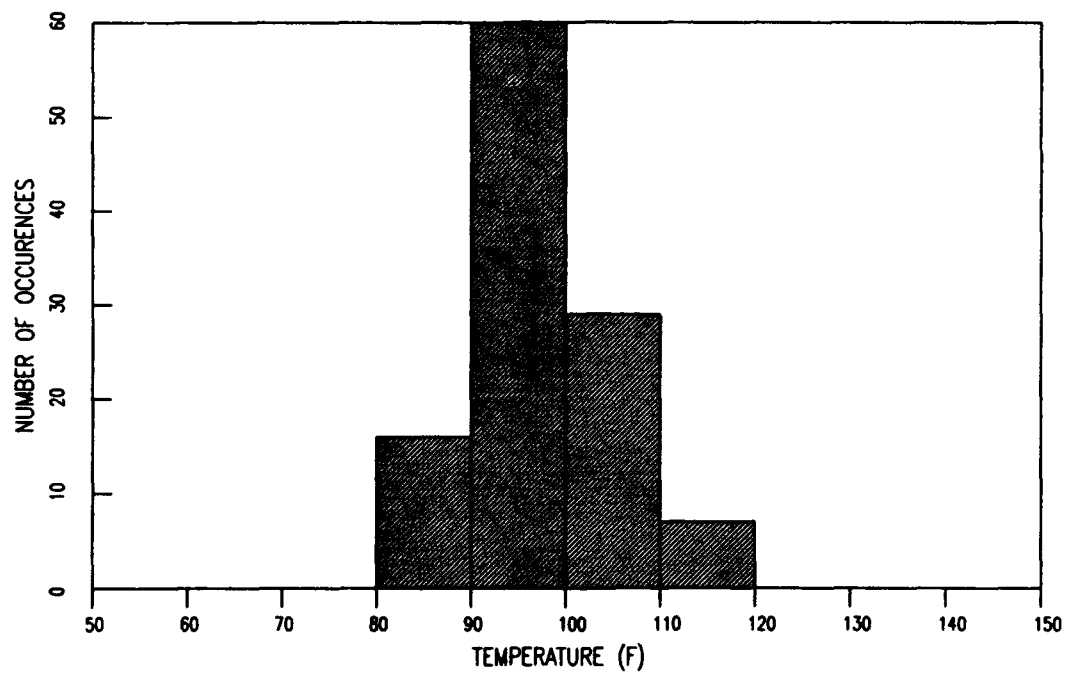
ASPHALT MIDHEIGHT TEMPERATURE HISTOGRAM FOR PASS LEVEL 10350



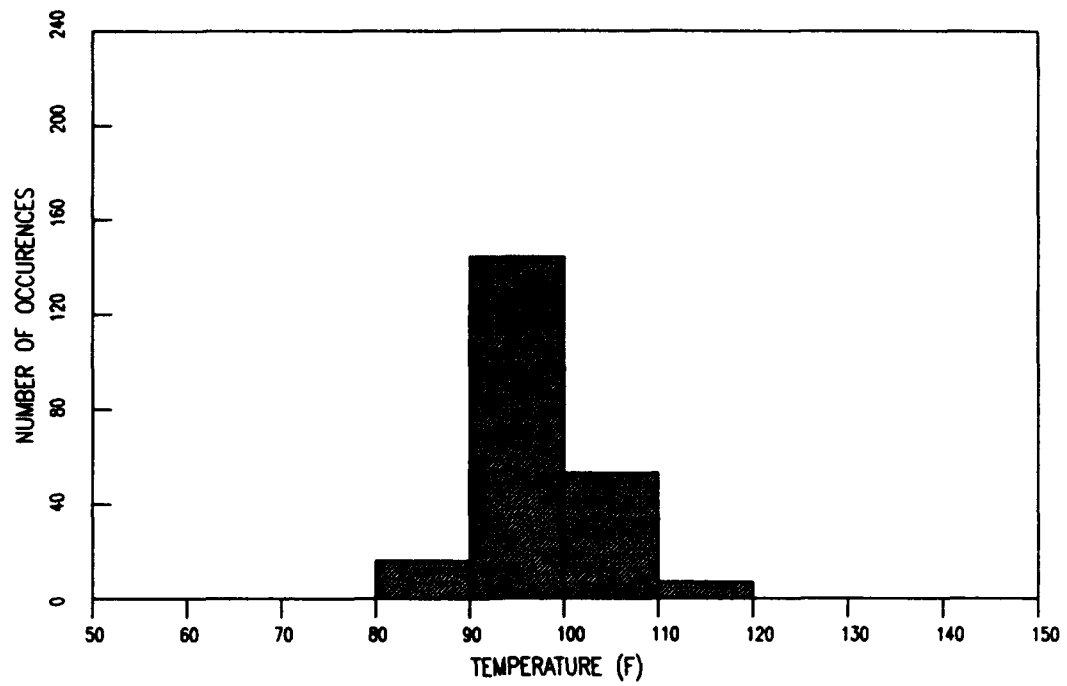
INTERFACE TEMPERATURE HISTOGRAM FOR PASS LEVEL 70



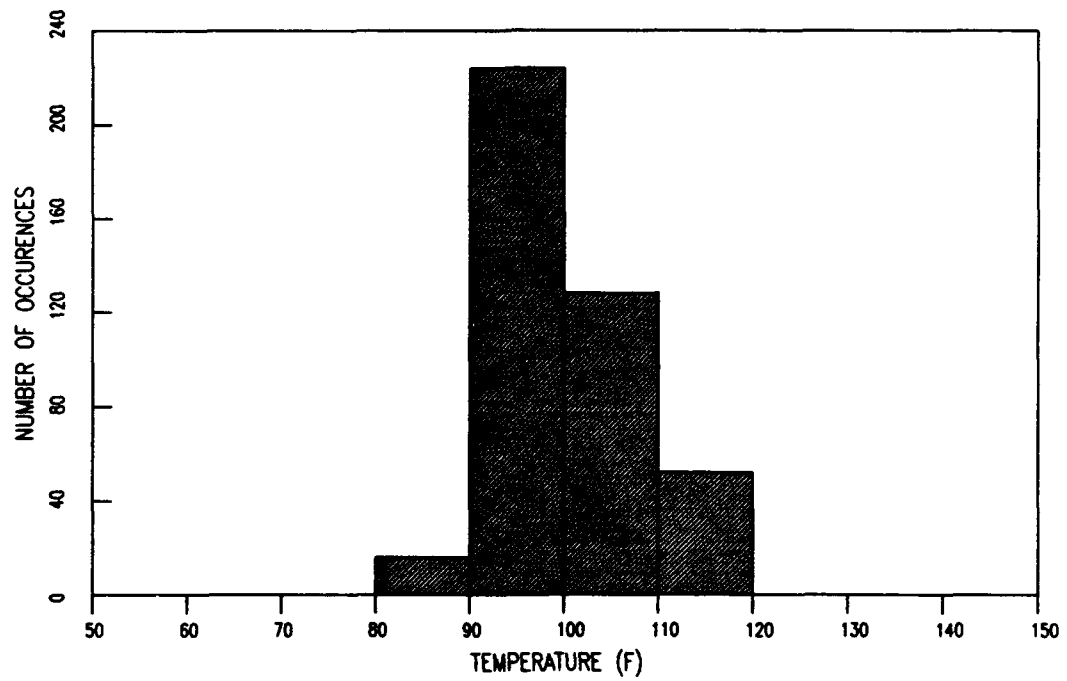
INTERFACE TEMPERATURE HISTOGRAM FOR PASS LEVEL 112



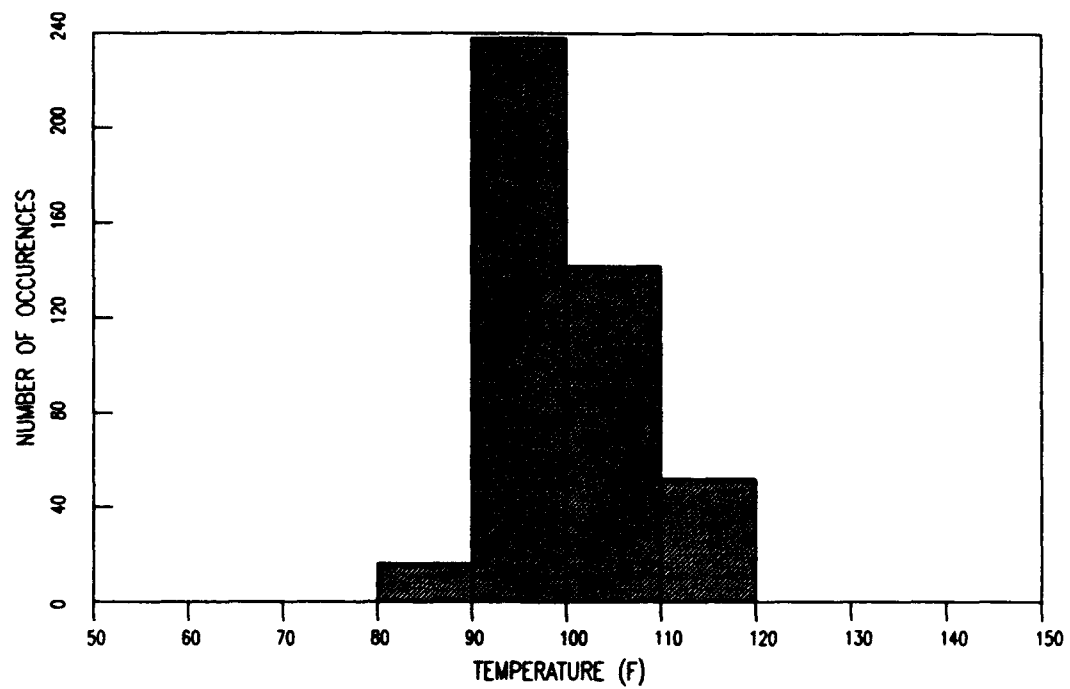
INTERFACE TEMPERATURE HISTOGRAM FOR PASS LEVEL 220



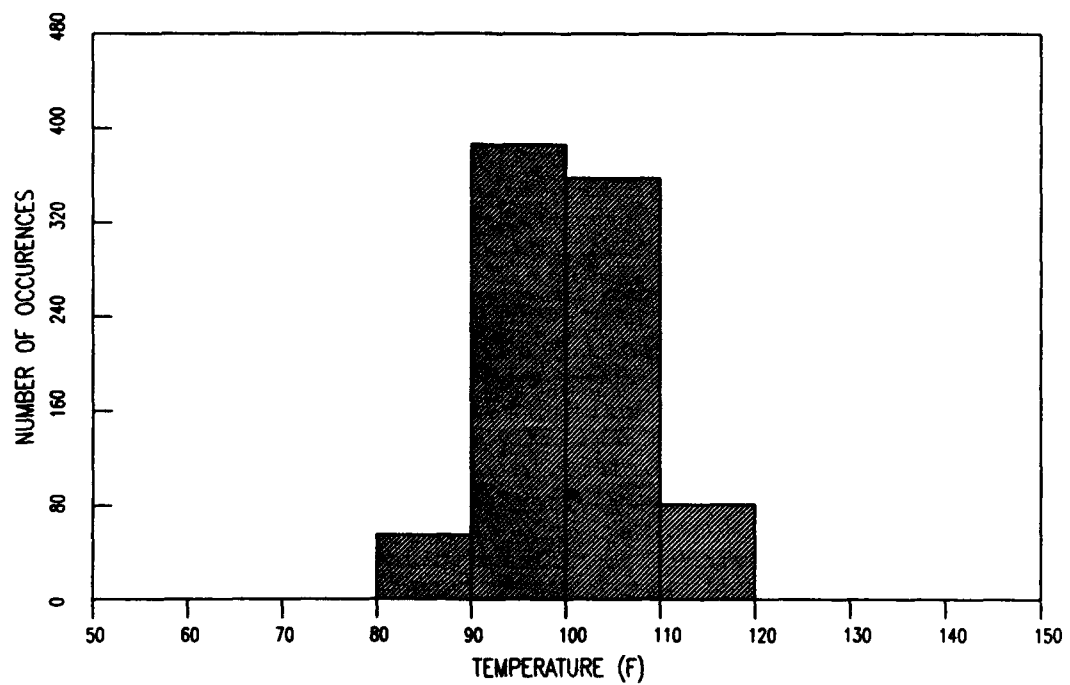
INTERFACE TEMPERATURE HISTOGRAM FOR PASS LEVEL 420



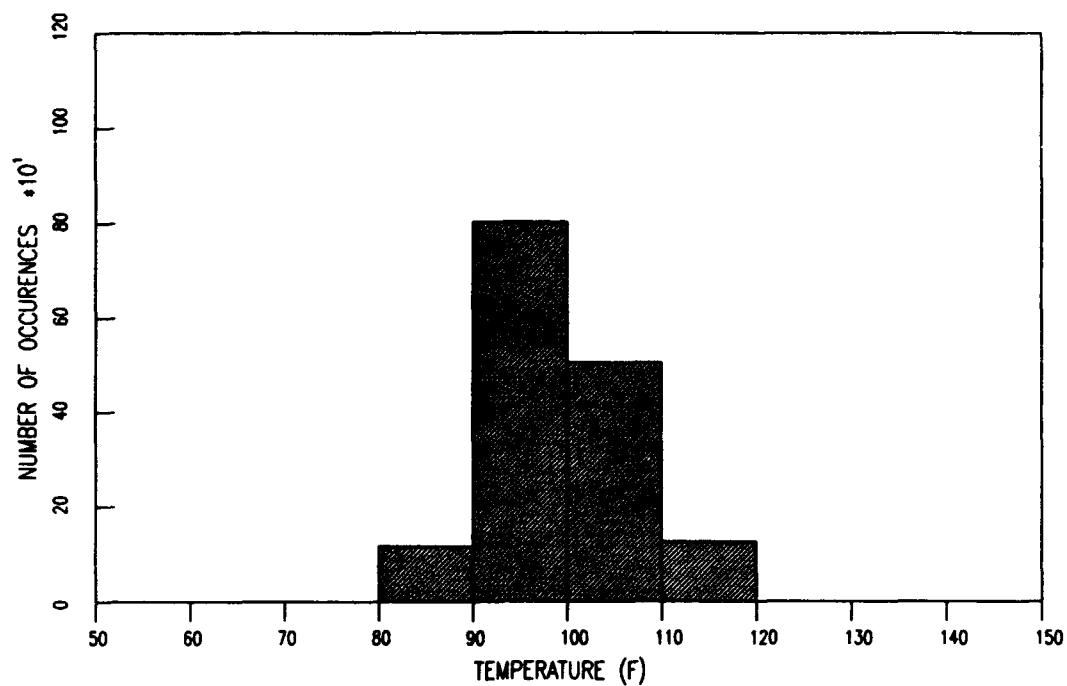
INTERFACE TEMPERATURE HISTOGRAM FOR PASS LEVEL 448



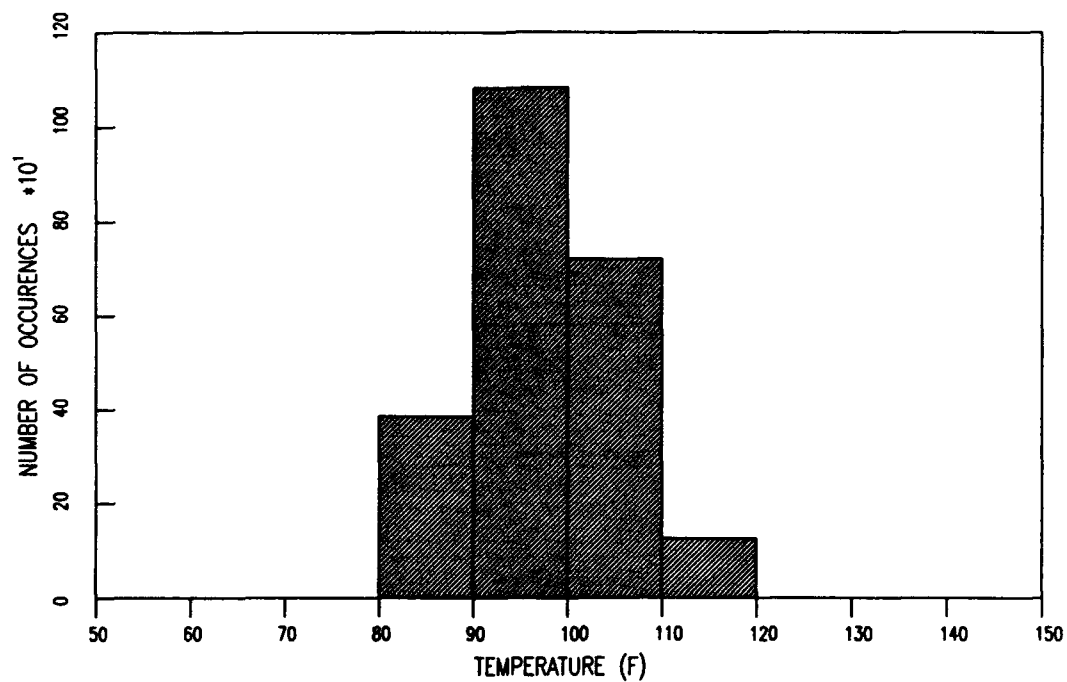
INTERFACE TEMPERATURE HISTOGRAM FOR PASS LEVEL 882



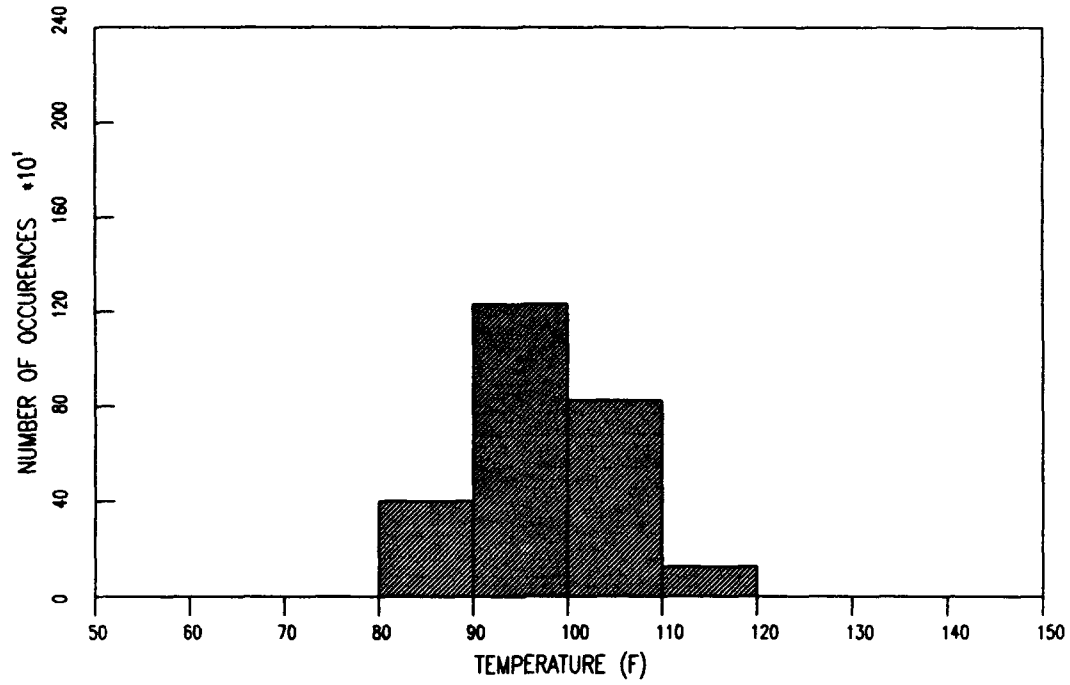
INTERFACE TEMPERATURE HISTOGRAM FOR PASS LEVEL 1554



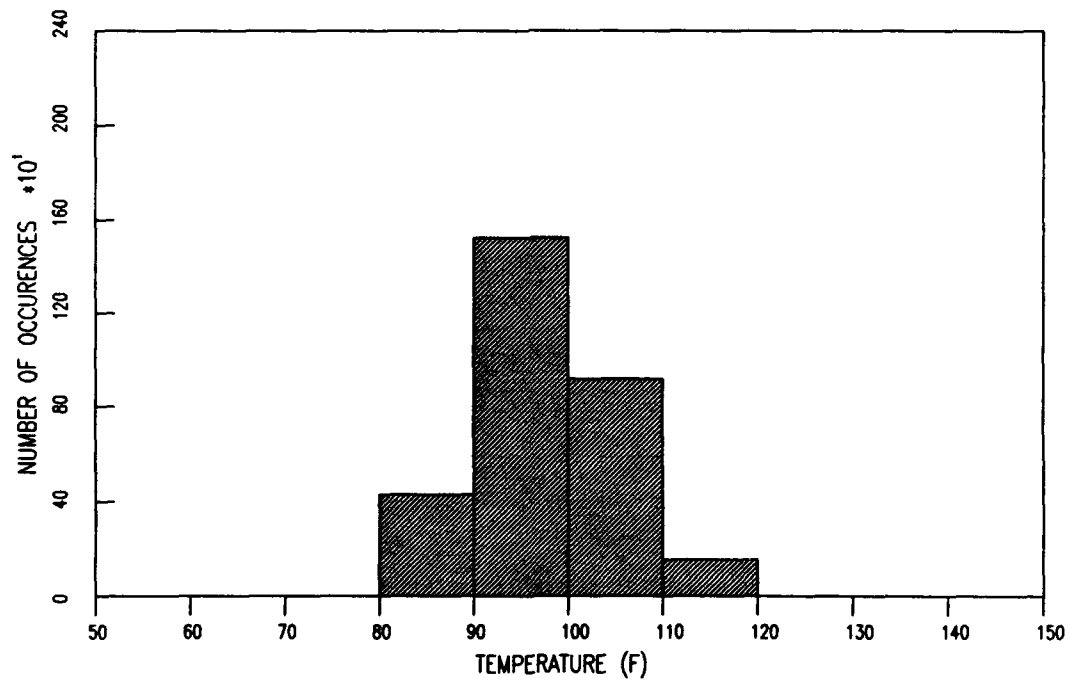
INTERFACE TEMPERATURE HISTOGRAM FOR PASS LEVEL 2324



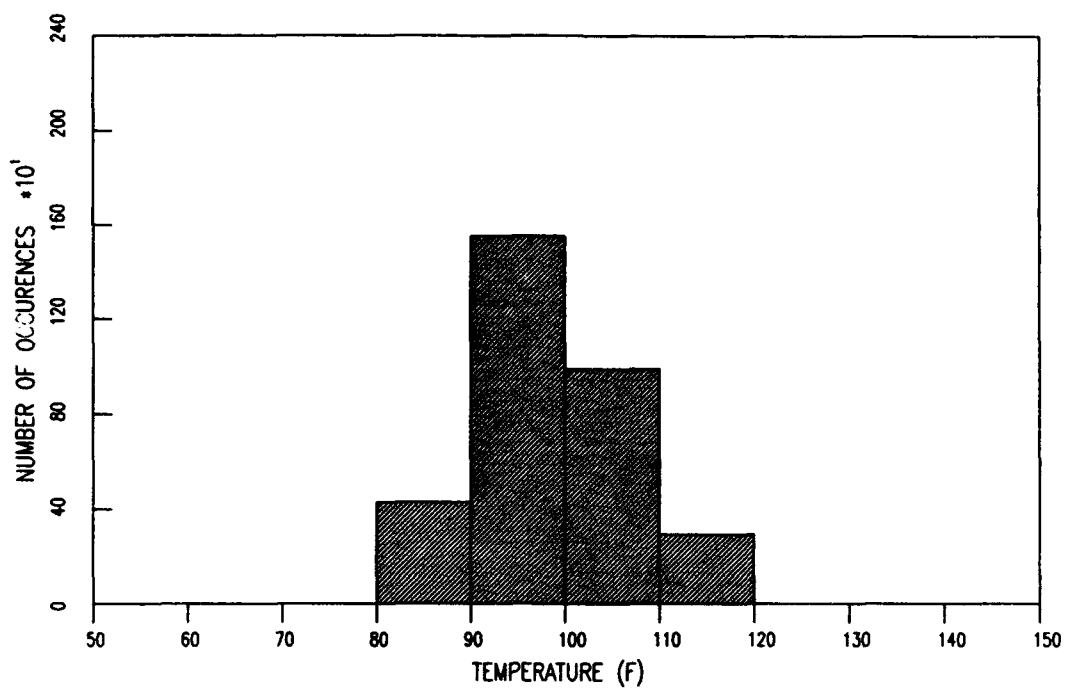
INTERFACE TEMPERATURE HISTOGRAM FOR PASS LEVEL 2589



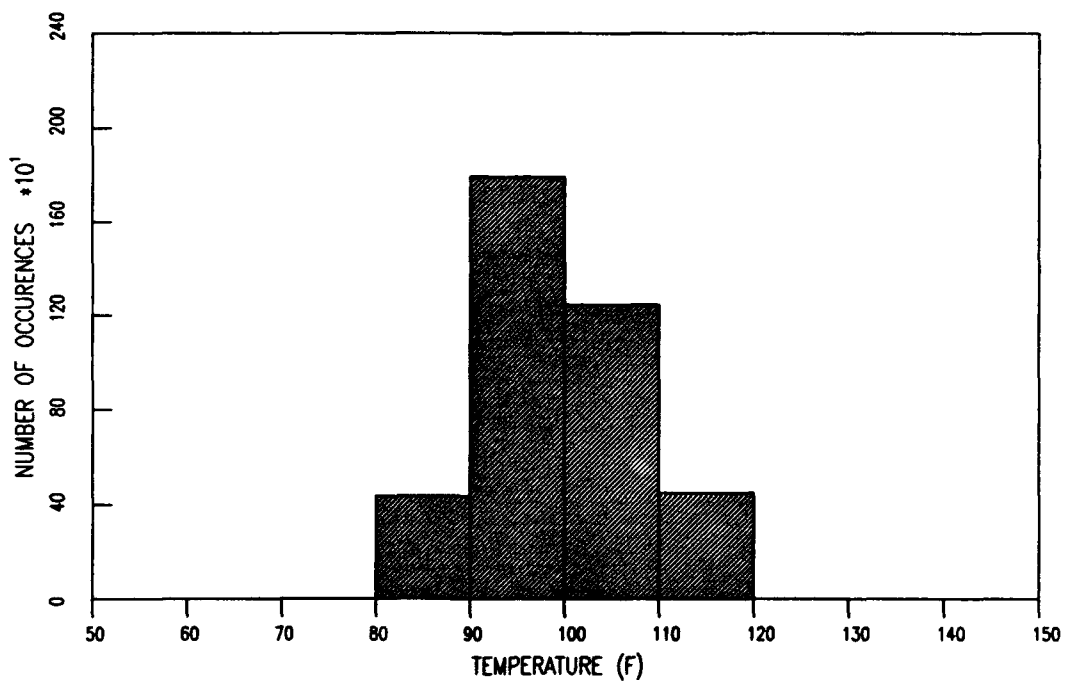
INTERFACE TEMPERATURE HISTOGRAM FOR PASS LEVEL 3049



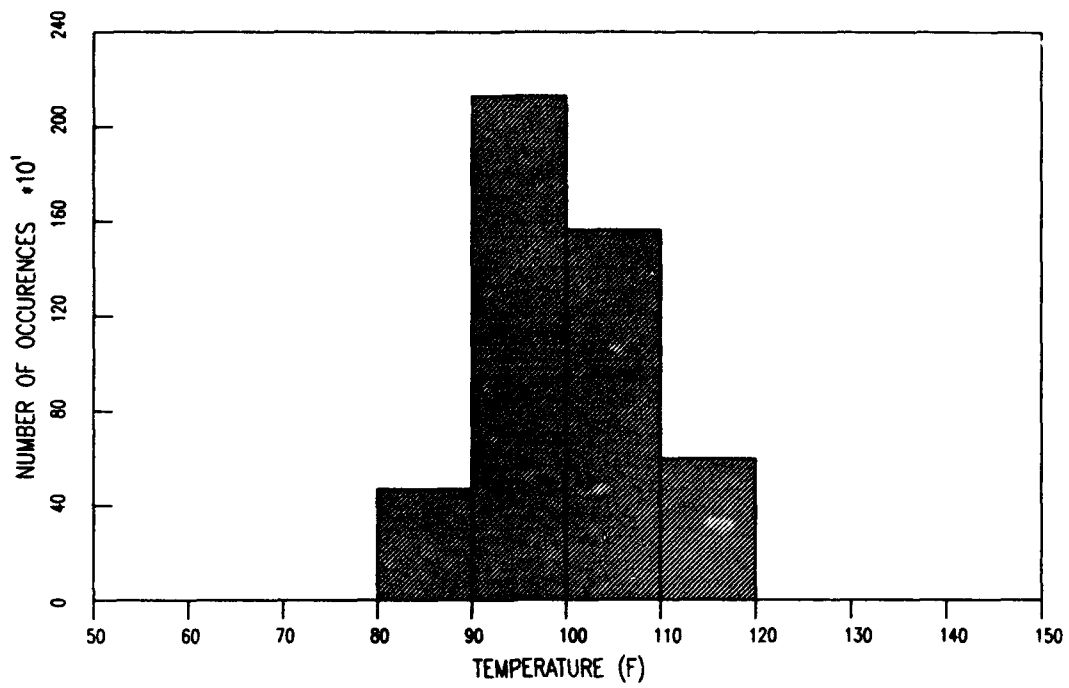
INTERFACE TEMPERATURE HISTOGRAM FOR PASS LEVEL 3286



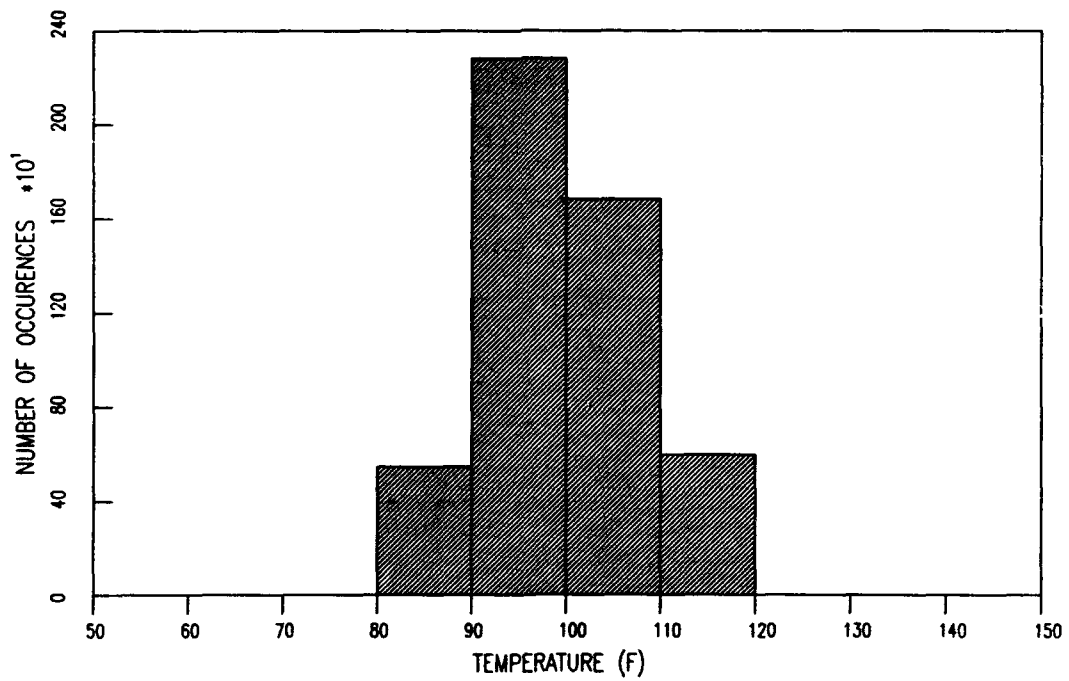
INTERFACE TEMPERATURE HISTOGRAM FOR PASS LEVEL 3942



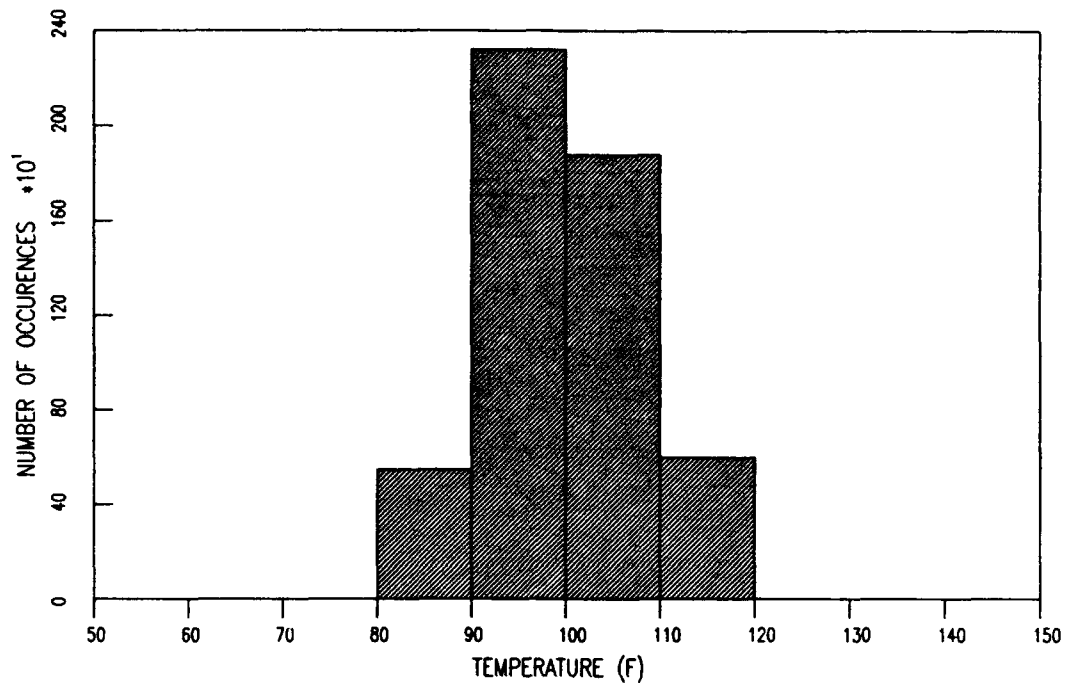
INTERFACE TEMPERATURE HISTOGRAM FOR PASS LEVEL 4784



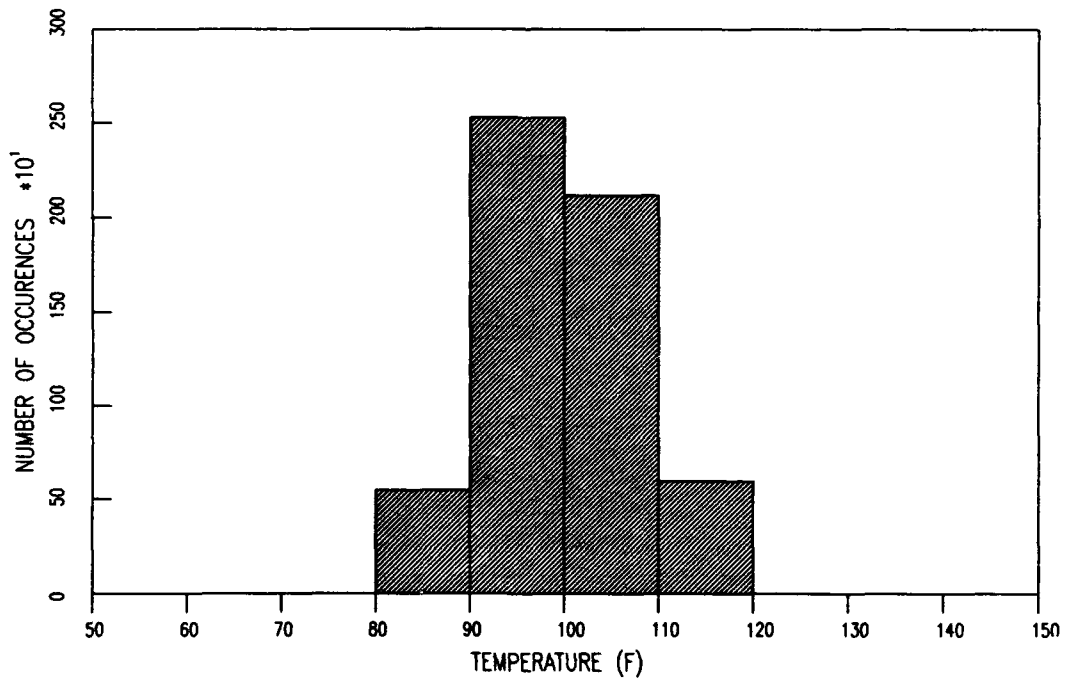
INTERFACE TEMPERATURE HISTOGRAM FOR PASS LEVEL 5137



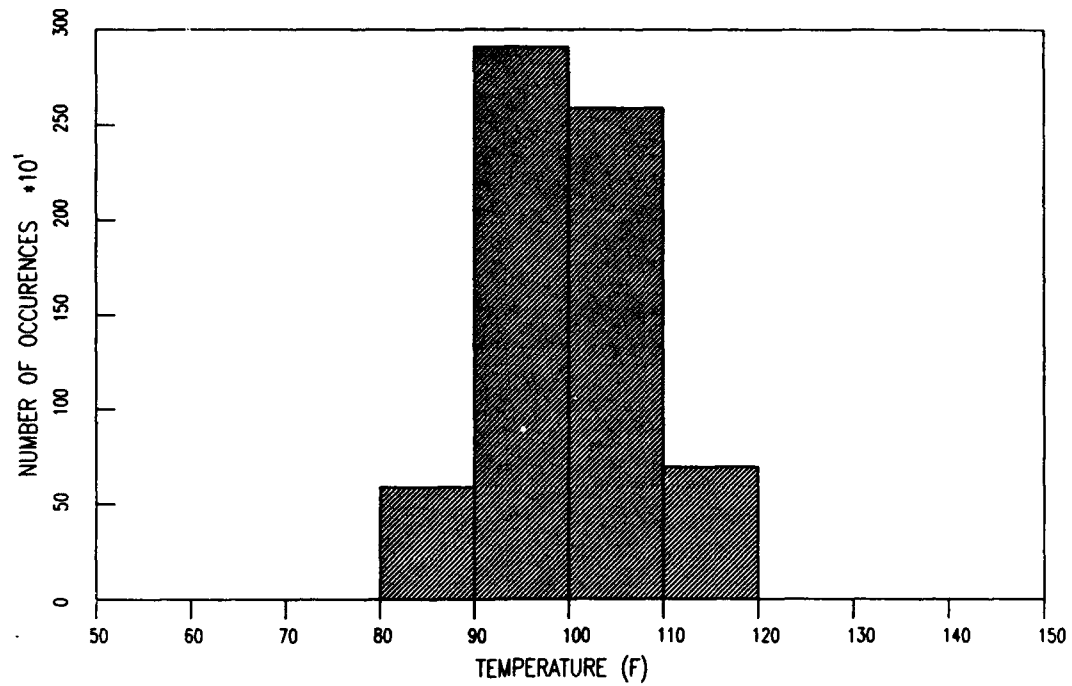
INTERFACE TEMPERATURE HISTOGRAM FOR PASS LEVEL 5370



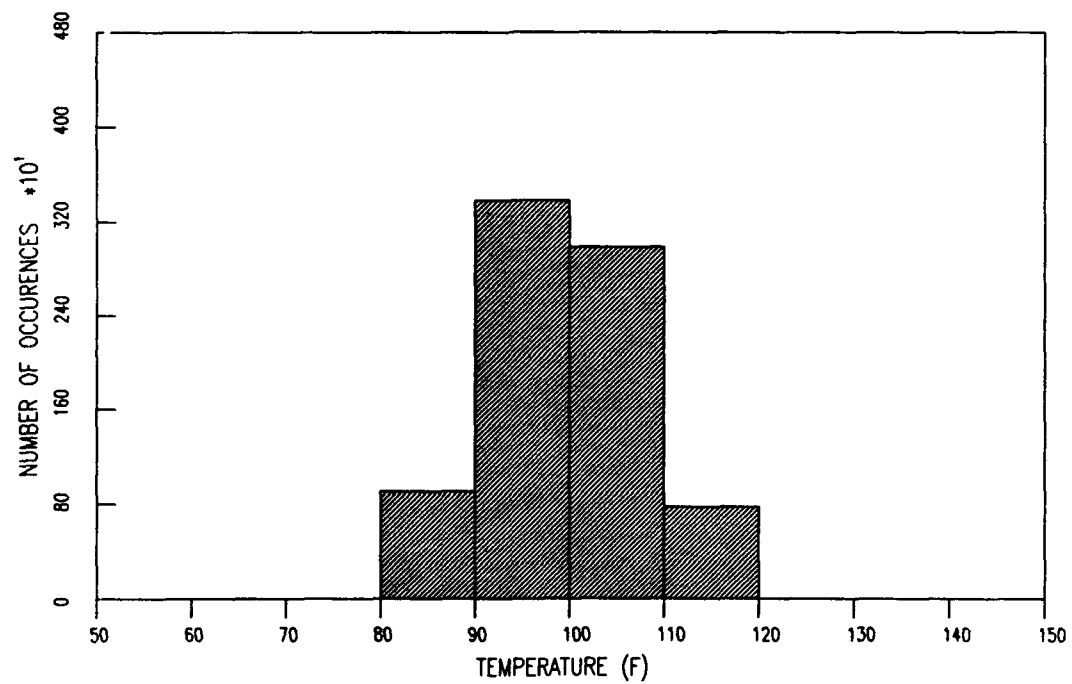
INTERFACE TEMPERATURE HISTOGRAM FOR PASS LEVEL 5817



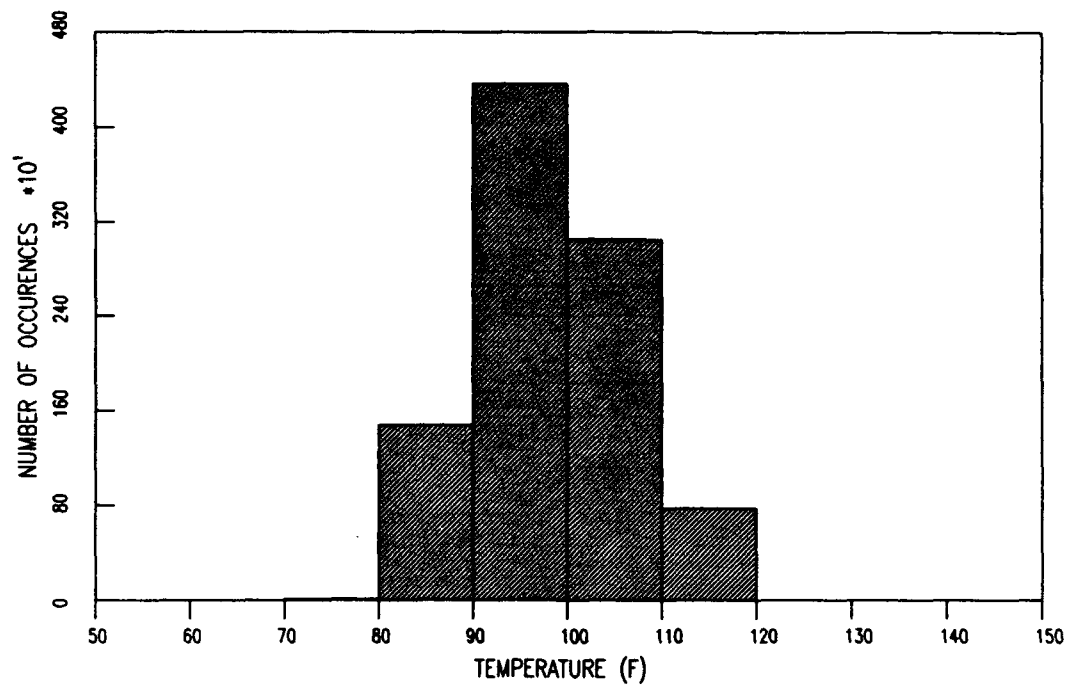
INTERFACE TEMPERATURE HISTOGRAM FOR PASS LEVEL 6808



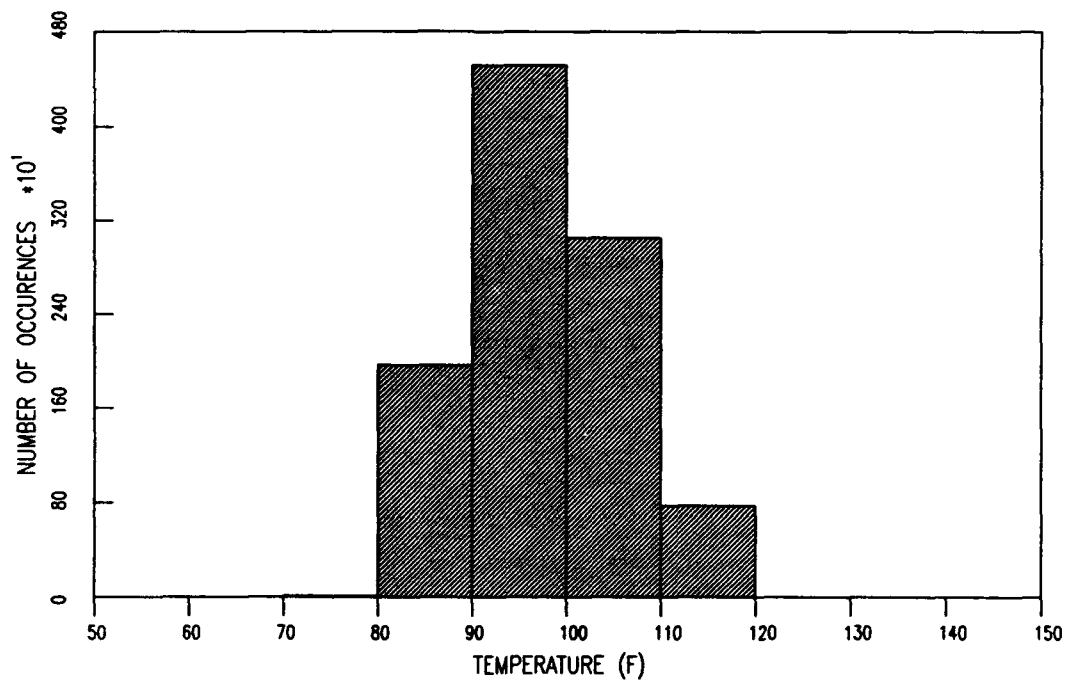
INTERFACE TEMPERATURE HISTOGRAM FOR PASS LEVEL 8080



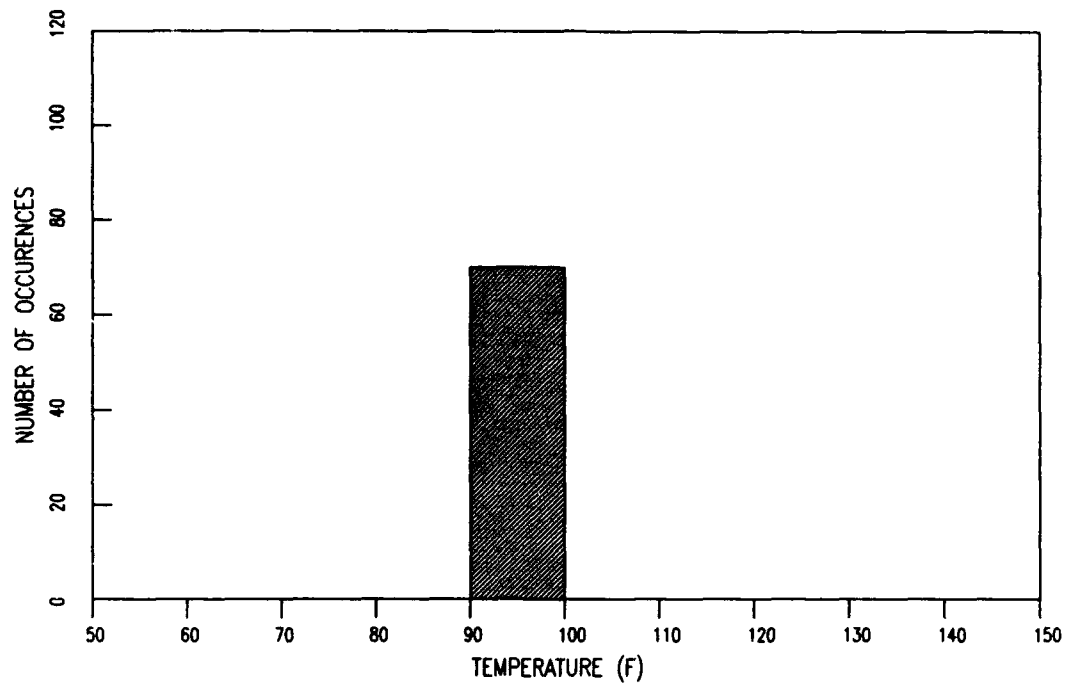
INTERFACE TEMPERATURE HISTOGRAM FOR PASS LEVEL 9715



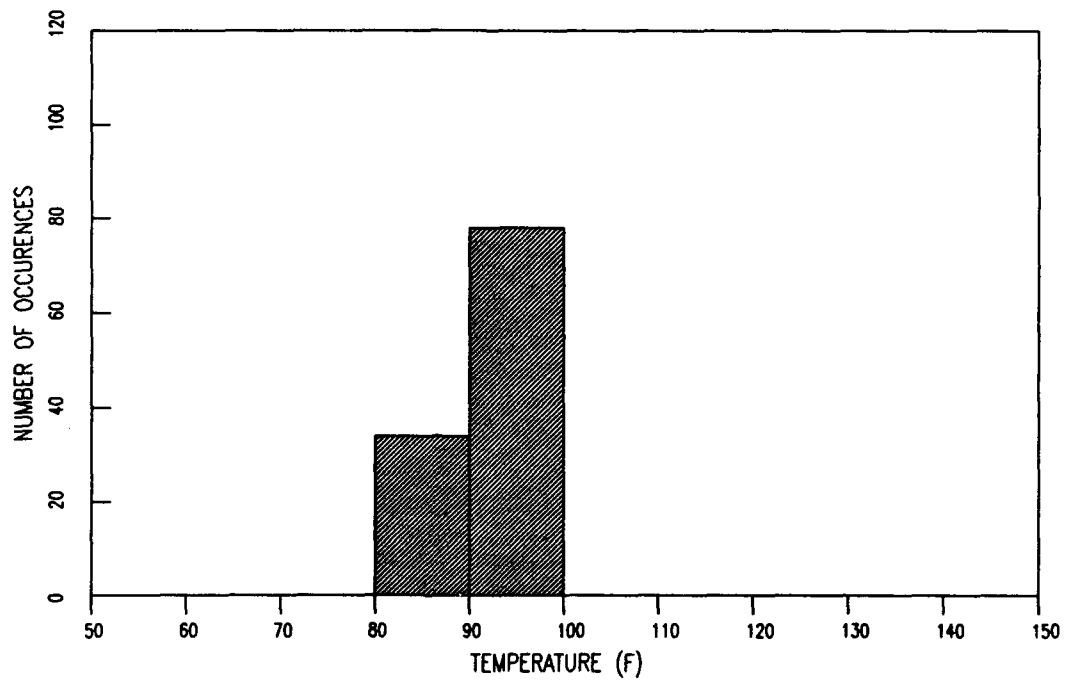
INTERFACE TEMPERATURE HISTOGRAM FOR PASS LEVEL 10350



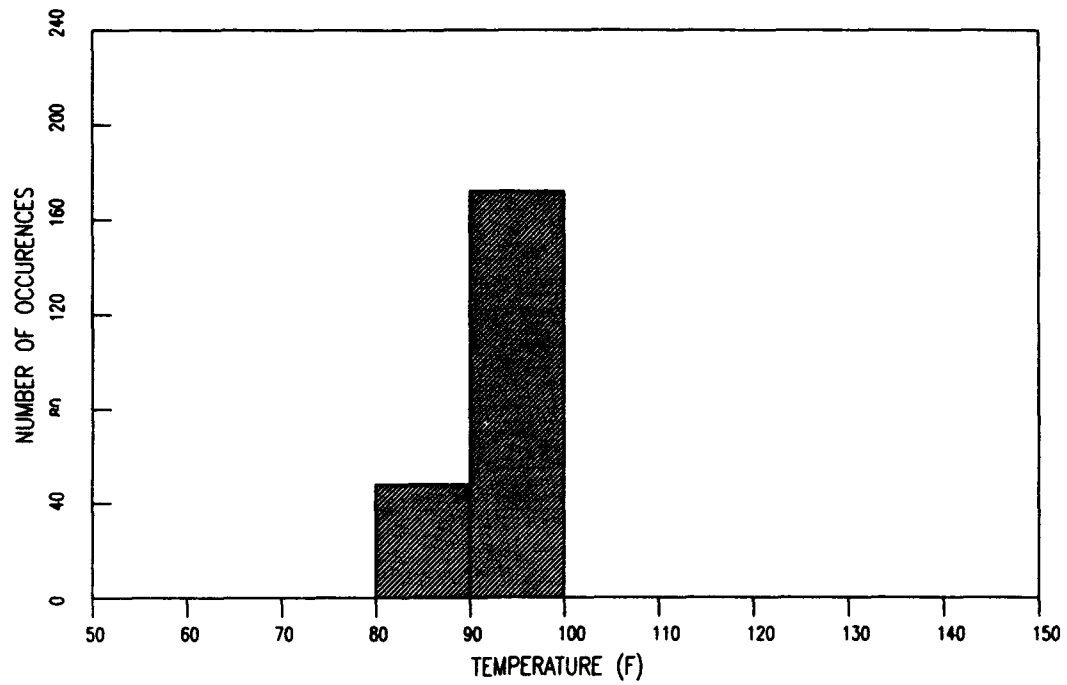
6-INCH TEMPERATURE HISTOGRAM FOR PASS LEVEL 70



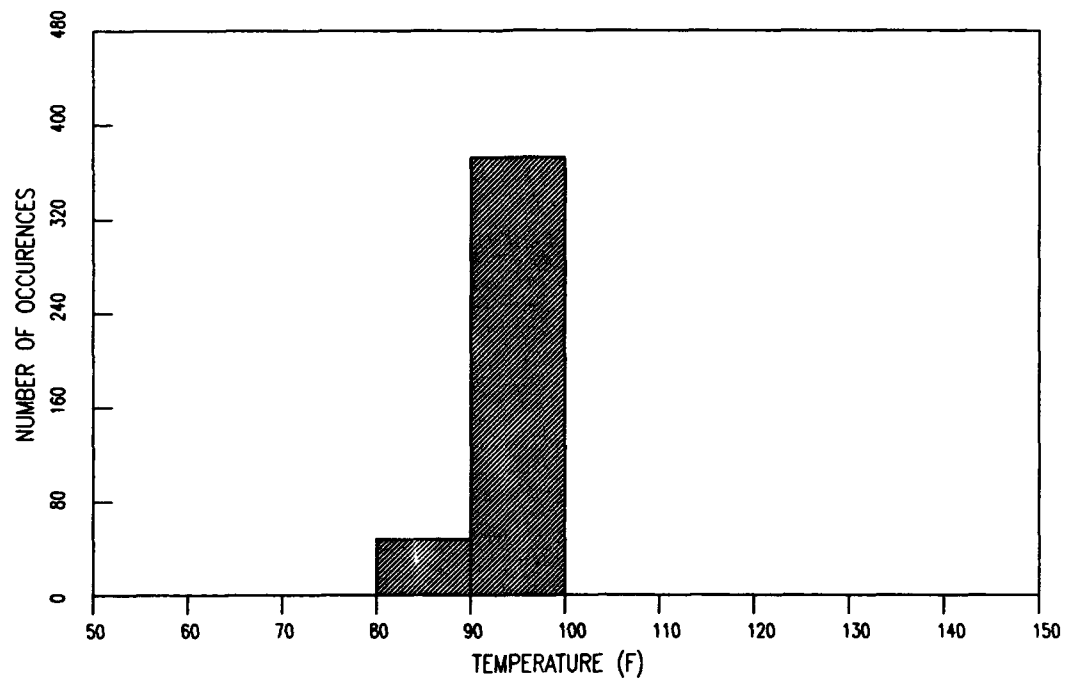
6-INCH TEMPERATURE HISTOGRAM FOR PASS LEVEL 112



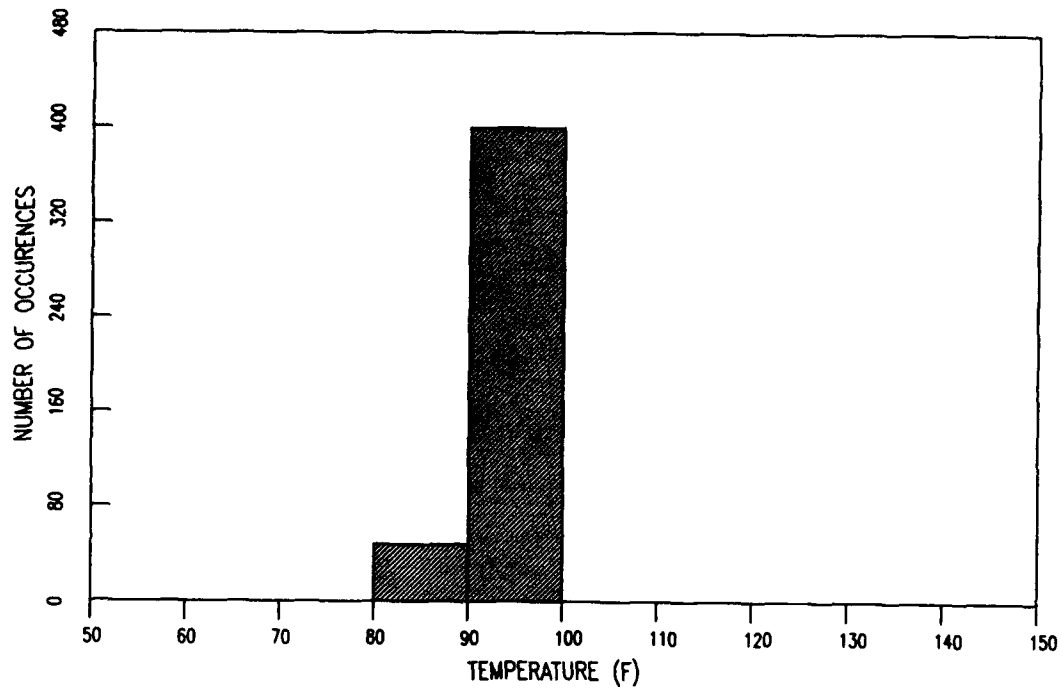
6-INCH TEMPERATURE HISTOGRAM FOR PASS LEVEL 220



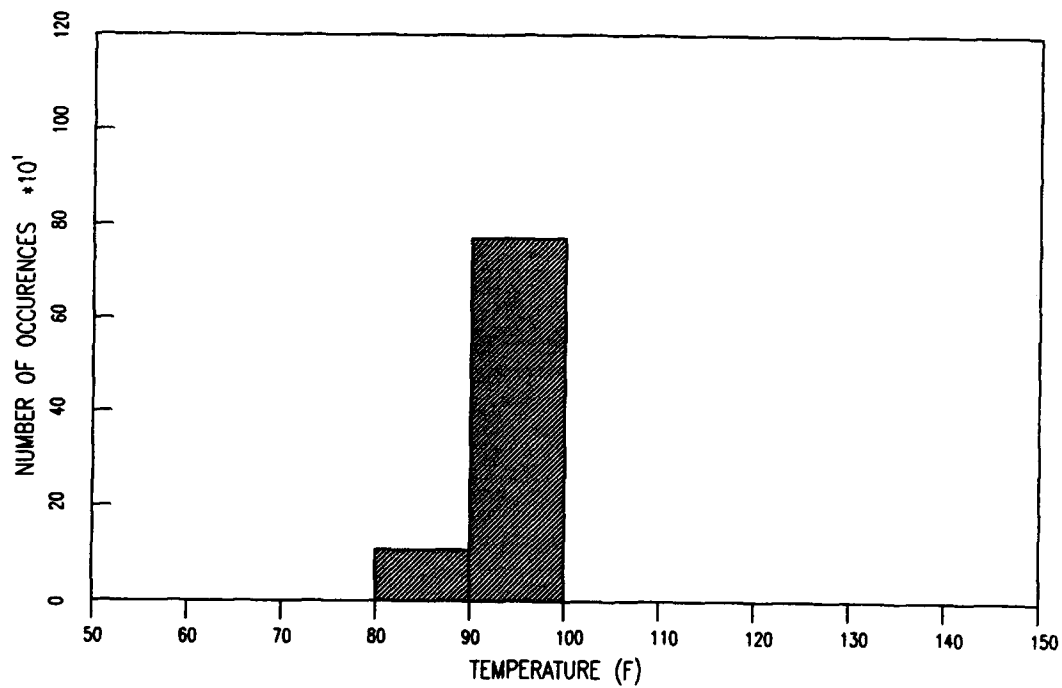
6-INCH TEMPERATURE HISTOGRAM FOR PASS LEVEL 420



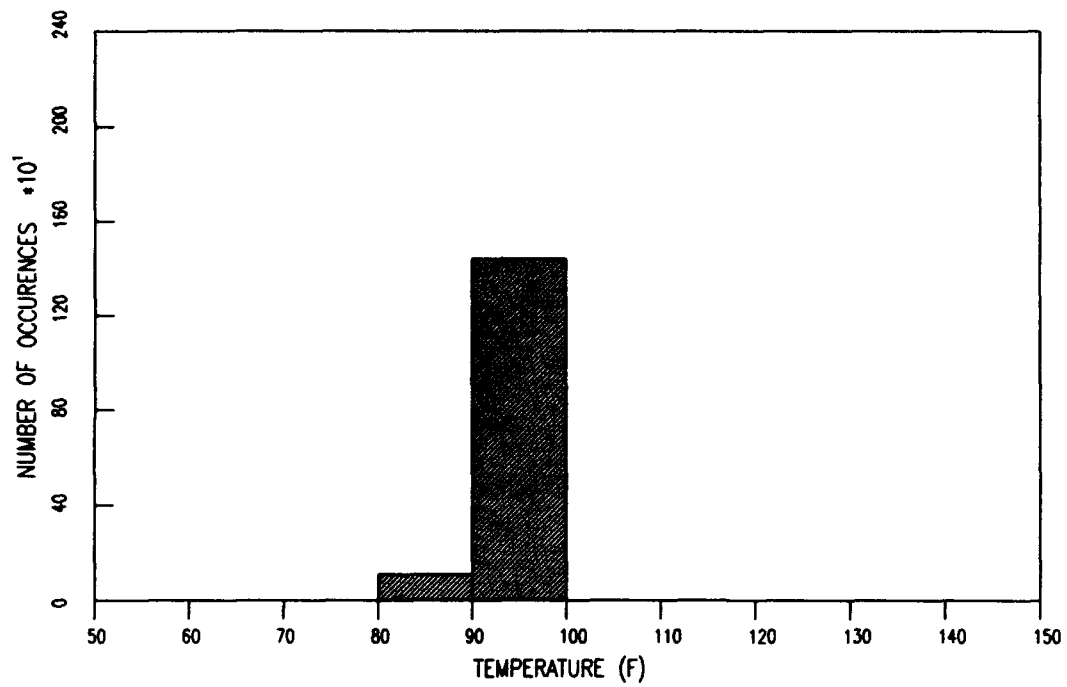
6-INCH TEMPERATURE HISTOGRAM FOR PASS LEVEL 448



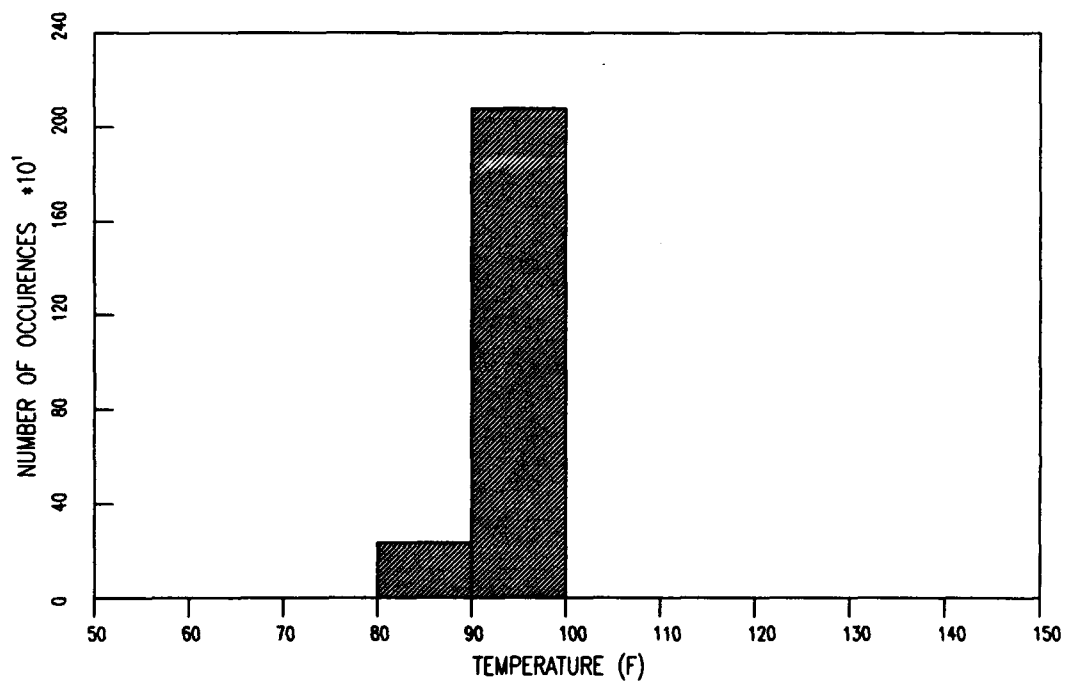
6-INCH TEMPERATURE HISTOGRAM FOR PASS LEVEL 882



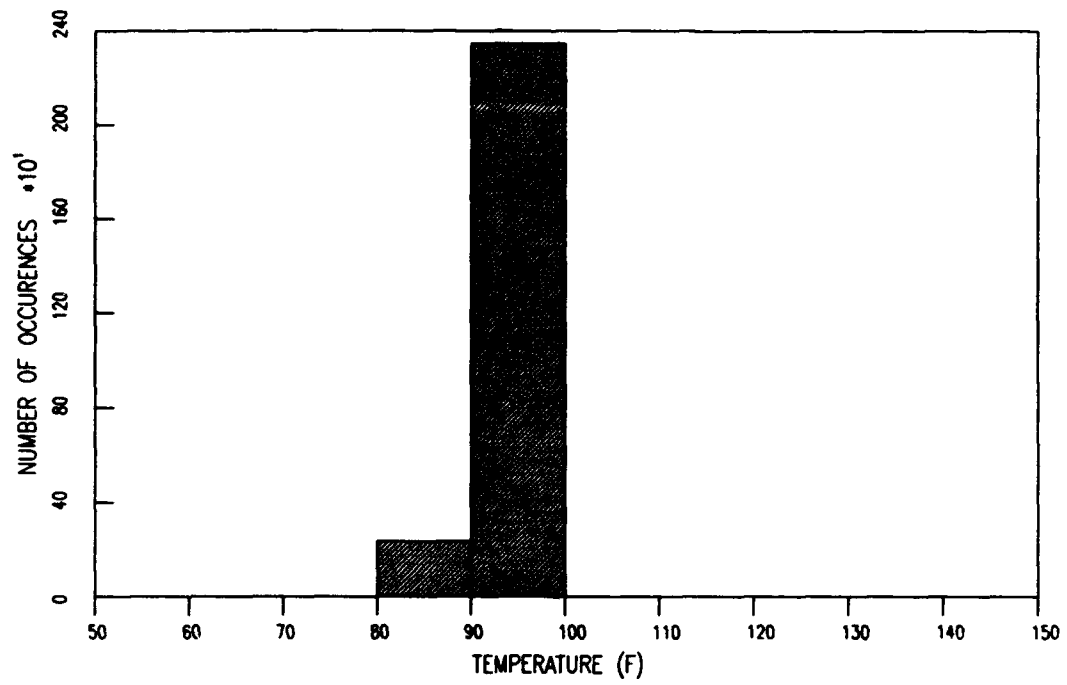
6-INCH TEMPERATURE HISTOGRAM FOR PASS LEVEL 1554



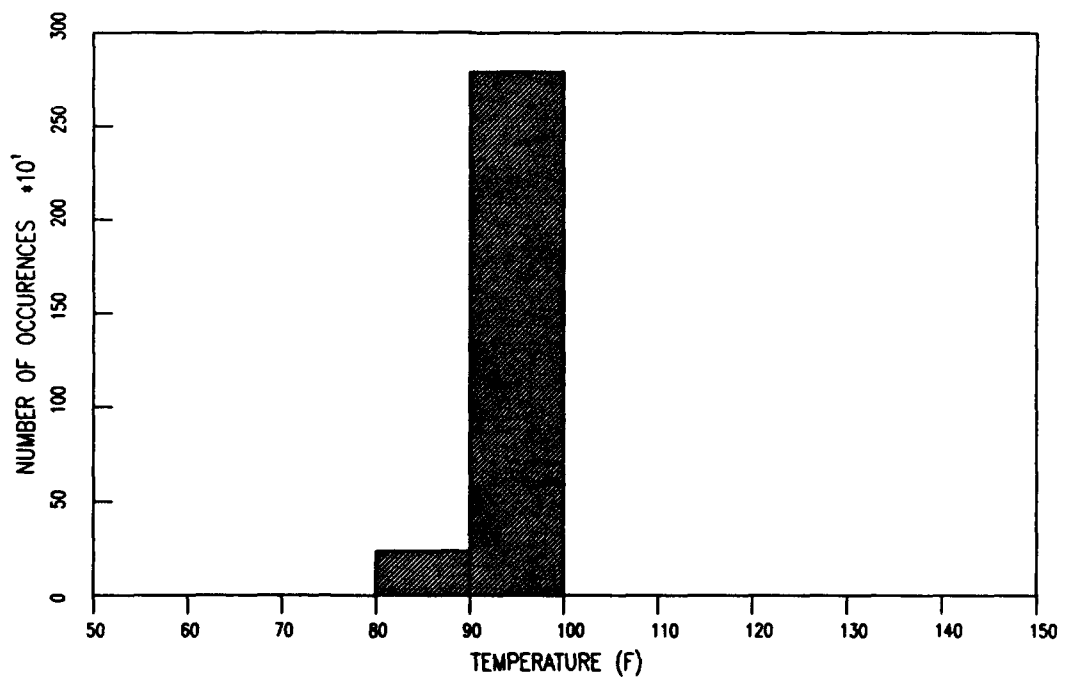
6-INCH TEMPERATURE HISTOGRAM FOR PASS LEVEL 2324



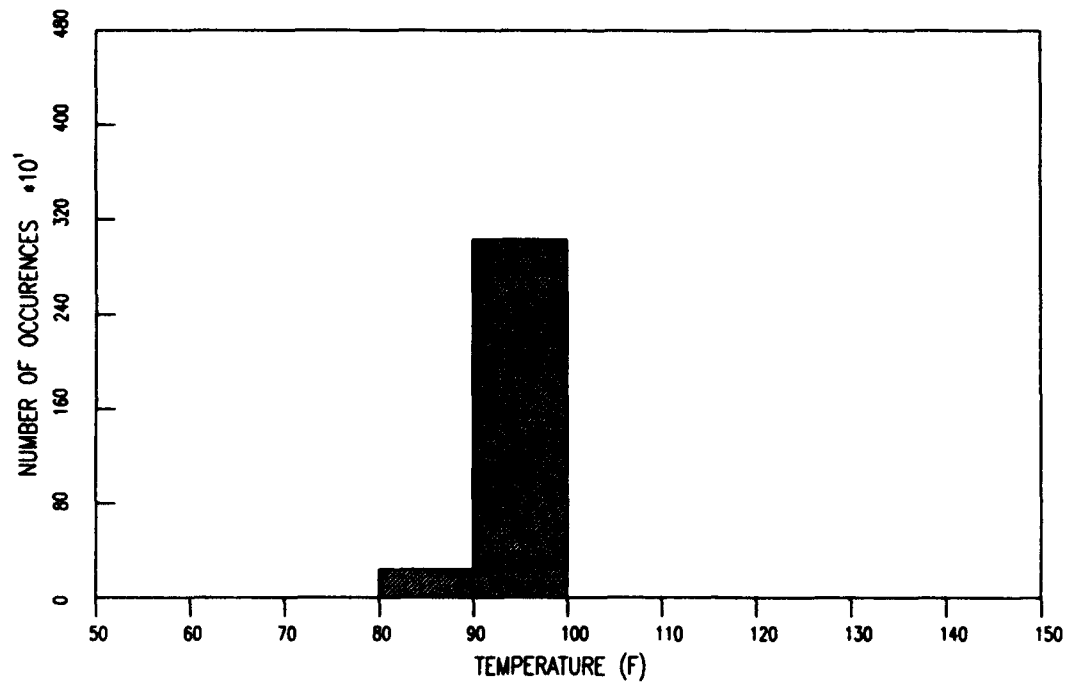
6-INCH TEMPERATURE HISTOGRAM FOR PASS LEVEL 2589



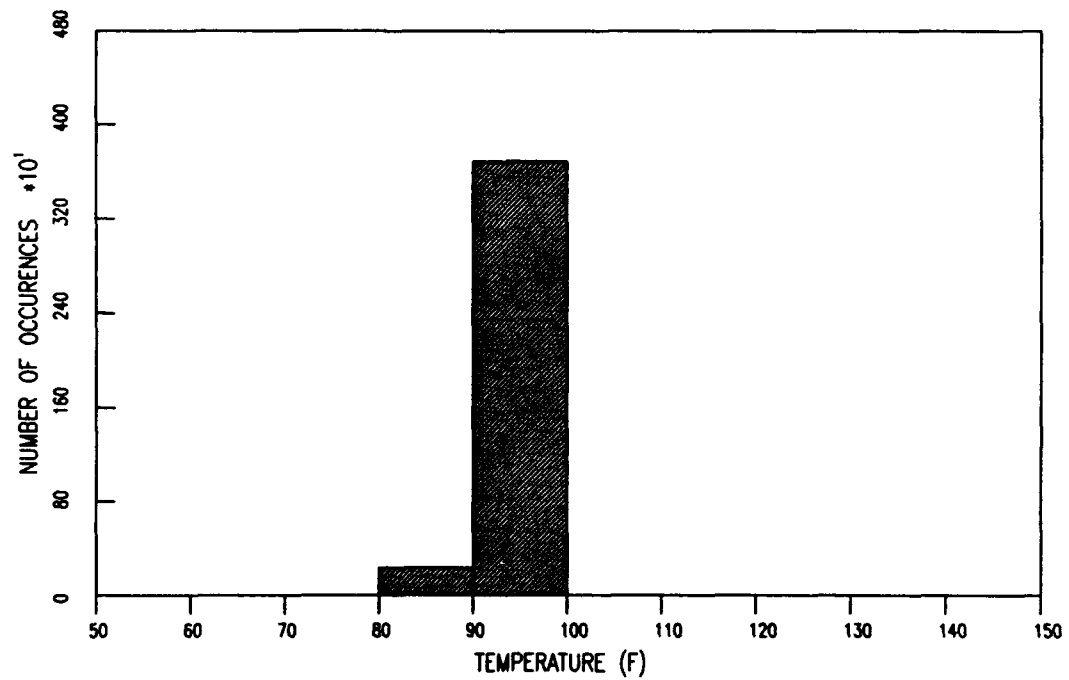
6-INCH TEMPERATURE HISTOGRAM FOR PASS LEVEL 3049



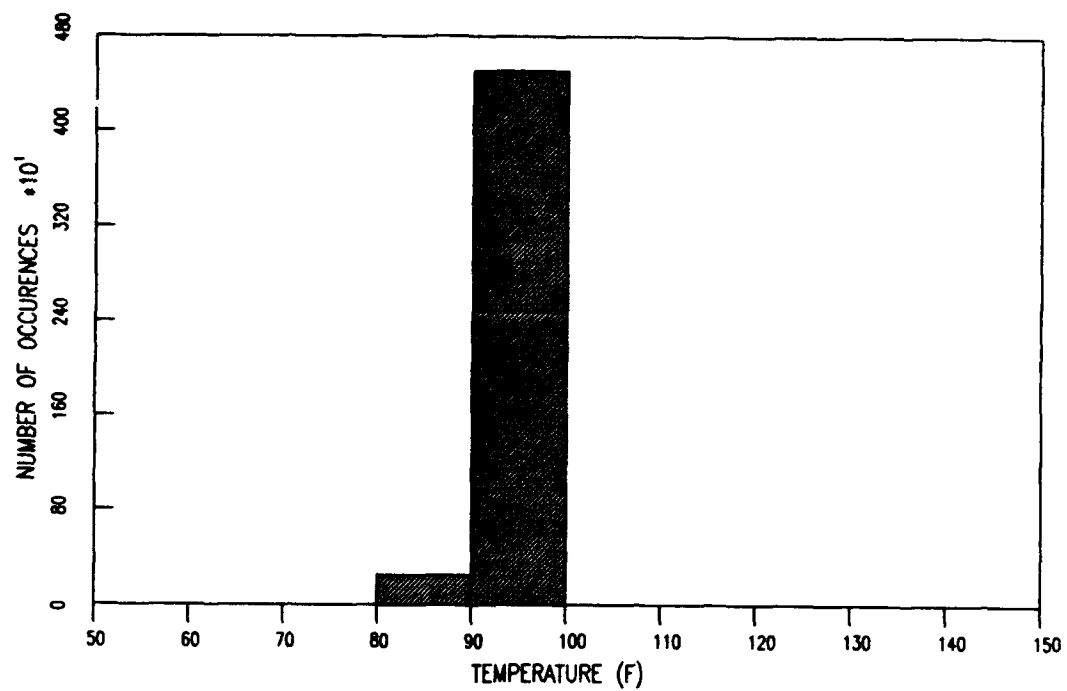
6-INCH TEMPERATURE HISTOGRAM FOR PASS LEVEL 3286



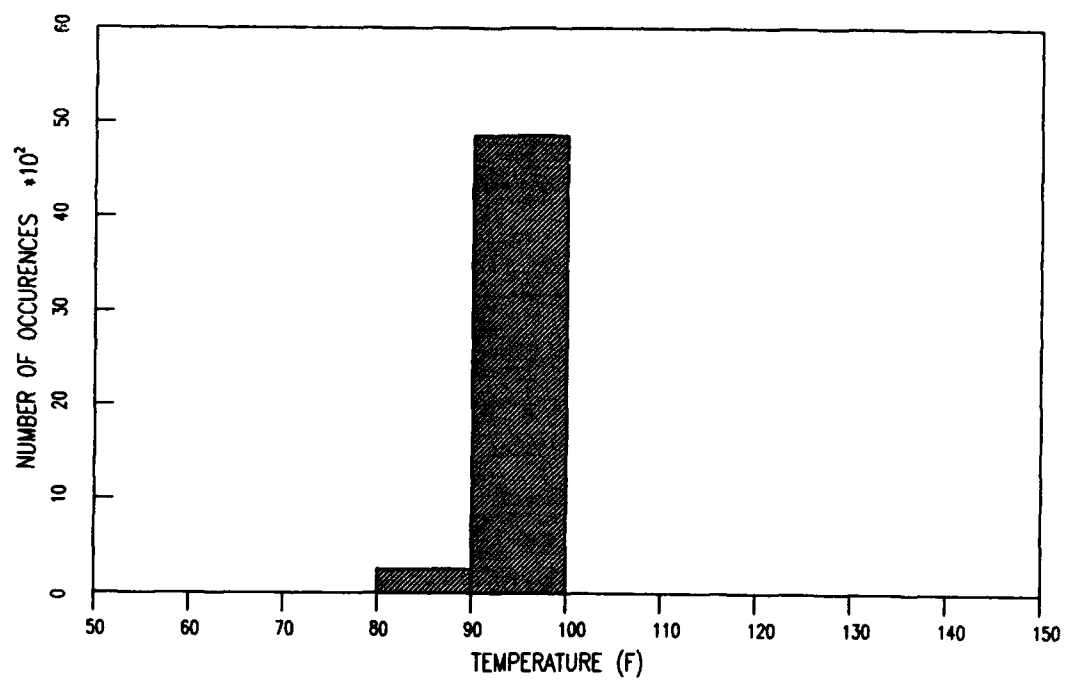
6-INCH TEMPERATURE HISTOGRAM FOR PASS LEVEL 3942



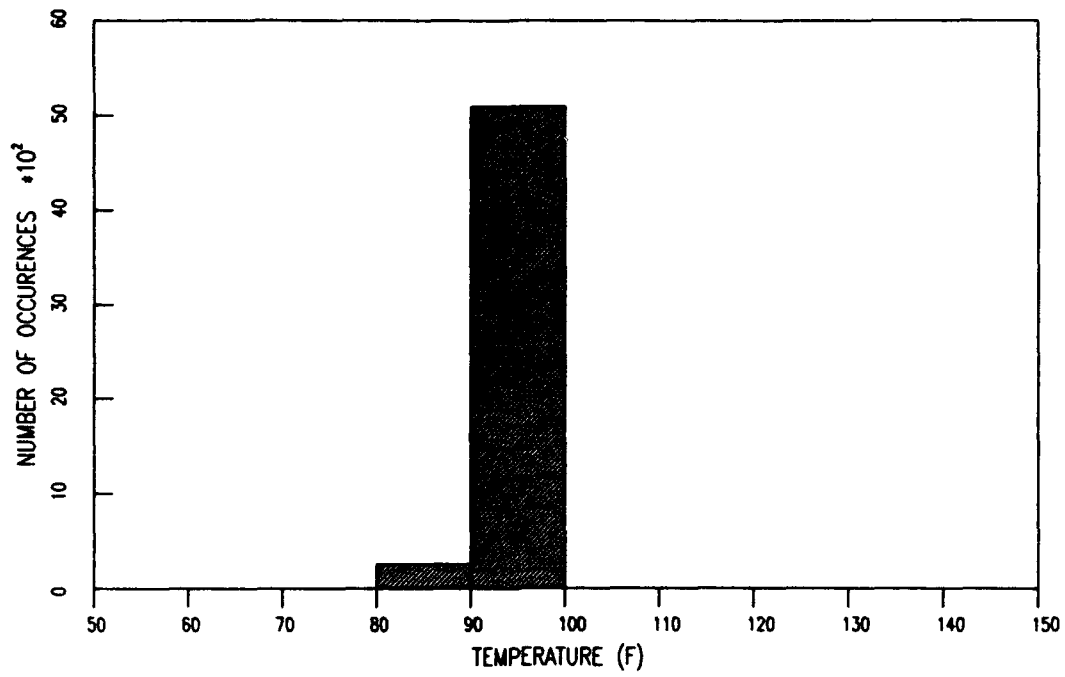
6-INCH TEMPERATURE HISTOGRAM FOR PASS LEVEL 4784



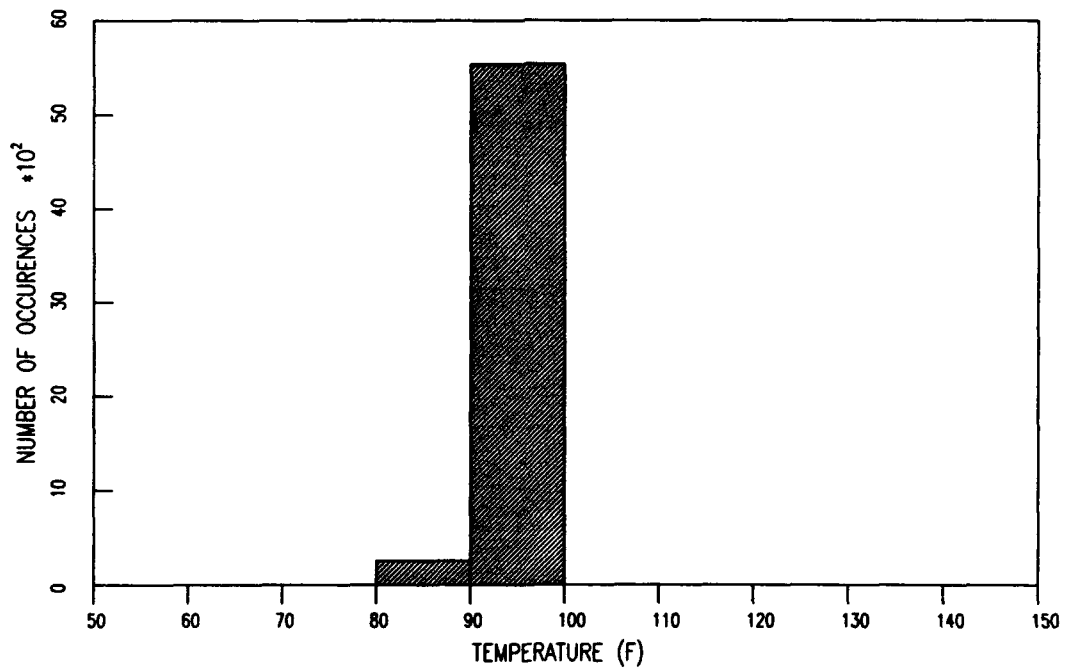
6-INCH TEMPERATURE HISTOGRAM FOR PASS LEVEL 5137



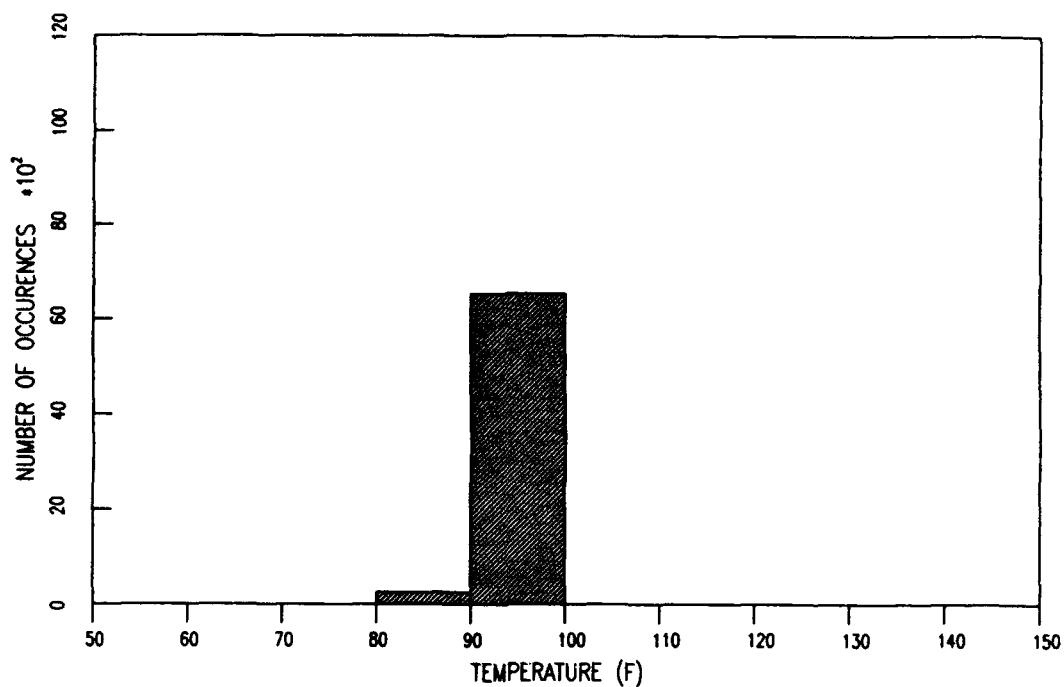
6-INCH TEMPERATURE HISTOGRAM FOR PASS LEVEL 5370



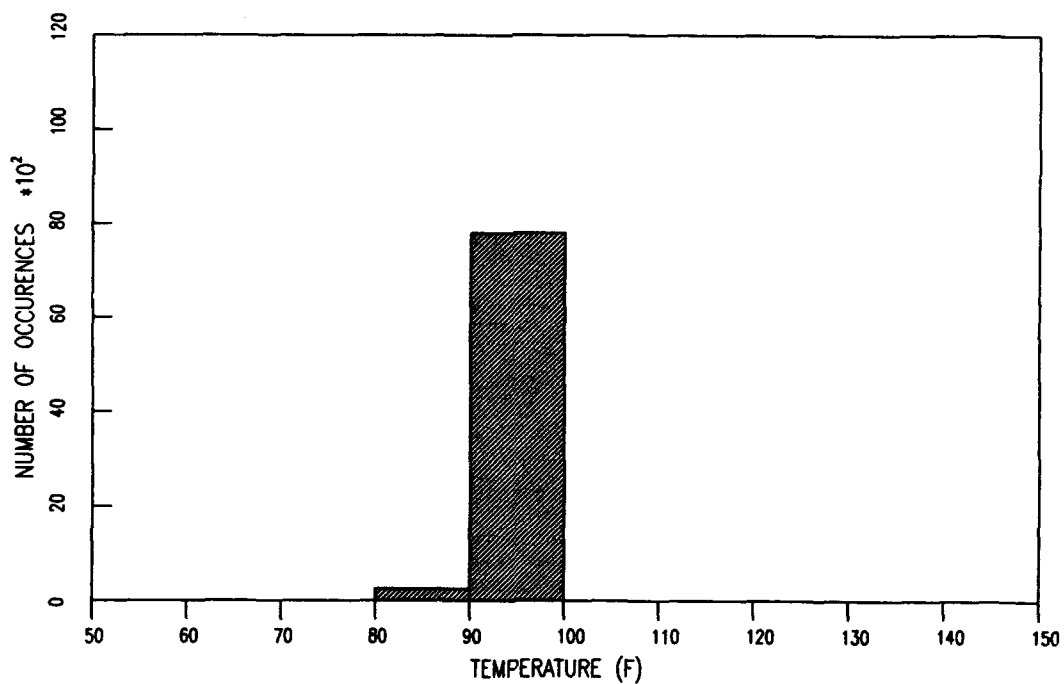
6-INCH TEMPERATURE HISTOGRAM FOR PASS LEVEL 5817



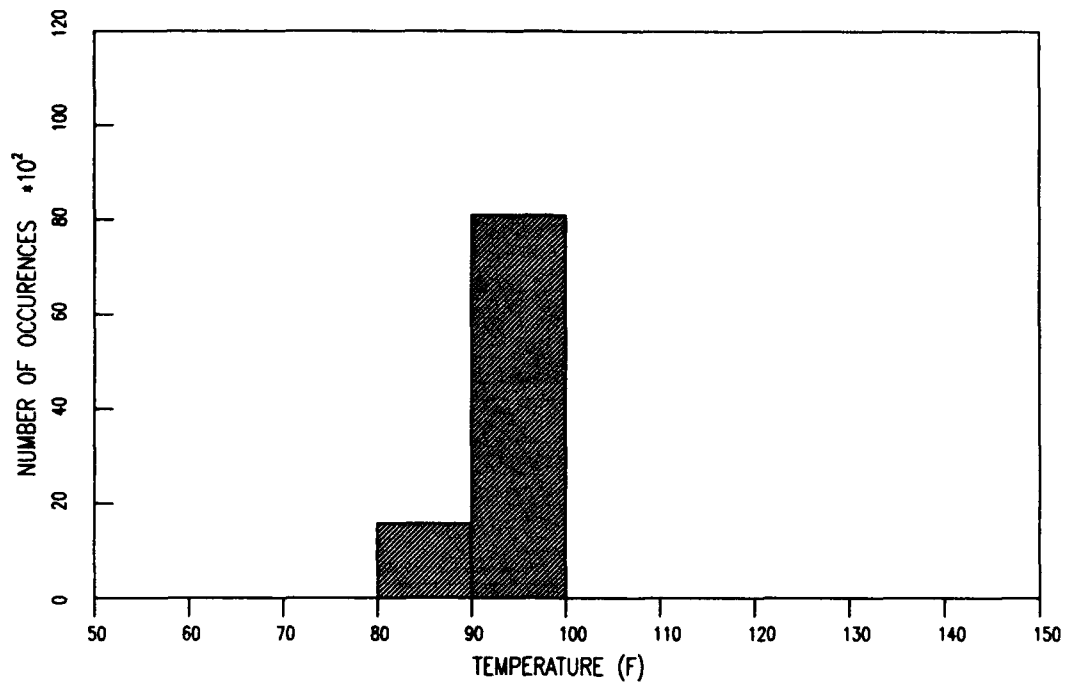
6-INCH TEMPERATURE HISTOGRAM FOR PASS LEVEL 6808



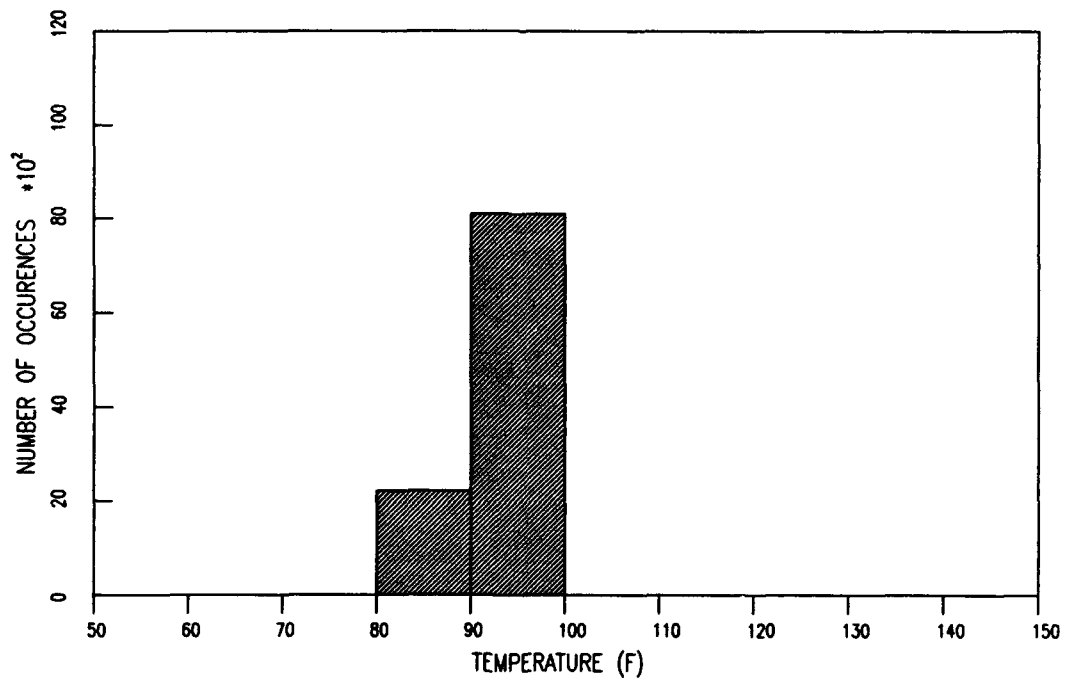
6-INCH TEMPERATURE HISTOGRAM FOR PASS LEVEL 8080



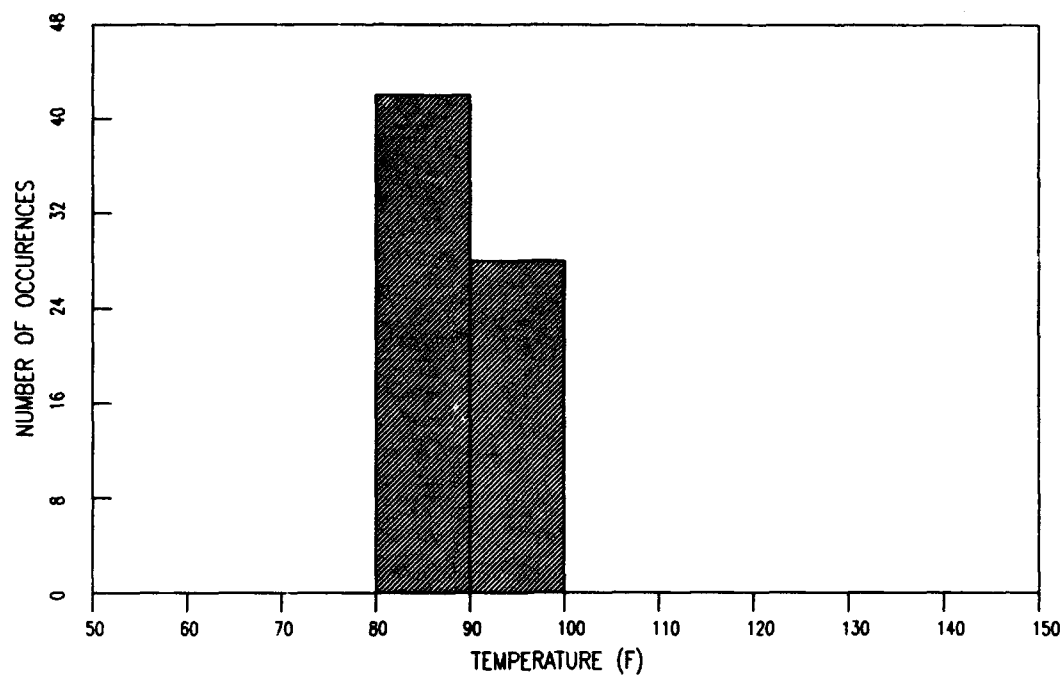
6-INCH TEMPERATURE HISTOGRAM FOR PASS LEVEL 9715



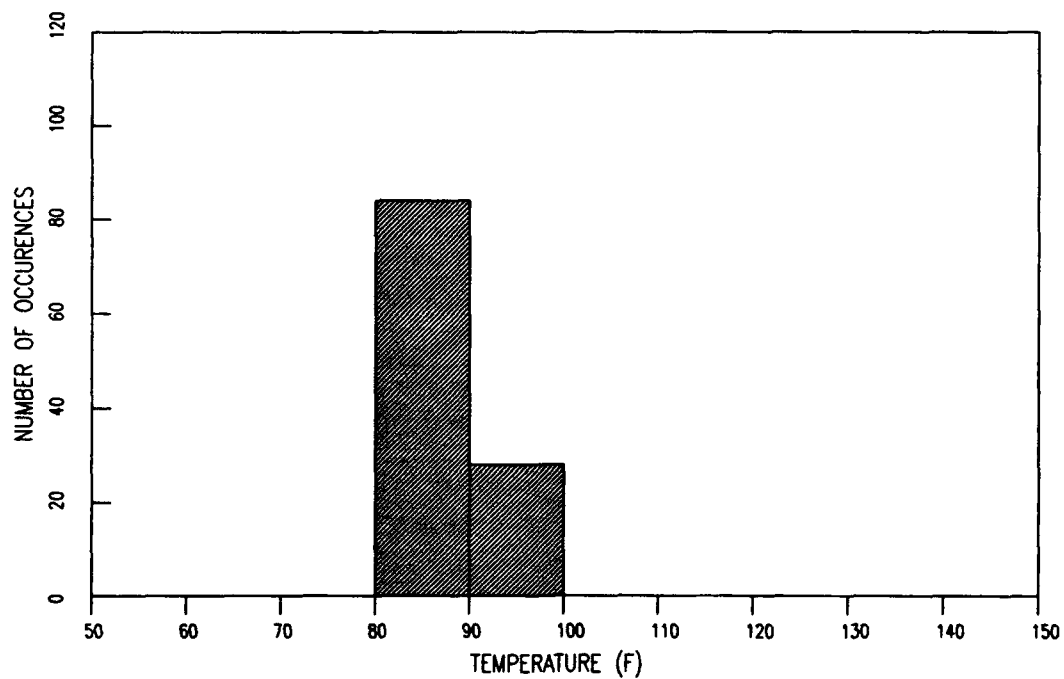
6-INCH TEMPERATURE HISTOGRAM FOR PASS LEVEL 10350



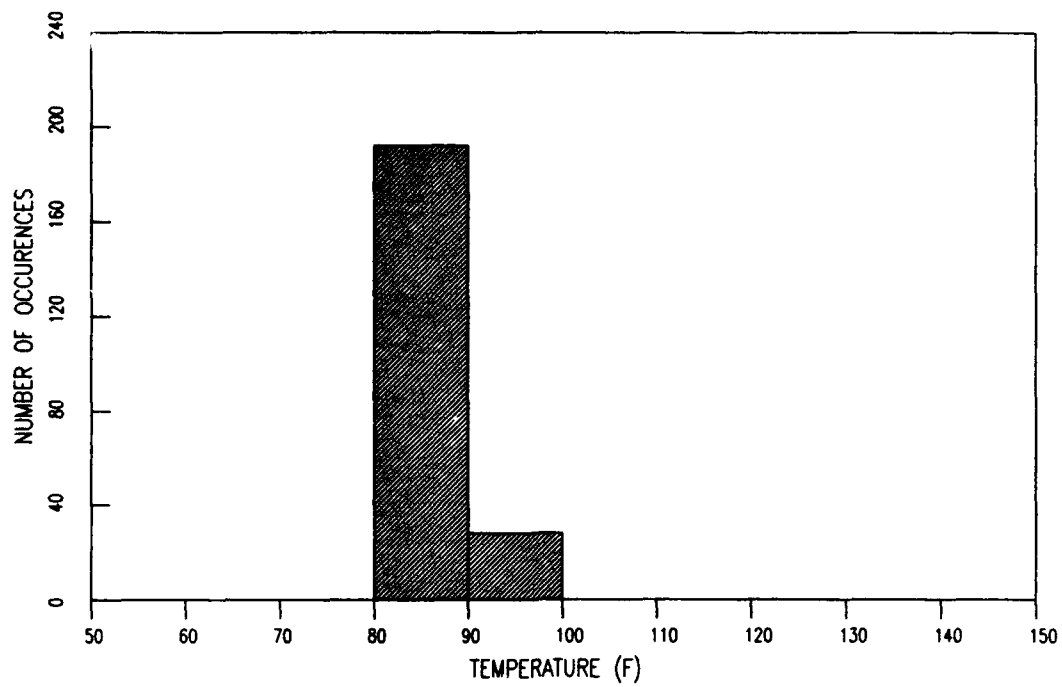
12-INCH TEMPERATURE HISTOGRAM FOR PASS LEVEL 70



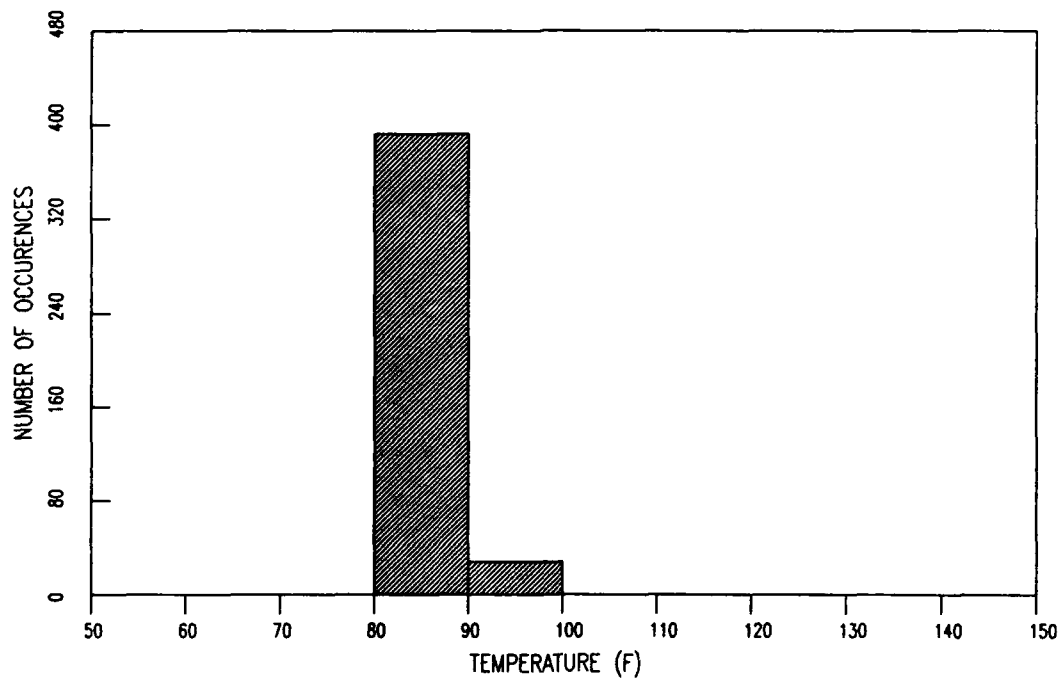
12-INCH TEMPERATURE HISTOGRAM FOR PASS LEVEL 112



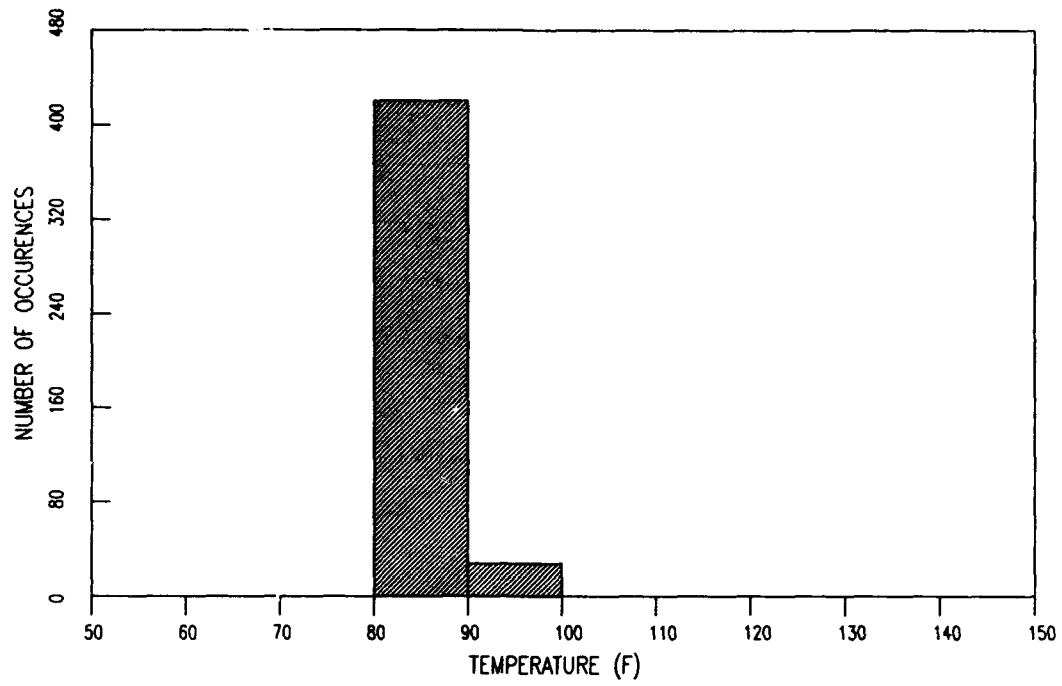
12-INCH TEMPERATURE HISTOGRAM FOR PASS LEVEL 220



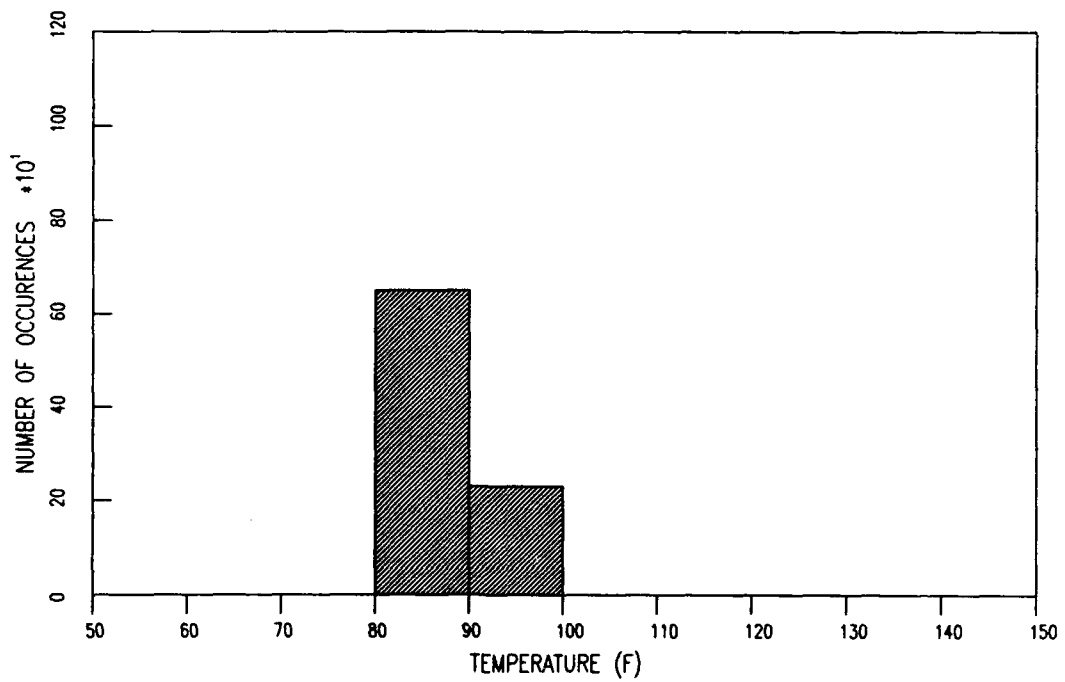
12-INCH TEMPERATURE HISTOGRAM FOR PASS LEVEL 420



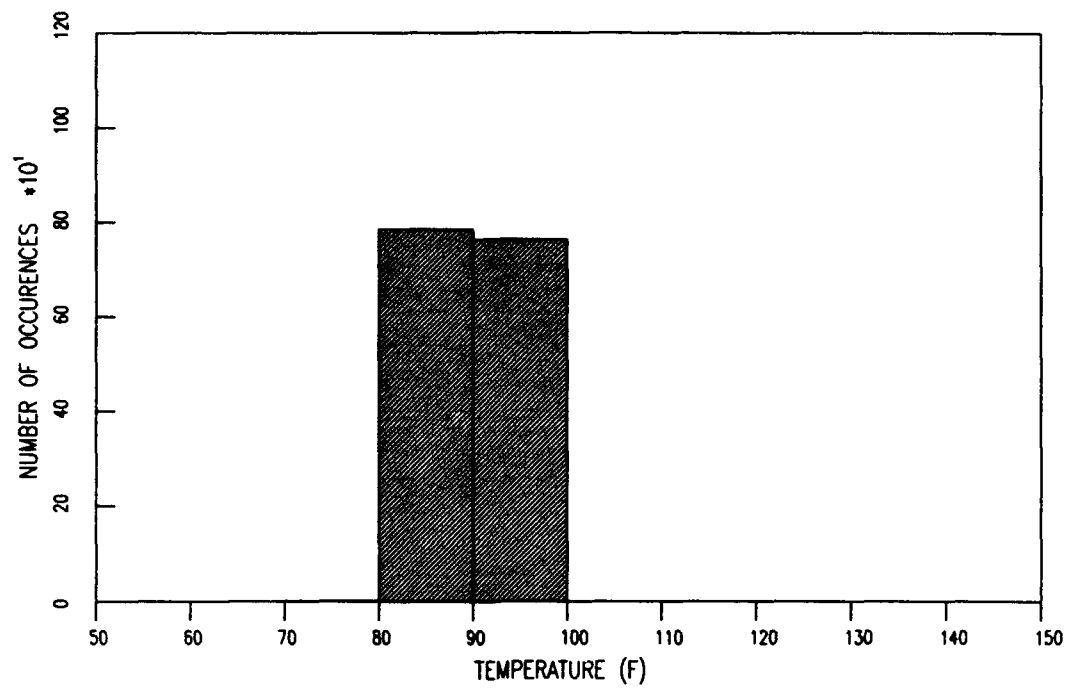
12-INCH TEMPERATURE HISTOGRAM FOR PASS LEVEL 448



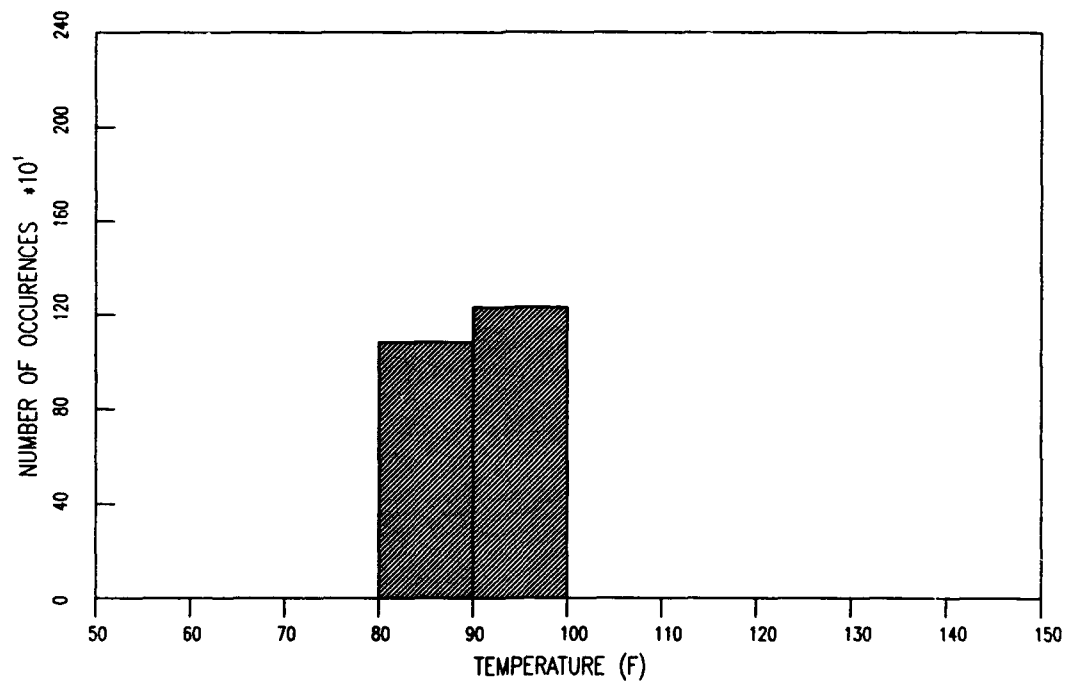
12-INCH TEMPERATURE HISTOGRAM FOR PASS LEVEL 882



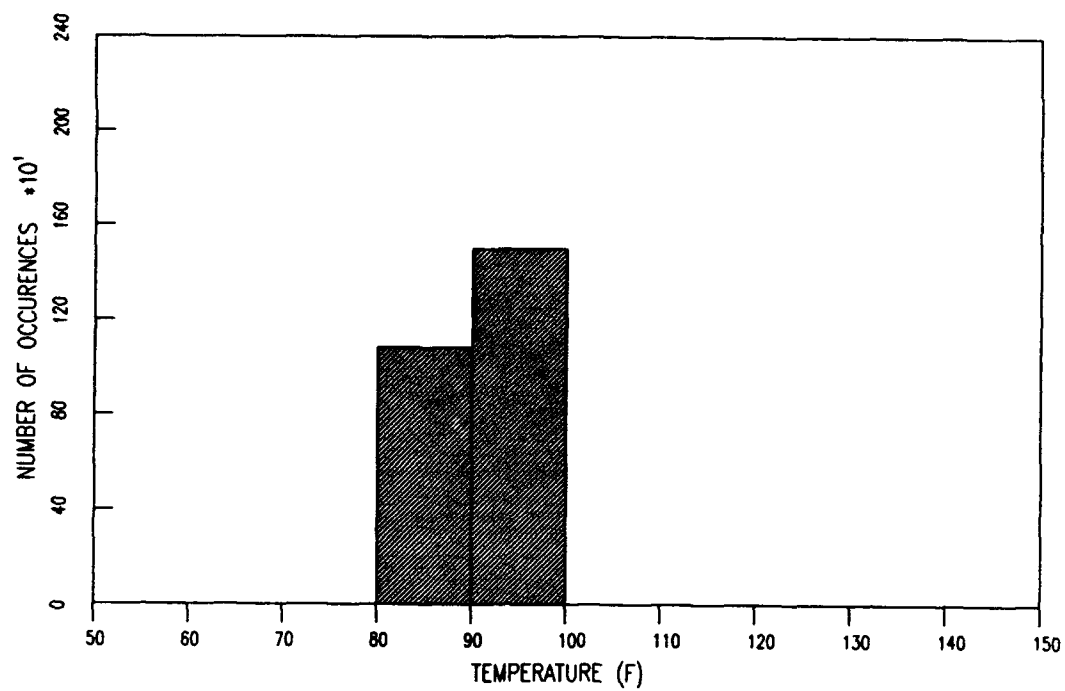
12-INCH TEMPERATURE HISTOGRAM FOR PASS LEVEL 1554



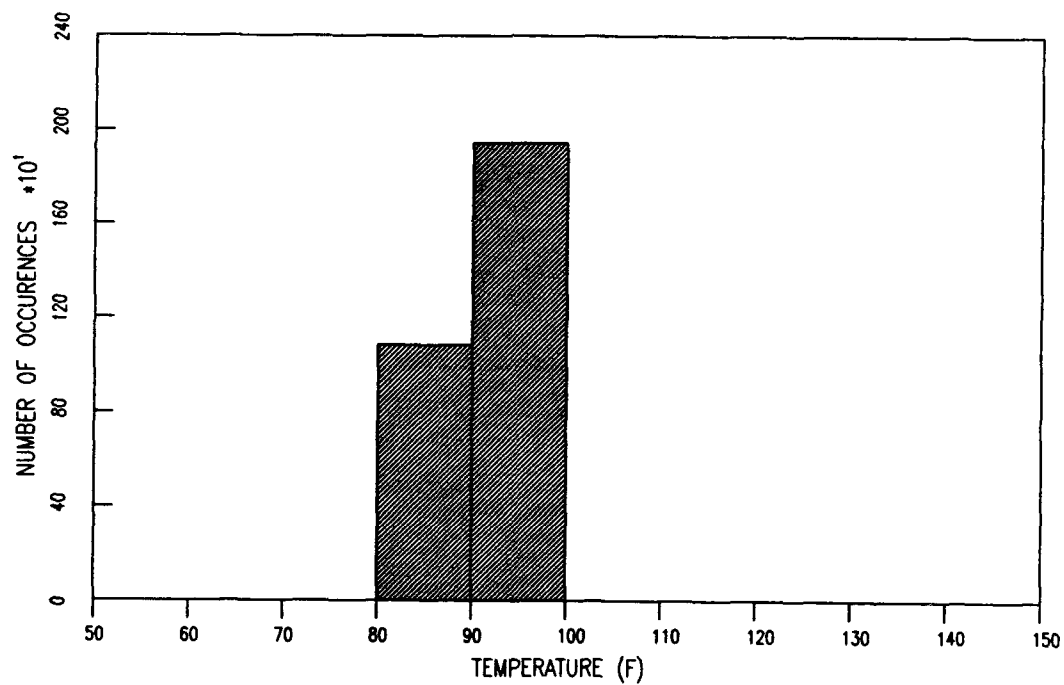
12-INCH TEMPERATURE HISTOGRAM FOR PASS LEVEL 2324



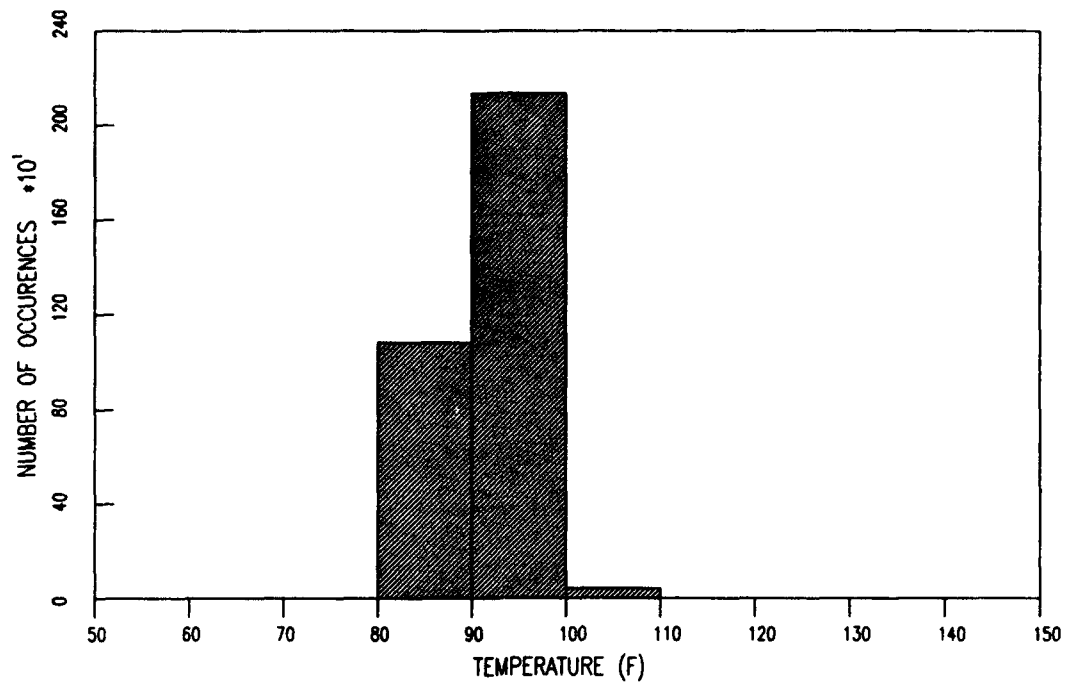
12-INCH TEMPERATURE HISTOGRAM FOR PASS LEVEL 2589



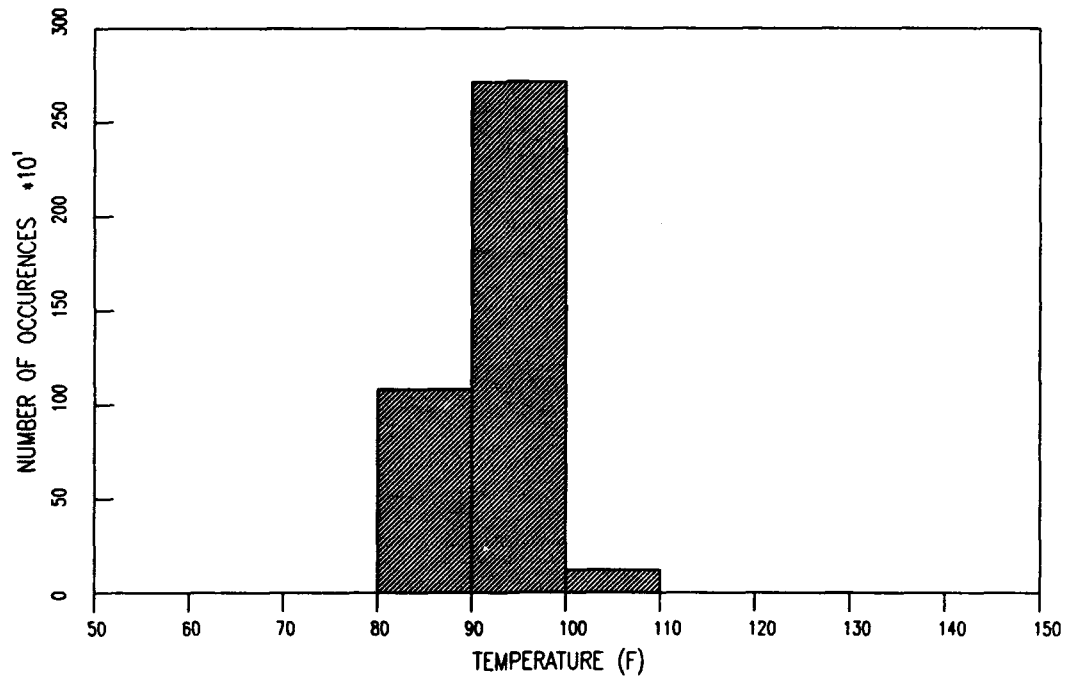
12-INCH TEMPERATURE HISTOGRAM FOR PASS LEVEL 3049



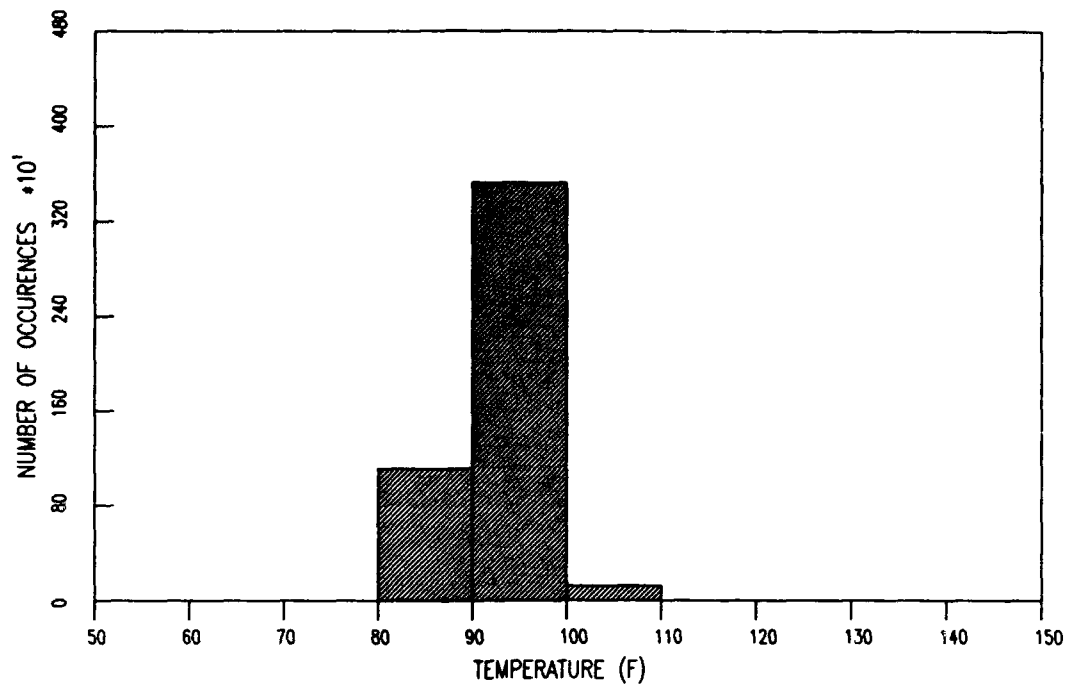
12-INCH TEMPERATURE HISTOGRAM FOR PASS LEVEL 3286



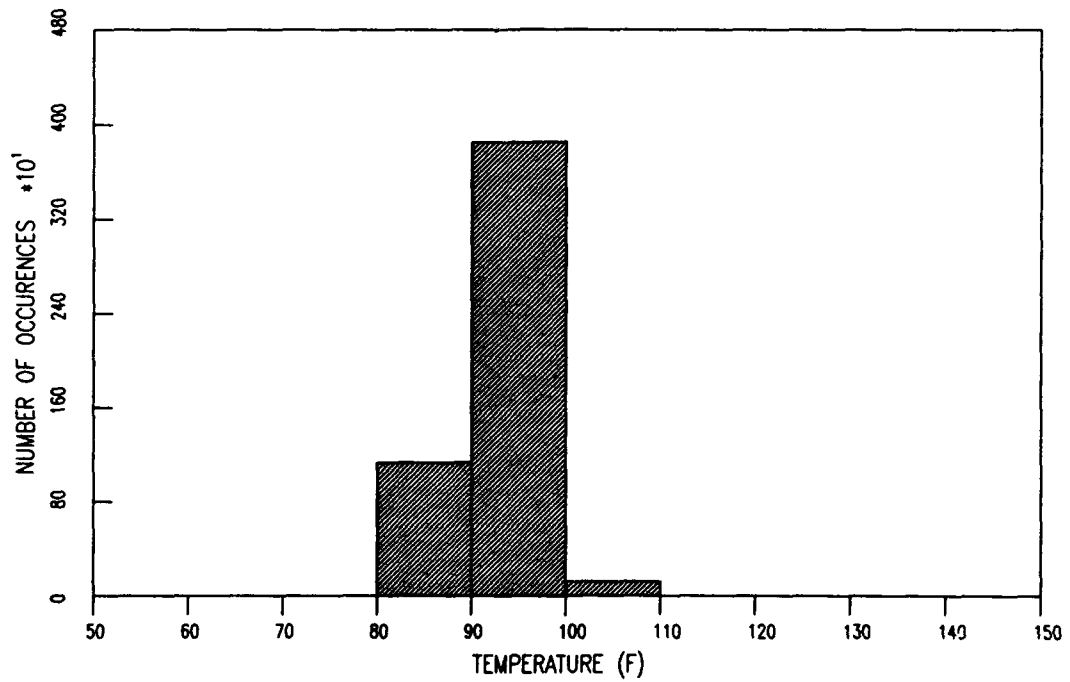
12-INCH TEMPERATURE HISTOGRAM FOR PASS LEVEL 3942



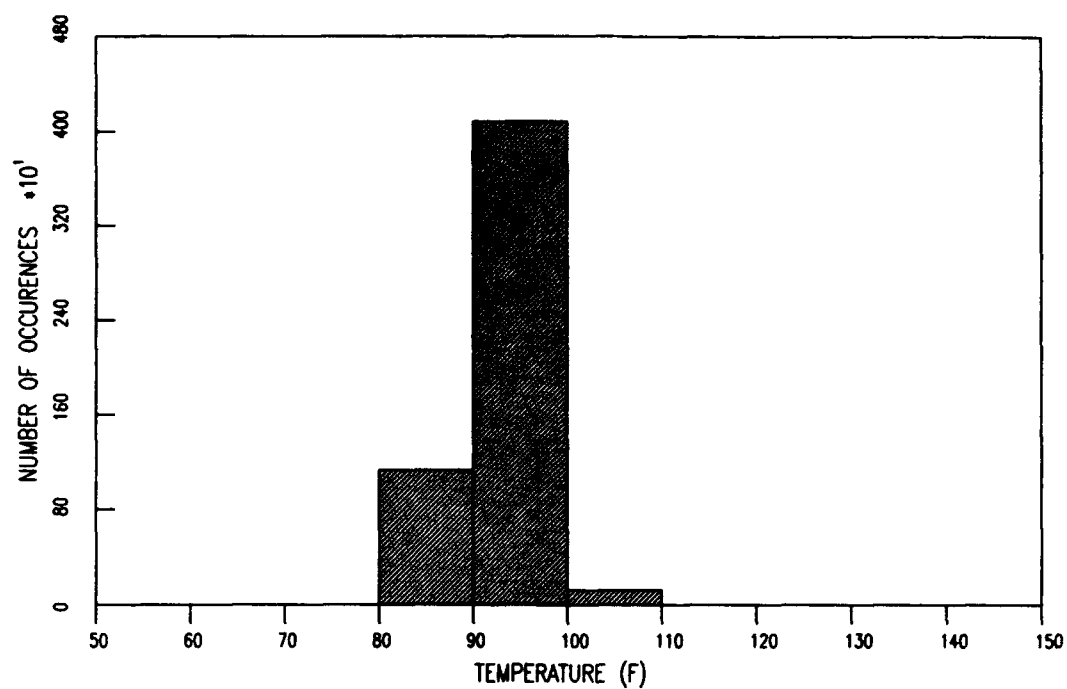
12-INCH TEMPERATURE HISTOGRAM FOR PASS LEVEL 4784



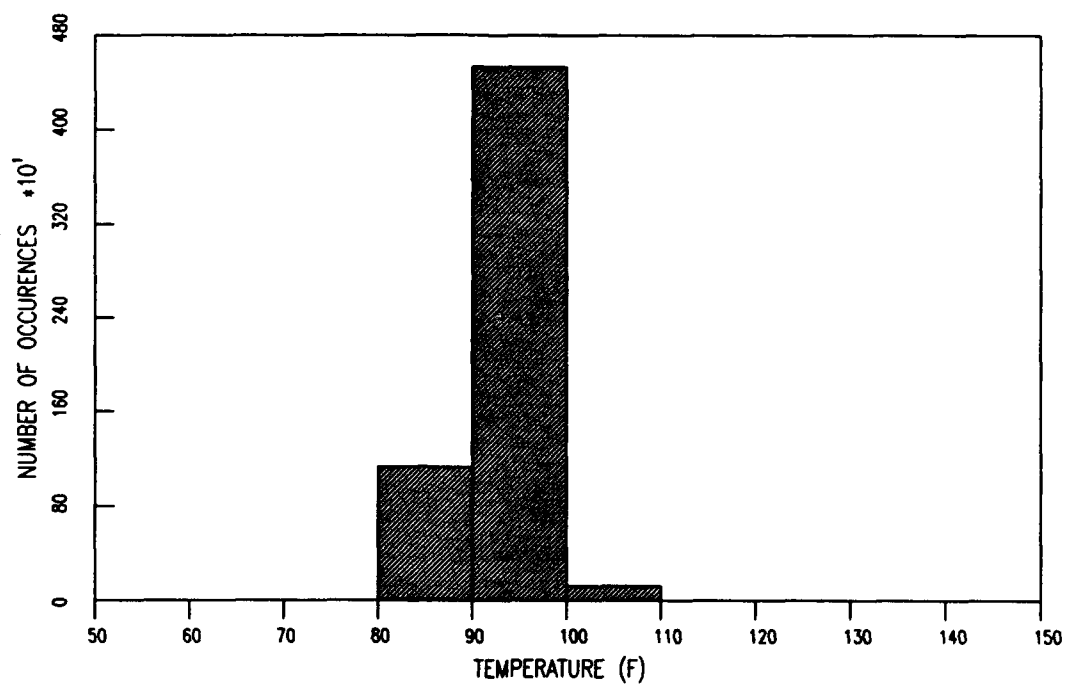
12-INCH TEMPERATURE HISTOGRAM FOR PASS LEVEL 5137



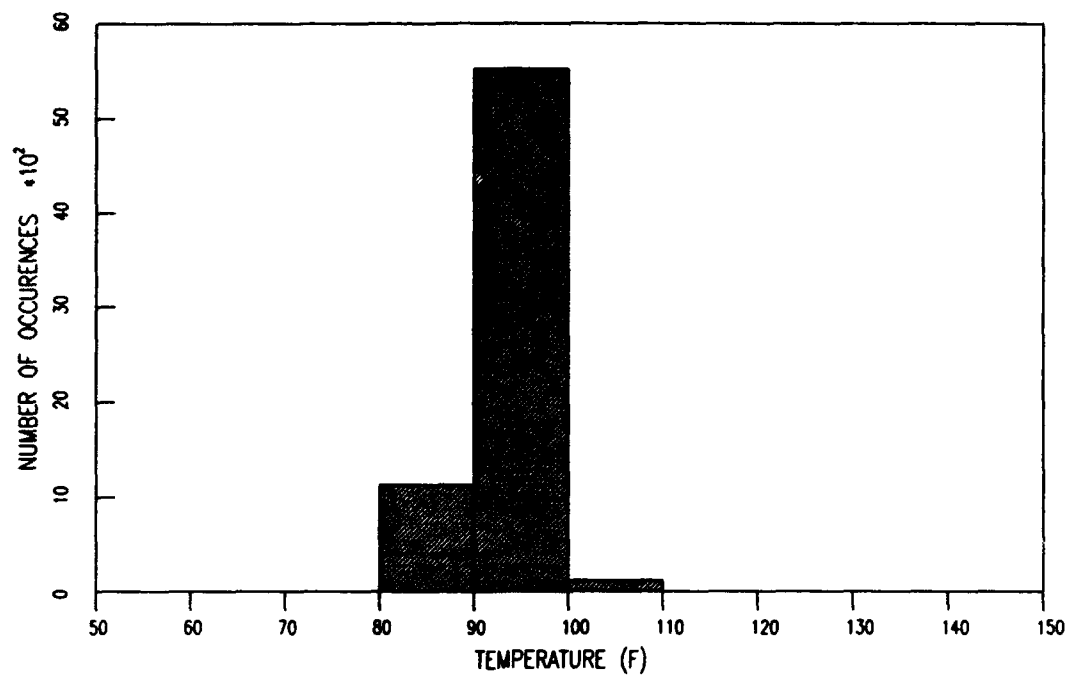
12-INCH TEMPERATURE HISTOGRAM FOR PASS LEVEL 5370



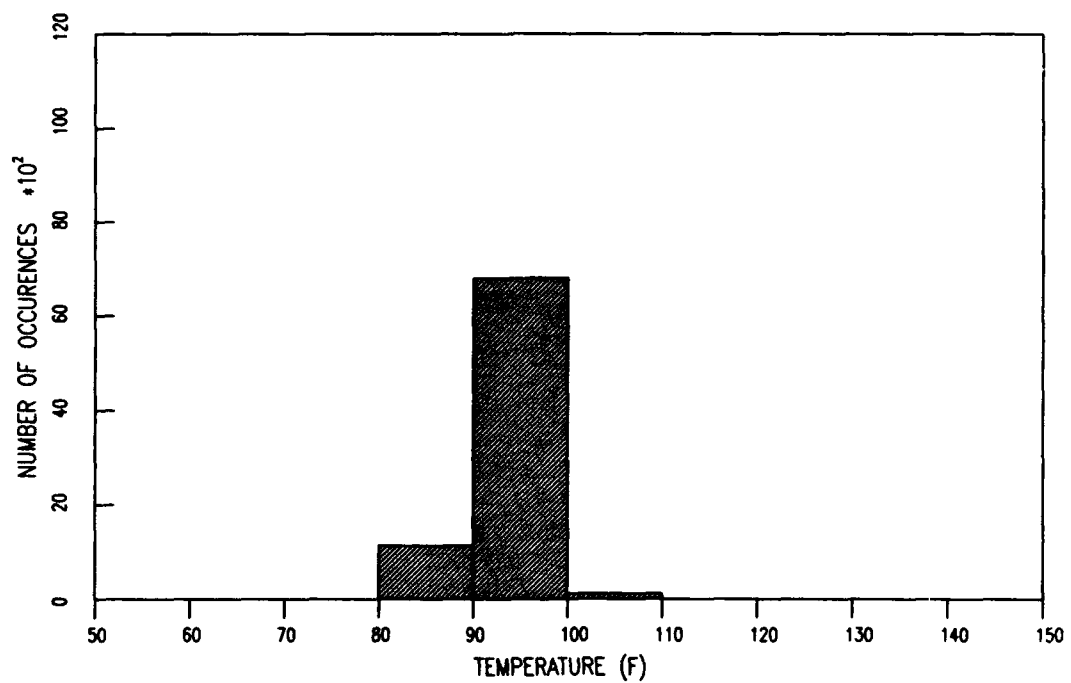
12-INCH TEMPERATURE HISTOGRAM FOR PASS LEVEL 5817



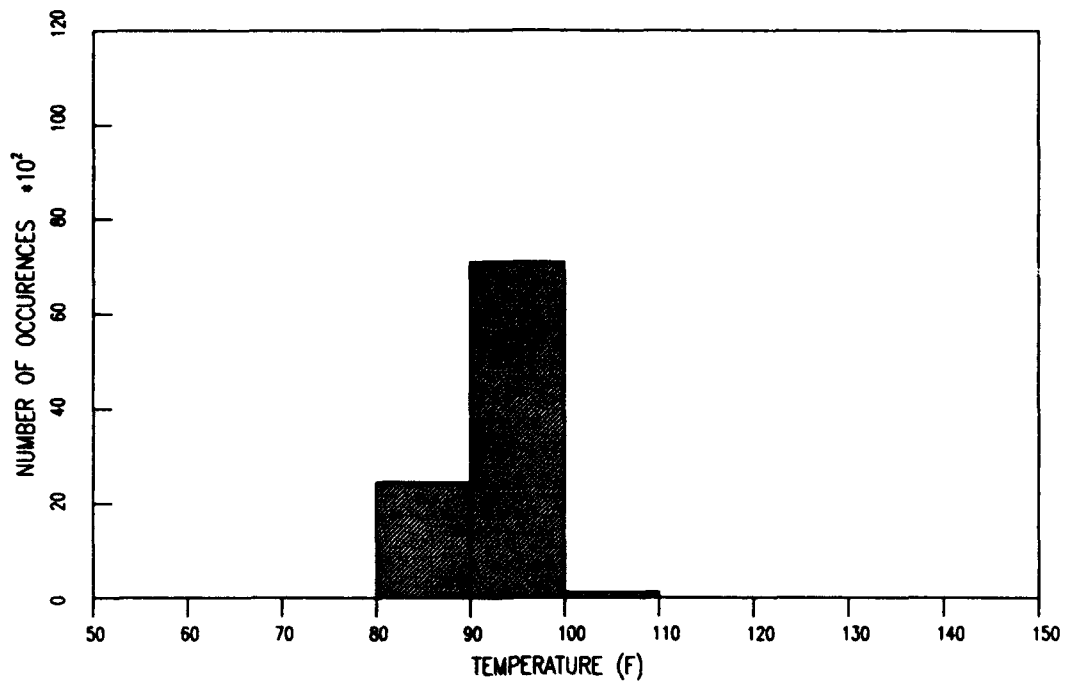
12-INCH TEMPERATURE HISTOGRAM FOR PASS LEVEL 6808



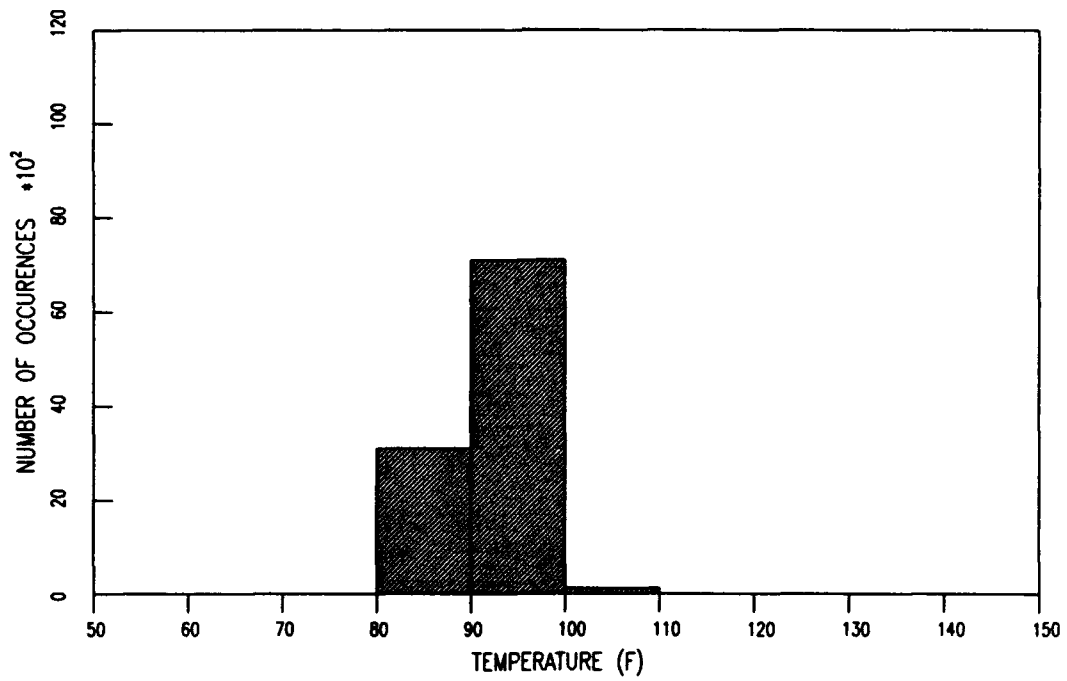
12-INCH TEMPERATURE HISTOGRAM FOR PASS LEVEL 8080



12-INCH TEMPERATURE HISTOGRAM FOR PASS LEVEL 9715



12-INCH TEMPERATURE HISTOGRAM FOR PASS LEVEL 10350

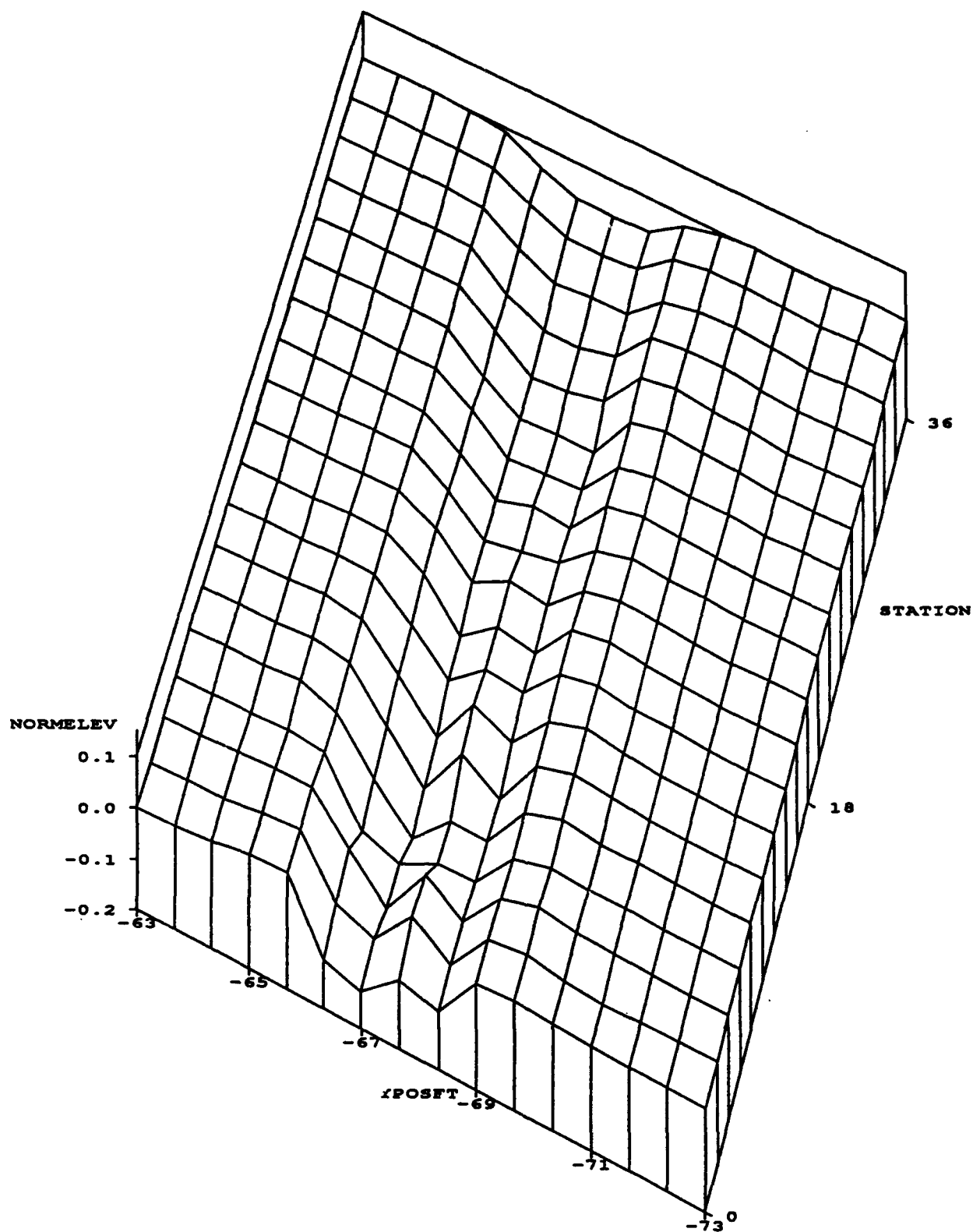


APPENDIX D

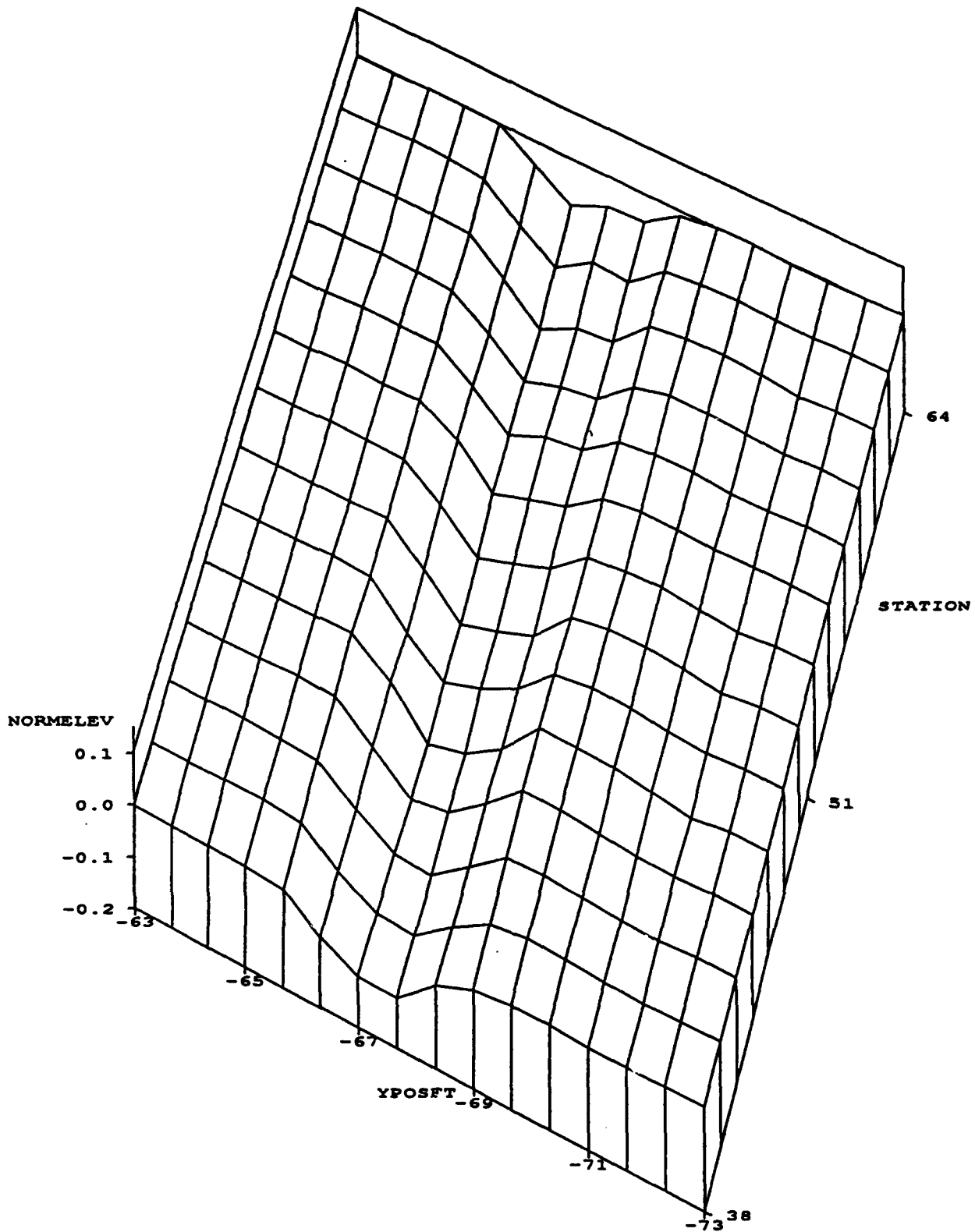
THREE DIMENSIONAL PROFILOGRAPH PLOTS

Representative Profiles Using 2/3-Foot Intervals

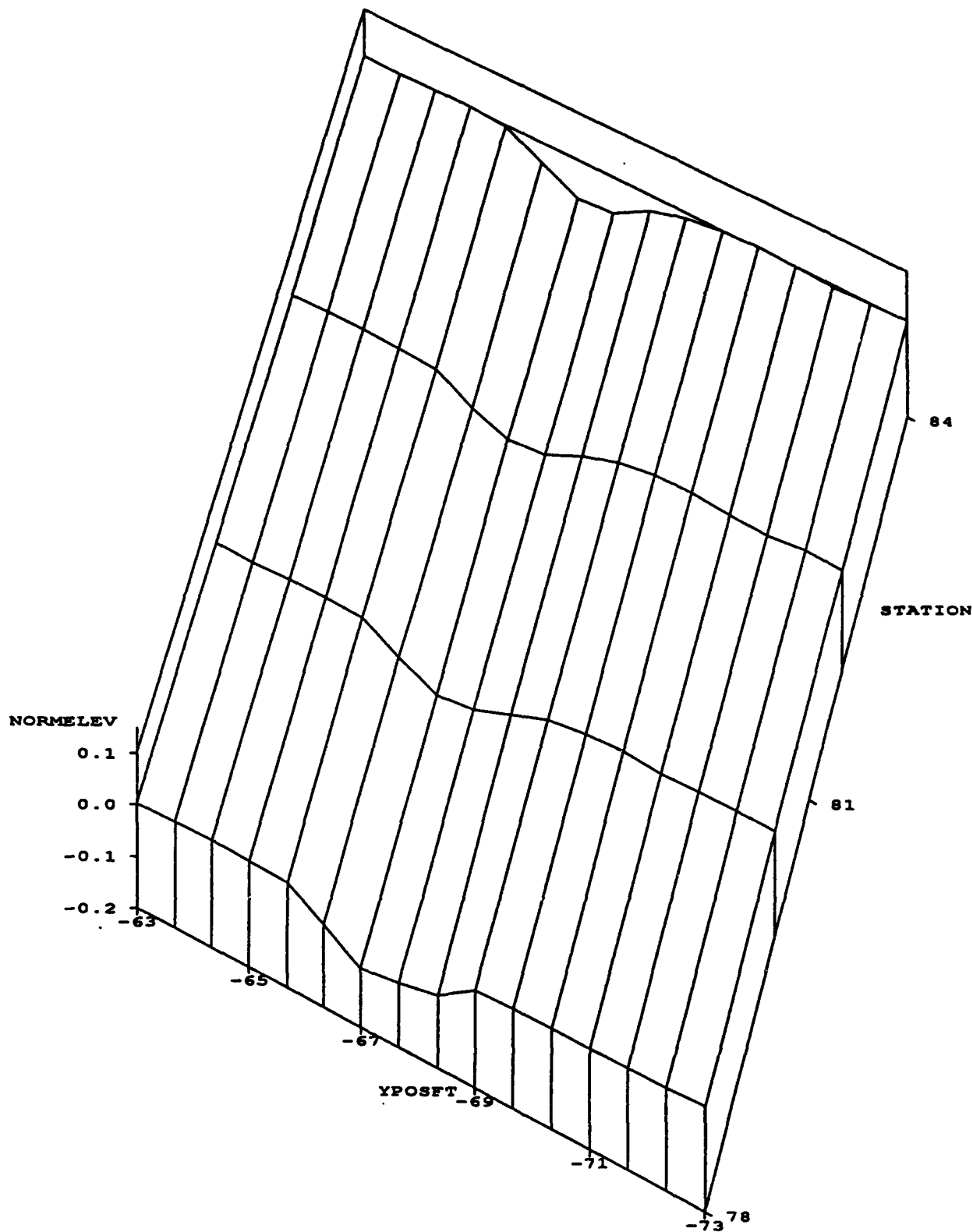
SECTION-1 START=0 MIXTURE-MARSHALL DEPTH-4 DESIGN-FLEXIBLE PASSES-2589



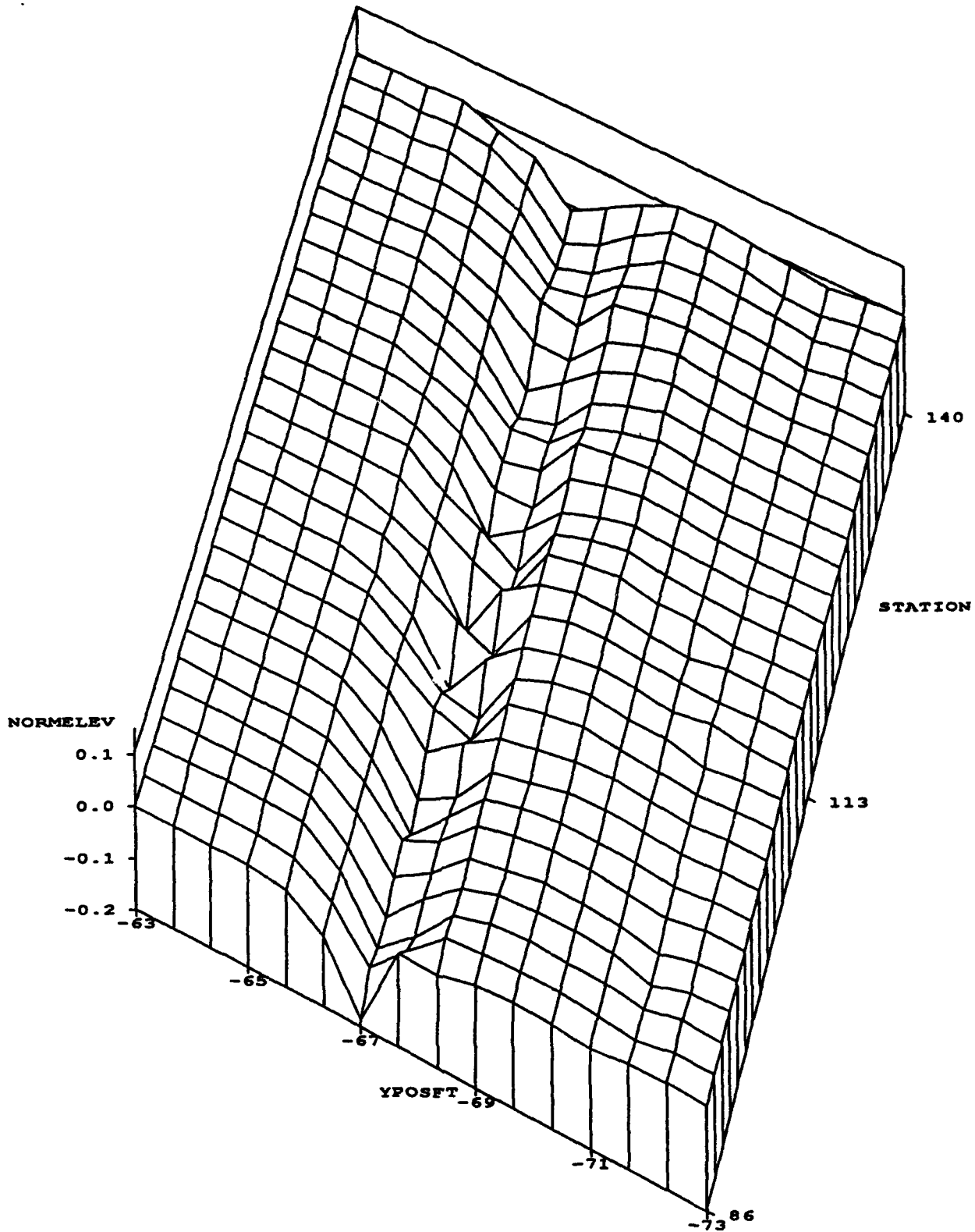
Representative Profiles Using 2/3-Foot Intervals
SECTION-1 START-38 MIXTURE-MARSHALL DEPTH-4 DESIGN-FLEXIBLE PASSES-3049



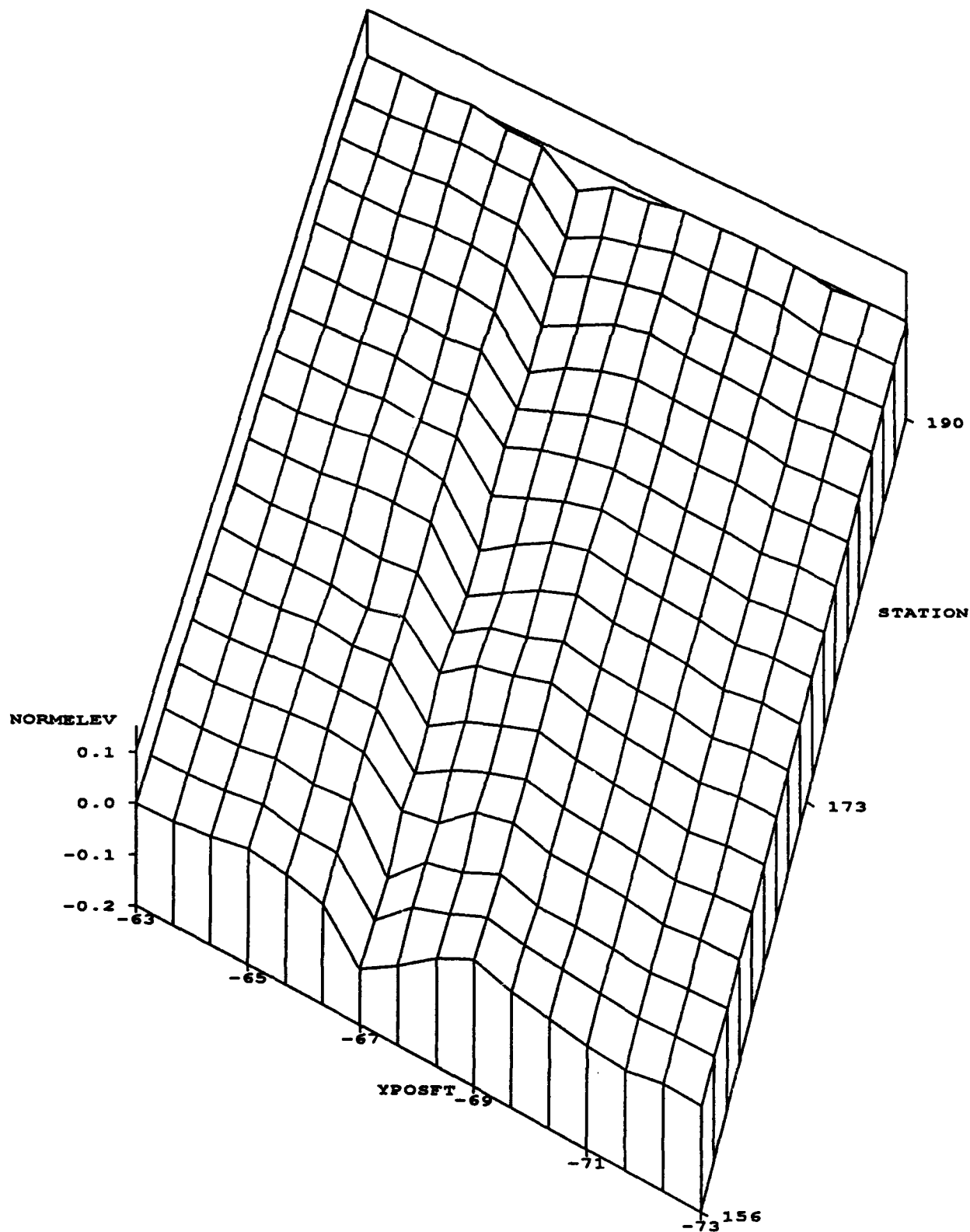
Representative Profiles Using 2/3-Foot Intervals SECTION-2 START-78 MIXTURE-MARSHALL DEPTH-6 DESIGN-FLEXIBLE PASSES-3049



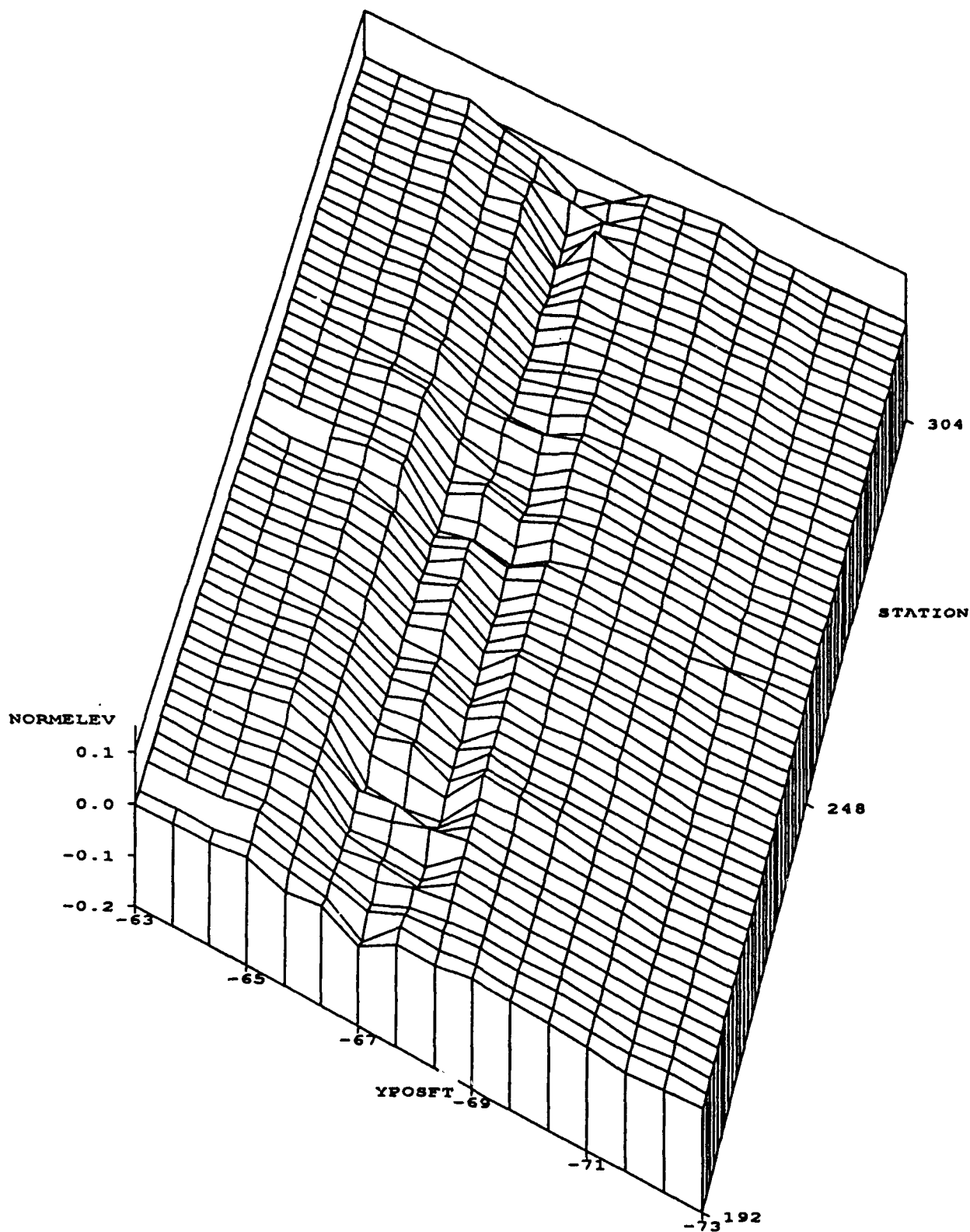
Representative Profiles Using 2/3-Foot Intervals
SECTION-2 START-86 MIXTURE-MARSHALL DEPTH-6 DESIGN-FLEXIBLE PASSES-5137



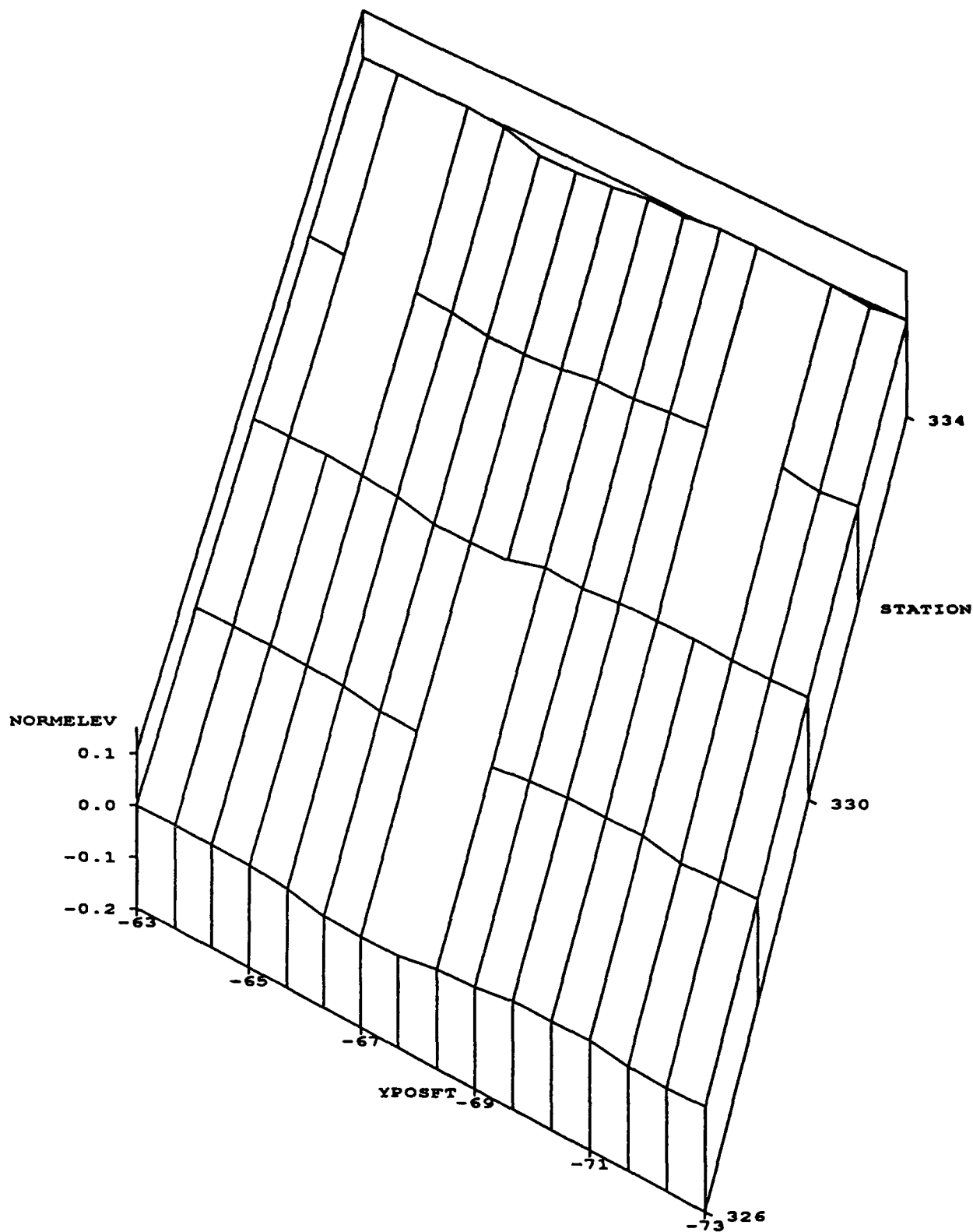
Representative Profiles Using 2/3-Foot Intervals
SECTION-3 START-156 MIXTURE-MARSHALL DEPTH-6 DESIGN-COMPOSIT PASSES-5137



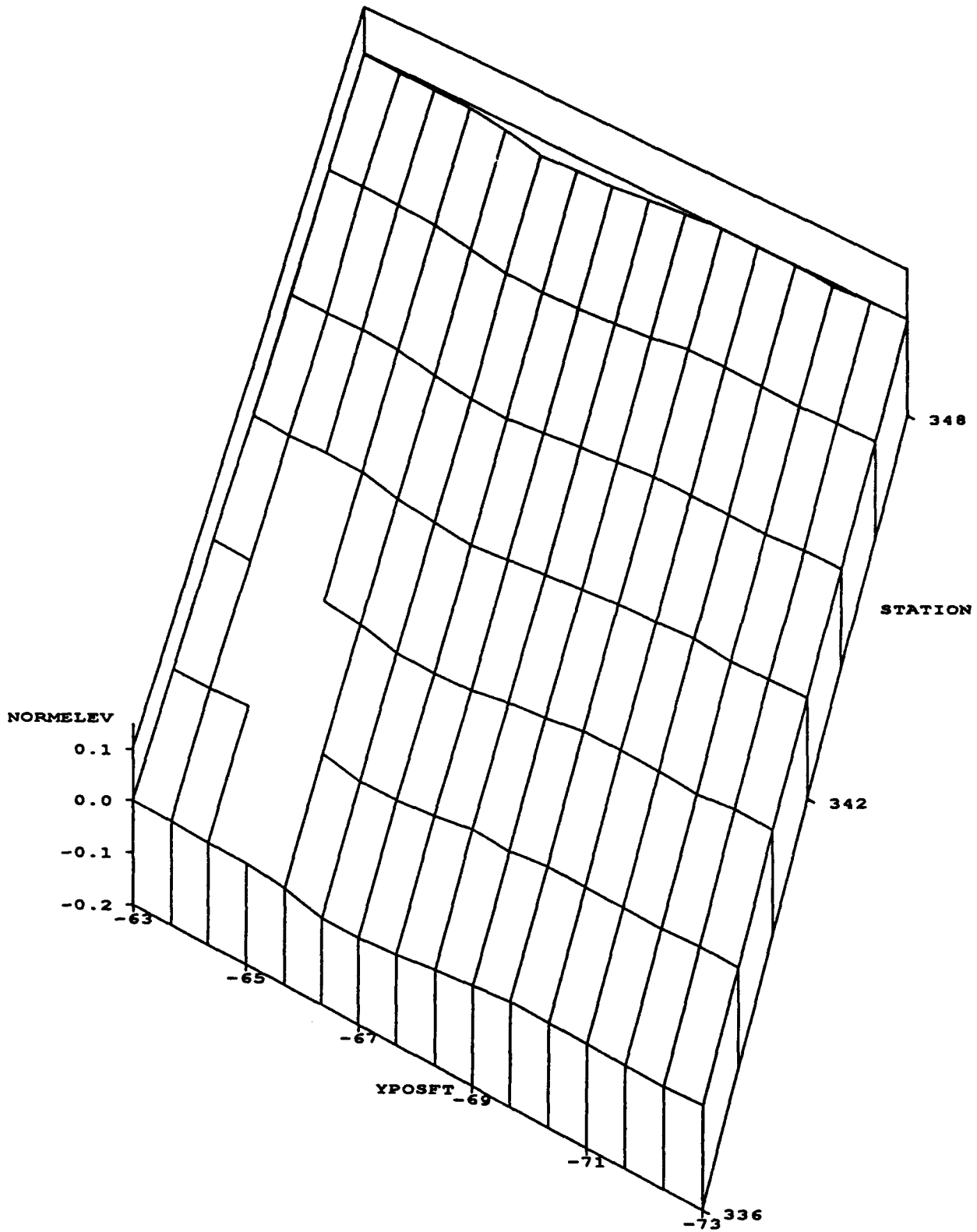
Representative Profiles Using 2/3-Foot Intervals
SECTION-3 START-192 MIXTURE-MARSHALL DEPTH-6 DESIGN-COMPOSIT PASSES-5817



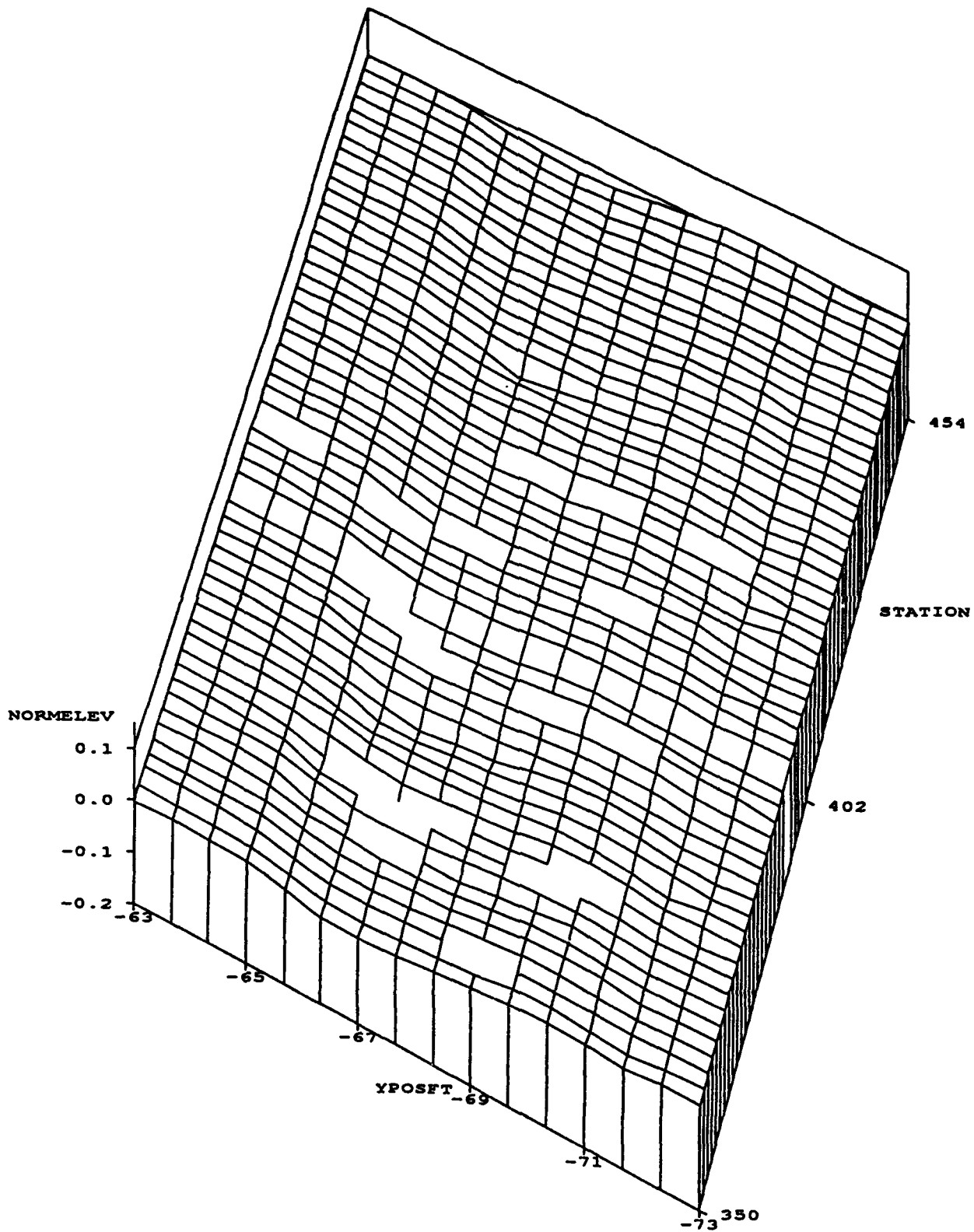
Representative Profiles Using 2/3-Foot Intervals SECTION-4 START-326 MIXTURE-GYRATORY DEPTH-6 DESIGN-COMPOSIT PASSES-5817



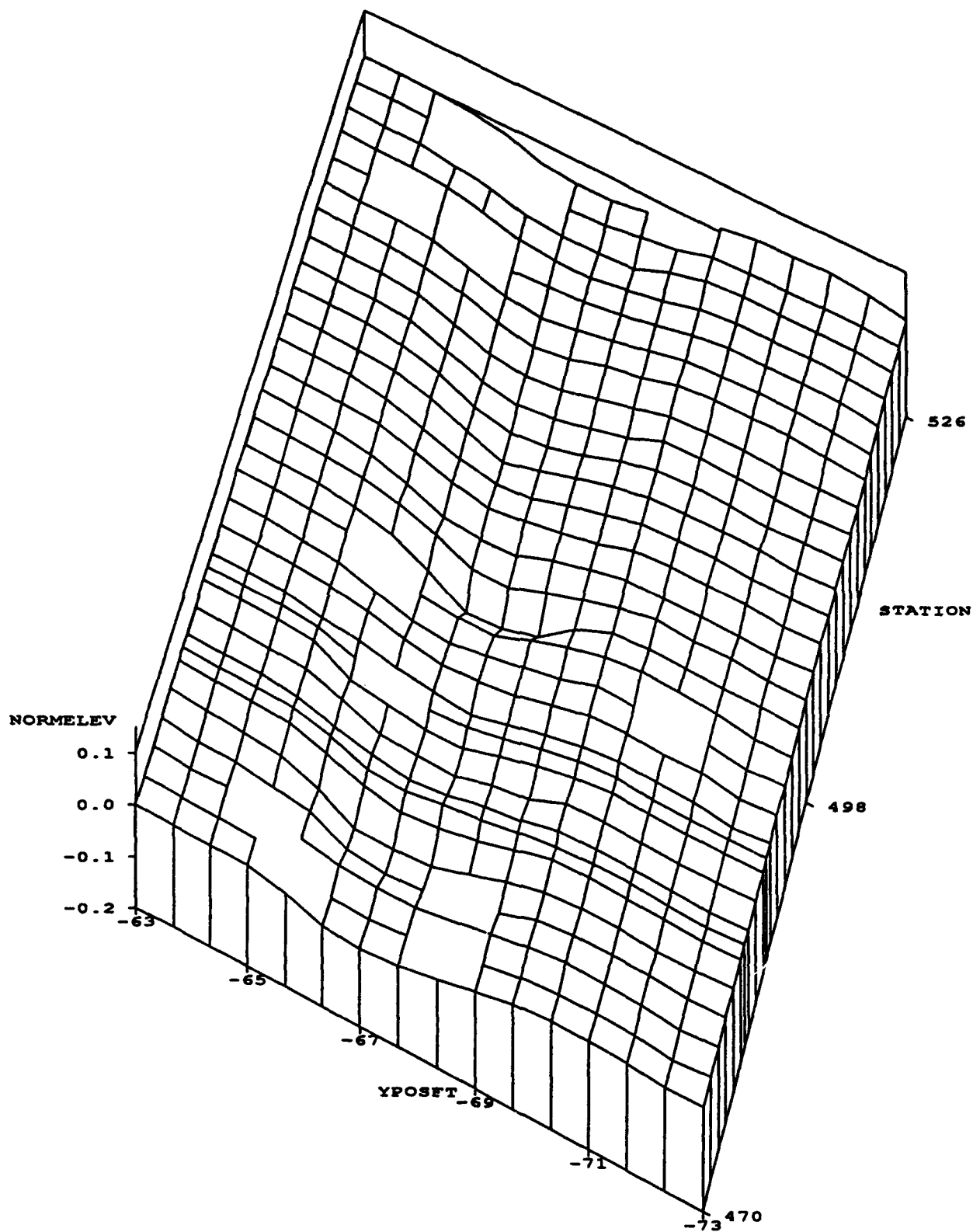
Representative Profiles Using 2/3-Foot Intervals
SECTION-4 START-336 MIXTURE-GYRATORY DEPTH-6 DESIGN-COMPOSIT PASSES-9715



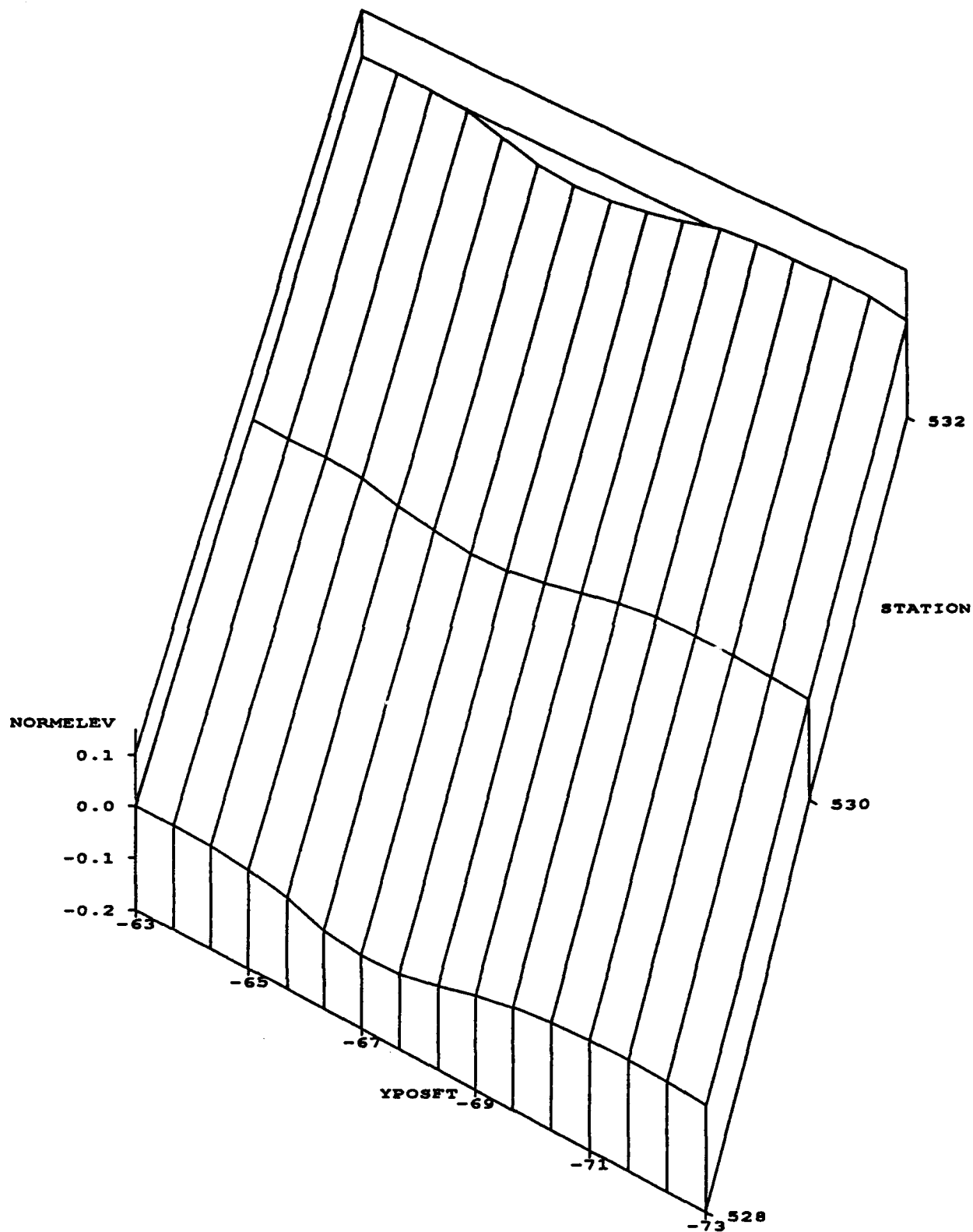
Representative Profiles Using 2/3-Foot Intervals
SECTION-4 START-350 MIXTURE-GYRATORY DEPTH-6 DESIGN-COMPOSIT PASSES-10350



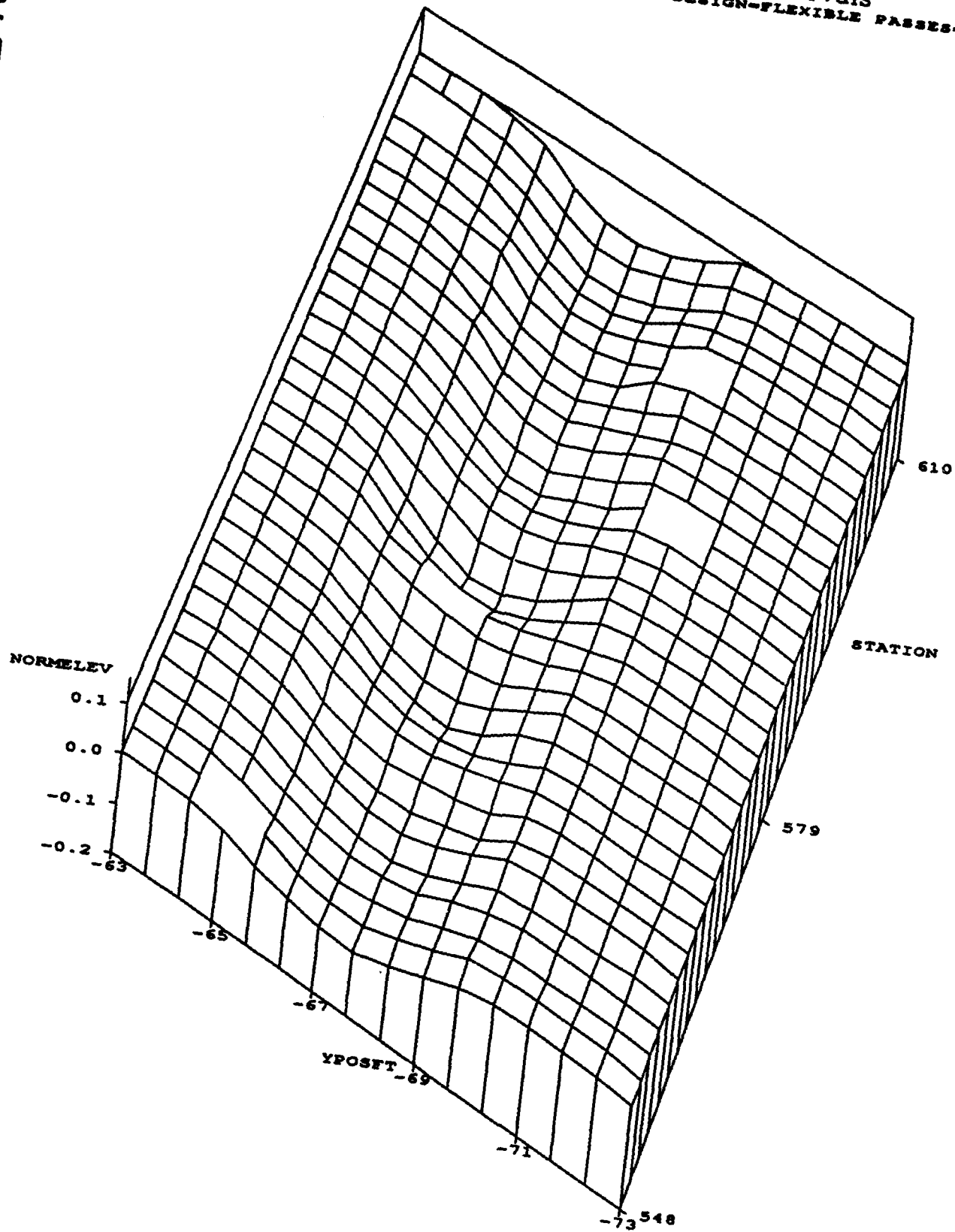
Representative Profiles Using 2/3-Foot Intervals
SECTION-5 START-470 MIXTURE-GYRATORY DEPTH-6 DESIGN-FLEXIBLE PASSES-10350



Representative Profiles Using 2/3-Foot Intervals SECTION-5 START-528 MIXTURE-GYRATORY DEPTH-6 DESIGN-FLEXIBLE PASSES-9715



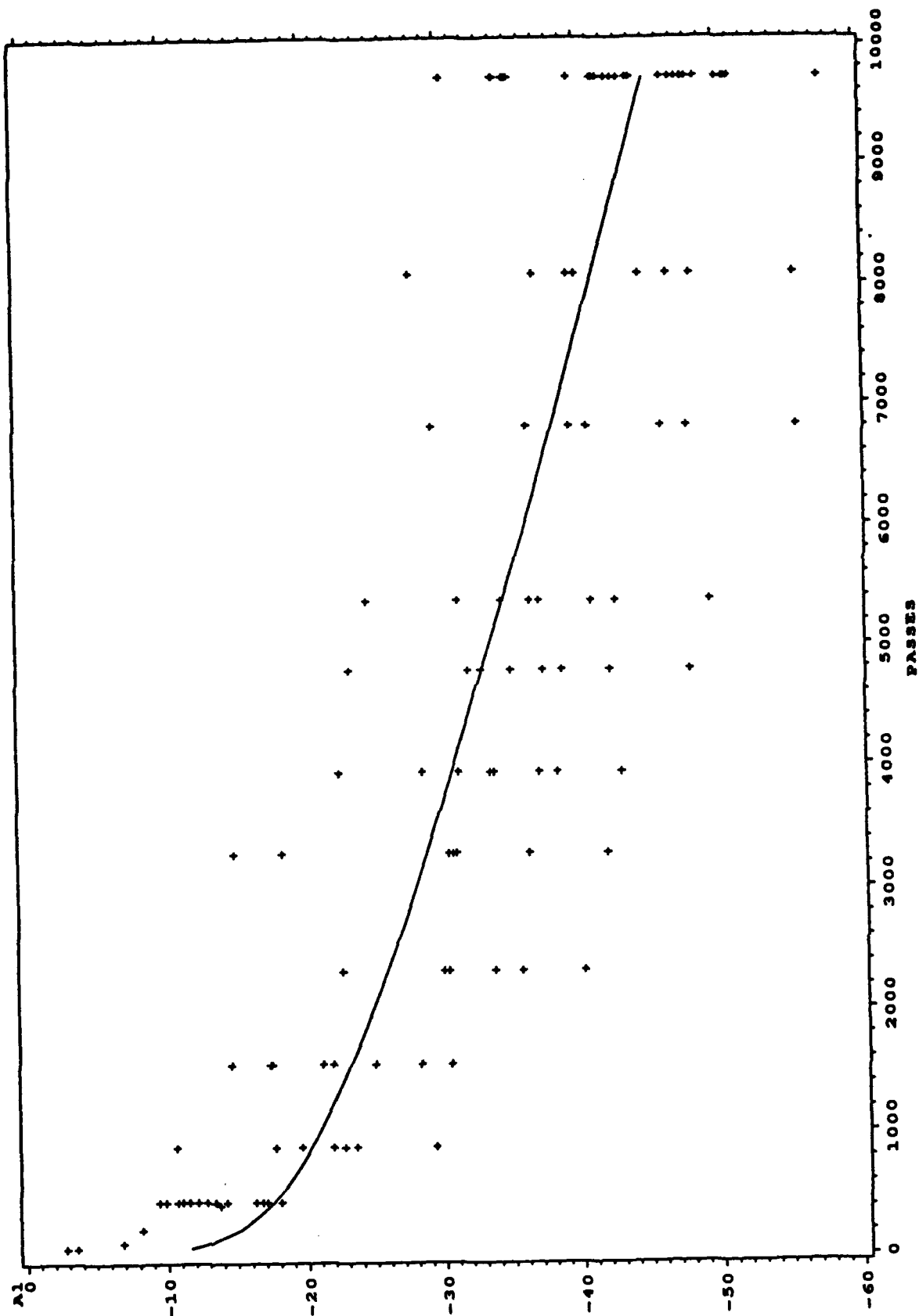
Representative Profiles Using 2/3-Foot Intervals
SECTION-6 START-548 MIXTURE-GRATORY DEPTH-4 DESIGN-FLEXIBLE PASSES-9715



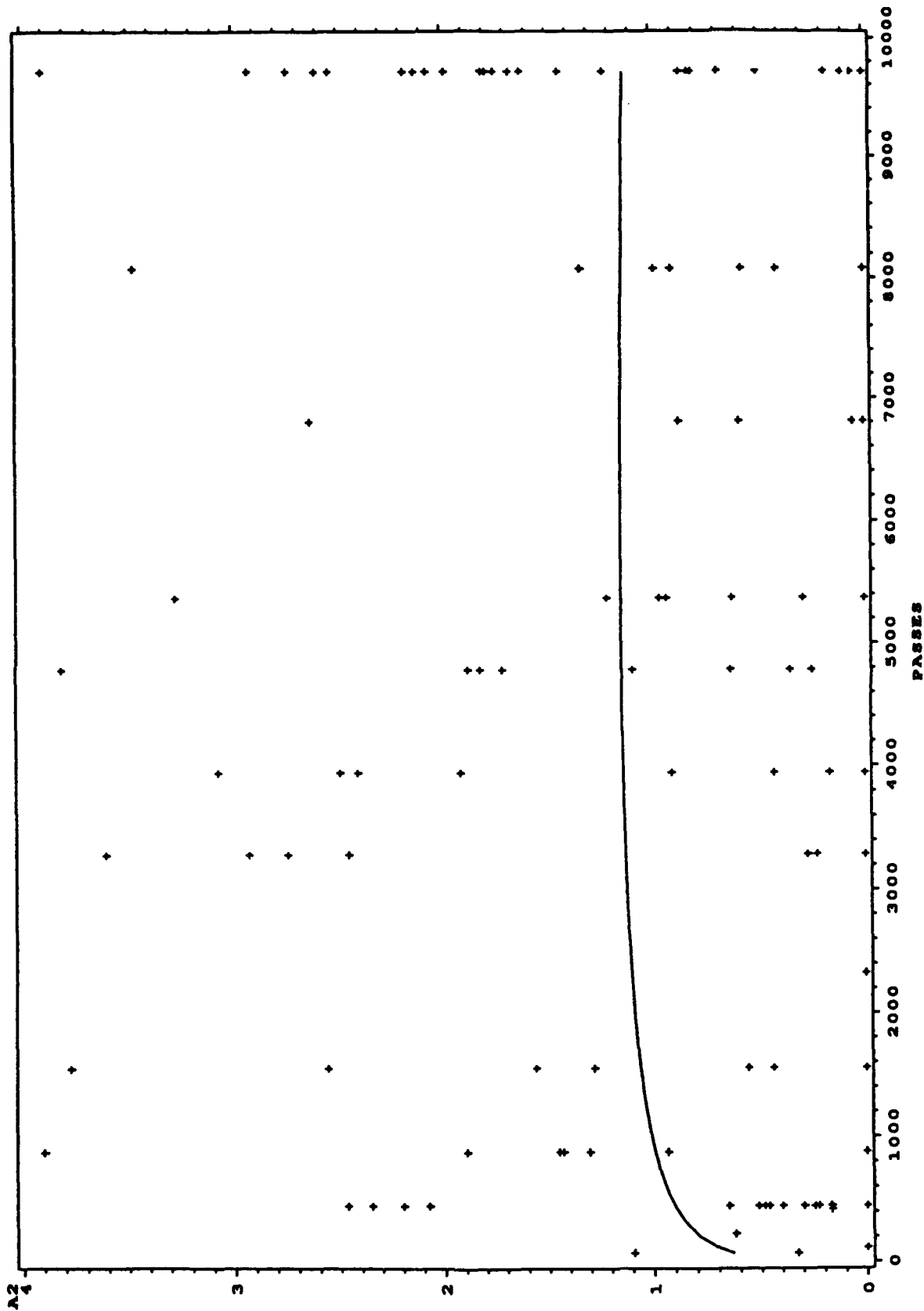
APPENDIX E

REGRESSION PLOTS OF DAMAGE PARAMETERS VERSUS TRAFFIC

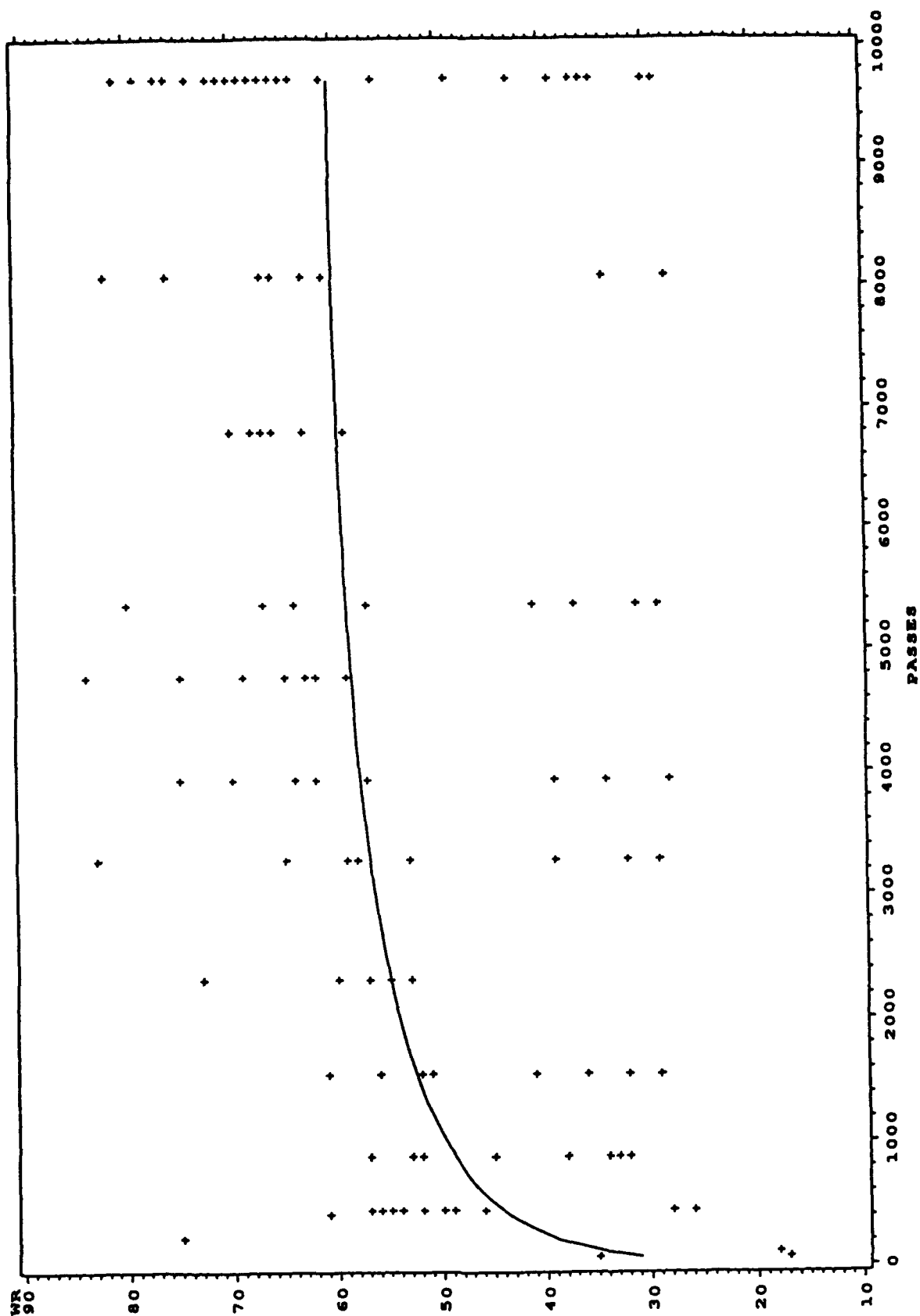
Linear Models of Damage Parameters vs. Number of Passes and Its Log SECTION-6 MIXTURE-GYRATORY DEPTH-4 DESIGN-FLEXIBLE



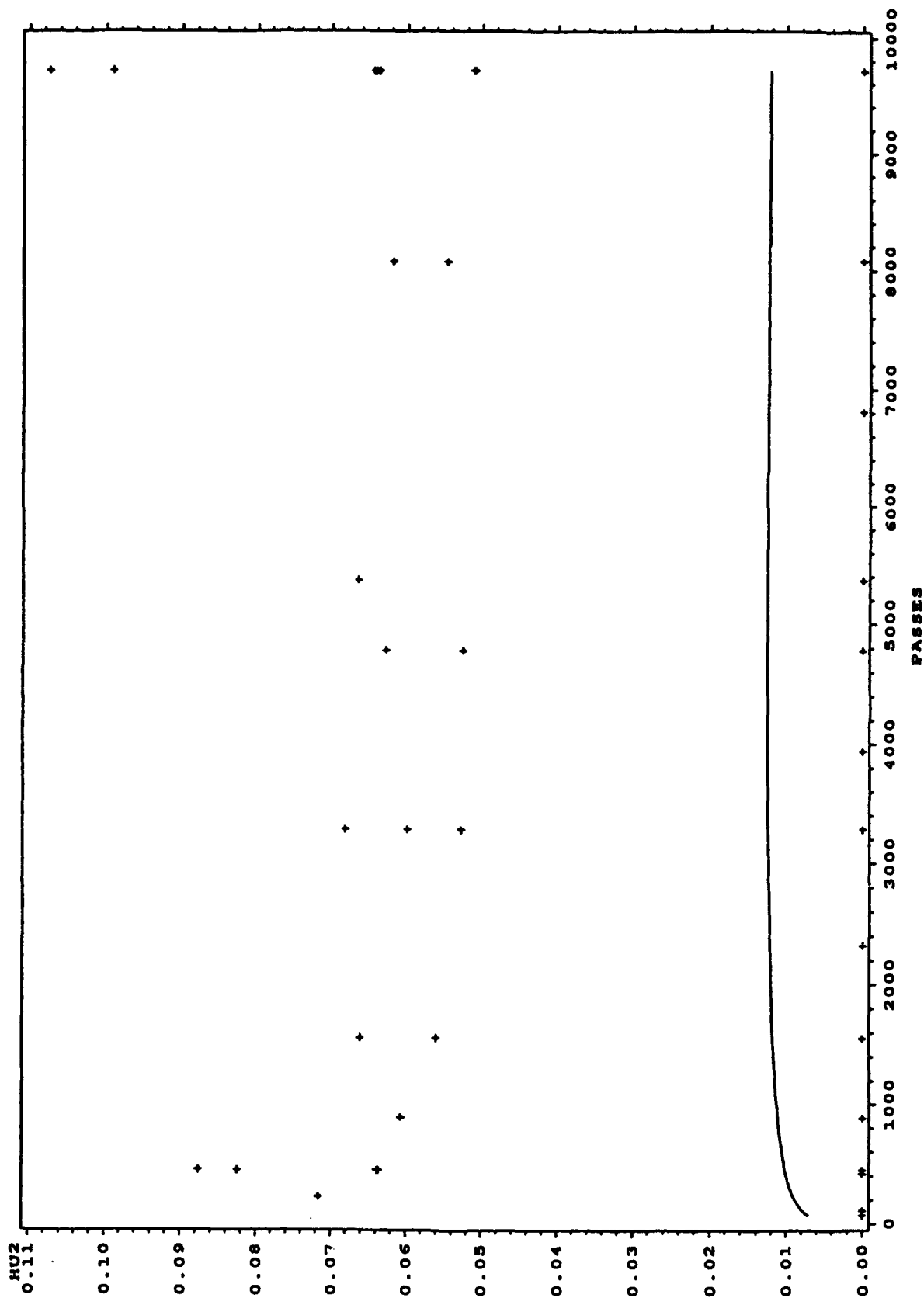
Linear Models of Damage Parameters vs. Number of Passes and Its Log SECTION-6 MIXTURE-GYRATORY DEPTH-4 DESIGN-FLEXIBLE



Linear Models of Damage Parameters vs. Number of Passes and Its Log SECTION-6 MIXTURE-GYRATORY DEPTH-4 DESIGN-FLEXIBLE

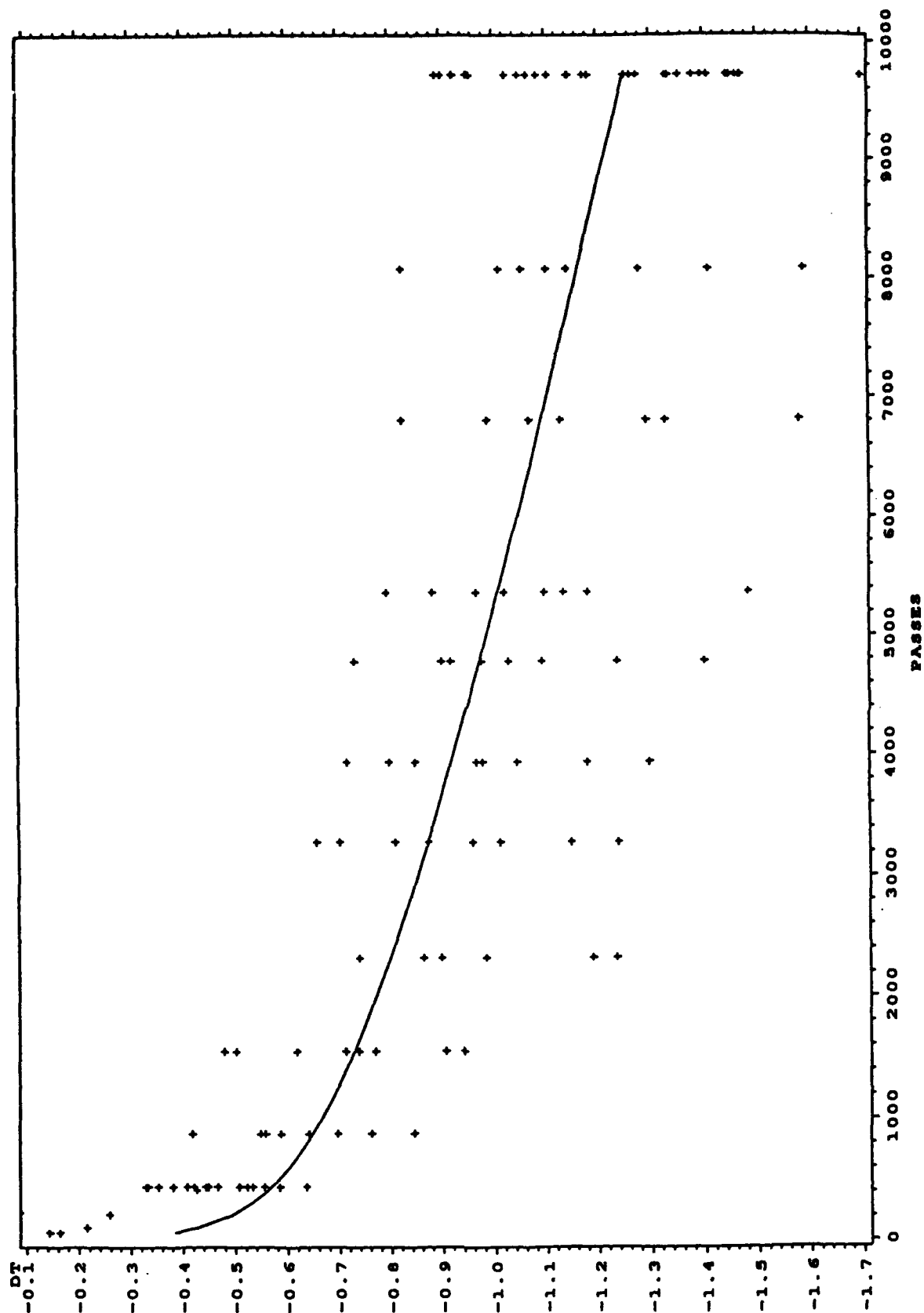


Linear Models of Damage Parameters vs. Number of Passes and Its Log SECTION-6 MIXTURE-GYRATORY DEPTH-4 DESIGN-FLEXIBLE

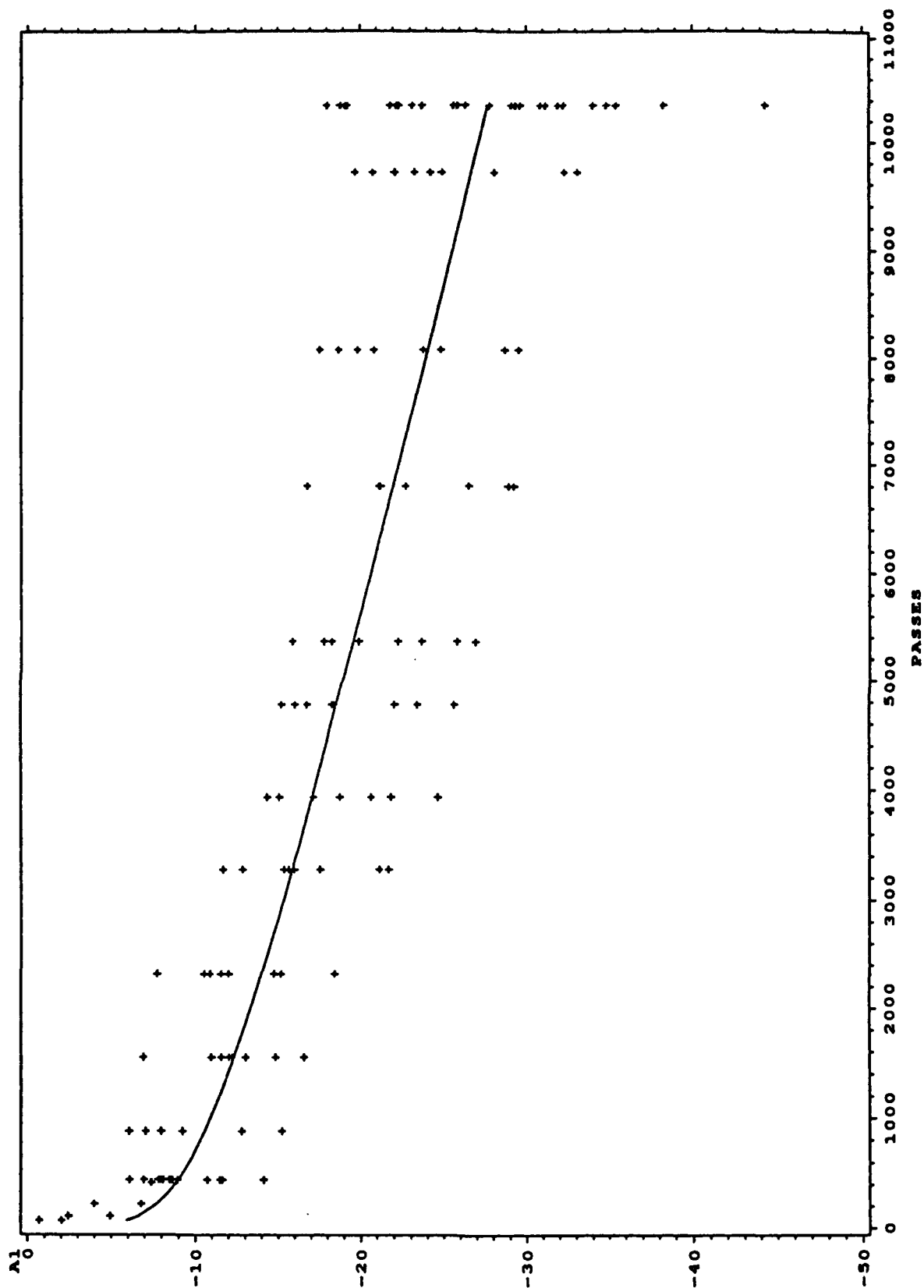


Linear Models of Damage Parameters vs. Number of Passes and Its Log

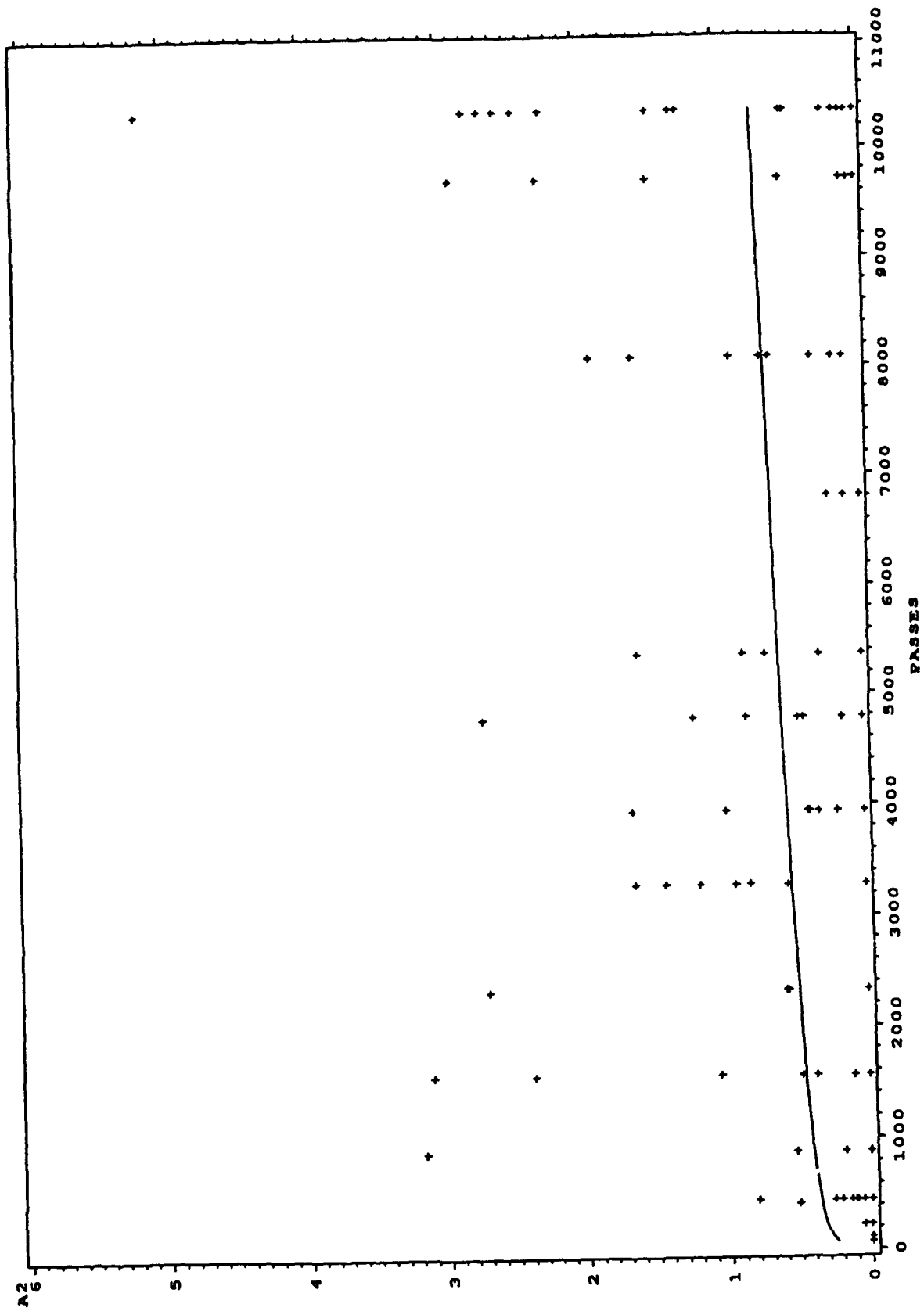
SECTION-6 MIXTURE-GYRATORY DEPTH-4 DESIGN-FLEXIBLE



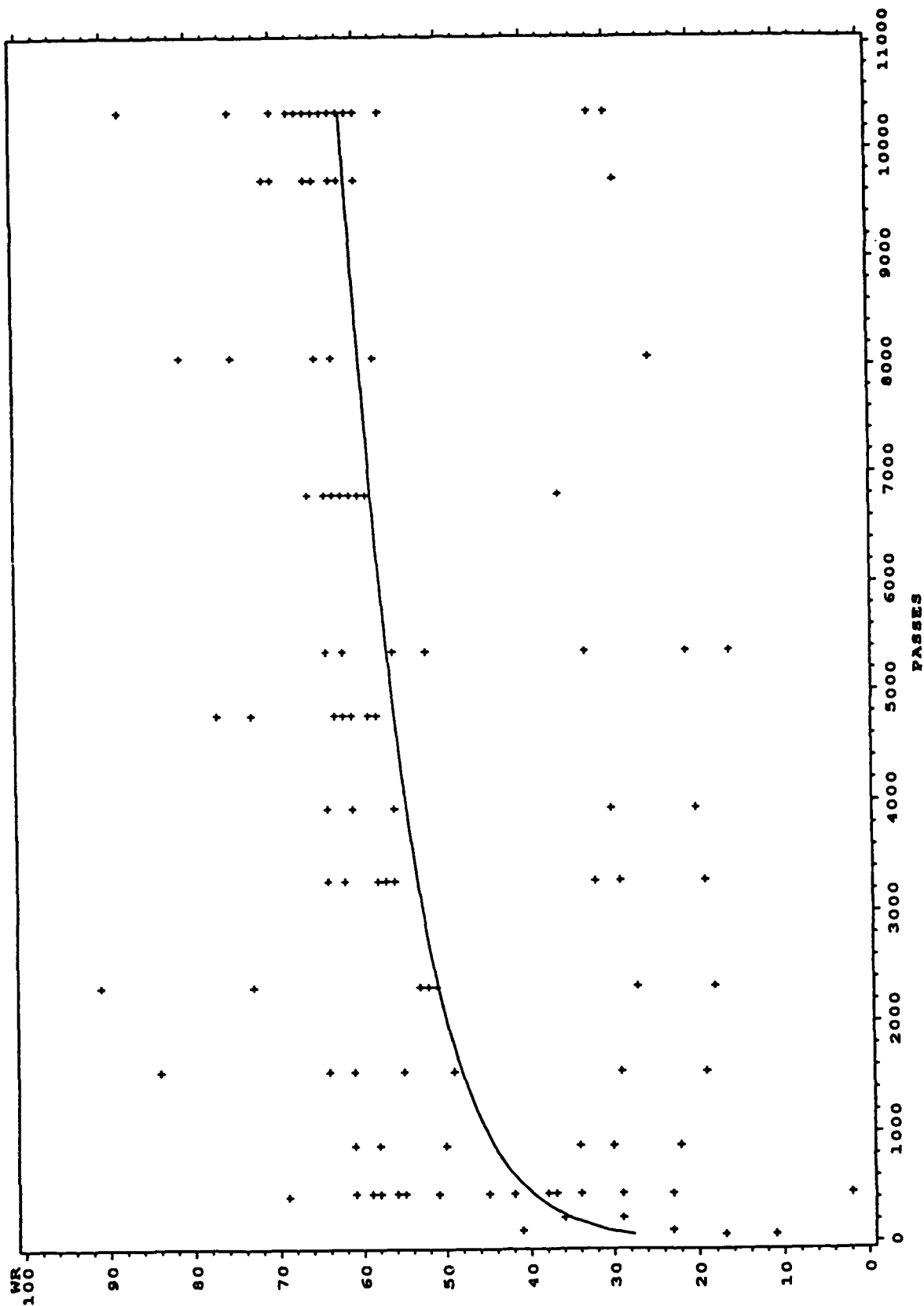
Linear Models of Damage Parameters vs. Number of Passes and Its Log SECTION-5 MIXTURE-GYRATORY DEPTH-6 DESIGN-FLEXIBLE



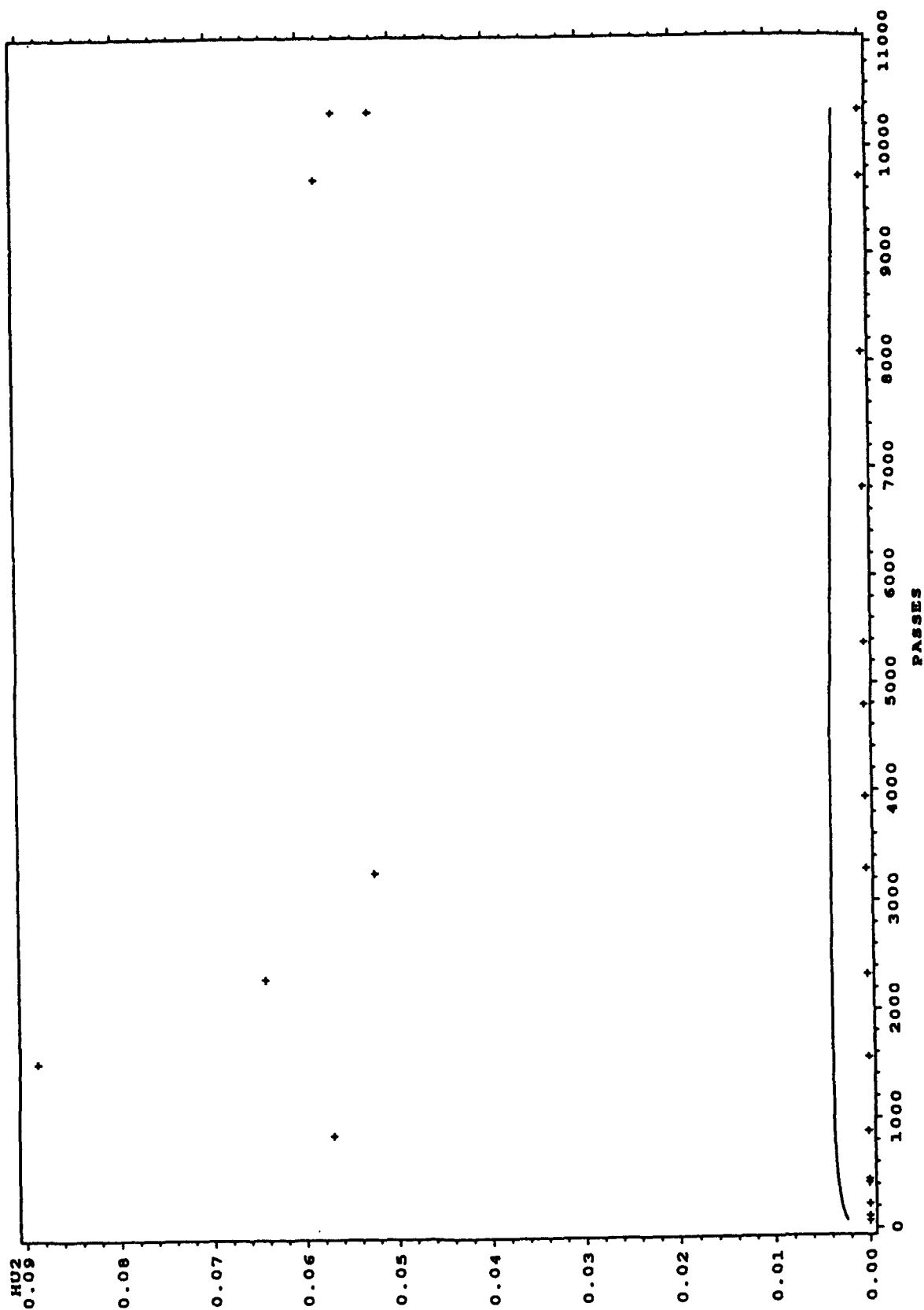
Linear Models of Damage Parameters vs. Number of Passes and Its Log SECTION-5 MIXTURE-GYHATORY DEPTH-6 DESIGN-FLEXIBLE



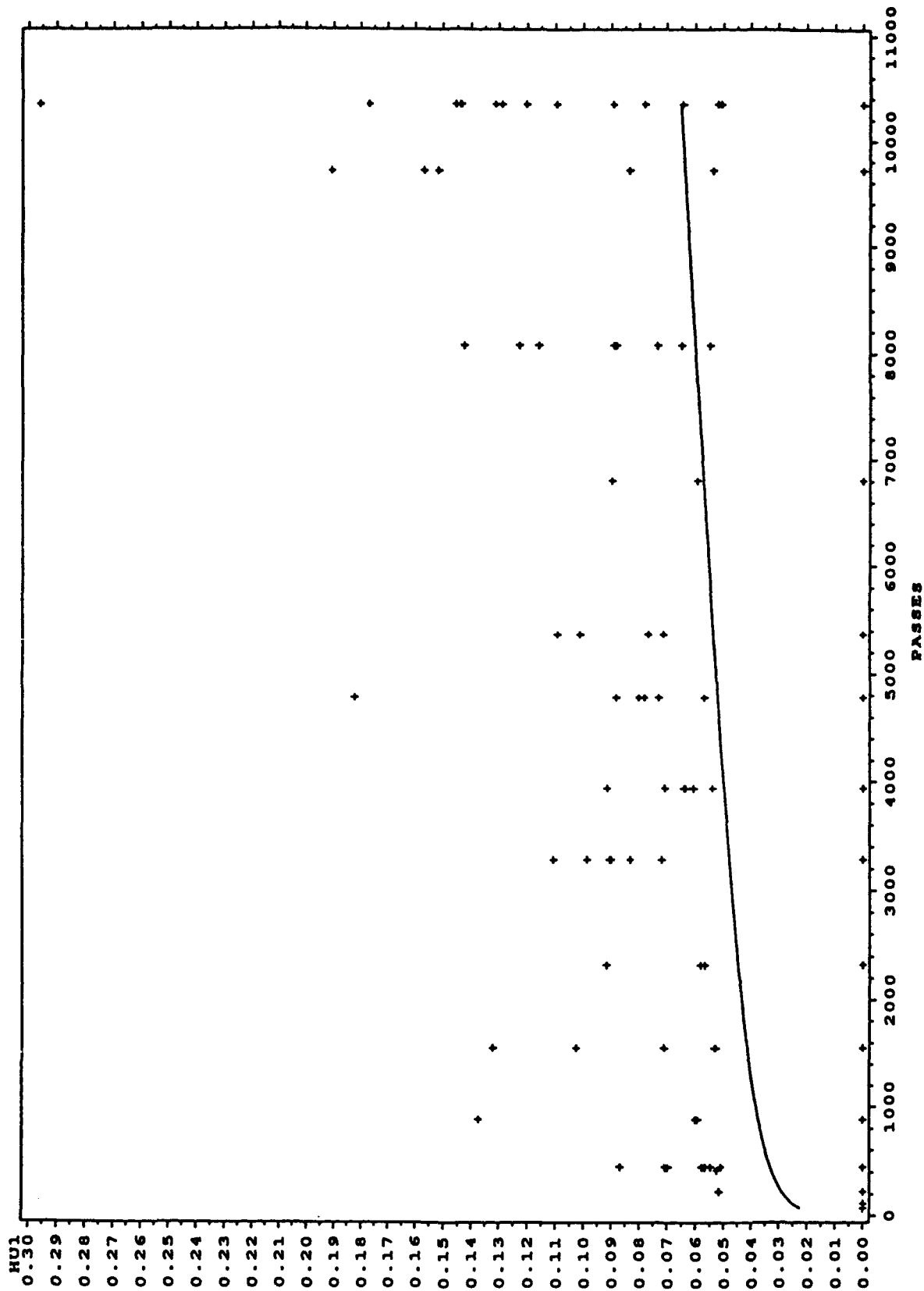
Linear Models of Damage Parameters vs. Number of Passes and Its Log SECTION-5 MIXTURE-GYRATORY DEPTH-6 DESIGN-FLEXIBLE



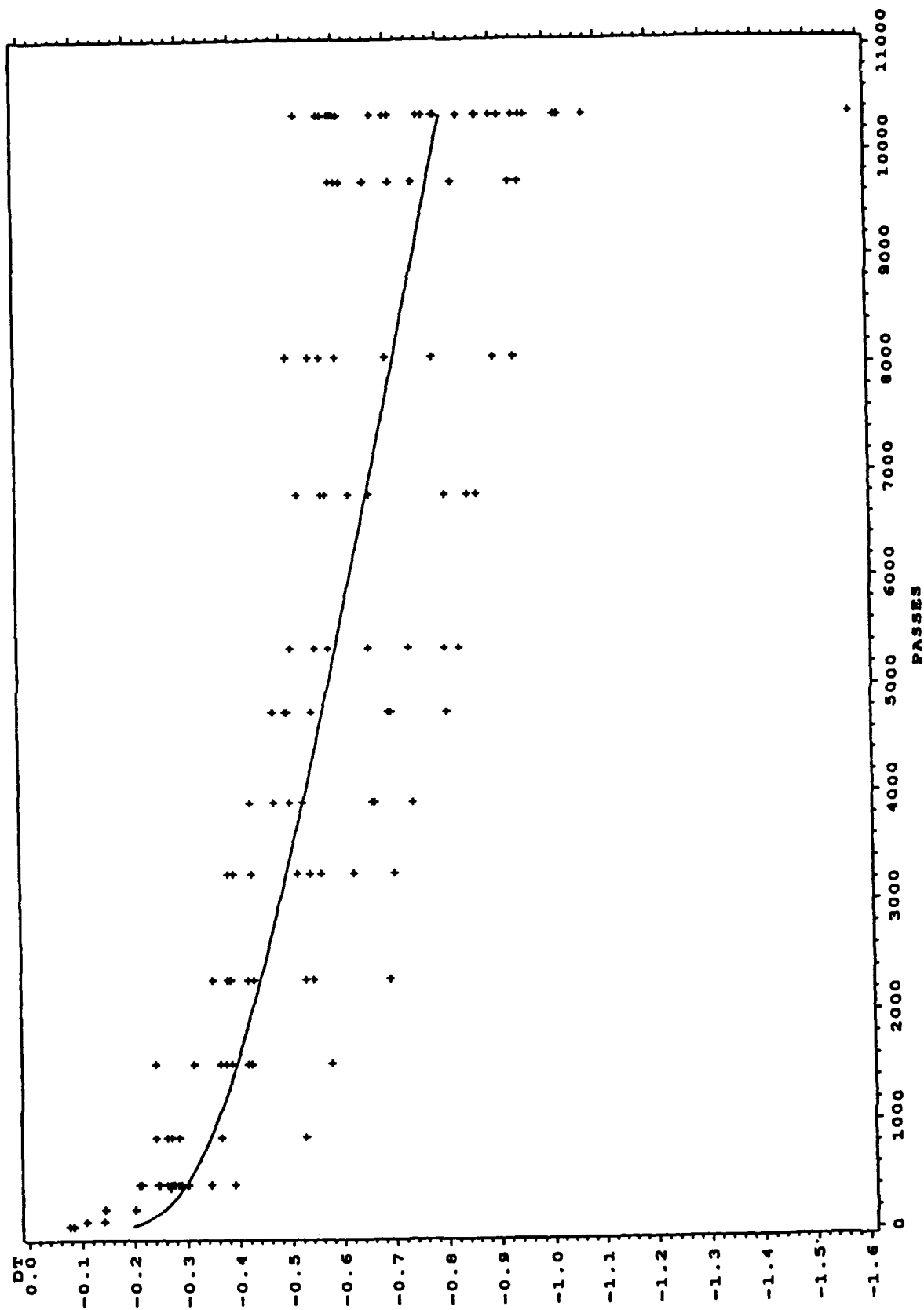
Linear Models of Damage Parameters vs. Number of Passes and Its Log SECTION-5 MIXTURE-GYRATORY DEPTH-6 DESIGN-FLEXIBLE



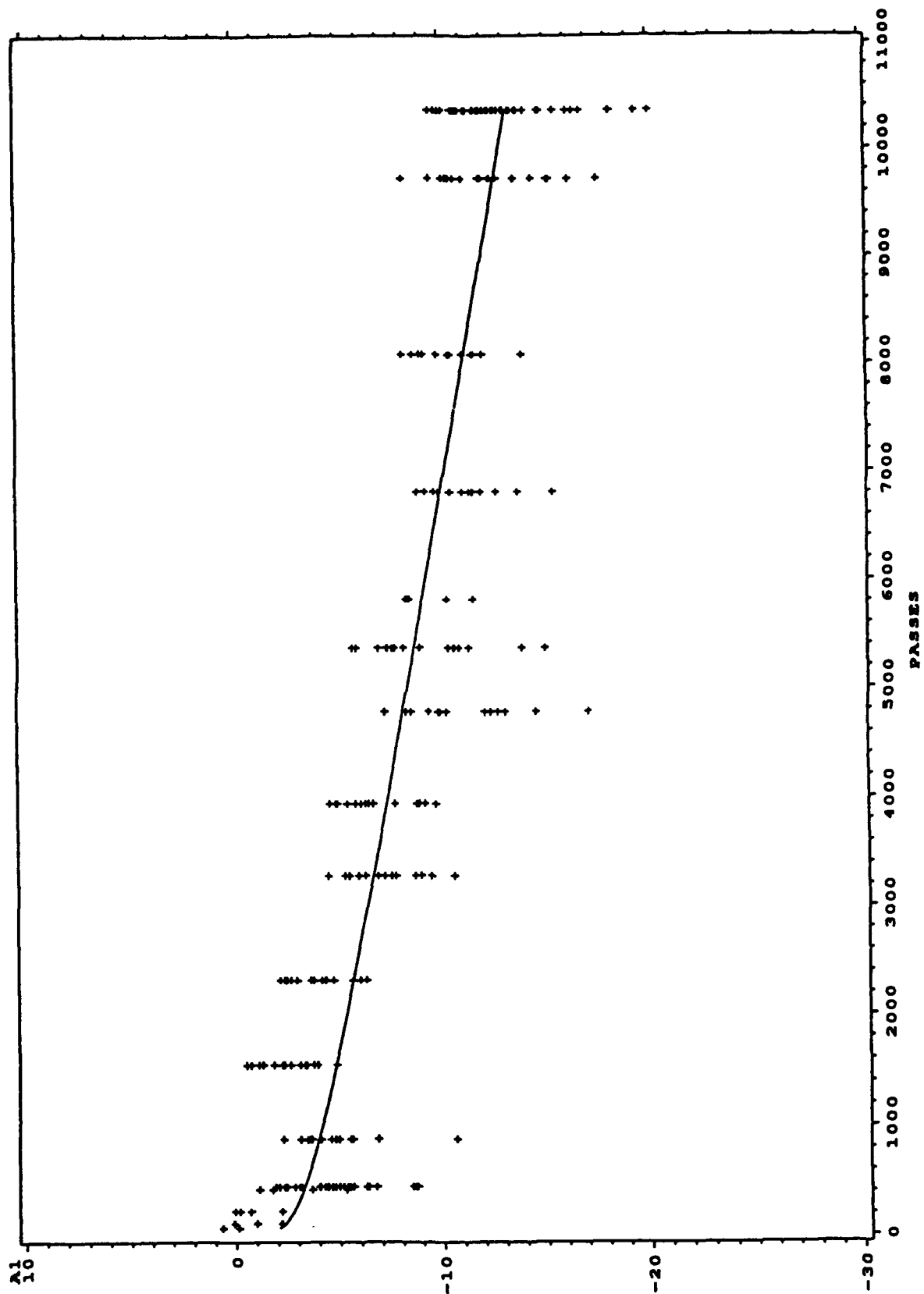
Linear Models of Damage Parameters vs. Number of Passes and Its Log SECTION-5 MIXTURE-GYRATORY DEPTH-6 DESIGN-FLEXIBLE



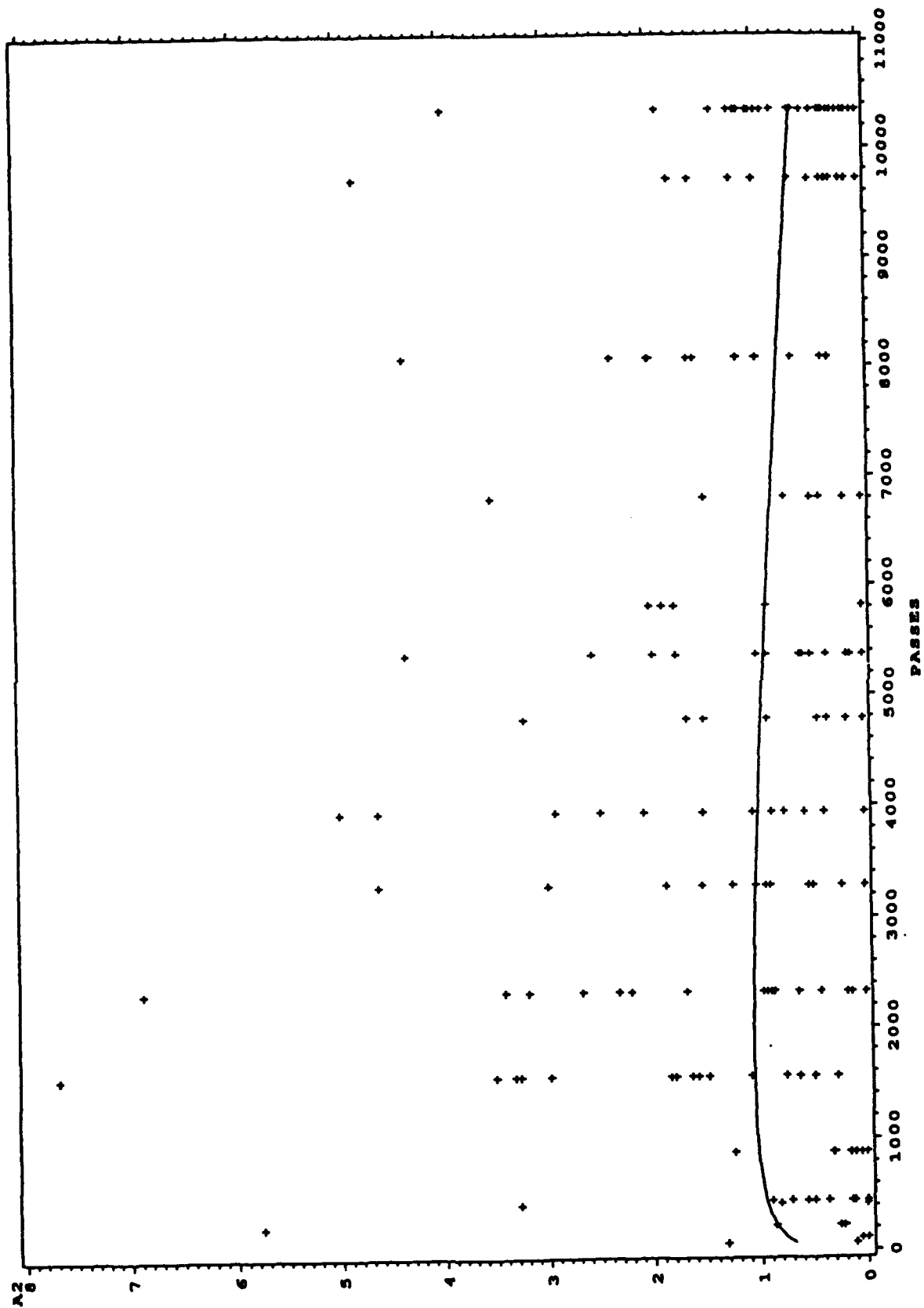
Linear Models of Damage Parameters vs. Number of Passes and Its Log SECTION-5 MIXTURE-GYRATORY DEPTH-6 DESIGN-FLEXIBLE



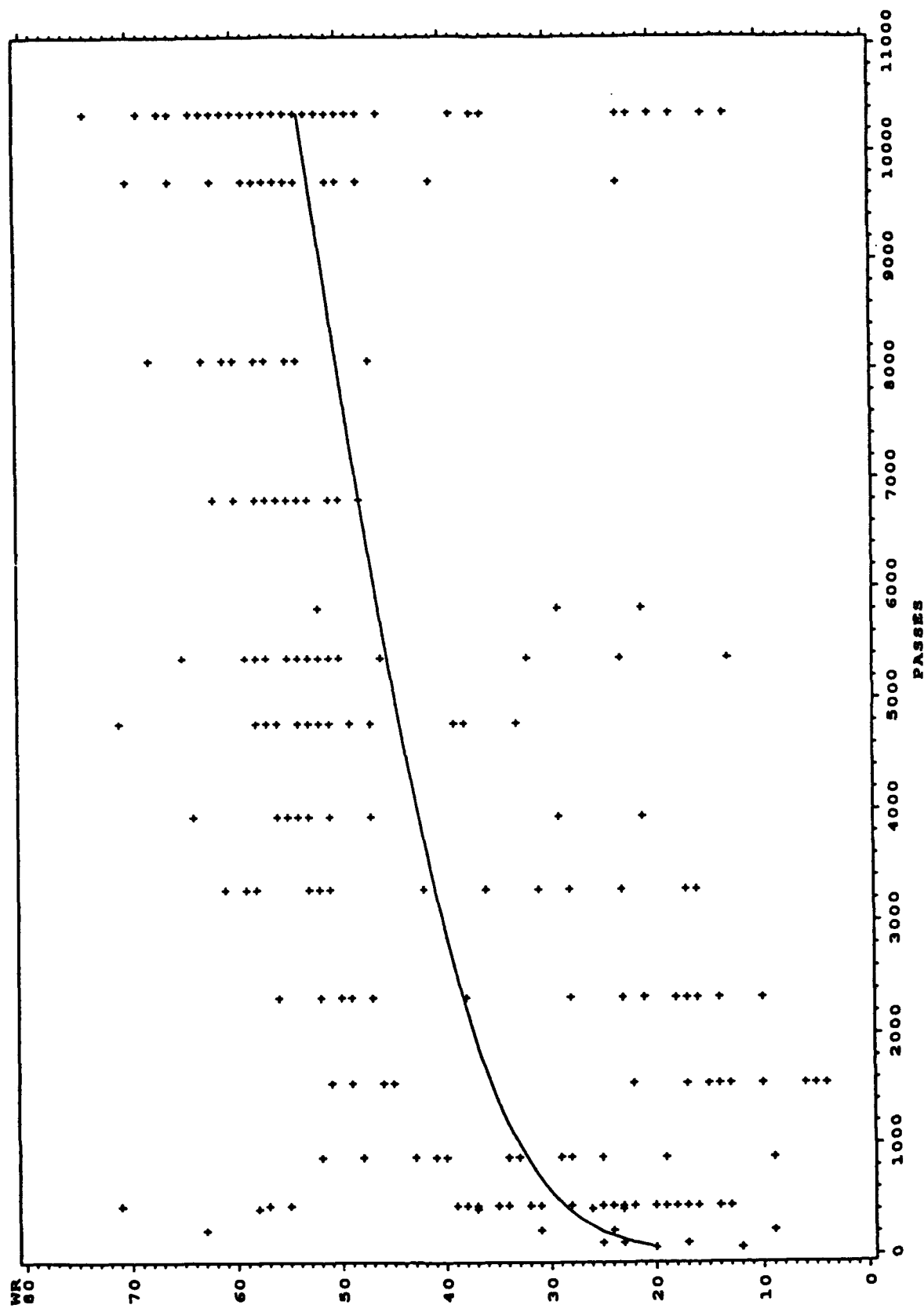
Linear Models of Damage Parameters vs. Number of Passes and Its Log SECTION-4 MIXTURE-GYRATORY DEPTH-6 DESIGN-COMPOSIT



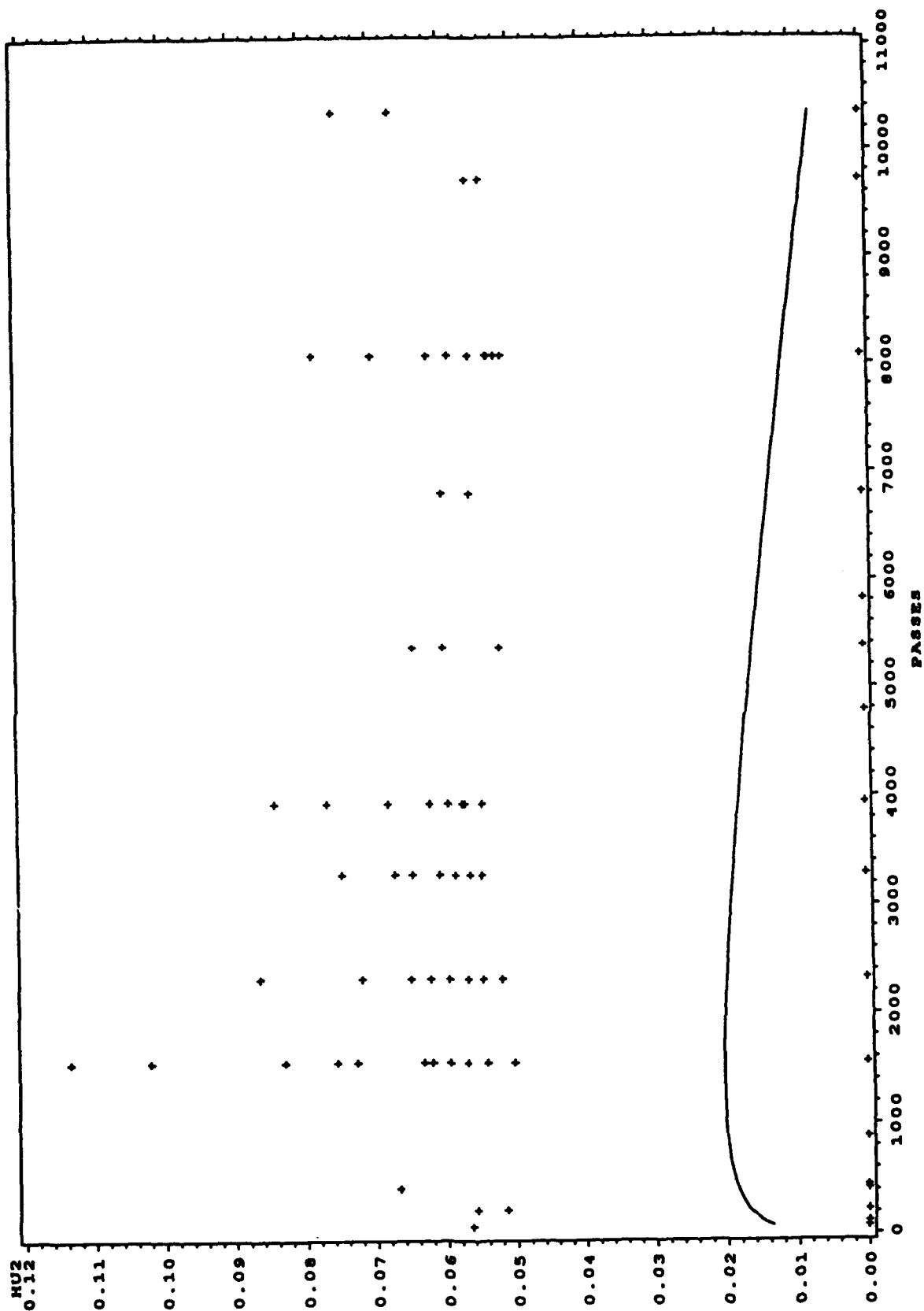
Linear Models of Damage Parameters vs. Number of Passes and Its Log SECTION-4 MIXTURE-GYRATORY DEPTH-6 DESIGN-COMPOSIT



Linear Models of Damage Parameters vs. Number of Passes and Its Log SECTION-4 MIXTURE-GYRATORY DEPTH-6 DESIGN-COMPOSIT

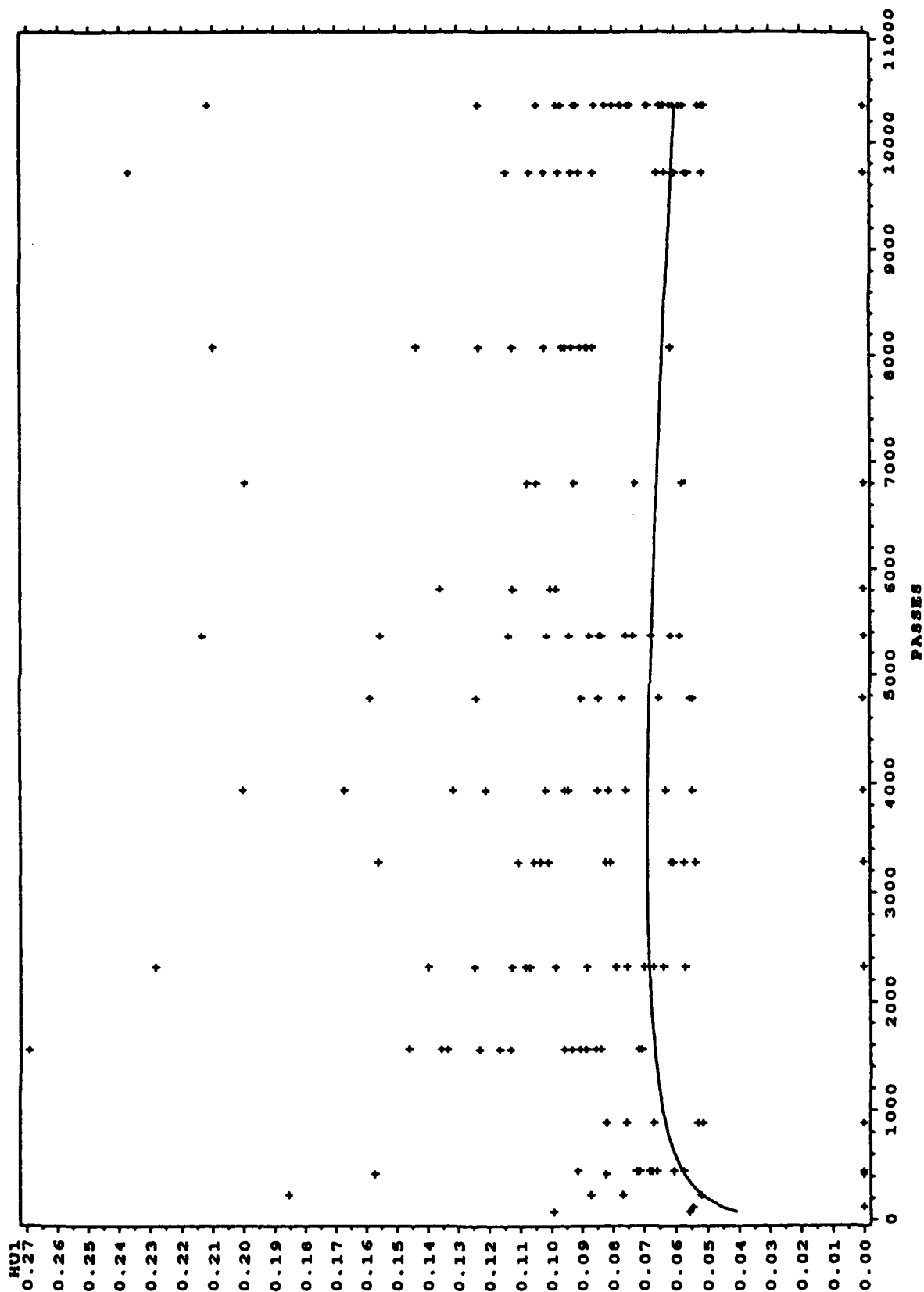


Linear Models of Damage Parameters vs. Number of Passes and Its Log SECTION-4 MIXTURE-GYRATORY DEPTH-6 DESIGN-COMPOSIT

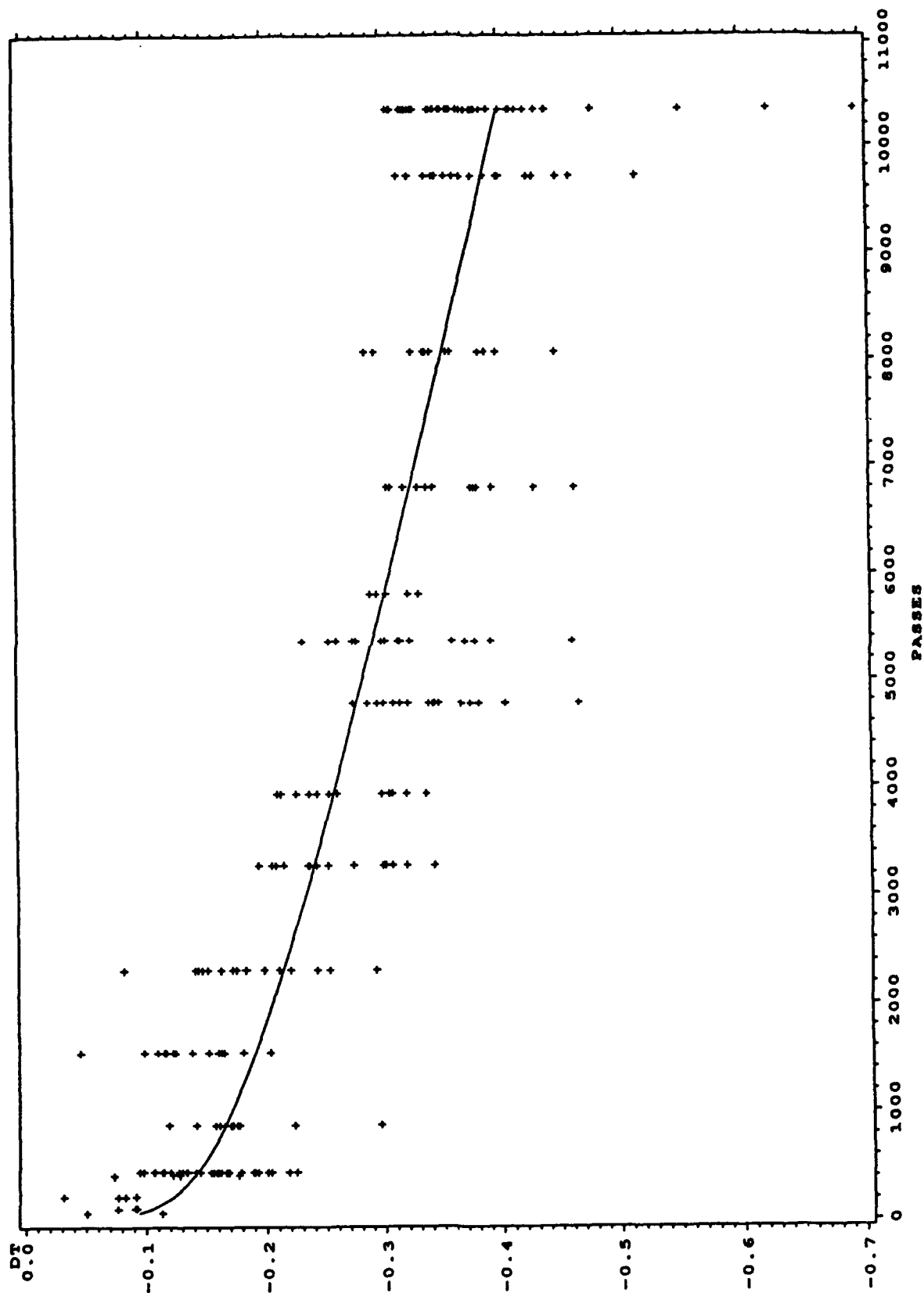


Linear Models of Damage Parameters vs. Number of Passes and Its Log

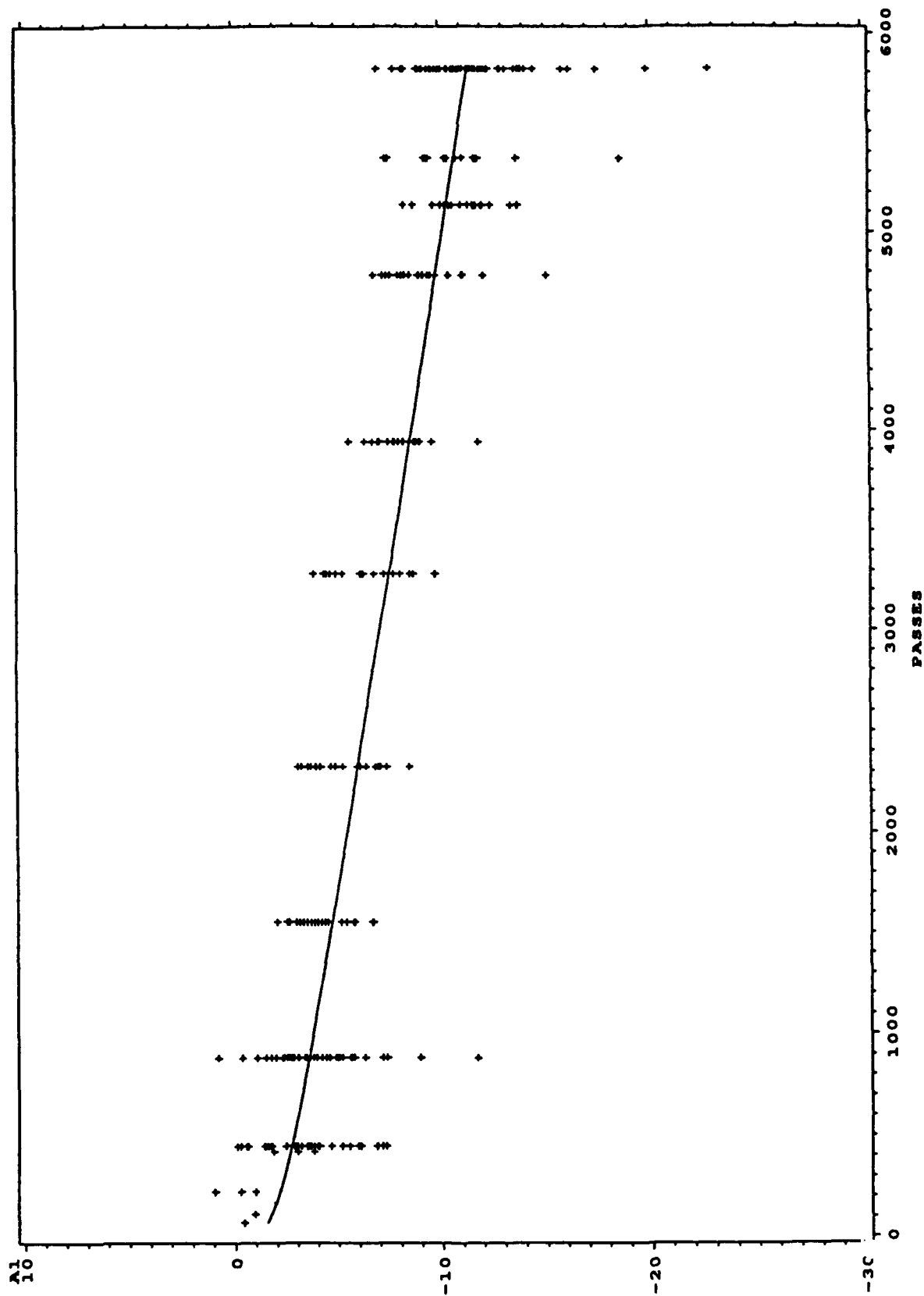
SECTION-4 MIXTURE-GYRATORY DEPTH-6 DESIGN-COMPOSIT



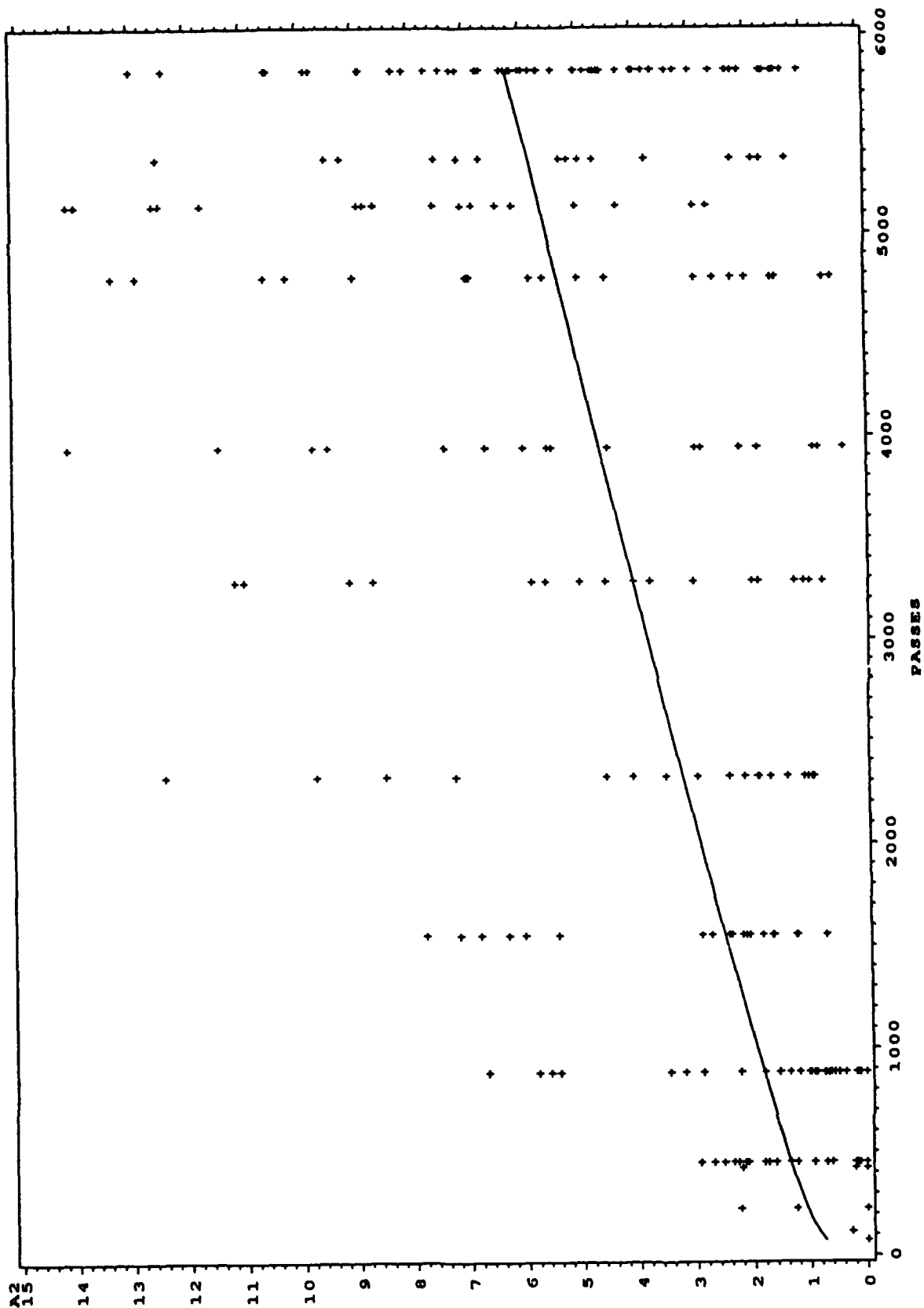
Linear Models of Damage Parameters vs. Number of Passes and Its Log SECTION-4 MIXTURE-GYRATORY DEPTH-6 DESIGN-COMPOSIT



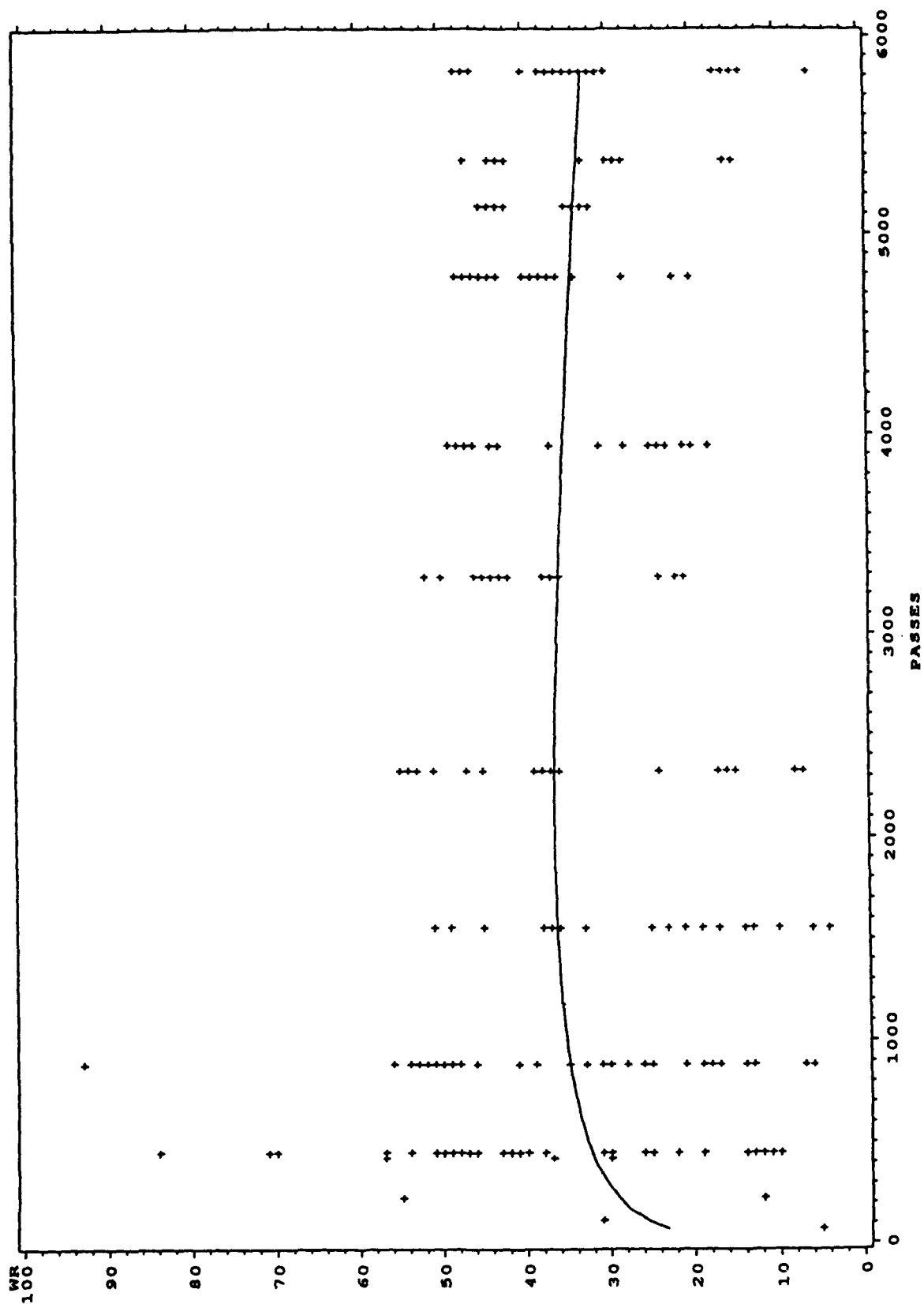
Linear Models of Damage Parameters vs. Number of Passes and Its Log SECTION-3 MIXTURE-MARSHALL DEPTH-6 DESIGN-COMPOSIT



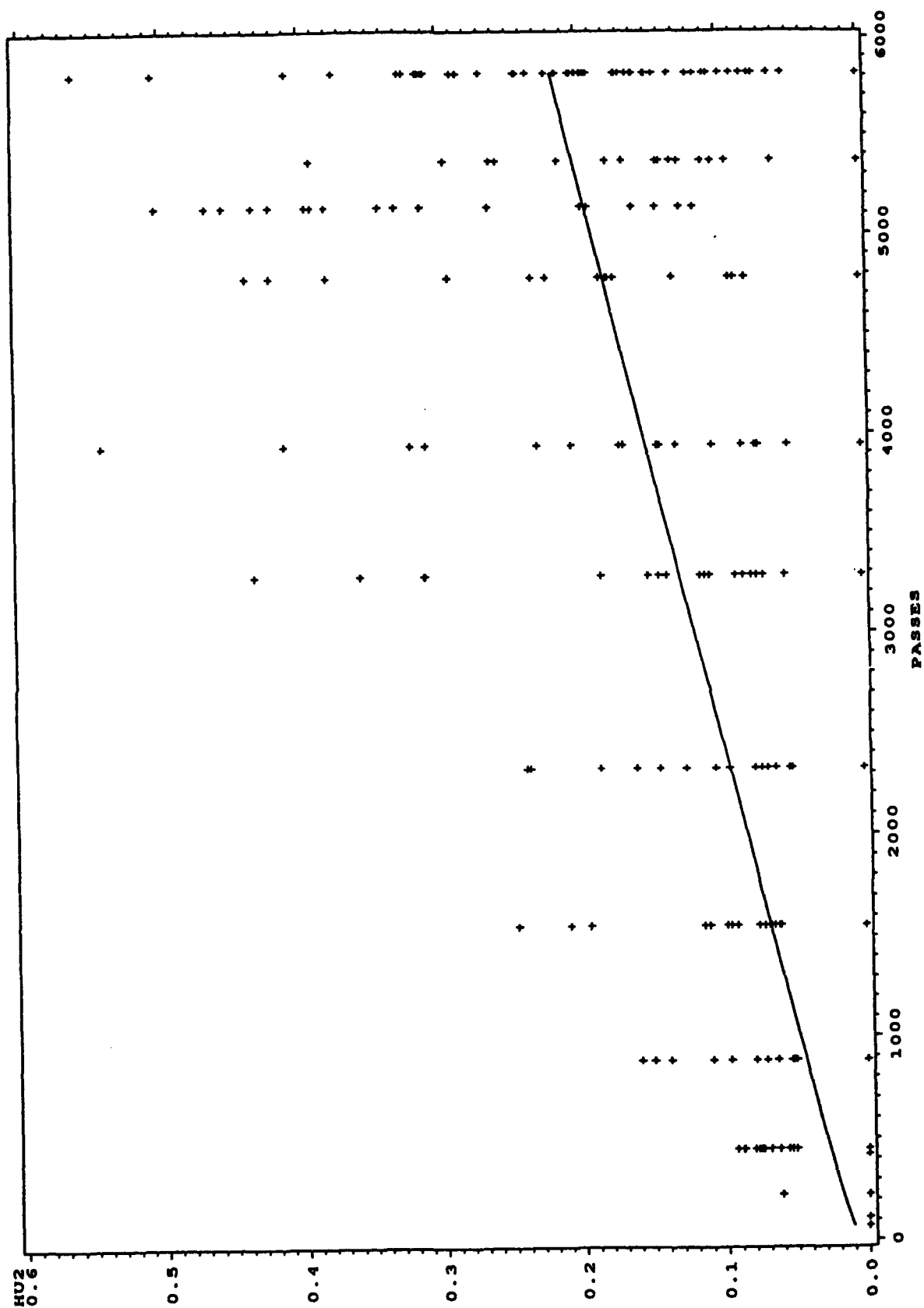
Linear Models of Damage Parameters vs. Number of Passes and Its Log SECTION-3 MIXTURE-MARSHALL DEPTH-6 DESIGN-COMPOSIT



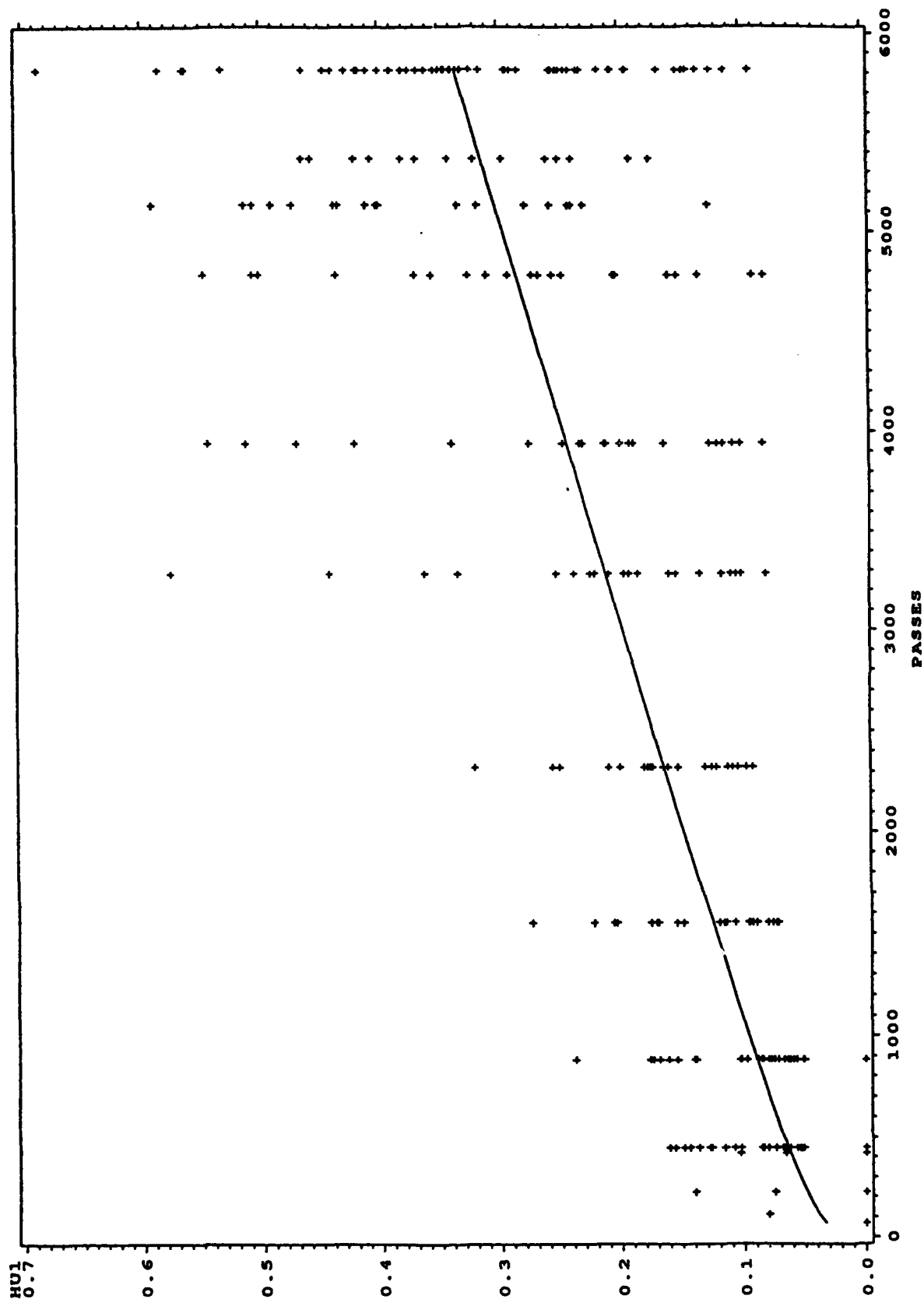
Linear Models of Damage Parameters vs. Number of Passes and Its Log SECTION-3 MIXTURE-MARSHALL DEPTH-6 DESIGN-COMPOSIT



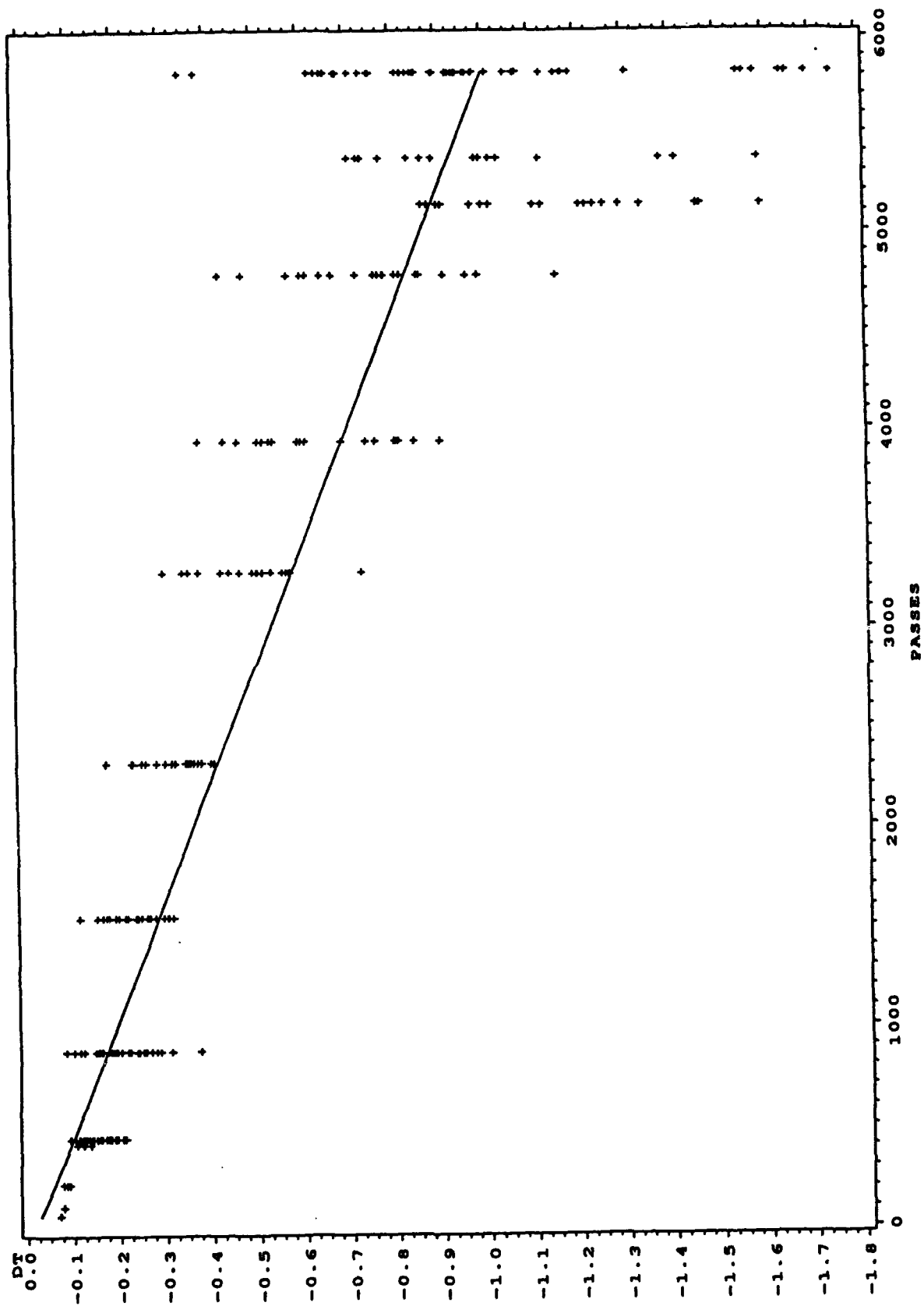
Linear Models of Damage Parameters vs. Number of Passes and Its Log SECTION-3 MIXTURE-MARSHALL DEPTH-6 DESIGN-COMPOSIT



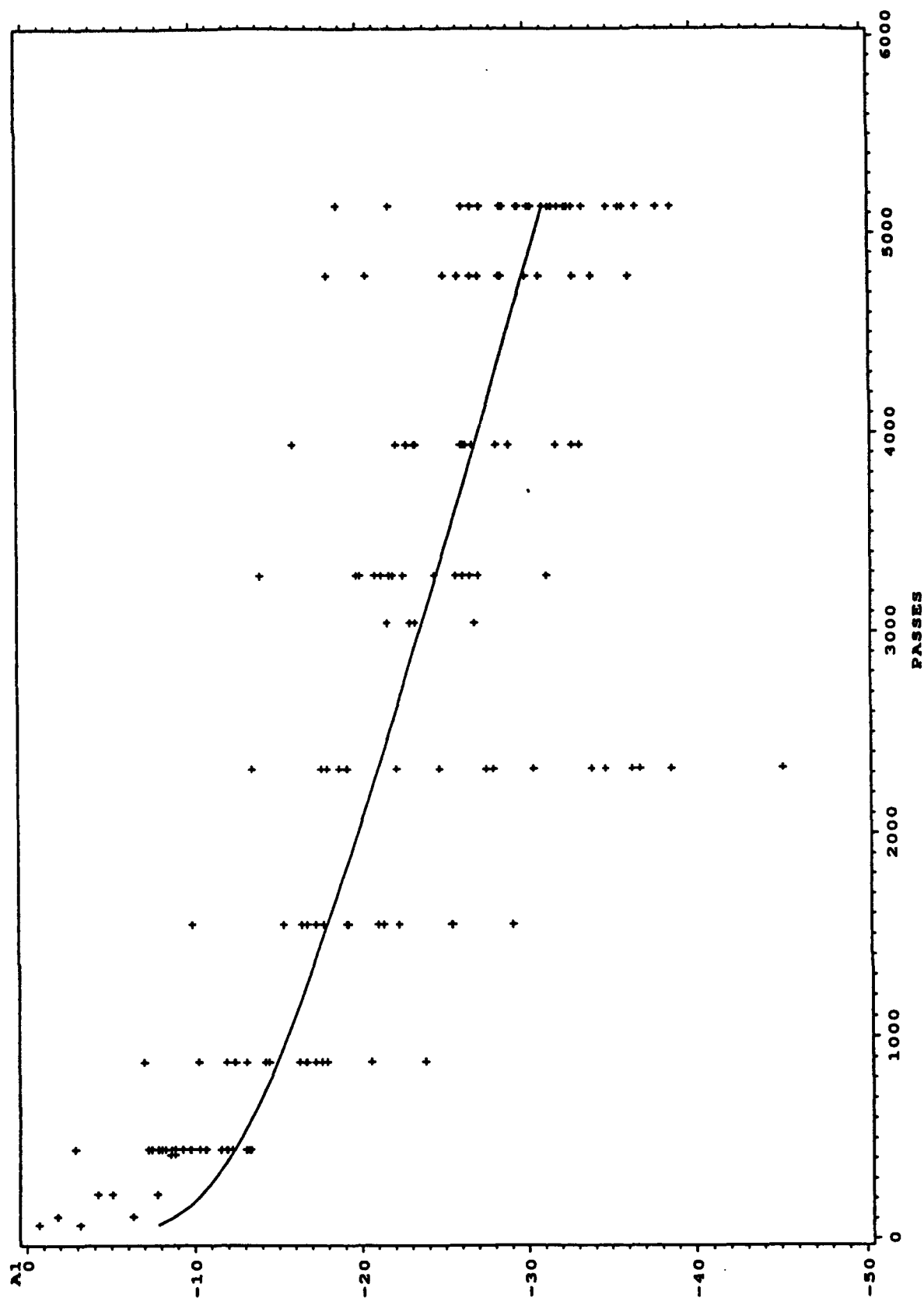
Linear Models of Damage Parameters vs. Number of Passes and Its Log SECTION-3 MIXTURE-MARSHALL DEPTH-6 DESIGN-COMPOSIT



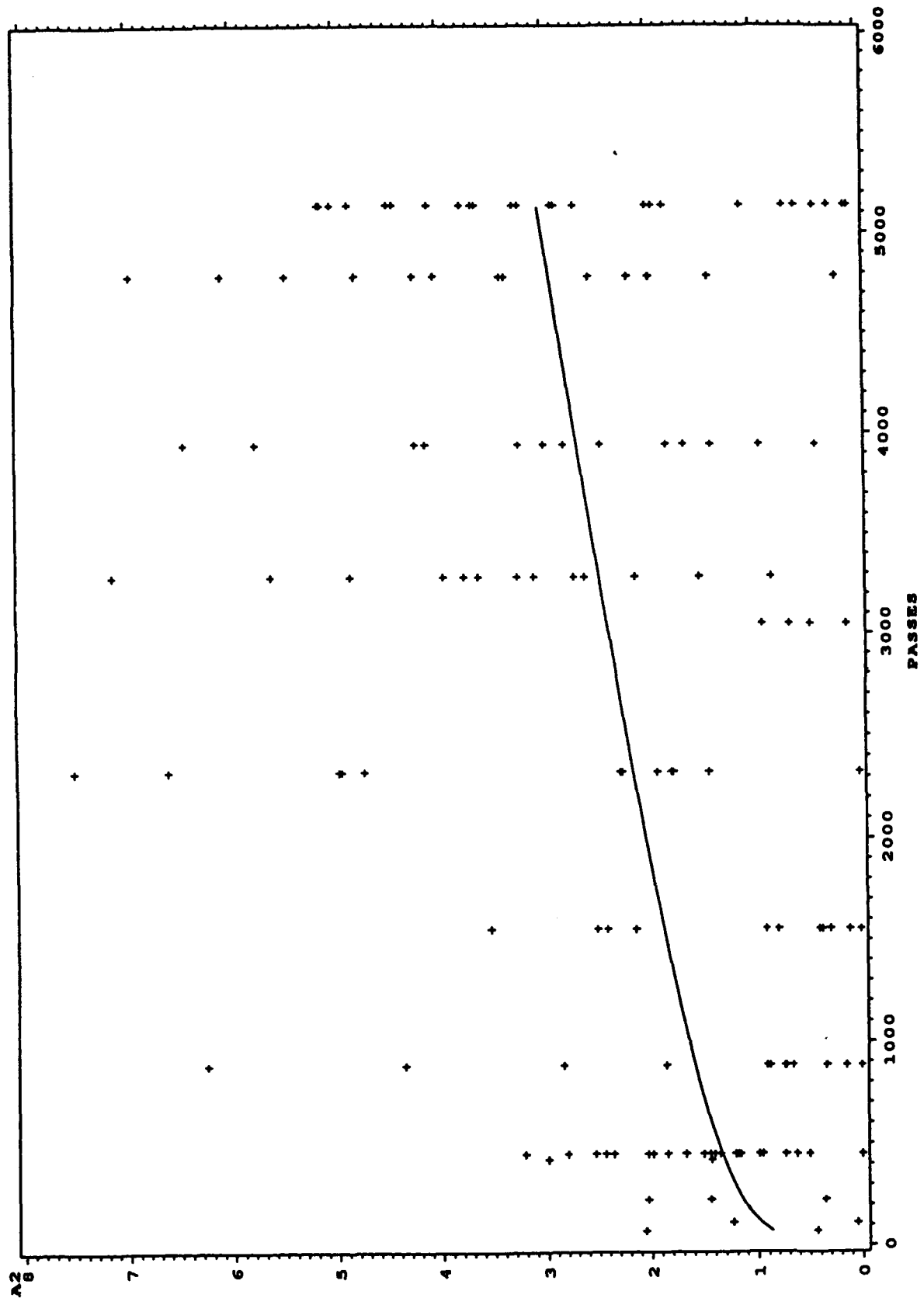
Linear Models of Damage Parameters vs. Number of Passes and Its Log SECTION-3 MIXTURE-MARSHALL DEPTH-6 DESIGN-COMPOSIT



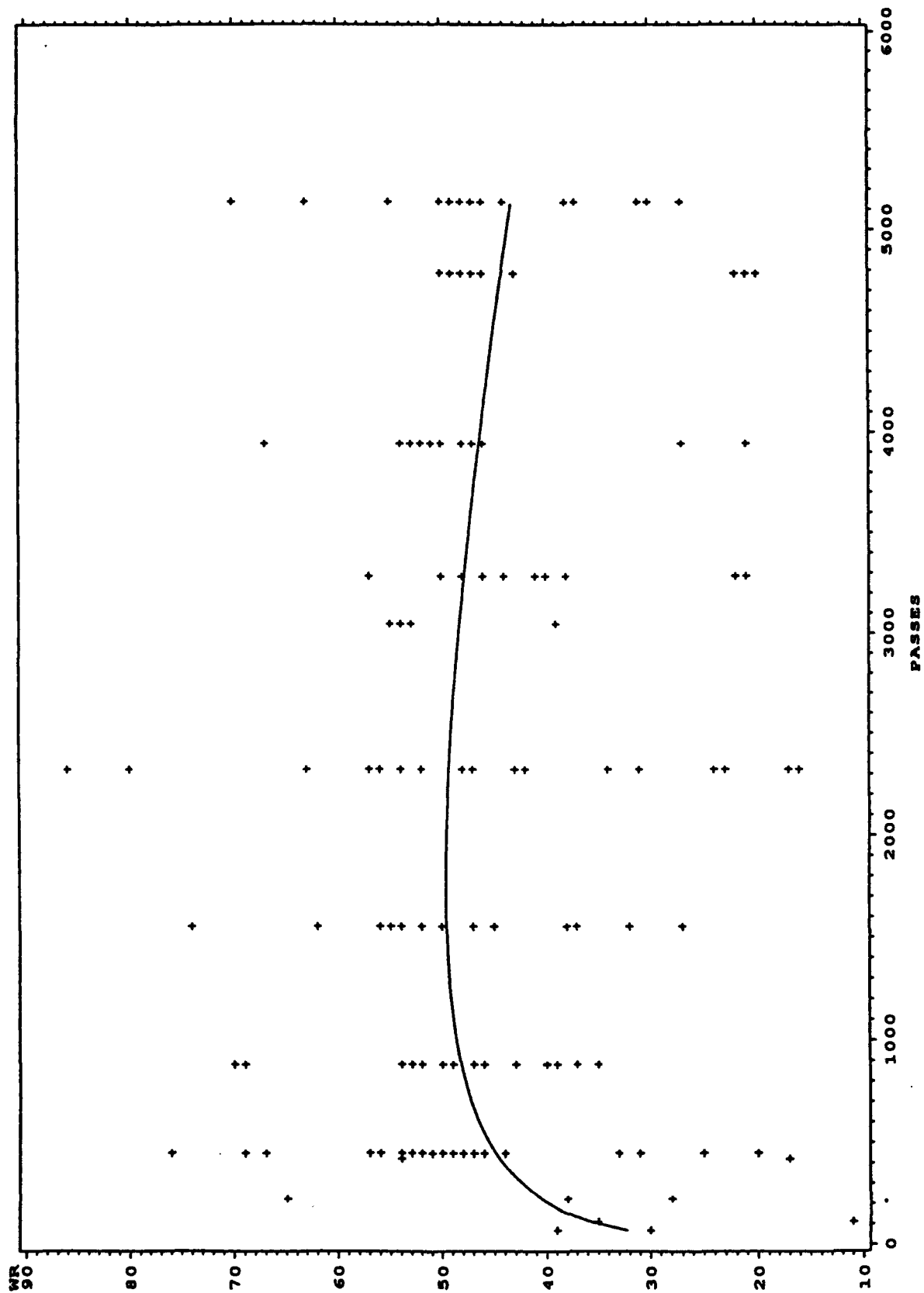
Linear Models of Damage Parameters vs. Number of Passes and Its Log SECTION-2 MIXTURE-MARSHALL DEPTH-6 DESIGN-FLEXIBLE



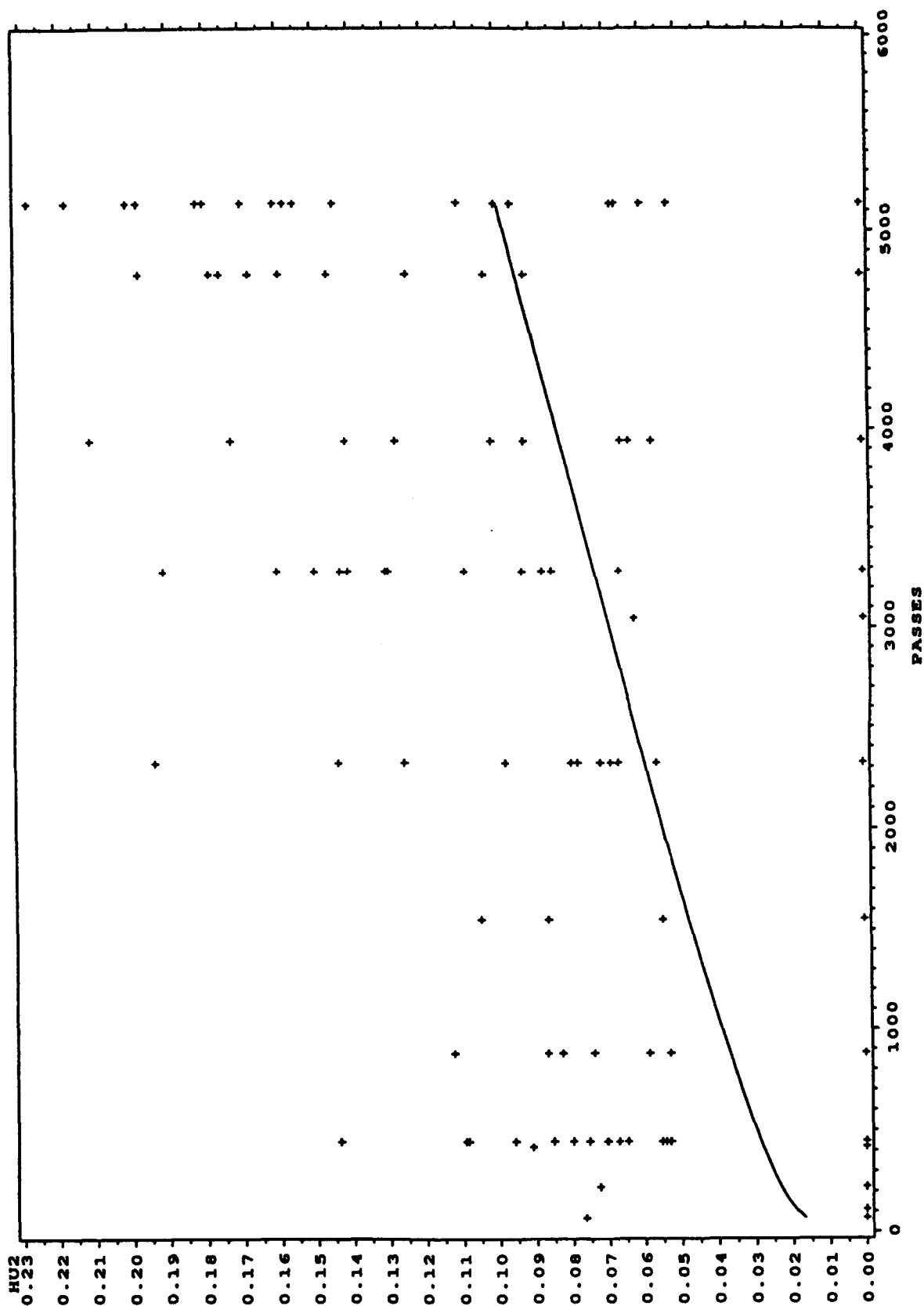
Linear Models of Damage Parameters vs. Number of Passes and Its Log SECTION-2 MIXTURE-MARSHALL DEPTH-6 DESIGN-FLEXIBLE



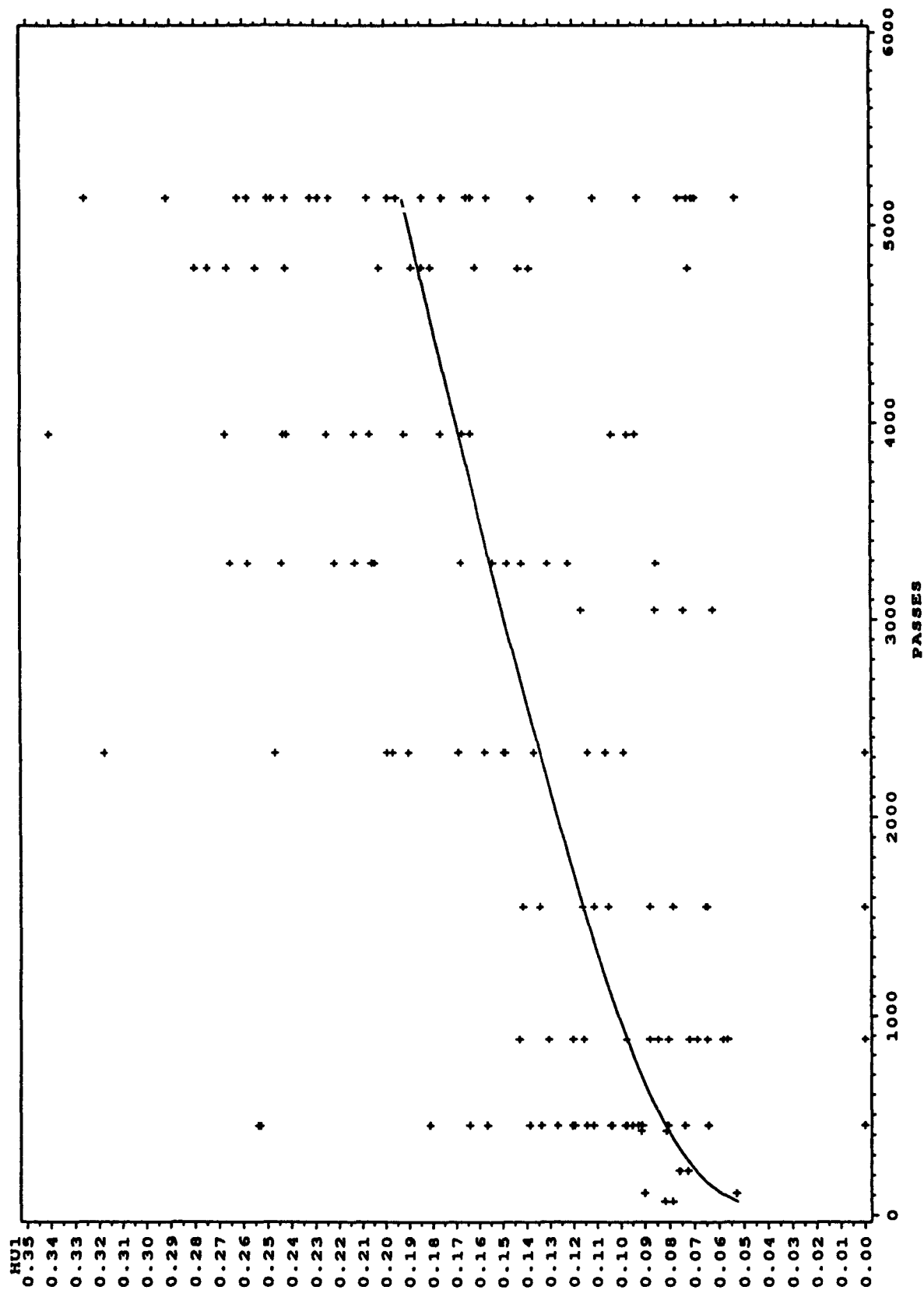
Linear Models of Damage Parameters vs. Number of Passes and Its Log SECTION-2 MIXTURE-MARSHALL DEPTH-6 DESIGN-FLEXIBLE



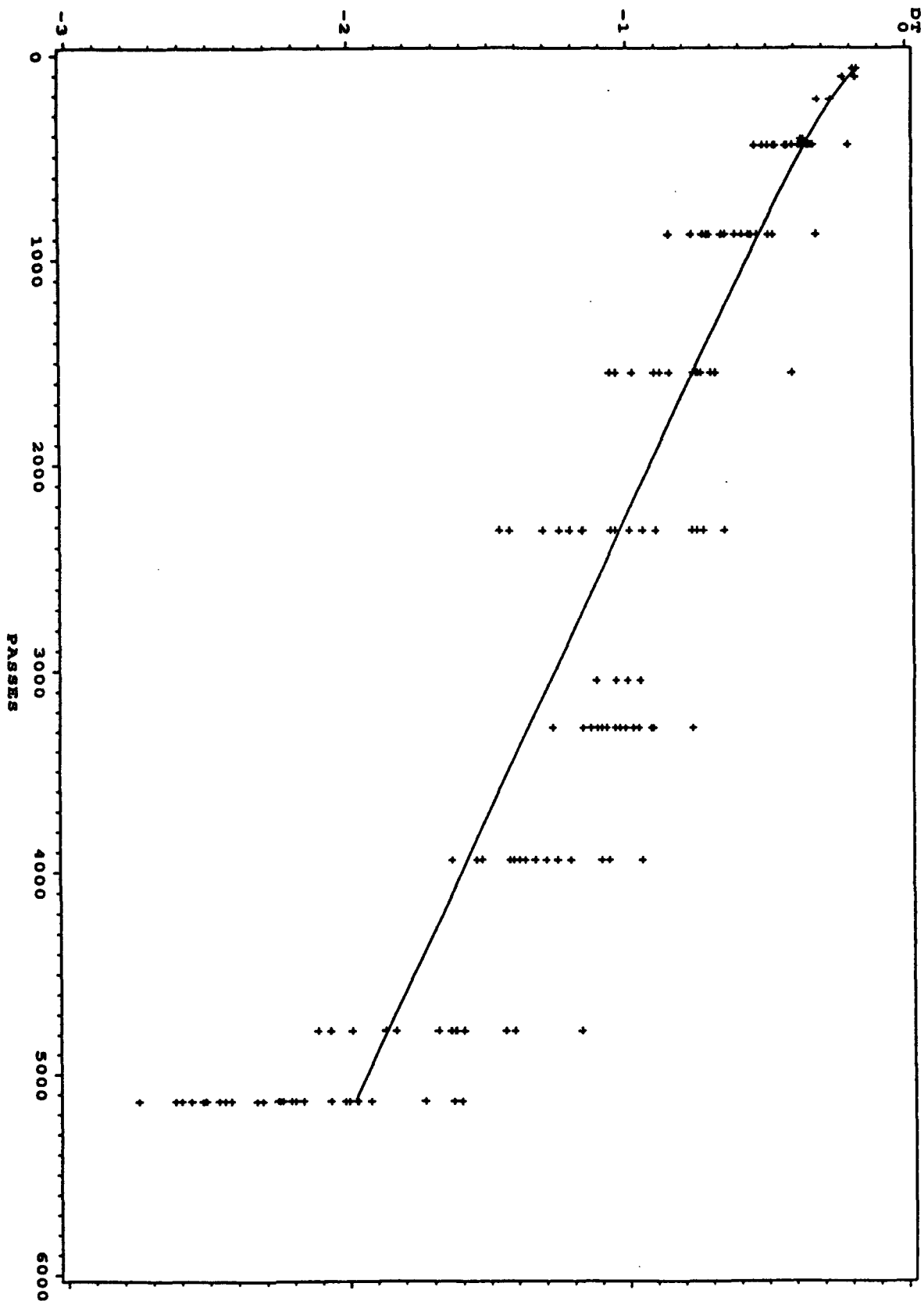
Linear Models of Damage Parameters vs. Number of Passes and Its Log SECTION-2 MIXTURE-MARSHALL DEPTH-6 DESIGN-FLEXIBLE



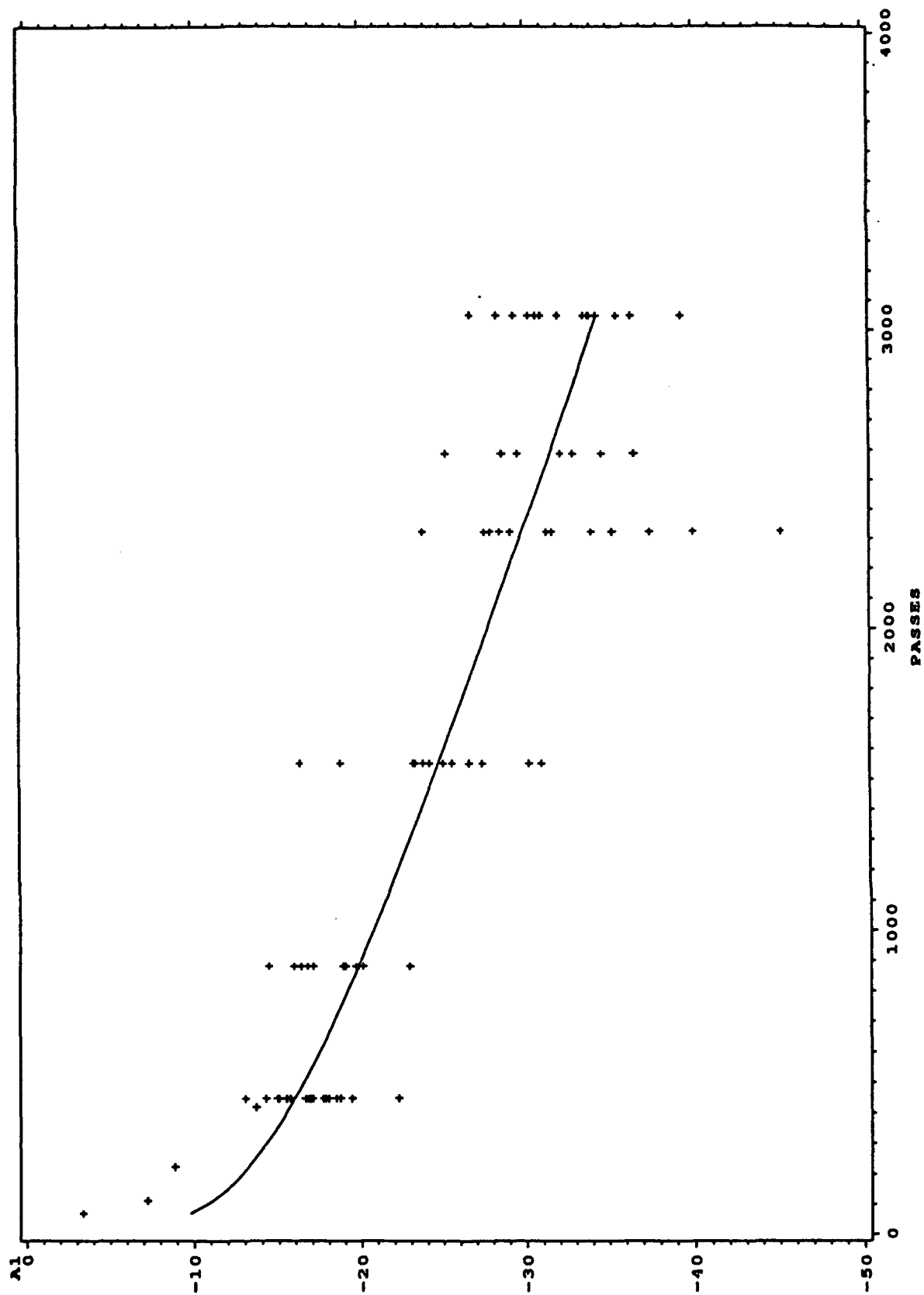
Linear Models of Damage Parameters vs. Number of Passes and Its Log SECTION-2 MIXTURE-MARSHALL DEPTH-6 DESIGN-FLEXIBLE



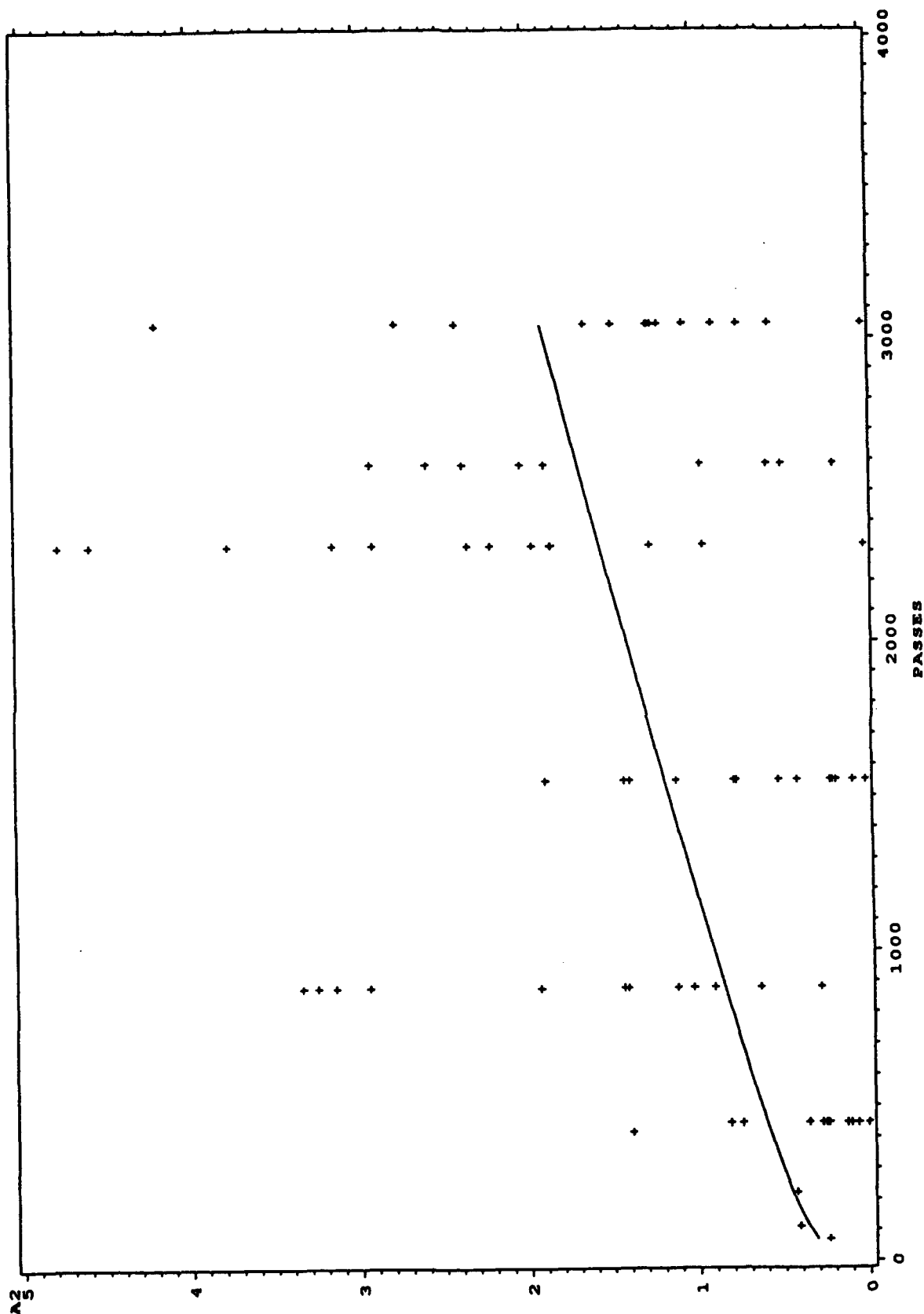
Linear Models of Damage Parameters vs. Number of Passes and Its Log SECTION-2 MIXTURE-MARSHALL DEPTH-6 DESIGN-FLEXIBLE



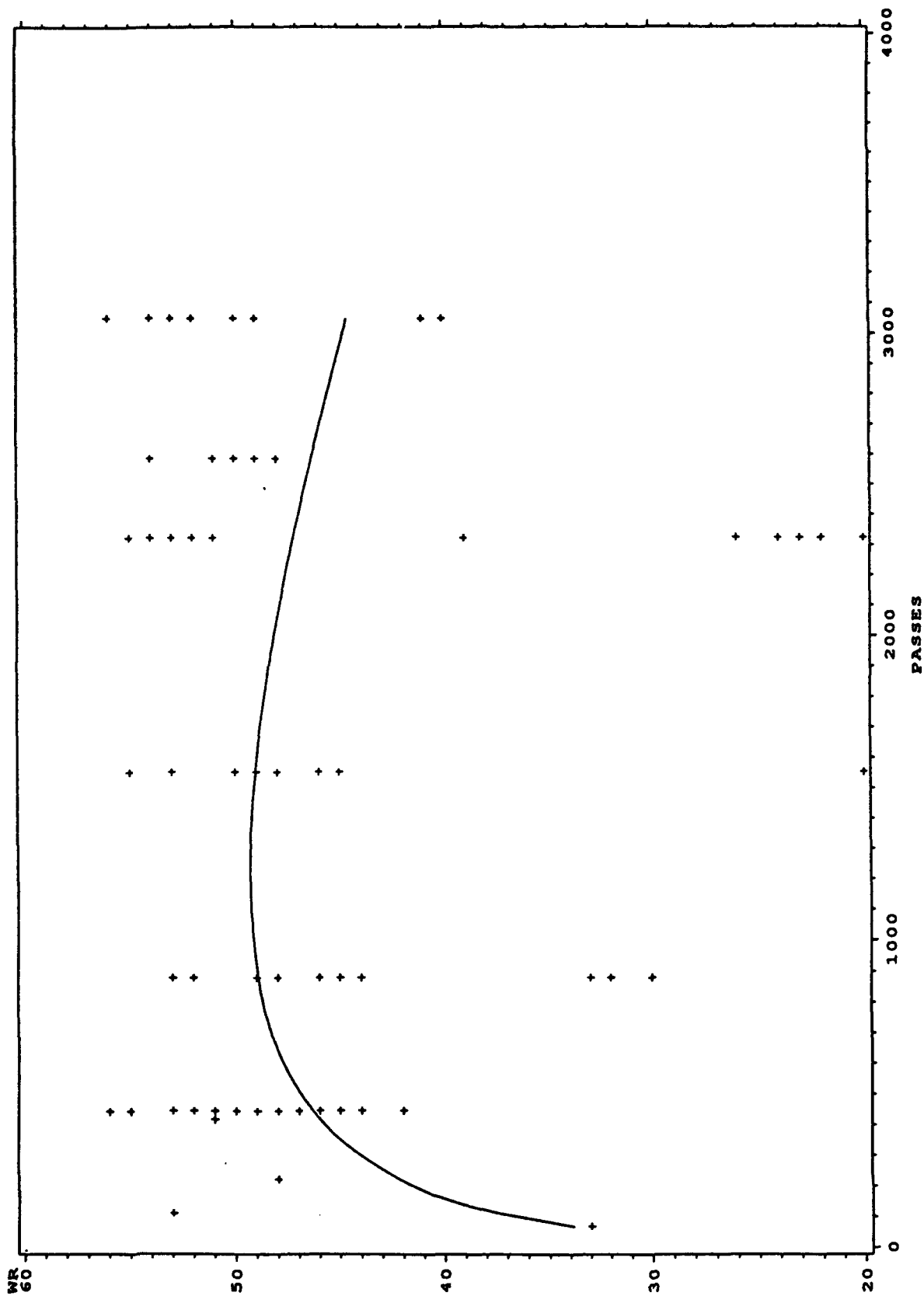
Linear Models of Damage Parameters vs. Number of Passes and Its Log SECTION-1 MIXTURE-MARSHALL DEPTH-4 DESIGN-FLEXIBLE



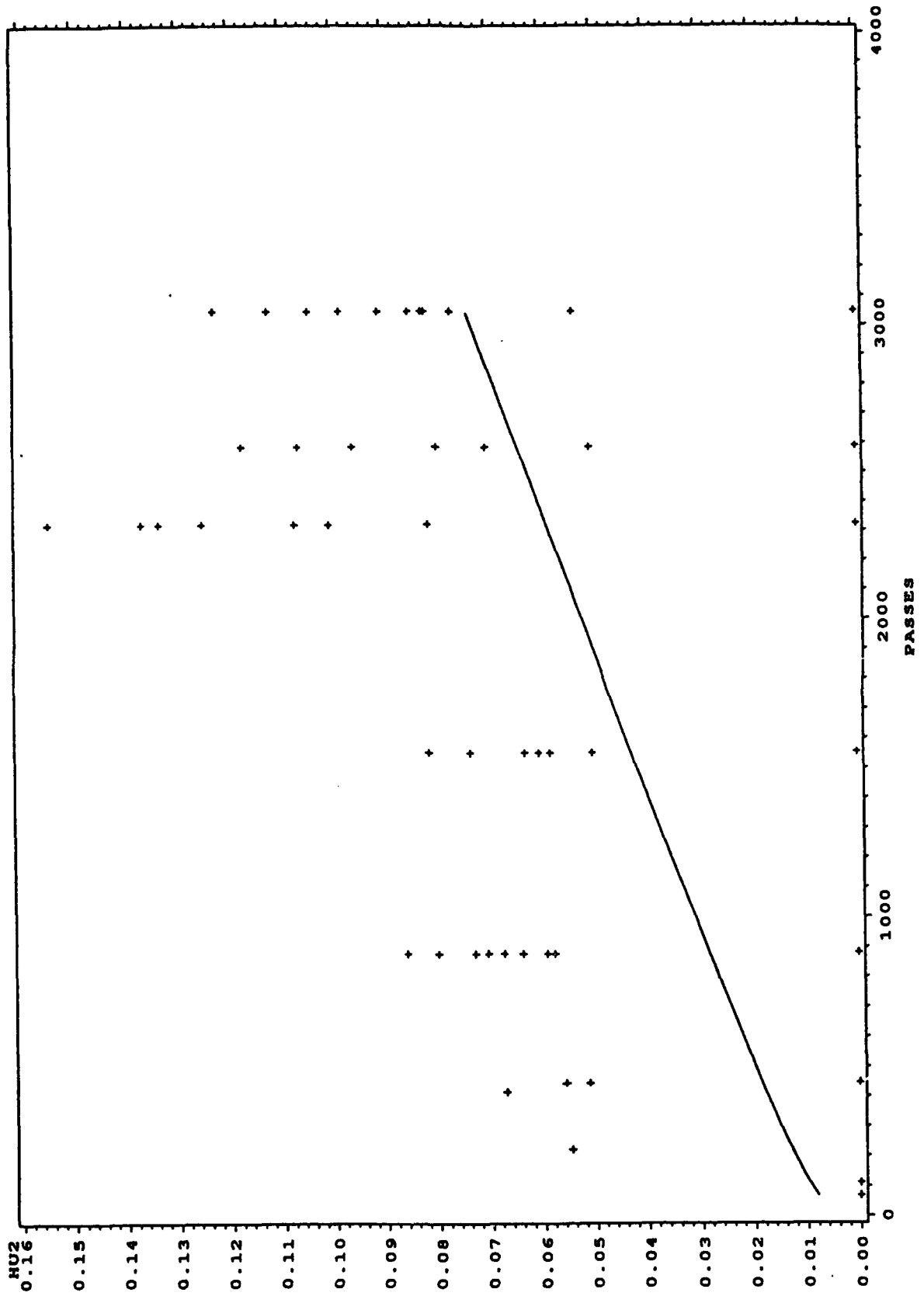
Linear Models of Damage Parameters vs. Number of Passes and Its Log SECTION-1 MIXTURE-MARSHALL DEPTH-4 DESIGN-FLEXIBLE



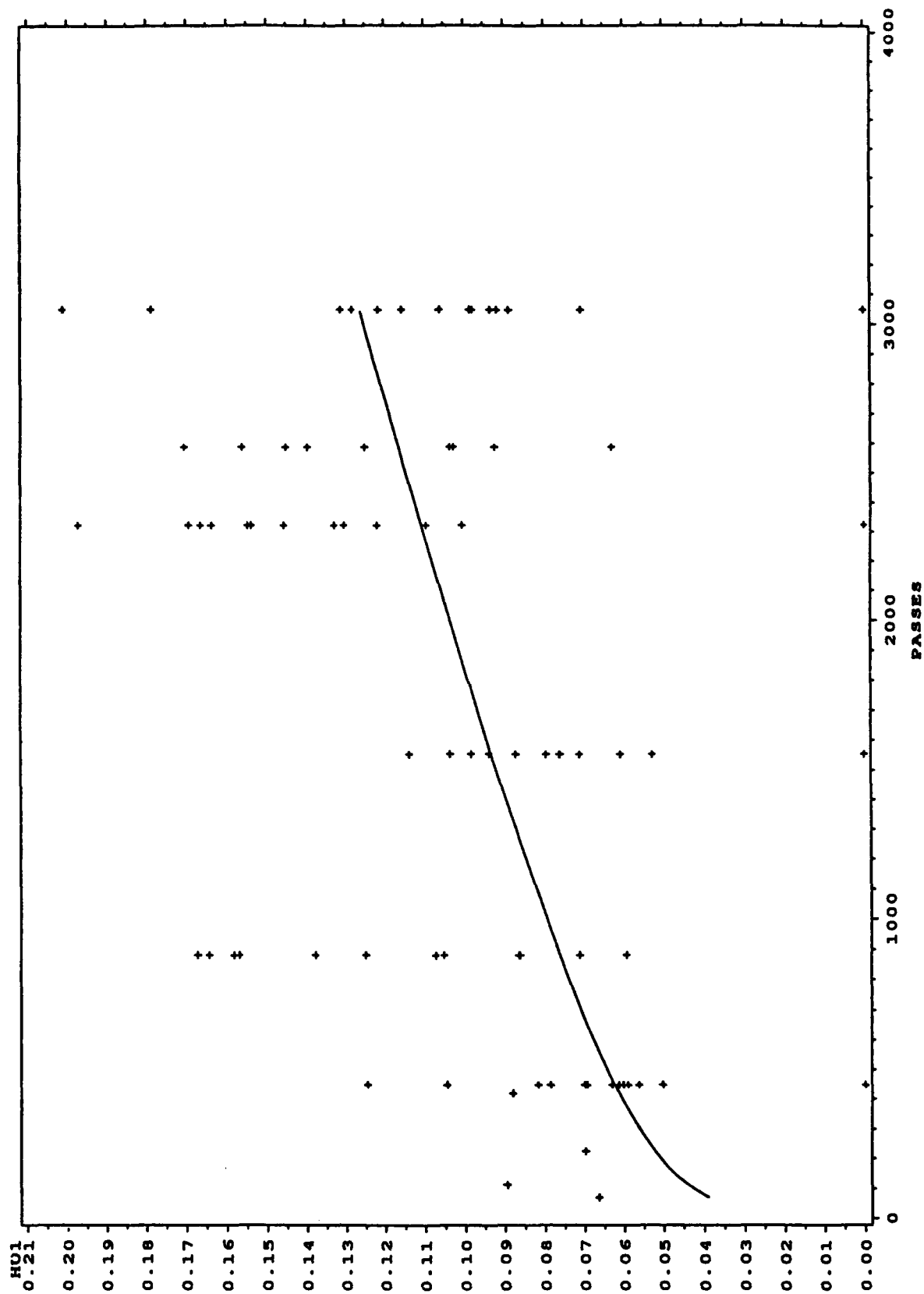
Linear Models of Damage Parameters vs. Number of Passes and Its Log SECTION-1 MIXTURE-MARSHALL DEPTH-4 DESIGN-FLEXIBLE



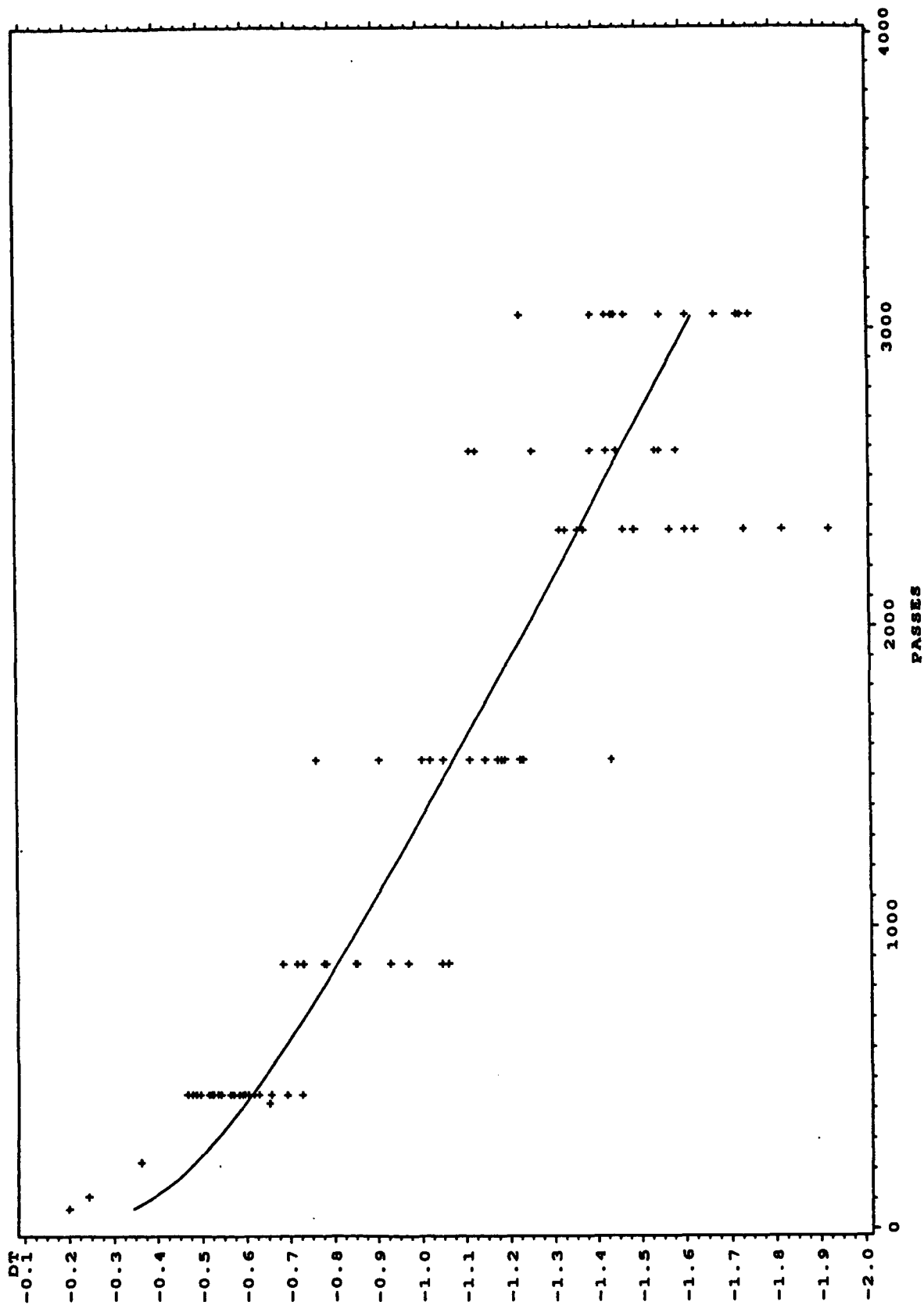
Linear Models of Damage Parameters vs. Number of Passes and Its Log SECTION-1 MIXTURE-MARSHALL DEPTH-4 DESIGN-FLEXIBLE



Linear Models of Damage Parameters vs. Number of Passes and Its Log SECTION-1 MIXTURE-MARSHALL DEPTH-4 DESIGN-FLEXIBLE



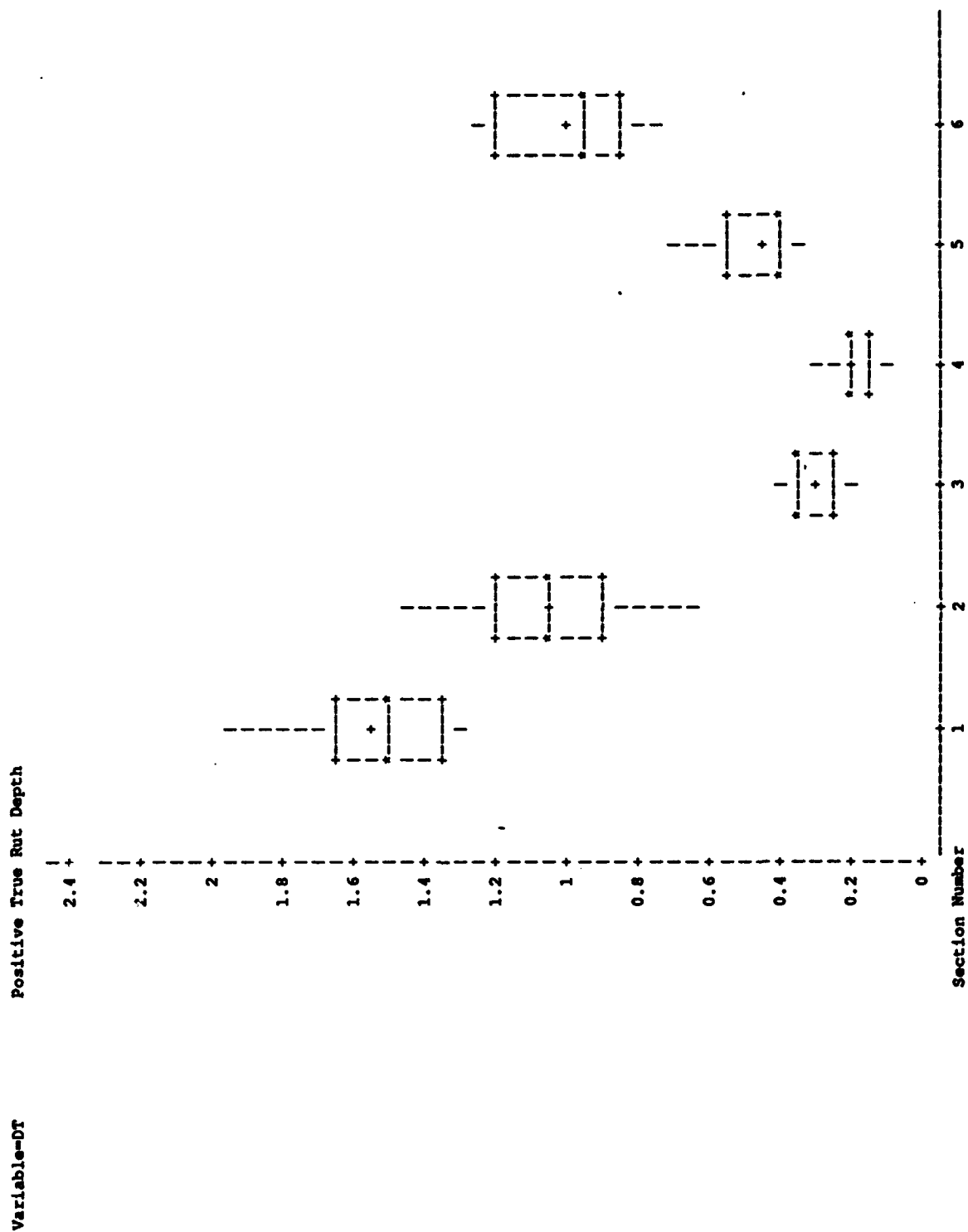
Linear Models of Damage Parameters vs. Number of Passes and Its Log SECTION-1 MIXTURE-MARSHALL DEPTH-4 DESIGN-FLEXIBLE



APPENDIX F

BOXPLOTS OF DAMAGE PARAMETERS

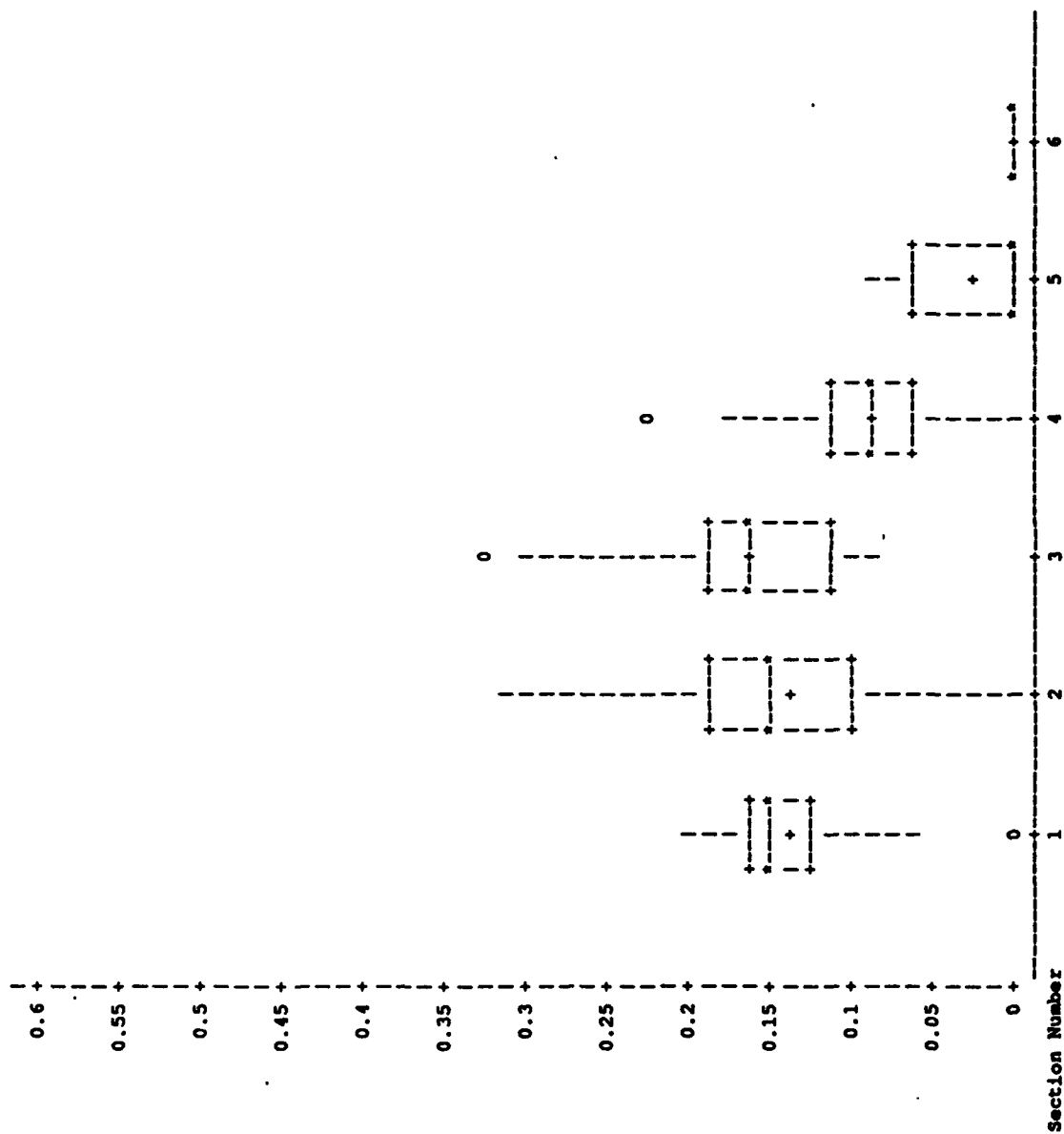
Damage at 2324 Passes
UNIVARIATE PROCEDURE
Schematic Plots



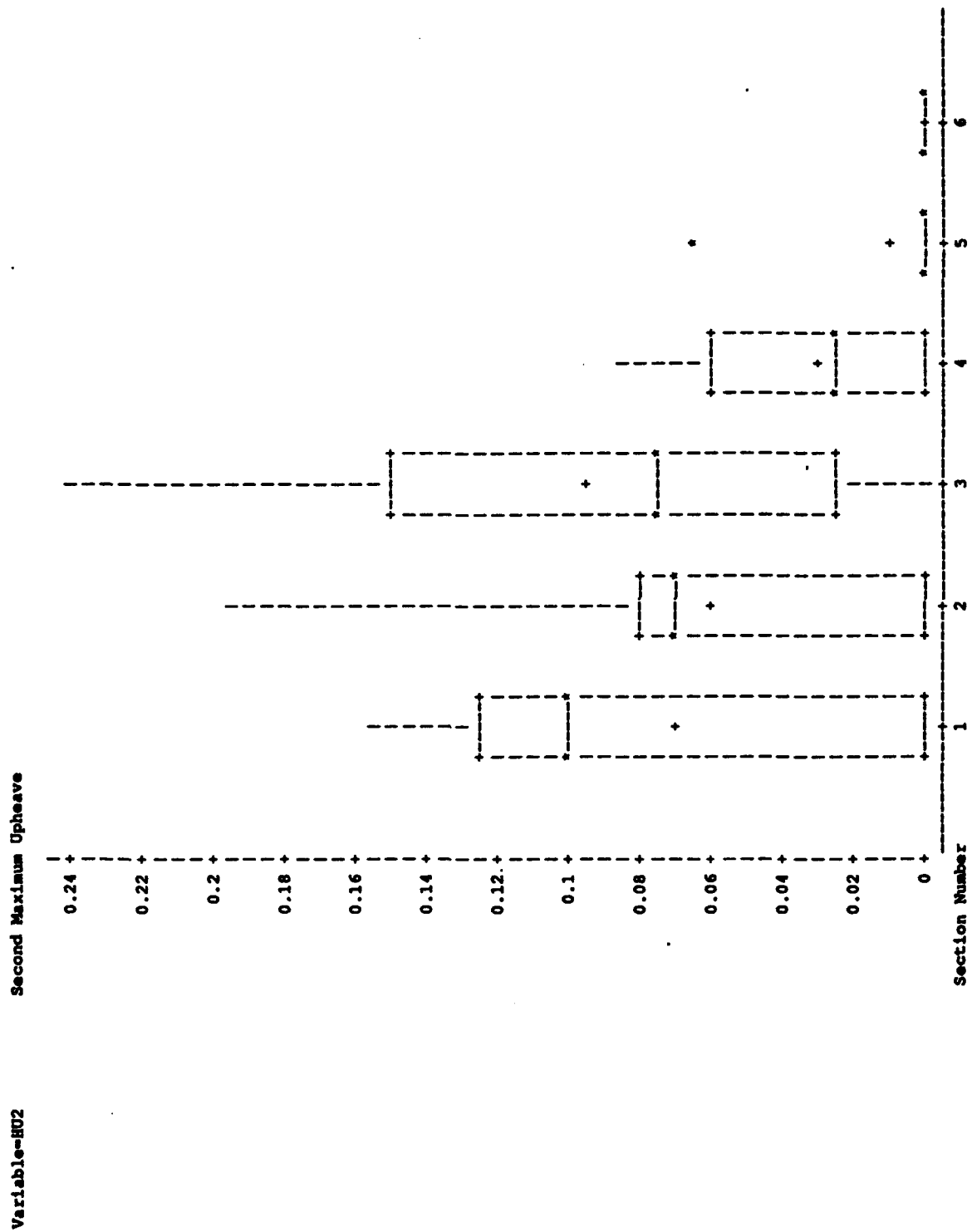
Damage at 2324 Passes

UNIVARIATE PROCEDURE
Schematic Plots

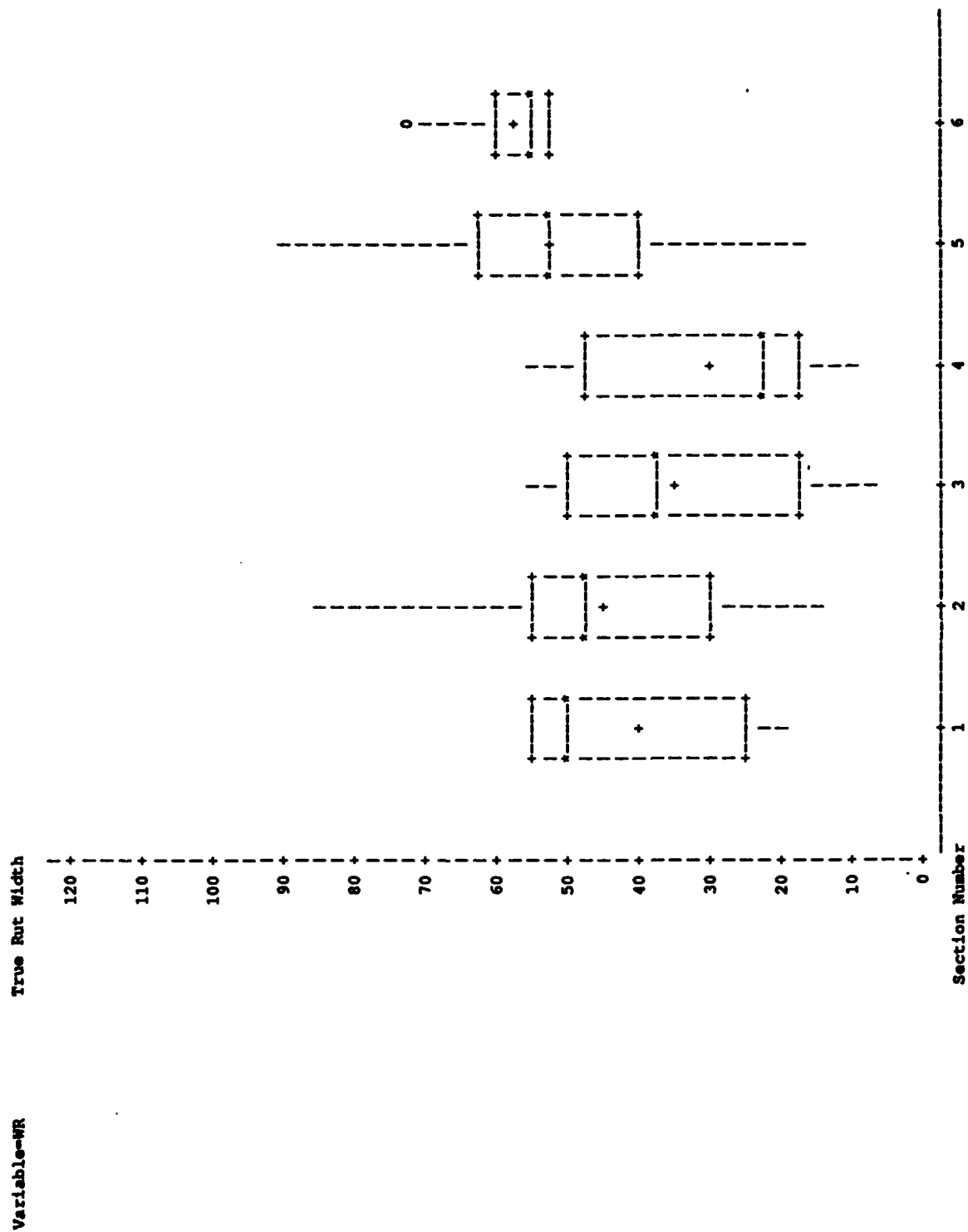
Variable=HV1 First Maximum Upheave



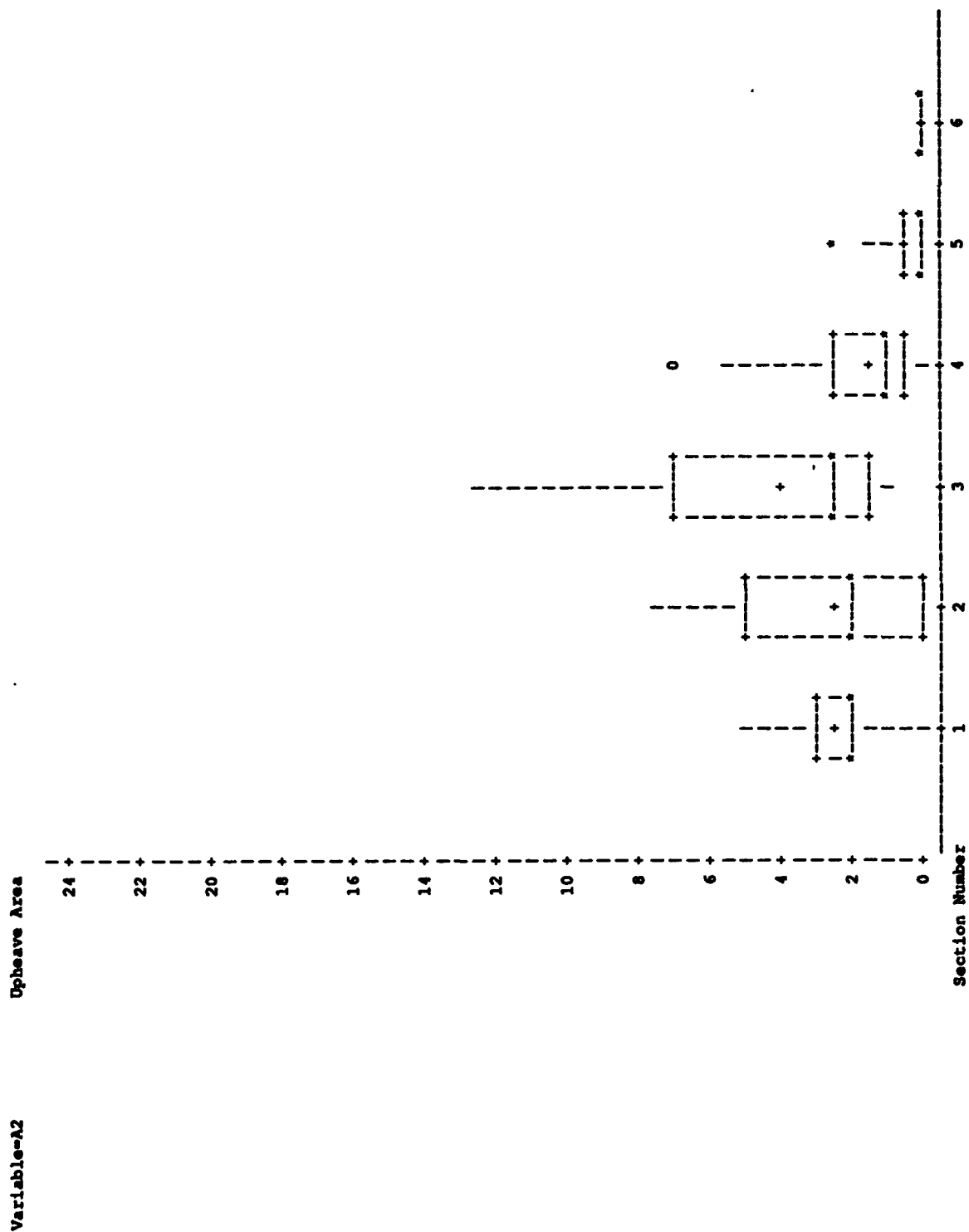
Damage at 2324 Passes
UNIVARIATE PROCEDURE
Schematic Plots



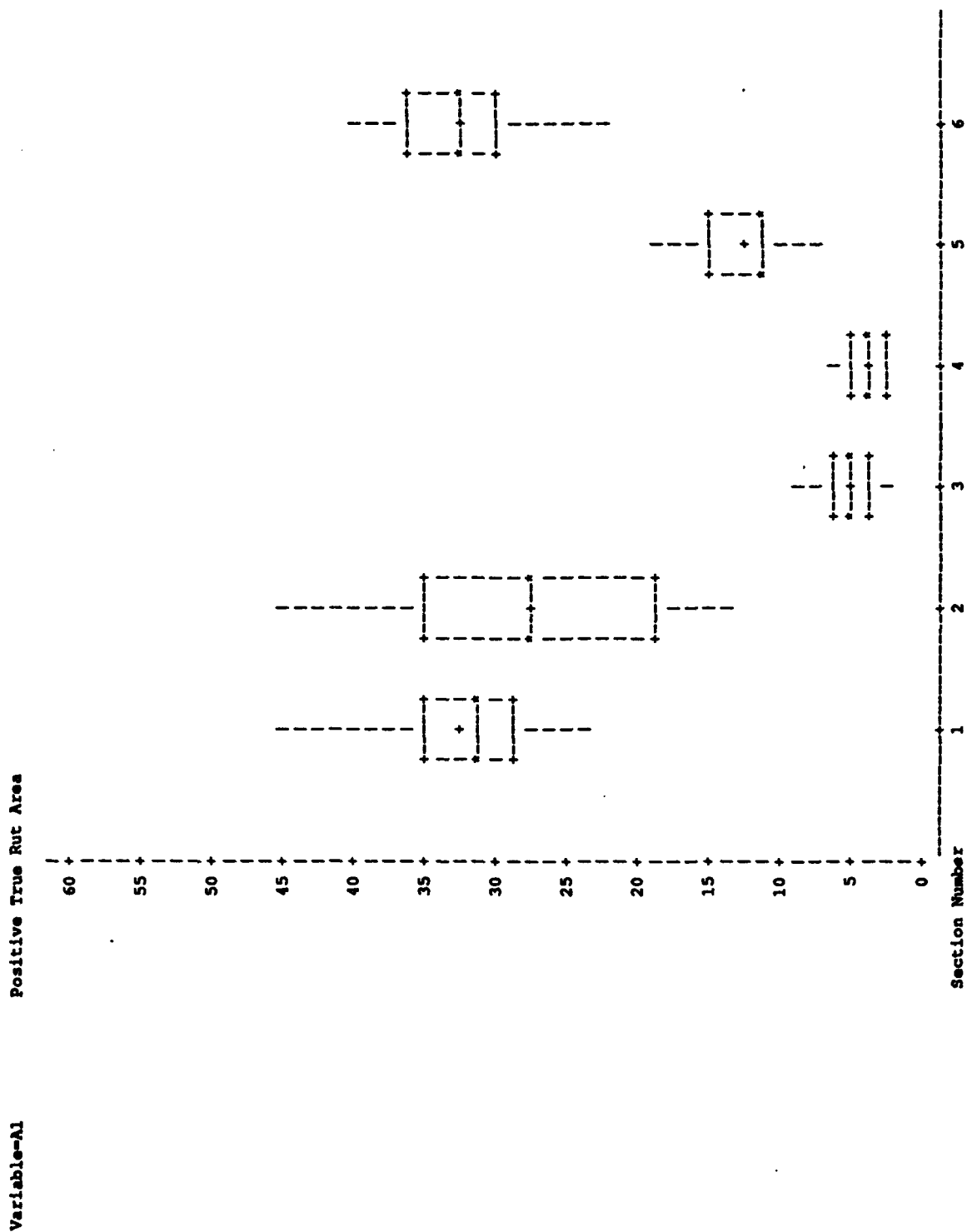
Damage at 2324 Passes
UNIVARIATE PROCEDURE
Schematic Plots



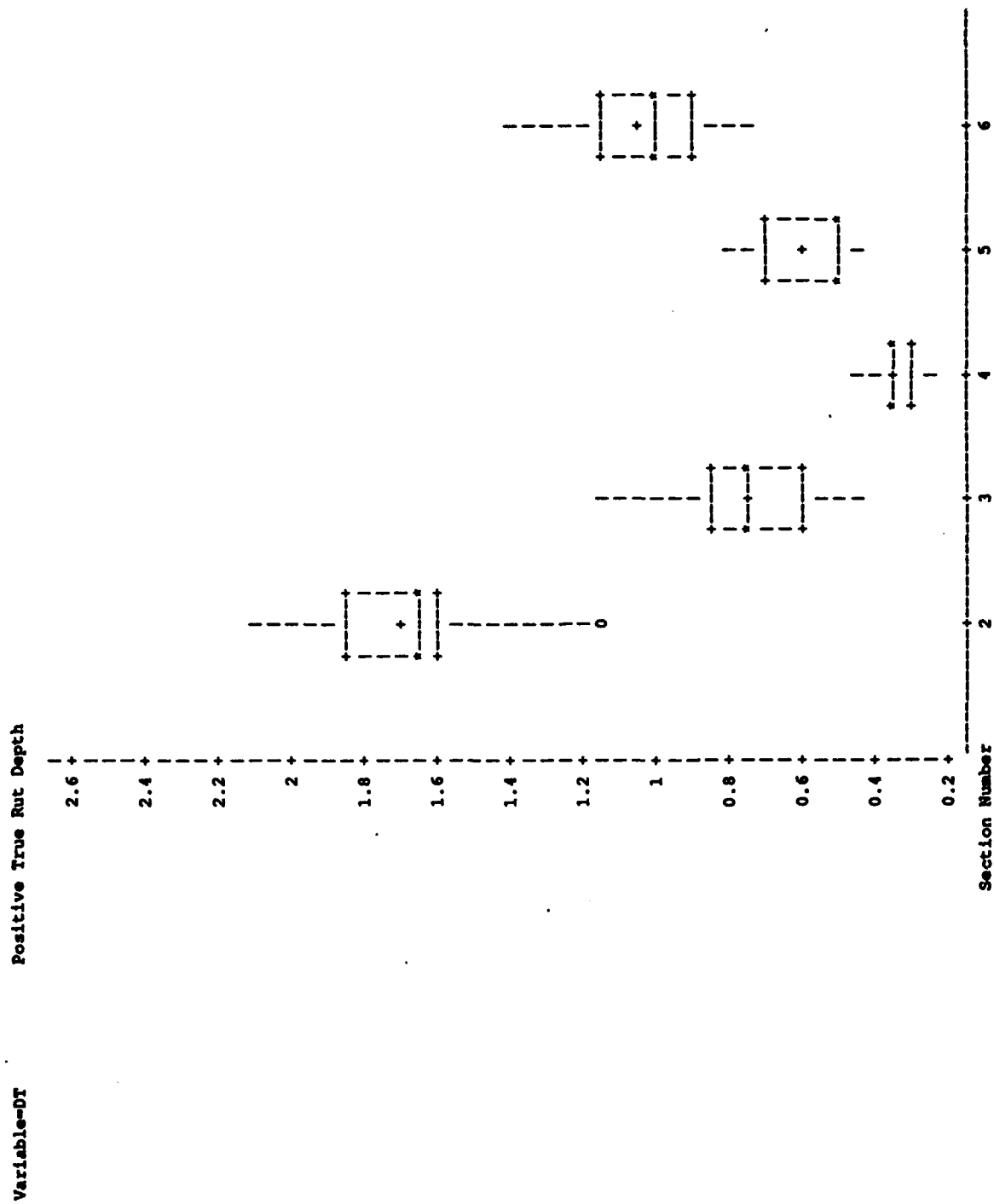
Damage at 2324 Passes
 UNIVARIATE PROCEDURE
 Schematic Plots



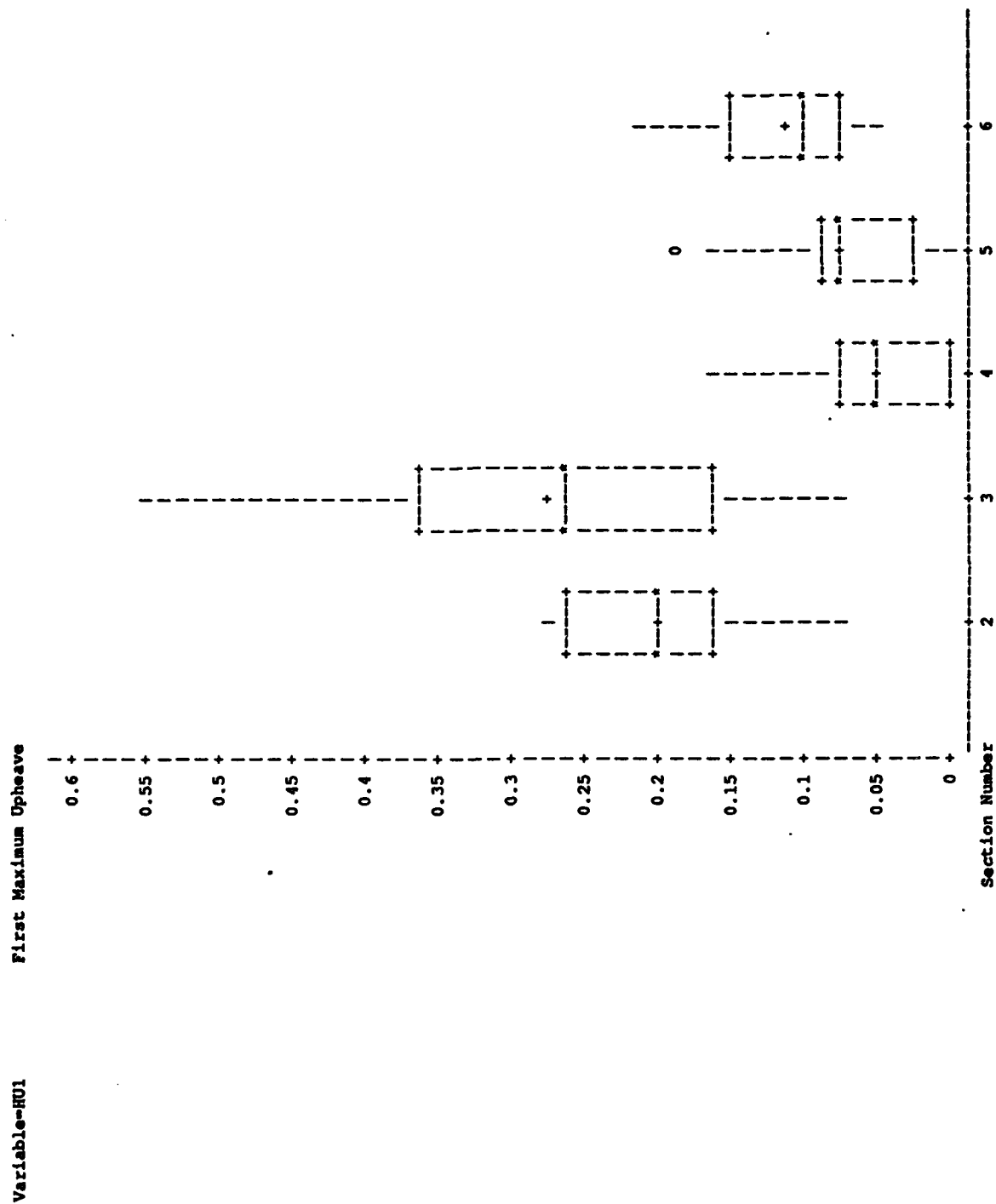
Damage at 2324 Passes
UNIVARIATE PROCEDURE
Schematic Plots



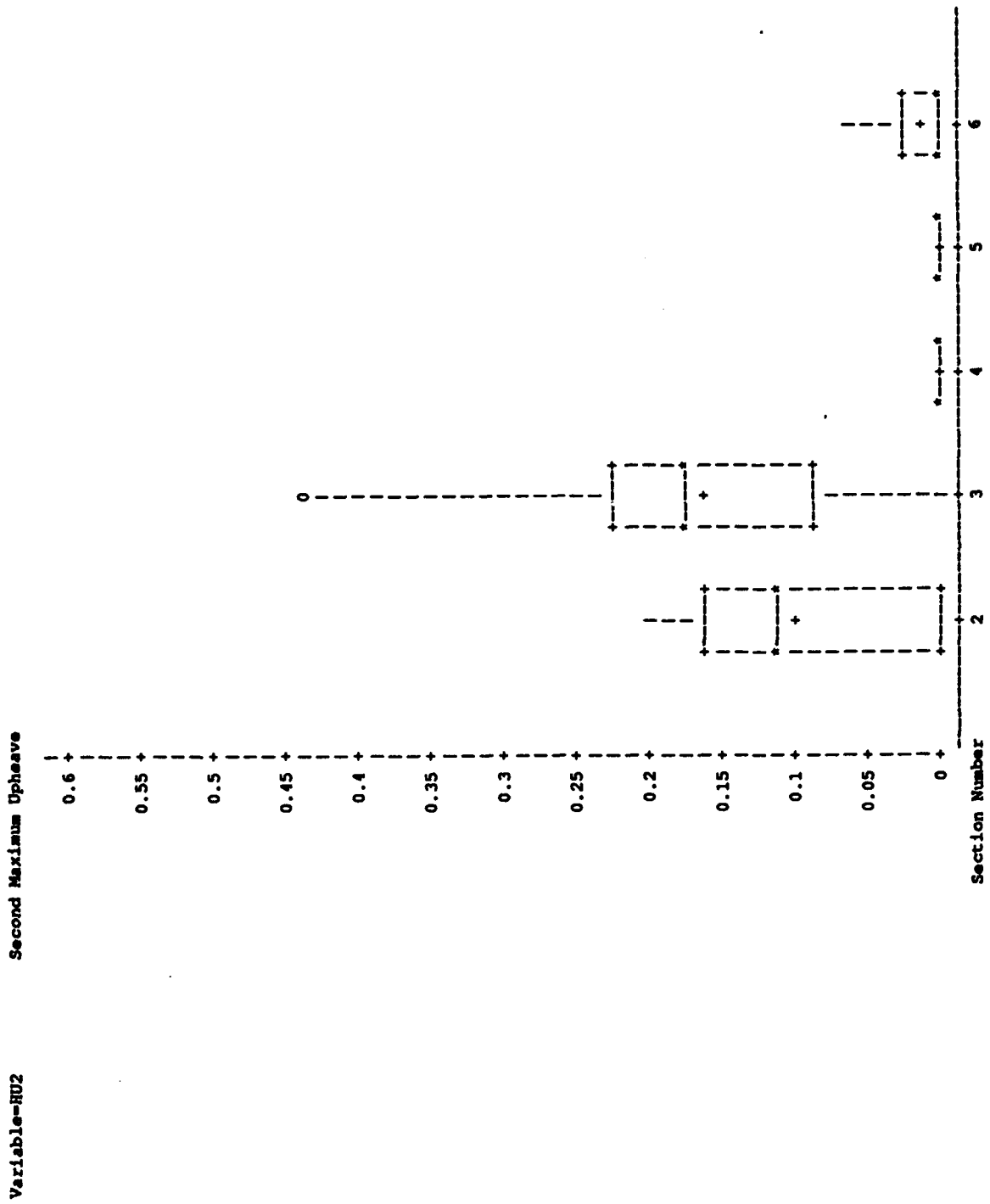
Damage at 4784 Passes
UNIVARIATE PROCEDURE
Schematic Plots



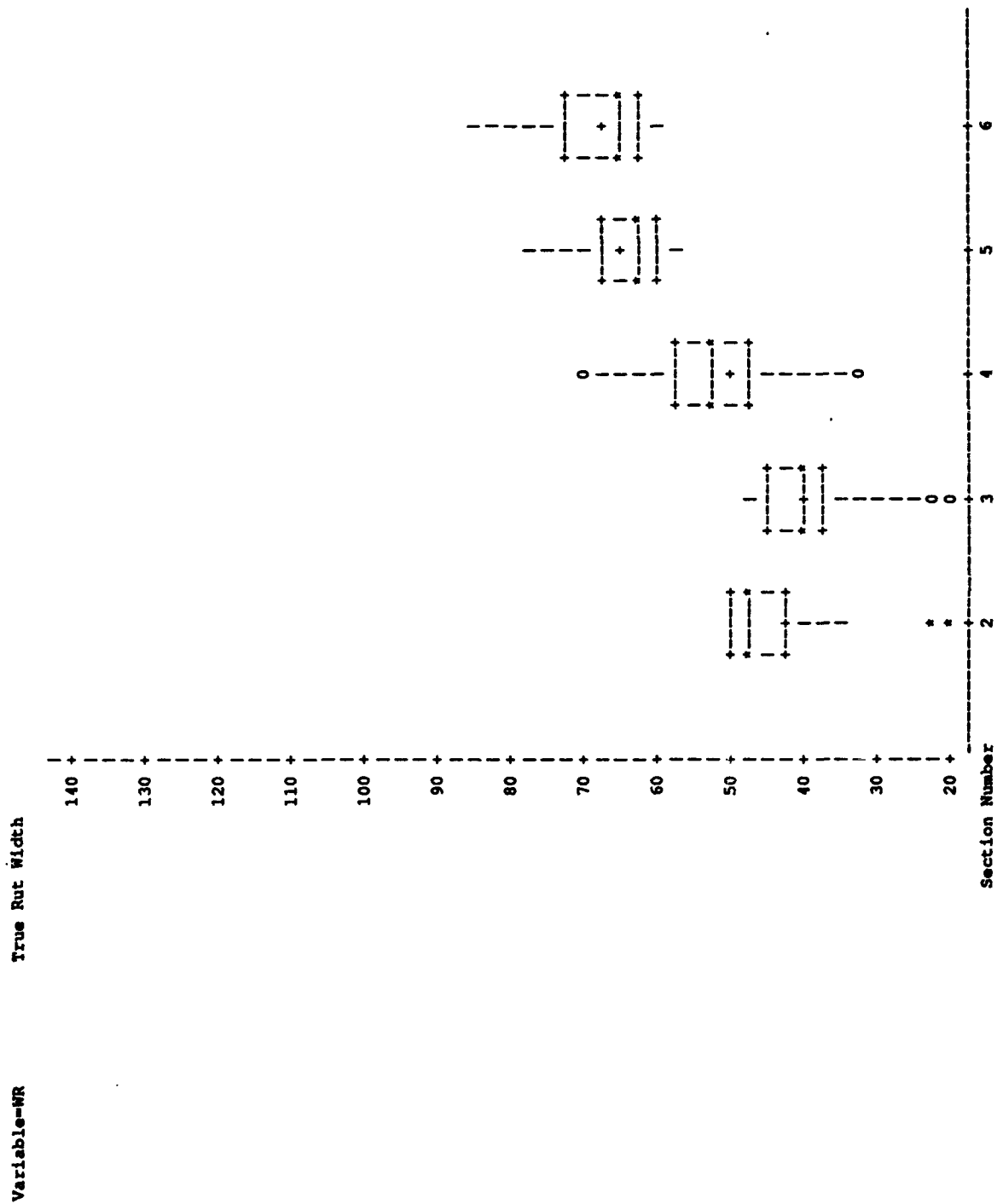
Damage at 4784 Passes
UNIVARIATE PROCEDURE
Schematic Plots



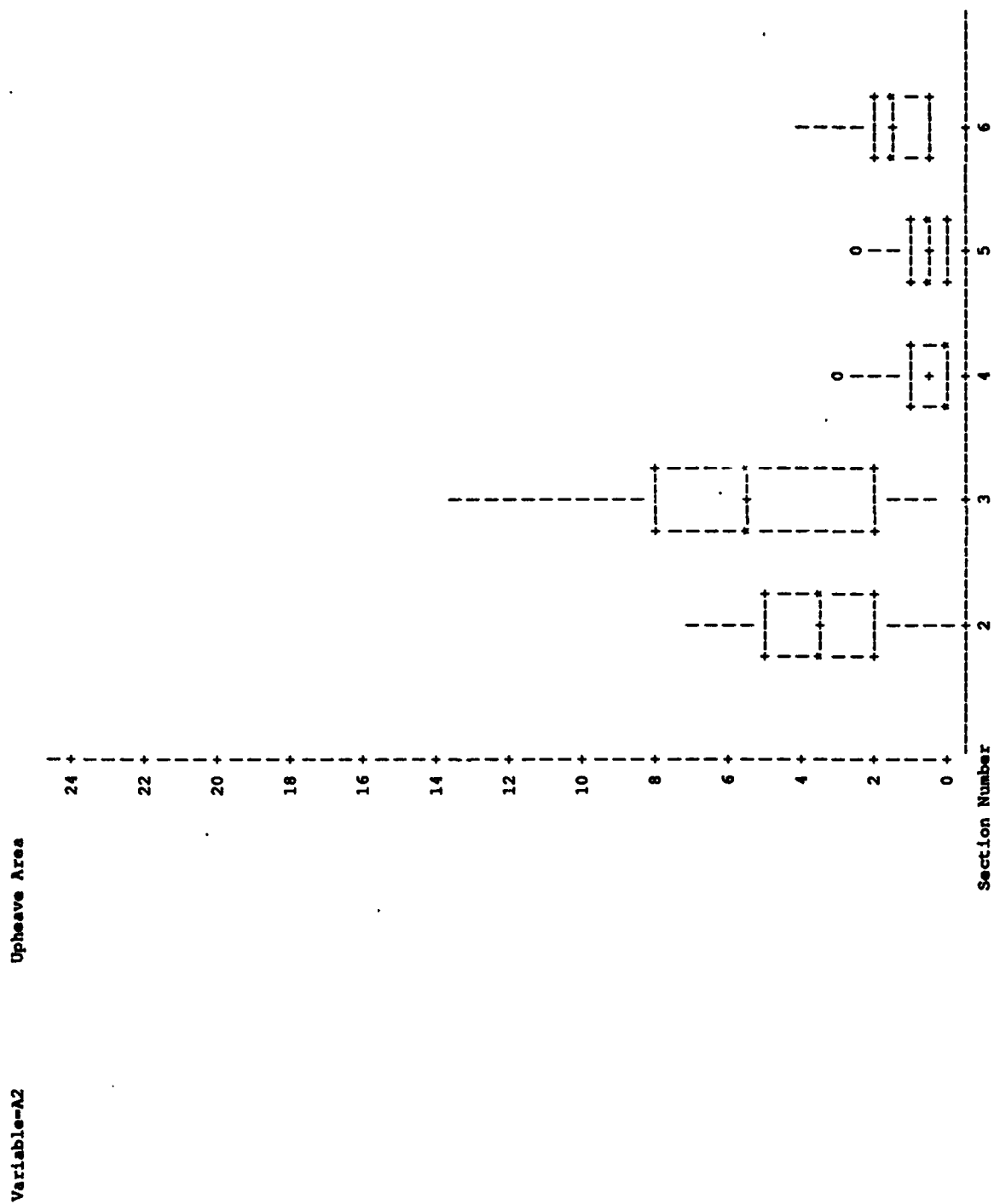
Damage at 4784 Passes
UNIVARIATE PROCEDURE
Schematic Plots



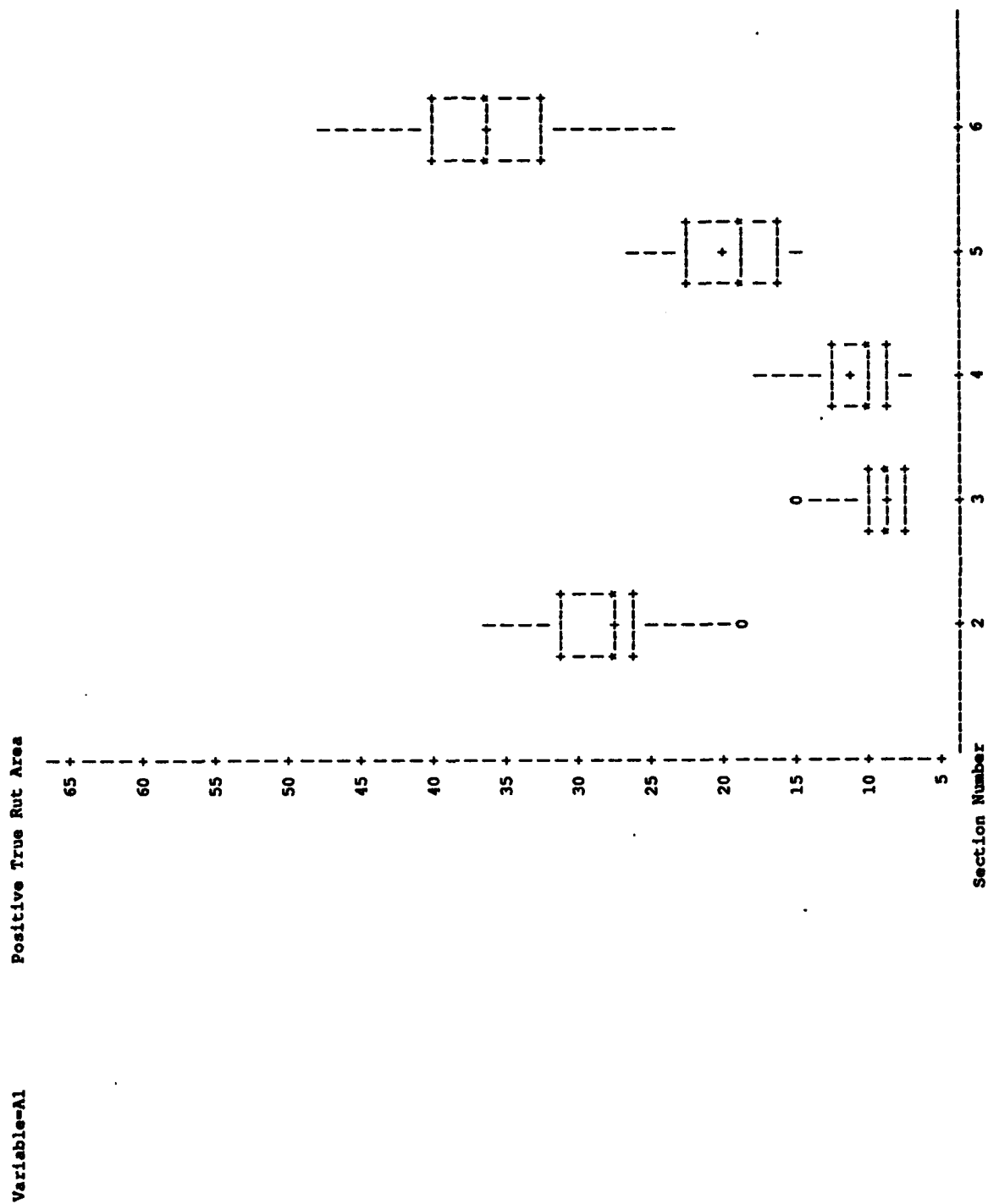
Damage at 4784 Passes
UNIVARIATE PROCEDURE
Schematic Plots



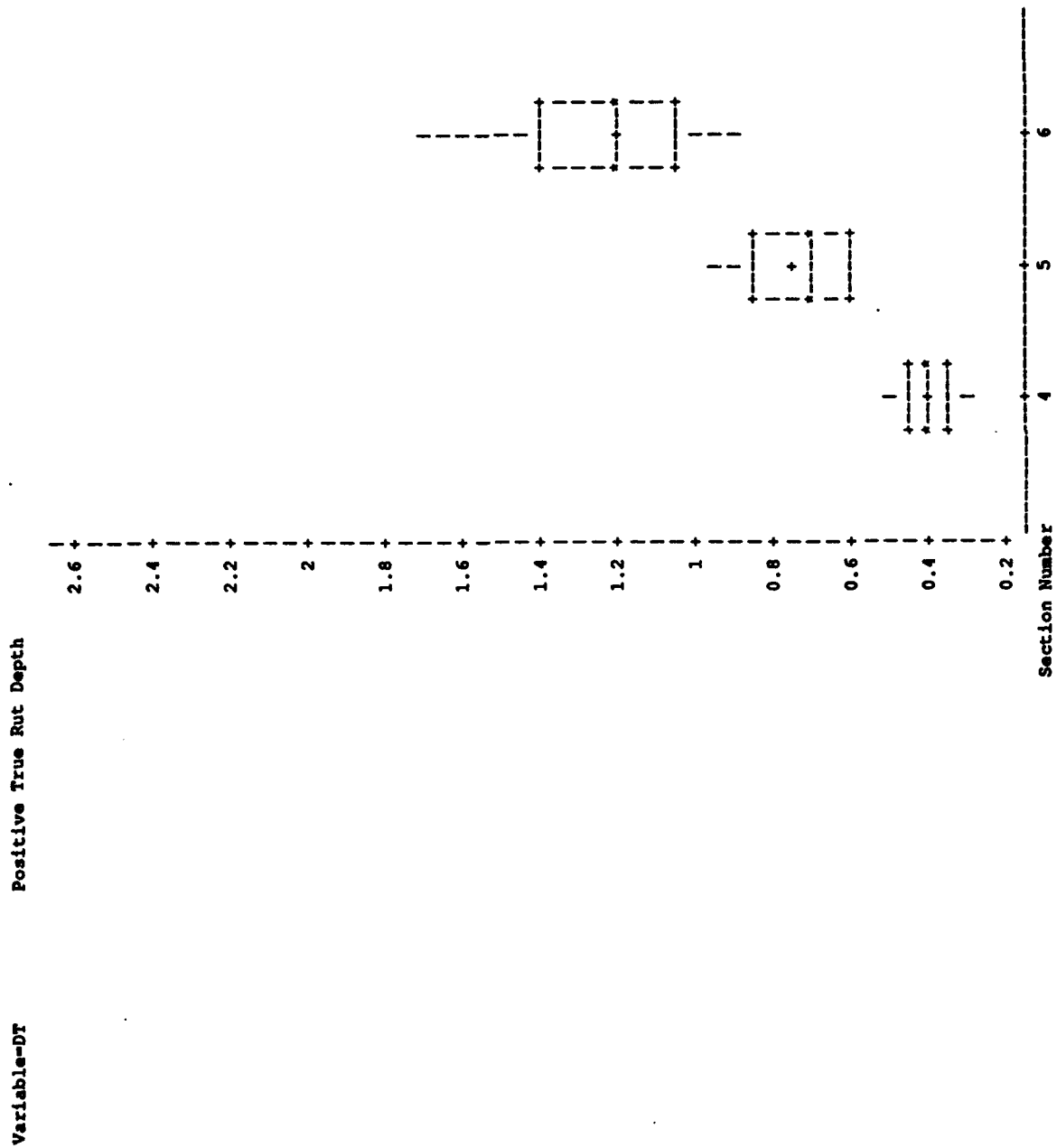
Damage at 4784 Passes
UNIVARIATE PROCEDURE
Schematic Plots



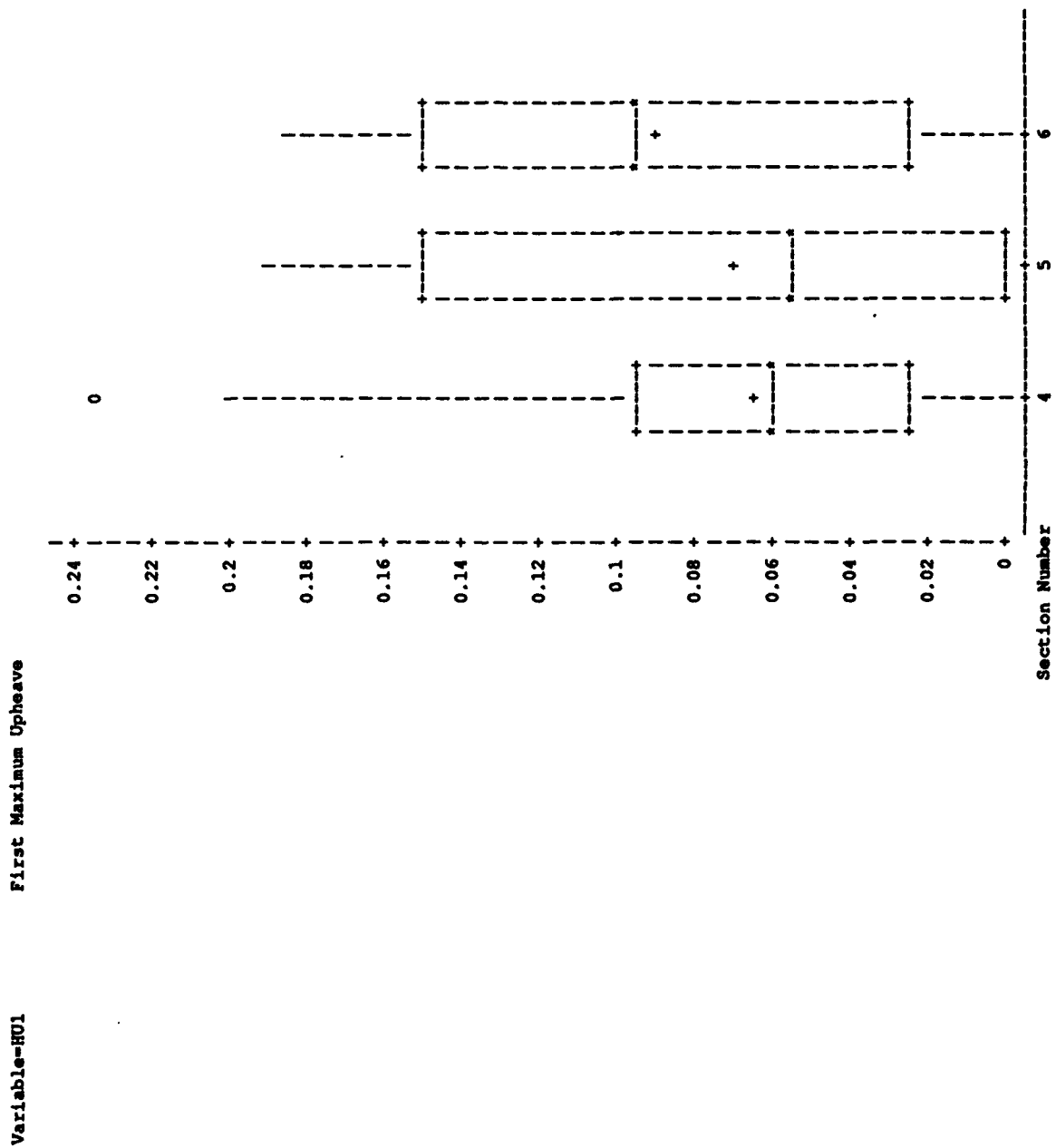
Damage at 4784 Passes
UNIVARIATE PROCEDURE
Schematic Plots



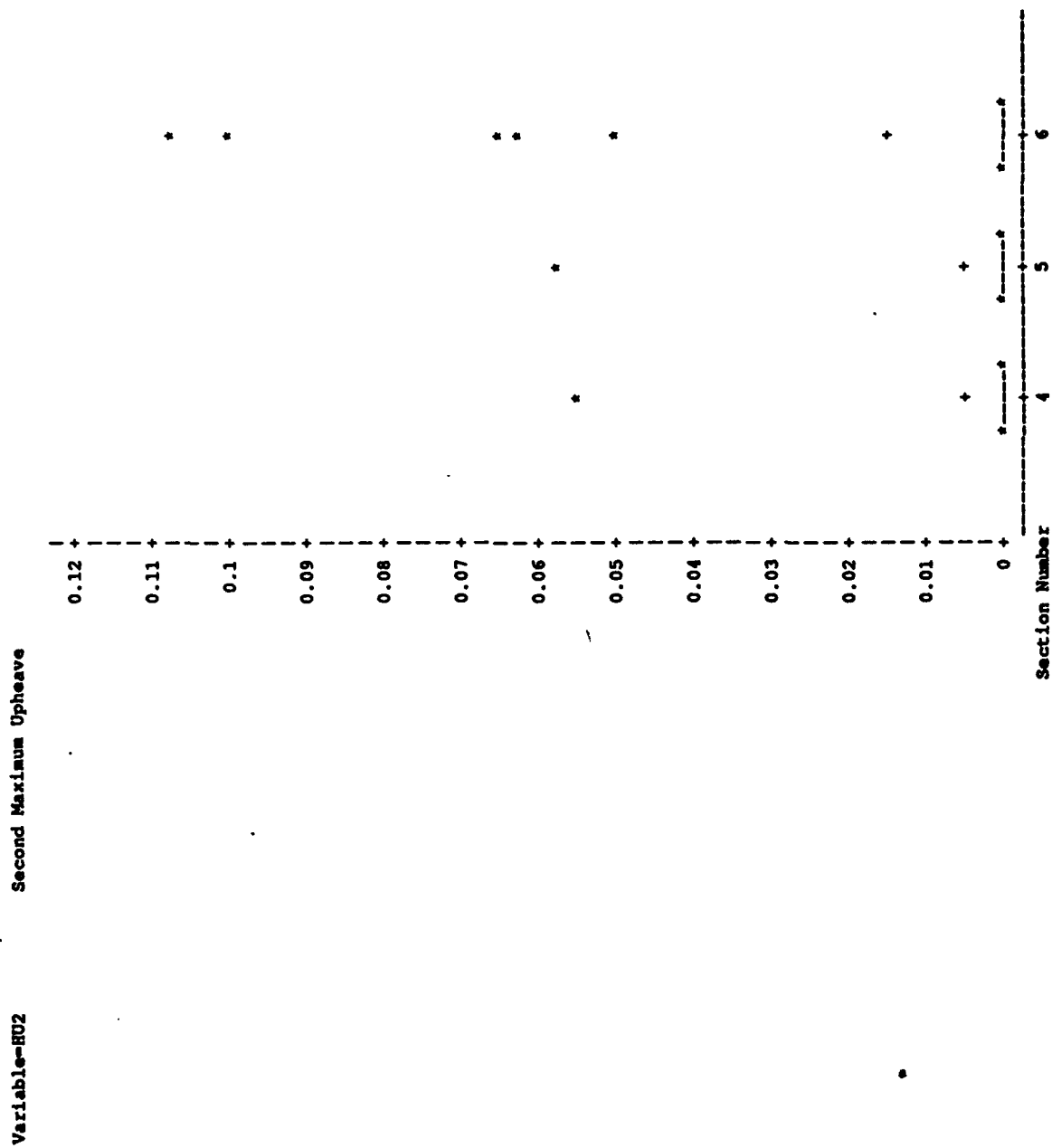
Damage at 9715 Passes
UNIVARIATE PROCEDURE
Schematic Plots



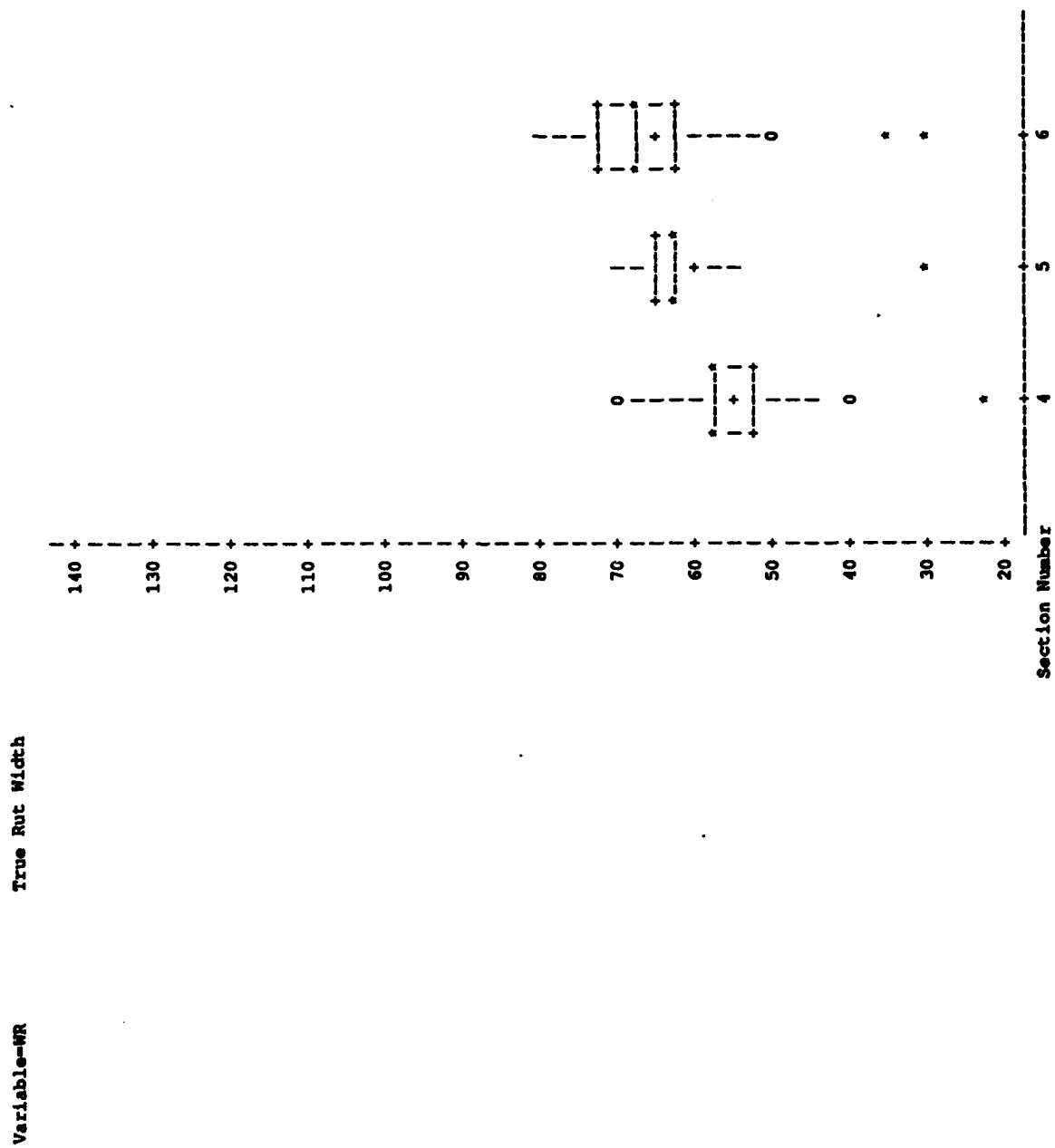
Damage at 9715 Passes
UNIVARIATE PROCEDURE
Schematic Plots



Damage at 9715 Passes
UNIVARIATE PROCEDURE
Schematic Plots

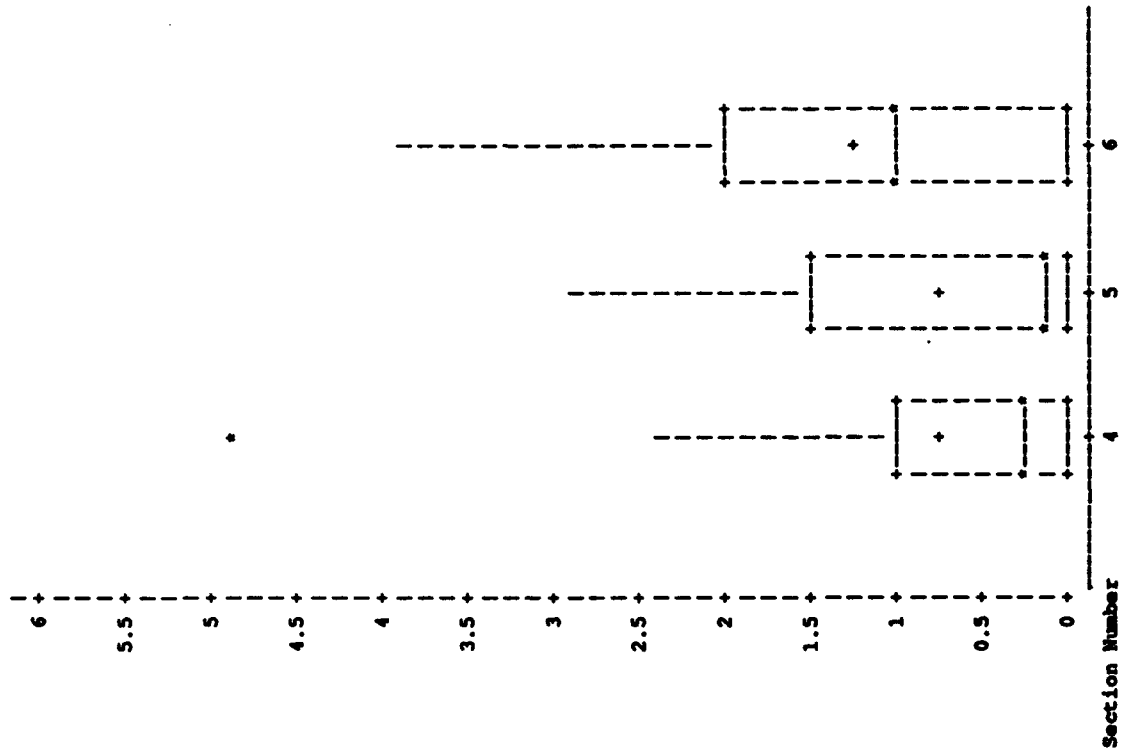


Damage at 9715 Passes
UNIVARIATE PROCEDURE
Schematic Plots

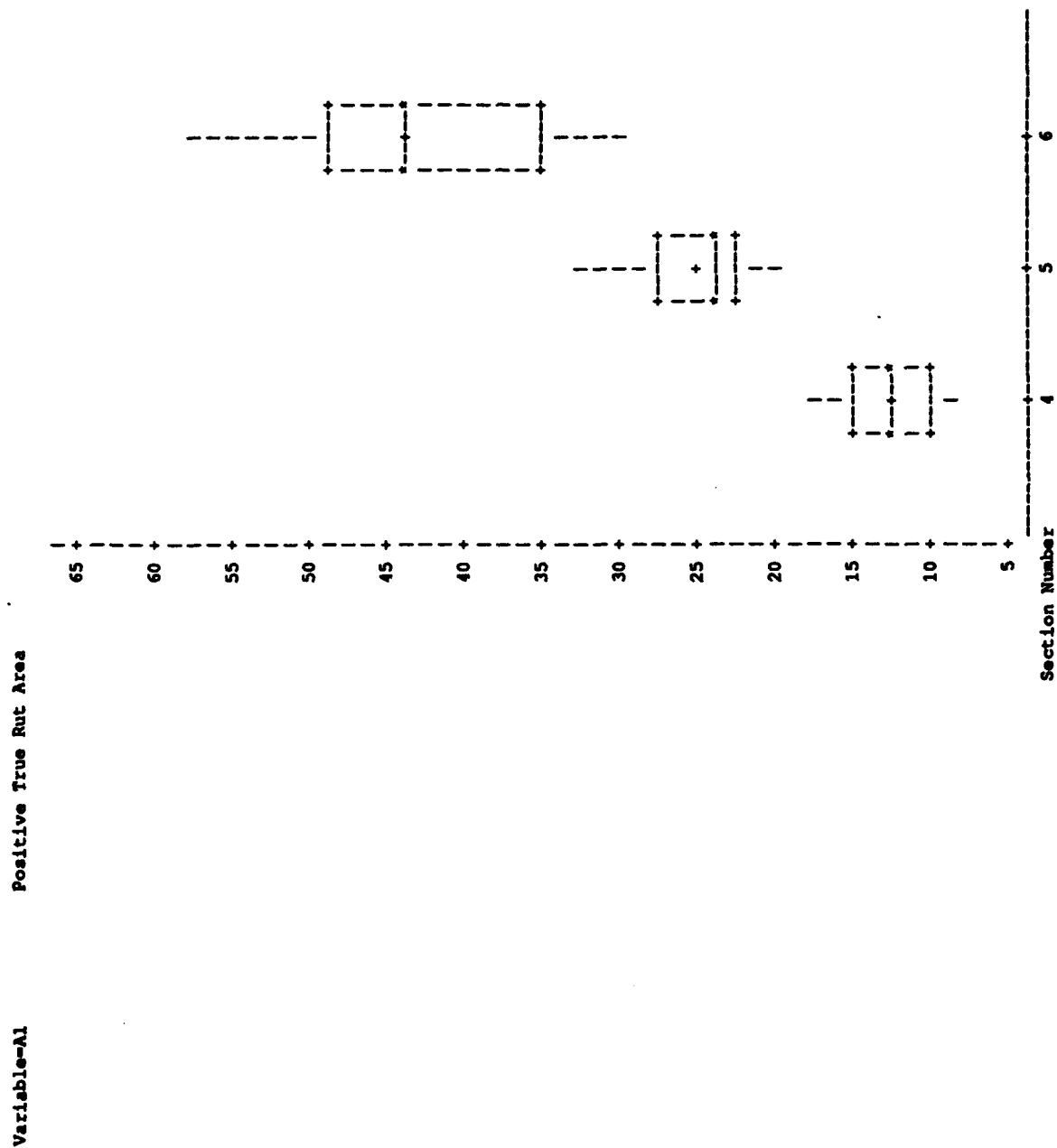


Damage at 9715 Passes
UNIVARIATE PROCEDURE
Schematic Plots

Variable-A2 Upheave Area



Damage at 9715 Passes
UNIVARIATE PROCEDURE
Schematic Plots



APPENDIX G

RESULTS FROM PEARSON PAIRWISE CORRELATION ANALYSIS

Pairwise Correlations of All Possible Pairs of Non-Zero Variables

1

CORRELATION ANALYSIS

60 Damage Measures
and Experimental
Variables

MODE	MEAN	ST_DEV	PASSES	DT	HU1	HU2	WR	A2	A1	BSFMDISM	PVFMIDISM	BULDDEMS	ASPHCONT
THAXDENS	ASPHVOLM	VOIDSTOT	VOIDSFIL	SIX_85	SIX_95	SIXAVE	INT_75	INT_85	INT_95	INT105	INT115	INTAVE	MID_85
MID_95	MID105	MID115	MID125	MIDAVE	SUR_85	SUR_95	SUR105	SUR115	SUR125	SUR135	SUR145	SURAVE	AMB_75
AMB_85	AMB_95	AMB105	AMBAVE	FT_75	FT_85	FT_95	FT_105	FT_AVE	VARIANCE	LM_PASS	O_SKEW	THICKNES	MIX_1MO
DES_1MO	TRUTHICK	PCTSMALL	PCHEDIUM										

Pairwise Correlations of All Possible Pairs of Non-Zero Variables

CORRELATION ANALYSIS

Simple Statistics

Variable	N	Mean	Std Dev	Sum	Minimum	Maximum
MODE	1030	31.503883	3.455040	32449	23.000000	41.000000
MEAN	1030	32.207506	2.899476	33174	2.404511	36.864739
ST DEV	1030	10.665465	0.923589	10985	8.272568	18.711740
PASSSES	1030	3965.832039	3211.415340	4084807	70.000000	18350
DT	1030	0.665259	0.500460	685.216940	0.030960	2.749320
HU1	1030	0.115753	0.110889	119.225550	0	0.686280
HU2	1030	0.053019	0.088965	54.609640	0	0.561850
WR	1030	45.079612	16.351326	46432	2.000000	93.000000
A2	1009	1.883631	2.506212	1900.583830	0	14.116650
A1	1030	15.544185	11.611349	16011	-0.951660	57.591700
BSFWDISM	1030	2192.791301	1719.179116	2258575	299.325000	4572.966667
PVFWDISM	1030	2682.786097	1779.585647	2763270	654.330000	4915.269444
BULKDENS	1030	149.876403	2.595003	154373	144.840278	154.607681
ASPHCONT	1030	5.728164	0.653381	5900.008545	4.621875	6.758889
THAXDENS	1030	160.290214	1.742446	165099	157.100000	163.200000
ASPHVOLM	1030	13.383743	1.67917	13785	10.869097	15.542130
VOIDSTOT	1030	6.473661	2.406886	6667.870804	2.472971	10.425694
VOIDSFIL	1030	67.962467	10.577895	70001	52.472917	86.132246
SIX_85	1030	418.558252	625.719874	431115	0	2211.000000
SIX_95	1030	3529.615534	2706.727183	3635504	70.000000	8099.000000
SIXAVE	1030	94.036285	0.552616	96857	91.964286	95.000000
INT_75	1030	1.249515	3.113480	1287.000000	0	9.000000
INT_85	1030	513.042718	553.909915	528434	0	1963.000000
INT_95	1030	1773.362136	1388.034254	1826563	42.000000	4515.000000
INT105	1030	1295.048544	1025.105136	133900	21.000000	3050.000000
INT115	1030	365.470874	283.595608	376435	7.000000	773.000000
INTAVE	1030	99.160071	0.997499	102135	97.318182	100.284091
MID_85	1030	390.134951	427.937309	401839	0	1443.000000
MID_95	1030	1064.111650	782.640859	1096035	24.000000	2554.000000
MID105	1030	1041.220388	820.360688	1072457	20.000000	2781.000000
MID115	1030	1122.633981	1011.918816	1156313	19.000000	2969.000000
MID125	1030	330.072816	223.751462	339975	7.000000	563.000000
MIDAVE	1030	105.165536	1.009809	108321	103.239181	106.840909
SUR_85	1030	173.643689	128.219747	178853	0	351.000000
SUR_95	1030	529.910680	535.237097	545808	4.000000	1820.000000
SUR105	1030	734.975728	569.593150	757025	18.000000	1869.000000
SUR115	1030	927.411650	688.147687	955234	22.000000	2291.000000
SUR125	1030	1113.528155	942.963819	1146934	10.000000	2955.000000
SUR135	1030	452.618447	370.069217	466197	16.000000	946.000000
SUR145	1030	11.917476	12.492485	12275	0	25.000000
SURAVE	1030	114.978416	1.530781	118428	112.234886	117.693182
AMB_75	1030	185.253398	161.198659	190811	0	535.000000
AMB_85	1030	2468.574757	1883.365166	2542632	44.000000	6455.000000
AMB_95	1030	1285.677670	1179.159153	1324248	26.000000	3308.000000
AMB105	1030	8.667961	5.376807	8928.000000	0	12.000000
AMB115	1030	87.301836	0.997928	89921	85.580357	88.802921
AMB125	1030	0.722330	0.448067	744.000000	0	1.000000
FT_75	1030	1140.479612	742.646623	1174694	42.000000	3094.000000
FT_85	1030	2746.577670	2489.686159	2828975	28.000000	7094.000000
FT_95	1030	60.394175	58.753128	62206	0	121.000000
FT105	1030	90.350948	2.762431	93267	85.625000	93.740216

Pairwise Correlations of All Possible Pairs of Non-Zero Variables

3

CORRELATION ANALYSIS

Simple Statistics

Variable	N	Mean	Std Dev	Sum	Minimum	Maximum
VARIANCE	1030	114.604323	23.715738	118042	68.435377	350.129233
LN PASS	1030	7.794134	1.158166	8027.957914	4.248495	9.244742
Q_SKEW	1030	0.262991	0.240365	270.880354	0.00004631	2.876263
THICKNES	1030	5.594175	0.804727	5762.000000	4.000000	6.000000
MIX_IND	1030	0.494175	0.500209	509.000000	0	1.000000
DES_IND	1030	0.517476	0.499937	533.000000	0	1.000000
TRUTHICK	1030	5.360650	0.901792	5521.470000	2.970000	6.670000
PCTSMALL	1030	9.942395	1.207181	10241	8.200000	12.566667
PCMEDIUM	1030	41.028366	2.990429	42259	37.900000	48.800000

Pairwise Correlations of All Possible Pairs of Non-Zero Variables

CORRELATION ANALYSIS

Pearson Correlation Coefficients / Prob > |R| under Ho: Rho=0 / Number of Observations

	MODE	MEAN	ST_DEV	PASSES	DT	HU1	HU2	WR	A2	A1	BSFWDISM	PVTWDISM
MODE	1.00000 0.0 1030	0.21311 0.0001 1030	0.17598 0.0001 1030	-0.27296 0.0001 1030	0.16868 0.0001 1030	-0.18372 0.0001 1030	-0.16975 0.0001 1030	0.02203 0.4800 1030	-0.17790 0.0001 1009	0.27795 0.0001 1030	-0.48273 0.0001 1030	-0.47657 0.0001 1030
MEAN	0.21311 0.0001 1030	1.00000 0.0 1030	-0.41425 0.0001 1030	-0.09678 0.0019 1030	0.01354 0.6642 1030	-0.31322 0.0001 1030	-0.31399 0.0001 1030	0.08724 0.0051 1030	-0.30336 0.0001 1009	0.17831 0.0001 1030	-0.35910 0.0001 1030	-0.36506 0.0001 1030
ST_DEV	0.17598 0.0001 1030	-0.41425 0.0001 1030	1.00000 0.0 1030	-0.01169 0.7078 1030	-0.07683 0.0136 1030	-0.05302 0.0890 1030	-0.06066 0.0516 1030	0.03475 0.2652 1030	-0.05071 0.1075 1009	-0.00198 0.9495 1030	-0.03800 0.2230 1030	-0.04131 0.1852 1030
PASSES	-0.27296 0.0001 1030	-0.09678 0.0019 1030	-0.01169 0.7078 1030	1.00000 0.0 1030	0.27804 0.0001 1030	0.09728 0.0018 1030	0.02444 0.4333 1030	0.41901 0.0001 1030	0.04060 0.1976 1009	0.40984 0.0001 1030	0.08278 0.0079 1030	0.07438 0.0170 1030
DT	0.16868 0.0001 1030	0.01354 0.6642 1030	-0.07683 0.0136 1030	0.27804 0.0001 1030	1.00000 0.0 1030	0.35883 0.0001 1030	0.31126 0.0001 1030	0.19473 0.0001 1030	0.27138 0.0001 1009	0.77592 0.0001 1030	-0.50010 0.0001 1030	-0.50261 0.0001 1030
HU1	-0.18372 0.0001 1030	-0.31322 0.0001 1030	-0.05302 0.0890 1030	0.35883 0.0001 1030	1.00000 0.0 1030	0.83311 0.0001 1030	-0.15926 0.0001 1030	0.90350 0.0 1009	-0.04413 0.1570 1030	0.18818 0.0001 1030	0.19557 0.0001 1030	0.19557 0.0001 1030
HU2	-0.16975 0.0001 1030	-0.31399 0.0001 1030	-0.06066 0.0516 1030	0.4333 0.0001 1030	0.31126 0.0001 1030	0.83311 0.0001 1030	1.00000 0.0 1030	-0.16907 0.0001 1030	0.88794 0.0 1009	-0.10816 0.0005 1030	0.21197 0.0001 1030	0.23102 0.0001 1030
WR	0.02203 0.4800 1030	0.08724 0.0001 1030	0.03475 0.2652 1030	0.41901 0.0001 1030	0.19473 0.0001 1030	-0.15926 0.0001 1030	-0.16907 0.0001 1030	1.00000 0.0 1030	-0.17821 0.0001 1009	0.44509 0.0001 1030	-0.30782 0.0001 1030	-0.32780 0.0001 1030
A2	-0.17790 0.0001 1009	-0.30336 0.0001 1009	-0.05071 0.1075 1009	0.04060 0.1976 1009	0.27138 0.0001 1009	0.90350 0.0 1009	0.88794 0.0 1009	-0.17821 0.0001 1009	1.00000 0.0 1009	-0.09746 0.0019 1009	0.21164 0.0001 1009	0.22082 0.0001 1009
A1	0.27795 0.0001 1030	0.17831 0.0001 1030	-0.00198 0.9495 1030	0.40984 0.0001 1030	0.77592 0.0001 1030	-0.04413 0.1570 1030	-0.10816 0.0005 1030	0.44509 0.0001 1030	-0.09746 0.0019 1009	1.00000 0.0 1030	-0.67977 0.0001 1030	-0.68878 0.0001 1030
BSFWDISM	-0.48273 0.0001 1030	-0.35910 0.0001 1030	-0.03800 0.2230 1030	0.08278 0.0079 1030	-0.50010 0.0001 1030	0.19557 0.0001 1030	0.18818 0.0001 1030	-0.30782 0.0001 1030	0.21164 0.0001 1009	1.00000 0.0 1030	0.99228 0.0 1030	0.99228 0.0 1030
PVTWDISM	-0.47657 0.0001 1030	-0.36506 0.0001 1030	-0.04131 0.1852 1030	0.07438 0.0170 1030	-0.50261 0.0001 1030	0.50261 0.0001 1030	-0.04131 0.1852 1030	-0.50261 0.0001 1030	-0.50261 0.0001 1030	-0.67977 0.0001 1030	0.99228 0.0 1030	0.99228 0.0 1030
BULKDENS	-0.17711 0.0001 1030	-0.16486 0.0001 1030	-0.12288 0.0001 1030	-0.24728 0.0001 1030	0.08822 0.0046 1030	0.39851 0.0001 1030	0.47434 0.0001 1030	-0.26597 0.0001 1030	0.42220 0.0001 1009	-0.32205 0.0001 1030	0.16871 0.0001 1030	0.21177 0.0001 1030

Pairwise Correlations of All Possible Pairs of Non-Zero Variables

CORRELATION ANALYSIS

Pearson Correlation Coefficients / Prob > |R| under Ho: Rho=0 / Number of Observations

	MODE	MEAN	ST_DEV	PASSES	DT	HU1	HU2	WR	A2	A1	BSFMDISM	PVFMDISM
ASPHCONT	-0.13484 0.0001 1030	-0.14612 0.0001 1030	-0.09608 0.0020 1030	-0.35627 0.0001 1030	0.23628 0.0001 1030	0.47372 0.0001 1030	0.46662 0.0001 1030	-0.32241 0.0001 1030	0.42677 0.0001 1009	-0.17837 0.0001 1030	0.12503 0.0001 1030	0.13920 0.0001 1030
THAXDENS	0.04305 0.11674 1030	0.11830 0.0001 1030	0.06874 0.0274 1030	0.33783 0.0001 1030	-0.27793 0.0001 1030	-0.44027 0.0001 1030	-0.43456 0.0001 1030	0.21144 0.0001 1030	-0.39202 0.0001 1009	0.07459 0.0166 1030	0.06805 0.0290 1030	0.04907 0.1155 1030
ASPHVOLM	-0.14474 0.0001 1030	-0.15519 0.0001 1030	-0.10276 0.0010 1030	-0.35730 0.0001 1030	0.22960 0.0001 1030	0.48736 0.0001 1030	0.49126 0.0001 1030	-0.32759 0.0001 1030	0.44886 0.0001 1009	-0.20234 0.0001 1030	0.13346 0.0001 1030	0.15185 0.0001 1030
VOIDSTOT	0.13653 0.0001 1030	0.16192 0.0001 1030	0.11135 0.0003 1030	0.30874 0.0001 1030	-0.17642 0.0001 1030	-0.45509 0.0001 1030	-0.50343 0.0001 1030	0.26779 0.0001 1030	-0.45139 0.0001 1009	0.24829 0.0001 1030	-0.08637 0.0055 1030	-0.12297 0.0001 1030
VOIDSFIL	-0.14095 0.0001 1030	-0.16873 0.0001 1030	-0.10543 0.0007 1030	-0.32968 0.0001 1030	0.20458 0.0001 1030	0.48938 0.0001 1030	0.52748 0.0001 1030	-0.28769 0.0001 1030	0.48066 0.0001 1009	-0.23311 0.0001 1030	0.09658 0.0019 1030	0.12738 0.0001 1030
SIX_85	-0.14164 0.0001 1030	0.00857 0.7836 1030	0.03456 0.2678 1030	0.82161 0.0001 1030	0.05229 0.0935 1030	-0.13849 0.0001 1030	-0.16685 0.0001 1030	0.36230 0.0001 1030	-0.14380 0.0001 1009	0.28069 0.0001 1030	0.03499 0.2619 1030	0.02771 0.3744 1030
SIX_95	-0.28956 0.0001 1030	-0.11610 0.0002 1030	-0.02169 0.4868 1030	0.99140 0.0 1030	0.31579 0.0001 1030	0.14627 0.0001 1030	0.06684 0.0320 1030	0.41135 0.0001 1030	0.08078 0.0103 1009	0.41915 0.0001 1030	0.08963 0.0040 1030	0.08138 0.0090 1030
SIXAVE	-0.08379 0.0026 1030	-0.12004 0.0001 1030	-0.07530 0.0156 1030	-0.21490 0.0001 1030	0.25013 0.0001 1030	0.34811 0.0001 1030	0.31612 0.0001 1030	-0.12586 0.0001 1030	0.30096 0.0001 1009	0.01193 0.7022 1030	0.02621 0.4007 1030	0.02953 0.3437 1030
INT_75	-0.09111 0.0034 1030	0.03386 0.2776 1030	0.06261 0.0445 1030	0.76415 0.0001 1030	0.01287 0.6798 1030	-0.18567 0.0001 1030	-0.21036 0.0001 1030	0.35350 0.0001 1030	-0.18609 0.0001 1009	0.27797 0.0001 1030	0.00313 0.9201 1030	-0.00574 0.8540 1030
INT_85	-0.21481 0.0001 1030	-0.03644 0.2426 1030	0.00175 0.9552 1030	0.94482 0.0 1030	0.17535 0.0001 1030	-0.02501 0.4226 1030	-0.07565 0.0152 1030	0.40546 0.0001 1030	-0.05443 0.0840 1009	0.36235 0.0001 1030	0.05439 0.0810 1030	0.04641 0.1366 1030
INT_95	-0.26950 0.0001 1030	-0.09274 0.0029 1030	-0.01480 0.6352 1030	0.99904 0.0 1030	0.28516 0.0001 1030	0.09744 0.0017 1030	0.02514 0.4203 1030	0.41953 0.0001 1030	0.04215 0.1810 1009	0.41813 0.0001 1030	0.07595 0.0148 1030	0.06748 0.0303 1030
INT105	-0.28333 0.0001 1030	-0.11299 0.0003 1030	-0.01502 0.6301 1030	0.99009 0.0 1030	0.29037 0.0001 1030	0.12655 0.0001 1030	0.04904 0.1158 1030	0.41218 0.0001 1030	0.06167 0.0502 1009	0.40818 0.0001 1030	0.09474 0.0023 1030	0.08623 0.0056 1030
INT115	-0.31236 0.0001 1030	-0.15607 0.0001 1030	-0.00817 0.7933 1030	0.95268 0.0 1030	0.34146 0.0001 1030	0.20702 0.0001 1030	0.11958 0.0001 1030	0.38630 0.0001 1030	0.13220 0.0001 1009	0.38707 0.0001 1030	0.11223 0.0003 1030	0.10530 0.0007 1030

Pairwise Correlations of All Possible Pairs of Non-Zero Variables

CORRELATION ANALYSIS

Pearson Correlation Coefficients / Prob > |R| under Ho: Rho=0 / Number of Observations

	MODE	MEAN	ST_DEV	PASSES	DT	HUI	HU2	WR	A2	A1	BSFWDISH	PVFWDISH
INTAVE	0.02982 0.3390 1030	-0.08928 0.0041 1030	0.09548 0.0022 1030	-0.41406 0.0001 1030	-0.11010 0.0004 1030	0.08044 0.0098 1030	0.08313 0.0076 1030	-0.15817 0.0001 1030	0.04997 0.1126 1009	-0.25172 0.0001 1030	0.06934 0.0261 1030	0.07358 0.0182 1030
MID_85	-0.22044 0.0001 1030	-0.04011 0.1984 1030	0.00486 0.8761 1030	0.96283 0.0 1030	0.18308 0.0001 1030	-0.01856 0.5519 1030	-0.07379 0.0179 1030	0.41848 0.0001 1030	-0.05192 0.0993 1009	0.37823 0.0001 1030	0.05241 0.0928 1030	0.04359 0.1621 1030
MID_95	-0.28975 0.0001 1030	-0.11476 0.0002 1030	-0.02785 0.3719 1030	0.99289 0.0 1030	0.32210 0.0001 1030	0.14639 0.0001 1030	0.07251 0.0199 1030	0.40694 0.0691 1030	0.08375 0.0078 1009	0.41220 0.0001 1030	0.09307 0.0028 1030	0.08578 0.0039 1030
MID105	-0.25603 0.0001 1030	-0.07624 0.0144 1030	-0.01141 0.7146 1030	0.98939 0.0 1030	0.25871 0.0001 1030	0.06460 0.0362 1030	-0.00455 0.8840 1030	0.41808 0.0001 1030	0.01778 0.5727 1009	0.41383 0.0001 1030	0.06520 0.0364 1030	0.05659 0.0694 1030
MID115	-0.26258 0.0001 1030	-0.09607 0.0020 1030	-0.00010 0.9976 1030	0.98927 0.0 1030	0.25119 0.0001 1030	0.07912 0.0111 1030	0.00643 0.8366 1030	0.42083 0.0001 1030	0.01935 0.5392 1009	0.39843 0.0001 1030	0.08613 0.0057 1030	0.07691 0.0135 1030
MID125	-0.33756 0.0001 1030	-0.18838 0.0001 1030	-0.03541 0.2562 1030	0.87474 0.0 1030	0.40500 0.0001 1030	0.31089 0.0001 1030	0.21704 0.0001 1030	0.32974 0.0001 1030	0.22858 0.0001 1009	0.36910 0.0001 1030	0.12776 0.0001 1030	0.12320 0.0001 1030
MIDAVE	0.05739 0.0656 1030	-0.09390 0.0026 1030	0.10383 0.0008 1030	-0.39341 0.0001 1030	-0.16344 0.0001 1030	0.04229 0.1750 1030	0.04345 0.1635 1030	-0.17856 0.0001 1030	0.01784 0.5713 1009	-0.28045 0.0001 1030	0.08281 0.0078 1030	0.08625 0.0056 1030
SUR_85	-0.30144 0.0001 1030	-0.11550 0.0002 1030	-0.07286 0.0194 1030	0.92817 0.0 1030	0.39322 0.0001 1030	0.22507 0.0001 1030	0.14156 0.0001 1030	0.37375 0.0001 1030	0.16182 0.0001 1009	0.44603 0.0001 1030	0.08797 0.0292 1030	0.06119 0.0496 1030
SUR_95	-0.25375 0.0001 1030	-0.08258 0.0080 1030	0.00581 0.8523 1030	0.98393 0.0 1030	0.23227 0.0001 1030	0.05593 0.0728 1030	-0.00623 0.8417 1030	0.40778 0.0001 1030	0.00556 0.8601 1009	0.38510 0.0001 1030	0.08879 0.0043 1030	0.08153 0.0089 1030
SUR105	-0.26782 0.0001 1030	-0.09179 0.0032 1030	-0.01762 0.5722 1030	0.99735 0.0 1030	0.28798 0.0001 1030	0.09691 0.0018 1030	0.02600 0.4046 1030	0.41843 0.0001 1030	0.04320 0.1703 1009	0.42101 0.0001 1030	0.07430 0.0171 1030	0.06600 0.0342 1030
SUR115	-0.27212 0.0001 1030	-0.09244 0.0030 1030	-0.02152 0.4903 1030	0.99723 0.0 1030	0.29573 0.0001 1030	0.09957 0.0014 1030	0.02745 0.3789 1030	0.41937 0.0001 1030	0.04657 0.1394 1009	0.42605 0.0001 1030	0.07137 0.0220 1030	0.06295 0.0434 1030
SUR125	-0.25248 0.0001 1030	-0.07447 0.0168 1030	-0.00334 0.9146 1030	0.98932 0.0 1030	0.22681 0.0001 1030	0.04357 0.1823 1030	-0.02526 0.4181 1030	0.42806 0.0001 1030	-0.00685 0.8281 1009	0.40526 0.0001 1030	0.07156 0.0216 1030	0.06176 0.0475 1030
SUR135	-0.30945 0.0001 1030	-0.16667 0.0001 1030	-0.00896 0.7740 1030	0.93452 0.0 1030	0.34573 0.0001 1030	0.22660 0.0001 1030	0.14023 0.0001 1030	0.36752 0.0001 1030	0.14731 0.0001 1009	0.37127 0.0001 1030	0.12569 0.0001 1030	0.11951 0.0001 1030

Pairwise Correlations of All Possible Pairs of Non-Zero Variables

CORRELATION ANALYSIS

Pearson Correlation Coefficients / Prob > |R| under Ho: Rho=0 / Number of Observations

	MODE	MEAN	ST_DEV	PASSES	DT	HU1	HU2	WR	A2	A1	BSFWDISM	PVTWDISM
SUR145	-0.30306 0.0001 1030	-0.18344 0.0001 1030	0.00335 0.9145 1030	0.83235 0.0001 1030	0.35507 0.0001 1030	0.27344 0.0001 1030	0.18149 0.0001 1030	0.31565 0.0001 1030	0.18801 0.0001 1009	0.32129 0.0001 1030	0.13110 0.0001 1030	0.12655 0.0001 1030
SURAVE	0.19431 0.0001 1030	0.02564 0.4111 1030	0.16578 0.0001 1030	-0.51846 0.0001 1030	-0.37257 0.0001 1030	-0.19015 0.0001 1030	-0.15306 0.0001 1030	-0.18859 0.0001 1030	-0.17841 0.0001 1009	-0.36104 0.0001 1030	0.02858 0.3596 1030	0.03000 0.3362 1030
AMB_75	-0.23494 0.0001 1030	-0.05962 0.0558 1030	-0.03986 0.2012 1030	0.96367 0.0 1030	0.27278 0.0001 1030	0.06730 0.0308 1030	0.00201 0.9486 1030	0.40510 0.0001 1030	0.02827 0.3697 1009	0.42258 0.0001 1030	0.04852 0.1196 1030	0.04033 0.1960 1030
AMB_85	-0.26613 0.0001 1030	-0.08542 0.0061 1030	-0.01571 0.6146 1030	0.99619 0.0 1030	0.27351 0.0001 1030	0.08283 0.0078 1030	0.01377 0.6588 1030	0.41878 0.0001 1030	0.03134 0.3199 1009	0.41209 0.0001 1030	0.07522 0.0158 1030	0.06700 0.0315 1030
AMB_95	-0.27859 0.0001 1030	-0.11681 0.0002 1030	-0.00020 0.9949 1030	0.98585 0.0 1030	0.27651 0.0001 1030	0.11941 0.0001 1030	0.04159 0.1823 1030	0.41122 0.0001 1030	0.05372 0.0881 1009	0.39331 0.0001 1030	0.09735 0.0018 1030	0.08881 0.0043 1030
AMB105	-0.28995 0.0001 1030	-0.11997 0.0001 1030	-0.15871 0.0001 1030	0.65825 0.0001 1030	0.43413 0.0001 1030	0.29808 0.0001 1030	0.22574 0.0001 1030	0.22215 0.0001 1030	0.26060 0.0001 1009	0.39669 0.0001 1030	0.04094 0.1892 1030	0.03742 0.2302 1030
AMBAVE	-0.23704 0.0001 1030	-0.20795 0.0001 1030	-0.05033 0.1064 1030	0.65590 0.0001 1030	0.30680 0.0001 1030	0.27382 0.0001 1030	0.19431 0.0001 1030	0.17376 0.0001 1030	0.20759 0.0001 1009	0.24678 0.0001 1030	0.12595 0.0001 1030	0.12211 0.0001 1030
FT_75	-0.28995 0.0001 1030	-0.11997 0.0001 1030	-0.15871 0.0001 1030	0.65825 0.0001 1030	0.43413 0.0001 1030	0.29808 0.0001 1030	0.22574 0.0001 1030	0.22215 0.0001 1030	0.26060 0.0001 1009	0.39669 0.0001 1030	0.04094 0.1892 1030	0.03742 0.2302 1030
FT_85	-0.21620 0.0001 1030	-0.03696 0.2359 1030	-0.01967 0.5283 1030	0.90848 0.0 1030	0.18264 0.0001 1030	-0.02466 0.4293 1030	-0.07067 0.0233 1030	0.38799 0.0001 1030	-0.04324 0.1699 1009	0.36500 0.0001 1030	0.04988 0.1096 1030	0.04266 0.1713 1030
FT_95	-0.27822 0.0001 1030	-0.10862 0.0005 1030	-0.00902 0.7726 1030	0.99322 0.0 1030	0.29340 0.0001 1030	0.12460 0.0001 1030	0.04706 0.1312 1030	0.41495 0.0001 1030	0.05937 0.0585 1009	0.40959 0.0001 1030	0.08013 0.0047 1030	0.07959 0.0106 1030
FT_105	-0.32357 0.0001 1030	-0.18623 0.0001 1030	0.00061 0.9843 1030	0.84679 0.0001 1030	0.36051 0.0001 1030	0.29313 0.0001 1030	0.19949 0.0001 1030	0.31927 0.0001 1030	0.20754 0.0001 1009	0.32591 0.0001 1030	0.13679 0.0001 1030	0.13228 0.0001 1030
FT_AVE	-0.30870 0.0001 1030	-0.17558 0.0001 1030	-0.12399 0.0001 1030	0.76555 0.0001 1030	0.46004 0.0001 1030	0.34768 0.0001 1030	0.25977 0.0001 1030	0.25050 0.0001 1030	0.28217 0.0001 1009	0.39740 0.0001 1030	0.08601 0.0037 1030	0.09191 0.0085 1030
VARIANCE	0.17695 0.0001 1030	-0.43359 0.0001 1030	0.99132 0.0 1030	-0.01229 0.6937 1030	-0.02847 0.3614 1030	-0.04452 0.1533 1030	-0.05155 0.0982 1030	0.03260 0.2959 1030	-0.04404 0.1622 1009	0.03396 0.2762 1030	-0.05875 0.0594 1030	-0.06182 0.0473 1030

Pairwise Correlations of All Possible Pairs of Non-Zero Variables

CORRELATION ANALYSIS

Pearson Correlation Coefficients / Prob > |R| under Ho: Rho=0 / Number of Observations

	MODE	MEAN	ST_DEV	PASSES	DT	HU1	HU2	WR	A2	A1	ESTWDSH	PVTWDSH
LN_PASS	-0.33379 0.0001 1030	-0.14341 0.0001 1030	-0.10726 0.0006 1030	0.88732 0.0 1030	0.41960 0.0001 1030	0.25104 0.0001 1030	0.16998 0.0001 1030	0.36015 0.0001 1030	0.19437 0.0001 1009	0.44705 0.0001 1030	0.08702 0.0048 1030	0.08198 0.0085 1030
Q_SKEW	-0.24173 0.0001 1030	-0.58660 0.0001 1030	0.24008 0.0001 1030	-0.12342 0.0001 1030	-0.06552 0.0328 1030	0.05751 0.0650 1030	0.05406 0.0829 1030	0.00675 0.8286 1030	0.03870 0.2193 1009	-0.11082 0.0004 1030	0.04538 0.1456 1030	0.04802 0.1235 1030
THICKNES	-0.30178 0.0001 1030	-0.24139 0.0001 1030	0.03362 0.2810 1030	0.06083 0.0510 1030	-0.32614 0.0001 1030	0.13915 0.0001 1030	0.15885 0.0001 1030	-0.22472 0.0001 1030	0.15593 0.0001 1009	-0.57829 0.0001 1030	0.52271 0.0001 1030	0.56021 0.0001 1030
MIX_IND	0.06665 0.0325 1030	0.11501 0.0002 1030	0.09188 0.0032 1030	0.37650 0.0001 1030	-0.30754 0.0001 1030	-0.46448 0.0001 1030	-0.46856 0.0001 1030	0.26573 0.0001 1030	-0.42055 0.0001 1009	0.10213 0.0010 1030	0.00951 0.7605 1030	-0.00754 0.8090 1030
DES_IND	-0.47123 0.0001 1030	-0.36684 0.0001 1030	-0.03696 0.2359 1030	0.06750 0.0303 1030	-0.49201 0.0001 1030	0.19943 0.0001 1030	0.23116 0.0001 1030	-0.32519 0.0001 1030	0.22369 0.0001 1009	-0.68737 0.0001 1030	0.98677 0.0 1030	0.98963 0.0 1030
TRUTHICK	-0.29284 0.0001 1030	-0.23510 0.0001 1030	0.05178 0.0967 1030	0.10673 0.0006 1030	-0.36595 0.0001 1030	0.12575 0.0001 1030	0.16189 0.0001 1030	-0.22538 0.0001 1030	0.16905 0.0001 1009	-0.56608 0.0001 1030	0.52173 0.0001 1030	0.55337 0.0001 1030
PCTSMALL	0.01488 0.6334 1030	0.01924 0.5374 1030	0.08682 0.0053 1030	0.27379 0.0001 1030	-0.24396 0.0001 1030	-0.20191 0.0001 1030	-0.21936 0.0001 1030	0.00404 0.8970 1030	-0.17091 0.0001 1009	0.00379 0.9033 1030	0.13309 0.0001 1030	0.13858 0.0001 1030
PCMEDIUM	0.27535 0.0001 1030	0.09260 0.0029 1030	0.19552 0.0001 1030	0.16362 0.0001 1030	0.07688 0.0136 1030	-0.13897 0.0001 1030	-0.22319 0.0001 1030	0.23553 0.0001 1030	-0.15050 0.0001 1009	0.39478 0.0001 1030	-0.28526 0.0001 1030	-0.32490 0.0001 1030

Pairwise Correlations of All Possible Pairs of Non-Zero Variables

CORRELATION ANALYSIS

Pearson Correlation Coefficients / Prob > |R| under Ho: Rho=0 / Number of Observations

	BULKDENS	ASPHCONT	TMAXDENS	ASPHVOLM	VOIDSTOT	VOIDSFIL	SIX_85	SIX_95	SIXAVE	INT_75	INT_95	INT_95
MODE	-0.17711 0.0001 1030	-0.13484 0.0001 1030	0.04305 0.1674 1030	-0.14474 0.0001 1030	0.13853 0.0001 1030	-0.14095 0.0001 1030	-0.14164 0.0001 1030	-0.28956 0.0001 1030	-0.09379 0.0026 1030	-0.09111 0.0034 1030	-0.21481 0.0001 1030	-0.26950 0.0001 1030
MEAN	-0.16486 0.0001 1030	-0.14612 0.0001 1030	0.11830 0.0001 1030	-0.15519 0.0001 1030	0.16192 0.0001 1030	-0.16873 0.0001 1030	0.08857 0.7836 1030	-0.11610 0.0002 1030	-0.12004 0.0001 1030	0.03386 0.2776 1030	-0.03644 0.2426 1030	-0.09274 0.0029 1030
ST_DEV	-0.12288 0.0001 1030	-0.09608 0.0001 1030	0.06874 0.0274 1030	-0.10276 0.0010 1030	0.11135 0.0003 1030	-0.10543 0.0007 1030	0.03456 0.2678 1030	-0.02169 0.4868 1030	-0.01 0.0133 1030	0.06261 0.0445 1030	0.00175 0.9552 1030	-0.01480 0.6352 1030
PASSES	-0.24728 0.0001 1030	-0.35627 0.0001 1030	0.33783 0.0001 1030	-0.35730 0.0001 1030	0.30874 0.0001 1030	-0.32968 0.0001 1030	0.82161 0.0001 1030	0.99140 0.0 1030	-0.21490 0.0001 1030	0.76415 0.0001 1030	0.94482 0.0 1030	0.99904 0.0 1030
DT	0.08822 0.0046 1030	0.23628 0.0001 1030	-0.27793 0.0001 1030	0.22960 0.0001 1030	-0.17642 0.0001 1030	0.20458 0.0001 1030	0.05229 0.0935 1030	0.31579 0.0001 1030	0.25013 0.0001 1030	0.01287 0.6798 1030	0.17535 0.0001 1030	0.28516 0.0001 1030
HU1	0.39851 0.0001 1030	0.47372 0.0001 1030	-0.44027 0.0001 1030	0.48736 0.0001 1030	-0.45509 0.0001 1030	0.48938 0.0001 1030	-0.13849 0.0001 1030	0.14627 0.0001 1030	0.34811 0.0001 1030	-0.18567 0.0001 1030	-0.02501 0.4226 1030	0.09744 0.0017 1030
HU2	0.47434 0.0001 1030	0.46662 0.0001 1030	-0.43458 0.0001 1030	0.49126 0.0001 1030	-0.50343 0.0001 1030	0.52748 0.0001 1030	-0.16685 0.0001 1030	0.06684 0.0320 1030	0.31612 0.0001 1030	-0.21036 0.0001 1030	-0.07565 0.0152 1030	0.02514 0.4203 1030
WR	-0.26597 0.0001 1030	-0.32241 0.0001 1030	0.21144 0.0001 1030	-0.32759 0.0001 1030	0.26779 0.0001 1030	-0.28769 0.0001 1030	0.36230 0.0001 1030	0.41135 0.0001 1030	-0.12586 0.0001 1030	0.35350 0.0001 1030	0.40546 0.0001 1030	0.41953 0.0001 1030
A2	0.42220 0.0001 1009	0.42677 0.0001 1009	-0.39202 0.0001 1009	0.44886 0.0001 1009	-0.45139 0.0001 1009	0.48066 0.0001 1009	-0.14380 0.0001 1009	0.08078 0.0103 1009	0.30096 0.0001 1009	-0.18609 0.0001 1009	-0.05443 0.0840 1009	0.04215 0.1810 1009
A1	-0.32205 0.0001 1030	-0.17837 0.0001 1030	0.07459 0.0166 1030	-0.20234 0.0001 1030	0.24829 0.0001 1030	-0.23311 0.0001 1030	0.28069 0.0001 1030	0.41915 0.0001 1030	0.01193 0.7022 1030	0.27797 0.0001 1030	0.36235 0.0001 1030	0.41813 0.0001 1030
BSTWDISM	0.16871 0.0001 1030	0.12503 0.0001 1030	0.06805 0.0290 1030	0.13346 0.0001 1030	-0.08637 0.0055 1030	0.09658 0.0019 1030	0.03499 0.2619 1030	0.08963 0.0040 1030	0.02621 0.4007 1030	0.00313 0.9201 1030	0.05439 0.0810 1030	0.07595 0.0148 1030
PVTWDISM	0.21177 0.0001 1030	0.13920 0.0001 1030	0.04907 0.1155 1030	0.15185 0.0001 1030	-0.12297 0.0001 1030	0.12738 0.0001 1030	0.02771 0.3744 1030	0.08138 0.0090 1030	0.02953 0.3437 1030	-0.00574 0.8540 1030	0.04641 0.1366 1030	0.06748 0.0303 1030
BULKDENS	1.00000 0.0 1030	0.63181 0.0001 1030	-0.65090 0.0001 1030	0.70831 0.0001 1030	-0.94684 0.0 1030	0.90233 0.0 1030	-0.25383 0.0001 1030	-0.23373 0.0001 1030	0.16315 0.0001 1030	-0.28842 0.0001 1030	-0.25442 0.0001 1030	-0.24715 0.0001 1030

Pairwise Correlations of All Possible Pairs of Non-Zero Variables

CORRELATION ANALYSIS

Pearson Correlation Coefficients / Prob > |R| under Ho: Rho=0 / Number of Observations

	BULKDENS	ASPHCONT	TMXDENS	ASPHVOLM	VOIDSTOT	VOIDSFIL	SIX_85	SIX_95	SIXAVE	INT_75	INT_85	INT_95
ASPHCONT	0.63181 0.0001 1030	1.00000 0.0 1030	-0.89699 0.0 1030	0.99461 0.0 1030	-0.80409 0.0001 1030	0.88212 0.0 1030	-0.38472 0.0001 1030	-0.33230 0.0001 1030	0.25194 0.0001 1030	-0.39512 0.0001 1030	-0.38613 0.0001 1030	-0.35411 0.0001 1030
TMXDENS	-0.65090 0.0001 1030	-0.89699 0.0 1030	1.00000 0.0 1030	-0.90432 0.0 1030	0.86048 0.0001 1030	-0.90073 0.0 1030	0.36421 0.0001 1030	0.31524 0.0001 1030	-0.24298 0.0001 1030	0.37386 0.0001 1030	0.36567 0.0001 1030	0.33548 0.0001 1030
ASPHVOLM	0.70831 0.0001 1030	0.99461 0.0 1030	-0.90432 0.0 1030	1.00000 0.0 1030	-0.85858 0.0001 1030	0.92416 0.0 1030	-0.38454 0.0001 1030	-0.33356 0.0001 1030	0.25188 0.0001 1030	-0.39836 0.0001 1030	-0.38575 0.0001 1030	-0.35528 0.0001 1030
VOIDSTOT	-0.94684 0.0 1030	-0.80409 0.0001 1030	0.86048 0.0001 1030	-0.85858 0.0001 1030	1.00000 0.0 1030	-0.98745 0.0 1030	0.32462 0.0001 1030	0.29003 0.0001 1030	-0.21270 0.0001 1030	0.35190 0.0001 1030	0.32552 0.0001 1030	0.30767 0.0001 1030
VOIDSFIL	0.90233 0.0 1030	0.88212 0.0 1030	-0.90073 0.0 1030	0.92416 0.0 1030	-0.98745 0.0 1030	1.00000 0.0 1030	-0.35245 0.0001 1030	-0.30835 0.0001 1030	0.23374 0.0001 1030	-0.37558 0.0001 1030	-0.35233 0.0001 1030	-0.32822 0.0001 1030
SIX_85	-0.25383 0.0001 1030	-0.38472 0.0001 1030	0.36421 0.0001 1030	-0.38454 0.0001 1030	0.32462 0.0001 1030	1.00000 0.0 1030	0.73994 0.0001 1030	0.73994 0.0001 1030	-0.65662 0.0001 1030	0.97400 0.0 1030	0.95413 0.0 1030	0.82873 0.0001 1030
SIX_95	-0.23373 0.0001 1030	-0.33230 0.0001 1030	0.31524 0.0001 1030	-0.33356 0.0001 1030	0.29003 0.0001 1030	-0.35245 0.0001 1030	1.00000 0.0 1030	1.00000 0.0 1030	-0.10295 0.0009 1030	0.67816 0.0001 1030	0.89585 0.0 1030	0.90860 0.0 1030
SIXAVE	0.16315 0.0001 1030	0.25194 0.0001 1030	-0.24298 0.0001 1030	0.25188 0.0001 1030	-0.21270 0.0001 1030	0.23374 0.0001 1030	-0.65662 0.0001 1030	-0.10295 0.0009 1030	1.00000 0.0 1030	-0.69587 0.0001 1030	-0.46483 0.0001 1030	-0.22057 0.0001 1030
INT_75	-0.28842 0.0001 1030	-0.39512 0.0001 1030	0.37386 0.0001 1030	-0.39836 0.0001 1030	0.35190 0.0001 1030	-0.37558 0.0001 1030	0.97400 0.0 1030	0.67816 0.0001 1030	-0.69587 0.0001 1030	1.00000 0.0 1030	0.89937 0.0 1030	0.77452 0.0001 1030
INT_85	-0.25442 0.0001 1030	-0.38613 0.0001 1030	0.36567 0.0001 1030	-0.38575 0.0001 1030	0.32552 0.0001 1030	-0.35233 0.0001 1030	0.95413 0.0 1030	0.89585 0.0 1030	-0.46483 0.0001 1030	0.89937 0.0 1030	1.00000 0.0 1030	0.94809 0.0 1030
INT_95	-0.24715 0.0001 1030	-0.35411 0.0001 1030	0.33548 0.0001 1030	-0.35528 0.0001 1030	0.30767 0.0001 1030	-0.32822 0.0001 1030	0.82873 0.0001 1030	0.98860 0.0 1030	-0.22057 0.0001 1030	0.77452 0.0001 1030	0.94809 0.0 1030	1.00000 0.0 1030
INT105	-0.24506 0.0001 1030	-0.34184 0.0001 1030	0.32464 0.0001 1030	-0.34384 0.0001 1030	0.30163 0.0001 1030	-0.32031 0.0001 1030	0.74509 0.0001 1030	0.99734 0.0 1030	-0.12254 0.0001 1030	0.68772 0.0001 1030	0.89516 0.0 1030	0.98549 0.0 1030
INT115	-0.19531 0.0001 1030	-0.29311 0.0001 1030	0.27855 0.0001 1030	-0.29252 0.0001 1030	0.24856 0.0001 1030	-0.26410 0.0001 1030	0.64490 0.0001 1030	0.97604 0.0 1030	0.00671 0.0001 1030	0.57727 0.0001 1030	0.81640 0.0001 1030	0.94713 0.0 1030

Pairwise Correlations of All Possible Pairs of Non-Zero Variables

CORRELATION ANALYSIS

Pearson Correlation Coefficients / Prob > |R| under Ho: Rho=0 / Number of Observations

	BULDENS	ASPHCONT	THAXDENS	ASPHVOLM	VOIDSTOT	VOIDSFIL	SIX_85	SIX_95	SIXAVE	INT_75	INT_85	INT_95
INTAVE	0.12755 0.0001 1030	0.19887 0.0001 1030	-0.18971 0.0001 1030	0.19864 0.0001 1030	-0.16626 0.0001 1030	0.18376 0.0001 1030	-0.58196 0.0001 1030	-0.35491 0.0001 1030	0.52709 0.0001 1030	-0.53748 0.0001 1030	-0.57689 0.0001 1030	-0.43447 0.0001 1030
MID_85	-0.27196 0.0001 1030	-0.39753 0.0001 1030	0.37669 0.0001 1030	-0.39838 0.0001 1030	0.34192 0.0001 1030	-0.36765 0.0001 1030	0.93712 0.0001 1030	0.92105 0.0001 1030	-0.42605 0.0001 1030	0.89107 0.0001 1030	0.99593 0.0001 1030	0.96586 0.0001 1030
MID_95	-0.21454 0.0001 1030	-0.32212 0.0001 1030	0.30541 0.0001 1030	-0.32183 0.0001 1030	0.27302 0.0001 1030	-0.29290 0.0001 1030	0.77296 0.0001 1030	0.99410 0.0001 1030	-0.13905 0.0001 1030	0.69797 0.0001 1030	0.91674 0.0001 1030	0.99129 0.0001 1030
MID105	-0.25507 0.0001 1030	-0.36403 0.0001 1030	0.34434 0.0001 1030	-0.36540 0.0001 1030	0.31677 0.0001 1030	-0.33821 0.0001 1030	0.87828 0.0001 1030	0.96584 0.0001 1030	-0.29897 0.0001 1030	0.83155 0.0001 1030	0.97229 0.0001 1030	0.99287 0.0001 1030
MID115	-0.26698 0.0001 1030	-0.36963 0.0001 1030	0.35130 0.0001 1030	-0.37211 0.0001 1030	0.32766 0.0001 1030	-0.34802 0.0001 1030	0.77994 0.0001 1030	0.98842 0.0001 1030	-0.18878 0.0001 1030	0.73298 0.0001 1030	0.91243 0.0001 1030	0.98413 0.0001 1030
MID125	-0.12413 0.0001 1030	-0.20237 0.0001 1030	0.19199 0.0001 1030	-0.20027 0.0001 1030	0.16406 0.0001 1030	-0.17414 0.0001 1030	0.50414 0.0001 1030	0.91621 0.0001 1030	0.16949 0.0001 1030	0.41819 0.0001 1030	0.70276 0.0001 1030	0.87105 0.0001 1030
MIDAVE	0.10038 0.0013 1030	0.16611 0.0001 1030	-0.15549 0.0001 1030	0.16511 0.0001 1030	-0.13357 0.0001 1030	0.15018 0.0001 1030	-0.51717 0.0001 1030	-0.34539 0.0001 1030	0.36039 0.0001 1030	-0.46089 0.0001 1030	-0.53634 0.0001 1030	-0.41617 0.0001 1030
SUR_85	-0.17921 0.0001 1030	-0.26407 0.0001 1030	0.24943 0.0001 1030	-0.26409 0.0001 1030	0.22559 0.0001 1030	-0.24048 0.0001 1030	0.64150 0.0001 1030	0.94777 0.0001 1030	0.01560 0.6169 1030	0.55566 0.0001 1030	0.83048 0.0001 1030	0.93232 0.0001 1030
SUR_95	-0.23321 0.0001 1030	-0.36268 0.0001 1030	0.34462 0.0001 1030	-0.36174 0.0001 1030	0.30359 0.0001 1030	-0.32821 0.0001 1030	0.88854 0.0001 1030	0.95704 0.0001 1030	-0.32772 0.0001 1030	0.82313 0.0001 1030	0.97359 0.0001 1030	0.98261 0.0001 1030
SUR105	-0.24429 0.0001 1030	-0.34982 0.0001 1030	0.33119 0.0001 1030	-0.35099 0.0001 1030	0.30394 0.0001 1030	-0.32430 0.0001 1030	0.83755 0.0001 1030	0.98457 0.0001 1030	-0.23618 0.0001 1030	0.78328 0.0001 1030	0.95305 0.0001 1030	0.98093 0.0001 1030
SUR115	-0.24235 0.0001 1030	-0.35006 0.0001 1030	0.33105 0.0001 1030	-0.35092 0.0001 1030	0.30256 0.0001 1030	-0.32306 0.0001 1030	0.83189 0.0001 1030	0.98574 0.0001 1030	-0.22327 0.0001 1030	0.77526 0.0001 1030	0.95139 0.0001 1030	0.98071 0.0001 1030
SUR125	-0.28128 0.0001 1030	-0.38697 0.0001 1030	0.36695 0.0001 1030	-0.38983 0.0001 1030	0.34393 0.0001 1030	-0.36551 0.0001 1030	0.82648 0.0001 1030	0.97781 0.0001 1030	-0.25016 0.0001 1030	0.78449 0.0001 1030	0.94162 0.0001 1030	0.98728 0.0001 1030
SUR135	-0.18402 0.0001 1030	-0.27144 0.0001 1030	0.25896 0.0001 1030	-0.27142 0.0001 1030	0.23271 0.0001 1030	-0.24692 0.0001 1030	0.60466 0.0001 1030	0.96433 0.0001 1030	0.04250 0.1729 1030	0.53557 0.0001 1030	0.78258 0.0001 1030	0.92745 0.0001 1030

Pairwise Correlations of All Possible Pairs of Non-Zero Variables

CORRELATION ANALYSIS

Pearson Correlation Coefficients / Prob > |R| under Ho: Rho=0 / Number of Observations

	BULDEMS	ASPHCONT	TRAXDEMS	ASPHVOLM	VOIDSTOT	VOIDSFIL	SIX_85	SIX_95	SIXAVE	INT_75	INT_85	INT_95
SUR145	-0.13115 0.0001 1030	-0.20665 0.0001 1030	0.19865 0.0001 1030	-0.20316 0.0001 1030	0.17160 0.0001 1030	-0.18130 0.0001 1030	0.48920 0.0001 1030	0.86975 0.0 1030	0.11345 0.0003 1030	0.42069 0.0001 1030	0.66287 0.0001 1030	0.82316 0.0001 1030
SURAVE	0.03431 0.2713 1030	0.08812 0.0047 1030	-0.07998 0.0102 1030	0.08484 0.0064 1030	-0.05697 0.0676 1030	0.06724 0.0310 1030	-0.41601 0.0001 1030	-0.51589 0.0001 1030	0.01895 0.5435 1030	-0.31362 0.0001 1030	-0.53918 0.0001 1030	-0.53948 0.0001 1030
AMB_75	-0.23827 0.0001 1030	-0.35379 0.0001 1030	0.33421 0.0001 1030	-0.35394 0.0001 1030	0.30128 0.0001 1030	-0.32420 0.0001 1030	0.85917 0.0001 1030	0.93987 0.0 1030	-0.28809 0.0001 1030	0.79163 0.0001 1030	0.96747 0.0 1030	0.96874 0.0 1030
AMB_85	-0.24419 0.0001 1030	-0.35582 0.0001 1030	0.33680 0.0001 1030	-0.35651 0.0001 1030	0.30627 0.0001 1030	-0.32795 0.0001 1030	0.85685 0.0001 1030	0.97876 0.0 1030	-0.26255 0.0001 1030	0.79841 0.0001 1030	0.96460 0.0 1030	0.99758 0.0 1030
AMB_95	-0.24832 0.0001 1030	-0.34975 0.0001 1030	0.33279 0.0001 1030	-0.35144 0.0001 1030	0.30724 0.0001 1030	-0.32628 0.0001 1030	0.74153 0.0001 1030	0.99317 0.0 1030	-0.12725 0.0001 1030	0.68896 0.0001 1030	0.88731 0.0 1030	0.96024 0.0 1030
AMB105	-0.06592 0.0344 1030	-0.11048 0.0604 1030	0.10164 0.0011 1030	-0.10909 0.0005 1030	0.08703 0.0052 1030	-0.09363 0.0026 1030	0.34954 0.0001 1030	0.69629 0.0001 1030	0.27033 0.0001 1030	0.24894 0.0001 1030	0.54259 0.0001 1030	0.67182 0.0001 1030
AMBAVE	-0.09933 0.0014 1030	-0.13485 0.0001 1030	0.13171 0.0001 1030	-0.13563 0.0001 1030	0.12193 0.0001 1030	-0.12469 0.0001 1030	0.27147 0.0001 1030	0.71159 0.0001 1030	0.28240 0.0001 1030	0.20990 0.0001 1030	0.44925 0.0001 1030	0.64590 0.0001 1030
FT_75	-0.06592 0.0344 1030	-0.11048 0.0004 1030	0.10164 0.0011 1030	-0.10909 0.0005 1030	0.08703 0.0052 1030	-0.09363 0.0026 1030	0.34954 0.0001 1030	0.69629 0.0001 1030	0.27033 0.0001 1030	0.24894 0.0001 1030	0.54259 0.0001 1030	0.67182 0.0001 1030
FT_85	-0.23036 0.0001 1030	-0.35314 0.0001 1030	0.33225 0.0001 1030	-0.35247 0.0001 1030	0.29523 0.0001 1030	-0.32043 0.0001 1030	0.96209 0.0 1030	0.85107 0.0001 1030	-0.47910 0.0001 1030	0.90778 0.0 1030	0.98258 0.0 1030	0.91661 0.0 1030
FT_95	-0.24610 0.0001 1030	-0.34762 0.0001 1030	0.33037 0.0001 1030	-0.34920 0.0001 1030	0.30475 0.0001 1030	-0.32391 0.0001 1030	0.75716 0.0001 1030	0.99823 0.0 1030	-0.13732 0.0001 1030	0.70146 0.0001 1030	0.90462 0.0 1030	0.98971 0.0 1030
FT_105	-0.13024 0.0001 1030	-0.21097 0.0001 1030	0.20174 0.0001 1030	-0.20890 0.0001 1030	0.17225 0.0001 1030	-0.18223 0.0001 1030	0.48995 0.0001 1030	0.88650 0.0 1030	0.13689 0.0001 1030	0.41438 0.0001 1030	0.67324 0.0001 1030	0.83978 0.0001 1030
FT_AVE	-0.08603 0.0057 1030	-0.13163 0.0001 1030	0.12430 0.0001 1030	-0.13088 0.0001 1030	0.10995 0.0004 1030	-0.11518 0.0002 1030	0.33856 0.0001 1030	0.82078 0.0001 1030	0.30933 0.0001 1030	0.25681 0.0001 1030	0.58792 0.0001 1030	0.76795 0.0001 1030
VARIANCE	-0.11701 0.0002 1030	-0.08079 0.0095 1030	0.05559 0.0745 1030	-0.08811 0.0047 1030	0.10191 0.0011 1030	-0.09506 0.0023 1030	0.02273 0.4663 1030	-0.01969 0.5278 1030	-0.05425 0.0818 1030	0.04476 0.1511 1030	-0.00239 0.9389 1030	-0.01453 0.6413 1030

Pairwise Correlations of All Possible Pairs of Non-Zero Variables

13

CORRELATION ANALYSIS

Pearson Correlation Coefficients / Prob > |R| under Ho: Rho=0 / Number of Observations

	BULKDENS	ASPHCONT	THAXDENS	ASPHVOLM	VOIDSTOT	VOIDSFIL	SIX_85	SIX_95	SIXAVE	INT_75	INT_85	INT_95
LN_PASS	-0.13381 0.0001 1030	-0.20588 0.0001 1030	0.19049 0.0001 1030	-0.20496 0.0001 1030	0.17009 0.0001 1030	-0.18211 0.0001 1030	0.58744 0.0001 1030	0.91204 0.0 1030	0.08894 0.0043 1030	0.43363 0.0001 1030	0.76959 0.0001 1030	0.89111 0.0 1030
Q_SKEW	0.11326 0.0003 1030	0.12102 0.0001 1030	-0.07132 0.0221 1030	0.12403 0.0001 1030	-0.10613 0.0006 1030	0.10574 0.0007 1030	-0.09985 0.0013 1030	-0.12275 0.0001 1030	-0.00069 0.9824 1030	-0.08815 0.0016 1030	-0.11273 0.0003 1030	-0.12560 0.0001 1030
THICKNES	0.48828 0.0001 1030	0.11641 0.0002 1030	-0.05962 0.0558 1030	0.16824 0.0001 1030	-0.35329 0.0001 1030	0.30289 0.0001 1030	0.03433 0.2710 1030	0.06378 0.0407 1030	0.01581 0.6122 1030	-0.02083 0.5043 1030	0.05103 0.1017 1030	0.05374 0.0847 1030
MIX_IND	-0.70906 0.0001 1030	-0.97195 0.0 1030	0.93397 0.0 1030	-0.97972 0.0 1030	0.87132 0.0 1030	-0.92741 0.0 1030	0.39660 0.0001 1030	0.35345 0.0001 1030	-0.25195 0.0001 1030	0.40622 0.0001 1030	0.40092 0.0001 1030	0.37349 0.0001 1030
DES_IND	0.19200 0.0001 1030	0.16599 0.0001 1030	0.01635 0.6001 1030	0.17372 0.0001 1030	-0.12354 0.0001 1030	0.13479 0.0001 1030	0.02054 0.5102 1030	0.07491 0.0162 1030	0.03404 0.2751 1030	-0.01123 0.7188 1030	0.03874 0.2141 1030	0.06083 0.0510 1030
TRUTHICK	0.39938 0.0001 1030	0.01171 0.7073 1030	0.06182 0.0473 1030	0.06229 0.0456 1030	-0.24249 0.0001 1030	0.19760 0.0001 1030	0.07592 0.0148 1030	0.10841 0.0005 1030	-0.00946 0.7618 1030	0.02678 0.3806 1030	0.09425 0.0025 1030	0.09926 0.0014 1030
PCTSMALL	-0.59166 0.0001 1030	-0.52061 0.0001 1030	0.64961 0.0001 1030	-0.55463 0.0001 1030	0.67338 0.0001 1030	-0.66321 0.0001 1030	0.24089 0.0001 1030	0.26793 0.0001 1030	-0.12141 0.0001 1030	0.25409 0.0001 1030	0.25705 0.0001 1030	0.26939 0.0001 1030
PCMEDIUM	-0.73333 0.0001 1030	-0.41907 0.0001 1030	0.32517 0.0001 1030	-0.47367 0.0001 1030	0.62816 0.0001 1030	-0.57570 0.0001 1030	0.12581 0.0001 1030	0.16430 0.0001 1030	-0.04998 0.1089 1030	0.17496 0.0001 1030	0.13728 0.0001 1030	0.16536 0.0001 1030

Pairwise Correlations of All Possible Pairs of Non-Zero Variables

CORRELATION ANALYSIS

Pearson Correlation Coefficients / Prob > |R| under Ho: Rho=0 / Number of Observations

	INT105	INT115	INTAVE	MID_85	MID_95	MID105	MID115	MID125	MIDAVE	SUR_85	SUR_95	SUR105
MODE	-0.28333 0.0001 1030	-0.31236 0.0001 1030	0.02982 0.3390 1030	-0.22044 0.0001 1030	-0.28975 0.0001 1030	-0.25603 0.0001 1030	-0.26258 0.0001 1030	-0.33756 0.0001 1030	0.05739 0.0656 1030	-0.30144 0.0001 1030	-0.25375 0.0001 1030	-0.26782 0.0001 1030
MEAN	-0.11299 0.0003 1030	-0.15607 0.0001 1030	-0.08928 0.0041 1030	-0.04011 0.1984 1030	-0.11476 0.0002 1030	-0.07624 0.0144 1030	-0.09607 0.0020 1030	-0.18838 0.0001 1030	-0.09390 0.0026 1030	-0.11550 0.0002 1030	-0.04258 0.0002 1030	-0.09179 0.0032 1030
ST_DEV	-0.01502 0.6301 1030	-0.00817 0.7933 1030	0.09548 0.0022 1030	0.00486 0.8761 1030	-0.02785 0.3719 1030	-0.01141 0.7146 1030	-0.00010 0.9976 1030	-0.03541 0.2562 1030	0.10383 0.0008 1030	-0.07286 0.0194 1030	0.00581 0.8523 1030	-0.01762 0.5722 1030
PASSES	0.99009 0.0 1030	0.95268 0.0 1030	-0.41406 0.0001 1030	0.96283 0.0 1030	0.99289 0.0 1030	0.98939 0.0 1030	0.98927 0.0 1030	0.87474 0.0 1030	-0.39341 0.0001 1030	0.92817 0.0 1030	0.98393 0.0 1030	0.99735 0.0 1030
DT	0.29037 0.0001 1030	0.34146 0.0001 1030	-0.11010 0.0004 1030	0.18308 0.0001 1030	0.32210 0.0001 1030	0.25871 0.0001 1030	0.25119 0.0001 1030	0.40500 0.0001 1030	-0.16344 0.0001 1030	0.39322 0.0001 1030	0.23227 0.0001 1030	0.28798 0.0001 1030
HU1	0.12655 0.0001 1030	0.20702 0.0001 1030	0.08044 0.0098 1030	-0.01856 0.5519 1030	0.14639 0.0001 1030	0.06460 0.0382 1030	0.07912 0.0111 1030	0.31089 0.0001 1030	0.04229 0.1750 1030	0.22507 0.0001 1030	0.05593 0.0728 1030	0.09691 0.0018 1030
HU2	0.04904 0.1158 1030	0.11958 0.0001 1030	0.08313 0.0076 1030	-0.07379 0.0179 1030	0.07251 0.0199 1030	-0.00455 0.8840 1030	0.00643 0.8366 1030	0.21704 0.0001 1030	0.04345 0.1635 1030	0.14156 0.0001 1030	-0.00623 0.8417 1030	0.02600 0.4046 1030
WR	0.41218 0.0001 1030	0.38630 0.0001 1030	-0.15817 0.0001 1030	0.41848 0.0001 1030	0.40684 0.0001 1030	0.41808 0.0001 1030	0.42083 0.0001 1030	0.32974 0.0001 1030	-0.17856 0.0001 1030	0.37375 0.0001 1030	0.40778 0.0001 1030	0.41843 0.0001 1030
A2	0.06167 0.0502 1009	0.13220 0.0001 1009	0.04997 0.1126 1009	-0.05192 0.0993 1009	0.08375 0.0078 1009	0.01778 0.5727 1009	0.01935 0.5392 1009	0.22858 0.0001 1009	0.01784 0.5713 1009	0.16182 0.0001 1009	0.00556 0.8601 1009	0.04320 0.1703 1009
A1	0.40818 0.0001 1030	0.38707 0.0001 1030	-0.25172 0.0001 1030	0.37923 0.0001 1030	0.41220 0.0001 1030	0.41383 0.0001 1030	0.39843 0.0001 1030	0.36910 0.0001 1030	-0.28045 0.0001 1030	0.44603 0.0001 1030	0.38510 0.0001 1030	0.42101 0.0001 1030
BSFWDISH	0.09474 0.0023 1030	0.11223 0.0003 1030	0.06934 0.0261 1030	0.05241 0.0928 1030	0.09307 0.0028 1030	0.08520 0.0364 1030	0.08613 0.0057 1030	0.12776 0.0001 1030	0.08281 0.0078 1030	0.06797 0.0292 1030	0.08879 0.0043 1030	0.07430 0.0171 1030
PVTWDISH	0.08623 0.0056 1030	0.10530 0.0007 1030	0.07358 0.0182 1030	0.04359 0.1621 1030	0.08578 0.0059 1030	0.05659 0.0694 1030	0.07691 0.0135 1030	0.12320 0.0001 1030	0.08625 0.0056 1030	0.06119 0.0496 1030	0.08153 0.0089 1030	0.06600 0.0342 1030
BULKDEINS	-0.24506 0.0001 1030	-0.19531 0.0001 1030	0.12755 0.0001 1030	-0.27196 0.0001 1030	-0.21454 0.0001 1030	-0.25507 0.0001 1030	-0.26698 0.0001 1030	-0.12413 0.0001 1030	0.10038 0.0013 1030	-0.17921 0.0001 1030	-0.23521 0.0001 1030	-0.24429 0.0001 1030

Pairwise Correlations of All Possible Pairs of Non-Zero Variables

CORRELATION ANALYSIS

Pearson Correlation Coefficients / Prob > |R| under Ho: Rho=0 / Number of Observations

	INT115	INTAVE	MID_85	MID_95	MID105	MID115	MID125	MIDAVE	SUR_85	SUR_95	SUR105
ASPHCONT	-0.34184 0.0001 1030	0.19887 0.0001 1030	-0.39753 0.0001 1030	-0.32212 0.0001 1030	-0.36403 0.0001 1030	-0.36963 0.0001 1030	-0.20237 0.0001 1030	0.16511 0.0001 1030	-0.26407 0.0001 1030	-0.36268 0.0001 1030	-0.34982 0.0001 1030
TMXNDENS	0.32464 0.0001 1030	-0.18971 0.0001 1030	0.37669 0.0001 1030	0.30541 0.0001 1030	0.34434 0.0001 1030	0.35130 0.0001 1030	0.19199 0.0001 1030	-0.15349 0.0001 1030	0.24943 0.0001 1030	0.34462 0.0001 1030	0.33119 0.0001 1030
ASPHVOLM	-0.34384 0.0001 1030	0.19864 0.0001 1030	-0.39838 0.0001 1030	-0.32183 0.0001 1030	-0.36540 0.0001 1030	-0.37211 0.0001 1030	-0.20027 0.0001 1030	0.16511 0.0001 1030	-0.26409 0.0001 1030	-0.36174 0.0001 1030	-0.35099 0.0001 1030
VOIDSTOT	0.30163 0.0001 1030	-0.16626 0.0001 1030	0.34192 0.0001 1030	0.27302 0.0001 1030	0.31677 0.0001 1030	0.32766 0.0001 1030	0.16406 0.0001 1030	-0.13357 0.0001 1030	0.22559 0.0001 1030	0.30359 0.0001 1030	0.30394 0.0001 1030
VOIDSPIL	-0.32031 0.0001 1030	0.18376 0.0001 1030	-0.36765 0.0001 1030	-0.29290 0.0001 1030	-0.33821 0.0001 1030	-0.34802 0.0001 1030	-0.17414 0.0001 1030	0.15018 0.0001 1030	-0.24048 0.0001 1030	-0.32821 0.0001 1030	-0.32430 0.0001 1030
STX_85	0.74509 0.0001 1030	-0.58196 0.0001 1030	0.93712 0.0001 1030	0.77296 0.0001 1030	0.87828 0.0001 1030	0.77994 0.0001 1030	0.50414 0.0001 1030	-0.51717 0.0001 1030	0.64150 0.0001 1030	0.88854 0.0001 1030	0.83755 0.0001 1030
STX_95	0.99734 0.0001 1030	-0.35491 0.0001 1030	0.92105 0.0001 1030	0.99410 0.0001 1030	0.96584 0.0001 1030	0.98842 0.0001 1030	0.91621 0.0001 1030	-0.34539 0.0001 1030	0.94777 0.0001 1030	0.95704 0.0001 1030	0.98457 0.0001 1030
SIXAVE	-0.12254 0.0001 1030	0.52709 0.0001 1030	-0.42605 0.0001 1030	-0.13905 0.0001 1030	-0.29897 0.0001 1030	-0.18878 0.0001 1030	0.16949 0.0001 1030	0.36039 0.0001 1030	0.01560 0.0001 1030	-0.32772 0.0001 1030	-0.23618 0.0001 1030
INT_75	0.68772 0.0001 1030	-0.53748 0.0001 1030	0.89107 0.0001 1030	0.68797 0.0001 1030	0.83155 0.0001 1030	0.73298 0.0001 1030	0.41819 0.0001 1030	-0.46089 0.0001 1030	0.55566 0.0001 1030	0.82313 0.0001 1030	0.78328 0.0001 1030
INT_85	0.89516 0.0001 1030	-0.57689 0.0001 1030	0.99593 0.0001 1030	0.91674 0.0001 1030	0.97229 0.0001 1030	0.91243 0.0001 1030	0.70276 0.0001 1030	-0.53634 0.0001 1030	0.83048 0.0001 1030	0.97359 0.0001 1030	0.95305 0.0001 1030
INT_95	0.98549 0.0001 1030	-0.43447 0.0001 1030	0.96586 0.0001 1030	0.99129 0.0001 1030	0.99287 0.0001 1030	0.98413 0.0001 1030	0.87105 0.0001 1030	-0.41617 0.0001 1030	0.93232 0.0001 1030	0.98261 0.0001 1030	0.99893 0.0001 1030
INT105	1.00000 0.0001 1030	-0.33502 0.0001 1030	0.92162 0.0001 1030	0.98902 0.0001 1030	0.96210 0.0001 1030	0.99526 0.0001 1030	0.89787 0.0001 1030	-0.31774 0.0001 1030	0.92606 0.0001 1030	0.95720 0.0001 1030	0.98102 0.0001 1030
INT115	0.96883 0.0001 1030	-0.20131 0.0001 1030	0.84472 0.0001 1030	0.96847 0.0001 1030	0.91080 0.0001 1030	0.95020 0.0001 1030	0.97092 0.0001 1030	-0.19951 0.0001 1030	0.92251 0.0001 1030	0.91480 0.0001 1030	0.93967 0.0001 1030

Pairwise Correlations of All Possible Pairs of Non-Zero Variables

CORRELATION ANALYSIS

Pearson Correlation Coefficients / Prob > |R| under Ho: Rho=0 / Number of Observations

	INT105	INT115	INTAVE	MID_85	MID_95	MID105	MID115	MID125	MIDAVE	SUR_85	SUR_95	SUR105
INTAVE	-0.33502 0.0001 1030	-0.20131 0.0001 1030	1.00000 0.0 1030	-0.55081 0.0001 1030	-0.39080 0.0001 1030	-0.49338 0.0001 1030	-0.34301 0.0001 1030	-0.14023 0.0001 1030	0.95095 0.0 1030	-0.47433 0.0001 1030	-0.43791 0.0001 1030	-0.45382 0.0001 1030
MID_85	0.92162 0.0 1030	0.84472 0.0001 1030	-0.55081 0.0001 1030	1.00000 0.0 1030	0.93405 0.0 1030	0.98450 0.0 1030	0.93820 0.0 1030	0.73032 0.0001 1030	-0.51383 0.0001 1030	0.85053 0.0001 1030	0.97956 0.0 1030	0.96895 0.0 1030
MID_95	0.98902 0.0 1030	0.96847 0.0 1030	-0.39080 0.0001 1030	0.93405 0.0 1030	1.00000 0.0 1030	0.97197 0.0 1030	0.97871 0.0 1030	0.91314 0.0 1030	-0.38293 0.0001 1030	0.95012 0.0 1030	0.97207 0.0 1030	0.98948 0.0 1030
MID105	0.96210 0.0 1030	0.91080 0.0 1030	-0.49338 0.0001 1030	0.98450 0.0 1030	0.97197 0.0 1030	1.00000 0.0 1030	0.96551 0.0 1030	0.82435 0.0001 1030	-0.47020 0.0001 1030	0.91084 0.0 1030	0.98337 0.0 1030	0.99451 0.0 1030
MID115	0.99526 0.0 1030	0.95020 0.0 1030	-0.34301 0.0001 1030	0.93820 0.0 1030	0.97871 0.0 1030	0.96551 0.0 1030	1.00000 0.0 1030	0.85795 0.0001 1030	-0.31315 0.0001 1030	0.89624 0.0 1030	0.96395 0.0 1030	0.97914 0.0 1030
MID125	0.89787 0.0 1030	0.97092 0.0 1030	-0.14023 0.0001 1030	0.73032 0.0001 1030	0.91314 0.0 1030	0.82435 0.0001 1030	0.85795 0.0001 1030	1.00000 0.0 1030	-0.16210 0.0001 1030	0.91634 0.0 1030	0.82360 0.0001 1030	0.86392 0.0 1030
MIDAVE	-0.31774 0.0001 1030	-0.19951 0.0001 1030	0.95095 0.0 1030	-0.51383 0.0001 1030	-0.38293 0.0001 1030	-0.47020 0.0001 1030	-0.31315 0.0001 1030	-0.16210 0.0001 1030	1.00000 0.0 1030	-0.49954 0.0001 1030	-0.40763 0.0001 1030	-0.43623 0.0001 1030
SUR_85	0.92606 0.0 1030	0.92251 0.0 1030	-0.47433 0.0001 1030	0.85053 0.0001 1030	0.95012 0.0 1030	0.91084 0.0 1030	0.89624 0.0 1030	0.91634 0.0 1030	-0.49954 0.0001 1030	1.00000 0.0 1030	0.87585 0.0 1030	0.93304 0.0 1030
SUR_95	0.95720 0.0 1030	0.91480 0.0 1030	-0.43791 0.0001 1030	0.97956 0.0 1030	0.97207 0.0 1030	0.98337 0.0 1030	0.96395 0.0 1030	0.82360 0.0001 1030	-0.40763 0.0001 1030	0.87585 0.0 1030	1.00000 0.0 1030	0.98216 0.0 1030
SUR105	0.98102 0.0 1030	0.93967 0.0 1030	-0.45382 0.0001 1030	0.96895 0.0 1030	0.98948 0.0 1030	0.99451 0.0 1030	0.97914 0.0 1030	0.86392 0.0 1030	-0.43623 0.0001 1030	0.93304 0.0 1030	0.98216 0.0 1030	1.00000 0.0 1030
SUR115	0.98098 0.0 1030	0.94293 0.0 1030	-0.45347 0.0001 1030	0.96706 0.0 1030	0.98979 0.0 1030	0.99457 0.0 1030	0.97800 0.0 1030	0.86973 0.0 1030	-0.43768 0.0001 1030	0.93736 0.0 1030	0.98089 0.0 1030	0.99907 0.0 1030
SUR125	0.98363 0.0 1030	0.92073 0.0 1030	-0.41404 0.0001 1030	0.96419 0.0 1030	0.97045 0.0 1030	0.97998 0.0 1030	0.99266 0.0 1030	0.81903 0.0001 1030	-0.37985 0.0001 1030	0.89429 0.0 1030	0.96838 0.0 1030	0.98398 0.0 1030
SUR135	0.96039 0.0 1030	0.99276 0.0 1030	-0.16608 0.0001 1030	0.81213 0.0001 1030	0.95604 0.0 1030	0.88404 0.0 1030	0.93994 0.0 1030	0.96703 0.0 1030	-0.16721 0.0001 1030	0.90258 0.0 1030	0.89512 0.0 1030	0.91947 0.0 1030

Pairwise Correlations of All Possible Pairs of Non-Zero Variables

CORRELATION ANALYSIS

Pearson Correlation Coefficients / Prob > |R| under Ho: Rho=0 / Number of Observations

	INT105	INT115	INTAVE	MID_95	MID_95	MID105	MID115	MID125	MIDAVE	SUR_85	SUR_95	SUR105
SUR145	0.86014 0.0001 1030	0.94317 0.0 1030	-0.02933 0.3471 1030	0.69261 0.0001 1030	0.85930 0.0001 1030	0.77971 0.0001 1030	0.82801 0.0001 1030	0.95567 0.0 1030	-0.03549 0.2552 1030	0.81522 0.0001 1030	0.78914 0.0001 1030	0.81406 0.0001 1030
SURAVE	-0.47127 0.0001 1030	-0.44127 0.0001 1030	0.78416 0.0001 1030	-0.52798 0.0001 1030	-0.55119 0.0001 1030	-0.55814 0.0001 1030	-0.42375 0.0001 1030	-0.49453 0.0001 1030	0.86293 0.0001 1030	-0.72728 0.0001 1030	-0.48961 0.0001 1030	-0.55559 0.0001 1030
AMB_75	0.92947 0.0 1030	0.86654 0.0 1030	-0.61220 0.0001 1030	0.97290 0.0 1030	0.95123 0.0 1030	0.98081 0.0 1030	0.92839 0.0 1030	0.78960 0.0001 1030	-0.60107 0.0001 1030	0.93293 0.0 1030	0.95569 0.0 1030	0.97308 0.0 1030
AMB_85	0.97533 0.0 1030	0.93135 0.0 1030	-0.46328 0.0001 1030	0.97697 0.0 1030	0.98679 0.0 1030	0.99632 0.0 1030	0.97527 0.0 1030	0.85261 0.0001 1030	-0.44300 0.0001 1030	0.92403 0.0 1030	0.98852 0.0 1030	0.99848 0.0 1030
AMB_95	0.99686 0.0 1030	0.97359 0.0 1030	-0.29757 0.0001 1030	0.91552 0.0 1030	0.98274 0.0 1030	0.95474 0.0 1030	0.99539 0.0 1030	0.89753 0.0 1030	-0.27492 0.0001 1030	0.90747 0.0 1030	0.95616 0.0 1030	0.97363 0.0 1030
AMB105	0.66142 0.0001 1030	0.67538 0.0001 1030	-0.50159 0.0001 1030	0.56162 0.0001 1030	0.70224 0.0001 1030	0.65076 0.0001 1030	0.60609 0.0001 1030	0.74310 0.0001 1030	-0.57018 0.0001 1030	0.84006 0.0001 1030	0.58385 0.0001 1030	0.67030 0.0001 1030
AMBAVE	0.71250 0.0001 1030	0.77402 0.0001 1030	0.05422 0.0820 1030	0.48659 0.0001 1030	0.69138 0.0001 1030	0.57998 0.0001 1030	0.68424 0.0001 1030	0.79730 0.0001 1030	0.14205 0.0001 1030	0.66041 0.0001 1030	0.58978 0.0001 1030	0.62932 0.0001 1030
FT_75	0.66142 0.0001 1030	0.67538 0.0001 1030	-0.50159 0.0001 1030	0.56162 0.0001 1030	0.70224 0.0001 1030	0.65076 0.0001 1030	0.60609 0.0001 1030	0.74310 0.0001 1030	-0.57018 0.0001 1030	0.84006 0.0001 1030	0.58385 0.0001 1030	0.67030 0.0001 1030
FT_85	0.84749 0.0001 1030	0.76686 0.0001 1030	-0.60198 0.0001 1030	0.97219 0.0 1030	0.88138 0.0 1030	0.95108 0.0 1030	0.86028 0.0001 1030	0.66602 0.0001 1030	-0.56686 0.0001 1030	0.80092 0.0001 1030	0.94129 0.0 1030	0.92548 0.0 1030
FT_95	0.99806 0.0 1030	0.97172 0.0 1030	-0.35103 0.0001 1030	0.93015 0.0 1030	0.99123 0.0 1030	0.96825 0.0 1030	0.99417 0.0 1030	0.90077 0.0 1030	-0.33462 0.0001 1030	0.93226 0.0 1030	0.96386 0.0 1030	0.98510 0.0 1030
FT_105	0.87134 0.0 1030	0.95882 0.0 1030	-0.06055 0.0521 1030	0.70401 0.0001 1030	0.88000 0.0 1030	0.79293 0.0001 1030	0.83559 0.0001 1030	0.98348 0.0 1030	-0.07047 0.0237 1030	0.86036 0.0001 1030	0.80678 0.0001 1030	0.83127 0.0001 1030
FT_AVE	0.79495 0.0001 1030	0.84164 0.0001 1030	-0.30400 0.0001 1030	0.61570 0.9001 1030	0.81709 0.0001 1030	0.72019 0.0001 1030	0.74077 0.0001 1030	0.90554 0.0 1030	-0.31882 0.0001 1030	0.90927 0.0 1030	0.88248 0.0001 1030	0.76345 0.0001 1030
VARIANCEZ	-0.01521 0.6259 1030	-0.00755 0.8088 1030	0.07534 0.0156 1030	-0.00003 0.9992 1030	-0.02441 0.4339 1030	-0.01192 0.7023 1030	-0.00414 0.8945 1030	-0.02683 0.3898 1030	0.08167 0.0087 1030	-0.05729 0.0661 1030	0.00095 0.9757 1030	-0.01663 0.5939 1030

Pairwise Correlations of All Possible Pairs of Non-Zero Variables

18

CORRELATION ANALYSIS

Pearson Correlation Coefficients / Prob > |R| under Ho: Rho=0 / Number of Observations

	INT105	INT115	INTAVE	MID_85	MID_95	MID105	MID115	MID125	MIDAVE	SUR_85	SUR_95	SUR105
LN_PASS	0.89460 0.0 1030	0.89718 0.0 1030	-0.36692 0.0001 1030	0.78798 0.0001 1030	0.91655 0.0 1030	0.86704 0.0 1030	0.85701 0.0001 1030	0.90797 0.0 1030	-0.40161 0.0001 1030	0.94895 0.0 1030	0.82714 0.0001 1030	0.89129 0.0 1030
Q_SKEW	-0.12382 0.0001 1030	-0.10832 0.0005 1030	0.06635 0.0332 1030	-0.11568 0.0002 1030	-0.12083 0.0001 1030	-0.12783 0.0001 1030	-0.12134 0.0001 1030	-0.10283 0.0009 1030	0.05094 0.1023 1030	-0.11603 0.0002 1030	-0.11173 0.0003 1030	-0.12551 0.0001 1030
THICKNES	0.05995 0.0544 1030	0.10533 0.0007 1030	0.05583 0.0733 1030	0.03887 0.2126 1030	0.07975 0.0105 1030	0.04356 0.1624 1030	0.04908 0.1155 1030	0.13260 0.0001 1030	0.06701 0.0315 1030	0.05844 0.0608 1030	0.08472 0.0065 1030	0.05202 0.0952 1030
MIX_IND	0.36430 0.0001 1030	0.31619 0.0001 1030	-0.19157 0.0001 1030	0.41353 0.0001 1030	0.34192 0.0001 1030	0.38233 0.0001 1030	0.39158 0.0001 1030	0.22524 0.0001 1030	-0.15522 0.0001 1030	0.28002 0.0001 1030	0.38173 0.0001 1030	0.36893 0.0001 1030
DES_IND	0.07990 0.0103 1030	0.09822 0.0016 1030	0.07638 0.0142 1030	0.03625 0.2450 1030	0.07883 0.0114 1030	0.05007 0.1083 1030	0.07029 0.0241 1030	0.11712 0.0002 1030	0.08833 0.0046 1030	0.05582 0.0733 1030	0.07356 0.0182 1030	0.05950 0.0363 1030
TRUTHICK	0.10586 0.0007 1030	0.14944 0.0001 1030	0.04723 0.1299 1030	0.08520 0.0062 1030	0.12104 0.0001 1030	0.08914 0.0042 1030	0.09811 0.0016 1030	0.16692 0.0001 1030	0.06483 0.0375 1030	0.09188 0.0032 1030	0.12893 0.0001 1030	0.09675 0.0019 1030
PCTSMALL	0.27842 0.0001 1030	0.25891 0.0001 1030	-0.06062 0.0518 1030	0.27220 0.0001 1030	0.25194 0.0001 1030	0.26874 0.0001 1030	0.29137 0.0001 1030	0.20988 0.0001 1030	-0.02501 0.4226 1030	0.20779 0.0001 1030	0.26626 0.0001 1030	0.26562 0.0001 1030
PCMEDM	0.16913 0.0001 1030	0.15499 0.0001 1030	-0.02423 0.4373 1030	0.15810 0.0001 1030	0.14066 0.0001 1030	0.16676 0.0001 1030	0.18042 0.0001 1030	0.11765 0.0002 1030	-0.00555 0.8588 1030	0.12852 0.0001 1030	0.13609 0.0001 1030	0.16314 0.0001 1030

Pairwise Correlations of All Possible Pairs of Non-Zero Variables

19

CORRELATION ANALYSIS

Pearson Correlation Coefficients / Prob > |R| under Ho: Rho=0 / Number of Observations

	SUR115	SUR125	SUR135	SUR145	SURAVE	AMB_75	AMB_85	AMB_95	AMBAVE	FT_75	FT_85
MODE	-0.27212 0.0001 1030	-0.25248 0.0001 1030	-0.30945 0.0001 1030	-0.30306 0.0001 1030	0.19431 0.0001 1030	-0.25494 0.0001 1030	-0.26613 0.0001 1030	-0.27859 0.0001 1030	-0.23704 0.0001 1030	-0.28995 0.0001 1030	-0.21620 0.0001 1030
MEAN	-0.09244 0.0030 1030	-0.07447 0.0168 1030	-0.16667 0.0001 1030	-0.18344 0.0001 1030	0.02564 0.4111 1030	-0.05962 0.0558 1030	-0.08542 0.0061 1030	-0.11681 0.0002 1030	-0.20795 0.0001 1030	-0.11997 0.0001 1030	-0.03696 0.2359 1030
ST_DEV	-0.02152 0.4903 1030	-0.00334 0.9146 1030	-0.00896 0.7740 1030	0.00335 0.9145 1030	0.16578 0.0001 1030	-0.03986 0.2012 1030	-0.01571 0.6146 1030	-0.00020 0.9949 1030	-0.05033 0.1064 1030	-0.15871 0.0001 1030	-0.01967 0.5283 1030
PASSES	0.99723 0.0 1030	0.98932 0.0 1030	0.93492 0.0 1030	0.93235 0.0001 1030	-0.51846 0.0001 1030	0.96367 0.0 1030	0.99619 0.0 1030	0.98585 0.0 1030	0.65590 0.0001 1030	0.65825 0.0001 1030	0.90848 0.0 1030
DT	0.29573 0.0001 1030	0.22681 0.0001 1030	0.34573 0.0001 1030	0.35507 0.0001 1030	-0.37257 0.0001 1030	0.27278 0.0001 1030	0.27351 0.0001 1030	0.27651 0.0001 1030	0.30680 0.0001 1030	0.43413 0.0001 1030	0.18264 0.0001 1030
HU1	0.09957 0.0014 1030	0.04357 0.1623 1030	0.22860 0.0001 1030	0.27344 0.0001 1030	-0.19015 0.0001 1030	0.06730 0.0308 1030	0.08283 0.0078 1030	0.11941 0.0001 1030	0.27382 0.0001 1030	0.29808 0.0001 1030	-0.02466 0.4293 1030
HU2	0.02745 0.3789 1030	-0.02526 0.4181 1030	0.14023 0.0001 1030	0.18149 0.0001 1030	-0.15306 0.0001 1030	0.00201 0.9486 1030	0.01377 0.6598 1030	0.04159 0.1823 1030	0.19431 0.0001 1030	0.22574 0.0001 1030	-0.07067 0.0233 1030
WR	0.41937 0.0001 1030	0.42806 0.0001 1030	0.36752 0.0001 1030	0.31565 0.0001 1030	-0.18859 0.0001 1030	0.40510 0.0001 1030	0.41878 0.0001 1030	0.41122 0.0001 1030	0.17376 0.0001 1030	0.22215 0.0001 1030	0.38799 0.0001 1030
A2	0.04657 0.1394 1009	-0.00685 0.8281 1009	0.14731 0.0001 1009	0.18801 0.0001 1009	-0.17841 0.0001 1009	0.02827 0.3697 1009	0.03134 0.3199 1009	0.05372 0.0881 1009	0.26660 0.0001 1009	0.26060 0.0001 1009	-0.04324 0.1699 1009
A1	0.42605 0.0001 1030	0.40526 0.0001 1030	0.37127 0.0001 1030	0.32129 0.0001 1030	-0.36104 0.0001 1030	0.42258 0.0001 1030	0.41209 0.0001 1030	0.39331 0.0001 1030	0.24678 0.0001 1030	0.39669 0.0001 1030	0.36500 0.0001 1030
BSFWDISM	0.07137 0.0220 1030	0.07156 0.0216 1030	0.12569 0.0001 1030	0.13110 0.0001 1030	0.02858 0.3596 1030	0.04852 0.1196 1030	0.07522 0.0158 1030	0.09735 0.0018 1030	0.12595 0.0001 1030	0.04094 0.1892 1030	0.04988 0.1096 1030
PVFWDISM	0.06295 0.0434 1030	0.06176 0.0475 1030	0.11951 0.0001 1030	0.12655 0.0001 1030	0.03000 0.3362 1030	0.04033 0.1960 1030	0.06700 0.0315 1030	0.08881 0.0043 1030	0.12211 0.0001 1030	0.03742 0.2302 1030	0.04266 0.1713 1030
BULKDEMS	-0.24235 0.0001 1030	-0.18402 0.0001 1030	-0.19402 0.0001 1030	-0.13115 0.0001 1030	0.03431 0.2713 1030	-0.23827 0.0001 1030	-0.24419 0.0001 1030	-0.24832 0.0001 1030	-0.09933 0.0014 1030	-0.06592 0.0344 1030	-0.23036 0.0001 1030

Pairwise Correlations of All Possible Pairs of Non-Zero Variables

CORRELATION ANALYSIS

Pearson Correlation Coefficients / Prob > |R| under Ho: Rho=0 / Number of Observations

	SUR115	SUR125	SUR135	SUR145	SURAVE	AMB_75	AMB_85	AMB_95	AMB105	AMBAVE	FT_75	FT_85
ASPHCONT	-0.35006 0.0001 1030	-0.38697 0.0001 1030	-0.27144 0.0001 1030	-0.20665 0.0001 1030	0.08812 0.0047 1030	-0.35379 0.0001 1030	-0.35582 0.0001 1030	-0.34975 0.0001 1030	-0.11048 0.0004 1030	-0.13485 0.0001 1030	-0.11048 0.0004 1030	-0.35314 0.0001 1030
TMAXDENS	0.33105 0.0001 1030	0.36695 0.0001 1030	0.25896 0.0001 1030	0.19865 0.0001 1030	-0.07998 0.0102 1030	0.33421 0.0001 1030	0.33680 0.0001 1030	0.33279 0.0001 1030	0.10164 0.0011 1030	0.13171 0.0011 1030	0.10164 0.0011 1030	0.33225 0.0001 1030
ASPHVOLM	-0.35092 0.0001 1030	-0.38983 0.0001 1030	-0.27142 0.0001 1030	-0.20516 0.0001 1030	0.08484 0.0064 1030	-0.35394 0.0001 1030	-0.35651 0.0001 1030	-0.35144 0.0001 1030	-0.10909 0.0005 1030	-0.13563 0.0001 1030	-0.10909 0.0005 1030	-0.35247 0.0001 1030
VOIDSTOT	0.30256 0.0001 1030	0.34393 0.0001 1030	0.23271 0.0001 1030	0.17160 0.0001 1030	-0.05697 0.0676 1030	0.30128 0.0001 1030	0.30627 0.0001 1030	0.30724 0.0001 1030	0.08703 0.0052 1030	0.12193 0.0001 1030	0.08703 0.0052 1030	0.29523 0.0001 1030
VOIDSFIL	-0.32306 0.0001 1030	-0.36551 0.0001 1030	-0.24692 0.0001 1030	-0.18130 0.0001 1030	0.06724 0.0310 1030	-0.32420 0.0001 1030	-0.32795 0.0001 1030	-0.32628 0.0001 1030	-0.09363 0.0026 1030	-0.12469 0.0001 1030	-0.09363 0.0026 1030	-0.32043 0.0001 1030
SIX_85	0.83189 0.0001 1030	0.82648 0.0001 1030	0.60466 0.0001 1030	0.48920 0.0001 1030	-0.41601 0.0001 1030	0.85917 0.0001 1030	0.85685 0.0001 1030	0.74153 0.0001 1030	0.34954 0.0001 1030	0.27147 0.0001 1030	0.34954 0.0001 1030	0.98269 0.0 1030
SIX_95	0.98574 0.0 1030	0.97781 0.0 1030	0.96433 0.0 1030	0.86975 0.0 1030	-0.51589 0.0001 1030	0.93987 0.0 1030	0.97876 0.0 1030	0.99317 0.0 1030	0.69629 0.0001 1030	0.71158 0.0001 1030	0.69629 0.0001 1030	0.85107 0.0001 1030
SIXAVE	-0.22327 0.0001 1030	-0.25046 0.0001 1030	0.04250 0.1729 1030	0.11345 0.0003 1030	0.01895 0.5435 1030	-0.28809 0.0001 1030	-0.26255 0.0001 1030	-0.12725 0.0001 1030	0.27033 0.0001 1030	0.28240 0.0001 1030	0.27033 0.0001 1030	-0.47910 0.0001 1030
INT_75	0.77526 0.0001 1030	0.78449 0.0001 1030	0.53557 0.0001 1030	0.42069 0.0001 1030	-0.31362 0.0001 1030	0.79163 0.0001 1030	0.79841 0.0001 1030	0.68896 0.0001 1030	0.24894 0.0001 1030	0.20990 0.0001 1030	0.24894 0.0001 1030	0.90778 0.0 1030
INT_85	0.95139 0.0 1030	0.94162 0.0 1030	0.78258 0.0001 1030	0.66287 0.0001 1030	-0.53918 0.0001 1030	0.96747 0.0 1030	0.96460 0.0 1030	0.88731 0.0 1030	0.54259 0.0001 1030	0.44925 0.0001 1030	0.54259 0.0001 1030	0.98258 0.0 1030
INT_95	0.99871 0.0 1030	0.98728 0.0 1030	0.92745 0.0 1030	0.82316 0.0001 1030	-0.53948 0.0001 1030	0.96874 0.0 1030	0.99758 0.0 1030	0.98024 0.0 1030	0.67182 0.0001 1030	0.64590 0.0001 1030	0.67182 0.0001 1030	0.91661 0.0 1030
INT105	0.98098 0.0 1030	0.98363 0.0 1030	0.96039 0.0 1030	0.86014 0.0001 1030	-0.47127 0.0001 1030	0.92947 0.0 1030	0.97533 0.0 1030	0.99686 0.0 1030	0.66142 0.0001 1030	0.71250 0.0001 1030	0.66142 0.0001 1030	0.84749 0.0001 1030
INT115	0.94293 0.0 1030	0.92073 0.0 1030	0.99276 0.0 1030	0.94317 0.0 1030	-0.44127 0.0001 1030	0.86654 0.0 1030	0.93135 0.0 1030	0.97359 0.0 1030	0.67538 0.0001 1030	0.77402 0.0001 1030	0.67538 0.0001 1030	0.76686 0.0001 1030

Pairwise Correlations of All Possible Pairs of Non-Zero Variables

CORRELATION ANALYSIS

Pearson Correlation Coefficients / Prob > |R| under Ho: Rho=0 / Number of Observations

	SUR115	SUR125	SUR135	SUR145	SURAVZ	AMB_75	AMB_85	AMB_95	AMB105	ANRAVZ	PT_75	PT_85
INTAVZ	-0.45347 0.0001 1030	-0.41404 0.0001 1030	-0.16608 0.0001 1030	-0.02933 0.3471 1030	0.78416 0.0001 1030	-0.61220 0.0001 1030	-0.46328 0.0001 1030	-0.29757 0.0001 1030	-0.50159 0.0001 1030	0.05422 0.0820 1030	-0.50159 0.0001 1030	-0.60198 0.0001 1030
MID_85	0.96706 0.0 1030	0.96419 0.0 1030	0.81213 0.0001 1030	0.69261 0.0001 1030	-0.52798 0.0001 1030	0.97290 0.0 1030	0.97697 0.0 1030	0.91552 0.0 1030	0.56162 0.0001 1030	0.48659 0.0001 1030	0.56162 0.0001 1030	0.97219 0.0 1030
MID_95	0.98979 0.0 1030	0.97045 0.0 1030	0.95604 0.0 1030	0.85930 0.0001 1030	-0.55119 0.0001 1030	0.95123 0.0 1030	0.98679 0.0 1030	0.98274 0.0 1030	0.70224 0.0001 1030	0.69138 0.0001 1030	0.70224 0.0001 1030	0.88138 0.0 1030
MID105	0.99457 0.0 1030	0.97998 0.0 1030	0.88404 0.0 1030	0.77971 0.0001 1030	-0.55814 0.0001 1030	0.98081 0.0 1030	0.99632 0.0 1030	0.95474 0.0 1030	0.65076 0.0001 1030	0.57998 0.0001 1030	0.65076 0.0001 1030	0.95108 0.0 1030
MID115	0.97800 0.0 1030	0.92666 0.0 1030	0.93994 0.0 1030	0.82801 0.0001 1030	-0.42575 0.0001 1030	0.92839 0.0 1030	0.97527 0.0 1030	0.99539 0.0 1030	0.60609 0.0001 1030	0.68424 0.0001 1030	0.60609 0.0001 1030	0.86028 0.0001 1030
MID125	0.86973 0.0 1030	0.81903 0.0001 1030	0.96703 0.0 1030	0.95567 0.0 1030	-0.49453 0.0001 1030	0.78960 0.0001 1030	0.85261 0.0001 1030	0.89753 0.0 1030	0.74310 0.0001 1030	0.79730 0.0001 1030	0.74310 0.0001 1030	0.66602 0.0001 1030
MIDAVE	-0.43768 0.0001 1030	-0.37985 0.0001 1030	-0.16721 0.0001 1030	-0.03549 0.2552 1030	0.86293 0.0001 1030	-0.60107 0.0001 1030	-0.44300 0.0001 1030	-0.27492 0.0001 1030	-0.57018 0.0001 1030	0.14205 0.0001 1030	-0.57018 0.0001 1030	-0.56686 0.0001 1030
SUR_85	0.93736 0.0 1030	0.89429 0.0 1030	0.90258 0.0 1030	0.81522 0.0001 1030	-0.72728 0.0001 1030	0.93293 0.0 1030	0.92483 0.0 1030	0.90747 0.0 1030	0.84006 0.0001 1030	0.66041 0.0001 1030	0.84006 0.0001 1030	0.80092 0.0001 1030
SUR_95	0.98089 0.0 1030	0.96838 0.0 1030	0.89512 0.0 1030	0.79914 0.0001 1030	-0.48961 0.0001 1030	0.95569 0.0 1030	0.98852 0.0 1030	0.95616 0.0 1030	0.58385 0.0001 1030	0.58978 0.0001 1030	0.58385 0.0001 1030	0.94129 0.0 1030
SUR105	0.99907 0.0 1030	0.98398 0.0 1030	0.91947 0.0 1030	0.81406 0.0001 1030	-0.53559 0.0001 1030	0.97308 0.0 1030	0.99848 0.0 1030	0.97363 0.0 1030	0.67030 0.0001 1030	0.62932 0.0001 1030	0.67030 0.0001 1030	0.92548 0.0 1030
SUR115	1.00000 0.0 1030	0.98296 0.0 1030	0.92099 0.0 1030	0.82117 0.0001 1030	-0.56342 0.0001 1030	0.97561 0.0 1030	0.99821 0.0 1030	0.97335 0.0 1030	0.68311 0.0001 1030	0.63247 0.0001 1030	0.68311 0.0001 1030	0.92398 0.0 1030
SUR125	0.98296 0.0 1030	1.00000 0.0 1030	0.90014 0.0 1030	0.77819 0.0001 1030	-0.46282 0.0001 1030	0.95235 0.0 1030	0.98302 0.0 1030	0.98006 0.0 1030	0.60994 0.0001 1030	0.63444 0.0001 1030	0.60994 0.0001 1030	0.89900 0.0 1030
SUR135	0.92099 0.0 1030	0.90014 0.0 1030	1.00000 0.0 1030	0.94190 0.0 1030	-0.41141 0.0001 1030	0.83432 0.0001 1030	0.90859 0.0 1030	0.96616 0.0 1030	0.66518 0.0001 1030	0.79009 0.0001 1030	0.66518 0.0001 1030	0.72910 0.0001 1030

Pairwise Correlations of All Possible Pairs of Non-Zero Variables

CORRELATION ANALYSIS

Pearson Correlation Coefficients / Prob > |R| under Ho: Rho=0 / Number of Observations

	SUR115	SUR125	SUR135	SUR145	SURAVE	AMB_75	AMB_85	AMB_95	AMB105	AMBAVE	FT_75	FT_85
SUR145	0.82117 0.0001 1030	0.77819 0.0001 1030	0.94190 0.0 1030	1.00000 0.0 1030	-0.33810 0.0001 1030	0.71648 0.0001 1030	0.80528 0.0001 1030	0.86923 0.0 1030	0.59176 0.0001 1030	0.76308 0.0001 1030	0.59176 0.0001 1030	0.60957 0.0001 1030
SURAVE	-0.56342 0.0001 1030	-0.46282 0.0001 1030	-0.41141 0.0001 1030	-0.33810 0.0001 1030	1.00000 0.0 1030	-0.67995 0.0001 1030	-0.55350 0.0001 1030	-0.42411 0.0001 1030	-0.84410 0.0001 1030	-0.18776 0.0001 1030	-0.84410 0.0001 1030	-0.57445 0.0001 1030
AMB_75	0.97561 0.0 1030	0.95235 0.0 1030	0.83432 0.0001 1030	0.71648 0.0001 1030	-0.67995 0.0001 1030	1.00000 0.0 1030	0.97683 0.0 1030	0.91319 0.0 1030	0.71287 0.0001 1030	0.52113 0.0001 1030	0.71287 0.0001 1030	0.94698 0.0 1030
AMB_85	0.99821 0.0 1030	0.98302 0.0 1030	0.90859 0.0 1030	0.80528 0.0001 1030	-0.55350 0.0001 1030	0.97683 0.0 1030	1.00000 0.0 1030	0.96766 0.0 1030	0.65752 0.0001 1030	0.61168 0.0001 1030	0.65752 0.0001 1030	0.93839 0.0 1030
AMB_95	0.97335 0.0 1030	0.98006 0.0 1030	0.96616 0.0 1030	0.86923 0.0 1030	-0.42411 0.0001 1030	0.91319 0.0 1030	0.96766 0.0 1030	1.00000 0.0 1030	0.63159 0.0001 1030	0.72656 0.0001 1030	0.63159 0.0001 1030	0.83330 0.0001 1030
AMB105	0.68311 0.0001 1030	0.60994 0.0001 1030	0.66518 0.0001 1030	0.59176 0.0001 1030	-0.84410 0.0001 1030	0.71287 0.0001 1030	0.65752 0.0001 1030	0.63159 0.0001 1030	1.00000 0.0 1030	0.58956 0.0001 1030	1.00000 0.0 1030	0.56685 0.0001 1030
AMBAVE	0.63247 0.0001 1030	0.63444 0.0001 1030	0.79009 0.0001 1030	0.76308 0.0001 1030	-0.18776 0.0001 1030	0.52113 0.0001 1030	0.61168 0.0001 1030	0.72656 0.0001 1030	0.58956 0.0001 1030	1.00000 0.0 1030	0.58956 0.0001 1030	0.41025 0.0001 1030
FT_75	0.68311 0.0001 1030	0.60994 0.0001 1030	0.66518 0.0001 1030	0.59176 0.0001 1030	-0.84410 0.0001 1030	0.71287 0.0001 1030	0.65752 0.0001 1030	0.63159 0.0001 1030	1.00000 0.0 1030	0.58956 0.0001 1030	1.00000 0.0 1030	0.56685 0.0001 1030
FT_85	0.92398 0.0 1030	0.89900 0.0 1030	0.72910 0.0001 1030	0.60957 0.0001 1030	-0.57445 0.0001 1030	0.94698 0.0 1030	0.93839 0.0 1030	0.83330 0.0001 1030	0.56685 0.0001 1030	0.41025 0.0001 1030	0.56685 0.0001 1030	1.00000 0.0 1030
FT_95	0.98526 0.0 1030	0.98385 0.0 1030	0.96027 0.0 1030	0.86333 0.0001 1030	-0.48461 0.0001 1030	0.93764 0.0 1030	0.98001 0.0 1030	0.99672 0.0 1030	0.66053 0.0001 1030	0.70104 0.0001 1030	0.66053 0.0001 1030	0.85395 0.0001 1030
FT_105	0.83685 0.0001 1030	0.79038 0.0001 1030	0.95301 0.0 1030	0.98501 0.0 1030	-0.39430 0.0001 1030	0.74128 0.0001 1030	0.82188 0.0001 1030	0.87796 0.0 1030	0.63763 0.0001 1030	0.77631 0.0001 1030	0.63763 0.0001 1030	0.62374 0.0001 1030
FT_AVE	0.77227 0.0001 1030	0.71587 0.0001 1030	0.83906 0.0001 1030	0.79439 0.0001 1030	-0.67379 0.0001 1030	0.74062 0.0001 1030	0.74653 0.0001 1030	0.77659 0.0001 1030	0.90938 0.0 1030	0.82425 0.0001 1030	0.90938 0.0 1030	0.57278 0.0001 1030
VARIANCE	-0.01954 0.5310 1030	-0.00674 0.8289 1030	-0.00878 0.7783 1030	0.00266 0.9319 1030	0.12807 0.0001 1030	-0.03365 0.2806 1030	-0.01533 0.6231 1030	-0.00351 0.9105 1030	-0.12280 0.0001 1030	-0.03901 0.2110 1030	-0.12280 0.0001 1030	-0.01886 0.5455 1030

Pairwise Correlations of All Possible Pairs of Non-Zero Variables

CORRELATION ANALYSIS

Pearson Correlation Coefficients / Prob > |R| under Ho: Rho=0 / Number of Observations

	SUR115	SUR125	SUR135	SUR145	SURAVE	AMB_75	AMB_85	AMB_95	AMBAYZ	FT_75	FT_85
LN_PASS	0.89884 0.0 1030	0.85276 0.0001 1030	0.88174 0.0 1030	0.79759 0.0001 1030	-0.66949 0.0001 1030	0.87232 0.0 1030	0.88353 0.0 1030	0.87091 0.0 1030	0.86118 0.0001 1030	0.86118 0.0001 1030	0.77939 0.0001 1030
Q_SKEW	-0.12749 0.0001 1030	-0.12806 0.0001 1030	-0.10388 0.0008 1030	-0.08211 0.0084 1030	0.07911 0.0111 1030	-0.12395 0.0001 1030	-0.12449 0.0001 1030	-0.11836 0.0001 1030	-0.13606 0.0001 1030	-0.13606 0.0001 1030	-0.12850 0.0001 1030
THICKNES	0.05258 0.0917 1030	0.03366 0.2805 1030	0.10798 0.0005 1030	0.13355 0.0001 1030	-0.00314 0.9198 1030	0.04050 0.1940 1030	0.05708 0.0671 1030	0.06773 0.0297 1030	0.04295 0.1684 1030	0.04295 0.1684 1030	0.04565 0.1432 1030
MIX_IND	0.36860 0.0001 1030	0.40742 0.0001 1030	0.29607 0.0001 1030	0.23079 0.0001 1030	-0.08323 0.0075 1030	0.36814 0.0001 1030	0.37457 0.0001 1030	0.37266 0.0001 1030	0.11852 0.0001 1030	0.11852 0.0001 1030	0.36845 0.0001 1030
DES_IND	0.05624 0.0712 1030	0.05525 0.0763 1030	0.11309 0.0003 1030	0.12028 0.0001 1030	0.03248 0.2977 1030	0.03355 0.2821 1030	0.06016 0.0536 1030	0.08202 0.0084 1030	0.03470 0.2659 1030	0.03470 0.2659 1030	0.03587 0.2500 1030
TRUTHICK	0.09698 0.0018 1030	0.08304 0.0077 1030	0.15004 0.0001 1030	0.17067 0.0001 1030	0.00005 0.9987 1030	0.08030 0.0099 1030	0.10148 0.0011 1030	0.11585 0.0002 1030	0.05115 0.1009 1030	0.05115 0.1009 1030	0.08310 0.0076 1030
PCTSMALL	0.26267 0.0001 1030	0.29231 0.0001 1030	0.25477 0.0001 1030	0.21985 0.0001 1030	-0.01199 0.7007 1030	0.24188 0.0001 1030	0.26469 0.0001 1030	0.28662 0.0001 1030	0.08805 0.0047 1030	0.08805 0.0047 1030	0.22877 0.0001 1030
PCMEDIUM	0.16210 0.0001 1030	0.18568 0.0001 1030	0.14484 0.0001 1030	0.12123 0.0001 1030	0.00684 0.8265 1030	0.14112 0.0001 1030	0.15647 0.0001 1030	0.17447 0.0001 1030	0.04991 0.1094 1030	0.04991 0.1094 1030	0.12094 0.0001 1030

Pairwise Correlations of All Possible Pairs of Non-Zero Variables

CORRELATION ANALYSIS

Pearson Correlation Coefficients / Prob > |R| under Ho: Rho=0 / Number of Observations

	FT_95	FT_105	FT_AVE	VARIANCE	LN_PASS	Q_SKEW	THICKNES	MIX_IND	DES_IND	TRUTHICK	PCTSMALL	PCTMEDIUM
MODE	-0.27822 0.0001 1030	-0.32357 0.0001 1030	-0.30870 0.0001 1030	0.17695 0.0001 1030	-0.33379 0.0001 1030	-0.24173 0.0001 1030	-0.30178 0.0001 1030	0.06665 0.0325 1030	-0.47123 0.0001 1030	-0.29284 0.0001 1030	0.01488 0.6334 1030	0.27535 0.0001 1030
MEAN	-0.10862 0.0005 1030	-0.18623 0.0001 1030	-0.17558 0.0001 1030	-0.43359 0.0001 1030	-0.14341 0.0001 1030	-0.58660 0.0001 1030	-0.24139 0.0001 1030	0.11501 0.0002 1030	-0.36684 0.0001 1030	-0.23510 0.0001 1030	0.01924 0.5374 1030	0.09260 0.0029 1030
ST_DEV	-0.00902 0.7726 1030	0.00061 0.9843 1030	-0.12399 0.0001 1030	0.99132 0.0 1030	-0.10726 0.0006 1030	0.24008 0.0001 1030	0.03362 0.2810 1030	0.09188 0.0032 1030	-0.03696 0.2359 1030	0.05178 0.0967 1030	0.08682 0.0053 1030	0.19552 0.0001 1030
PASSES	0.99322 0.0 1030	0.84679 0.0001 1030	0.76555 0.0001 1030	-0.01229 0.6937 1030	0.88732 0.0 1030	-0.12342 0.0001 1030	0.06083 0.0510 1030	0.37650 0.0001 1030	0.06750 0.0303 1030	0.10673 0.0006 1030	0.27379 0.0001 1030	0.16362 0.0001 1030
DT	0.29340 0.0001 1030	0.36051 0.0001 1030	0.46004 0.0001 1030	-0.02847 0.3614 1030	0.41960 0.0001 1030	-0.06652 0.0328 1030	-0.32614 0.0001 1030	-0.30754 0.0001 1030	-0.49201 0.0001 1030	-0.36595 0.0001 1030	-0.24396 0.0001 1030	0.07688 0.0136 1030
HU1	0.12460 0.0001 1030	0.29313 0.0001 1030	0.34768 0.0001 1030	-0.04457 0.1531 1030	0.25104 0.0001 1030	0.05751 0.0650 1030	0.13915 0.0001 1030	-0.46448 0.0001 1030	0.19943 0.0001 1030	0.12575 0.0001 1030	-0.20191 0.0001 1030	-0.13897 0.0001 1030
HU2	0.04706 0.1312 1030	0.19949 0.0001 1030	0.25977 0.0001 1030	-0.05155 0.0982 1030	0.16998 0.0001 1030	0.05406 0.0829 1030	0.15885 0.0001 1030	-0.46856 0.0001 1030	0.23116 0.0001 1030	0.16189 0.0001 1030	-0.21936 0.0001 1030	-0.22319 0.0001 1030
WR	0.41495 0.0001 1030	0.31927 0.0001 1030	0.25050 0.0001 1030	0.03260 0.2959 1030	0.36015 0.0001 1030	0.00675 0.8286 1030	-0.22472 0.0001 1030	0.26573 0.0001 1030	-0.32519 0.0001 1030	-0.22538 0.0001 1030	0.00404 0.8970 1030	0.23553 0.0001 1030
A2	0.05957 0.0595 1009	0.20754 0.0001 1009	0.28217 0.0001 1009	-0.04404 0.1622 1009	0.19437 0.0001 1009	0.03870 0.2193 1009	0.15593 0.0001 1009	-0.42055 0.0001 1009	0.22369 0.0001 1009	0.16905 0.0001 1009	-0.17091 0.0001 1009	-0.15050 0.0001 1009
A1	0.40959 0.0001 1030	0.32591 0.0001 1030	0.39740 0.0001 1030	0.03396 0.2762 1030	0.44705 0.0001 1030	-0.11082 0.0004 1030	-0.57829 0.0001 1030	0.10213 0.0010 1030	-0.68737 0.0001 1030	-0.56608 0.0001 1030	0.00379 0.9033 1030	0.39478 0.0001 1030
BSFWDISM	0.08813 0.0047 1030	0.13679 0.0001 1030	0.08601 0.0057 1030	-0.05875 0.0594 1030	0.08782 0.0048 1030	0.04538 0.1456 1030	0.52271 0.0001 1030	0.00951 0.7605 1030	0.98677 0.0 1030	0.52173 0.0001 1030	0.13309 0.0001 1030	-0.28526 0.0001 1030
PVFWDISM	0.07959 0.0106 1030	0.13228 0.0001 1030	0.08191 0.0085 1030	-0.06182 0.0473 1030	0.08198 0.0085 1030	0.04802 0.1235 1030	0.56021 0.0001 1030	-0.00754 0.8090 1030	0.98963 0.0 1030	0.55537 0.0001 1030	0.13858 0.0001 1030	-0.32490 0.0001 1030
BULADENS	-0.24610 0.0001 1030	-0.13024 0.0001 1030	-0.08603 0.0057 1030	-0.11701 0.0002 1030	-0.13361 0.0001 1030	0.11326 0.0003 1030	0.48828 0.0001 1030	-0.70906 0.0001 1030	0.19200 0.0001 1030	0.39938 0.0001 1030	-0.59166 0.0001 1030	-0.73333 0.0001 1030

Pairwise Correlations of All Possible Pairs of Non-Zero Variables

CORRELATION ANALYSIS

Pearson Correlation Coefficients / Prob > |R| under Ho: Rho=0 / Number of Observations

	FT_95	FT_105	FT_AVE	VARIANCE	LN_PASS	Q_SKEW	THICKNES	MIX_IND	DES_IND	TRUTHICK	PCTSMALL	PCTMEDIUM
ASPHCONT	-0.34762 0.0001 1030	-0.21097 0.0001 1030	-0.13163 0.0001 1030	-0.08079 0.0095 1030	-0.20588 0.0001 1030	0.12102 0.0001 1030	0.11641 0.0002 1030	-0.97195 0.0 1030	0.16599 0.0001 1030	0.01171 0.7073 1030	-0.52061 0.0001 1030	-0.41907 0.0001 1030
THAXDENS	0.33037 0.0001 1030	0.20174 0.0001 1030	0.12430 0.0001 1030	0.05559 0.0745 1030	0.19049 0.0001 1030	-0.07132 0.0221 1030	-0.05962 0.0558 1030	0.93397 0.0 1030	0.01635 0.6001 1030	0.06182 0.0473 1030	0.64961 0.0001 1030	0.32517 0.0001 1030
ASPHVOLM	-0.34920 0.0001 1030	-0.20890 0.0001 1030	-0.13088 0.0001 1030	-0.08811 0.0047 1030	-0.20496 0.0001 1030	0.12403 0.0001 1030	0.16824 0.0001 1030	-0.97972 0.0 1030	0.17372 0.0001 1030	0.06229 0.0456 1030	-0.55463 0.0001 1030	-0.47367 0.0001 1030
VOIDSTOT	0.30475 0.0001 1030	0.17225 0.0001 1030	0.10995 0.0004 1030	0.10191 0.0011 1030	0.17009 0.0001 1030	-0.10613 0.0006 1030	-0.35329 0.0001 1030	0.97132 0.0 1030	-0.12354 0.0001 1030	-0.24249 0.0001 1030	0.67338 0.0001 1030	0.62816 0.0001 1030
VOIDSPIL	-0.32391 0.0001 1030	-0.18223 0.0001 1030	-0.11518 0.0002 1030	-0.09506 0.0023 1030	-0.18211 0.0001 1030	0.10574 0.0007 1030	0.30289 0.0001 1030	-0.92741 0.0 1030	0.13479 0.0001 1030	0.19760 0.0001 1030	-0.66321 0.0001 1030	-0.57570 0.0001 1030
SIX_85	0.75716 0.0001 1030	0.48995 0.0001 1030	0.35856 0.0001 1030	0.02273 0.4663 1030	0.58744 0.0001 1030	-0.09985 0.0013 1030	0.03433 0.2710 1030	0.39660 0.0001 1030	0.02034 0.5102 1030	0.07592 0.0148 1030	0.24089 0.0001 1030	0.12581 0.0001 1030
SIX_95	0.99823 0.0 1030	0.88650 0.0 1030	0.82078 0.0001 1030	-0.01969 0.5278 1030	0.91204 0.0 1030	-0.12275 0.0001 1030	0.06378 0.0407 1030	0.35345 0.0001 1030	0.07491 0.0162 1030	0.10841 0.0005 1030	0.26793 0.0001 1030	0.16430 0.0001 1030
SIXAVE	-0.13732 0.0001 1030	0.13689 0.0001 1030	0.30933 0.0001 1030	-0.05425 0.0818 1030	0.08894 0.0043 1030	-0.00069 0.9824 1030	0.01581 0.6122 1030	-0.25195 0.0001 1030	0.03404 0.2751 1030	-0.00946 0.7618 1030	-0.12141 0.0001 1030	-0.04998 0.1089 1030
INT_75	0.70146 0.0001 1030	0.41438 0.0001 1030	0.25681 0.0001 1030	0.04476 0.1511 1030	0.49363 0.0001 1030	-0.09815 0.0016 1030	-0.02083 0.5043 1030	0.40622 0.0001 1030	-0.01123 0.7188 1030	0.02678 0.3906 1030	0.25409 0.0001 1030	0.17496 0.0001 1030
INT_85	0.90462 0.0 1030	0.67524 0.0001 1030	0.58792 0.0001 1030	-0.00239 0.9389 1030	0.76959 0.0001 1030	-0.11273 0.0003 1030	0.05103 0.1017 1030	0.40092 0.0001 1030	0.03874 0.2141 1030	0.09425 0.0025 1030	0.25705 0.0001 1030	0.13728 0.0001 1030
INT_95	0.98971 0.0 1030	0.83978 0.0001 1030	0.76795 0.0001 1030	-0.01453 0.6413 1030	0.89111 0.0 1030	-0.12560 0.0001 1030	0.05374 0.0847 1030	0.37349 0.0001 1030	0.06083 0.0510 1030	0.09926 0.0014 1030	0.26939 0.0001 1030	0.16536 0.0001 1030
INT105	0.99806 0.0 1030	0.87134 0.0001 1030	0.79495 0.0001 1030	-0.01521 0.6259 1030	0.89460 0.0 1030	-0.12382 0.0001 1030	0.05995 0.0544 1030	0.36430 0.0001 1030	0.07990 0.0103 1030	0.10586 0.0007 1030	0.27842 0.0001 1030	0.16913 0.0001 1030
INT115	0.97172 0.0 1030	0.95882 0.0 1030	0.84164 0.0001 1030	-0.00755 0.8088 1030	0.89718 0.0 1030	-0.10832 0.0005 1030	0.10533 0.0007 1030	0.31619 0.0001 1030	0.09822 0.0016 1030	0.14944 0.0001 1030	0.25891 0.0001 1030	0.15499 0.0001 1030

Pairwise Correlations of All Possible Pairs of Non-Zero Variables

CORRELATION ANALYSIS

Pearson Correlation Coefficients / Prob > |R| under Ho: Rho=0 / Number of Observations

	FT_95	FT_105	FT_AVE	VARIANCE	LN_PASS	Q_SKEW	THICKNES	MIX_IND	DES_IND	TRUTHICK	PCTSMALL	PCHMEDUM
INTAVE	-0.35103 0.0001 1030	-0.06055 0.0521 1030	-0.30400 0.0001 1030	0.07534 0.0156 1030	-0.36692 0.0001 1030	0.06635 0.0332 1030	0.05503 0.0733 1030	-0.19157 0.0001 1030	0.07638 0.0142 1030	0.04723 0.1299 1030	-0.06062 0.0518 1030	-0.02423 0.4373 1030
MID_85	0.93015 0.0 1030	0.70401 0.0001 1030	0.61570 0.0001 1030	-0.00003 0.9992 1030	0.78798 0.0001 1030	-0.11568 0.0002 1030	0.03887 0.2126 1030	0.41353 0.0001 1030	0.03625 0.2450 1030	0.08520 0.0062 1030	0.27220 0.0001 1030	0.15810 0.0001 1030
MID_95	0.99123 0.0 1030	0.88000 0.0 1030	0.81709 0.0001 1030	-0.02441 0.4339 1030	0.91655 0.0 1030	-0.12083 0.0001 1030	0.07975 0.0105 1030	0.34192 0.0001 1030	0.07883 0.0114 1030	0.12104 0.0001 1030	0.25194 0.0001 1030	0.14066 0.0001 1030
MID105	0.96825 0.0 1030	0.79293 0.0001 1030	0.72019 0.0001 1030	-0.01192 0.7023 1030	0.86704 0.0 1030	-0.12783 0.0001 1030	0.04356 0.1624 1030	0.38233 0.0001 1030	0.05007 0.1083 1030	0.08914 0.0042 1030	0.26874 0.0001 1030	0.16676 0.0001 1030
MID115	0.99417 0.0 1030	0.83559 0.0001 1030	0.74077 0.0001 1030	-0.00414 0.8945 1030	0.85701 0.0001 1030	-0.12134 0.0001 1030	0.04908 0.1155 1030	0.39158 0.0001 1030	0.07029 0.0241 1030	0.09811 0.0016 1030	0.29137 0.0001 1030	0.18042 0.0001 1030
MID125	0.90077 0.0 1030	0.98348 0.0 1030	0.90554 0.0 1030	-0.02683 0.3898 1030	0.90797 0.0 1030	-0.10283 0.0009 1030	0.13260 0.0001 1030	0.22524 0.0001 1030	0.11712 0.0002 1030	0.16692 0.0001 1030	0.20988 0.0001 1030	0.11765 0.0002 1030
MIDAVE	-0.33462 0.0001 1030	-0.07047 0.0237 1030	-0.31882 0.0001 1030	0.08167 0.0087 1030	-0.40161 0.0001 1030	0.05094 0.1023 1030	0.06701 0.0315 1030	-0.15522 0.0001 1030	0.08833 0.0046 1030	0.06483 0.0375 1030	-0.02501 0.4236 1030	-0.00555 0.8588 1030
SUR_85	0.93226 0.0 1030	0.86036 0.0001 1030	0.90927 0.0 1030	-0.05729 0.0661 1030	0.94895 0.0 1030	-0.11603 0.0002 1030	0.05844 0.0608 1030	0.28002 0.0001 1030	0.05582 0.0733 1030	0.09188 0.0032 1030	0.20779 0.0001 1030	0.12852 0.0001 1030
SUR_95	0.96386 0.0 1030	0.80678 0.0001 1030	0.68248 0.0001 1030	0.00095 0.9757 1030	0.82714 0.0001 1030	-0.11173 0.0003 1030	0.08472 0.0065 1030	0.38173 0.0001 1030	0.07356 0.0182 1030	0.12893 0.0001 1030	0.26626 0.0001 1030	0.13609 0.0001 1030
SUR105	0.98510 0.0 1030	0.83127 0.0001 1030	0.76345 0.0001 1030	-0.01663 0.5939 1030	0.89129 0.0 1030	-0.12551 0.0001 1030	0.05202 0.0952 1030	0.36893 0.0001 1030	0.05950 0.0563 1030	0.09675 0.0019 1030	0.26562 0.0001 1030	0.16314 0.0001 1030
SUR115	0.98526 0.0 1030	0.83685 0.0001 1030	0.77227 0.0001 1030	-0.01954 0.5310 1030	0.89884 0.0 1030	-0.12749 0.0001 1030	0.05258 0.0917 1030	0.36860 0.0001 1030	0.05624 0.0712 1030	0.09698 0.0018 1030	0.26267 0.0001 1030	0.16210 0.0001 1030
SUR125	0.98385 0.0 1030	0.79038 0.0001 1030	0.71587 0.0001 1030	-0.00674 0.8289 1030	0.85276 0.0001 1030	-0.12806 0.0001 1030	0.03366 0.2805 1030	0.40742 0.0001 1030	0.05525 0.0763 1030	0.08304 0.0077 1030	0.29231 0.0001 1030	0.18568 0.0001 1030
SUR135	0.96027 0.0 1030	0.95301 0.0 1030	0.83906 0.0001 1030	-0.00878 0.7783 1030	0.88174 0.0 1030	-0.10388 0.0008 1030	0.10798 0.0005 1030	0.29607 0.0001 1030	0.11309 0.0003 1030	0.15004 0.0001 1030	0.25477 0.0001 1030	0.14484 0.0001 1030

Pairwise Correlations of All Possible Pairs of Non-Zero Variables

CORRELATION ANALYSIS

Pearson Correlation Coefficients / Prob > |R| under Ho: Rho=0 / Number of Observations

	FT_95	FT_105	FT_AVE	VARIANCE	LN_PASS	Q_SKEW	THICKNES	MIX_IND	DES_IND	TRUTHICK	PCTSMALL	POWEDIUM
SUR145	0.86333 0.0001 1030	0.98501 0.0 1030	0.79439 0.0001 1030	0.00266 0.9319 1030	0.79759 0.0001 1030	-0.08211 0.0084 1030	0.13355 0.0001 1030	0.23079 0.0001 1030	0.12028 0.0001 1030	0.17067 0.0001 1030	0.21985 0.0001 1030	0.12123 0.0001 1030
SURAVE	-0.48461 0.0001 1030	-0.39430 0.0001 1030	-0.67379 0.0001 1030	0.12807 0.0001 1030	-0.66949 0.0001 1030	0.07911 0.0111 1030	-0.00314 0.9198 1030	-0.08323 0.0075 1030	0.03248 0.2377 1030	0.00005 0.9987 1030	-0.01199 0.7007 1030	0.00684 0.8265 1030
AMB_75	0.93764 0.0 1030	0.74128 0.0001 1030	0.74062 0.0001 1030	-0.03365 0.2806 1030	0.87232 0.0 1030	-0.12395 0.0001 1030	0.04050 0.1940 1030	0.36814 0.0001 1030	0.03355 0.2821 1030	0.08030 0.0099 1030	0.24188 0.0001 1030	0.14112 0.0001 1030
AMB_85	0.98001 0.0 1030	0.82188 0.0001 1030	0.74653 0.0001 1030	-0.01533 0.8231 1030	0.88353 0.0 1030	-0.12449 0.0001 1030	0.05708 0.0671 1030	0.37457 0.0001 1030	0.06016 0.0536 1030	0.10148 0.0011 1030	0.26469 0.0001 1030	0.15647 0.0001 1030
AMB_95	0.99672 0.0 1030	0.87796 0.0 1030	0.77659 0.0001 1030	-0.00351 0.9105 1030	0.87091 0.0 1030	-0.11836 0.0001 1030	0.06773 0.0297 1030	0.37266 0.0001 1030	0.08202 0.0084 1030	0.11585 0.0002 1030	0.28662 0.0001 1030	0.17447 0.0001 1030
AMB105	0.66053 0.0001 1030	0.63763 0.0001 1030	0.90938 0.0 1030	-0.12280 0.0001 1030	0.86118 0.0001 1030	-0.13606 0.0001 1030	0.04295 0.1684 1030	0.11852 0.0001 1030	0.03470 0.2659 1030	0.05115 0.1009 1030	0.08805 0.0047 1030	0.04991 0.1094 1030
AMBAVE	0.70104 0.0001 1030	0.77631 0.0001 1030	0.82425 0.0001 1030	-0.03901 0.2110 1030	0.68382 0.0001 1030	-0.12803 0.0001 1030	0.11313 0.0003 1030	0.15821 0.0001 1030	0.11784 0.0002 1030	0.13902 0.0001 1030	0.18337 0.0001 1030	0.10568 0.0007 1030
FT_75	0.66053 0.0001 1030	0.63763 0.0001 1030	0.90938 0.0 1030	-0.12280 0.0001 1030	0.86118 0.0001 1030	-0.13606 0.0001 1030	0.04295 0.1684 1030	0.11852 0.0001 1030	0.03470 0.2659 1030	0.05115 0.1009 1030	0.08805 0.0047 1030	0.04991 0.1094 1030
FT_85	0.85395 0.0001 1030	0.62374 0.0001 1030	0.57278 0.0001 1030	-0.01886 0.5455 1030	0.77939 0.0001 1030	-0.12850 0.0001 1030	0.04585 0.1432 1030	0.36645 0.0001 1030	0.03587 0.2500 1030	0.08310 0.0076 1030	0.22877 0.0001 1030	0.12094 0.0001 1030
FT_95	1.00000 0.0 1030	0.87715 0.0 1030	0.79164 0.0001 1030	-0.01009 0.7463 1030	0.88689 0.0 1030	-0.11823 0.0001 1030	0.06089 0.0508 1030	0.36904 0.0001 1030	0.07293 0.0192 1030	0.10778 0.0005 1030	0.27822 0.0001 1030	0.17118 0.0001 1030
FT_105	0.87715 0.0 1030	1.00000 0.0 1030	0.83854 0.0001 1030	0.00170 0.9566 1030	0.83292 0.0001 1030	-0.08317 0.0076 1030	0.14661 0.0001 1030	0.23592 0.0001 1030	0.12572 0.0001 1030	0.18515 0.0001 1030	0.22652 0.0001 1030	0.12637 0.0001 1030
FT_AVE	0.79164 0.0001 1030	0.83854 0.0001 1030	1.00000 0.0 1030	-0.09527 0.0022 1030	0.90940 0.0 1030	-0.13077 0.0001 1030	0.08296 0.0077 1030	0.14775 0.0001 1030	0.07813 0.0121 1030	0.10144 0.0011 1030	0.14138 0.0001 1030	0.08340 0.0074 1030
VARIANCE	-0.01009 0.7463 1030	0.00170 0.9566 1030	-0.09527 0.0022 1030	1.00000 0.0 1030	-0.08489 0.0064 1030	0.25548 0.0001 1030	0.00576 0.8536 1030	0.07392 0.0177 1030	-0.05728 0.0661 1030	0.01555 0.6182 1030	0.07040 0.0238 1030	0.18916 0.0001 1030

Pairwise Correlations of All Possible Pairs of Non-Zero Variables

28

CORRELATION ANALYSIS

Pearson Correlation Coefficients / Prob > |R| under Ho: Rho=0 / Number of Observations

	FT_95	FT_105	FT_AVE	VARIANCE	LN_PASS	Q_SKEW	THICKNES	MIX_IND	DES_IND	TRUTHICK	PCTSMALL	PCMEDM
LN_PASS	0.88689 0.0 1030	0.83292 0.0001 1030	0.90940 0.0 1030	-0.08489 0.0064 1030	1.00000 0.0 1030	-0.14865 0.0001 1030	0.06915 0.0265 1030	0.22242 0.0001 1030	0.07749 0.0129 1030	0.09419 0.0025 1030	0.17087 0.0001 1030	0.10118 0.0001 1030
Q_SKEW	-0.11823 0.0001 1030	-0.08317 0.0076 1030	-0.13077 0.0001 1030	0.25548 0.0001 1030	-0.14865 0.0001 1030	1.00000 0.0 1030	-0.03011 0.3344 1030	-0.12501 0.0001 1030	0.04443 0.1542 1030	-0.08006 0.0102 1030	-0.16718 0.0001 1030	-0.18581 0.0001 1030
THICKNES	0.06089 0.0508 1030	0.14661 0.0001 1030	0.08296 0.0077 1030	0.00576 0.8536 1030	0.06915 0.0265 1030	-0.03011 0.3344 1030	1.00000 0.0 1030	-0.09038 0.0037 1030	0.52250 0.0001 1030	0.92181 0.0 1030	-0.01528 0.6242 1030	-0.52125 0.0001 1030
MIX_IND	0.36904 0.0001 1030	0.23592 0.0001 1030	0.14775 0.0001 1030	0.07392 0.0177 1030	0.22242 0.0001 1030	-0.12501 0.0001 1030	-0.09038 0.0037 1030	1.00000 0.0 1030	-0.02874 0.3568 1030	0.03309 0.2887 1030	0.63156 0.0001 1030	0.45387 0.0001 1030
DES_IND	0.07293 0.0192 1030	0.12572 0.0001 1030	0.07813 0.0121 1030	-0.05728 0.0661 1030	0.07749 0.0129 1030	0.04443 0.1542 1030	0.52250 0.0001 1030	-0.02874 0.3568 1030	1.00000 0.0 1030	0.51469 0.0001 1030	0.12942 0.0001 1030	-0.29779 0.0001 1030
TRUTHICK	0.10778 0.0005 1030	0.18515 0.0001 1030	0.10144 0.0011 1030	0.01555 0.6182 1030	0.09419 0.0025 1030	-0.08006 0.0102 1030	0.92181 0.0 1030	0.03309 0.2887 1030	0.51469 0.0001 1030	1.00000 0.0 1030	0.14681 0.0001 1030	-0.39715 0.0001 1030
PCTSMALL	0.27822 0.0001 1030	0.22652 0.0001 1030	0.14138 0.0001 1030	0.07040 0.0238 1030	0.17087 0.0001 1030	-0.16718 0.0001 1030	-0.01528 0.6242 1030	0.63156 0.0001 1030	0.12942 0.0001 1030	0.14681 0.0001 1030	1.00000 0.0 1030	0.32136 0.0001 1030
PCMEDM	0.17118 0.0001 1030	0.12637 0.0001 1030	0.08340 0.0074 1030	0.18916 0.0001 1030	0.10118 0.0011 1030	-0.18581 0.0001 1030	-0.52125 0.0001 1030	0.45387 0.0001 1030	-0.29779 0.0001 1030	-0.39715 0.0001 1030	0.32136 0.0001 1030	1.00000 0.0 1030

APPENDIX H

RESULTS OF STEPWISE REGRESSION MODELS

Stepwise Regression Results for Dependent Variable DT

R-square = 0.69537191 C(p) = 10.62977138

	DF	Sum of Squares	Mean Square	F	Prob>F
Regression	10	177.01685943	17.70168594	227.81	0.0001
Error	998	77.54743560	0.07770284	-mse	
Total	1008	254.56429503			

Variable	Parameter Estimate	Standard Error	Type II Sum of Squares	F	Prob>F
intercept	-27.46644280	3.29647395	5.39439121	69.42	0.0001
LN_PASS	0.23553798	0.00819384	64.20727273	826.32	0.0001
ST_DEV	-0.38563620	0.07995716	1.80749794	23.26	0.0001
VARIANCE	0.01585799	0.00308606	2.05175020	26.41	0.0001
Q_SKEW	-0.12211429	0.04019436	0.71719913	9.23	0.0024
PVFWDISM	-0.00015742	0.00000663	43.75173900	563.06	0.0001
BULKDENS	0.05792197	0.00732821	4.85431126	62.47	0.0001
ASPHCONT	0.48164218	0.03505400	14.66934495	188.79	0.0001
TMAXDENS	0.10870507	0.01427616	4.50519510	57.98	0.0001
TRUTHICK	-0.10545457	0.01478513	3.95291344	50.87	0.0001
PCMEDIUM	0.01826960	0.00487709	1.09036693	14.03	0.0002

Stepwise Regression Results for Dependent Variable HU1

R-square = 0.44344981 C(p) = 15.64541534

	DF	Sum of Squares	Mean Square	F	Prob>F
Regression	9	5.52039498	0.61337722	88.44	0.0001
Error	999	6.92835310	0.00693529	-mse	
Total	1008	12.44874808			

Variable	Parameter Estimate	Standard Error	Type II Sum of Squares	F	Prob>F
intercept	-4.83864348	0.36895435	1.19279690	171.99	0.0001
PASSES	-0.00000602	0.00000193	0.06737175	9.71	0.0019
LN_PASS	0.04763292	0.00511533	0.60135626	86.71	0.0001
Q_SKEW	0.04240207	0.01139746	0.09598929	13.84	0.0002
PVFWDISM	0.00000750	0.00000190	0.10857124	15.65	0.0001
BULKDENS	0.02332974	0.00225872	0.73987613	106.68	0.0001
ASPHCONT	0.06654293	0.00585521	0.89574281	129.16	0.0001
TRUTHICK	-0.00686042	0.00441094	0.01677660	2.42	0.1202
PCMEDIUM	0.01405719	0.00136412	0.73647272	106.19	0.0001
PCTSMALL	0.01593107	0.00320824	0.17100947	24.66	0.0001

Stepwise Regression Results for Dependent Variable A2

R-square = 0.41058484 C(p) = 14.23994920

	DF	Sum of Squares	Mean Square	F	Prob>F
Regression	9	2599.55512808	288.83945868	77.32	0.0001
Error	999	3731.79188451	3.73552741	=mse	
Total	1008	6331.34701259			

Variable	Parameter Estimate	Standard Error	Type II Sum of Squares	F	Prob>F
intercept	-128.19288355	8.56281056	837.23444724	224.13	0.0001
PASSES	-0.00020221	0.00004482	76.03712417	20.36	0.0001
LN_PASS	1.06923425	0.11871819	303.01427682	81.12	0.0001
Q_SKEW	0.72186403	0.26451583	27.82014550	7.45	0.0065
PVFWDISM	0.00021697	0.00004402	90.76029514	24.30	0.0001
BULKDENS	0.65517030	0.05242113	583.50910627	156.21	0.0001
ASPHCONT	1.02529012	0.13588960	212.65375400	56.93	0.0001
TRUTHICK	-0.18597876	0.10237046	12.32904070	3.30	0.0696
PCMEDIUM	0.34876876	0.03165892	453.35139590	121.36	0.0001
PCTSMALL	0.44414649	0.07445790	132.91768790	35.58	0.0001

Stepwise Regression Results for Dependent Variable A1

R-square = 0.82356787 C(p) = 12.28329668

	DF	Sum of Squares	Mean Square	F	Prob>F
Regression	11	113131.43886897	10284.67626082	423.08	0.0000
Error	997	24236.03602934	24.30896292	=mse	
Total	1008	137367.47489831			

Variable	Parameter Estimate	Standard Error	Type II Sum of Squares	F	Prob>F
intercept	-377.28036258	58.54883824	1009.38830544	41.52	0.0001
PASSES	0.00050598	0.00012118	423.80398839	17.43	0.0001
LN_PASS	4.01861935	0.33329459	3533.97638182	145.38	0.0001
ST_DEV	-2.45176964	1.49439686	65.43255298	2.69	0.1012
VARIANCE	0.11974458	0.05743266	105.67209951	4.35	0.0373
Q_SKEW	-2.56905291	0.71210518	316.39108763	13.02	0.0003
PVFWDISM	-0.00395845	0.00011734	27665.82206725	1138.09	0.0001
BULKDENS	0.49918104	0.12978246	359.62557251	14.79	0.0001
ASPHCONT	4.72153434	0.62254634	1398.26461326	57.52	0.0001
TMAXDENS	1.78509208	0.25278137	1212.26490420	49.87	0.0001
TRUTHICK	-3.90395080	0.26160671	5413.48996051	222.70	0.0001
PCMEDIUM	0.39399180	0.08638314	505.68820851	20.80	0.0001

Stepwise Regression Results for Dependent Variable HU2

R-square = 0.42016959 C(p) = 10.62453987

	DF	Sum of Squares	Mean Square	F	Prob>F
Regression	9	3.33721118	0.37080124	80.44	0.0001
Error	999	4.60532260	0.00460993 =mse		
Total	1008	7.94253378			

Variable	Parameter Estimate	Standard Error	Type II Sum of Squares	F	Prob>F
intercept	-4.47261989	0.30080681	1.01916204	221.08	0.0001
PASSES	-0.00000508	0.00000157	0.04800810	10.41	0.0013
LN_PASS	0.03184627	0.00417050	0.26880327	58.31	0.0001
Q_SKEW	0.02328770	0.00929230	0.02895355	6.28	0.0124
PVFWDISM	0.00000809	0.00000155	0.12617165	27.37	0.0001
BULKDENS	0.02376895	0.00184153	0.76799660	166.60	0.0001
ASPHCONT	0.03662013	0.00477373	0.27128088	58.85	0.0001
TRUTHICK	-0.01187245	0.00359622	0.05024389	10.90	0.0010
PCMEDIUM	0.00983680	0.00111216	0.36063464	78.23	0.0001
PCTSMALL	0.01584263	0.00261567	0.16911608	36.69	0.0001

Stepwise Regression Results for Dependent Variable WR

R-square = 0.36151213 C(p) = 19.61208843

	DF	Sum of Squares	Mean Square	F	Prob>F
Regression	6	98162.83239196	16360.47206533	94.56	0.0001
Error	1002	173371.16166155	173.02511144 =mse		
Total	1008	271533.99405352			

Variable	Parameter Estimate	Standard Error	Type II Sum of Squares	F	Prob>F
intercept	231.22301551	36.14714326	7079.83764301	40.92	0.0001
PASSES	0.00212137	0.00013938	40078.85801817	231.64	0.0001
Q_SKEW	4.58598165	1.75005817	1188.14322475	6.87	0.0089
PVFWDISM	-0.00252858	0.00025802	16616.91815383	96.04	0.0001
BULKDENS	-0.87724708	0.23601574	2390.40275840	13.82	0.0002
ASPHCONT	-4.43946888	0.86553516	4551.99463681	26.31	0.0001
PCTSMALL	-3.22328768	0.47118347	8097.05666926	46.80	0.0001